



NARASARAOPETA
ENGINEERING COLLEGE
(AUTONOMOUS)



PROCEEDINGS

INTERNATIONAL CONFERENCE

EMERGING TRENDS IN MECHANICAL ENGINEERING AND INDUSTRIAL AUTOMATION

NEC-ICETMEIA-2K22

29th & 30th July, 2022

Editors-in-Chief

Dr. M.Sreenivasa Kumar

Principal & Professor, Dept. of Mechanical Engineering

Dr.D.Jagadish

Professor, Dept. of Mechanical Engineering

Editors

Dr. D.Suneel

Vice-Principal

Dr. B.Venkata Siva,

Professor, HoD Dept. of ME

Dr. P.Suresh Babu

Professor, Dept. of ME

Dr. M.Venkanna Babu

Associate Professor, Dept. of ME



Organized by

Department of Mechanical Engineering

In Association with *The Institution of Engineers (India)*



ISBN: 978-93-91420-07-9

Proceedings of
**International Conference on
Emerging Trends in Mechanical Engineering and Industrial Automation
NEC-ICETMEIA- 2K22
29th – 30th JULY 2022**

Chief Editors

Dr.M.Sreenivasa Kumar Principal and Professor Department of Mechanical Engineering Narasaraopeta Engineering College Narasaraopet-522601	Dr.D.Jagadish Professor Department of Mechanical Engineering Narasaraopeta Engineering College Narasaraopet-522601
---	---

Editors

Dr.D.Suneel
Dr.B.Venkata Siva
Dr.P.Suresh Babu
Dr.M.Venkanna Babu



Organized By

Department of Mechanical Engineering
NARASARAOPETA ENGINEERING COLLEGE (AUTONOMOUS)
NARASARAOPET-522 601, ANDHRA PRADESH, INDIA
www.nrtec.in

Every effort has been made to avoid errors or omissions in this publication. In spite of this, some errors might have crept in. Any mistake, error or discrepancy noted may be brought to our notice which shall be taken care of in the next edition. It is notified that neither the publisher nor the authors or seller will be responsible for any damage or loss of action to any one, of any kind, in any manner, there from.

No part of this book may be reproduced or copied in any form or by any means (graphic, electronic or mechanical, including **Photocopying**, recording, taping, or information retrieval system) or reproduced on any disc, tape, perforated media or other information storage device, etc., without the written permission of the publishers. Breach of this condition is liable for legal action.

For binding mistakes, misprints or for missing pages, etc., the publisher's liability is limited to replacement within one month of purchase by similar edition. All expenses in this connection are to be borne by the purchaser.

"Copying of the book and selling it after photocopying or reselling it as **Second Hand Book** is illegal and is not allowed, under the copyright act".

This book is sold subject to the condition that it shall not, by way of trade or otherwise, be **lent, hired** out, or otherwise circulated without the publisher's prior written consent.

All disputes are subject to Pakala jurisdiction only.

Note: Please inform if any one encourage to photocopy of this book, along with the Proof and get attractive Reward. Names will be kept Confidential.

©Authors

Rs. /-

ISBN: 978-93-91420-07-9

First Edition: 2022

Published by Surneni Mohan Naidu for Spectrum Publications and printed at Students Helpline Group, Hyderabad-38



SPECTRUM PUBLICATIONSTM
knowledge at your hands...

#326/C, Surneni Nilayam, Near BK Guda Park, S.R. Nagar

Hyderabad-500038, India

Tel: +914023710657, 32494570, 23800657

Cell: +919440575657, 9392575657

Fax: +914023810657

E-mail: studentshelpline.org@gmail.com

ACKNOWLEDGEMENT

It is my pleasure to record my sincere thanks to **Mr M.S.Chakravarthi, Hon'ble Vice Chairman, NEC Group** for his valuable guidance and encouragement throughout the proceedings of the conference. My sincere thanks to **Dr.M.Sreenivasa Kumar, Principal, NEC, Dr D. Suneel, Vice Principal NEC** and **Dr.B.Venkata Siva H.O.D., Mech.** for their whole hearted administrative support.

It's my privilege to thank the Keynote Speakers, Invited Speakers and Chairpersons of various technical sessions for their support in organizing the event. My sincere thanks to all the individual members of the Scientific Advisory Committee and Organizing Committee for their constructive ideas while designing the Conference Program. My special thanks to **Dr.Sergio Gonzalez Horcas**, Research Engineering in CFD, CIMNE, **Spain** and **Dr. Siddharth Pitta**, Fatigue and Damage Tolerance Engineer, Altran Innovations, Madrid, **Spain** for sparing their valuable time. I thank all the participants who submitted the scientific and technical papers for sharing their ideas.

NEC-ICETMEIA 2K21 conference would have been impossible without the support of academic institutions and industrial organizations both in terms of manpower and ideas. This support is greatly acknowledged. I thank my management **Sri M.V.Koteswara Rao** Garu, Chairman and **Sri M.Ramesh Babu** Garu Secretary for their kind support and encouragement for the conference.

My heartfelt thanks to my colleagues and all my research team members whose efforts and hard work in organizing and managing the conference are gratefully acknowledged. I thank Co-Conveners and Organizing Committee for rendering their support to the conference.

I sincerely thank M/S Spectrum Publications Hyderabad for bringing out the Souvenir and Pre Conference Proceedings well in time.

Finally, I thank all the people and institutions who are directly and indirectly involved in organizing the Conference.

I thank one and all

Dr.D.Jagadish

Professor

Department of Mechanical Engineering

Narasaraopeta Engineering College

(Autonomous)

Co-Convener, NEC-ICETMEIA- 2K22

Chief Patron

SrM.S.Chakravarthi, B.Tech, MS(US),eMBA(ISB-Hyd)

Vice -Chairman, NEC Group

Patrons

Sri M.V.Koteswara Rao, B.Sc

Chairman, NEC Group

Sri M.Ramesh Babu, B.Com

Secretary, NEC Group

Co-Patrons

Dr.M.Sreenivasa Kumar, M.Tech, Ph.D(UK),MISTEE,FIE(I)

Principal, NEC

Dr.D.Suneel, M.Tech, Ph.D, FIE(I),MISTEE,MRSI

Vice Principal, NEC

Convener

Dr.B.Venkata Siva, M.Tech, Ph.D, FIE (I), MISTE, ISNT

Head, Dept. of ME

Co-Conveners

Dr.D.Jagadish,M.E, Ph.D,

Professor, Dept. of ME

Dr. P.Suresh Babu,M.Tech, Ph.D

Professor, Dept. of ME

Organizing Committee

Dr.M.Venkanna Babu

Mrs.P.Sravani

Mr.M.Venkaiah

Mrs.D.Raghavendra

Mr.P.Srinivasa Rao

Mr.Shaik Bajan

Mr.Ch.Sekhar

Mr.A.Pavan Kumar

Mr.T.Ashok Kumar

Mr.K.Kiran Chand

Mr.N.Vijaya Sekhar

Mr.K.JohnBabu

Mr. SK.Nagul Meeravali

Conference Advisory Committee

Prof. Marina L. Galano,
Dept. of Material Science, UNIVERSITY OF OXFORD, UK

Dr. Rukmini Srikant Revuru,
Assoc Prof. University of Northern Iowa, Cedar Falls, IA, USA

Jose I. Rojas,
Department of Physics – Division of Aerospace Engineering,
Universitatpolitecnica de catalunya, Spain

Kishore Kumar Sadasivuni,
Department of ME & IE, Qatar University, Qatar

Prof. N Siva Prasad,
Pro Vice Chancellor, GITAM University, Hyderabad

Dr. K. Srinivasa Reddy,
Professor, Dept of ME, IIT Madras

Prof. V.V. Subbarao,
Principal, UCEN, JNTUK, Narasaraopet

Dr. A. Gopala Krishna,
Professor, Director (R&D), JNTUK

Dr. D. Chakradhar,
Asst. Prof. Dept. of ME, IIT, Palakkad

Dr. K.L. Sahoo,
Sr. Principal Scientist, CSIR, NML, Jamshedpur

Dr. Y. Ravi Kumar,
Asoc. Prof. Dept. of ME, NIT, Warangal

Dr. Y. Naresh,
Asst. Prof. Dept. of ME, SVNIT, Surat

Dr. Ramakrishna Ramachandran,
Assoc. Prof. Dept. of D&A, VIT, Vellore

Dr. P.S. Rama Sreekanth,
Dept. of ME, VIT, A.P

Mr. Jnanananda Rao Kadi,
Deputy Manager, Bharat Dynamics Ltd., Hyderabad

Dr. Srinivasu Gangisetty,
Asst. Prof. Dept. of ME, NIT, Raipur

Conference Papers Review Board

Dr.M.Sreenivasa Kumar, Professor, Principal, NEC

Dr.D.Suneel, Professor, Vice Principal, NEC

Dr.B.Venkata Siva, Professor, Head, Dept. of ME, NEC

Dr.D.Jagadish, Professor

Dr.P.SureshBabu, Professor

Dr.M.Venkanna Babu, Associate Professor

M.Venkaiah, Associate Professor

P.Srinivasarao, Assistant Professor

Ch.Sekhar, Assistant Professor

K.Kiran Chand, Assistant Professor

P.Sravani, Assistant Professor

T.Ashok Kumar, Assistant Professor

N.Vijaya Sekhar, Assistant Professor

K.John Babu, Assistant Professor

Shaik Bajan, Assistant Professor

SK.Nagul Meeravali, Assistant Professor

D.Raghavendra, Assistant Professor

PREFACE

International Conference on “**Emerging Trends in Mechanical Engineering and Industrial Automation**” **NEC-ICETMEIA-2K22** provides an excellent international forum for sharing knowledge and results in theory, methodology and applications impacts and challenges of Mechanical Engineering. The purpose of this conference is to bring together the mechanical engineering community to explore, disseminate and strengthen initiatives in new directions under the broad areas of Manufacturing, Thermal Sciences, Mechanical Design, Robotics, Mechatronics and Industrial Automation.

The objective of this conference is to create an international conglomeration of scientists, engineers and institutional experts. This forum serves as platform where people can share information about latest diverse technological advancements, innovations and achievements in the areas of Mechanical Engineering and allied fields of Engineering. Further it would also facilitate the discussion that centers on the developments and challenges in the fields of design, manufacturing, thermal, robotics, mechatronics fields of Engineering. The focus of this conference is to provide technical platform that encourages the scientific research and educational activities that would cater the needs of both society and the industry. Most importantly, NEC-ICEMEIA-2K22 is invested in the advancement of a common man’s life by utilizing the theory and practice of mechanical engineering and allied streams of Engineering. The conference includes Keynote addresses and guest lectures by eminent speakers around the globe who would deliberate the recent trends and challenges in the fields of Mechanical Engineering and Industrial Automation.

Message from Vice Chairman



I am glad to know that Department of Mechanical Engineering of Narasaraopeta Engineering College is organizing “International Conference on **Emerging Trends in Mechanical Engineering and Industrial Automation [NEC-ICETMEIA2K22]**. I hope this e-conference can congregate academicians, industry personnel and research scholars to share their findings and insights about innovations in Mechanical Engineering. The theme of the conference emphasizes on key aspects of Manufacturing, Thermal Sciences, Mechanical Design, Robotics, Mechatronics and Industrial Automation. I hope this initiative by Department of Mechanical Engineering will pave way to exceptional deliberations and other activities to enhance the power of knowledge and ideology in the field of engineering.

I wish the organizers great success for the conference.

Mr.M.S.Chakravarthi
Vice Chairman
NEC-Group

Message from Principal



I am glad to know that the Department of Mechanical Engineering of Narasaraopeta Engineering College organizing an International Virtual Conference on “**Emerging Trends in Mechanical Engineering and Industrial Automation [NEC-ICETMEIA2K22]**” during 29th & 30th of July 2022. The unprecedented ongoing pandemic situation prevailing all over the globe has driven the professionals to continue their research and knowledge dissemination virtually. I believe that such virtual conferences will be one of the finest opportunities for academicians, scientists, professionals, students and researchers from all over the globe to share and express their views, discuss the practical challenges and possible solutions in Science & Engineering fields.

The theme of the conference emphasizes the necessity of engineering innovation Mechanical Engineering in these difficult times all over the globe. I hope the scientific deliberations, discussions and other activities that happen during the conference will enrich the participants and definitely leave new milestones.

I wish the organizers the very best for the success of the Conference

Dr. M.Sreenivasa Kumar
Principal
Narasaraopeta Engineering College

Message from Vice Principal



It gives immense pleasure to write a message for the International Conference on “**Emerging Trends in Mechanical Engineering and Industrial Automation [NEC-ICETMEIA2K22]**” organized by Department of Mechanical Engineering, Narasaraopeta Engineering College (Autonomous) during 29th& 30th of July 2022. There are truly amazing innovations and breakthrough nowadays in the selected fields of Mechanical Engineering. I expect the present International Conference will explore students and research scholars to focus much on the field of Mechanical Engineering and Industrial Automation. I have gone through some of the abstracts and could see its rich qualitative academic content. I am also able to envisage its great potential to discuss and learn some new innovations in the fields of Mechanical Engineering.

It is important to inculcate an attitude towards research in the minds of younger generation and this conference would be a stepping stone towards this attainment in the field of Mechanical Engineering.

I wish the conference a great success. I am sure the conference is a grand scientific extravaganza and great feast for the student community.

Dr.D.Suneel
Vice Principal
Narasaraopeta Engineering College

Message from Head of the Department



I am very much delighted in welcoming the delegates for the 2 day virtual international conference on “**Emerging Trends in Mechanical Engineering and Industrial Automation [NEC-ICETMEIA2K22]**”. The pursuit for knowledge has been from the beginning of time but knowledge only becomes valuable when it is disseminated and applied to benefit of humankind. The prime focus of this conference is to bring together academicians, researchers and industry professional to join hands in finding the scope, challenges and opportunities and solutions that are encountered in the fields of Mechanical Engineering. Our technical sessions are rich and varied in the domains of **Machine Design, Production Engineering, Thermal Engineering and Automation**. As a conference Convener, I know that the success of the conference depends ultimately on the many people who have worked with us in planning and organizing both the technical program and virtual technical deliberations. In particular, we thank the review and advisory committee for their wise advice and brilliant suggestion on organizing the technical program; the Program Committee for their thorough and timely reviewing of the papers and publishing them in a conference proceeding. It is envisaged that the intellectual discourse will result in future collaborations between Universities, research institutions and industry globally towards the recent technological developments of Mechanical Engineering, during this pandemic situation.

Dr.B.Venkata Siva
Head, Department of ME

LIST OF FULL LENGTH PAPERS SELECTED FOR PROCEEDINGS
International Conference on Emerging Trends in Mechanical Engineering and
Industrial Automation
NEC-ICETMEIA- 2K22

Paper No.	TITLE OF THE PAPER	Page No.
NECICETMEIA-01	Camera Based Color Identification Robot For Segregation	01
NECICETMEIA-02	PLC Based Water Level Indicator & Controlling System	07
NECICETMEIA-03	Design Of Automatic Colour Code Sorting Machine Based On Pneumatics And PLC	11
NECICETMEIA-04	Design and Fabrication of Inversion of Slider Crank Mechanism by using 3D Printing	16
NECICETMEIA-05	Manipulation of Robotic Arm by using QR code	23
NECICETMEIA-06	Design And Fabrication of App Controlled Robot	28
NECICETMEIA-07	WI-FI controlled ward Sanitization robot car	34
NECICETMEIA-08	Influence of Core-Face Plates and Cell geometry on the strength of Sandwich Honeycomb Structure	45
NECICETMEIA-09	Design And Fabrication of 3D Printed Swiveling Vise	51
NECICETMEIA-10	Modelling and Fabrication of Finger Flywheel Engine Using 3D Printing	55
NECICETMEIA-11	Design And Fabrication of Prosthetic Hybrid Hand Using 3D Printing Technique	60
NECICETMEIA-12	Design and Fabrication of Geneva Mechanism using 3D printer	63
NECICETMEIA-13	Design and fabrication of Industrial time controller	68
NECICETMEIA-14	Evaluation and Comparison of Mechanical Properties of 3D Printed PLA Material With Different Filling Patterns	72
NECICETMEIA-15	Photoluminescence Investigations of Cd ₃ (BO ₃) ₂ Nano-Composite and transition metal ions doped Cd ₃ (BO ₃) ₂ Nano-Composites	80
NECICETMEIA-16	Synthesis And Characterization of Stir Casted Al 2024-Sic Metal Matrix Composites	84

NECICETMEIA-17	Comprehensive review on mechanism accountable for dispersion stability of ultra-fine particle suspensions in heat transfer applications	91
NECICETMEIA-18	Fracture, Fatigue Growth Rate And Vibration Analysis Of Cam Shafts Used In Railways	96
NECICETMEIA-19	Design And Fabrication of Multi-Purpose Operations Machine of Drilling, Sawing, Grinding And Cutting	104
NECICETMEIA-20	Preparation of al/brass composite (mmc) by using stir casting technique and its characterization	109
NECICETMEIA-21	Multi optimization of process parameters using grey relational analysis	114
NECICETMEIA-22	Optimization of Wear behavior of A7075-Flyash-Silicon Carbide metal matrix composite using Taguchi Method	117
NECICETMEIA-23	Optical and Luminescence futures of PbO-Al ₂ O ₃ -B ₂ O ₃ glasses doped with rare earth oxides	121
NECICETMEIA-24	Finite Element Analysis of Sheet Molding Compound Panels	126
NECICETMEIA-25	Design and fabrication of agriculture cutting machine using crank and slotted lever mechanism	130
NECICETMEIA-26	Design And Analysis of Helical Coil Spring In Two Wheeler Suspension System	135
NECICETMEIA-27	FE Analysis Knuckle Joint Used In Tractor Trailer	140
NECICETMEIA-28	The Aerodynamic analysis on car body and drag reduction by modifying the Design	145
NECICETMEIA-29	Design and Analysis of Bumper Assembly to Improve the Design for Impact	149
NECICETMEIA-30	Convertible Four Wheel Steering Mechanism	154
NECICETMEIA-31	Design And Analysis of Connecting Rod Using Generative Design	163
NECICETMEIA-32	Structural Analysis of Cam Mechanism With Different Load Applications	170
NECICETMEIA-33	Traffic Signal Control Using Programmable Logic Controller (PLC)	175
NECICETMEIA-34	PLC based automatic liquid filling and mixing system	180
NECICETMEIA-35	Designing And Modelling of Go-Kart Vehicle	186
NECICETMEIA-36	Experimental observation of Mechanical and microstructure properties of Corn /Coconut Hybrid composites with Alkali Treatment	189

NECICETMEIA-37	Fabrication and analysis of Heliotropic Smart Flower Solar Collector	194
NECICETMEIA-38	Fabrication And Performance Analysis Of Portable Vertical Axis Wind Turbine	198
NECICETMEIA-39	Effect of Titanium Oxide Nano Lubricant on the Performance of VCR System	202
NECICETMEIA-40	IoT based gas leakage detector robot	206
NECICETMEIA-41	Sterilization of Watercourse Contrivance	211
NECICETMEIA-42	Performance Monitoring of Heat Exchanger Using IoT	216
NECICETMEIA-43	Mathematical Modelling of Cooling Rates of Mango Fruits During Unsteady State Cooling in an Artificial ripening chamber	221
NECICETMEIA-44	Effect of Aluminum Oxide Nano lubricant on the performance of VCR system	226
NECICETMEIA-45	Transient thermal and structural analysis of disc brake	230
NECICETMEIA-46	A study of boundary layer flow over bullet shaped object	238
NECICETMEIA-47	Optimization of Steam turbine bland and its analysis	244
NECICETMEIA-48	Port Fuel Injection with Fuel Vaporizer and Early Pilot Injection Techniques in HCCI Combustion Engine	252
NECICETMEIA-49	Investigation of Mechanical, Thermal Properties and SEM analysis of Jute/Coconut Hybrid Composites with Alkali Treatment	257
NECICETMEIA-50	Design of gear assembly Using catia v5 software	261
NECICETMEIA-51	Optimization of properties of 3d printed abs material by 19 orthogonal array method	264
NECICETMEIA-52	Production of 4 inch cleat grey iron casting by full mould dry sand casting process	269
NECICETMEIA-53	Design and fabrication of injection moulding die using wire edm	270
NECICETMEIA-54	Conversion of high-density polyethylene (hdpe) to useful materials	271
NECICETMEIA-55	Design and fabrication of air purifier using hepa air filter	272
NECICETMEIA-56	The numerical analysis of bubble growth and bubble frequency in nucleate boiling	273

CAMERA BASED COLOR IDENTIFICATION ROBOT FOR SEGREGATION

VENKAI AH MANDULA¹, Y.VENKATA REDDY², K.PRAVEEN REDDY³

¹Assistant Professor, Department of Mechanical Engineering, Narasaraopeta Engineering College, Narasaraopet, India

^{2,3} Student, Department of Mechanical Engineering, Narasaraopeta Engineering College, Narasaraopet, India

Abstract— Recently, the use of has become significant to industries, especially when involving the routine works in industries. A robot is a machine designed to execute one or more tasks automatically with speed and precision. In our project work, by using the pneumatic gripper and the programming given pick and place operation will performed by color sensor. By using a robotic arm with pneumatic gripper Manipulation of a robot arm can be utilized for different purposes innovatively, here in this work, for pick and placing. IGUS robot with pneumatic gripper is used to hold the object and moves from one place to another place.

The goal of this project is to implement a programmable industrial robot for color sorting. This investigates the development of an intelligent and low-cost monitoring system for color identification and segregation. The main purpose is to optimize the productivity and avoid human mistakes. A serial image acquisition device (camera) is used to capture the image and are sent to SD card through a microcontroller. The microcontroller performs color detection algorithm to recognize the dominant color of the object, and it sends commands to the robotic arm to pick and place the objects to their respective locations. A robotic arm is a manipulator, which has about same number of degrees of freedom as in human arm. DC motors are used for joint rotations involved in the robotic arm; these motors are interfaced with microcontroller through motor driver circuits. These motor drivers are able to efficiently control the speed and direction of motors.

Keywords— pneumatic gripper, microcontroller, manipulator, robotic arm.

I. INTRODUCTION

Industrial robot is defined by ISO as an automatically controlled, reprogrammable, multipurpose manipulator, programmable in three or more axes, which can be either fixed in place or m Visual input, in the form of color images from a camera, can be a rich source of information, considering the sophisticated algorithms recently developed in the field of computer vision, for extracting information from images. Even so, most robots continue to rely on non-visual sensors such as tactile sensors, sonar, and laser. This preference for relatively low-fidelity sensors rather than vision can be attributed to three major discrepancies between the needs of robots and the capabilities of state-of-the-art vision algorithms .Pick And Place Robotics for use in industrial. This paper aims to address these challenges by exploiting the structure that is often present in a robot's environment. We define structure as the objects of unique shapes and colors that exist at known locations – a color-coded world model. We show that a robot can use this structure to model the color distributions, thereby achieving efficient color segmentation. Specifically, knowing that it is looking at an object of known color allows it to treat certain image pixels as labeled training samples. The domain knowledge also helps develop object recognition algorithms that can be used by the robot to localize and navigate in its

complex world towards additional sources of color information. We have developed a mobile robot vision system that learns colors using the uniquely color-coded objects at known locations, and adapts to illumination changes. Specifically, this article makes the following contributions: automation applications.

It describes a baseline vision system that tackles color segmentation and object recognition on-board a robot with constrained computational and memory resources. The baseline system is robust to jerky nonlinear camera motion and noisy images. However, it relies on manually labeled training data and operates in constant and uniform illumination conditions. And then it exploits the structure inherent in the environment to eliminate the need for manual labeling. The image regions corresponding to known objects are used as labeled training samples. The learned color distributions are used to better identify the objects, thereby localizing and possibly moving to other sources of color information. We introduce a hybrid color representation that allows for color learning both within the controlled lab settings and in un-engineered indoor corridors, it provides robustness to changing illumination 2 conditions. We introduce an algorithm that enables the robot to detect significant changes in illumination. When a change in illumination is detected, the robot autonomously adapts by revising its current representation of color distributions. As a result, the robot is able to function over a wide range of illuminations. The focus of this article is on the design of efficient robot vision algorithms that address challenging problems such as color segmentation, object recognition, color learning and illumination invariance. Using our algorithms the robot is able to operate autonomously in an uncontrolled environment with changing illumination over an extended period of time. The vision system is fully implemented and tested on a commercial off-the-shelf four-legged robot. We also illustrate the general applicability of our algorithms with the running example of a vision-based autonomous car on the road; we refer to it as the car-on-the-road task. The remainder of the article is organized as follows. After a brief description of our test platform, we present our baseline vision system, which tackles the problems of color segmentation, object recognition and line detection, in real-time.it extends the baseline system by eliminating the offline color calibration phase: the robot uses the environmental structure to autonomously generate a suitable motion sequence to learn the desired colors. Further enables the robot to detect significant illumination changes and adapt to them.

II. USE OF ROBOTS

There are many different reasons for using a robot but the central reason for most applications is to eliminate a human operator. The most obvious reason is: To save labor and reduce cost. Human is bad for the product for example semiconductor handling. Within this class are other reasons for using robots for example food handling, pharmaceuticals, etc. Product is bad for the human for example radioactive product. Within the above are other reasons for using robots for example robots can be used to replace human operators where the dangers are:

1. Repetitive strain syndrome.
2. Working with machinery that is dangerous for example presses, winders.
3. Working with materials which might be harmful in the short or long term. Quality the main reason for using a robot is to save labor the biggest impact a robot has can be on quality. Applications where quality will be improved are:
 1. gluing,
 2. spraying (glue or paint),
 3. trimming and de-burring,
 4. Testing and gauging.
 5. assembly
 6. laboratory routines

A. Robot anatomy:

Controller:

The Joint movements must be controlled if the robot is to perform as desired. Microprocessor-based controllers are regularly used to perform this control action. Controller is organized in a hierarchical fashion. Each joint can feed back control data individually, with an overarching supervisory controller coordinating the combined actuations of the joints according to the sequence of the robot program.

Manipulators:

Robot manipulators are created from a sequence of link and joint combinations. The links are the rigid members connecting the joints, or axes. The axes are the movable components of the robotic manipulator that cause relative motion between adjoining links. The mechanical joints used to construct the robotic arm manipulator consist of five principal types. Two of the joints are linear, in which the relative motion between adjacent links is no rotational, and three are rotary types, in which the relative motion involves rotation between links.

End effector:

Grippers grasp and manipulate objects during the work cycle. Typically, the objects grasped are work parts that need to be loaded or unloaded from one station to another. It may be custom-designed to suit the physical specifications of the work parts they have to grasp. End effectors, grippers are described in detail in below:

- ❖ Mechanical gripper: Two or more fingers that can be actuated by robot controller to open and close on a work part.

- ❖ Vacuum gripper: Suction cups are used to hold flat objects
- ❖ Magnetized devices making use of the principles of Magnetism, these are used for holding ferrous work parts.
- ❖ Adhesive devices Deploying adhesive substances these hold flexible materials, such as fabric
- ❖ Simple mechanical devices for example, hooks and scoops.

End effectors – tools:

The robot end effector may also use tools. Tools are used to perform processing operations on the work part. Typically, the robot uses the tool relative to a stationary or slowly moving object. In this way the process is carried out.

Examples of the tools used as end effectors by robots to perform processing applications include.

- Spot welding gun
- Arc welding tool
- Spray painting gun
- Rotating spindle for drilling, routing, grinding.
- Assembly tool (e.g., automatic screwdriver)
- Heating torch.

III. LITERATURE REVIEW

Dipak Aphale , Vikas Kusekar “PLC Based Pick and Place Robot with 4DOF” The pick and place robot is one of the technologies in manufacturing industry and designed to perform various functions. The system is very important to eliminate human errors and to get more precise work. It can also save the cost in long term and help to solve problems and tasks that cannot be done such as on high temperature area, narrow area and very heavy load thing. This project is a basic development and modification for that type of robot where it use the peripheral interface Programmable Logic Control (PLC) as the robot brain to control all of the robot movement. The rotation of till robots 360 degree (clockwise) and -360 degree (counter clockwise). The electromagnetic gripper will move horizontally to pick up and hold the object from one place to another place. This robot is used to pick and place the object only in their specifications (up to 300mm horizontal and 300mm vertically). The benefit of this project is the robot can pick the object using electromagnetic gripper which is simple in construction and also cost effective.

S Premkumar, Vikas Kusekar “Design and Implementation of multi handling Pick and Place Robotic Arm” Robot manipulator is an essential motion subsystem component of robotic system for positioning, orientating object so that robot can perform useful task of our work is to collaborate the gripper mechanism and

Vacuum sucker mechanism working in a single pick and place robotic arm. This robot can be self-operational in controlling, stating with simple tasks such as gripping, sucking, lifting, placing and releasing in a single robotic arm. The main focus of our work is to design the robotic arm for the above-mentioned purpose. Robotic arm consists of revolute joints that allowed angular movement between adjacent joint. Three double acting cylinders were used to actuate the arm of the robot. Robot manipulators are designed to execute required movements. By using this collaborated mechanism, the success rate of pick and place robots are increased.

Shirine El Zaatari, Mohamed Marei, Weidong Li, Zahid Usman: “Cobot Programming for Collaborative Industrial Tasks”, Collaborative robots (cobots) have been increasingly adopted in industries to facilitate human-robot collaboration. Despite this, it is challenging to program cobots for collaborative industrial tasks as the programming has two distinct elements that are difficult to implement: (1) an intuitive element to ensure that the operations of a cobot can be composed or altered dynamically by an operator, and (2) a human-aware element to support cobots in producing flexible and adaptive behaviors dependent on human partners. In this area, some research works have been carried out recently, but there is a lack of a systematic summary on the subject. In this paper, an overview of collaborative industrial scenarios and programming requirements for cobots to implement effective collaboration is given. Then, detailed reviews on cobot programming, which are categorized into communication, optimization, and learning, are conducted. Additionally, a significant gap between cobot programming implemented in industry and in research is identified.

De-socialisation For Turkle :, the advance of the robot for social purposes is worrying, and she fears that people will lose their social skills and become even lonelier. She is concerned that children will get used to perfect friendships with perfectly programmed positive robots, so they will not learn to deal with real-life people with all their complexities, problems, and bad habits. These ideas remain speculations, because there has been only limited research on the actual effects of the impact of social robots on children and adults. In addition, Turkle sees the sex robot as a symbol of a great danger, namely that the robot’s influence stops us from being willing to exert the necessary effort required for regular human relations: “Dependence on a robot presents itself as risk free. But when one becomes accustomed to ‘companionship’ without demands, life with people may seem overwhelming. Dependence on a person is risky—because it makes us the subject of rejection—but it also opens us to deeply knowing another.” She states that the use of sex robots leads to de-socialisation based on turkle point of view.

IV: PROGRAMMABLE LOGIC CONTROLLER:

A programmable logic controller (PLC) is an industrial computer control system that continuously monitors the state of input devices and makes decisions based upon a custom program to control the state of output devices. PLCs were first developed in the automobile manufacturing

industry to provide flexible, rugged and easily programmable controllers to replace hard-wired relays. Since then, they have been widely adopted as high reliability automation controllers suitable for harsh environments.

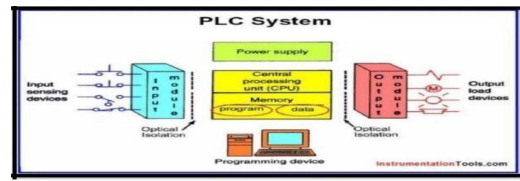


FIGURE 1 : PLC ARCHITECTURE

A.Connections from plc to robot:

In programmable logic controller they are six modules present in the system, they are power supply, communication module and four servo motors for four axis movements. The output of the plc give connection to the input of robot. a compressor is connected to the robot to hold the objects.



FIGURE 2: Programmable Logic Controller to Robot

V: EXPERIMENTAL PROCEDURE:

A.The following figure showing the block diagram of robot manipulation.

- The robot manipulation is based on c programming and PLC the control of manipulation of robot is controlled by PLC.
- In our work they two relays i.e. relay 1 is related to beverage one and relay 2 is related to beverage two.
- The two relays are getting signal from PLC, When the relay 1 get the signal, the submersible motor 1 activate similarly submersible motor 2 will be activate.

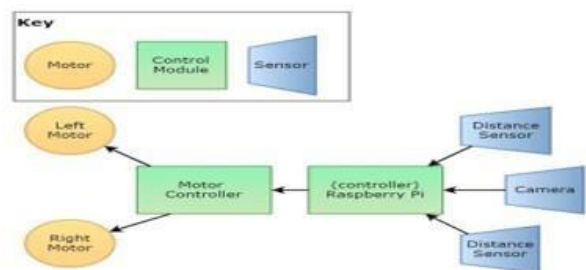


FIGURE 3 :Block diagram

B.SEQUENCE OF OPERATION:

- The sequence of operation is initiated from cprog software. The required operation of robot should be written in a code in cprog software.
- After execution code in cprog software, the plc controls the robot manipulation and robot get signal from PLC.
- The robot comes to home position and after that robot moves to a specific distance and pic the glass.
- The robot returns to its home position and wait for it command.
- The operator gives the command has switch. They are two switches and two relays.

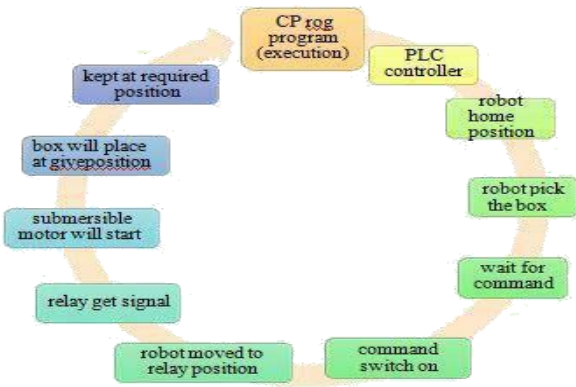


FIGURE 4: Sequence of Operation

C. CIRCUIT DIAGRAM OF PROJECT:

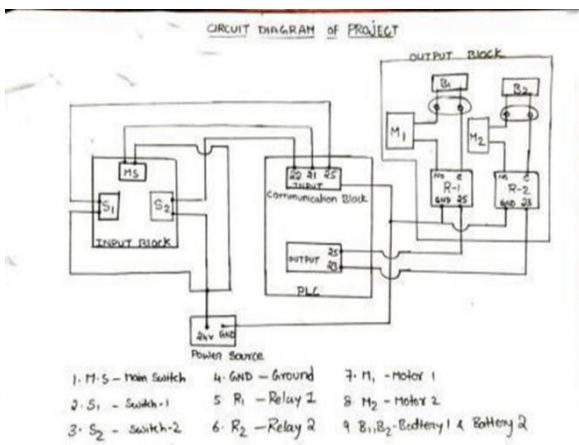


FIGURE 5: Circuit Diagram

The circuit diagram of the system working with PLC and relays has been schematically.

D. Step by Step Procedure of Code:

After completion of connecting circuits to robot and PLC. Then Switch on the robots, PLC and computer. Later Open CProg software and connect the hardware. Now reference the robot after it by using jog jogging command moving the robot in required axis and angle. Fix all the positions in the program editor and save it in the .xml format then run the program.

VI: EXPERIMENTAL RESULTS:

A. Step by step procedure to write the Main program in software:

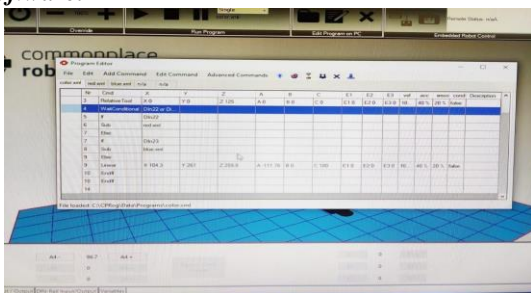


FIGURE 6 : Main Program

Explanation for the above program:

```
<Program>
<Header RobotName="igus Arm"
RobotType="igus_4DOF_BV" GripperType="
Software="CPRog V902-10-033"/>
```

```
<Linear Nr="0" x="281.1" y="0" z="518.1" a="-180" b="0"
c="180" e1="0" e2="0"
e3="0" vel="100" acc="40" smooth="20" AbortCondition="false"
Descr=""/>
<Joint Nr="1" a1="68.22" a2="1.89" a3="1.4"
a4="86.71" a5="0" a6="0" e1="0" e2="0"
e3="0"
velPercent="50" acc="40" smooth="20"
AbortCondition="false" Descr=""/>
<Linear Nr="2" x="104.3" y="261" z="259.8" a="-111.78"
b="0" c="180" e1="0" e2="0"
e3="0"
vel="100" acc="40" smooth="20"
AbortCondition="false" Descr=""/>
<Relative Nr="3"
MoType="CartTool" x="0" y="0" z="125" a="0.0"
b="0.0" c="0.0" vel="100"
acc="40" smooth="20"
AbortCondition="false" Descr=""/>
<Wait Nr="4" Type="Conditional"
Condition="DIn22 or Din23"
Descr=""/>
<If Nr="5"
Condition="DIn22" Descr=""/>
<Sub Nr="6" File="red.xml"
Descr=""/>
<Else/>
<If Nr="7" Condition="DIn23" Descr=""/>
<Sub Nr="8" File="blue.xml" Descr=""/>
<Else/>
<Linear Nr="9" x="104.3" y="261" z="259.8"
a="-111.78" b="0" c="180" e1="0" e2="0"
e3="0"
vel="100" acc="40" smooth="20" AbortCondition="false"
Descr=""/>
<EndIf/>
<EndIf/>
</Program>
```

B. Python Code For Color Recognition With Open Cv:

```
import cv2
from PIL import Image import os
import RPi.GPIO as GPIO import time
GPIO.setwarnings(False) GPIO.setmode(GPIO.BCM)
GPIO.setup(21,GPIO.OUT)
GPIO.setup(20,GPIO.OUT)
GPIO.output(20,False) # Turn on Led
GPIO.output(21,False)
cap = cv2.VideoCapture(0)
cap.set(cv2.CAP_PROP_FRAME_WIDTH, 640)
cap.set(cv2.CAP_PROP_FRAME_HEIGHT, 480)
while True:
_, frame = cap.read()
hsv_frame = cv2.cvtColor(frame, cv2.COLOR_BGR2HSV)
height, width, _ = frame.shape
cx = int(width / 2) cy = int(height / 2) # Pick
pixel value
pixel_center = hsv_frame[cy, cx] hue_value =
pixel_center[0] color = "Undefined" if hue_value < 5:
color = "RED" GPIO.output(21,True) #Turn on Led
time.sleep(1) GPIO.output(20,False) GPIO.output(21,False)
print("PASS TO RED TRAY") elif hue_value < 22: color =
"ORANGE"
elif hue_value < 33: color = "YELLOW"
```

C. Step by step procedure to write the red color program in CProg:

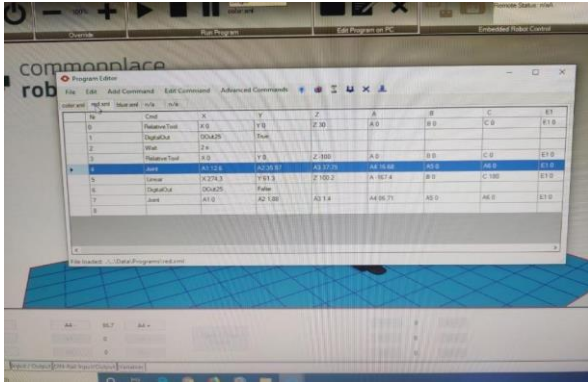


FIGURE 7: Red Color Box 1.xml

Explanation for the above program:

```

<Program>
<Header      RobotName="igus      Arm"
RobotType="igus_4DOF_BV"      GripperType=""
Software="CPRog V902-10-033"/>
<Relative Nr="0" MoType="CartTool" x="0" y="0" z="30"
a="0.0" b="0.0" c="0.0" vel="100" acc="40" smooth="20"
AbortCondition="false" Descr=""/>
<Output Nr="1" Channel="DOut25" State="True"
Descr=""/>
<Wait Nr="2" Type="Time" Seconds="2" Descr=""/>
<Relative Nr="3" MoType="CartTool" x="0" y="0" z="-
60" a="0.0" b="0.0" c="0.0" vel="100" acc="40"
smooth="20" AbortCondition="false" Descr=""/>
<Joint Nr="4" a1="-39.83" a2="33.43" a3="25.47"
a4="31.09" a5="0" a6="0" e1="0" e2="0"
e3="0"
velPercent="50" acc="40" smooth="20"
AbortCondition="false" Descr=""/>
<Relative Nr="5" MoType="CartTool" x="0" y="0"
z="130" a="0.0" b="0.0" c="0.0" vel="100" acc="40"
smooth="20" AbortCondition="false" Descr=""/>
<Output Nr="6" Channel="DOut25" State="False"
Descr=""/>
<Joint Nr="7" a1="0" a2="1.88" a3="1.4" a4="86.71"
a5="0" a6="0" e1="0" e2="0"
e3="0" velPercent="50" acc="40" smooth="20"
AbortCondition="false" Descr=""/>
</Program>
    
```

D. Step by step procedure to write the blue color program in CProg:

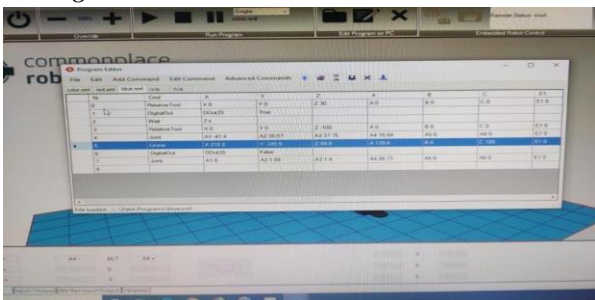


FIGURE 8: Blue Color Box 2.xml

Explanation for the above program:

```

<Program>
<Header      RobotName="igus      Arm"
RobotType="igus_4DOF_BV"      GripperType=""
Software="CPRog V902-10-033"/>
    
```

```

<Relative Nr="0" MoType="CartTool" x="0" y="0" z="30"
a="0.0" b="0.0" c="0.0" vel="100" acc="40" smooth="20"
AbortCondition="false" Descr=""/>
    
```

```

<Output Nr="1" Channel="DOut25" State="True" Descr=""/>
<Wait Nr="2" Type="Time" Seconds="2" Descr=""/>
    
```

```

<Relative Nr="3" MoType="CartTool" x="0" y="0" z="-100"
a="0.0" b="0.0" c="0.0" vel="100" acc="40" smooth="20"
AbortCondition="false" Descr=""/>
    
```

```

<Joint Nr="4" a1="-2.95" a2="35.58" a3="27.83" a4="26.58"
a5="0" a6="0"
e1="0" e2="0" e3="0" velPercent="50" acc="40" smooth="20"
AbortCondition="false" Descr=""/>
    
```

```

<Relative Nr="5" MoType="CartTool" x="0.0" y="0.0"
z="100.0" a="0.0" b="0.0" c="0.0" vel="100" acc="40.0"
smooth="20" AbortCondition="false" Descr=""/>
<Output Nr="6" Channel="DOut25" State="False" Descr=""/>
    
```

```

<Joint Nr="7" a1="0" a2="1.88" a3="1.4" a4="86.71" a5="0"
a6="0" e1="0" e2="0"
e3="0" velPercent="50" acc="40" smooth="20"
AbortCondition="false" Descr=""
    
```

VII. WORKING PHOTOS:



FIGURE 9: Explaining About Project

CONCLUSIONS:

A manually operated dispatching machine system has been designed for non- contact servicing of beverages using robot arm manipulated by PLC has been developed and implemented.

Robotics is a technology with a future, and it is a technology for the future. In this project we are introducing a robot which can pick and place objects based on the color. Earlier this was done using color sensors but we have improved the entire project by using a serial jpeg camera which can capture and identify or recognize the color of the image and eventually the robot picks and places that object accordingly. By doing so the speed and the accuracy of the color sorting process is increased. The cost for the color sorting process is considerably reduced. And most importantly there is overall optimization in the productivity if an industry. This robot arm can perform an action which is much similar to human. Although there is significant progress in robotics, still its usage is limited due to less availability of resources and high cost of production. If we able to overcome these restrictions, more benefits can be achieved from robotics.

Hence, the Pick and Place operation by using color sensor on IGUS Robot arm with 4-axis is successfully achieved. The PLC with combination of relays attached to the system of motors for picking and placing operations is used in this system to get more productivity with less time high reliability for and flexible in work.

Hence, the picking and placing operation by using color code on IGUS Robot arm with 4- axis is successfully achieved.

REFERENCES

1. A. K. Bejezy, Robot arm dynamics and control, 1974.
2. B. C. Mcinnis and C. K. F. Liu, "Kinematics and dynamics in robotics: A tutorial based upon classical concepts of vectorial mechanics", IEEE J. Robotics Automat., vol. RA-2, no. 4, Dec.1986.
3. C. S. G. Lee, "Robot arm kinematics dynamics and control", IEEE Computer, pp. 62-80, Dec.1982.
4. Denavit and R. S. Hartenberg, "A kinematic notation for lower-pair mechanisms based on matrices", ASME J. Appl. Mech, vol. 22, pp. 215-221, June 1955.
5. J. M. HoIIerbach, "A recursive formulation of Lagrangian manipulator dynamics", IEEE Trans.Syst. Man Cybern., vol. SMC-10, no. 11, pp. 730-736, 1980.
6. J. R. Birk and R. S. Kelly, "An overview of the basic research needed to advance the state of knowledge in robotics", IEEE Trans. Syst. Man Cybern., vol. SMC-11, no.8, pp. 574-579, 1981.
7. J. Y. S. Luh, M. W. Walker and R. P. C. Paul, "On-line computational scheme for mechanical manipulators", Trans. ASME J. Dyn. Syst. Meas. Contr., vol. 102, pp. 69-76, June 1980.
8. M. C. Leu and N. Hemati, "Automated symbolic derivation of dynamic equations of motion for robotic manipulators", Trans. ASME J. Dyn. Syst. Meas. Contr., vol. 108, pp. 172-179, Sept. 1986.
9. P. E. Nikravesh, R. A. Wehage and O. K. Kwon, "Euler parameters in computational kinematics and dynamics. Part 1", ASME J. Mech. Transmissions Automat. Des., vol. 107, pp. 358-365, Sept. 1985.
10. P. Paul, Robot Manipulators: Mathematics Programming and Control, MA, Cambridge:MIT Press, 1981. W. O. Schiehlen and E. J. Kreuzer, "Symbolic computerized derivation of equations of motion", Proc. IUTAM Symp., 1977.81.

PLC BASED WATER LEVEL INDICATOR & CONTROLLING SYSTEM

D.Raghavendra¹, K B M Murthy², M V S Kishore Kumar³, Shaik Shabber⁴

Assistant Professor, Department of Mechanical Engineering, Narasaraopeta Engineering College, Narasaraopet, India

Student, Department of Mechanical Engineering, Narasaraopeta Engineering College, Narasaraopet, India

Abstract—Automation has been an integral part of industries which provides safety, accuracy, efficiency and less human intervention with dangerous chemical process. In this project water level management using PLC is design to control the level of water and avoid wastage of water in the tank. The system has an automatic pumping attachment. The water level is controlled by using PLC, Sensors and motors. The purpose of doing this project to reduce time consumption and human resource consumption, increase product revenue and greater accessibility or more security. Also by using this project the wastage of water occurred by overflowing of tanks can be avoided. The logic of the project with minor changes can be used in different industries related to fluids like petroleum industries or oil refineries for controlling the level of filling the tanks and to avoid wastage.

Keywords— PLC, Sensors and motors, water level management, Float Sensor, Relay card

I. INTRODUCTION

In today’s fast-moving, highly competitive industrial world, a company must be flexible, cost effective and efficient if it wishes to survive. In the process and manufacturing industries, this has resulted in a great demand for industrial control systems/ automation in order to streamline operations in terms of speed, reliability and product output. Automation plays an increasingly important role in the world economy and in daily experience. Automation is the use of control systems and information technologies to reduce the need for human work in the production of goods and services. In the scope of industrialization, automation is a step beyond mechanization. Whereas mechanization provided human operators with machinery to assist them with the muscular requirements of work, automation greatly decreases the need for human sensory and mental requirements as well.

Automation Control System - system that is able to control a process with minimal human assistance or without manual and have the ability to initiate, adjust, action show or measures the variables in the process and stop the process in order to obtain the desired output.

The main objective of Automation Control System used in the industry are:

1. To increase productivity
2. To improve quality of the product
3. Control production cost

Programmable logic controllers are small industrial computers. Their design uses modular components in a single device to automate customized control processes. They differ from most other computing devices, as they are intended for and tolerant of severe conditions of factory settings such as dust, moisture, and extreme temperatures.

Industrial automation began long before PLCs. In the early 1900s until their invention, the only way to control machinery was through the use of complicated electro mechanical relay circuits. Each motor would need to be turned ON/OFF

individually. This resulted in factories needing massive cabinets full of power relays. As industrial automation continued to grow, modern factories of the time needed dozens of motors with ON/OFF switches to control one machine, and all these relays had to be hardwired in a very specific way. PLCs were developed as a solution to have one solid control as an electronic replacement for hard-wired relay systems. The term PLC architecture refers to the design specification of the various PLC hardware and software components and the how they interact with one another to form the overall PLC system. The architecture of a PLC is based on the same principles of that used in standard computer architecture.

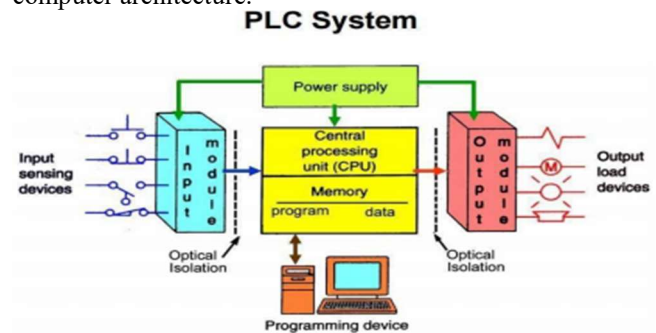


Figure 1: PLC Architecture

A Programmable Logic Controller, PLC or Programmable Controller may be a computer used for automation of Mechanical device processes. It is used to convert previously used “Relay Logic” or “Wired Logic” for automation of industrial purposes into “Ladder Logic”.

The system has associate automatic pumping system hooked up thereto thus on refill the tank once the liquid gets to the lower threshold, while offing the pump once the liquid gets to the higher threshold. Sustainability of available water resources in many reasons of the world is now dominant issue. This problem is quietly related to poor water allocation, inefficient use lack of adequate and integrated water management. Water is often used for agriculture, industry and domestic consumption. Therefore, efficient use and water monitoring and controlling are potential constraint for home or office water management system. Our planned system are often divided into 3 main modules sensing, decision making and implementation. Level sensors are used to implement the system. These sensors detect the presence of water. The readings of the sensors are utilized by the PLC to require the specified call. Finally the choice is enforced by the PLC through a relay switch. The ladder logic was implemented in WPS Delta software. The proposed system will control the liquid level of the tank continuously and will ensure that a sufficient level of water is maintained in tanks. This system can be used in industrial application. It can be used to prevent industrial accident by overflowing of any open container and

to prevent overflowing of any closed container thereby creating overpressure condition. The high number of the input output port of the PLC will enable this single system to control large number of tanks single handedly. The system is operated by PLC so there is no need of human

Interference this could save the human resources and provides protections to individuals from danger of industrial accidents. The system is highly reliable, once programmed it does not need any inspections.

II. COMPONENTS USED

A. *PLC Board:* A programmable logic controller (PLC) is an industrial computer control system that continuously monitors the state of input devices and makes decisions based upon a custom program to control the state of output devices

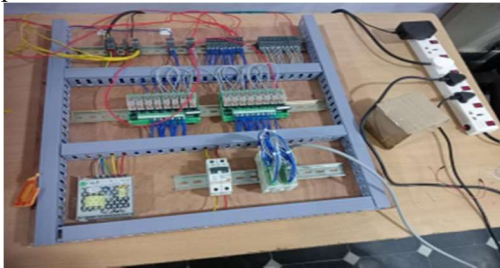


Figure 2: Programmable logic controller Board

B. *SUBMERSIBLE PUMP MOTOR:* The motor is hermetically sealed and close-coupled to the body of the pump. A submersible pump pushes water to the surface by converting rotary energy into kinetic energy into pressure energy.



Figure 2: 24V-DC Motor

C. *WATER LEVEL SWITCH SENSOR:* Float level switches are general liquid level switches, and are used to detect liquids.. These level switches have been used in various locations where liquid levels must be detected. A float switch is a device used to sense the level of liquid within a tank. The switch may actuate a pump, an indicator, an alarm, or other device.



Figure 3 : Water Level Switch Sensor

D. *CONTAINERS:* These containers made with plastic .These are used to passing the liquids from one container into another containers with the help of the water tubes. The liquid flow into the containers by the ladder diagram (time management). In this containers we arrange the 2- motors in two containers with water tubes.



Figure 4: Containers

E. *WATER TUBES:* The water tubes are helpful to pumping the water one container to another container. The pipe -1 is placed in first container, which is attached to pump motor-1 The pipe-2 is placed in second container, which is attached to pump motor-2 The pipe-2 is dropped in first container. The pipe-1 is dropped to second container



Figure 5: Water Tubes

F. *RUBBER TAPES AND INSULATION TAPES:* Rubber tapes are designed for use I NHY6n splicing and terminating wires and cables with options rated up to 69Kv. Electrical tape is a safety tape for wires, used to cover and insulate a broad range of cables, wires and other materials that conduct electricity.

G. *ELECTRICAL WIRES:* Stranded wire is composed of a number of small wires bundled or wrapped together to form a larger conductor. Stranded wire is more flexible than solid wire of the same total cross-sectional area.



Figure 6: Electrical wires

IV. EXPERIMENTAL PROCEDURE:

- ❖ Make the arrangement of required material of the plastic containers, float sensors, motors, wires, and PLC board and computer system.
- ❖ As to fulfil the need of two water tanks as we use two plastic containers.
- ❖ One bucket is used for purpose of a water tank from where water is to be fetched.
- ❖ The other one is use to fill the water until a specific quantity.
- ❖ The first tank comprises of a motor M0 to fetch water for second tank.



Figure 7: Water transfers from container

- ❖ The second tank comprises of two float sensors attached inside that serve as lower level and upper level for water.
- ❖ The float sensor detect the level of water

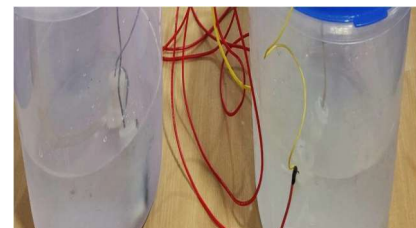


FIGURE 8: Float Sensors detect

- ❖ When the program set to run the computer system by using WPL software.
- ❖ The input of main switch at X0 and Y0 input red wires at x1, x2, x3 and output yellow wires at Y1, Y2 and Y3.
- ❖ As power is set on, the water is at low level then water starts adding in to required tank.
- ❖ When the water reaches required up to upper level sensor detects and stops the water supply.
- ❖ Automatically the supply set to off position when water level is reached up to the tank.
- ❖ The flow of water will start from outside tank.
- ❖ The cycle will repeat according to the program burned in PLC.

SCHEMATIC DIAGRAM:

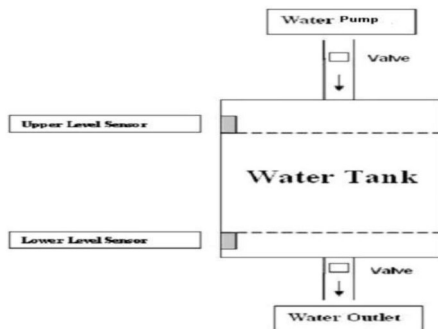


Figure 9: Schematic diagram

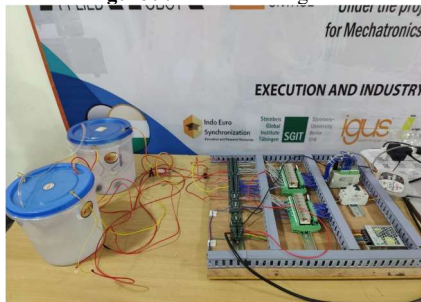


Figure 10: Water level indicator and controlling system connections

V. EXPERIMENTAL RESULTS

A. Ladder diagram:

Ladder diagrams are specialized schematics commonly used to document industrial control logic systems. They are called “ladder” diagrams because they resemble a ladder, with two vertical rails (supply power) and as many “rungs” (horizontal lines) as there are control circuits to represent.

The four components of ladder diagrams are:

- ❖ Power Supply (rails).
- ❖ Input Devices (components).
- ❖ Output Devices (components).
- ❖ Conductors (rungs)

B. Ladder Logic:

Ladder logic was originally a written method to document the design and construction of relay racks as used in manufacturing and process control. Each device in the relay rack would be represented by a symbol on the ladder diagram with connections between those devices shown. In addition, other items external to the relay rack such as pumps, heaters, and so forth would also be shown on the ladder diagram.

Ladder logic has evolved into a programming language that represents a program by a graphical diagram based on the circuit diagrams of relay logic hardware. Ladder logic is used to develop software for programmable logic controllers

(PLCs) used in industrial control applications. The name is based on the observation that programs in this language resemble ladders, with two vertical rails and a series of horizontal rungs between them.

C. ALGORITHM:

STEP-1

Arrange all the parts and give the connection.

STEP-2

Fill the plastic containers with water.

STEP-3

Switch on the power.

STEP-4

Container-1, Power motor-1 will start and pump the liquid to the other container from the source to the tank.

STEP-5

Fill the water to reach the high level.

STEP-6

Automatically the water supply stops.

STEP-7

Repeat the process up to requirement.

D. Ladder Diagram Of Water Level Indicator And

Controlling System:

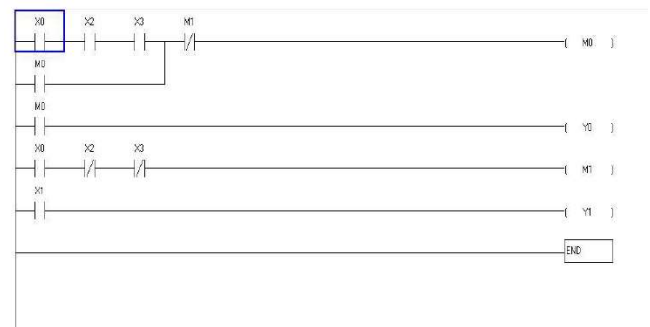


Figure 11: Ladder diagram of Water level indicator and controlling system. Ladder diagram usually starts from top to bottom and left to right. Inputs placed at left side and outputs at right side of ladder diagram.

Here the,

- X0 is Main Switch
- X1 is Secondary Switch
- X2 is Low Level Sensor
- X3 is High Level Sensor
- Y0 is Inlet Motor
- Y1 is Outlet Motor

CONCLUSION

This prototype is specifically designed for the transfer of accurate amount of water desired in any process or system that involves the measurement of a certain amount of water. The adaptability in industry of our research is due to its automatic process. It is more probable that our research is accepted due to ease of usability and very low cost. In today’s world industries can only grow by making themselves advance in technology and by upgrading their machineries and plants. The water level control system using PLC and wireless sensors is a simple one and combines wireless sensors and programmable logic controllers. The program was made on an experimental panel with a DELTA WPL software. 24RL programmable logic Controller conducted in the laboratory. Wireless sensors and PLC are modern technologies that can be used for several control systems such as water tank level process.

A solution for water level control system using PLC and wireless sensors is proposed, designed, implemented and tested. The advantages of a design based on a PLC are simplicity, flexibility.

FUTURE SCOPE

Automatic water level monitoring system has a good scope in future especially for agriculture sector. There are any areas where we need water level controller. It could be agricultural fields, overhead tanks. We can make this project wireless by using NRF transmitter and receiver. In future, the proposed system can be used to monitor and analyse water usage of the specific water source thus require developing such logic for the application. The system can also be used to collect and study the environmental data of water source and its surrounding area by integrating other sensor to the system.

REFERENCES

- [1]. Aamir, M. and Mahmood, A. (2008). Performance Analysis of Wide area operation, control and protection using High Scale SCADA System. 978- 1-4244-2895-3/08/\$25.00 ©2008 IEEE .
- [2].Austin, H. (2005). Electric Motor and Drives, Newness; 3rd Edition.
- [3].Birbir, Y. and Nogay, H. S. (2008). Design and Implementation of PLC Based Monitoring Control System for Three-Phase Induction Motors Fed by PWM Inverter.
- [4]. International Journal of Systems Applications, Engineering & Development, 2,128-135.
- [5]. Bolton, W. (2006). Programmable Logic Controllers. 4th ed., North Carolina: Elsevier Newnes.
- [6]. Bover, S. A. (2004). SCADA: Supervisory Control and Data Acquisition. ,3rd ed., North Carolina: ISA, 9-21.
- [7]. Hao, L. and Ruilin, P. (2005). Application of Centralized PLC Automation Control in Painting Line of Steel Plant. Proceeding of the 4th Asian Conference on Industrial Automation and Robotics, Landmark Hotel, Thailand.
- [8]. Hugh, J (2008). Automated manufacturing system with PLCVersion 5.1
www.freeinfosociety.com/media/pdf/2908.pdf.
- [9]. Jay, H. (2003). Basic Pneumatics, Carolina Academic Press.
- [10]. James, H. (1993). Industrial control electronics. James Humphries, Delmar CengageLearning; 4th edition.
- [11]. PLC LOGO Instruction manual Siemens.

Design Of Automatic Colour Code Sorting Machine Based On Pneumatics and PLC

Sivasankara Raju R¹, Sreeramulu D², Sagar Yanda³, Srihari P⁴, Raghuvveer D⁵

Department of Mechanical Engineering, Aditya Institute of Technology and Management, Tekkali - 532201, Andhra Pradesh, India

Abstract—Industrial automation has become more important in all production processes over the past few decades. Therefore, saving time, money, and human effort is our key goal. As a result, the "Colour Sensing Punching Machine" was created to satisfy the aforementioned needs. Instead of having separate conveyors for each colour, have a single conveyor with a colour sensor, which saves both money and space. PLC programming is employed to make labour easier than with other equipment, and a pick-and-place robot is used to accurately box finished goods. This work is also accelerating manufacturing at a high rate of precision. The entire procedure is carried out in stages. Layout is first created by sketching, followed by simulations of PLC programming in WPL software, PLC assembly, completion of all parts with minor components like lights to prevent loss, testing, and approval. So that small-scale industries like food production and soft-ball manufacturing can begin as soon as the entire process is ready. The top outcomes in the sectors are produced by these kinds of industrial machinery with skilled workers.

Keywords: Color Detection, PLC, Photoelectric Sensor, WPL Software, Microcontroller.

I. INTRODUCTION

Automation is largely converting the role of people in plenty of systems, and riding isn't always any exception. A developing amount of automobiles are being prepared with pace manipulate structure. This device use ultrasonic sensor to discover the impediment or affecting automobile beforehand and warn toward motive force on crash risk. When subsequent a few other car, the velocity manage device (SCS) will mechanically offers sign about distance among vehicle with obstruction during LED show to the driver to lessen the pace of vehicle[1]–[3].

Nowadays manufacturers of Cars similarly to Motor cycles moreover anticipate such technology and machine's which assures safety at immoderate pace. The use of right braking gadget and via the use of managed tempo discount strategies is the important thing to solve such troubles. The utilization of Anti-lock braking mechanism in motors is the present day style to boom protection of the car. There are also different answers like Automatic Braking Systems which can be beneficial as well as useful. Automatic braking technology coalesce sensors and brake controls to assist save human immoderate momentum impact. Some computerized braking structures can save collisions on the whole, but maximum of them are intended to actually reduce the cost of a medium earlier than it hits some component[4]–[7].

Automation has been accomplished by a variety of methods, including mechanical, hydraulic, pneumatic, electrical, electronic, and computer systems, frequently in conjunction. Complex systems, including contemporary factories, aircraft, and ships, frequently employ all four strategies in combination. Automation has several advantages, including reduced labour expenses, lower electricity and

material prices, and higher levels of precision, accuracy, and quality. In general there are 3 types of automations such as flexible, programmable and fixed automations. Figure 1 is shows levels in industrial automation.

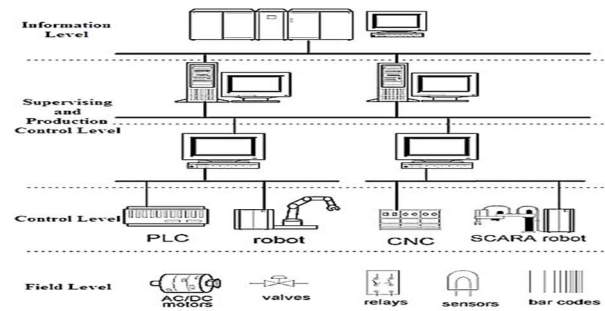


Fig. 1. Levels in industrial Automation

Pneumatics is the study of system operated under Air pressure. In a boarder classification, air comes under the terminology of fluids. In industrial fluid power technology, pneumatic system holds a significant place and is widely used, various components of pneumatics as shown in Figure 2.



Fig. 2. Various components in Pneumatics

Dhanya et al. [8] proposed an era of improve automatic braking with sensor fusion idea. In this they represent operation of the residences of every capacitive and ultrasonic sensor for identifying the difficulty for measuring the distance many of the car and the interference. This distance range is applied to deal with computerized braking system for security program. In this apparatus they adopt the 32-bit micro-controller with ARM processor (LPC2138) because the thoughts of this gadget for controlling performance and complete the register through using c-language.

Bhumkar et al. [9] implements a scheme of about accidents avoidance and disclosure on streets. This technology is prepared for growth production in vehicles to execute it more intelligently and interactively to prevent accidents on highways. ARM7 is the usage of making this design more active, steady and powerful. In this process, they heard described real-time online protection prototypes that rule the

car pace underneath motive pressure exhaust. The principle of this machine is to avoid injuries.

Sairam et al. [10] provides a technique which can adorn the security of an automobile. This machine offer solution can reinforce the operator via caution the purpose force impediment and gathering adjacent to a vehicle that could produce collision to this. Moreover implementing and automobile are retarding in device, which supports in heading off calamities. In this device ultrasonic sensor, motor purpose of pressure and LCD are adopted.

Muqaddas Bin Tahir [11] have come up with an ingenious method distance measuring (Hurdle Detection) for comfy surroundings in car via ultrasonic rays. In this strategy, 8 ultrasonic sensors are employed to sense the unique find of a thing. By enforcing a rise in safety strategy in automobile, sensor may be able of achievement typically until the sensor detects workable possibility. Until the car reaches 75 feet inside of an object in this situation, the sensor will not permit output or sign, at which point the timer will give the driver a record of the obstruction. The sensor clearly displays an object; it is up to person or goal pressure to overcome the obstacle.

In order to help identify important process factors, Oram and Strine [12] devised colour assessment of a solid active drug component. An investigational drug's powdered pharmaceutically active ingredient (API) was found to have a colour as a result of several manufacturing variables. A sphere spectrophotometer's reflectance data was used to determine the solid material's colour. These data offered a practical and non-destructive tool to monitor how changes in the process parameters affected the final product. Visual evaluation was unable to offer a quantitative, impartial evaluation of the information. Even as visual variations were obvious, Colour of Solution (COS) analyses lacked the sensitivity to identify a few of the data from one another.

The primary objective of this work is to reduce the space occupied by the machinery in industries. In order to sort objects of various colours, multiple conveyor belt devices are equipped and used in a variety of industries, such as the food processing industry and the pharmaceutical industry. This is accomplished by establishing up a single conveyor belt that transports goods, followed by a PLC module and sensor module that recognises the objects and sorts them appropriately. By only slightly increasing the inputs for the PLC, the expenditures, labour costs, and cost of installation are drastically decreased.

The objective of this work is:

- To develop a colour detection system using Photoelectric sensor
- To suggest a cost effective automation solution that is simple to apply in today's businesses in order to reduce periodical or manual accuracy testing.

II. DESIGN AND IMPLEMENTATION

a. PLC Programming

It is simple to calculate with Programmable Logic Controllers (PLCs). They use relay ladders, which are strikingly similar to hypnotic relay circuits. Without a lot of practise or study, engineers, consultants, and electricians can figure out how to compute the PLC. The decision to use programmable logic controllers rather than relays or solid-state electronics is

influenced by a variety of factors. Transformations are possible in a PLC, and in most cases, they don't need changing the controller's hardware. PLCs are recyclable, and indicator lights at key diagnostic locations on the PLC aid in regulation. It is dependable, effective in the current environment, and simple to maintain. The PLC is adaptable and able to produce a variety of functionalities in addition to cost savings.

b. PLC Wiring

Generally, in electrical wiring concept we have two major types. They are Sourcing and Sinking: When choosing the type of input or output module for your PLC system, it is very significant to have a firm sympathetic of sinking and sourcing concepts. Uses of these terms occur often in conversation of input or output circuits.

A series or parallel connection (Figure 3) can be used to connect a number of inputs (I1, I2, I3, I4,.....In) with a variety of outputs (Q1, Q2,.....Qn). The three inputs (I1, I2, and I3) are connected in series with the single output (Q1 and Q2), whereas the four inputs (I1, I2, I3, and I4) are connected in parallel. As a result, we can link the inputs in series or parallel depending on the needs of our code.

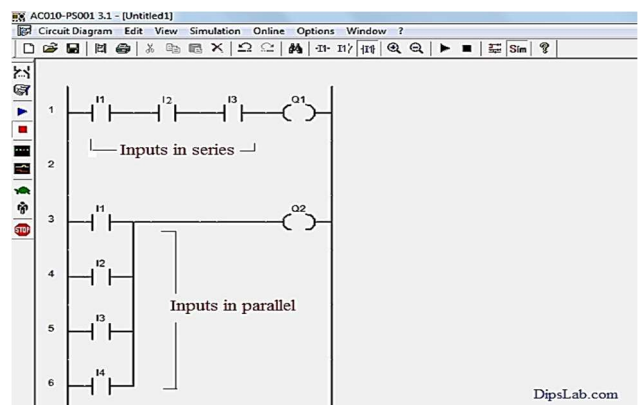


Fig. 3. Inputs Representations in Series and Parallel Connection

The second rule states that the single input and all of the outputs (Q1, Q2, Q3, Q4,.....Qn) are connected in parallel (I1). See the illustration Figure 4. The single output (Q1) will activate if the single input (I1) is ordinarily closed (NC contact) (On).

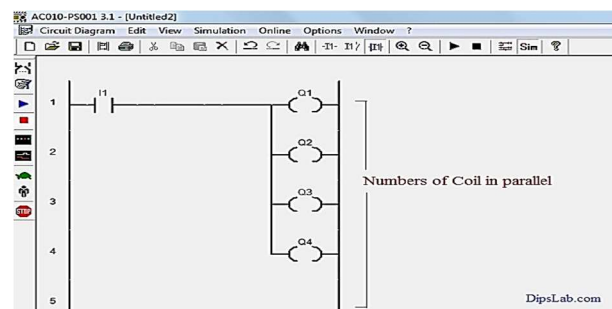


Fig. 4. Outputs in Parallel Connection

The third rule states that a just been can be used repeatedly in several rungs. As you can see from the graphic Figure 5, the programme is attached to the very same input (switch) but various outputs.

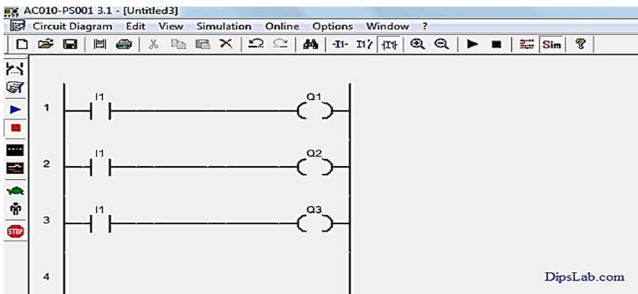


Fig. 5. Single Input with a different form of Outputs

Figure 6 shows the working in the latch/unlatch function is identical to that in the set/reset function. The sole distinction is that the second input (I2) is generally closed whereas the first input (I1) is usually opened (NO) (NC). The cycling process can benefit from the launch/unlatch operation.

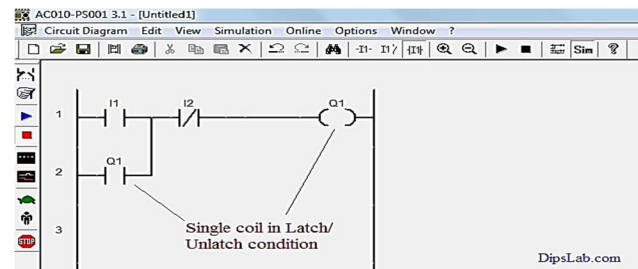


Fig. 6. Latch Coil or Unlatch Coil (Same Output Address)

c. WPL SOFTWARE

WPLSoft, shown in Fig. 7, is program-editing software created for the Delta DVP-PLC series used with Windows. In addition to general programme design and distinct general Windows features (such as cut, paste, copy, and multi-windows), WPL Soft has included a wide range of Chinese/English commentary-editing and special features.

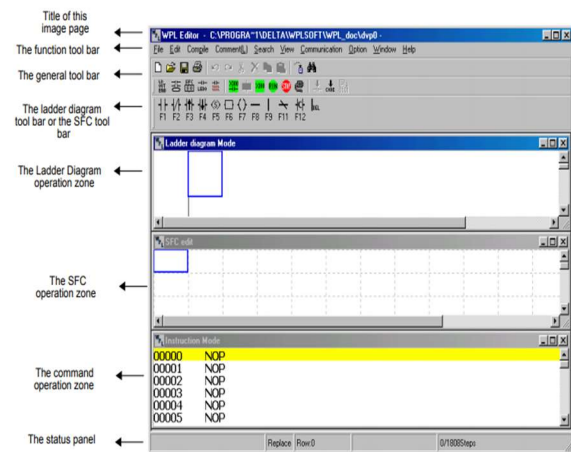


Fig. 7. WPL Editor Window

d. PNEUMATIC ACTUATOR

A piston or a diaphragm that generates the motive force makes up the majority of a pneumatic actuator. It maintains the air in the top part of the cylinder, allowing air pressure to drive the piston or diaphragm to turn the valve control element or move the valve stem. Valves function with low pressure and often multiply or triple the input force. The output pressure might increase with the size of the piston. If

the air supply is poor, having a larger piston can help because it will produce the same forces with less effort. These pressures are high enough to cause pipe-bound objects to be crushed. You could easily move a compact automobile (weighing up to 1,000 lbs) with 100 kPa input, and this is merely the beginning. A schematic layout is shown in Figure 8.

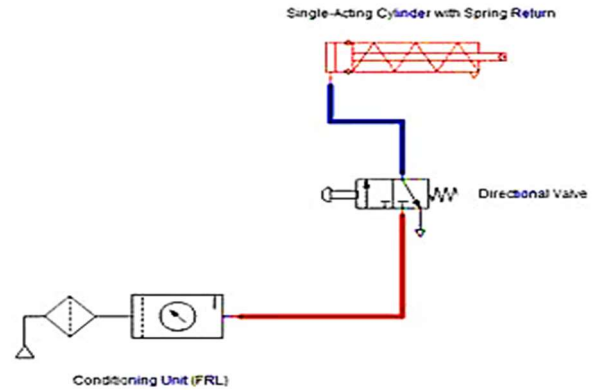


Fig. 8. Working circuit of single acting cylinder developed in Automation studio software

e. PHOTOELECTRIC SENSOR

Photo-optical workpieces are found via photoelectric sensors. There are numerous types of sensors, such as diffuse-reflective, through-beam, retro-reflective, and distance-settable sensors. Additionally, there are sensors with integrated or external amplifiers and fibre units. An Emitter for generating light and a Receiver for receiving light make up the majority of a photoelectric sensor. The amount of light that reaches the receiver changes, when emitted light is stopped or reflected by the detecting device. This change is picked up by the receiver, which transforms it into an electrical output. Most photoelectric sensors use infrared or visible light as their light source (often red or green/blue for distinguishing colours). Triangulation is the general operating mechanism for distance-settable sensors. Figure 9 provides an illustration of this idea.

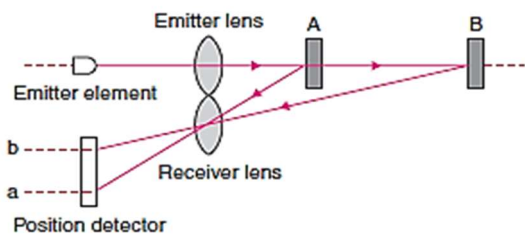


Fig. 9. Principle of triangulation

The Emitter and Receiver are mounted in the same housing, as shown in Figure 10, and the Reflector is generally installed on the contrary direction to reflect light back to the Receiver from the Emitter. The detecting device reduces the amount of light received when it interrupts the light. The object is found using this decrease in light intensity.

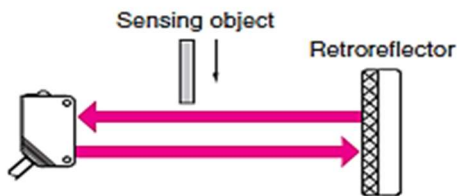


Fig. 10. Sensing Method

f. ROBOTICS SYSTEMS

Servo motors are used to drive the robotic arm, and the timer of the pulse rail that appears at its control inputs regulates how much they rotate. Different degrees of rotation for the servomotor are assigned to perform the actions in accordance with the design of the robotic arm. The robot's arm is created utilizing brackets made of aluminium. For this, four different sorts of brackets are arranged. The complexity and manufacturing process of the robotic arms makes them extremely expensive and complicated. Two different types of brackets are used for the robotic arm's extensions and interconnections, as well as two different types for holding the servo motors.

III. STEPS IN CIRCUIT DESIGNING

The layout of circuit and assembled panel are presented in Figure 11 and Figure 12. The lists of components such as STOP push button (X1), START push button (X0), Red light treated as pistons (Y2, Y4, Y6), Terminal block, 220V AC power supply, 220V AC to 12V DC converter, RELAY, proximity sensor treated as colour sensor (X2, X3, X4), USB port, RS 32 cable, TRUFF, MCB (miniature circuit breaker), Buzzer treated as holding devices (Y1, Y3, and Y5), PLC (programmable logic controller), SMPS (switch mode power supply), and DC motor treated as motor for conveyor (Y0), Dend Rail.

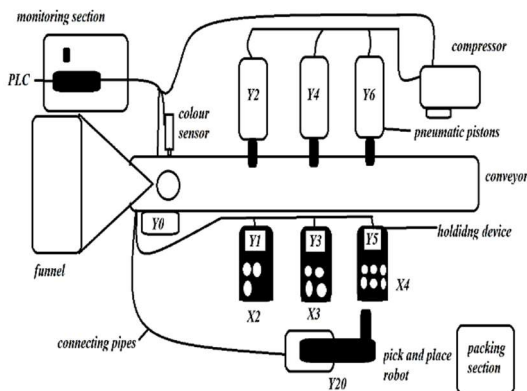


Fig. 11. Layout of colour code sensing punching machine

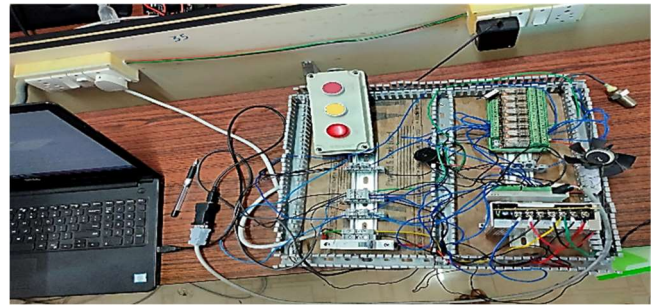


Fig. 12. Automatic colour code sensing punching machine based on pneumatics with PLC

a. CIRCUIT DIAGRAM AND EXPLANATION

- The PLC programming is done through the WPL software and then simulation is also done in the same software.
- Then the programming is imported to the PLC and make sure that the connections are tightly fixed as mentioned in the layout.
- At first the objects are manufactured in the separated block then at last those all mixed in the funnel for packing section.
- Then these objects are placed in the conveyor.
- The colour sensor is located at first in the conveyor it detects the colour. Once it detects the colour based on the time delay the conveyor stops and object is placed at the respective position exactly In-front of the pistons.
- The three pistons and three holding devices are there for three colours which are RED, GREEN, and BLUE.
- The time delay for Red sensor and piston 1 is 5 seconds, the time delay for Green sensor and piston 2 is 10 seconds, the time delay for Blue sensor and piston 3 is 15 seconds.
- The holding devices are ON before 3 seconds of the piston ON and conveyor stops in the respective positions and OFF after 2 seconds of piston return backs.
- After printing the logo, description of company, ingredients and price details on the components the piston goes its actual position then after the holding device releases the object to the container.
- The sensor in the container counts the objects when it reaches to 5, 10, 15 objects of Red, Green, Blue coloured objects the pick and place robot is ON and it places in the packing section.
- While operating the robot the remaining process is stopped.
- This operation is done until the production stops.

IV. CONCLUSIONS

The entire PLC programming (ladder diagram) is done through WPL software and later the simulation is also done by using WPL software. So that the program is imported to the PLC and verified by using the above connection and concluded that the program for Automatic colour code sensing punching machine based on pneumatics gives the accurate results. Hence this code is used for the medium scale industries to meet Good results.

Acknowledgements. The Authors are grate thankful to the management of Aditya Institute of Technology and Management, for establishing ARC laboratory collaborating with APSSDC – European centre for Mechatronics APS GMBH, Aachen.

REFERENCES

- [1] A. P. Correia, C. H. Llanos, R. W. de Carvalho, S. A. Alfaro, C. Koike, and E. D. Moreno, "A control design approach for controlling an autonomous vehicle with FPGAs," *J. Comput.*, vol. 5, no. 3, pp. 360–371, 2010.
- [2] D. Webster, "A Pulsed Ultrasonic Distance Measurement System based upon Phase Digitizing," *IEEE Trans. Instrum. Meas.*, vol. 43, no. 4, pp. 578–582, 1994.
- [3] H. Ahmad Al_Issa, "Sensors Application Using PIC16F877A Microcontroller," *Am. J. Remote Sens.*, vol. 4, no. 3, p. 13, Jul. 2016.
- [4] C. C. Chang, C. Y. Chang, and Y. T. Cheng, "Distance measurement technology development at remotely teleoperated robotic manipulator system for underwater constructions," in *International Symposium on Underwater Technology, UT'04 - Proceedings*, 2004, pp. 333–338.
- [5] D. H. K. Hoomod and S. M. M. Al-Chalabi, "Achieving Real-Time Tracking Mobile Wireless Sensors Using SE-KFA," in *Journal of Physics: Conference Series*, 2018, vol. 1003, no. 1, p. 012039.
- [6] N. Amin and M. Borschbach, "Quality of obstacle distance measurement using Ultrasonic sensor and precision of two Computer Vision-based obstacle detection approaches," in *International Conference on Smart Sensors and Systems, IC-SSS 2015*, 2017, pp. 1–6.
- [7] G. L. Gissinger, C. Menard, and A. Constans, "A mechatronic conception of a new intelligent braking system," *Control Eng. Pract.*, vol. 11, pp. 163–170, 2003.
- [8] D. Thakur and A. P. Thakare, "A Review on Implementation of FPGA for Automatic Reverse Braking System," *Int. J. Sci. Res. ISSN (Online Index Copernicus Value Impact Factor)*, vol. 14, no. 1, pp. 2319–7064, 2013.
- [9] S. P. Bhumkar, V. V. Deotare, and R. V. Babar, "Accident Avoidance and Detection on Highways," *Int. J. Eng. Trends Technol.*, vol. 3, no. 2, pp. 247–252, 2012.
- [10] G. V. Sairam, B. Suresh, C. H. S. Hemanth, and K. Krishna, "Intelligent Mechatronic Braking System," *Int. J. Emerg. Technol. Adv. Eng.*, vol. 3, no. 4, pp. 3–8, 2013.
- [11] M. Bin Tahir and M. Abdullah, "Distance Measuring (Hurdle detection System) for Safe Environment in Vehicles through Ultrasonic Rays," *Glob. J. Res. Eng. Automot. Eng.*, vol. 12, no. 1, pp. 1–5, 2012.

Design and Fabrication of Inversions of Slider Crank Mechanism by Using 3d Printing

Kiran Chand Kopila and Konda Babu, Shaik Fayaz, Kondu Naveen Reddy

¹Assistant Professor, Department of Mechanical Engineering, Narasaraopeta Engineering College (A), Narasaraopet, A.P. India
^{2, 3, 4} Student, Department of Mechanical Engineering, Narasaraopeta Engineering College (A), Narasaraopet, A.P. India

Abstract— Mechanism in which the rotary motion of the crank is converted into the linear motion of the piston or any other integral elements the crank is the main element in crank mechanism. A slider crank is most widely used to convert reciprocating to rotary motion (as in an engine) or to convert rotary to reciprocating motion (as in pumps), but it has numerous other applications. A mechanism is a kinematic chain with one fixed link. The fixed link is called frame. Different mechanism is obtained by fixing different link in kinematic chain. Inversion is the process of choosing different links in a kinematic chain for the frame. Now a day's smart work is the best result for the output. The additive manufacturing is the advanced product manufacturing process of producing 3-dimensional objects from a computer file. 3D printing is overall method of manufacturing parts directly from digital model by layer- by-layer material built-up approach. 3D printing is called as desktop fabrication. It is process of prototyping where by a structure is synthesizes from a 3D model. 3D printing process is derived from inject desktop printer in which multiple deposit jets and the printing material layer by layer derived from the CAD 3D data. In this project slider crank mechanism is designed in CATIA software and fabricated by using 3D printer. Generates properties and estimating time is done by using Ultimaker Cura S5. Acrylonitrile Butadiene Styrene (ABS) material is used as a 3D printing material. Slider crank mechanism 3D printing time is 18 hours 35 minutes and volume of material consumed is 134.4 grams. Rotary engine mechanism 3D printing is 20 hours 40 minutes and volume of material consumed is 80 grams.

Keywords: 3D printing, Catia, ultimaker cura s5.

I. INTRODUCTION

Mechanism in which rotary motion of crank is converted into the linear motion of the piston or any other integral element. Crank is the main element used in crank mechanism. A slider crank (see illustration) is most widely used to convert reciprocating to rotary motion (as in an engine) or to convert rotary to reciprocating motion (as in pumps), but it has numerous other applications.

Slider-crank mechanism, arrangement of mechanical parts designed to convert straight line motion to rotary motion, as in a reciprocating piston engine, or to convert rotary motion to straight line motion, as in reciprocating piston pump. The basic nature of the mechanism and the relative motion of the parts can best be described with the aid of the accompanying figure, in which the moving parts are lightly shaded. The darkly shaded part 1, the **fixed** frame or block of the pump or engine, contains a cylinder, depicted in cross section by its walls DE and FG, in which the piston, part 4, slides back and forth. The small circle at A represents the main crankshaft bearing, which is also in part 1. The crankshaft, part 2, is shown as a straight member extending from the main bearing at A to the crankpin bearing at B, which connects it to the connecting rod, part 3. The connecting rod is shown as a straight member extending

from the crankpin bearing at B to the wristpin bearing at C, which connects it to the piston, part 4, which is shown as a rectangle.

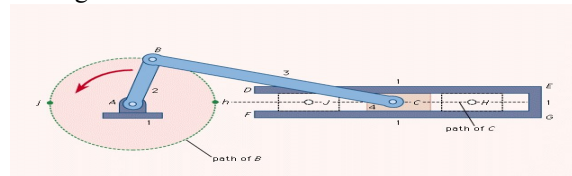


Fig:1 Slider Crank Mechanism

II. LITERATURE SURVEY

Van Der Putten, J.; De Schutter, G.; Van Tittelboom, K. Surface modification as a technique to improve inter-layer bonding strength in 3D printed cementitious materials. RILEM Tech. Lett. 2019, 4, 33–38. [Google Scholar] [CrossRef]: The structural capacity of 3D printed components mainly depends on the inter-layer bonding strength between the different layers. This bond strength is affected by many parameters (e.g. moisture content of the substrate, time gap, and surface roughness) and any mismatch in properties of the cementitious material may lead to early failure. A common technique to improve inter-layer bonding strength between a substrate and a newly added layer is modifying the substrate surface. For the purpose of this research, a custom-made 3D printing.

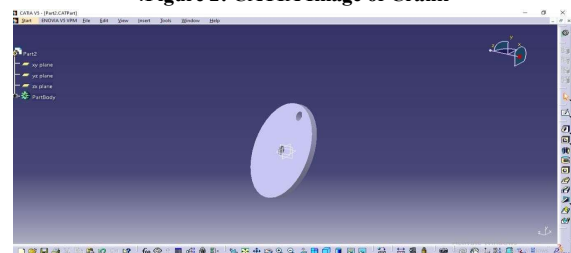
III. MODELLING

List of Components: Slider Crank

Crank, Connecting Rod, Slider Pin and Slider Case.

Crank: Diameter= 100mm, Thickness = 5mm

Figure 2: CATIA Image of Crank



Connecting Rod: length = 200mm, Thickness = 5mm

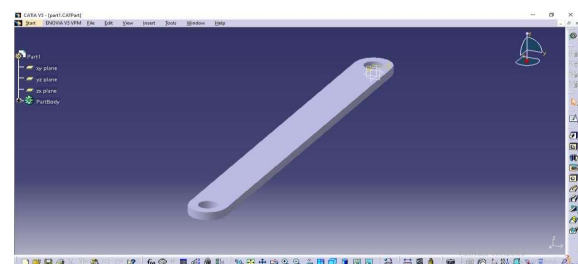
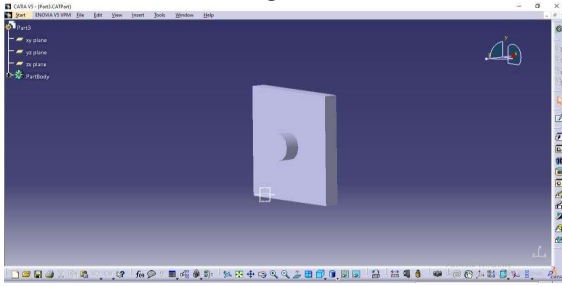


Fig: 3 Connecting Rod

Slider: length = 40mm, Width = 40, Thickness = 5mm

.Figure 4: Slider



Pin: Diameter = 10mm, Height = 12mm

Figure 5: Pin

Slider Case: Length = 160mm, Height=80mm, Depth =15mm.

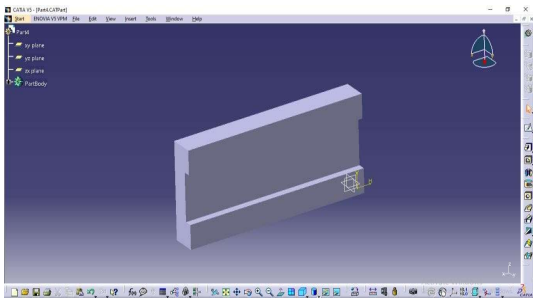


Figure 6: Slider Case

Rotary Engine Components

Connecting Rod: Width =63 mm, Height = 7mm, Depth =16mm.

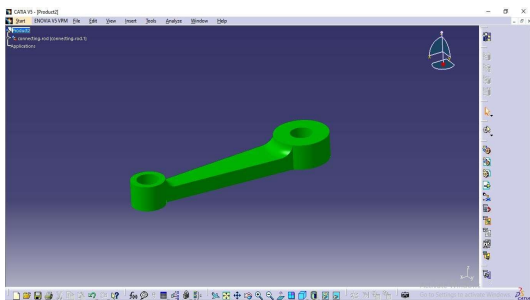


Figure 7: Connecting Rod

Crank shaft Pin: Diameter = 10mm, Height=20mm.

Fig: 8 Crank shaft pin

Crank Bearing: Diameter = 22mm, Height = 9mm

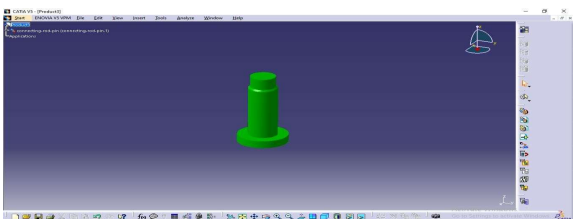


Fig: 8 Crank Bearing

Crank Shaft: Height = 24 mm, Width =45mm, Thickness = 5mm

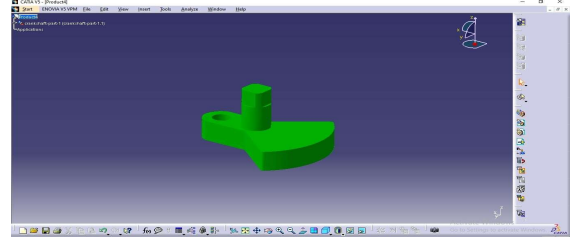


Fig: 9 Crank Shaft

Engine Case: Bore diameter = 50 mm and fin length = 10mm, Stroke length = 40mm

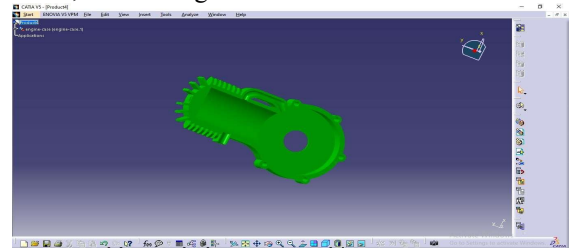


Figure 10: Engine Case

Gudgen Pin: Diameter = 10mm, Length = 20mm

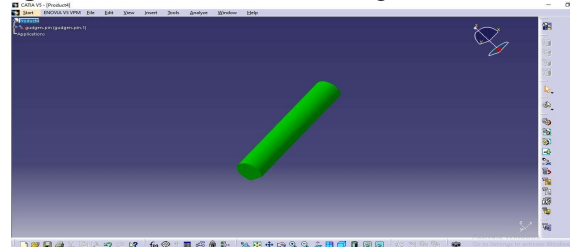


Figure 11: Gudgin Pin

Handle: Thickness = 5mm

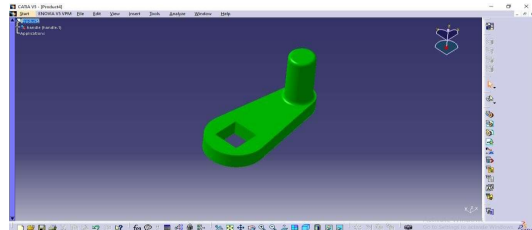


Figure 12: Handle

Piston: Diameter = 25mm and height= 30mm

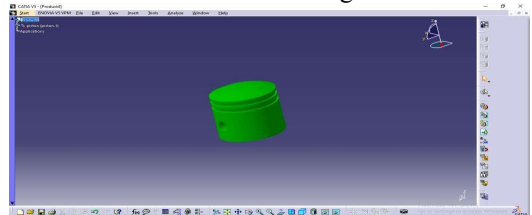


Figure 13: Piston

Piston Rings:Diameter =25mm and thickness = 2mm



Figure 14: Piston Rings

Washer: Diameter = 20mm, internal diameter = 10mm and thickness = 3mm

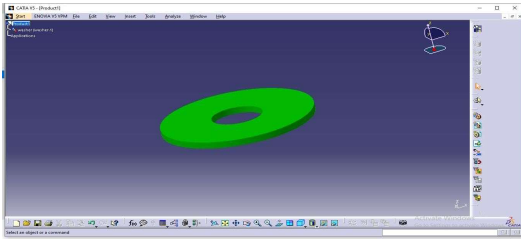


Figure 15: Washer CURA SOFTWARE

Cura 3D is slicing software for 3D printers. It takes a 3D model and slices it into layers to create a file known as G-Code, which is the code that a 3D printer understands. Curaslices 3D models. It translates the 3D STL, OBJ or 3MF file into a format that the printer can understand. Fused filament fabrication (FFF) 3D printers print one layer upon another to build up the 3D object. Cura 3D takes the 3D model and works out how those layers are placed on the print bed and creates a set of instructions for the printer to follow layer on layer. Cura generates instructions for your 3D printer. They are called G-Code, a text document that ends with the file extension. G-code. Open the file and you 'll actually be able to read through quite a bit of the code and understand what it's telling the printer to do.

IV. STAGES OF 3D PRINTING:

4.2.1 MODELING: This is carried out in any 3D modeling application such as cad or Sketch-Up, which are just two of many example applications. These applications have their own file format and these enable you to open, edit, save, and export those 3D printer files from the application.

4.2.2 3D FILE EXPORT: Once you have created your model, it then needs to be exported as eitheran STL, OBJ, or 3MF file. These are the file formats that are recognized by Cura. They differ from the file formats that are native to the 3D modeling applications as they just hold the final geometry and not the individual primitives and editable content. Still, you can change the size of the 3D model, but not the geometry.

4.2.3 SLICING FILE EXPORT: The STL or OBJ file can then be imported into the Cura software where it is sliced and output as G-Code. This G-Code is just a text document (in essence) with a list of commands for the 3D printer to read and follow such as hot-end temperature, move to the left this much, right that much etc.

4.2.4 CURA SET UP OF 3D PRINTER:

On first loading Cura, it will be asked to select a printer. If not, or if you want to set up a new printer, then select Settings > Printer.

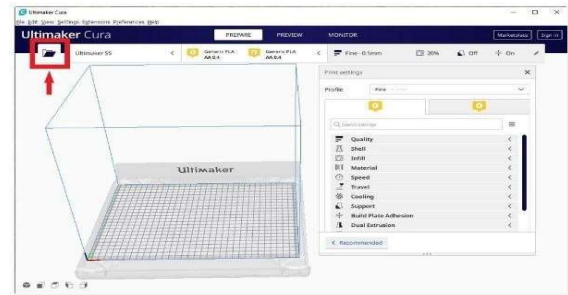


Figure 16: Adding 3D printing model.

4.2.5 MODEL VIEWS IN CURA:

In the Cura software, there are three basic ways to view the model. Each is useful for different reasons, especially when a problem arises with your prints.

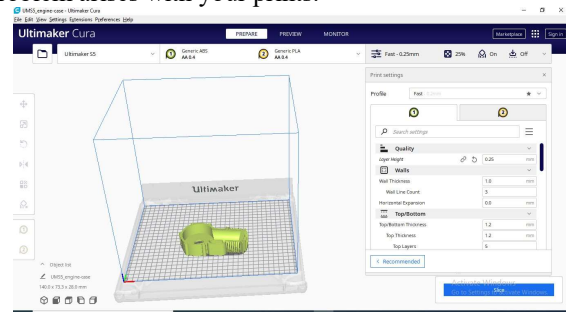


Figure 17: Cura software adding STL component.

4.2.6 LAYERS: Also under Preview, if a print is failing every time at a certain point, or you 've done something clever and just want to check that part of the print is OK, you can switch to Layer view. An accurate way to do this is with the arrow keys. Alternatively, there's a slider for quickly looking through all of the layers that build up your print. As you get more advanced with Cura, this feature is handy for pinpointing layers where you want to change settings in the G-code, such as to increase fan speed, layer height or flow.

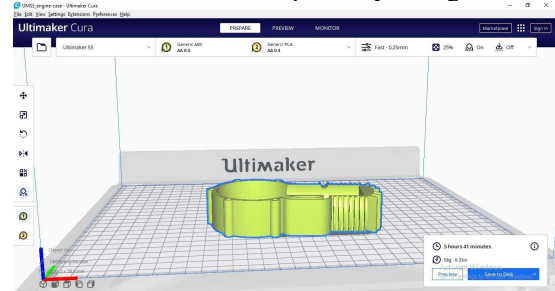


Figure 18: cura software 3d printing layer settings

4.3 CURA: Sometimes, you may want to move the model along Cura 's build area because you don 't want to print the model right at the center of the printer platform. At other times, the imported model might have the wrong orientation on the build area. If your model needs adjusting, all you need to do is click on the model so that it is highlighted and then select one of the options from the tools on the left. Here you can quickly move, rotate, and scale the model.

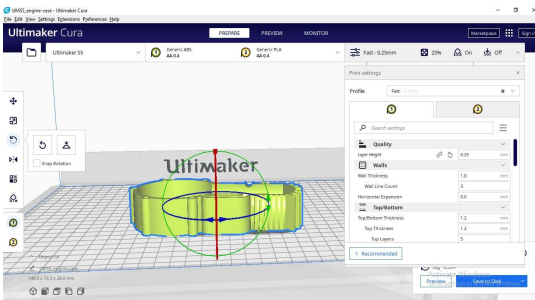


Figure 19: cura software settings

4.4 PRINTER SETTING: This section lets you select the right printer and material.

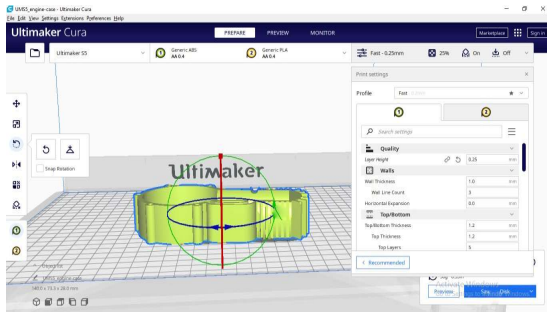


Figure 20: 3D printing Settings

V. 3D PRINTING MATERIALS

5.1 PLASTICS: Nylon, or Polyamide, is commonly used in powder form with the sintering process Orin filament form with the FDM process. It is a strong, flexible and durable plastic material that has proved reliable for 3Dprinting. It is naturally white in colour but it can be coloured pre- or post-printing. This material can also be combined (in powder format) with powdered aluminum to produce another common 3D printing material for sintering Alumide
 ABS is another common plastic used for 3D printing, and is widely used on the entry-level FDM 3D printers in filament form. It is a particularly strong plastic and comes in a wide range of colours. ABS can be bought in filament form from a number of nonproprietary sources, which is another reason why it is so popular

5.2 METALS: Two of the most common are aluminum and cobalt derivatives. One of the strongest and therefore most commonly used metals for 3D printing is Stainless Steel in powder form. It is in the last couple of years Gold and Silver have been added to the range of metal materials that can be 3D printed directly, with obvious applications across the jewellery sector. These are both very strong materials and are processed in powder form. Titanium is one of the strongest possible metal materials and has been used for 3D printing industrial applications for some time. Supplied in powder form, it can be used for the sintering/melting/EBM processes.

5.3 CERAMICS: Ceramics are a relatively new group of materials that can be used for 3Dprinting with various levels of success. The particular thing to note with these materials is that, post printing, the ceramic parts need to undergo the same processes as any ceramic part made using traditional methods of production namely firing and glazing.

First, let ‘s define what exactly the two materials are. Both ABS and PLA are thermoplastics. Thermoplastics become malleable when superheated, thus allowing you to mold and sculpt them into different shapes prior to cooling. Moreover, you can repeat the process without affecting the integrity of the material. While both are used for making objects in 3D printing via similar processes, ABS and PLA differ in some key ways, and therefore some printers will only utilize ABS or PLA or both, depending on the machine at hand. That said, below is a quick glance at the merits of each thermoplastic in case you ‘re wondering why the distinction exists to begin with.

5.4 ABS: ABS, short for Acylonitrile Butadiene Styrene, is an oil-based plastic. It is a strong, sturdy material that businesses widely used for constructing things such as plastic car parts, musical instruments, and the ever-popular Lego building blocks. ABS has a high melting point, and can experience warping if cooled while printing. Because of this, ABS objects must be printed on a heated surface, which is something many at-home printers do not have. ABS also requires ventilation when in use, as the fumes can be unpleasant. The aforementioned factors make ABS printing difficult for hobbyist printers, though, it’s the preferred material for professional applications.

5.5 PLA:
 PLA, or Poly Lactic Acid, is made from organic material — specifically cornstarch and sugarcane. This makes the material both easier and safer to use, while giving it a smoother and shinier appearance that’s more aesthetically pleasing. The thermoplastic is also more pleasant on the nose, as the sugar-based material smells slightly sweet when heated opposed to the harsh smell often associated with ABS. However, while PLA might seem like a better overall choice at first glance, it features a far lower melting point than ABS. This means that using printed parts for mechanical operations, or even storing them in high-temperature locations, can result in the part warping, cracking, or melting.

The table below compares the main properties of PLA vs. ABS:

Properties	ABS	PLA
Tensile Strength	27 MPa	37 MPa
Elongation	3.5 - 50%	6%
Flexural Modulus	2.1 - 7.6 GPa	4 GPa
Density	1.0 - 1.4 g/cm ³	1.3 g/cm ³
Melting Point	N/A (amorphous)	173 °C
Biodegradable	No	Yes, under the correct conditions
Glass Transition Temperature	105 °C	60 °C

Table2 shows properties of ABS material

Properties	ABS
Tensile Strength	27 MPa
Elongation	3.5 - 50%
Flexural Modulus	2.1 - 7.6 GPa
Density	1.0 - 1.4 g/cm ³
Melting Point	85 °C (amorphous)
Biodegradable	No
Glass Transition Temperature	105

VI. SPECIFICATIONS OF 3D PRINTER USED:

- Build volume: 330 x 240 x 300 mm (13 x 9.4 x 11.8 inches)
- Physical dimensions: 495 x 500 x 1197 mm (19.5 x 19.5 x 47.1 inches)
- Print technology: Fused filament fabrication (FFF)
- Weight: 41.9 kg (92.4 lbs.)
- Power input: 100-240 VAC, 50-60 Hz
- Maximum power output: 600W

**FABRICATION OF COMPONENTS USING 3D PRINTER
SLIDER CRANK:**

Crank:



Figure 21:3D Printed Crank

Slider Case:



Figure 22:3D Printed Slider Case

Connecting Rod:



Figure 23:3D Printed Connecting Rod

Crank Support:

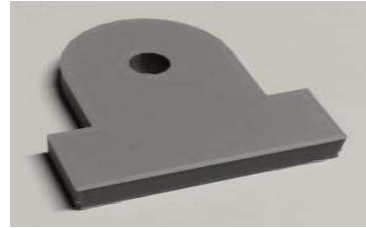


Figure 24:3D Printed Crank Support

Slider:

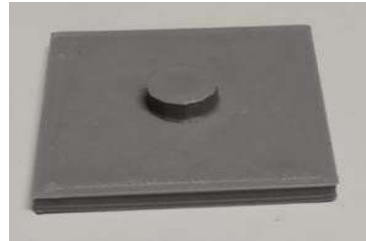


Figure 25:3D Printed Slider
ROTARY ENGINE

Engine Case:



Figure 26:3D Printed Engine Case

Handle:



Figure 26:3D Printed Handle

Bearing:



Figure 27:3D Printed bearing

Crank Shaft:



Figure 28:3D Printed Crank Shaft

Piston:



Figure 29:3D Printed Piston

1. Washer:



Figure 30:3D Printed Washer

Gudgen Pin:



Figure 31:3D Printed Gudgen Pin

Piston Rings:

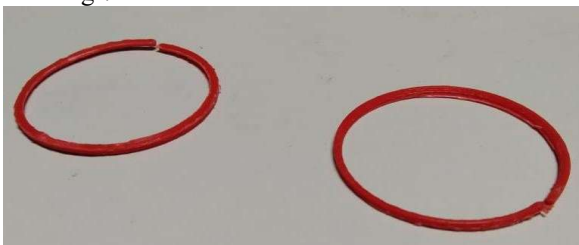


Figure 32:3D Printed Piston Rings

Connecting Rod:



Figure 33:3D Printed Connecting Rod

ASSEMBLING OF THE COMPONENTS AND PRINTING TIME Slider Crank



Figure 34: Assembled Component in single slider crank mechanism

Table 3 shows time taken to print the components

S. No	Name Of the Component	Printed Time
1	Crank	4:30
2	Slider case	5:32
3	Connecting Rod	2:43
4	Slider	2:38
5	Crank support	3:38
6	Pin and handle	2:00
Total:		21:38 minutes

ROTARY ENGINE



Figure 35: Assembled Component in single Rotary Engine

Table 4 shows time taken to print the components

S. No	Name Of the Component	Printed Time
1	Engine case	6:40
2	Handle	1:32
3	Washer	1:03
4	Piston	3:38
5	Bearing	1:38

6	Connecting rod	3:25
7	Gudgen pin	2:00
8	Piston rings	0:25
9	Crank shaft	2:30
Total:		23:1mi nutes

CONCLUSION

The world is forever changing with the help of 3D printing. The use of 3D printing for medicinal purposes today is beyond astonishing but what the future holds is unknown, however it is certain that additive layer manufacturing will be a large corporate in solving our problems. 3D printing really is limitless and only the surface has been scratched, there is still much more to be uncovered. As shown in throughout the web page. 3D printing bones is still new and continuously improving and adjusting but it has already enhanced the life of many patients around the world and more specifically in Australia. It is evident that the more funding and research put into 3D printing, the further 3D printing will take us. 3D is forever unpredictable.

In this project work, design is done by using CATIA software and then file is transformed to STL format which is used for production of the component in 3D printing machine. CURA software is used for slicing of the component produced in CATIA and it also helps in adjustment of dimensions, solidification time, material selection, printing speed and printing time. In this project ABS material is used for the production of the component in 3D printing machine. Slider

crank mechanism 3D printing time is 18 hours 35 minutes and volume of material consumed is 134.4 grams. Rotary engine mechanism 3D printing is 20 hours 40 minutes and volume of material consumed is 80 grams.

REFERENCES

1. ALABOODI, Abdulaziz S.; SIVASANKARAN, S. Experimental design and investigation on the mechanical behaviour of novel 3D printed biocompatibility polycarbonate scaffolds for medical applications. *Journal of Manufacturing Processes*, v. 35, p. 479-491, 2018.
2. ALBERTI, E. A.; BUENO, B. M. P.; D'OLIVEIRA, A. S. C. M. Additive manufacturing using plasma transferred arc. *The International Journal of Advanced Manufacturing Technology*, v. 83, n. 9-12, p. 1861-1871, 2016.
3. ALI, M Hazrat; MIR-NASIRI, Nazim; KO, Wai Lun. Multi nozzle extrusion system for 3D printer and its control mechanism. *The International Journal of Advanced Manufacturing Technology*, v. 86, n. 1-4, p. 999-1010, 2016.
4. AREIR, Milad et al. A study of 3D printed active carbon electrode for the manufacture of electric double layer capacitors. *Journal of Manufacturing Processes*, v. 25, p. 351-356, 2017.
5. CHONG, Li; RAMAKRISHNA, Seeram; SINGH, Sunpreet. A review of digital manufacturing-based hybrid additive manufacturing processes. *The International Journal of Advanced Manufacturing Technology*, v. 95, n. 5-8, p. 2281-2300, 2018.
6. CORREA, Jorge E. et al. Laminated micro-machine: Design and fabrication of a flexure-based Delta robot. *Journal of Manufacturing Processes*, v. 24, p. 370-375, 2016.
7. DAWOUD, Michael; TAHA, Iman; EBEID, Samy J. Mechanical behaviour of ABS: An experimental study using FDM and injection moulding techniques. *Journal of Manufacturing Processes*, v. 21, p. 39-45, 2016.
8. GUO, Liang; QIU, Jingxiong. Combination of cloud manufacturing and 3D printing: research progress and prospect. *The International Journal of Advanced Manufacturing Technology*, v. 96, n. 5-8, p. 1929- 1942, 2018.

MANIPULATION OF ROBOTIC ARM BY USING QR CODE

Ch.Shekhar¹, Y.Siva Reddy², B.Gopi³

Assistant Professor, Department of Mechanical Engineering, Narasaraopeta Engineering College, Narasaraopet,
Student, Department of Mechanical Engineering, Narasaraopeta Engineering College, Narasaraopet, India

ABSTRACT—Recently, the use of has become significant to industries, especially when involving the routine works in industries. A robotize machine designed to execute one or more tasks automatically with speed and precision. In our project work, by using the pneumatic gripper and the programming given pick and place operation will performed by color sensor. By using a robotic arm with pneumatic gripper Manipulation of a robot arm can be utilized for different purposes innovatively, here in this work, for pick and placing. IGUS robot with pneumatic gripper is used to hold the object and moves from one place to another place. The goal of this project is to implement a programmable industrial robot for color sorting. This investigates the development of an intelligent and low-cost monitoring system for color identification and segregation. The main purpose is to optimize the productivity and avoid human mistakes. A serial image acquisition device (camera) is used to capture the image and are sent to SD card through a microcontroller .The microcontroller performs color detection algorithm to recognize the dominant color of the object, and it sends commands to the robotic arm topic and place the objects to their respective locations. A robotic arm is a manipulator which has a bout same number of degrees of freedom as in human arm. DC motors are used for joint rotations involved in the robotic arm; these motors are interfaced with microcontroller through motor driver circuits. These motor drivers are able to efficiently control the speed and direction of motors. **Keywords**—pneumatic gripper, microcontroller, manipulator, robotic arm.

Keywords: Colour Detection, PLC, Photoelectric Sensor, WPL Software, Microcontroller.

I. INTRODUCTION

Industrial robotics defined by ISO as an automatically controlled, reprogrammable, multipurpose manipulator, programmable in three or more axes, which can be either fixed in place or visual input, in the form of color images from a camera, can be a rich source of information, considering the sophisticated algorithms recently developed in the field of computer vision, for extracting information from images. Even so, most robots continue to rely on non-visual sensors such as tactile sensors, sonar, and laser. This preference for relatively low-fidelity sensors rather than vision can be attributed to three major discrepancies between the needs of robots and the capabilities of state-of-the-art vision algorithms. Pick And Place Robotics for use in industrial. This paper aims to address these challenges by exploiting the structure that is often present in a robot's environment. We define structure as the objects of unique shapes and colors that exist at known locations – a color-coded world model. We show that a robot can use this structure to model the color distributions, thereby achieving efficient color segmentation. Specifically, knowing that it is looking at an object of known

Dhanya et al. [8] proposed an era of improve automatic braking with sensor fusion idea. In this they represent operation of the residences of every capacitive and

color allows it to treat certain image pixels as labeled training samples. The domain knowledge also helps develop object recognition algorithms that can be used by the robot to localize and navigate in its complex world towards additional sources of color information. We have developed a mobile robot vision system that learns colors using the uniquely color-coded objects at known locations, and adapts to illumination changes. Specifically, this article makes the following contributions: automation applications.

It describes a baseline vision system that tackles color segmentation and object recognition on-board a robot with constrained computational and memory resources. The baseline system is robust to jerky nonlinear camera motion and noisy images. However, it relies on manually labeled training data and operates in constant and uniform illumination conditions. And then it exploits the structure inherent in the environment to eliminate the need for manual labeling. The image regions corresponding to known objects are used as labeled training samples. The learned color distributions are used to better identify the objects, thereby localizing and possibly moving to other sources of color information. We introduce a hybrid color representation that allows for color learning both within the controlled lab settings and in un-engineered indoor corridors, it provides robustness to changing illumination 2 conditions.

We introduce an algorithm that enables the robot to detect significant changes in illumination. When a change in illumination is detected, the robot autonomously adapts by revising its current representation of color distributions. As a result, the robot is able to function over a wide range of illuminations. The focus of this article is on the design of efficient robot vision algorithms that address challenging problems such as color segmentation, object recognition, color learning and illumination invariance. Using our algorithms the robot is able to operate autonomously in an uncontrolled environment with changing illumination over an extended period of time. The vision system is fully implemented and tested on a commercial off-the-shelf four-legged robot. We also illustrate the general applicability of our algorithms with the running example of a vision-based autonomous car on the road; we refer to it as the car-on-the-road task. The remainder of the article is organized as follows.

After a brief description of our test platform, we present our baseline vision system, which tackles the problems of color segmentation, object recognition and line detection, in real-time. it extends the baseline system by eliminating the offline color calibration phase: the robot uses the environmental structure to autonomously generate a suitable motion sequence to learn the desired colors. Further enables the robot to detect significant illumination changes and adapt to them

ultrasonic sensor for identifying the difficulty for measuring the distance

II. USE OF ROBOTS

There are many different reasons for using a robot but the central reason for most applications is to eliminate a human operator. The most obvious reason is: To save labour and reduce cost. Human is bad for the product for example semiconductor handling. Within this class are other reasons for using robots for example food handling, pharmaceuticals, etc. Product is bad for the human for example radioactive product. Within the above are other reasons for using robots for example robots can be used to replace human operators where the dangers are:

1. Repetitive strain syndrome.
2. Working with machinery that is dangerous for example presses, winders.
3. Working with materials which might be harmful in the short or long term.

Quality the main reason for using a robot is to save labour the biggest impact a robot has can be on quality. Applications where quality will be improved are:

- gluing,
- spraying (glue or paint),
- trimming and de- burring,
- testing and gauging.
- assembly
- laboratory routines

A. Robot Anatomy:

Controller:

The Joint movements must be controlled if the robot is to perform as desired. Microprocessor-based controllers are regularly used to perform this control action. Controller is organized in a hierarchical fashion. Each joint can feed back control data individually, with an overarching supervisory controller coordinating the combined actuations of the joints according to the sequence of the robot program.

Manipulators:

Robot manipulators are created from a sequence of link and joint combinations. The links are the rigid members connecting the joints, or axes. The axes are the movable components of the robotic manipulator that cause relative motion between adjoining links. The mechanical joints used to construct the robotic arm manipulator consist of five principal types. Two of the joints are linear, in which the relative motion between adjacent links is no rotational, and three are rotary types, in which the relative motion involves rotation between links.

End effector:

Grippers grasp and manipulate objects during the work cycle. Typically, the objects grasped are work parts that need to be loaded or unloaded from one station to another. It may be custom-designed to suit the physical specifications of the work parts they have to grasp. End effectors, grippers are described in detail in below:

Mechanical gripper: Two or more fingers that can be actuated by robot controller to open and close on a work part.

•Vacuum gripper: Suction cups are used to hold flat objects

•Magnetized devices making use of the principles of magnetism, these are used for holding ferrous work parts.

Endeffectors–tools:

The robot end effector may also use tools. Tools are used to perform processing operations on the work part. Typically,

the robot uses the tool relative to a stationary or slowly moving object. In this way the process is carried out.

Examples of the tools used as end effectors by robots to perform processing applications include.

- Spot welding gun
- Arc welding tool
- Spray painting gun
- Rotating spindle for drilling, routing, grinding.
- Assembly tool (e.g., automatic screwdriver)
- Heating torch.

III. LITERATUREREVIEW

Dipak Aphale , Vikas Kusekar “PLC Based Pick and Place Robot with 4DOF” The pick and place robot is one of the technologies in manufacturing industry and designed to perform various functions. The system is very important to eliminate human errors and to get more precise work. It can also save the cost in long term and help to solve problems and tasks that cannot be done such as on high temperature area, narrow area and very heavy load thing. This project is a basic development and modification for that type of robot where it use the peripheral interface Programmable Logic Control (PLC) as the robot brain to control all of the robot movement. The rotation of till robotics 360 degree (clockwise) and -360 degree (counter clockwise). The electromagnetic gripper will move horizontally top and hold the object from one place to another place. This robot is used to pick and place the object only in their specifications (up to 300mm horizontal and 300mm vertically). The benefit of this project is the robot can pick the object using electromagnetic gripper which is simple in construction and also cost effective.

SPremkumar, Vikas Kusekar “Design and Implementation of multi handling Pick and Place Robotic Arm ” Robot manipulator is an essential motion subsystem component of robotic system for positioning, orientating objects that robot can perform useful task The main aim of our work is to collaborate the gripper mechanism and vacuum sucker mechanism working in a single pick and place robotic arm. This robot can be self-operational in controlling, stating with simple tasks such as gripping, sucking, lifting, placing and releasing in a single robotic arm. The main focus of our work is to design the robotic arm for the above-mentioned purpose. Robotic arm consists of revolute joints that allowed angular movement between adjacent joint. Three double acting cylinders were used to actuate the arm .Robot manipulators are designed to execute required movements. By using this collaborated mechanism, the success rate of pick and place robots are increased. Shirine El Zaatari, Mohamed Marei, Weidong Li, Zahid Usman: “Cobot Programming for Collaborative Industrial Tasks”, Collaborative robots (cobots) have been increasingly adopted in industries to facilitate human-robot collaboration. Despite this, it is challenging to program cobots for collaborative industrial tasks as the programming has two distinct elements that are difficult to implement: (1) an intuitive element to ensure that the operations of a cobot can be composed or altered dynamically by an operator, and (2) a human-aware element to support cobots in producing flexible and adaptive behaviors dependent on human partners. In this area, some research works have been carried out recently, but there is a lack of a systematic summary on the subject. In this paper, an overview of collaborative industrial scenarios and programming requirements for cobots to implement effective

collaboration is given. Then, detailed reviews on cobot programming, which are categorized into communication, optimization, and learning, are conducted. Additionally, a significant gap between cobot programming implemented in industry and in research is identified.

De-socialisation For Turkle:, the advance of the robot for social purposes is worrying, and she fears that people will lose their social skills and become even lonelier. She is concerned that children will get used to perfect friendships with perfectly programmed positive robots, so they will not learn to deal with real-life people with all their complexities, problems, and bad habits. These ideas remain speculations, because there has been only limited research on the actual effects of the impact of social robots on children and adults. In addition, Turkle sees the sex robot as a symbol of a great danger, namely that the robot's influence stops us from being willing to exert the necessary effort required for regular human relations: "Dependence on a robot presents itself as risk free. But when one becomes accustomed to 'companionship' without demands, life with people may seem overwhelming. Dependence on a person is risky—because it makes us the subject of rejection—but it also opens us to deeply knowing another." She states that the use of sex robots leads to de-socialisation based on turkle point of view.

IV. PROGRAMMABLE LOGIC CONTROLLER:

A programmable logic controller (PLC) is an industrial computer control system that continuously monitors the state of input devices and makes decisions based upon a custom program to control the state of output devices. PLCs were first developed in the automobile manufacturing industry to provide flexible, rugged and easily programmable controllers to replace hard-wired relays. Since then, they have been widely adopted as high reliability automation controllers suitable for harsh environments.

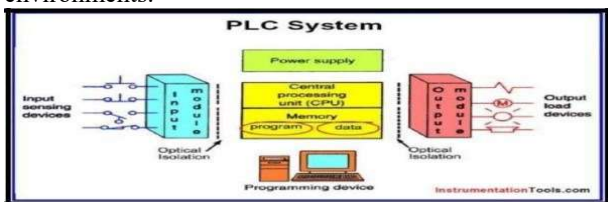


FIG 1 :PLC ARCHITECTURE

A. Connections from PLC to robot:

In programmable logic controller they are six modules present in the system, they are power supply, communication module and four servo motors for four axis movements. The output of the PLC give connection to the input of robot. A compressor is connected to the robot to hold the objects.



Fig 2: Programmable Logic Controller to Robot

V. EXPERIMENTAL PROCEDURE:

A. the Following Figure Show in the Block Diagram of Robot Manipulation

The robot manipulation is based on c programming and PLC the control of manipulation of robot is controlled by PLC.

In our work they two relays i.e. relay 1 is related to beverage one and relay 2 is related to beverage two.

The two relays are getting signal from PLC, when the relay 1 get the signal, the submersible motor1 activate similarly submersible emotor2 will be activate.

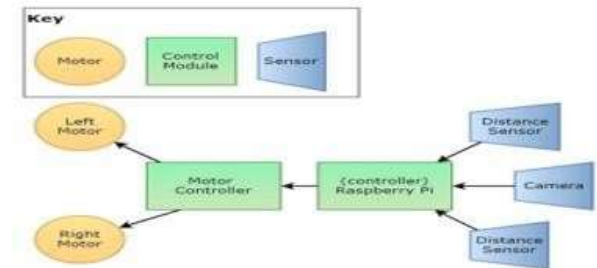


Fig 3 :Block diagram

B. SEQUENCE OF OPERATIONS:

- The sequence of operation is initiated from c prog software. The required operation of robot should be written in a code in cprog software.
- After execution code in cprog software, the plc controls the robot manipulation and robot get signal from PLC.
- The robot comes to home position and after that robot moves to a specific distance and pic the glass.
- The robot returns to its home position and wait for it command.
- The operator gives the command has switch They are two switches and two relays

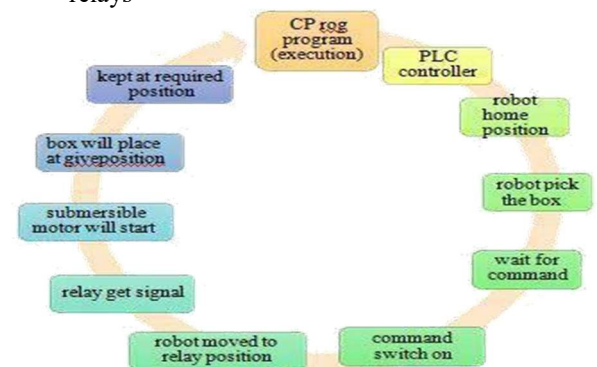


Fig 4: Sequence of Operation

C. CIRCUIT DIAGRAM OF PROJECT:

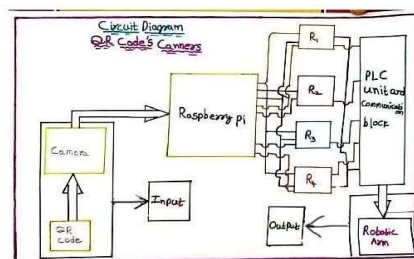


Fig 5 : Circuit Diagram

The circuit diagram of the system working with PLC and relays has been schematically.

D. Step by Step Procedure of Code:

After completion of connecting circuits to robot and PLC. Then Switch on the robots, PLC and computer. Later Open C Prog software and connect the hardware. Now reference the robot after it by using jog jogging command moving the robot in required axis and angle. Fix all the positions in the programed it or and save it in the.xml format then run the program.

VI. EXPERIMENTAL RESULTS:

A .Step by step procedure to write the Main program in software

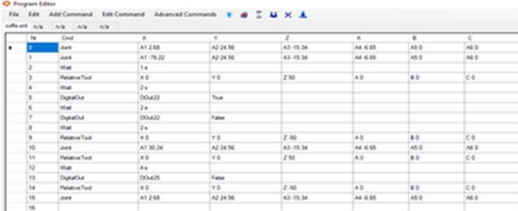


Fig 6: Main Program

Explanation for the above program:

```
<Program>
<Header RobotName="igus Arm"
RobotType="igus_4DOF_BV"
GripperType="" Software="CPRog V902-10-033"/>
<LinearNr="0" x="281.1" y="0" z="518.1" a="-180" b="0" c="180" e1="0" e2="0"
e3="0" vel="100" acc="40" smooth="20" AbortCondition="false" Descr="" />
<Joint Nr="1" a1="68.22" a2="1.89" a3="1.4"
a4="86.71" a5="0" a6="0" e1="0" e2="0"
e3="0"
velPercent="50" acc="40" smooth="20" AbortCondition="false" Descr="" />
<LinearNr="2" x="104.3" y="261" z="259.8" a="-111.78" b="0" c="180" e1="0" e2="0"
e3="0"
vel="100" acc="40" smooth="20"
AbortCondition="false"
Descr="" />
<RelativeNr="3" MoType="CartTool"
x="0" y="0" z="125" a="0.0" b="0.0" c="0.0"
vel="100"
acc="40" smooth="20" AbortCondition="false"
Descr="" />
<Wait Nr="4" Type="Conditional"
Condition="DIn22 orDin23"
Descr="" />
<If Nr="5" Condition="DIn22"
Descr="" />
<Sub Nr="6" File="red.xml" Descr="" />
<Else/>
<IfNr="7" Condition="DIn23" Descr="" />
<SubNr="8" File="blue.xml" Descr="" />
<Else/>
<Linear Nr="9" x="104.3" y="261" z="259.8" a="-111.78" b="0" c="180" e1="0" e2="0"
e3="0"
vel="100" acc="40" smooth="20" AbortCondition="false"
Descr="" />
<EndIf/>
<EndIf/>
</Program>
```

C. Step by step procedure to write the red color program in C prog:

Fig 7: QR code 1Box1.xml

Explanation for the above program:

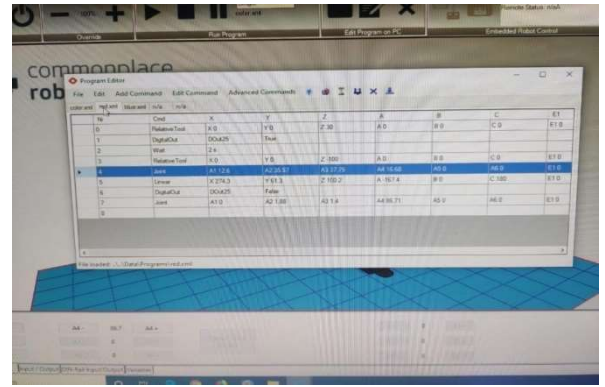
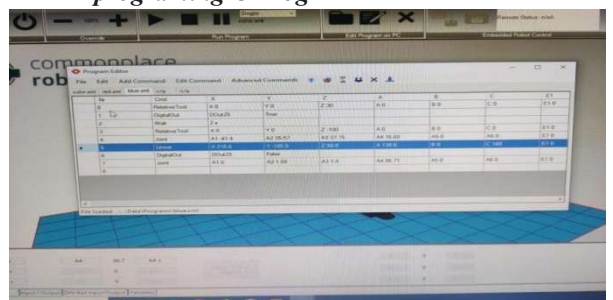


Fig 8 : QR code 1 Box 2.xml

D. Step by step procedure to write the blue color programming C Prog



Explanation for the above program:

```
<Program>
<Header RobotName="igus Arm"
RobotType="igus_4DOF_BV" GripperType=""
Software="CPRog V902-10-033"/>
```

```
<Relative Nr="0" MoType="CartTool" x="0" y="0" z="30" a="0.0" b="0.0" c="0.0" vel="100" acc="40" smooth="20" AbortCondition="false" Descr=""/>
```

```
<Output Nr="1" Channel="DOut25" State="True" Descr=""/><Wait Nr="2" Type="Time" Seconds="2" Descr=""/>
```

```
<Relative Nr="3" MoType="CartTool" x="0" y="0" z="100" a="0.0" b="0.0" c="0.0" vel="100" acc="40" smooth="20" AbortCondition="false" Descr=""/>
```

```
<Joint Nr="4" a1="-2.95" a2="35.58" a3="27.83" a4="26.58" a5="0" a6="0"
```

```
e1="0" e2="0" e3="0" velPercent="50" acc="40" smooth="20" AbortCondition="false" Descr=""/>
```

```
<Relative Nr="5" MoType="CartTool" x="0.0" y="0.0" z="100.0" a="0.0" b="0.0" c="0.0" vel="100" acc="40.0" smooth="20" AbortCondition="false" Descr=""/><Output Nr="6" Channel="DOut25" State="False" Descr=""/>
```

```
<Joint Nr="7" a1="0" a2="1.88" a3="1.4" a4="86.71" a5="0" a6="0" e1="0" e2="0"
```

```
e3="0" velPercent="50" acc="40" smooth="20" AbortCondition="false" Descr="
```



CONCLUSIONS

A manually operated dispatching machine system has been designed for non- contact servicing of beverages using robot arm manipulated by PLC has been developed and implemented.

Robotics is a technology with a future, and it is a technology for the future. In this project we are introducing a robot which can pick and place objects based on the color. Earlier this was done using color sensors but we have improved the entire project by using a serial jpeg camera which can capture

and identify or recognize the color of the image and eventually the robot picks and places that object accordingly. By doing so the speed and the accuracy of the color sorting process is increased. The cost for the color sorting process is considerably reduced. And most importantly there is overall optimization in the productivity if an industry. This robot arm can perform an action which is much similar to human. Although there is significant progress in robotics, still its usage is limited due to less availability of resources and high cost of production. If we able to overcome these restrictions, more benefits can be achieved from robotics.

Hence, the Pick and Place operation by using color sensor on IGUS Robot arm with 4-axis is successfully achieved. The PLC with combination of relays attached to the system of motors for picking and placing operations is used in this system to get more productivity with less time high reliability for and flexible in work.

Hence, the picking and placing operation by using color code on IGUS Robot arm with 4- axis is successfully achieved.

REFERENCES

- [1] A.K.Bejezy, Robot arm dynamics and control,1974.
- [2] B. C. Mcinnis and C. K. F. Liu, "Kinematics and dynamics in robotics: A tutorial based upon classical concepts of vectorial mechanics", IEEE J. Robotics Automat., vol. RA-2, no. 4, Dec.1986.
- [3] C. S. G. Lee, "Robot kinematics dynamics and control", IEEE Computer, pp. 62-80, Dec.1982.
- [4] Denavit and R. S. Hartenberg, "A kinematic notation for lower-pair mechanisms based on matrices", ASMEJ. Appl. Mech, vol.22,pp.215-221, June1955.
- [5]J. M. HoIlerbach, "A recursive formulation of Lagrangian manipulator dynamics", IEEE Trans.Syst.ManCybern.,vol. SMC-10, no. 11, pp. 730-736,1980.
- [6] J. R. Birk and R. S. Kelly, "An overview of the basic research needed to advance the state of knowledge in robotics",IEEETrans.Syst.Man Cybern.,vol.SMC-11,no.8,pp.574-579,1981.
- [7] J. Y. S. Luh, M. W. Walker and R. P. C. Paul, "On-line computational scheme for mechanical manipulators", Trans.ASMEJ.Dyn. Syst.Meas. Contr.,vol.102,pp.69-76, June1980.
- [8] M. C. Leu and N. Hemati, "Automated symbolic derivation of dynamic equations of motion for robotic manipulators", Trans. ASME J. Dyn. Syst. Meas. Contr., vol. 108, pp. 172-179, Sept.1986.
- [9] P. E. Nikravesh, R. A. Wehage and O. K. Kwon, "Euler parameters in computational kinematics and dynamics. Part 1", ASME J. Mech. Transmissions Automat. Des., vol. 107, pp. 358-365, Sept.1985.
- [10] R. P. Paul, Robot Manipulators: Mathematics Programming and Control, MA, Cambridge:MIT Press, 1978. W. O. Schiehlen and E. J. Kreuzer, "Symbolic computerized derivation of equations of motion", Proc. IUTAM Symp., 1977.81.

DESIGN AND FABRICATION OF APP CONTROLLED ROBOT

Ch. Sekhar, Vaka.Venkata Tarun, K. G N D V Prasanth

*Assistant Professor, Department of Mechanical Engineering, Narasaraopeta Engineering College, Narasaraopeta, India
Student, Department of Mechanical Engineering, Narasaraopeta Engineering College, Narasaraopeta, India*

ABSTRACT: Carrying a load with a human effort is not an easy task it increases the chances of contracting injuries. Robots can play a vital role during the critical situation as they can minimize some works of humans where humans should not step in. This robot carries the load in home and industrial proposes. A working prototype has been designed to control a car wirelessly using an Android Application. This is done with the help of Wi-Fi module for better connectivity. Android application is used by the User to send data wirelessly either by Wi-Fi This data is an input to the microcontroller system and the microcontroller uses it as the controlling parameter to the underlying hardware. This project is aimed to design and develop a Wi-Fi-controlled robot using node MCU ESP8266, Wi-Fi, and L298N Motor Driver Module. An android app named Node MCU car developed to control robot car. By using this app, robot can be controlled in all directions.

I. INTRODUCTION

Designing a Wi-Fi-controlled wireless car is the main motto of this project. Wi-Fi technology used has an average range of 10 m, due to which the car cannot travel a binger distance. So, Bluetooth-controlled automated cars have a limited range of issues. This limitation has been solved by using a Wi-Fi Module with a better range and wireless connectivity. Another key point behind developing the project is the use of Android Applications rather than traditional hardware controllers, which effectively reduces cost. The wireless car is controlled via a smartphone which is connected to the Wi-Fi module. This Android application has been developed with the required software tools (Android Studio) and it works as a controller that controls the movement of the car. Node MUC has been used as a microcontroller to drive this project. Node MCU board provides ease in terms of hardware interfacing and the coding is done using Arduino software In the last decade, with the development of technology, sensors used with electronic devices have been used in many areas to facilitate life. Sensors are devices that convert energy forms into electrical energy. The sensors serve as a bridge connecting the environment and various electronic devices. The environment can be any physical environment such as military areas, or airports. factories, hospitals, shopping malls, and electronic devices can be smartphones, robots, tablets, or smart clocks. These devices have a wide range of applications to control, protect, image, and identification in the industrial process. Today, there are hundreds of types of sensors produced by the development of technology such as heat, pressure, and obstacle recognizer. Human detecting. Sensors were used for lighting purposes in the past, but now they are used to make life easier. Thanks to technology in the field of electronics, incredibly fast developments are experienced. In this respect, it is possible to develop an invention or a new application every day and make life easier. Today, robot systems are developed with the use of artificial intelligence algorithms. The robotics field is one of them The most important part of

the robot is perception Perceiving the environment will be important for a robot design. For instance, it is very important to identify explosives by a robot to detect a terrorist in the military field by using sensors. A robot must perceive some variables (liken invention around it, interpret it, and then decide to act accordingly.

In this article, a simple-designed mobile robot built up from cost effective parts is introduced. The mobile robot can be controlled via Wi-Fi wireless network with the help of a simple application. Due to the cheap and simple design of the robot, it may be a useful developing tool for those, who cannot afford a much more expensive robot.

Robotic evolution starts with some basic ideas. It minimizes the human efforts, and it can be deployed in a lot of fields like military, surveillance application, Industrial Pick and Place Robots latest Humanoid robots are developed in the modern world. Now a day's robotic cars are developed by using Wireless technology. Wireless technology in Robotics starts with Bluetooth, WIFI, and Zigbee Communication. Based on the Requirement and Application they deployed the communication in Projects. And we have numerous android Applications in Play store to control a robot car. Blynk is a Popular App used in this Project it has a lot of Features like buttons, gauges, Sliders and Plotting Features also. By using Wi Fi technology, we can connect a greater number of Robotic Car to control it very useful for surveillance application

Now a day's Indoor localization Technologies are developed on that case also we can deploy this type of Wi-Fi controlled Robotic Car. A robot is a machine especially one programmable by a computer capable of carrying out a complex series of actions automatically. Robots can be guided by an external control device, or the control may be embedded within. Robots may be constructed on the lines of human form, but most robots are machines designed to perform a task with no regard to their aesthetics.

Robots have replaced humans in performing repetitive and dangerous tasks which humans prefer not to do, or are unable to do because of size limitations, or which take place in extreme environments such as outer space or the bottom of the sea. There are concerns about the increasing use of robots and their role in society. Robots are blamed for rising technological unemployment as they replace workers in increasing numbers of functions. The use of robots in military combat raises ethical concerns. The possibilities of robot autonomy and potential repercussions have been addressed in fiction and may be a realistic concern in the future.

They are also employed for jobs which are too dirty, dangerous or dull to be suitable for humans. Robots are widely used in manufacturing, assembly and packing, transport, earth and space exploration, surgery, weaponry,

laboratory research, and mass production of consumer and industrial goods.

A robot is an electromechanical machine that is controlled by computer program to perform various operations. Industrial robots have designed to reduce human effort and time to improve productivity and to reduce manufacturing cost. Today human-machine interaction is moving away from mouse and pen and becoming much more pervasive and much more compatible with the physical world. Android app can control the robot motion from a long- distance using Bluetooth communication to interface controller and android. Microcontroller unit can be interfaced to the Bluetooth module through protocol and code is written in embedded C language.

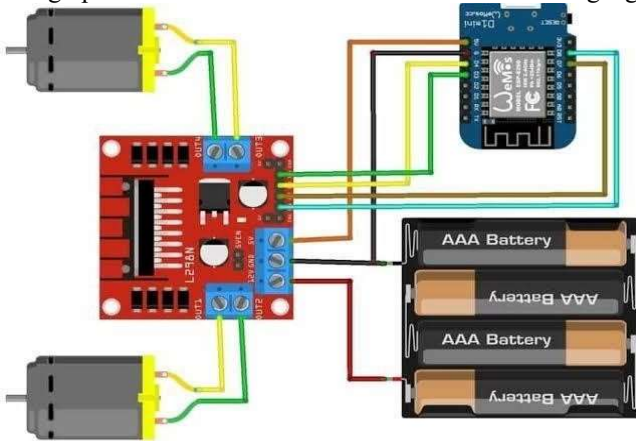


Figure.1. Basic Connections

As per the commands received from android app the robot motion can be controlled. The output motion of a robotic vehicle is accurate and repeatable. Pick and Place robots can be reprogrammable, and tool can be interchanged to provide for multiple applications. The purpose of this work is to design and implement an Android Controlled Bluetooth Robot which is used for Surveillance, home automation, wheelchairs, military and hostages Rescue applications.

Robots are smart machines that can be programmed and used in many areas such as industry, manufacturing, production lines, or health, etc. These robots perform hard, dangerous, and accurate work to facilitate our life and to increase the production because they can work 24 hours without rest and can do works like human but more precisely and with less time. Assistive mobile robots that perform different kinds of work over everyday activities in many areas such as industry, manufacturing, production lines, or health, etc. are very commonly used to improve our life. The idea of this research is to exploit robotics usage on healthcare field to help mobility disabled people.

INTRODUCTION OF EMBEDDED C PROGRAMMING

Before going into the details of Embedded C Programming Language and basics of Embedded C Program, we will first talk about the C Programming Language. The C Programming Language, developed by Dennis Ritchie in the late 60's and early 70's, is the most popular and widely used programming language. The C Programming Language provided low level memory access using an uncomplicated compiler (a software that converts programs to machine code) and achieved

efficient mapping to machine instructions. The C Programming Language became so popular that it is used in a wide range of applications ranging from Embedded Systems to Super Computers.

Embedded C Programming Language, which is widely used in the development of Embedded Systems, is an extension of C Program Language. The Embedded C Programming Language uses the same syntax and semantics of the C Programming Language like main function, declaration of data types, defining variables, loops, functions, statements, etc. The extension in Embedded C from standard C Programming Language include I/O Hardware Addressing, fixed point arithmetic operations, accessing address spaces, etc.

A. Keywords in Embedded C:

A Keyword is a special word with a special meaning to the compiler (a C Compiler for example, is a software that is used to convert program written in C to Machine Code). For example, if we take the Keil's Cx51 Compiler (a popular C Compiler for 8051 based Microcontrollers) the following are some of the keywords:

- bit
- sbit
- sfr
- small
- large

B. Data Types in Embedded C:

Data Types in C Programming Language (or any programming language for that matter) help us declaring variables in the program. There are many data types in C Programming Language like signed int, unsigned int, signed char, unsigned char, float, double, etc. In addition to these there few more data types in Embedded C.

The following are the extra data types in Embedded C associated with the Keil's Cx51 Compiler.

- bit
- sbit
- Sfr
- sfr16

FACTORS FOR SELECTING THE PROGRAMMING LANGUAGE

The following are few factors that are to be considered while selecting the Programming Language for the development of Embedded Systems.

- Size: The memory that the program occupies is very important as Embedded Processors like Microcontrollers have a very limited amount of ROM (Program Memory).
- Speed: The programs must be very fast i.e., they must run as fast as possible. The hardware should not be slowed down due to a slow running software.
- Portability: The same program can be compiled for different processors.
- Ease of Implementation.
- Ease of Maintenance.
- Readability.

Earlier Embedded Systems were developed mainly using Assembly Language. Even though Assembly Language is closest to the actual machine code instructions and produces

small size hex files, the lack of portability and high number of resources (time and manpower) spent on developing the code, made the Assembly Language difficult to work with. There are other high-level programming languages that offered the above-mentioned features, but none were close to C Programming Language. Some of the benefits of using Embedded C as the main Programming Language:

- Significantly easy to write code in C.
- Consumes less time when compared to Assembly.
- Maintenance of code (modifications and updates) is very simple.
- Make use of library functions to reduce the complexity of the main code.
- You can easily port the code to other architecture with very little modification.

II. COMPONENTS

This are the main important components used:

- Node MCU (esp82 66-12e v1.0) Wi-fi Board.
- L298N Motor Driver Module.
- DC geared motor.
- Wheels.
- Caster ball wheel.
- Micro USB cable.
- 14.8v rechargeable battery Li-Po battery.
- Jumper wires (female to a female).
- 2-wheel car chassis kit.

III. FABRICATION OF APP CONTROL ROBOT

Wi-Fi module for the system, which can be used as either master or slave. Generally, our master will be smartphone and slave will be Bluetooth module Bluetooth module will give the commands given by smartphone to the microcontroller. Microcontroller will act as the brain of the robot. The motor movement will he decided by the microcontroller. In this system we will using microcontroller named Arduino Uno which microcontroller chip. The microcontroller will be programmed with the help of the Embedded C programming Arduino has its own programming environment through which the microcontroller can be purpose we will be using a DC motor purpose we will be using a DC motor t will generate high amount of power and torque which will be sufficient to drive a human being. A motor driver will be used to control the DC motor will we connected to the microcontroller and the Bluetooth module will be connected to the same. In this proposed system we will be using any rechargeable battery to supply power to the electronic components of the system. Mainly the microcontroller and DC motor will be in need of power supply. The model represents a general idea how our robot will look like, and it is interfacing with the android smartphone. All the above-mentioned components will be mounted on the skateboard. And act mentioned in the system architecture the working will be processed. Motor driver is used to control DC motor. The microcontroller is the Brain of the robot and is used to connect the smartphone through the Bluetooth module. The motor belt driver is used to connect the wheels of the skateboard and the de motor through driving cog. The entire electronic component except the motor and belt will be kept in electronic component case.

In the operating system of the smart mobile phone android, we develop a remote-control program. The program connected with wi-fi to communicate with the robot. Wireless control is the most important basic need of all people. Wireless network-controlled robots use wi-fi modules.

Arduino blue control android application will transmit commands using wi-fi to the car so that it can move in the required direction like moving forward, reverse, turning left, turning right, and stop.

1 .LOAD CARRYING ROBOT

The wi-Fi-controlled robot is used to carry the load at Starting to require a location with controlling with the mobile. The application of the prototype car is maximum weight is carried 3kg and it is used in hazardous situations of the area i.e., for example for military weapons transfer, any fire accidents. etc.

2 .BLOCK DIAGRAM OF PROJECT

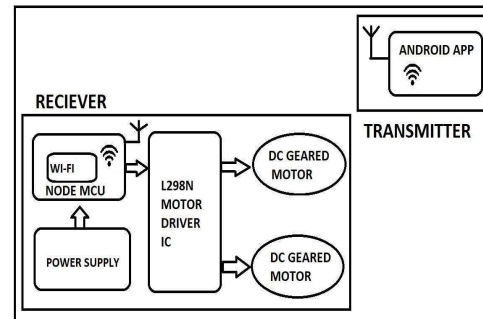


Fig 2.: Block diagram

Here is a block diagram, we have two sections one is the transmitter section and the receiver section. In the receiver section Node MCU is connected to two L298N motor drivers where one is connected to two dc geared motors. The power supply is also given to Node MCU. On the transmitter side, we have a simple android app.

SOFTWARE DEVELOPMENT:

To develop this software, we must install the software Arduino 1.8.13 and there we must write the program and compile it. Here in the code, we are given the wi-fi device name ARC BATCH: -B4, now our robot car will operate only for the device named ARC BATCH: - B4. If we want to change the device name, then we must change the name in code and dump or update it then compile. Now we can operate the machine with the changed name.

```

ESP8266 | Arduino 1.8.13
File: Sketch - Serial - Serial.ino

1 // Serial.ino
2 // Serial.ino
3 // Serial.ino
4 // Serial.ino
5 // Serial.ino
6 // Serial.ino
7 // Serial.ino
8 // Serial.ino
9 // Serial.ino
10 // Serial.ino
11 // Serial.ino
12 // Serial.ino
13 // Serial.ino
14 // Serial.ino
15 // Serial.ino
16 // Serial.ino
17 // Serial.ino
18 // Serial.ino
19 // Serial.ino
20 // Serial.ino
21 // Serial.ino
22 // Serial.ino
23 // Serial.ino
24 // Serial.ino
25 // Serial.ino
26 // Serial.ino
27 // Serial.ino
28 // Serial.ino
29 // Serial.ino
30 // Serial.ino
31 // Serial.ino
32 // Serial.ino
33 // Serial.ino
34 // Serial.ino
35 // Serial.ino
36 // Serial.ino
37 // Serial.ino
38 // Serial.ino
39 // Serial.ino
40 // Serial.ino
41 // Serial.ino
42 // Serial.ino
43 // Serial.ino
44 // Serial.ino
45 // Serial.ino
46 // Serial.ino
47 // Serial.ino
48 // Serial.ino
49 // Serial.ino
50 // Serial.ino
51 // Serial.ino
52 // Serial.ino
53 // Serial.ino
54 // Serial.ino
55 // Serial.ino
56 // Serial.ino
57 // Serial.ino
58 // Serial.ino
59 // Serial.ino
60 // Serial.ino
61 // Serial.ino
62 // Serial.ino
63 // Serial.ino
64 // Serial.ino
65 // Serial.ino
66 // Serial.ino
67 // Serial.ino
68 // Serial.ino
69 // Serial.ino
70 // Serial.ino
71 // Serial.ino
72 // Serial.ino
73 // Serial.ino
74 // Serial.ino
75 // Serial.ino
76 // Serial.ino
77 // Serial.ino
78 // Serial.ino
79 // Serial.ino
80 // Serial.ino
81 // Serial.ino
82 // Serial.ino
83 // Serial.ino
84 // Serial.ino
85 // Serial.ino
86 // Serial.ino
87 // Serial.ino
88 // Serial.ino
89 // Serial.ino
90 // Serial.ino
91 // Serial.ino
92 // Serial.ino
93 // Serial.ino
94 // Serial.ino
95 // Serial.ino
96 // Serial.ino
97 // Serial.ino
98 // Serial.ino
99 // Serial.ino
100 // Serial.ino
101 // Serial.ino
102 // Serial.ino
103 // Serial.ino
104 // Serial.ino
105 // Serial.ino
106 // Serial.ino
107 // Serial.ino
108 // Serial.ino
109 // Serial.ino
110 // Serial.ino
111 // Serial.ino
112 // Serial.ino
113 // Serial.ino
114 // Serial.ino
115 // Serial.ino
116 // Serial.ino
117 // Serial.ino
118 // Serial.ino
119 // Serial.ino
120 // Serial.ino
121 // Serial.ino
122 // Serial.ino
123 // Serial.ino
124 // Serial.ino
125 // Serial.ino
126 // Serial.ino
127 // Serial.ino
128 // Serial.ino
129 // Serial.ino
130 // Serial.ino
131 // Serial.ino
132 // Serial.ino
133 // Serial.ino
134 // Serial.ino
135 // Serial.ino
136 // Serial.ino
137 // Serial.ino
138 // Serial.ino
139 // Serial.ino
140 // Serial.ino
141 // Serial.ino
142 // Serial.ino
143 // Serial.ino
144 // Serial.ino
145 // Serial.ino
146 // Serial.ino
147 // Serial.ino
148 // Serial.ino
149 // Serial.ino
150 // Serial.ino
151 // Serial.ino
152 // Serial.ino
153 // Serial.ino
154 // Serial.ino
155 // Serial.ino
156 // Serial.ino
157 // Serial.ino
158 // Serial.ino
159 // Serial.ino
160 // Serial.ino
161 // Serial.ino
162 // Serial.ino
163 // Serial.ino
164 // Serial.ino
165 // Serial.ino
166 // Serial.ino
167 // Serial.ino
168 // Serial.ino
169 // Serial.ino
170 // Serial.ino
171 // Serial.ino
172 // Serial.ino
173 // Serial.ino
174 // Serial.ino
175 // Serial.ino
176 // Serial.ino
177 // Serial.ino
178 // Serial.ino
179 // Serial.ino
180 // Serial.ino
181 // Serial.ino
182 // Serial.ino
183 // Serial.ino
184 // Serial.ino
185 // Serial.ino
186 // Serial.ino
187 // Serial.ino
188 // Serial.ino
189 // Serial.ino
190 // Serial.ino
191 // Serial.ino
192 // Serial.ino
193 // Serial.ino
194 // Serial.ino
195 // Serial.ino
196 // Serial.ino
197 // Serial.ino
198 // Serial.ino
199 // Serial.ino
200 // Serial.ino
201 // Serial.ino
202 // Serial.ino
203 // Serial.ino
204 // Serial.ino
205 // Serial.ino
206 // Serial.ino
207 // Serial.ino
208 // Serial.ino
209 // Serial.ino
210 // Serial.ino
211 // Serial.ino
212 // Serial.ino
213 // Serial.ino
214 // Serial.ino
215 // Serial.ino
216 // Serial.ino
217 // Serial.ino
218 // Serial.ino
219 // Serial.ino
220 // Serial.ino
221 // Serial.ino
222 // Serial.ino
223 // Serial.ino
224 // Serial.ino
225 // Serial.ino
226 // Serial.ino
227 // Serial.ino
228 // Serial.ino
229 // Serial.ino
230 // Serial.ino
231 // Serial.ino
232 // Serial.ino
233 // Serial.ino
234 // Serial.ino
235 // Serial.ino
236 // Serial.ino
237 // Serial.ino
238 // Serial.ino
239 // Serial.ino
240 // Serial.ino
241 // Serial.ino
242 // Serial.ino
243 // Serial.ino
244 // Serial.ino
245 // Serial.ino
246 // Serial.ino
247 // Serial.ino
248 // Serial.ino
249 // Serial.ino
250 // Serial.ino
251 // Serial.ino
252 // Serial.ino
253 // Serial.ino
254 // Serial.ino
255 // Serial.ino
256 // Serial.ino
257 // Serial.ino
258 // Serial.ino
259 // Serial.ino
260 // Serial.ino
261 // Serial.ino
262 // Serial.ino
263 // Serial.ino
264 // Serial.ino
265 // Serial.ino
266 // Serial.ino
267 // Serial.ino
268 // Serial.ino
269 // Serial.ino
270 // Serial.ino
271 // Serial.ino
272 // Serial.ino
273 // Serial.ino
274 // Serial.ino
275 // Serial.ino
276 // Serial.ino
277 // Serial.ino
278 // Serial.ino
279 // Serial.ino
280 // Serial.ino
281 // Serial.ino
282 // Serial.ino
283 // Serial.ino
284 // Serial.ino
285 // Serial.ino
286 // Serial.ino
287 // Serial.ino
288 // Serial.ino
289 // Serial.ino
290 // Serial.ino
291 // Serial.ino
292 // Serial.ino
293 // Serial.ino
294 // Serial.ino
295 // Serial.ino
296 // Serial.ino
297 // Serial.ino
298 // Serial.ino
299 // Serial.ino
300 // Serial.ino
301 // Serial.ino
302 // Serial.ino
303 // Serial.ino
304 // Serial.ino
305 // Serial.ino
306 // Serial.ino
307 // Serial.ino
308 // Serial.ino
309 // Serial.ino
310 // Serial.ino
311 // Serial.ino
312 // Serial.ino
313 // Serial.ino
314 // Serial.ino
315 // Serial.ino
316 // Serial.ino
317 // Serial.ino
318 // Serial.ino
319 // Serial.ino
320 // Serial.ino
321 // Serial.ino
322 // Serial.ino
323 // Serial.ino
324 // Serial.ino
325 // Serial.ino
326 // Serial.ino
327 // Serial.ino
328 // Serial.ino
329 // Serial.ino
330 // Serial.ino
331 // Serial.ino
332 // Serial.ino
333 // Serial.ino
334 // Serial.ino
335 // Serial.ino
336 // Serial.ino
337 // Serial.ino
338 // Serial.ino
339 // Serial.ino
340 // Serial.ino
341 // Serial.ino
342 // Serial.ino
343 // Serial.ino
344 // Serial.ino
345 // Serial.ino
346 // Serial.ino
347 // Serial.ino
348 // Serial.ino
349 // Serial.ino
350 // Serial.ino
351 // Serial.ino
352 // Serial.ino
353 // Serial.ino
354 // Serial.ino
355 // Serial.ino
356 // Serial.ino
357 // Serial.ino
358 // Serial.ino
359 // Serial.ino
360 // Serial.ino
361 // Serial.ino
362 // Serial.ino
363 // Serial.ino
364 // Serial.ino
365 // Serial.ino
366 // Serial.ino
367 // Serial.ino
368 // Serial.ino
369 // Serial.ino
370 // Serial.ino
371 // Serial.ino
372 // Serial.ino
373 // Serial.ino
374 // Serial.ino
375 // Serial.ino
376 // Serial.ino
377 // Serial.ino
378 // Serial.ino
379 // Serial.ino
380 // Serial.ino
381 // Serial.ino
382 // Serial.ino
383 // Serial.ino
384 // Serial.ino
385 // Serial.ino
386 // Serial.ino
387 // Serial.ino
388 // Serial.ino
389 // Serial.ino
390 // Serial.ino
391 // Serial.ino
392 // Serial.ino
393 // Serial.ino
394 // Serial.ino
395 // Serial.ino
396 // Serial.ino
397 // Serial.ino
398 // Serial.ino
399 // Serial.ino
400 // Serial.ino
401 // Serial.ino
402 // Serial.ino
403 // Serial.ino
404 // Serial.ino
405 // Serial.ino
406 // Serial.ino
407 // Serial.ino
408 // Serial.ino
409 // Serial.ino
410 // Serial.ino
411 // Serial.ino
412 // Serial.ino
413 // Serial.ino
414 // Serial.ino
415 // Serial.ino
416 // Serial.ino
417 // Serial.ino
418 // Serial.ino
419 // Serial.ino
420 // Serial.ino
421 // Serial.ino
422 // Serial.ino
423 // Serial.ino
424 // Serial.ino
425 // Serial.ino
426 // Serial.ino
427 // Serial.ino
428 // Serial.ino
429 // Serial.ino
430 // Serial.ino
431 // Serial.ino
432 // Serial.ino
433 // Serial.ino
434 // Serial.ino
435 // Serial.ino
436 // Serial.ino
437 // Serial.ino
438 // Serial.ino
439 // Serial.ino
440 // Serial.ino
441 // Serial.ino
442 // Serial.ino
443 // Serial.ino
444 // Serial.ino
445 // Serial.ino
446 // Serial.ino
447 // Serial.ino
448 // Serial.ino
449 // Serial.ino
450 // Serial.ino
451 // Serial.ino
452 // Serial.ino
453 // Serial.ino
454 // Serial.ino
455 // Serial.ino
456 // Serial.ino
457 // Serial.ino
458 // Serial.ino
459 // Serial.ino
460 // Serial.ino
461 // Serial.ino
462 // Serial.ino
463 // Serial.ino
464 // Serial.ino
465 // Serial.ino
466 // Serial.ino
467 // Serial.ino
468 // Serial.ino
469 // Serial.ino
470 // Serial.ino
471 // Serial.ino
472 // Serial.ino
473 // Serial.ino
474 // Serial.ino
475 // Serial.ino
476 // Serial.ino
477 // Serial.ino
478 // Serial.ino
479 // Serial.ino
480 // Serial.ino
481 // Serial.ino
482 // Serial.ino
483 // Serial.ino
484 // Serial.ino
485 // Serial.ino
486 // Serial.ino
487 // Serial.ino
488 // Serial.ino
489 // Serial.ino
490 // Serial.ino
491 // Serial.ino
492 // Serial.ino
493 // Serial.ino
494 // Serial.ino
495 // Serial.ino
496 // Serial.ino
497 // Serial.ino
498 // Serial.ino
499 // Serial.ino
500 // Serial.ino
501 // Serial.ino
502 // Serial.ino
503 // Serial.ino
504 // Serial.ino
505 // Serial.ino
506 // Serial.ino
507 // Serial.ino
508 // Serial.ino
509 // Serial.ino
510 // Serial.ino
511 // Serial.ino
512 // Serial.ino
513 // Serial.ino
514 // Serial.ino
515 // Serial.ino
516 // Serial.ino
517 // Serial.ino
518 // Serial.ino
519 // Serial.ino
520 // Serial.ino
521 // Serial.ino
522 // Serial.ino
523 // Serial.ino
524 // Serial.ino
525 // Serial.ino
526 // Serial.ino
527 // Serial.ino
528 // Serial.ino
529 // Serial.ino
530 // Serial.ino
531 // Serial.ino
532 // Serial.ino
533 // Serial.ino
534 // Serial.ino
535 // Serial.ino
536 // Serial.ino
537 // Serial.ino
538 // Serial.ino
539 // Serial.ino
540 // Serial.ino
541 // Serial.ino
542 // Serial.ino
543 // Serial.ino
544 // Serial.ino
545 // Serial.ino
546 // Serial.ino
547 // Serial.ino
548 // Serial.ino
549 // Serial.ino
550 // Serial.ino
551 // Serial.ino
552 // Serial.ino
553 // Serial.ino
554 // Serial.ino
555 // Serial.ino
556 // Serial.ino
557 // Serial.ino
558 // Serial.ino
559 // Serial.ino
560 // Serial.ino
561 // Serial.ino
562 // Serial.ino
563 // Serial.ino
564 // Serial.ino
565 // Serial.ino
566 // Serial.ino
567 // Serial.ino
568 // Serial.ino
569 // Serial.ino
570 // Serial.ino
571 // Serial.ino
572 // Serial.ino
573 // Serial.ino
574 // Serial.ino
575 // Serial.ino
576 // Serial.ino
577 // Serial.ino
578 // Serial.ino
579 // Serial.ino
580 // Serial.ino
581 // Serial.ino
582 // Serial.ino
583 // Serial.ino
584 // Serial.ino
585 // Serial.ino
586 // Serial.ino
587 // Serial.ino
588 // Serial.ino
589 // Serial.ino
590 // Serial.ino
591 // Serial.ino
592 // Serial.ino
593 // Serial.ino
594 // Serial.ino
595 // Serial.ino
596 // Serial.ino
597 // Serial.ino
598 // Serial.ino
599 // Serial.ino
600 // Serial.ino
601 // Serial.ino
602 // Serial.ino
603 // Serial.ino
604 // Serial.ino
605 // Serial.ino
606 // Serial.ino
607 // Serial.ino
608 // Serial.ino
609 // Serial.ino
610 // Serial.ino
611 // Serial.ino
612 // Serial.ino
613 // Serial.ino
614 // Serial.ino
615 // Serial.ino
616 // Serial.ino
617 // Serial.ino
618 // Serial.ino
619 // Serial.ino
620 // Serial.ino
621 // Serial.ino
622 // Serial.ino
623 // Serial.ino
624 // Serial.ino
625 // Serial.ino
626 // Serial.ino
627 // Serial.ino
628 // Serial.ino
629 // Serial.ino
630 // Serial.ino
631 // Serial.ino
632 // Serial.ino
633 // Serial.ino
634 // Serial.ino
635 // Serial.ino
636 // Serial.ino
637 // Serial.ino
638 // Serial.ino
639 // Serial.ino
640 // Serial.ino
641 // Serial.ino
642 // Serial.ino
643 // Serial.ino
644 // Serial.ino
645 // Serial.ino
646 // Serial.ino
647 // Serial.ino
648 // Serial.ino
649 // Serial.ino
650 // Serial.ino
651 // Serial.ino
652 // Serial.ino
653 // Serial.ino
654 // Serial.ino
655 // Serial.ino
656 // Serial.ino
657 // Serial.ino
658 // Serial.ino
659 // Serial.ino
660 // Serial.ino
661 // Serial.ino
662 // Serial.ino
663 // Serial.ino
664 // Serial.ino
665 // Serial.ino
666 // Serial.ino
667 // Serial.ino
668 // Serial.ino
669 // Serial.ino
670 // Serial.ino
671 // Serial.ino
672 // Serial.ino
673 // Serial.ino
674 // Serial.ino
675 // Serial.ino
676 // Serial.ino
677 // Serial.ino
678 // Serial.ino
679 // Serial.ino
680 // Serial.ino
681 // Serial.ino
682 // Serial.ino
683 // Serial.ino
684 // Serial.ino
685 // Serial.ino
686 // Serial.ino
687 // Serial.ino
688 // Serial.ino
689 // Serial.ino
690 // Serial.ino
691 // Serial.ino
692 // Serial.ino
693 // Serial.ino
694 // Serial.ino
695 // Serial.ino
696 // Serial.ino
697 // Serial.ino
698 // Serial.ino
699 // Serial.ino
700 // Serial.ino
701 // Serial.ino
702 // Serial.ino
703 // Serial.ino
704 // Serial.ino
705 // Serial.ino
706 // Serial.ino
707 // Serial.ino
708 // Serial.ino
709 // Serial.ino
710 // Serial.ino
711 // Serial.ino
712 // Serial.ino
713 // Serial.ino
714 // Serial.ino
715 // Serial.ino
716 // Serial.ino
717 // Serial.ino
718 // Serial.ino
719 // Serial.ino
720 // Serial.ino
721 // Serial.ino
722 // Serial.ino
723 // Serial.ino
724 // Serial.ino
725 // Serial.ino
726 // Serial.ino
727 // Serial.ino
728 // Serial.ino
729 // Serial.ino
730 // Serial.ino
731 // Serial.ino
732 // Serial.ino
733 // Serial.ino
734 // Serial.ino
735 // Serial.ino
736 // Serial.ino
737 // Serial.ino
738 // Serial.ino
739 // Serial.ino
740 // Serial.ino
741 // Serial.ino
742 // Serial.ino
743 // Serial.ino
744 // Serial.ino
745 // Serial.ino
746 // Serial.ino
747 // Serial.ino
748 // Serial.ino
749 // Serial.ino
750 // Serial.ino
751 // Serial.ino
752 // Serial.ino
753 // Serial.ino
754 // Serial.ino
755 // Serial.ino
756 // Serial.ino
757 // Serial.ino
758 // Serial.ino
759 // Serial.ino
760 // Serial.ino
761 // Serial.ino
762 // Serial.ino
763 // Serial.ino
764 // Serial.ino
765 // Serial.ino
766 // Serial.ino
767 // Serial.ino
768 // Serial.ino
769 // Serial.ino
770 // Serial.ino
771 // Serial.ino
772 // Serial.ino
773 // Serial.ino
774 // Serial.ino
775 // Serial.ino
776 // Serial.ino
777 // Serial.ino
778 // Serial.ino
779 // Serial.ino
780 // Serial.ino
781 // Serial.ino
782 // Serial.ino
783 // Serial.ino
784 // Serial.ino
785 // Serial.ino
786 // Serial.ino
787 // Serial.ino
788 // Serial.ino
789 // Serial.ino
790 // Serial.ino
791 // Serial.ino
792 // Serial.ino
793 // Serial.ino
794 // Serial.ino
795 // Serial.ino
796 // Serial.ino
797 // Serial.ino
798 // Serial.ino
799 // Serial.ino
800 // Serial.ino
801 // Serial.ino
802 // Serial.ino
803 // Serial.ino
804 // Serial.ino
805 // Serial.ino
806 // Serial.ino
807 // Serial.ino
808 // Serial.ino
809 // Serial.ino
810 // Serial.ino
811 // Serial.ino
812 // Serial.ino
813 // Serial.ino
814 // Serial.ino
815 // Serial.ino
816 // Serial.ino
817 // Serial.ino
818 // Serial.ino
819 // Serial.ino
820 // Serial.ino
821 // Serial.ino
822 // Serial.ino
823 // Serial.ino
824 // Serial.ino
825 // Serial.ino
826 // Serial.ino
827 // Serial.ino
828 // Serial.ino
829 // Serial.ino
830 // Serial.ino
831 // Serial.ino
832 // Serial.ino
833 // Serial.ino
834 // Serial.ino
835 // Serial.ino
836 // Serial.ino
837 // Serial.ino
838 // Serial.ino
839 // Serial.ino
840 // Serial.ino
841 // Serial.ino
842 // Serial.ino
843 // Serial.ino
844 // Serial.ino
845 // Serial.ino
846 // Serial.ino
847 // Serial.ino
848 // Serial.ino
849 // Serial.ino
850 // Serial.ino
851 // Serial.ino
852 // Serial.ino
853 // Serial.ino
854 // Serial.ino
855 // Serial.ino
856 // Serial.ino
857 // Serial.ino
858 // Serial.ino
859 // Serial.ino
860 // Serial.ino
861 // Serial.ino
862 // Serial.ino
863 // Serial.ino
864 // Serial.ino
865 // Serial.ino
866 // Serial.ino
867 // Serial.ino
868 // Serial.ino
869 // Serial.ino
870 // Serial.ino
871 // Serial.ino
872 // Serial.ino
873 // Serial.ino
874 // Serial.ino
875 // Serial.ino
876 // Serial.ino
877 // Serial.ino
878 // Serial.ino
879 // Serial.ino
880 // Serial.ino
881 // Serial.ino
882 // Serial.ino
883 // Serial.ino
884 // Serial.ino
885 // Serial.ino
886 // Serial.ino
887 // Serial.ino
888 // Serial.ino
889 // Serial.ino
890 // Serial.ino
891 // Serial.ino
892 // Serial.ino
893 // Serial.ino
894 // Serial.ino
895 // Serial.ino
896 // Serial.ino
897 // Serial.ino
898 // Serial.ino
899 // Serial.ino
900 // Serial.ino
901 // Serial.ino
902 // Serial.ino
903 // Serial.ino
904 // Serial.ino
905 // Serial.ino
906 // Serial.ino
907 // Serial.ino
908 // Serial.ino
909 // Serial.ino
910 // Serial.ino
911 // Serial.ino
912 // Serial.ino
913 // Serial.ino
914 // Serial.ino
915 // Serial.ino
916 // Serial.ino
917 // Serial.ino
918 // Serial.ino
919 // Serial.ino
920 // Serial.ino
921 // Serial.ino
922 // Serial.ino
923 // Serial.ino
924 // Serial.ino
925 // Serial.ino
926 // Serial.ino
927 // Serial.ino
928 // Serial.ino
929 // Serial.ino
930 // Serial.ino
931 // Serial.ino
932 // Serial.ino
933 // Serial.ino
934 // Serial.ino
935 // Serial.ino
936 // Serial.ino
937 // Serial.ino
938 // Serial.ino
939 // Serial.ino
940 // Serial.ino
941 // Serial.ino
942 // Serial.ino
943 // Serial.ino
944 // Serial.ino
945 // Serial.ino
946 // Serial.ino
947 // Serial.ino
948 // Serial.ino
949 // Serial.ino
950 // Serial.ino
951 // Serial.ino
952 // Serial.ino
953 // Serial.ino
954 // Serial.ino
955 // Serial.ino
956 // Serial.ino
957 // Serial.ino
958 // Serial.ino
959 // Serial.ino
960 // Serial.ino
961 // Serial.ino
962 // Serial.ino
963 // Serial.ino
964 // Serial.ino
965 // Serial.ino
966 // Serial.ino
967 // Serial.ino
968 // Serial.ino
969 // Serial.ino
970 // Serial.ino
971 // Serial.ino
972 // Serial.ino
973 // Serial.ino
974 // Serial.ino
975 // Serial.ino
976 // Serial.ino
977 // Serial.ino
978 // Serial.ino
979 // Serial.ino
980 // Serial.ino
981 // Serial.ino
982 // Serial.ino
983 // Serial.ino
984 // Serial.ino
985 // Serial.ino
986 // Serial.ino
987 // Serial.ino
988 // Serial.ino
989 // Serial.ino
990 // Serial.ino
991 // Serial.ino
992 // Serial.ino
993 // Serial.ino
994 // Serial.ino
995 // Serial.ino
996 // Serial.ino
997 // Serial.ino
998 // Serial.ino
999 // Serial.ino
1000 // Serial.ino
    
```

Fig 3.: Program

Program for connecting wi-fi

```

Batch_4 | Arduino 1.8.13
File Edit Sketch Tools Help
Batch_4
// Starting Web-server
server.on ( "/", HTTP_handleRoot );
server.onNotFound ( HTTP_handleRoot );
server.begin();
}

void goAhead()
{
  digitalWrite(IN_1, LOW);
  digitalWrite(IN_2, HIGH);
  digitalWrite(IN_3, LOW);
  digitalWrite(IN_4, HIGH);
}

void goBack()
{
  digitalWrite(IN_1, HIGH);
  digitalWrite(IN_2, LOW);
  digitalWrite(IN_3, HIGH);
  digitalWrite(IN_4, LOW);
}

void goRight()
{
  digitalWrite(IN_1, HIGH);
  digitalWrite(IN_2, LOW);
  digitalWrite(IN_3, LOW);
  digitalWrite(IN_4, HIGH);
}

```

Fig. 4: Program

```

Batch_4 | Arduino 1.8.13
File Edit Sketch Tools Help
Batch_4
void goLeft()
{
  digitalWrite(IN_1, LOW);
  digitalWrite(IN_2, HIGH);
  digitalWrite(IN_3, HIGH);
  digitalWrite(IN_4, LOW);
}

void stopRobot()
{
  digitalWrite(IN_1, LOW);
  digitalWrite(IN_2, LOW);
  digitalWrite(IN_3, LOW);
  digitalWrite(IN_4, LOW);
}

void loop()
{
  server.handleClient();
  command = server.arg("State");
  if (command == "F")
  {
    goAhead();
  }
  else if (command == "B")
  {
    goBack();
  }
}

```

Fig 5: Program

```

Batch_4 | Arduino 1.8.13
File Edit Sketch Tools Help
Batch_4
goBack();
}
else if (command == "L")
{
  goRight();
}
else if (command == "R")
{
  goLeft();
}
else if (command == "I")
{
  //goAheadfgg();
}
//else if (command == "G") goAheadLeft();
//else if (command == "J") goBackRight();
//else if (command == "H") goBackLeft();

else if (command == "S")
{
  stopRobot();
}
}

void HTTP_handleRoot(void) {
if( server.hasArg("State") ){
  serial.println(server.arg("State"));
}
server.send ( 200, "text/html", "" );
delay(1);
}

```

Fig 6: Program

Program for moving the robot right, left, forward, backward and stop.

APP INSTALLATION:

Step.1. Install this app (Node MCU car) on your mobile.



Fig.7. Node MCU

Step.2 Open the app, then you can find.

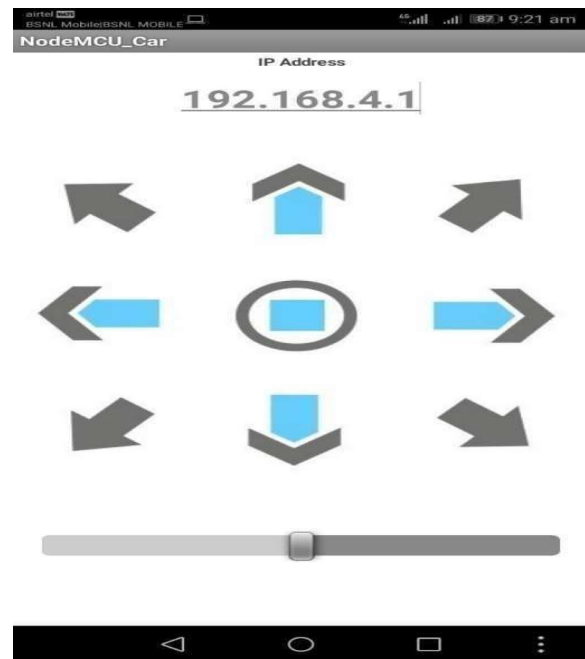


Fig 8. Image showing inside the app

The above arrow marks indicate the directions in which we can move the robot car in different directions. Console page consist of 5 buttons named as LEFT, RIGHT, FORWARD, BACKWARD & STOP. On pressing these buttons one can move the robot in the specified direction, for example on pressing Right the app will send an R output to the controller which will then process the signal and give the input to motor driver. While pressing the stop button the robot will stop its movements

IV. CIRCUIT DIAGRAM AND EXPLANATION:

Node MCU is connected to L298N motor driver where it is connected to two dc geared motors. Power supply bis also given to Node MCU. In IN1 transmitter side we have a simple android app.

- Connect the pin of the L298n motor driver module to the D1 pin of the Node MCU board.
- Connect the IN2 pin of the L298n motor driver module to the D2 pin of the Node MCU board.
- Connect the IN3 pin of the L298n motor driver module to the D3 pin of the Node MCU board.
- Connect the IN4 pin of the L298n motor driver module to the D4 pin of the Node MCU board.
- Connect the GND pin of the L298n motor driver module to the GND pin of the Node MCU board.
- Connect VCC pin of L298n motor driver module to Vin pin of Node MCU board.

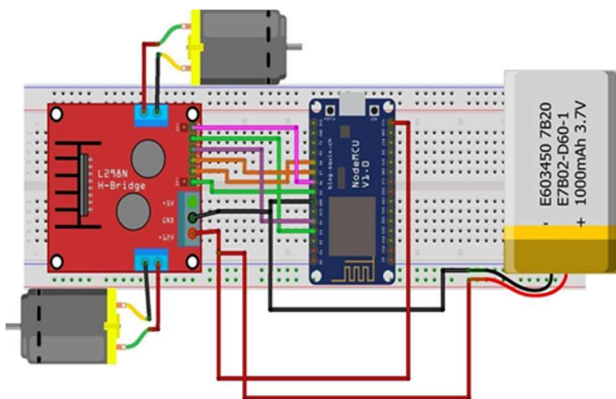


Fig.9.: circuit diagram

V. WORK EXPERIENCE AND FINAL PROJECT:

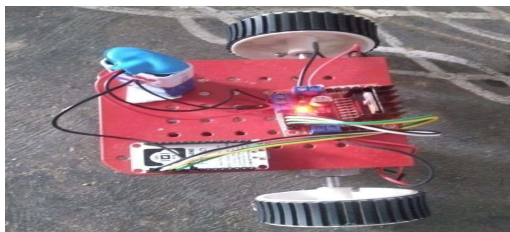


Fig 10.: Final project



Fig.11.: Load carrying

CONCLUSION

The project is Bluetooth Robot using Arduino is an application based on popular open-source technology Android and Arduino. The aim of the project was to create an Arduino integrated robot that has to be controlled through an application that runs on the android operating system. The project has been completed with success with the maximum satisfaction. Provisions are created to upgrade the code. The applying has been tested with live information and has provided a health result. Hence the code has proven to figure hasty. The system created met its objectives, by being straightforward to use, implement. Further modules may be simply other once necessary. The code is developed with standard approach. All modules within the system are tested with all the valid information for everything work with success.

Wireless control is one of the most important basic needs for all the people all over the world. But unfortunately, the technology is not fully utilized due to a huge amount of data and communication overheads. Generally, many of the wireless-controlled robots use RF modules. But our project. for robotic control make use of Android mobile phone which is very cheap and easily available. The available control commands are more than RF modules. For this purpose, the android mobile user must install a designed application on her/his mobile.

REFERENCES

- [1] Vermesan Ovidiu, Friess Peter. Guillemin Patrick. Sundmaecker Harald. Eisenhauer Markus. Moessner Klaus, Le Gall Franck and Cousin Philippe 2010 Internet of Things Strategic Research and Innovation Agenda (River Publishers Series in Communications) p 7.
- [2] Zheng Pei and Ni Lionel 2010 Smart Phone and Next Generation Mobile Computing (Elsevier)
- [3] Abed Faisal Theyab, ALRikabi Haider Th Salim and Ibrahim Isam Aameer 2020 Efficient Energy of Smart Grid Education Models for Modern Electric Power System Engineering in Iraq (IOP Conference Series: Materials Science and Engineering) vol 870 no 1 p 012049.
- [4] Singh Balkeshwar, Sellappan N and Kumara has P 2013 Evolution of Industrial Robots and Their Applications (J International Journal of emerging technology, and engineering advanced) vol 3 no 5 pp 763-768.
- [5] Hernandez-de-Menendez Marcela, Diaz Carlos A Escobar, MoralesMenendez Ruben 2020 Engineering Education for Smart 4.0 Technology: A Review (J International Journal on Interactive Design, and Manufacturing) vol 14, no 3 pp 789-803.
- [6] Marinoudi Vasso, Sorensen Claus G, Pearson Simon and Bochtis Dionysius 2019 Robotics and Labour in Agriculture. A Context Consideration (J Biosystems Engineering) vol 184 pp 111 121.
- [7] Maurtua Inaki, Ibarguren Aitor, Kildal Johan, Susperregi Loreto and Sierra Basilio 2017 Human-Robot Collaboration in Industrial Applications: Safety, Interaction And Trust (JInternational Journal of Advanced Robotic Systems) vol 14 no 4 pp 17298814-17716010.

- [8] Roa'a M Al airaji, Aljazaery Ibtisam A, Al Dulaimi Suha Kamal, Alrikabi Haider TH Salimand Informatics 2020 Generation of High Dynamic Range for Enhancing the Panorama Environment (Bulletin of Electrical Engineering) vol 10 no 1.
- [9] Smys S and Ranganathan G 2019 Robot Assisted Sensing Control and Manufacture in Automobile Industry (%J SMS ISMAC) vol 1 no 03 pp 180187.

WI-FI CONTROLLED WARD SANITIZATION ROBOT CAR

B. Venkata Siva¹, Venkannababu Mendi², D Raviteja³, Ch.V.L.Janardhan⁴

^{1,2} Professor, *Department of Mechanical Engineering, Narasaraopeta Engineering College, Narasaraopet.*

^{3,4} Student, *Department of Mechanical Engineering, Narasaraopeta Engineering College, Narasaraopet.*

ABSTRACT: This project describes the evolving role of robotics in healthcare and allied areas with special concerns relating to the management and control of the spread of the novel coronavirus disease 2019 (COVID-19). The prime utilization of such robots is to minimize person-to-person contact and to ensure cleaning, sterilization and support in hospitals and similar facilities such as quarantine. This will result in minimizing the life threat to medical staffs and doctors taking an active role in the management of the COVID-19 pandemic.

The intention of the present research is to highlight the importance of medical robotics in general and then to connect its utilization with the perspective of COVID-19 management so that the hospital management can direct themselves to maximize the use of medical robots for various medical procedures. This is despite the popularity of telemedicine, which is also effective in similar situations. In essence, the recent achievement of the Korean and Chinese health sectors in obtaining active control of the COVID-19 pandemic was not possible without the use of state of the art medical technology. In this project designing and developing a Wi-Fi-controlled robot using node MCU ESP8266, Wi-Fi, and L298N Motor Driver Module. To control this robot car was developed with a simple android app named Node MCU car. By using this app, robot can be controlled in all directions.

1. INTRODUCTION

Industrial robot is defined by ISO as an automatically controlled, reprogrammable, multipurpose manipulator, programmable in three or more axes, which can be either fixed in place or mobile for use in industrial automation applications.

2. HISTORY OF ROBOTICS: TIMELINE

This history of robotics is intertwined with the histories of technology, science and the basic principle of progress. Technology used in computing, electricity, even pneumatics and hydraulics can all be considered a part of the history of robotics. The timeline presented is therefore far from complete.

Robotics currently represents one of mankind’s greatest accomplishments and is the single greatest attempt of mankind to produce an artificial, sentient being. It is only in recent years that manufacturers are making robotics increasingly available and attainable to the general public. The focus of this timeline is to provide the reader with a general overview of robotics (with a focus more on mobile robots) and to give an appreciation for the inventors and innovators in this field who have helped robotics to become what it is today [2].

Medieval times:

Automatons, human-like figures run by hidden mechanisms, were used to impress peasant worshippers in church into believing in a higher power. [These mechanisms] created the illusion of self-motion (moving without assistance). The clock jack was a mechanical figure that could strike time on a bell

with its axe. This technology was virtually unheard of in the 13th century.

Science fiction writer Isaac Asimov first used the word "robotics" to describe the technology of robots and predicted the rise of a powerful robot industry.

The term robotics refers to the study and use of robots; it came about in 1941 and was first adopted by Isaac Asimov, a scientist and writer. It was Asimov who also proposed the following “Laws of Robotics” in his short story Run around in 1942. First Industrial Robot shown in fig 1.1, is introduced by George Devol it is used for transferring objects and also for transporting die casting [3].

A second largest robot shown in fig 1.2 arrived of on the scene in 1963. Designed by Harry Johnson & Veljko Milenkovic. It is the world first cylindrical robot and it is first commercial painting robot used in Ford Motors.

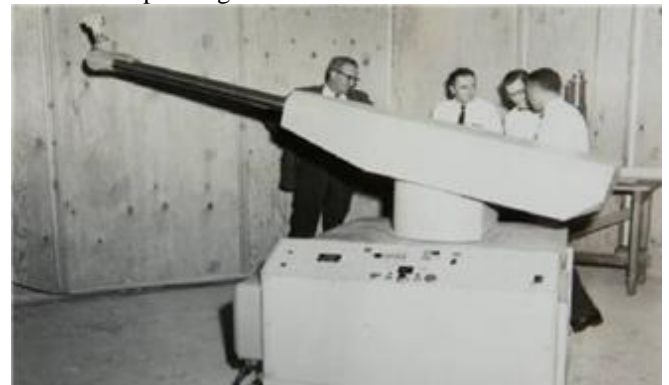


Figure: First Industrial Robot



Fig 1.2 Versatran robot

1.3 ROBOT PARAMETERS:

The following are the parameters for robots. The parameters are required when purchasing and handling a robot. A robot axis will move. When a force is applied to it.

Degrees of freedom	-	This is usually the same as the number of axes.
Working envelope	-	The region of space a robot can reach.
Kinematics	-	The actual arrangement of joints in the robot.
Payload	-	How much weight a robot can lift.
Speed	-	How fast the robot can position the end of its arm.
Acceleration	-	How quickly an axis can accelerate.
Accuracy	-	How closely a robot can reach a commanded position.
Repeatability	-	How well the robot will return to a programmed position.
Compliance	-	Measure of the amount in angle or distance that

- Assembly tool (e.g. automatic screwdriver)
 - Heating torch

Drive:

- The drive is the engine or motor that moves the links into their designated positions.

- The links are the sections between the joints.
- Industrial robot arms generally use one of the following types of drives:
 - Hydraulic drive
 - Electric drive
 - Pneumatic drive

Hydraulic drive:

It gives a robot great speed and strength. They provide high speed and strength, hence they are adopted for large industrial robots. This type of drives are preferred in environments in which the use of electric drive robots may cause fire hazards.

Pneumatic drive:

Generally used for smaller robots with fewer axes of movement. Used for Carry out simple pick-and-place material-handling operations, such as picking up an object at one location and placing it at another location. These operations are generally simple and have short cycle times. Here pneumatic power can be used for sliding or rotational joints.

Pneumatic robots are less expensive than electric or hydraulic robots.

Sensors:

Sensors receive feedback about its environment and also as a sense of sight and sound. and it collects information and sends it electronically to the robot controlled.

Vision sensors allow a pick and place robot to differentiate between items to choose and items to ignore [8].

1.5 Classification of robots:

According to operation of controller:

Limited sequence control

Limited sequence robots do not give servo controlled to inclined relative positions of the joints; instead they are controlled by setting limit switches & are mechanical stops. There is generally no feedback associated with a limited sequence robot to indicate that the desired position, has been achieved generally thin type of robots involves simple motion as pick & place operations.

Playback with point-to-point control

These type robots are capable of controlling velocity acceleration & path of motion, from the beginning to the end of the path. It uses complex control programs, PLC's (programmable logic controller's) computers to control the motion. The point to point control motion robots are capable of performing motion cycle that consists of a series of desired point location. The robot is tough & recorded, unit.

1.4 Robot anatomy:

Controller:

The Joint movements must be controlled if the robot is to perform as desired. Microprocessor-based controllers are regularly used to perform this control action. Controller is organised in a hierarchical fashion. Each joint can feed back control data individually, with an overarching supervisory controller co-ordinating the combined actuations of the joints according to the sequence of the robot program.

Manipulators:

Robot manipulators are created from a sequence of link and joint combinations. The links are the rigid members connecting the joints, or axes. The axes are the movable components of the robotic manipulator that cause relative motion between adjoining links. The mechanical joints used to construct the robotic arm manipulator consist of five principal types.

Two of the joints are linear, in which the relative motion between adjacent links is nonrotational, and three are rotary types, in which the relative motion involves rotation between links.

End effector:

Grippers grasp and manipulate objects during the work cycle. Typically the objects grasped are work parts that need to be loaded or unloaded from one station to another. It may be custom-designed to suit the physical specifications of the work parts they have to grasp. End effectors, grippers are described in detail in below:

Mechanical gripper: Two or more fingers that can be actuated by robot controller to open and close on a work part.

- Vacuum gripper: Suction cups are used to hold flat objects.
- Magnetised devices Making use of the principles of magnetism, these are used for holding ferrous work parts.
- Adhesive devices deploying adhesive substances these hold flexible materials, such as fabric.
- Simple mechanical devices for example, hooks and scoops.

End effectors – tools:

The robot end effector may also use tools. Tools are used to perform processing operations on the work part. Typically the robot uses the tool relative to a stationary or slowly moving object. In this way the process is carried out.

Examples of the tools used as end effectors by roots to perform processing applications include:

- Spot welding gun
- Arc welding tool
- Spray painting gun
- Rotating spindle for drilling, routing, grinding, etc.

CHAPTER-2

LITERATURE SURVEY:

The purpose of the project is to carry the load at starting to require a location with controlling the mobile. The application of the prototype car is maximum weight is carried 3kg and it is used in hazardous situations of the area i.e., for example for military weapons transfer, any fire accidents. etc.

The designing methodology of the system has two major portions: software design and hardware design. Hardware is designed by arranging microcontrollers whereas software design includes programming that is written and uploaded to the microcontroller.

Node MCU (Node Microcontroller Unit) is the central coordinator. This microcontroller has built-in support for Wi-Fi connectivity which allows it to send and receive data from the mobile application via an internet server. It reads data and sends them to mobile applications and receives commands from mobile applications to control the robot. It then drives the robotic directions. Mobile application- Node MCU_CAR is the simple software used to control the robotic directions. Internet server-mobile application in smartphones and Node MCU communicates by using Wi-Fi. Bidirectional transfer of data between Node MCU and mobile app occurs through this server.

This project is to limit the interaction between COVID-19 patients and health workers as well as to address the shortage of PPE kits. COVID-19 has not just added to the already heavy workload of healthcare professionals around the globe; it has also created the additional concern of medical workers getting infected due to direct contact with patients.

The aim of this research is to provide an automated mobile robot based solution to improve the effectiveness of ward management and medicine management and distribution processes. This system shows its use can improve the effectiveness of the present hospital ward management system. This will include helping with things like food and medication, something that nurses and doctors have been doing so far, putting them at larger risk of contracting the virus. The idea of robots taking up jobs previously done by humans may feel dystopian but scientists believe machines can free up human hospital medical staff while limiting the spread of the virus. "Robots can play a vital role during the present pandemic as they can minimise human intervention at all levels, starting from patient examination to patient care and drug delivery mechanism," The designing methodology of the system has two major portions: software design and hardware design. hardware is designed by arranging microcontroller whereas software design includes programming that is written and uploaded in the microcontroller.

Node MCU (Node Microcontroller Unit) it is the central coordinator. This microcontroller has built-in support for Wi-

Fi connectivity which allows it to send and receive data from mobile application via internet server. It reads data and sends them to mobile application and receives commands from mobile application to control robot. It then drives the robotic directions. Mobile application- Node MCU_CAR is the simple software used to control the robotic directions. Internet server-mobile application in Smartphone and Node MCU communicate by using Wi-Fi. Bidirectional transfer of data between Node MCU and mobile app occurs through this server. A few research papers related to medical robots have been reviewed and the following references show influence on the design of the smart medical assistant robot.

S Premkumar, Vikas Kusekar "Design and Implementation of multi handling Pick and Place Robotic Arm" Robot manipulator is an essential motion subsystem component of robotic system for positioning, orientating object so that robot can perform useful task The main aim of our work is to collaborate the gripper mechanism and vacuum sucker mechanism working in a single pick and place robotic arm. This robot can be selfoperational in controlling, stating with simple tasks such as gripping, sucking, lifting, placing and releasing in a single robotic arm. The main focus of our work is to design the robotic arm for the above mentioned purpose. Robotic arm consists of revolute joints that allowed angular movement between adjacent joint. Three double acting cylinders were used to actuate the arm of the robot. Robot manipulators are designed to execute required movements. By using this collaborated mechanism the success rate of pick and place robots are increased.

N. Rakesh, A. Pradeep Kumar, S. Ajay "Design And Manufacturing Of Low Cost Pneumatic Pick And Place Robot" The paper proposes a cheap and effective method for design and manufacturing of a three degree of freedom revolute jointed robotic arm. The design process begins by specifying top-level design criteria and passing down these criteria from the top level of the manipulator's structure to all subsequent components. With this proposed approach the sequential design intents are captured, organized and implemented based on the entire system objectives, as opposed to the conventional design process which aims at individual components optimization. By considering the mechanical arm's performance objectives, the design starts with modelling the integration of all the individual links constituting the manipulator. During the design process, modifications are made based on integrated information of kinematics, dynamics and structural analysis of the desired robot configuration as a whole. An optimum assembly design is then achieved with workable sub designs of the manipulator components. As a result, the proposed approach for manipulator design yields substantially less number of iterations, automatic propagation of design changes and great saving of design efforts.

Shirine El Zaatari, Mohamed Marei, Weidong Li, Zahid Usman "Cobot Programming for Collaborative Industrial Tasks", Collaborative robots (cobots) have been increasingly adopted in industries to facilitate human-robot collaboration.

Despite this, it is challenging to program cobots for collaborative industrial tasks as the programming has two distinct elements that are difficult to implement: (1) an intuitive element to ensure that the operations of a cobot can be composed or altered dynamically by an operator, and (2) a human-aware element to support cobots in producing flexible and adaptive behaviours dependent on human partners. In this area, some research works have been carried out recently, but there is a lack of a systematic summary on the subject. In this paper, an overview of collaborative industrial scenarios and programming requirements for cobots to implement effective collaboration is given. Then, detailed reviews on cobot programming, which are categorised into communication, optimisation, and learning, are conducted. Additionally, a significant gap between cobot programming implemented in industry and in research is identified, and research that works towards bridging this gap is pinpointed. Finally, the future directions of cobots for industrial collaborative scenarios are outlined, including potential points of extension and improvement.

CHAPTER-3 ROBOT MODULES

3.1. Node MCU:

NodeMCU is a low-cost open source IoT platform. It initially included firmware which runs on the ESP8266 Wi-Fi from Espressif Systems, and hardware which was based on the ESP-12 module. Later, support for the ESP32 32-bit MCU was added.

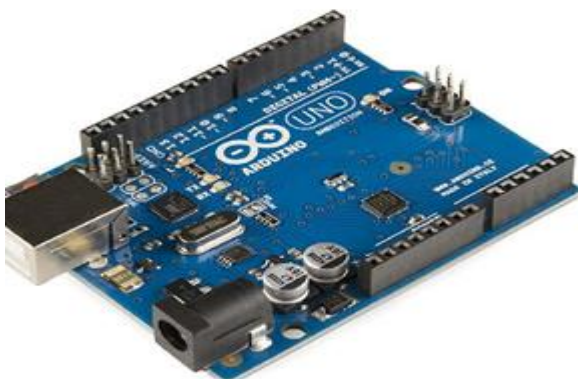


Fig 3.1 Node MCU

NodeMCU is an open source firmware for which open source prototyping board designs are available. The name "NodeMCU" combines "node" and "MCU" (micro-controller unit). The term "NodeMCU" strictly speaking refers to the firmware rather than the associated development kits. Both the firmware and prototyping board designs are open source.

The firmware uses the Lua scripting language. The firmware is based on the eLua project, and built on the Espressif Non-OS SDK for ESP8266. It uses many open source projects, such as lua-cjson and SPIFFS. Due to resource constraints, users need to select the modules relevant for their project and build a firmware tailored to their needs. Support for the 32-bit ESP32 has also been implemented.

The prototyping hardware typically used is a circuit board functioning as a dual in-line package (DIP) which integrates a USB controller with a smaller surface-mounted board

containing the MCU and antenna. The choice of the DIP format allows for easy prototyping on breadboards. The design was initially based on the ESP-12 module of the ESP8266, which is a Wi-Fi SoC integrated with a Tensilica Xtensa LX106 core, widely used in IoT applications.

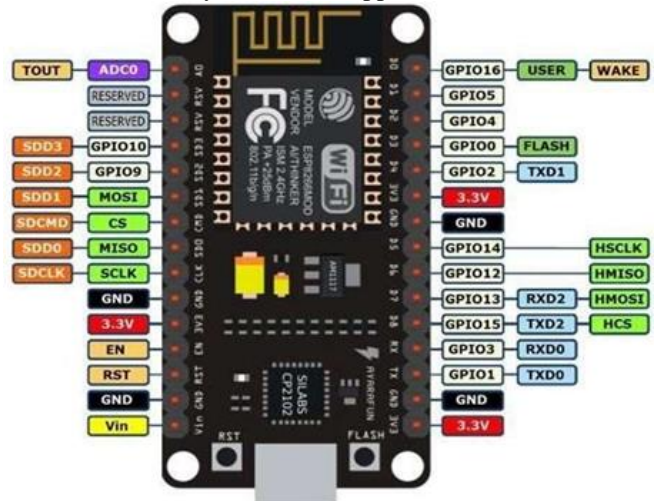


Fig 3.2 MCU Pin functions

Types :

There are two available versions of NodeMCU as version 0.9 & 1.0 where the version 0.9 contains **ESP-12** and version 1.0 contains **ESP-12E** where E stands for "Enhanced".

ESP8266 Arduino Core:

As Arduino.cc began developing new MCU boards based on non-AVR processors like the ARM/SAM MCU and used in the Arduino Due, they needed to modify the Arduino IDE so that it would be relatively easy to change the IDE to support alternate toolchains to allow Arduino C/C++ to be compiled for these new processors. They did this with the introduction of the Board Manager and the SAM Core. A "core" is the collection of software components required by the Board Manager and the Arduino IDE to compile an Arduino C/C++ source file for the target MCU's machine language. Some ESP8266 enthusiasts developed an Arduino core for the ESP8266 WiFi SoC, popularly called the "ESP8266 Core for the Arduino IDE". This has become a leading software development platform for the various ESP8266-based modules and development boards, including NodeMCUs.

General Pin Functions :

LED: There is a built-in LED driven by digital pin 13. When the pin is high value, the LED is on, when the pin is low, it is off.

VIN: The input voltage to the Arduino/Genuino board when it is using an external power source (as opposed to 5 volts from the USB connection or other regulated power source). You can supply voltage through this pin, or, if supplying voltage via the power jack, access it through this pin.

➤ **5V:** This pin outputs a regulated 5V from the regulator on the board. The board can be supplied with power either from the DC power jack (7 - 20V), the USB connector (5V)

➤ **VIN pin of the board (7-20V).** Supplying voltage via the 5V or 3.3V pins bypasses the regulator, and can damage the board.

- **3V3:** A 3.3 volt supply generated by the on-board regulator. Maximum current draw is 50 mA.

3.2. L298N MOTOR DRIVER:

This **L298N Motor Driver Module** is a high power motor driver module for driving DC and Stepper Motors. This module consists of an L298 motor driver IC and a 78M05 5V regulator. L298N Module can control up to 4 DC motors, or 2 DC motors with directional and speed control.

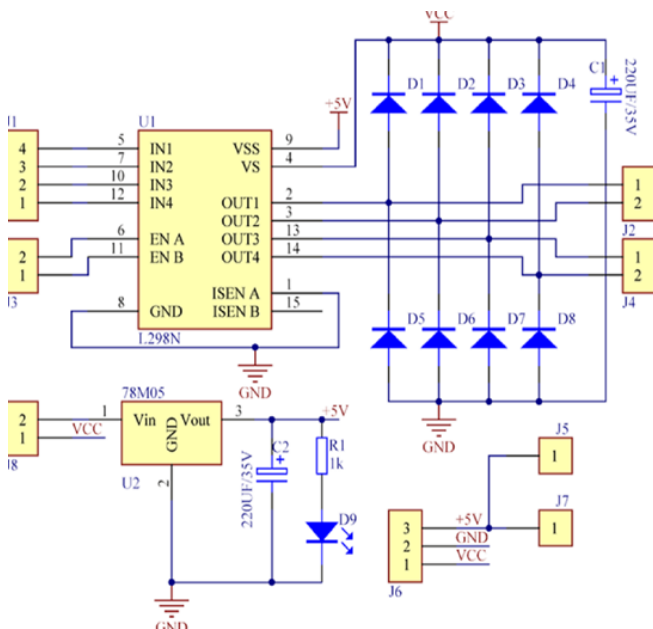
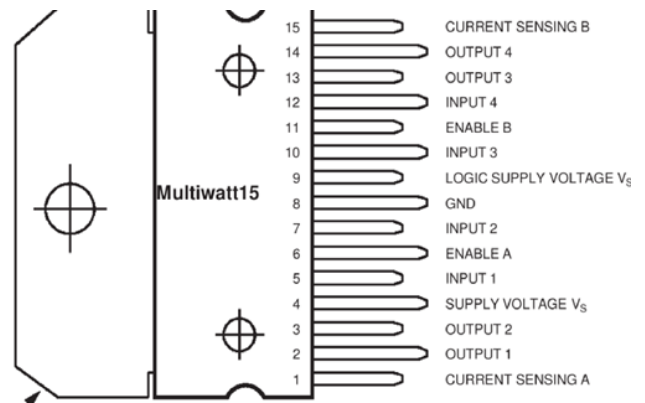
78M05 Voltage regulator will be enabled only when the jumper is placed. When the power supply is less than or equal to 12V, then the internal circuitry will be powered by the voltage regulator and the 5V pin can be used as an output pin to power the microcontroller. The jumper should not be placed when the power supply is greater than 12V and separate 5V should be given through SV terminal to power the internal circuitry.

ENA & ENB pins are speed control pins for Motor A and Motor B while IN1 & IN2 and IN3 & IN4 are direction control pins for Motor A and Motor B.

The L298N is an integrated monolithic circuit in a 15-lead Multiwatt and PowerSO20 packages. It is a high voltage, high current dual full-bridge driver de-signed to accept standard TTL logic level and drive inductive loads such as relays, solenoids, DC and stepping motors. Two enable inputs are provided to enable or disable the device independently of the in-put signals. The emitters of the lower transistors of each bridge are connected together and the corresponding external terminal can be used for the connection of an external sensing resistor. An additional Supply input is provided so that the logic works at a lower voltage.

Two built in H-bridge, high voltage, large current, full bridge driver, which can be used to drive DC motors, stepper motors, relay coils and other inductive loads. Using standard logic level signal to control.

1. Able to drive a two-phase stepper motor or four-phase stepper motor, and two-phase DC motors.
2. Adopt a high-capacity filter capacitor and a freewheeling diode that protects devices in the circuit from being damaged by the reverse current of an inductive load, enhancing reliability.
3. The module can utilize the built-in stabilivolt tube 78M05 to obtain 5v from the power supply. But to protect the chip of the 78M05 from damage, when the drive voltage is greater than 12v, an external 5v logic supply should be used.
4. Drive voltage: 5-35V; logic voltage: 5V.
5. PCB size: 4.2 x 4.2 cm.



High operating voltage, which can be up to 40 volts;
 Large output current, the instantaneous peak current can be up to 3A; With 25W rated power;

3.3.Wi-Fi Module:

Wi-Fi modules (wireless fidelity) also known as WLAN modules (wireless local area network) are electronic components used in many products to achieve a wireless connection to the internet.

There are two main categories of Wi-Fi modules for IoT: A “single” solution where the MCU runs the Wi-Fi stack and the host application in one chip. A “host processor + WiFi module” solution where the wireless connectivity solution contains the WiFi stack, and a separate processor runs the host application.

The Arduino Uno Wi-Fi is an Arduino Uno with an integrated WiFi module. The board is based on the ATmega328P with an ESP8266WiFi Module integrated. The ESP8266WiFi Module is a self contained So with integrated TCP/IP protocol stack that can give access to your Wi-Fi network (or the device can act as an access point).

An ESP8266 Wi-Fi module is a SOC microchip mainly used for the development of endpoint IoT (Internet of things) applications. It is referred to as a standalone wireless transceiver, available at a very low price. It is used to enable

the internet connection to various applications of embedded systems.

The module has a wireless Wi-Fi transceiver operating in an unlicensed frequency range of 2400-2484 MHz in the IEEE 802.11 b/g/n standard, with support for TCP/IP communication protocol stack and Wi-Fi security including WAP3.

The five Wi-Fi technologies are A, B, G, N and AC. B and G use the 2.4 GHz frequency; A and AC use the 5 GHz frequency; and N uses both 2.4 and 5 GHz frequencies. Your choice for your home or business will come down to three: Wireless G, N or AC. Routers that only support Wireless B are no longer manufactured.

The **ESP8266** is a very user friendly and low cost device to provide internet connectivity to your projects. The module can work both as a Access point (can create hotspot) and as a station (can connect to Wi-Fi), hence it can easily fetch data and upload it to the internet making Internet of **Things** as easy as possible.

The ESP8266 Integrates 802.11b/g/n HT40 Wi-Fi transceiver, so it can not only connect to a Wi-Fi network and interact with the Internet, but it can also set up a network of its own, allowing other devices to connect directly to it. This makes the ESP8266 Node MCU even more versatile Power to the ESP8266 Node MCU is supplied via the on-board Micro USB connector. Alternatively, if you have a regulated 9V voltage source, the VIN pin can be used to directly supply the ESP8266 and its peripherals.

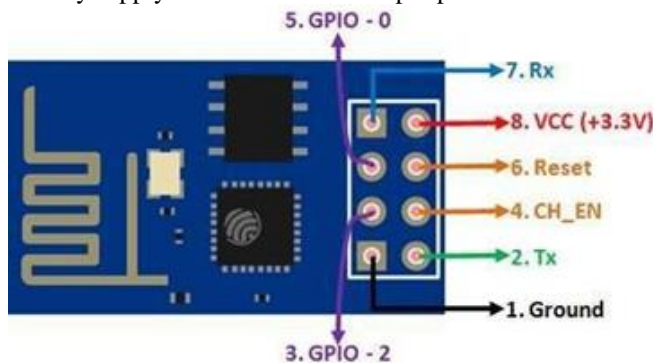


Fig.3.5 pin configuration of Wi-Fi module

V3 : -3.3 V Power Pin.

GND : - Ground Pin.

RST : - Active Low Reset Pin.

EN : Active High enable pin.

TX : Serial Transmit Pin Of UART.

RX : Serial Resive Pin Of UART.

Features :

- Processor: L106 32-bit RISC micro processor core based on the Tensilica Diamond Standard 106Micro running at 80 MHz.
- Memory: 32 KiB instruction RAM.
- 32 KiB instruction cache RAM
- 80 KiB user-data RAM

- 16 KiB ETS system-data RAM
- Integrated TR switch, balun, LNA, power amplifier and matching network

- WEP or WPA/WPA2 authentication, or open networks
- 17 GPIO pins
- Serial Peripheral Interface Bus (SPI)
- I²C (software implementation)
- I²S interfaces with DMA (sharing pins with GPIO)
- UART on dedicated pins, plus a transmit-only UART can be enabled on GPIO2
- 10-bit ADC (successive approximation ADC)

Pin Out of ESP -01:

The pinout is as follows for the common ESP-01 module:

- GND, Ground (0 V)
- GPIO 2, General-purpose input/output No. 2
- GPIO 0, General-purpose input/output No. 0
- RX, Receive data in, also GPIO3
- VCC, Voltage (+3.3 V; can handle up to 3.6 V)
- RST, Reset
- CH_PD, Chip power-down
- TX, Transmit data out, also GPIO1

3.4.Basics of Embedded C Program :

Embedded C is one of the most popular and most commonly used Programming Languages in the development of Embedded Systems. So, in this article, we will see some of the Basics of Embedded C Program and the Programming Structure of Embedded C.

Embedded C is perhaps the most popular languages among Embedded Programmers for programming Embedded Systems. There are many popular programming languages like Assembly, BASIC, C++, Python etc. that are often used for developing Embedded Systems but Embedded C remains popular due to its efficiency, less development time and portability.

Before digging in to the basics of Embedded C Program, we will first take a look at what an Embedded System is and the importance of Programming Language in Embedded Systems.

we have seen a little bit about Embedded Systems and Programming Languages, we will dive in to the basics of Embedded C Program. We will start with two of the basic features of the Embedded C Program: Keywords and Datatypes.

Embedded System :

An Embedded System can be best described as a system which has both the hardware and software and is designed to do a specific task. A good example for an Embedded System, which many households have, is a Washing Machine.

We use washing machines almost daily but wouldn't get the idea that it is an embedded system consisting of a Processor (and other hardware as well) and software.

Programming Embedded Systems:

As mentioned earlier, Embedded Systems consists of both Hardware and Software. If we consider a simple Embedded

System, the main Hardware Module is the Processor. The Processor is the heart of the Embedded System and it can be anything like a Microprocessor, Microcontroller, DSP, CPLD (Complex Programmable Logic Device) or an FPGA (Field Programmable Gated Array).

All these devices have one thing in common: they are programmable i.e., we can write a program (which is the software part of the Embedded System) to define how the device actually works.

Embedded Software or Program allow Hardware to monitor external events (Inputs / Sensors) and control external devices (Outputs) accordingly. During this process, the program for an Embedded System may have to directly manipulate the internal architecture of the Embedded Hardware (usually the processor) such as Timers, Serial Communications Interface, Interrupt Handling, and I/O Ports etc.

From the above statement, it is clear that the Software part of an Embedded System is equally important as the Hardware part. There is no point in having advanced Hardware Components with poorly written programs (Software).

There are many programming languages that are used for Embedded Systems like Assembly (low-level Programming Language), C, C++, JAVA (highlevel programming languages), Visual Basic, JAVA Script (Application level Programming Languages), etc.

In the process of making a better embedded system, the programming of the system plays a vital role and hence, the selection of the Programming Language is very important.

Factors for Selecting the Programming Language :

The following are few factors that are to be considered while selecting the Programming Language for the development of Embedded Systems.

➤ **Size:** The memory that the program occupies is very important as Embedded Processors like Microcontrollers have a very limited amount of ROM (Program Memory).

➤ **Speed:** The programs must be very fast i.e., they must run as fast as possible. The hardware should not be slowed down due to a slow running software.

➤ **Portability:** The same program can be compiled for different processors.

- Ease of Implementation
- Ease of Maintenance
- Readability

Earlier Embedded Systems were developed mainly using Assembly Language. Even though Assembly Language is closest to the actual machine code instructions and produces small size hex files, the lack of portability and high amount of resources (time and man power) spent on developing the code, made the Assembly Language difficult to work with.

There are other high-level programming languages that offered the above mentioned features but none were close to C Programming Language. Some of the benefits of using Embedded C as the main Programming Language:

- Significantly easy to write code in C
- Consumes less time when compared to Assembly
- Maintenance of code (modifications and updates) is very simple
- Make use of library functions to reduce the complexity of the main code
- You can easily port the code to other architecture with very little modifications

Introduction to Embedded C Programming Language :

Before going in to the details of Embedded C Programming Language and basics of Embedded C Program, we will first talk about the C Programming Language.

The C Programming Language, developed by Dennis Ritchie in the late 60's and early 70's, is the most popular and widely used programming language. The C Programming Language provided low level memory access using an uncomplicated compiler (a software that converts programs to machine code) and achieved efficient mapping to machine instructions.

The C Programming Language became so popular that it is used in a wide range of applications ranging from Embedded Systems to Super Computers.

Embedded C Programming Language, which is widely used in the development of Embedded Systems, is an extension of C Program Language. The Embedded C Programming Language uses the same syntax and semantics of the C Programming Language like main function, declaration of datatypes, defining variables, loops, functions, statements, etc.

The extension in Embedded C from standard C Programming Language include I/O Hardware Addressing, fixed point arithmetic operations, accessing address spaces, etc.

Keywords in Embedded C :

A Keyword is a special word with a special meaning to the compiler (a C Compiler for example, is a software that is used to convert program written in C to Machine Code). For example, if we take the Keil's Cx51 Compiler (a popular C Compiler for 8051 based Microcontrollers) the following are some of the keywords:

- bit
- sbit
- sfr
- small
- large

Data Types in Embedded C :

Data Types in C Programming Language (or any programming language for that matter) help us declaring variables in the program. There are many data types in C Programming Language like signed int, unsigned int, signed

char, unsigned char, float, double, etc. In addition to these there are few more data types in Embedded C.

The following are the extra data types in Embedded C associated with the Keil's Cx51 Compiler.

- bit
- sbit
- sfr
- sfr16

Basic Structure of an Embedded C Program (Template for Embedded C Program) :

The next thing to understand in the Basics of Embedded C Program is the basic structure or Template of Embedded C Program. This will help us in understanding how an Embedded C Program is written. The following part shows the basic structure of an Embedded C Program.

```

Multiline Comments . . . . . Denoted using /*.....*/
Single Line Comments . . . . . Denoted using //
Preprocessor Directives . . . . . #include<...> or #define
Global Variables . . . . . Accessible anywhere in the program
Function Declarations . . . . . Declaring Function
Main Function . . . . . Main Function, execution begins here
{
Local Variables . . . . . Variables confined to main function
Function Calls . . . . . Calling other Functions
Infinite Loop . . . . . Like while(1) or for(;;) Statements . . .
. . .
. . .
}
Function Definitions . . . . . Defining the Functions
{
Local Variables . . . . . Local Variables confined to this Function
Function Statements . . . . .
. . .
. . .
}
    
```

**CHAPTER-4
SANITIZATION ROBOT COMPONENTS**

4.1 : NODE MCU

Node MCU is an open source firmware for which open source prototyping board designs are available. The name "Node MCU" combines "node" and "MCU" (microcontroller unit).

The term "Node MCU" strictly speaking refers to the firmware rather than the associated development kits.

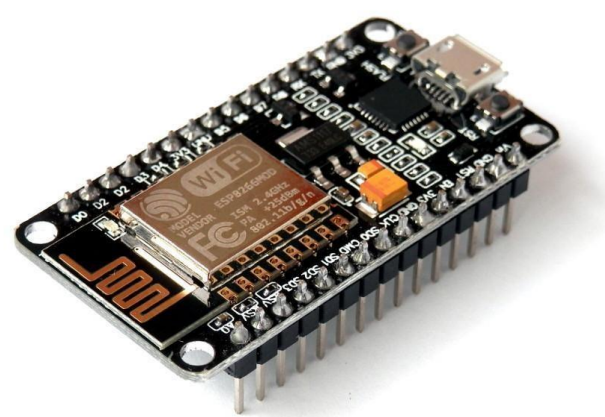


Fig 4.1 Node MCU

TABLE 1: SPECIFICATIONS OF NODE MCU :

specifications	NodeMCUv1.0	Arduino pro Mini
MCU	32 bit Tensilica	8 bit AT mega328P
frequency	80/160 MHz	16 MHz
Input-Output	17*DIO	14*DIO
ADC pin	1*10 bit	6*10 bit
Operating Voltage	3.0 ~ 3.6V	3.0 ~ 3.6V
Program Memory	4MB	32kb
Wi-Fi	IEEE 802.11 b/g/n	---



Fig 4.7 CASTER BALL WHELL

**CHAPTER-5
EXPERIMENTAL WORK AND EXECUTION
BLOCK DIAGRAM OF ROBOT :**

Node MCU is connected to two L298N motor drivers where one is connected to two dc geared motors and another is connected to the submersible pipe motor. Power supply bis also given to Node MCU. In transmitter side have a simple android app.

Connect the IN3 pin of the L298n motor driver module to the D3 pin of the NodeMCU board.
Connect the IN4 pin of the L298n motor driver module to the D4 pin of the NodeMCU board.
Connect the GND pin of the L298n motor driver module to the GND pin of the NodeMCU board.
Connect VCC pin of L298n motor driver module to Vin pin of NodeMCU board.

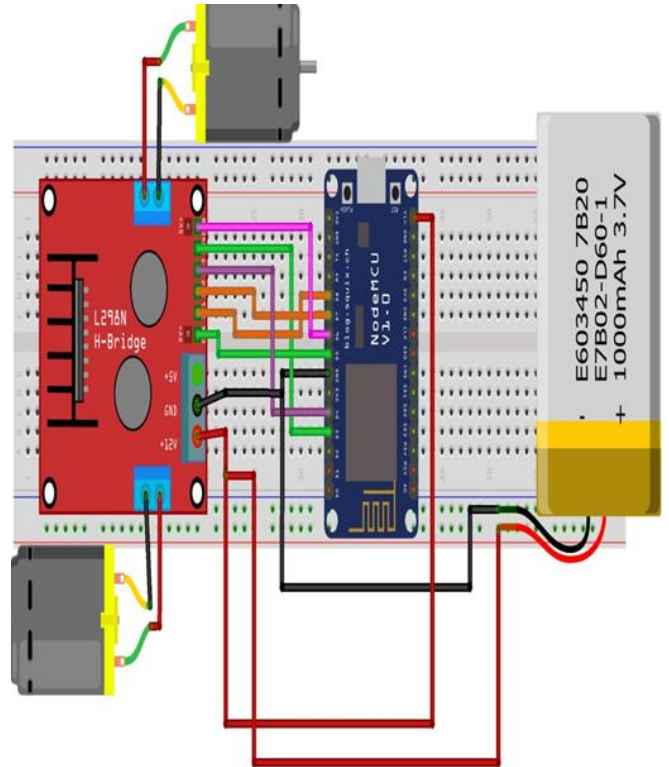
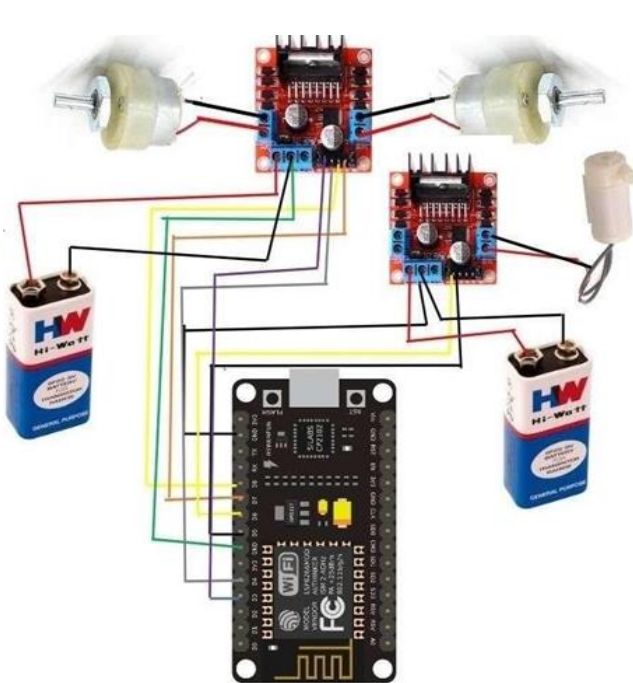
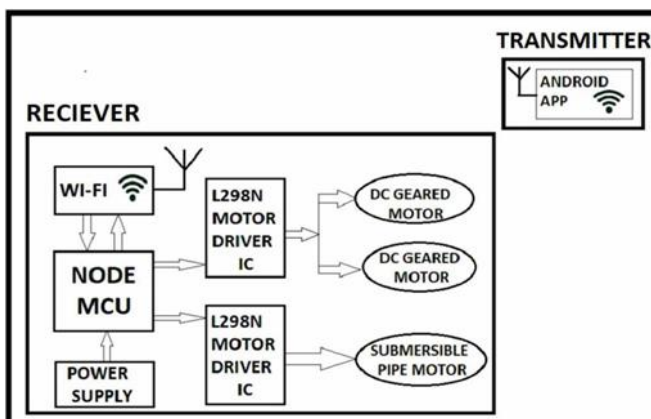


Fig.3.15 Image showing the circuit diagram

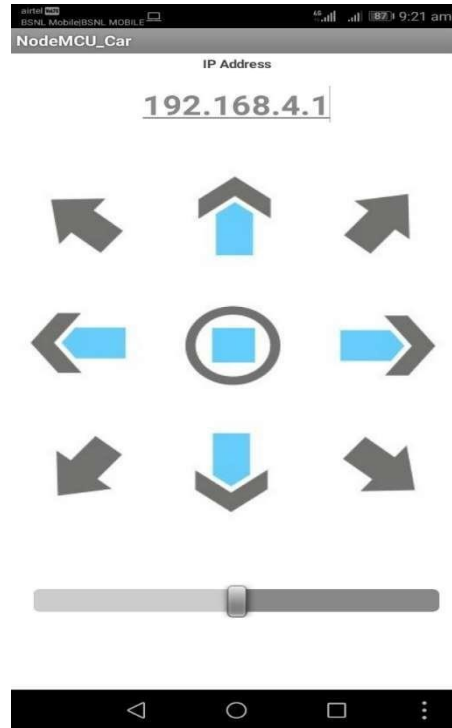


CIRCUIT DIAGRAM AND EXPLANATION:

Node MCU is connected to L298N motor driver where it is connected to two dc geared motors. Power supply bis also given to Node MCU. In transmitter side we have a simple android app.

Connect the IN1 pin of the L298n motor driver module to the D1 pin of the NodeMCU board.
Connect the IN2 pin of the L298n motor driver module to the D2 pin of the NodeMCU board.





- After uploading the code, open the application.
- The wi-fi address for the phone and board should be the same.
- In the operating system of the smart mobile phone android, we develop a remote-control program.
- The program connected with wi-fi to communicate with the robot. Wireless control is the most important basic need of all people.
- Wireless network-controlled robots use wi-fi modules.
- Arduino blue control android application will transmit commands using wi-fi to the car so that it can move in the required direction like moving forward, reverse, turning left, turning right, and stop.

App Installation:

Step.1. Install this app(NodeMCU_ car) in your mobile



Software Development :

To develop this software we have to install the software Arduino 1.8.13 and there we have to write the program and compile it. Here in the code we given the wi-fi device name venky, now our robot car will operate only for the device named venky. If we want change the device name then we have change the name in code and dump or update it then compile. Now we can operate the machine with the changed name.

To develop this software, we must install the software Arduino 1.8.13 and there we must write the program and compile it. Here in the code, we are given the wi-fi device name ARC BATCH: -B4, now our robot car will operate only for the device named ARC BATCH: -B4. If we want to change the device name, then we must change the name in code and dump or update it then compile. Now we can operate the machine with the changed name.

```

Batch_4
Batch_4j Arduino 1.8.13
File Edit Sketch Tools Help

Batch_4
#define IN_1 5 // L298N in1 motors Right GPIO15 (D1)
#define IN_2 4 // L298N in2 motors Right GPIO13 (D2)
#define IN_3 0 // L298N in3 motors Left GPIO2 (D3)
#define IN_4 2 // L298N in4 motors Left GPIO0 (D4)

#include <ESP8266WiFi.h>
#include <WiFiClient.h>
#include <ESP8266WebServer.h>

String command; //String to store app command state.

const char* ssid = "ARC BATCH:-B4";
ESP8266WebServer server(80);

void setup() {

  pinMode(IN_1, OUTPUT);
  pinMode(IN_2, OUTPUT);
  pinMode(IN_3, OUTPUT);
  pinMode(IN_4, OUTPUT);

  Serial.begin(115200);

  // Connecting WiFi
  WiFi.mode(WIFI_AP);
  WiFi.softAP(ssid);

  IPAddress myIP = WiFi.softAPIP();
  Serial.print("AP IP address: ");
  Serial.println(myIP);

  The sketch name had to be modified.
  Sketch names must start with a letter or number, followed by letters,
  numbers, dashes, dots and underscores. Maximum length is 63 characters.
  
```

CONCLUSION

As everything get automated and updated in this tech era, people usually look for easy and smart ways of using things and this wi-fi controlled robot car would come under one of the smart way to sanitize the hospital wards, schools and public places using mobile phone through nodemcu car app. The main advantage is that it is a cost effective ,simple manner and it's processing time is very less . One of the disadvantage is it is used for short distance.

Autonomous mobile sanitizing robot is becoming most useful in COVID-19 hospital environments. It reduces the human intervention in sanitization. The designed system is very compact, so easily can transport this robot to any place.

The COVID-19 pandemic presents even more reason to use mobile robots for safe cleaning in quarantine zones. The proposed model is fabricated and tested in a hospital environment. The system is capable of disinfecting an area of up to 100 m² per day.

By using the autonomous sprinkler system optimizes the disinfecting areas and reduces the wastage of sanitizer. The designed system is capable of sanitizing an area of up to 100 m² per day.

The application area can include hospital corridors, medical shop, operation theatre, walking pathways, doctor room, testing center, and patient room, etc.

SCOPE FOR FUTURE WORK

With the changing time, just like other technologies, robots are also playing an important role in fight against diseases like COVID-19. In the case of an outbreak, the robotic technology can play a crucial role in not just assisting the patients but also keeping the doctor and healthcare staff safe. Robots are all around us, making significant contributions to making our lives easier and more efficient.

Now, robotics and Internet of Things (IoT) technologies are being applied to help organizations battle the COVID-19 pandemic, by sanitizing the different places such as shopping malls, movie theatres, train stations, schools and grocery stores. Automation updates with AI for better business model and consumer experience.

Size and shape of the Robot can be modified according to the requirement. We can also mount the web camera in our robot, which can be used in various field such as spying, or for military uses.

A wireless camera is mounted on the robot vehicle for spying and surveillance purpose even in night time by using infrared lighting. Future modifications can be made to perform different tasks with precise control such as:

- A Robot Mounted with camera.
- A headset, with a full-color display

- A mission control centre
- Multiple sensor can be added in the robot.

REFERENCES

- 1) https://ifr.org/img/office/Industrial_Robots_2016_Chapter_1_2.pdf
- 2) <https://cs.stanford.edu/people/eroberts/courses/soco/projects/199899/robotics/history.html>
- 3) <https://www.robotshop.com/media/files/PDF/timeline.pdf>
- 4) <http://cyberneticzoo.com/early-industrial-robots/1958-62-versatran-industrial-robot-harryjohnson-veljko-milenkovic/>
- 6) <https://www.robots.com/articles/kuka-robot-history>
- 7) <https://www.google.com/search?q=PUMA&oq=PUMA&aqs=chrome..69i57l1847j0j8&sourceid=chrome&ie=UTF-8>
- 8) <https://www.britannica.com/technology/robot-technology>
- 9) <http://www.roboticsbible.com/anatomy-of-industrial-robots.html>
- 10) <https://www.robots.com/faq/what-are-the-main-types-of-robots>
- 11) <https://www.genesis-systems.com/blog/robots-automotive-manufacturing-top-6applications>
- 12) http://www.ijirset.com/upload/2016/february/56_10_PLC.pdf
- 13) <https://pdfs.semanticscholar.org/703c/e09d12cfe0c70dc33686b4bc7884fc06d7b6.pdf>
- 14) <http://www.ijstr.org/final-print/aug2013/Design-And-Manufacturing-Of-Low-CostPneumaticPick-And-Place-Robot.pdf>
- 15) https://www.researchgate.net/publication/331855439_Cobot_programming_for_collaborative_industrial_tasks_An_overview

Influence of Core-Face Plates and Cell geometry on the strength of Sandwich Honeycomb Structure

T Rama Krishna¹, T J Prasanna Kumar², B Teja³

*^{1, 2} Assistant professor, Department of Mechanical Engineering, PVPSIT, Vijayawada, India-520007. mail Id: tjpk.mech@gmail.com
³ UG student, Department of Mechanical Engineering, PVPSIT, Vijayawada, India-520007*

ABSTRACT Honeycomb sandwich structures are widely used in aerospace and space structures due to unique characteristics like high strength to weight ratio and High stiffness. Honeycomb sandwich structure consists of honeycomb core made of either metal or thin paper like materials. Core is sandwiched with metallic or composite face sheets. Core gives high compressive strength whereas face sheet gives shear strength. Generally, Honeycomb core is made up of aluminum, fiberglass and advanced composite materials. For nearly same weight honeycomb sandwich structure can give up to 30 time's higher stiffness than metallic sheets. Modelling of Honeycomb sandwich structures with actual cell configuration is difficult and time consuming. Hence sandwich structure is generally modelled as equivalent homogeneous structure. Honeycomb core sandwich structures are especially becoming more prevalent in the field of civil engineering where the need of high structural strength and low weight is necessary. So there is a constant increase in demand for lightweight, high strength and stiffness properties and cost economical materials. These factors are directly or indirectly related to the mechanical properties of honeycomb sandwich structures. Usually, the optimal geometrical structure at with higher mechanical properties is the main motive in this material research. Often there is a correlation to design and manufacture sandwich panels with much precise geometry and optimal properties. Normally the existing sandwich panels are designed and manufactured with the higher factor of safety in the thickness and mechanical properties required for the particular application. This may be a reasonable solution. But when we consider for complex geometry and larger design, it's not so comparatively easy, dimensional restrictions, and material consumption and production cost will be the major issues. The present work is to experimentally analyses the mechanical properties of the sandwich panels and find the optimal geometrical thickness of the sandwich with high strength and stiffness properties.

Keywords: Sandwich, Honeycomb, Aluminum, Balsa, face sheet, strength, stiffness

I. INTRODUCTION

1.1. Sandwich Structure with Balsa Core and Aluminum Face Sheets

1.1.1. Sandwich Structures:

Sandwich structured composites are a particular class of composite materials which have become very popular due to high specific strength and bending stiffness. The low density of these materials makes them especially suitable for use in aeronautical, space and marine applications. Sandwich panels are composite structural elements, consisting of two thin and stiff face sheets and separated by a thick layer of light weight and a stiff material called core. The faces and the core material are bonded together with an adhesive to facilitate the load transfer mechanisms between the components. This particular layered composition creates a structural element with both high bending stiffness, bending

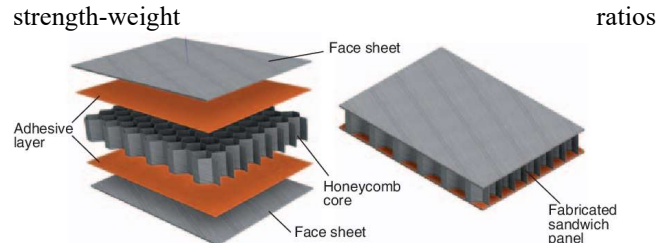


Fig 1.1. Construction of honeycomb core sandwich panel

The construction of honeycomb core sandwich structures is shown in Fig 1.1. The first layer is the face sheet. This layer is the primary layer of the sandwich structure called as skin and the skin is bonded with the honeycomb core by the adhesive layer. The adhesive may be thermoset plastic or thermoplastic. By splitting a solid laminate down the middle and separating the two halves with a core material the result is a sandwich panel. The new panel weighs little more than the laminate, but its flexural stiffness and strength are much greater by doubling the thickness of the core material the difference is, even more, striking.

1.1.2. Face sheet materials:

The primary functions of the face sheets are to provide the required bending and in-plane shear stiffness alongside to carry the axial, bending, and in-plane shear loading. There are various materials that can be used as face sheets. Some examples are given below:

- Aluminium
- Steel/Stainless Steel
- Carbon/Epoxy
- Fiberglass/Epoxy
- Aramid/Epoxy
- Plywood
- Galvanized iron



Fig.1.2. Aluminium sheet

1.1.3. Core materials

The main part of the sandwich structure is core material, in most of the sandwich structure in plain loads and bending loads are carried by the face sheets and the core carries the transverse shear load. The core materials are generally divided into four types solid, honeycomb, web core and truss core. The inner skin is laminated onto the top of the core material effectively sealing it. Sandwich core laminates of this type are used to stiffen various composite applications

such as boat hulls, automobile hoods, moulds, and aircraft panels. By increasing the core thickness, you can increase the stiffness of the sandwich without substantially increasing weight and cost.

The most common types of core materials are Honeycomb, Vinyl Sheet Foam, End Grain Balsa, Polyurethane Foam

Honeycomb:

Honeycomb is a series of cells, nested together to form panels similar in appearance to the cross-sectional slice of a beehive as shown in Fig 1.3. In its expanded form, honeycomb is 90-99 % open space. Honeycomb is fire retardant, flexible, lightweight, and has good impact resistance. It offers the best strength to weight ratio of the core materials. Honeycomb is used primarily for structural applications in the aerospace industry. Parts which require minimum weight often employ Honeycomb sandwich cores.

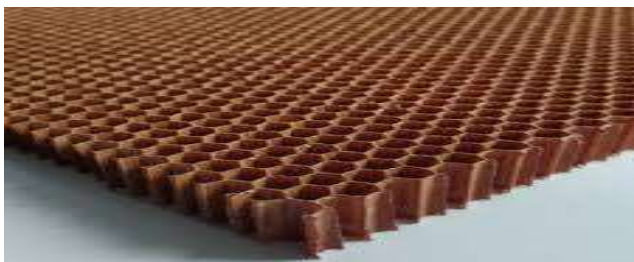


Fig: 1.3. Honeycomb core



Fig 1.4. Vinyl Sheet Foam

Vinyl Sheet Foam

Vinyl sheet foam is shown in Fig 1.4. is one of the most versatile core materials on the market. It is a rigid, closed cell material that resists hydrocarbons, alkalis, dilute acids, methyl alcohol, sea water, gasoline, diesel oil, and it is self-extinguishing. It has been used extensively in aircraft and performance automotive structures, but it can be applied anywhere that high properties and easy handling are needed. Vinyl foam can be thermoformed in an oven or with a heat gun while applying gentle pressure. For ultimate peel strength, use a perforation roller to increase the surface area of the foam. The peel strength will increase an additional 15-20% after perforation.

End Grain Balsa

End-grain balsa is the most widely used core material. It is both a relatively high strength core and less expensive than vinyl or honeycomb. It achieves its high compression strength because on a microscopic level it has a honeycomb type of structure yet is quite dense. It is easy to cut and bevel and is available in 29x49 inch sheets. The individual small blocks of end grain balsa are bonded to a light scrim fabric which makes the sheet quite flexible as shown in Fig 1.5.



Fig1.5. End Grain Balsas



Fig 1.6. Polyurethane Foam

Polyurethane Foam

This sheet foam shown in Fig 1.6 is a rigid, closed cell material with excellent thermal insulation and flotation properties. This core has been at the heart of the marine industry for decades and is fairly inexpensive when a lower property cored laminate is needed. It is compatible with both polyester and epoxy resin systems.

1.1.4. ADHESIVES

Adhesives' (or the bounding layer) role in the sandwich structures is to keep the faces and the core co-operating with each other. The adhesive between the faces and the core must be able to transfer the shear forces between the faces and the core. The adhesive must be able to carry shear and tensile stresses. It is hard to specify the demands on the joints; a simple rule is that the adhesive should be able to take up the same shear stress as the core [13]. Some adhesive types, such as phenolic, give out vapor during curing reaction. The vapor can cause several problems if this vapor is trapped; it may cause little or no bond in some areas, the pressure may damage the core material or it may cause the core to move to an undesired position. Common adhesives in current use are:

1. Nitrile Phenolic
2. Vinyl Phenolic
3. Epoxy
4. Urethane
5. Polyimide
6. Polyamide

1.2. Major Application Areas of Honeycomb Sandwich Structures

1.2.1 Aerospace Applications

In Commercial Aerospace, As Radome: Specialized glass Prepregs. Flexcore honeycomb, For Landing Gear Doors and Leg Fairings: Glass/carbon Prepregs, honeycomb and Redux bonded assembly. Special process honeycomb, For Galley, Wardrobes, Toilets: Fabricated Fibrelam panels, As Partitions: Fibrelam panel materials, For Wing to Body Fairing: Carbon/glass/aramid Prepregs. Honeycombs. Redux adhesive. In Wing Assembly: (Trailing Edge Shroud Box)

Carbon/glass Prepregs. Nomex honeycomb. Redux bonded assembly, Flying Control Surfaces - Ailerons, Spoilers, Vanes, and Flaps: Glass/carbon/aramid Prepregs. Honeycomb. Redux adhesive, Passenger Flooring: Fibrelam panels, Engine Nacelles and Thrust Reversers: Carbon/glass Prepregs. Nomex honeycomb. Special process parts, Cargo Flooring: Fibrelam panels

1.2.2. Space & Defence Applications

In Fuselage Panel Sections: Epoxy carbon Prepregs. Non-metallic honeycomb core and Redux adhesives, In Flying Control Surfaces: Epoxy carbon and glass Prepregs. Honeycomb core material and Redux adhesives, In Satellites, Solar Panels : Epoxy carbon prepregs, aluminum honeycomb, film adhesive , Reflectors Antennae : Epoxy/aramid prepreg, cyanate carbon prepreg, aramid/aluminum honeycomb, Satellite Structures : Carbon prepreg, aluminum honeycomb, film adhesive, As Energy Absorbers, Driver Protection: Pre-crushed metallic honeycomb assemblies and carbon prepregs, As Ceiling panels: Molded with prepreg or honeycomb sandwich, As Upper Deck and Lower Flooring: Molded with prepreg or honeycomb sandwich, As Connecting Archway: Molded component with honeycomb and prepreg materials, As External Doors: Bonded honeycomb sandwich construction.

The sandwich structures are used not only directly in automobiles but also indirectly as crash test barriers due to their high shock absorbance capacity such as A-Pillar, Front Side Rail, Other Side Rail, Front Header, B-Pillar, Rear Header, Rearmost Pillar, Upper Roof

II. METHOD OF APPROACH

2.1 Experimental Analysis

2.1.1. Tensile test carried out on sandwich honeycomb structure specimen with the following specifications:

Most sandwich constructions are loaded in tension perpendicular to the panel, which is through the thickness direction of the foam. This limits the number of tests standards to be used since the core thickness is typical. Tensile strength is calculated at maximum load, which normally occurs when the specimen breaks. Displacement, or strain, is measured by direct measurement on the specimen with an extensometer. Tensile modulus is calculated from the steepest part of the load-displacement curve in the elastic region.

SPECIMEN SPECIFICATIONS:

- Length - 160 mm
- Width - 12.5 mm
- Thickness - 0.60 mm



Fig.2.1. Tensile test specimen

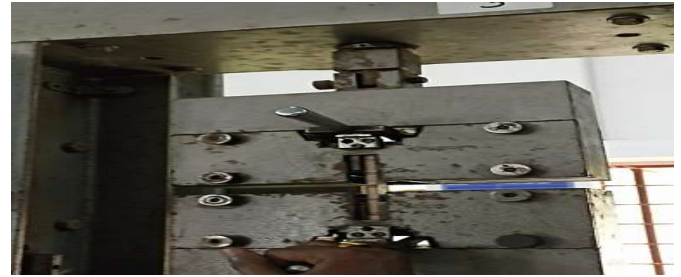


Fig.2.2. Specimen in the tensile test machine

2.1.2. Bending test carried out on sandwich honeycomb structure specimen with the following specifications:

Bending-testing sandwich panels, when testing solid laminates the support and loading cylinders usually have relatively small diameters. As discussed above, sandwich specimens are typically supported and loaded as wide flat plates. While the ASTM standards permit to use the steel cylinders, it is noted that there is a greater risk of local specimen crushing because of the more concentrated loading induced by a cylinder.

SPECIMEN SPECIFICATIONS:

- Length – 100 mm
- Width – 25 mm
- Thickness - 0.60 mm



Fig.2.3. Bending test specimens



Fig.2.4. Specimen in bending test machine



Fig.2.5. Specimen after bending test

2.1.3 Impact test carried out on sandwich honeycomb structure specimen with the following specifications:

Impact energy is described as the amount of energy required to fracture a material subject to a shock loading. Charpy,

Izod, and drop weight impact tests are generally used to get impact energy of a material. For a free-falling impactor case, the basic principle is that initial potential energy will be converted to maximum kinetic energy when the impactor collides into a target. This kinetic energy is converted to impact energy when a material is fractured. If there is an initial kinetic energy, impact energy is defined as potential energy and kinetic energy, ignoring friction and sound energies produced by the impact. In the following impact simulations to compare impact energies, the potential energy of the impactor is ignored due to the very short distance between the impactor and the target structure. Therefore, the impact energy is assumed to be calculated only from the kinetic energy.

SPECIMEN SPECIFICATIONS:

- Length - 63.5 mm
- Width - 12.7 mm
- Thickness - 0.60 mm



Fig.2.6 (a). Impact Test Machine, (b). Specimen fixed on testing machine



Fig.2.7. Specimens after impact test

III. Results and Discussions

3.1 Experimental Observations from Tensile, Bending and Impact Tests:

Table: 3.1 Tensile test results for G.I sheet

S. NO.	Cell height (mm)	Maximum load (KN)
1	5	3.3
2	6	4.03
3	7	5.5
4	8	5.2

Table: 3.2 Tensile test results for aluminium sheet

S. NO.	Cell height (mm)	Maximum load (KN)
1	5	2.4
2	6	2.9
3	7	2.0
4	8	1.7

Table: 3.3 bending test results for G.I sheet

S. NO.	Cell height (mm)	Maximum load (KN)
1	5	3.3
2	6	5.75
3	7	6.5
4	8	5.0

Table: 3.4 bending test results for aluminium sheet

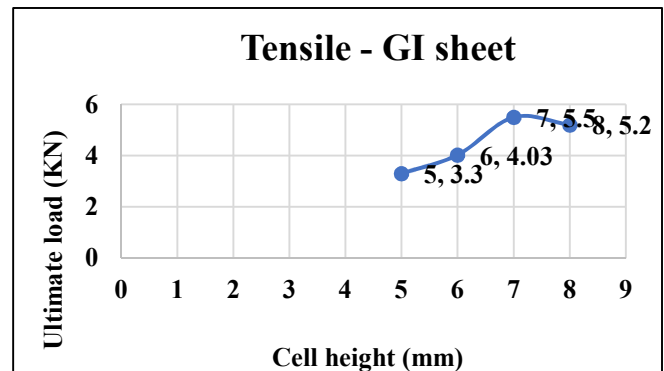
S. NO.	Cell height (mm)	Maximum load (KN)
1	5	3.3
2	6	2.6
3	7	2.46
4	8	2

Table: 3.5 Impact test results for G.I sheet

S. NO.	Cell height (mm)	Impact load (Joules)
1	5	6
2	6	6
3	7	6
4	8	6

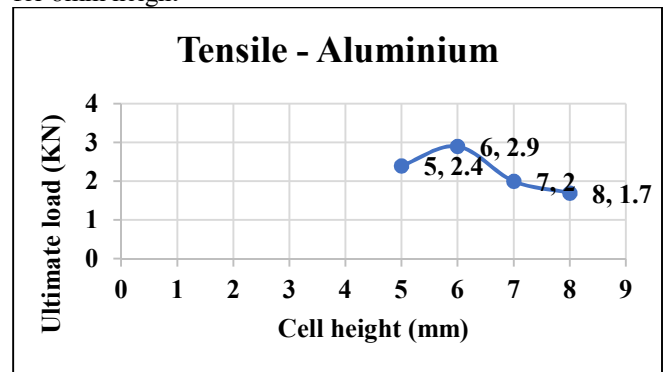
Table: 3.6 Impact test results for aluminium sheet

S. NO.	Cell height (mm)	Impact load (Joules)
1	5	4
2	6	4
3	7	6
4	8	6



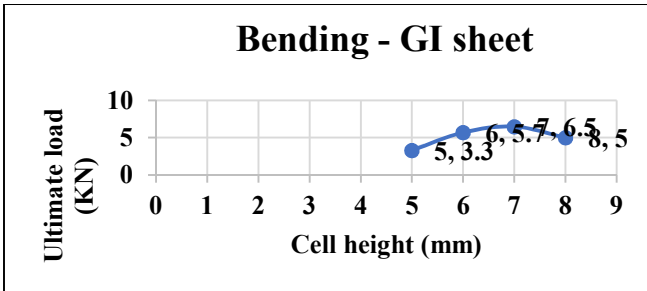
Plot: 3.1 Variation of Ultimate Load With Respect To Cell Height for GI Sheet

In the graph we observe that the ultimate load goes on increasing up to 7mm height of cell, but the load decreases for 8mm height



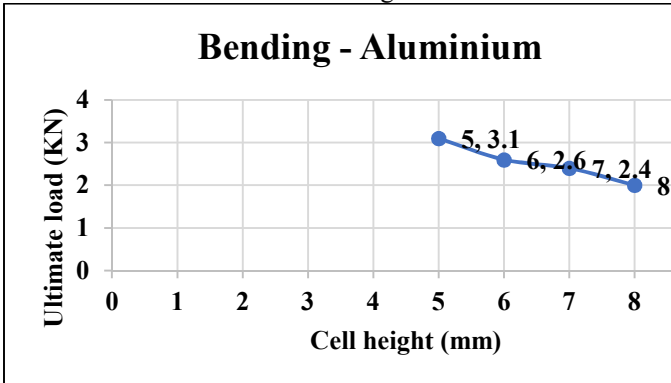
Plot: 3.2 Variation of Ultimate Load With Respect to Cell Height for Aluminium Sheet

The above graph shows that the load increases up to 6 mm height of the cell but the load decreases for the 7 mm and 8 mm height of the cell.



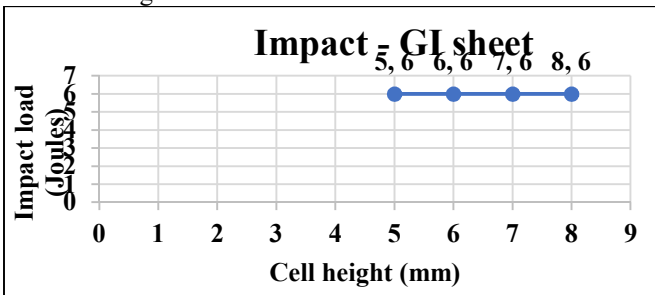
Plot: 3.3 Variation of Ultimate Load With Respect to Cell Height for GI Sheet

From the graph the ultimate load increases up to 7 mm height of cell but it decreases for 8mm height



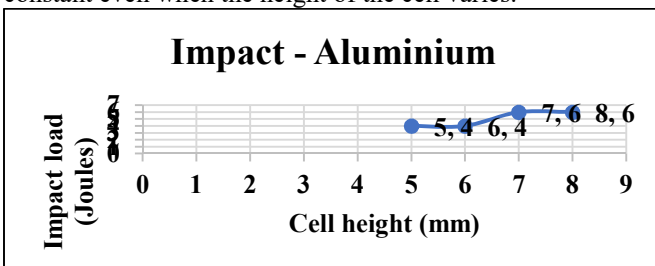
Plot: 3.4 Variation of Ultimate Load With Respect to Cell Height for Aluminium Sheet

The above graph shows that the load decreases gradually when the height of the cell increases.



Plot: 3.5 Variation of Ultimate Load With Respect to Cell Height for GI Sheet

From the above graph it shows that the impact load is constant even when the height of the cell varies.

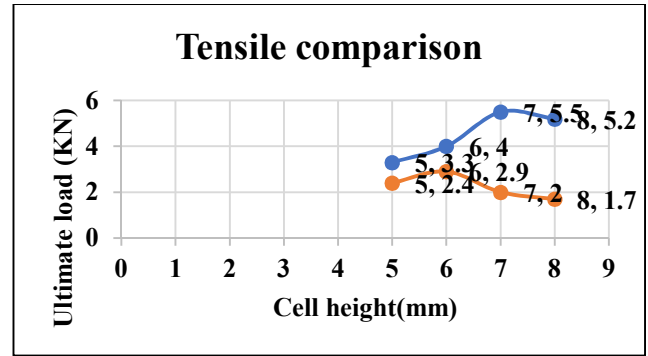


Plot: 3.6 Variation of Ultimate Load With Respect to Cell Height for Aluminium Sheet

It is observe that the Impact load is constant for 5 and 6mm height of cell but the load increases and is constant for 7 and 8mm height of cell.

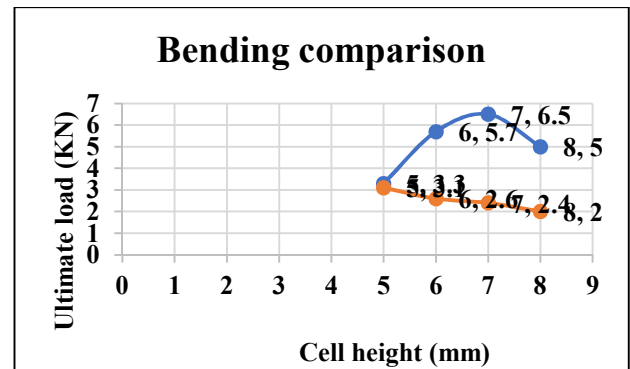
4. Comparative Plots between Various Test Carried Out on Specimens Made of Al/Balsa/Al and GI/Balsa/GI Sandwich Honeycomb Structures

3.1 Comparison between Tensile Plots:



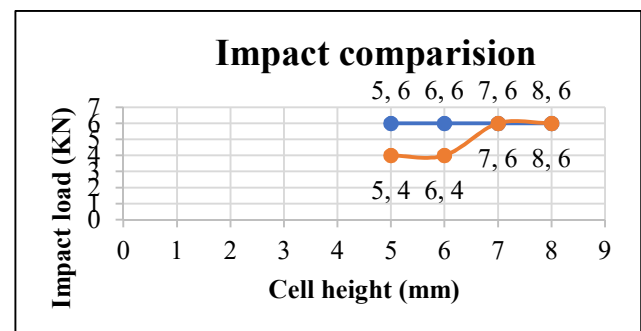
The above graph shows that the variation of Ultimate load in tensile test for different face plate materials.

3.2 Comparison between Bending Plots:



It shows that the variation of ultimate load in bending test for different types of face plate materials.

3.3 Comparison between Impact test plots:



The above graph shows that the variation of impact loads for GI material and Aluminium material.

CONCLUSIONS

From the experimentation analysis carried out on various testing's for specimen modelled using sandwich honeycomb structure with Aluminium/Balsa wood/ Aluminium and Galvanized Iron/ Balsa wood/Galvanized Iron face plates and core structures respectively; the following conclusions have been made:

1. When tensile test carried out on specimen made of GI as faceplates and Balsa wood as core structure the ultimate tensile strength increases as cell height of the core increases from (5/6/7) mm. 7 mm core cell height is observed as optimum, later the strength decreases with increases in height. Maximum load for specimen rupture is noted as 5.5 KN whereas for specimen made of Al as face plates and Balsa wood as core structure, the maximum load for specimen rupture is noted as 2.9 KN. Hence it is observed that

GI/Balsa/GI sandwich structure attains more tensile strength than Al/Balsa/Al sandwich structure.

2. When bending test carried out on specimen made of GI as faceplates and Balsa wood as core structure the ultimate bending strength increases as cell height of the core increases from (5/6/7) mm. 7 mm core cell height is observed as optimum, later the strength decreases with increases in height. Maximum load for specimen rupture is noted as 6.5 KN whereas for specimen made of Al as face plates and Balsa wood as core structure, the maximum load for specimen rupture is noted as 3.3 KN. Hence it is observed that GI/Balsa/GI sandwich structure attains more bending strength than Al/Balsa/Al sandwich structure.

3. When impact test carried out on specimen made of GI as faceplates and Balsa wood as core structure the ultimate impact strength is constant as cell height of the core increases from (5/6/7/8) mm. Maximum load for specimen rupture is noted as 6J whereas for specimen made of Al as face plates and Balsa wood as core structure, the maximum load for specimen rupture is noted as 6J for 7 and 8mm cell height, and 4J for 5 and 6mm cell height. Hence it is observed that GI/Balsa/GI sandwich structure attains more impact strength than Al/Balsa/Al sandwich structure.

REFERENCES

- [1] Shubham Upreti, Vishal K. Singh, Susheel K. Kamal, Arpit Jain, Anurag Dixit ; (2019) "Modelling and analysis of honeycomb sandwich structure using finite element method" *Materials Today: Proceedings* (ELSEVIER)
- [2] Shanyouming Sun, Dan Liu, Yinglong Sheng, Shangsheng Feng, Hongbin Zhu, Tian Jian Lu (2021) "Out-of-plane compression of a novel hybrid corrugated core sandwich panel" *Composite Structures* (ELSEVIER)
- [3] M Kamel, A F Nemnem and M Kassem (2020) "Experimental modal testing of a honeycomb sandwich plate" *IOP Conference Series: Materials Science and Engineering*(973)
- [4] Clément Audibert, Anne-Sophie Andréani, Éric Lainé, Jean-Claude Grandidier(2019) "Discrete modelling of low velocity impact on Nomex® honeycomb sandwich structures with CFRP skins" *Composite Structures* (ELSEVIER)
- [5] Meifeng He, Wenbin Hu (2008) "A study on composite honeycomb sandwich panel structure" *Materials and Design* vol.29
- [6] Qiancheng Zhang, Xiaohu Yang, Peng Li, Guoyou Huang (2015) "Bioinspired engineering of honeycomb structure Using nature to inspire human innovation" *Progress in Materials Science* vol.74
- [7] Junhua Zhang, Xiufang Zhu, Xiaodong Yang, Wei Zhang (2019) "Transient Nonlinear Responses of an Auxetic Honeycomb Sandwich Plate under Impact Loads" *International Journal of Impact Engineering*.
- [8] Mahammad Muzeeb Baig, Suresh Arjula (2019) "Bending Analysis of Honeycomb Sandwich Panels with Different combinations of Materials for Core and Face Plates" *Journal of engineering sciences* Vol 10, Issue 12.
- [9] Recep Gunes, Kemal Arslan, M Kemal Apalak and JN Reddy (2017) "Ballistic performance of honeycomb sandwich structures reinforced by functionally graded faceplates" *Journal of Sandwich Structures and Materials*.
- [10] K.Kantha Rao, K. Jayathirtha Rao (2012) "Thermostructural Analysis Of Honeycomb Sandwich Panels" *International Journal Ofengineering Science & Advanced Technology* Volume-2, Issue-5.
- [11] Shubham V. Rupani, Shivang S. Jani, G.D.Acharya (2017) "Design, Modelling and Manufacturing aspects of Honeycomb Sandwich Structures: A Review" *International Journal of Scientific Development and Research (IJS DR)* Vol- 2, Issue 4
- [12] Ondrej Flasar, Vaclav Triska, and Milan Junas (2017) "Experimental study of impact properties of aluminium honeycomb sandwich structure" *MATEC Web of Conferences* (133)
- [13] Zhi-jia Zhang, Bin Han, Qian-cheng Zhang, Feng Jin (2017) "Free vibration analysis of sandwich beams with honeycomb-corrugation hybrid cores" *Composite Structures* (ELSEVIER)
- [14] S P Zaoutsos (2017) "Mechanical behavior of aluminium honeycomb sandwich structures under extreme low temperature conditions" *IOP Conf. Series: Materials Science and Engineering*.
- [15] Mohsin Abdullah AL-Shammari & Muhannad AL-Waily (2018) "Analytical Investigation of Buckling Behavior of Honeycombs Sandwich Combined Plate Structure" *International Journal of Mechanical and Production Engineering Research and Development (IJMPERD)* Vol. 8, Issue 4,
- [16] Anil Kumar¹, Arindam Kumar Chanda, Surjit Angra(2021) "Numerical Modelling of a Composite Sandwich Structure Having Non Metallic Honeycomb Core" *EVERGREEN Joint Journal of Novel Carbon Resource Sciences & Green Asia Strategy*, Vol. 08, Issue 04, pp759-767.

DESIGN AND FABRICATION OF 3D PRINTED SWIVELLING VISE

N.Vijaya Sekhar¹, V.Yuvaraj², B.Vinod³

*Assistant professor, Narasaraopeta College of engineering, Narasaraopet, Andhra Pradesh, India
Student, Narasaraopeta College of engineering, Narasaraopet, Andhra Pradesh, India*

ABSTRACT: Swiveling vise is modification of regular bench vise, in regular bench vise the work piece can held only at standard position and the bench vise also does not have the feature of rotating, but in swiveling vise we can rotate the work piece. Now a days Prototyping or model making is one of the important steps to finalize a product design. Traditional 3D printing is commonly referred to as layered manufacturing or solid free form fabrication. It is used for the physical modelling of a new product design directly from computer aided design (CAD) data without the use of any special tooling or significant process engineering. This rapid procedure reduces the lead time required to produce a prototype of a product by eliminating much or all of the process engineering time and tooling requirements. It helps in conceptualization of a design. Designing a rigid, flexible, cost effective and highly durable vise is need of today's era. Safety should also be taken into consideration while designing the vise. This project is related to design and manufacturing of Swiveling vise by 3D printing process. Swiveling vise is designed in CATIA software and manufactured by using ULTIMAKER machine. Time taken to print swiveling vise is 74 hours 45 minutes and material consumed is 360 grams.

I. INTRODUCTION

Additive Manufacturing is the formalized term for what used to be called Rapid Prototyping and what is popularly called 3D Printing. The term Rapid Prototyping (or RP) is used in a variety of industries to describe a process for rapidly creating a system or part representation before final release or commercialization. In other words, the emphasis is on creating something quickly, and that the output is a prototype or basis model from which further models and eventually the final product will be derived. Management consultants and software engineers both also use the term Rapid Prototyping to describe a process of developing business and software solutions in a piecewise fashion that allows clients and other stakeholders to test ideas and provide feedback during the development process. In a product development context, the term Rapid Prototyping was used widely to describe technologies which created physical prototypes directly from digital model data. This text is about these latter technologies, first developed for prototyping but now used for many more purposes.

HISTORY OF 3D PRINTING TECHNOLOGY

In 1983 Charles W. Hull (Chuck Hull) invented stereolithography or 3D printing that year he created the first-ever 3D printed part. Hull coined the term stereolithography in his August 8, 1984 patent application for "Apparatus for production of three-dimensional objects by stereolithography" U.S. patent US4575330 A was granted on March 11, 1986. Hull defined stereolithography as a method and apparatus for making solid objects by successively printing thin layers of the ultraviolet curable material one on top of the other. It became widely used in Rapid prototyping and direct manufacturing.

Throughout the 1990's and early 2000's a host of new technologies continued to be introduced, still focused wholly on industrial applications and while they were still largely processes for prototyping applications, R&D was also being conducted by the more advanced technology providers for specific tooling, casting and direct manufacturing applications. This saw the emergence of new terminology, namely Rapid Tooling (RT), Rapid Casting and Rapid Manufacturing (RM) respectively.

During the mid-nineties the sector started to show signs of distinct diversification with two specific areas of emphasis that are much more clearly defined today. First, there was the high end of 3D printing, still very expensive systems, which were geared towards part production for high value, highly engineered, complex parts. This is still ongoing and growing but the results are only now really starting to become visible in production applications across the aerospace, automotive, medical and fine jewellery sectors, as years of R&D and qualification are now paying off.

3D PRINTING TECHNOLOGY NOWADAYS

The starting point for any 3D printing process is a 3D digital model, which can be created using a variety of 3D software programmers in industry this is 3D CAD, for Makers and Consumers there are simpler, more accessible programmers available or scanned with a 3D scanner.

Applications of 3-D printing Now a Days

- Automobiles • Jewelry • Spare & Replacements Parts • Aerospace • Glasses and Eyewear • Shoes • Proto type • Dentistry
- Surgery • Prosthetics • Construction

Working process of Fused Deposition Modelling

1. Heat the nozzle until it reaches the desired temperature. The filament will be fed to the extrusion head and then it will be melts in the nozzle.
2. The extrusion head can move in the X, Y and Z directions. The extrusion head extrudes melted material in very thin strands .The material is deposited layer-by-layer on the platform, and then will be cool and solid.
3. When one layer is finished, the build platform will move down (on some machines, the extrusion head moves up) and a new layer will be deposited. This process repeats until the part is completed.

Characteristics of Fused Deposition Modelling

1. Printer Parameters. 2. Warping 3. Layer Adhesion 4. Support Structure 5. Infill & Shell Thickness 6. Common FDM Materials 7. Post Processing 8. Benefits & Limitations of FDM

3D PRINTING MATERIALS

The materials available for 3D printing have come a long way since the early days of the technology. There is now a wide variety of different material types that are supplied in different states (powder, filament, pellets, granules, resin etc). Specific materials are now generally developed for specific platforms performing dedicated applications (an example would be the dental sector) with material properties that more precisely suit the application

However, there are now way too many proprietary materials from the many different 3D printer vendors to cover them all here. Instead, this article will look at the most popular types of material in a more generic way. And also a couple of materials that stand out.

ABS material's desired properties:

- Impact Resistance
- Structural Strength and Stiffness
- Chemical Resistance
- Excellent High and Low Temperature Performance
- Great Electrical Insulation Properties
- Easy to Paint and Glue

ABS plastic attains these physical attributes through the initial creation process. By polymerizing styrene and acrylonitrile in the presence of polybutadiene, chemical "chains" attract each other and bind together to make ABS stronger. This combination of materials and plastics provides ABS with superior hardness, gloss, toughness and resistance properties, greater than that of pure polystyrene

Advantages:

- Excellent impact, chemical and abrasion resistance
- Superior stiffness and strength
- Easily machined and thermoformed
- Easy to paint and glue
- Good dimensional stability
- Excellent electrical properties

ABS plastic is advantageous in a wide variety of industries; however, certain physical limitations restrict the materials use in certain products and applications.

Disadvantages:

- Weather ability (damaged by sunlight)
- Solvent Resistance
- Hazardous When Burned
- Limited Uses in Association with Food Industry
- Higher Price than Polystyrene or Polyethylene.

MODELLING OF A 3D PRINTED SWIVELLING VISE CATIA V5

CATIA stands for Computer Aided Three-Dimensional Interactive Application. It was developed by Dassault Systems, France. It is a complete re-engineered, next generation family of CAD/CAM/CAE software solution for PLM (Product Lifecycle Management). CATIA V5 delivers innovative technologies for maximum productivity and creativity. It allows the flexibility of using feature based design and parametric design

INDUSTRIES USING CATIA

- Automobile.
- Defence
- Ship building.
- Aerospace.

Companies like General Motors, TATA, Hyundai, Ford, Samsung, Ashok Leyland, Maruti, Honda, L & T, Wipro, IBM, Mahindra, Eicher etc. are using CATIA for designing purpose.

WORKBENCHES IN CATIA V5:

- Sketcher.
- Part Modelling.
- Assembly.
- Wire frame and surface design.
- Drafting. •

CURA SOFTWARE

CURA 3D

Cura is an open source slicing application for 3D printers. It was created by David Braam who was later employed by Ultimaker, a 3D printer manufacturing company, to maintain the software. Cura is available under LGPL license. Cura was initially released under the open source Affero General Public License version 3, but on 28 September 2017 the license was changed to v3. This change allowed for more integration with third-party CAD applications. Development is hosted on Ultimaker Cura is used by over one million users worldwide and handles 1.4 million print jobs per week. It is the preferred 3D printing software for Ultimaker 3D printers, but it can be used with other printers as well.

Z- SEAM ALIGNMENT CHOICES

There are four choices for the Z-Seam Alignment setting: Shortest, User Specified, Sharpest Corner and Random. Shortest is Cura's default value. When selected, the Cura slicer software instructs the printer to start printing a new layer from the endpoint of the previous layer. This often leads to a visible seam, so this choice should usually be avoided. User Specified lets you specify where exactly on the model surface you want the Z-Seam to appear. When selected, two more settings become available – Z-Seam X and Z-Seam Y. These Cura settings correspond to the X-Y coordinates of the Z-Seam. Sharpest Corner instructs the printer to start printing each layer from the sharpest corner on the model surface. A corner, by virtue of being sharp, can cover up a Z-Seam in many cases. However if your model does not have sharp corners, then this option is not too useful. Setting Z Seam Alignment to Random will start each layer at a random position. This will eliminate the seam completely, but will also lengthen the print time as the print head will require additional time to move to a new position between each layer

THREE STAGES OF 3D PRINTING

There are three basic stages to preparing files for 3D printing.

MODELING:

This is carried out in any 3D modelling application such as Tinker cad or Sketch Up, which are just two of many example applications. These applications have their own file format and these enable you to open, edit, save, and export those 3D printer files from the application.

3D FILE EXPORT:

Once you have created your model, it then needs to be exported as either an STL, OBJ, or 3MF file. These are the file formats that are recognized by Cura. They differ from the file formats that are native to the 3D modeling applications as they just hold the final geometry and not the individual

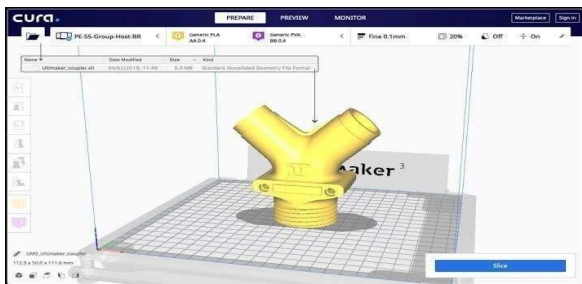
primitives and editable content. Still, you can change the size of the 3D model, but not the geometry.

SLICING FILE EXPORT:

The STL or OBJ file can then be imported into the Cura software where it is sliced and output as G-Code. This G-Code is just a text document (in essence) with a list of commands for the 3D printer to read and follow such as hot-end temperature, move to the left this much, right that much etc.

ADDING A 3D PRINTER MODEL TO CURA

Once you have set up Cura for your printer, it's time to import a model into the Cura software. To import a model, you can either click on the floating folder icon on the left or select File > Open File(s) from the top menu. Select an STL, OBJ, or 3MF file from your computer and Cura will import it.



Recommended print settings by software

GENERATE A G-CODE FILE WITH CURA:

The model is now print-ready and all you need to do is to export the file from Cura to either an SD card or send it directly to the printer. Cura will now handle everything converting the 3D STL or OBJ into the G-code file required by the printer.

Save the 3D print file: Click either Save to file, Save to SD or Send to Printer button on the bottom right of the window. Estimate of time for 3D print: Cura will give you a rough estimate on the length of time it will take for your printer to print the piece.

Start the 3D print: If tethered, sit back and wait for the printer to fire up and start printing. If you save to SD, then eject the SD card from your computer and transfer to your printer. Select print, select the file, and go.

THE Z-SEAM ALIGNMENT SETTING

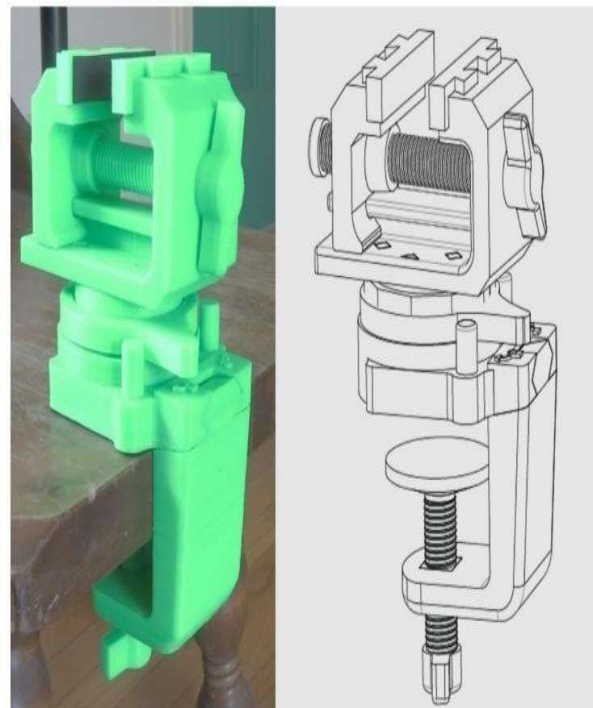
These can prevent a prominent Z-Seam on the 3D model surface. Sometimes, the printer will leave a mark on the model surface at the start of each layer. When these marks all align, the 3D model will have a prominent spurious line on its outer wall. This line is called a Z- Seam. The Z-Seam Alignment setting lets you choose where in the 3D model surface this line appears or lets you get rid of the line altogether.

COMPONENTS PRINTED USING 3D PRINTER



Total time taken for this print is 74 hours 45 minutes and the material consumed by the printer for this project is 360 grams. In cura software, arrangement of components were done in the effective way to reduce the time and material wastage.

ASSEMBLY OF A 3D PRINTING COMPONENTS



CONCLUSION

With the help of CATIA, design of Swivelling vise is developed including few sub- assemblies and fabrication of remaining parts components is completed by using 3D printing machine. 3D printing technology is the most advanced manufacturing process which is trending now a day which help in printing component at high speed and reduces production cost.

REFERENCES

- [1] M. Sabareeswaran, K. Padmanaban, and K. Sundararaman, "printing of 3D printed mechanical parts like swivelling vise by Design and fabrication using ulitmaker D.Kurniawan, "Recent Developments on Computer Aided Fixture Design: Case Based Reasoning Approaches fixture layout". International Journal of Machining and Machinability of Materials, Vol. 15 (2014)
- [2] H. Hashemi, A. Mohamed Shaharoun, S. ".Advances in Mechanical Engineering, Vol.2014 (2014) 15.
- [3] Jain Pranjai, KutheA. M., Feasibility Study of manufacturing using rapid prototyping: FDM Approach. MESIC 2013.
- [4] Dimension BST/SST 1200es 3D Printer user guide.

Modelling and Fabrication of Finger Flywheel Engine Using 3D Printing

Shaik Nagul Meeravali¹, B. Rambabu², M Venakta Sai Rajesh³

^{1,2} Assistant Professor, *Department of Mechanical Engineering, Narasaraopeta Engineering College, Narasaraopet, India*
³ IV Year Student, *Department of Mechanical Engineering, Narasaraopeta Engineering College, Narasaraopet, India*

Abstract— A flywheel is an energy storage device that is capable of storing kinetic energy in a spinning mass, and the energy stored is directly proportional to the square of the wheel speed and rotor’s mass moment of inertia. Flywheels continue to be used in all reciprocating engines and in all machines that require very high power for a small part of their working cycles. 3D Printing is a novel method of manufacturing parts directly from digital model by using layer by layer material build-up approach. II3D printing is called as desktop fabrication. It is process of prototyping where by a structure is synthesizes from a 3D model. 3D printing process is derived from inject desktop printer in which multiple deposit jets and the printing material layer by layer derived from the CAD 3D data. Generation of G-Codes and estimating time is done by using Cura Ultimate S5. Acrylonitrile Butadiene Styrene (ABS) material is used for fabrication. This project deals with the study of additive manufacturing, Cura software and Polymer, Acrylonitrile Butadiene Styrene (ABS) material is used as a 3D printing material. Finger Flywheel 3D printing time is 28 hours 5 minutes and volume of material consumed is 124.3 grams.

Keywords—Flywheel, 3D Printing, Infill Density and shape.

I. INTRODUCTION

In the 1980s, 3D printing techniques were considered suitable only for the production of functional or aesthetic prototypes, and a more appropriate term for it at the time was rapid prototyping. As of 2019, the precision, repeatability, and material range of 3D printing have increased to the point that some 3D printing processes are considered viable as an industrial- production technology. Product customization has been a challenge for manufacturers due to the high costs of producing custom-tailored products for end-users. On the other hand, AM is able to 3D print small quantities of customized products with relatively low costs. This is specifically useful in the biomedical field, whereby unique patient-customized products are typically required. Customized functional products are currently becoming the trend in 3D printing as predicted by Wohler’s Associates, who envisioned that about 50% of 3D printing will revolve around the manufacturing of commercial products in 2021.

Over the last 5 years, significant development has occurred in 3D printing. All over the world people are designing and printing new devices like human upper limbs, toys, mechanical parts and Mechanisms. Scientific papers have been published regarding research in 3D Printing Components and people are printing their own images and components and large communities have established for the global community. Digital fabrication technology, also referred to as 3D printing or additive manufacturing, creates physical objects from a geometrical representation by successive addition of materials. 3D printing technology is a fast-emerging technology. Nowadays, 3D Printing is widely used in the world. 3D printing technology increasingly used

for the mass customization, production of any types of open source designs in the field of agriculture, in healthcare, automotive industry, locomotive industry and aviation industries. 3D printing technology can print an object layer by layer deposition of material directly from a CAD model [1]. Numerous opportunities provided by this emerging technology as well as the risks and challenges related to it [2]. The basic concepts of flywheel energy storage systems are described in the first part of a two part paper. General equations for the charging and discharging characteristics of flywheel systems are developed and energy density formulas for flywheel rotors [3]. This is research paper on the 3D-printer in which reader introduced basic components operation materials used for making objects and applications. Now a day we are growing every day and every second. We adopt new technology with new invention and create new invention and create new things for enjoys life very easily. There are lots of new technologies we adopted in our daily life. In this technology one of them is 3D-printer. This is one of innovation on this we can make many objects [4]. The applications of 3D printing are ever increasing and it’s proving to be a very exciting technology to look out for. In this paper we seek to explore how it works and the current and future applications of 3D printing [5].

From the Literature review many researchers are studied on the Geneva Mechanism properties. This is an attempt of analyze the mechanism properties manufactured by the 3D Printer. In this work Ultimaker s5 Pro bundle 3D printer and the ABS material is used.

Table 01: ABS Material properties

Properties	Metric	units
Yield Strength	1.85e7 - 5.1e7	pa
Tensile strength	2.76e7 - 5.52e7	pa
Elongation	0.015 - 1	% strain
Hardness (Vickers)	5.49e7 - 1.5e8	pa
Fracture Toughness	1.19e6 - 4.29e6	Pa/m ^{0.5}
Young’s Modulus	1.19e9 - 2.9e9	pa
Max Service Temperature	61.9 - 76.9	°C
Specific Heat Capability	1.39e3 - 1.92e3	J/kg °C
Thermal Expansion Coefficient	8.46e-5 - 2.34e-4	strain/°C

II. EXPERIMENTAL WORK

Material used for this project work is ABS, short for Acrylonitrile Butadiene Styrene, is an oil-based plastic. It is a strong, sturdy material that businesses widely used for constructing things such as plastic car parts, musical instruments, and the ever-popular Lego building blocks. ABS has a high melting point, and can experience warping if cooled while printing. Because of this, ABS objects must be printed on a heated surface. ABS also requires ventilation when in use, as the fumes can be unpleasant. The material desired properties are:

- Impact resistance
- Structural strength & Stiffness
- Chemical Resistance
- Excellent high and low temperature performance.
- Great electrical insulation properties
- Easy to pain and glue

ABS plastic attains these physical attributes through the initial creation process. By polymerizing styrene and acrylonitrile in the presence of polybutadiene, chemical “chains” attract each other and bind together to make ABS stronger. This combination of materials and plastics provides ABS with superior hardness, gloss, toughness and resistance properties, greater than that of pure polystyrene.

III. METHODOLOGY

Step 1: Initially the components to be prepares are drawn using FUSION 360 software by using sketcher tool.

Step 2: Once the component is drawn as per required dimensions then the file is saved as STL file in FUSION 360software

Step 3: After completion of above procedure, STL file is loaded into cura software.

Step 4: Once the STL file is loaded, required parameters are set in cura software that is material used, layer thickness, infill density, infill shapes, fan speed, nozzle temperature, bed temperature, extrusion temperature, supports required all are selected and modified as per the requirement.

Step 5: After selection of the above parameters slicing is done by using slice option.

Step 6: Once slicing is done STL file is converted into G codes which is readable by 3D printer.

Step 7: G-code file is loaded in 3d printer by using pen drive and printing is done.

Step 8: Assembly of Printed Components.

For this research work ultimaker s5 pro bundle is used for to print the mechanism and analyzing the various print parameters. This is an attempt to establish the optimal properties for printing the objects using 3D printing technique. In this machine mainly three parts are present. Air Manager, Ultimaker s5 printer and material station. This printer has a variable nozzle diameters.

IV. MODELING OF GENEVA MECHANISM

Fusion 360 is an advanced software for shape designing, Styling, surface workflow, modeling and Simulation.

This Fusion 360 is used in many companies like Tata motors, Hyundai, Ford, Honda, Suzuki, Samsung etc...



Figure 1: Flywheel Rotating Wheel

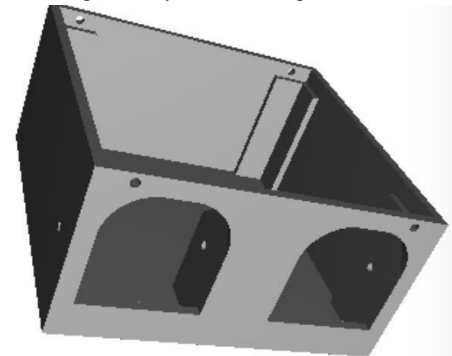


Figure 2: Base

The crank is designed in a Fusion 360 and saved in .prt file and converted this file to .stl file for preprocessing in ultimaker 3D printer software cura to analyze the properties like print time, material consumption and where supports are needed to print the components with accuracy. After completion of the preprocess convert this file into G codes and transferred to the printer.

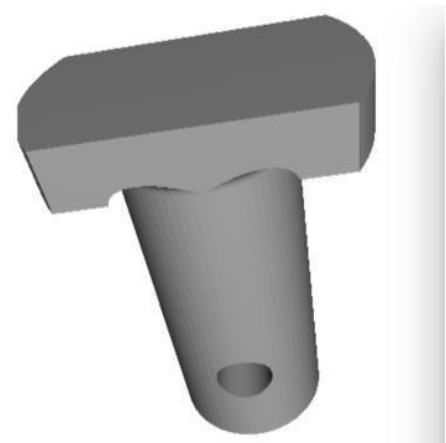


Figure 3: crank shaft

Same like above steps are followed and convert this body parts into G codes and saved in .ufp format after transferred into 3D printer.

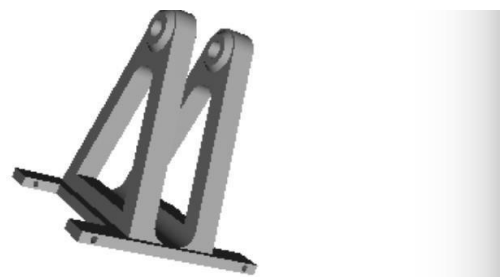


Figure 4: Supports

Same like above steps are followed and convert this body parts into G codes and saved in .ufp format after transferred into 3D printer.

V. PREPROCESSING THE COMPONENTS IN CURA

Cura 3D is slicing software for 3D printers. It takes a 3D model and slices it into layers to create a file known as

G-Code, which is the code that a 3D printer understands. Cura slices 3D models. It translates the 3D STL, OBJ or 3MF file into a format that the printer can understand. Fused filament fabrication (FFF) 3D printers print one layer upon another to build up the 3D object. Cura 3D takes the 3D model and works out how those layers are placed on the print bed and creates a set of instructions for the printer to follow layer on layer. Cura generates instructions for your 3D printer. They are called G-Code, a text document that ends with the file extension .ufp. Open the file and you'll actually be able to read through quite a bit of the code and understand what it's telling the printer to do. Here's a small snippet:

```
G0 F7200 X19.698 Y28.262 Z.36
G1 F1500 E0
G1 F1350 X22.467 Y26.175 E0.15654
G1 X23.338 Y25.568 E0.20447
G1 X24.246 Y25.027 E0.25218
```

Figure 5: sample G codes

As you become more adept at 3D printing you can go into this code and adjust fan speeds, layer heights and hot-end temperatures at different points. This can be handy when you need to troubleshoot some 3D print problems. As every printer has a different setup, print area, build plate and nozzle size, the slicing software needs to know these hardware details in a printer profile. Once it has the required details, you can then specify settings like layer height and thickness. Ultimaker Cura software will calculate the path the print head needs to take in order to print your model and produce a list of instructions for the printer. These instructions are saved in that G-Code file.

The G-Code be saved to an SD card or sent to the printer over wireless or cable depending on the printer directly from Ultimaker Cura software. There are many 3D slicing programs available on the market, Ultimaker Cura software is just one of many.

Ultimaker cura provides so many features and one is the infill patterns. Infill patterns affects model strength, material consumed and print time. By default, the Cura slicer prints a grid-shaped infill, printing in one diagonal direction per layer. This provides reasonable strength without eating up too much material. It is also one of the fastest patterns in terms of print time. Cura's standard infill pattern should be fine for most common applications. In some special applications though, the default pattern might not be best. In such cases, Cura offers a range of infill patterns to choose from.



Figure 6: Ultimaker Cura infill patterns

To change Cura infill pattern, enable the Infill Pattern hidden setting and it will appear under the Infill section. You have a choice of 13 different patterns. Some of the important patterns are

- Grid: A grid-shaped infill, with lines in both diagonal directions on each layer.
- Lines: Creates a grid-shaped infill, printing in one diagonal direction per layer.
- Triangles: Creates a triangular shaped infill pattern.

- Cubic: A 3D infill of tilted cubes.
- Tetrahedral: A 3D infill of pyramid shapes.
- Concentric: The infill prints from the outside towards the centre of the model. This way infill lines won't be visible through the walls of the print.
- Concentric 3D: The infill prints from the outside towards the centre of the model, with an incline over the entire print.
- Zig Zag: A grid-shaped infill, printing continuously in one diagonal direction.

Necessity of a control the speed of the machine. If machine speed increases it decreases the printing time but it decreases the quality of the print. For the above reason need to control the speed up to 40 to 60 mm/s gives good quality results.

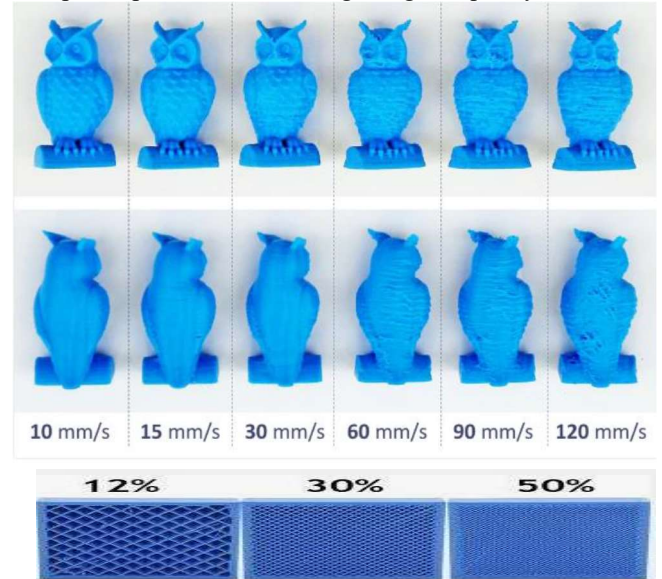


Figure 7: the quality effects by the print speed

	Fast	Normal	Fine	Extra Fine
Quality	0.2 mm	0.15mm	0.1 mm	0.06mm
Wall Thickness	1 mm	1.3 mm	1.3 mm	1.3 mm
Top Layer	6	8	12	20
Bottom Layer	6		12	20
Infill Density	20%	20%	20%	20%
Infill Pattern	Triangles	Triangles	Triangles	Triangles
Print Speed	60 mm/s	60 mm/s	55mm/s	50 mm/s
Estimated Time	9 hr 51 min	15 hr 5 min	1 day 2 hrs	1 day 19 hrs
Material Consumption	88g	95g	95g	95g
	Normal	Normal	Normal	Normal
Quality	0.16	0.17	0.18	0.19
Wall Thickness	1.3	1.3 mm	1.3 mm	1.3 mm
Top Layer	8	8	8	8
Bottom Layer	8	8	8	8
Infill Density	20%	20%	20%	20%
Infill Pattern	Triangles	Triangles	Triangles	Triangles
Print Speed	60 mm/s	60 mm/s	60 mm/s	60 mm/s
Estimated Time	14 hr 27 min	13hr 55min	12hr 54min	12hr 26min
Material Consumption	96g	97g	95g	95g

Table 2: Analyzed Ultimaker Cura parameters

After analysing the all parameters, normal with 0.15 mm layer thickness with supports and infill density 20% was selected. Because of it gives good strength and gives optimum values.

VI. PRINTING OF OBJECTS USING 3D PRINTER

Step 1: Once the modelling is done then STL file is loaded into cura software and slicing is done. After completion of the above process the G code file loaded in to 3D printer by using SD card or Pen drive.

Step 2: In order to print the component filament is loaded into the machine

Step 3: Initially bed is prepared by cleaning it with alcohol based solvent.

Step 4: After cleaning bed is preheated to 85°C temperature.

Step 5: Before printing the component, glue stick is applied because of avoiding the warping

Step 6: Once the above procedure is done select the G code file from the SD card by using select option.

Step 7: Each and every parameter setting is visible on the machine screen. Check for any errors and parameters and do modifications if necessary.

Step 8: After checking the parameters printing is started by giving start option in the machine.

Step 9: After completion of the component wait for at least 30 minutes in order to remove the component from the machine bed.

Step 10: Post processing is done to the components by removing of excess material and component supports.

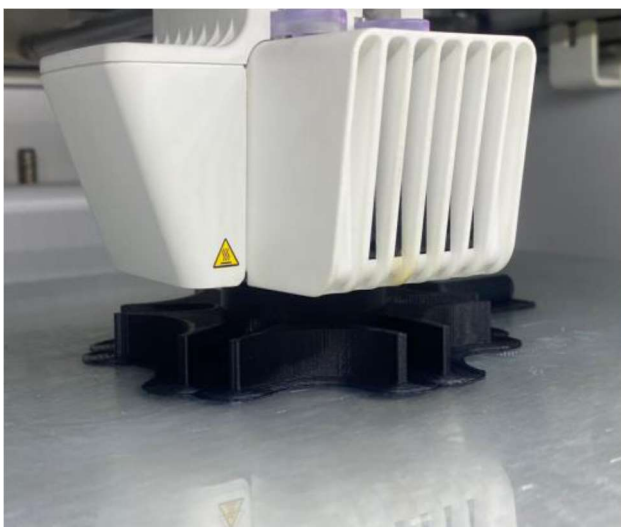


Figure 9: Components while 3D Printing



Figure 10: Finished Product

CONCLUSION

The world is forever changing with the help of 3D printing. The use of 3D printing for medicinal purposes today is beyond astonishing but what the future holds is unknown, however It is certain that additive layer manufacturing will be a large corporate in solving our problems. 3D printing really is limitless and only the surface has been scratched, there is still much more to be uncovered. As shown in throughout the web page. 3D printing bones is still new and continuously improving and adjusting but it has already enhanced the life of many patients around the world and more specifically in Australia. It is evident that the more funding and research put into 3D printing, the further 3D printing will take us. 3D is forever unpredictable. With the help of CATIA, design of actuator is developed including few sub-assemblies and fabrication of linear actuator components is completed by using 3D printing machine. 3D printing technology is the most advanced manufacturing process which is trending now a day which help in printing component at high speed and reduces production cost.

In this project work, design is done by using CATIA software and then file is transformed to STL format which is used for production of the component in 3D printing machine. CURA software is used for slicing of the component in CATIA and it also helps in adjustment of dimensions, solidification time, material selection, printing speed and printing time. In this project ABS material is used for the production of the component in 3D printing machine

REFERENCES

- [1] Goldfarb, V. Aspects of Gears and Reduction Drives Automated Design. Gearing and Transmissions, Izhevsk, Assoc. Engineers, 1991, No 1, 20-24 (in Russian).
- [2] Bulgarian Standard 17108 (CT, CIV 5744 - 86). Cylindrical Involute Gears with Externally Meshing. Standardization Strength Calculation of the Gear's Teeth, G-15,1999, Sofia, p. 124, (in Bulgarian)
- [3] Anchev, A., K. Minkov, D. Petrova, Kumchev. Synthesis and Analysis of Bevel Gears with Spiral Teeth, Publishing House of the Bulgarian Academy of Sciences, Sofia, 1980
- [4] Dudley, D., J. Springer's, D. Schroder, H. Yamashina. Gear Motor Handbook, Springer – Verlag, Berlin Heidelberg, 1995, 607

- [5] Review Paper on 3 Dimensional Printing Technology. Mr.Akash M. Patil, Miss. Neha U. Deshpande & Prof. V. A. Patil (2002)

Design and Fabrication of Prosthetic Hybrid Hand by using 3D Printing Technique

P. Pedda rajul¹, T. Ashok Kumar²

Department of Mechanical Engineering, Narasaraopeta Engineering College, Narasaraopet, India

Department of Mechanical Engineering, Narasaraopeta Engineering College, Narasaraopet, India

Abstract—Arising out of civil conflict, disease, birth defects, traumatic accidents, many people in developing countries lack hands or fingers. Prosthetic hands can help give these people a sense of agency and increased ability to perform everyday tasks. Unfortunately, many prostheses are prohibitively expensive and often require frequent maintenance and repair. Therefore, they are financially and geographically inaccessible to most people living in developing countries. A 3D printed, open-source hand is one possible solution owing to its low cost and potential for customization. However, the hand must be appropriate for the environmental conditions and lifestyles found in developing countries. To characterize the functionality of the 3D printed hand, a series of daily task and object tests were carried out. While the prosthesis was able to successfully complete a number of tasks, it had difficulty with those that required intricate movements and with heavy objects.

Keywords—3D Printer, Cura Software, Prosthetic Hand, Ultimaker Cura Machine, Abs Material

I. INTRODUCTION

The World Health Organization estimates that 650 million people worldwide have a physical disability. Of those, 80% live in low-income countries where only 1-2% of the disabled population have access to rehabilitative services [1]. In the developing world, a portion of the disabled population are upper limb amputees due to war, disease, or traumatic injury, or are otherwise missing hands or fingers due to birth defects. As the majority of jobs in these low-resource settings require manual labour, many upper limb amputees are at a severe economic disadvantage because they are unable to work. They may also face social stigma due to their condition.

Many of these people could benefit from a prosthetic device, which can aid in daily tasks and provide psychological benefits. However, most of the prosthetic hands on the market are too expensive, complex, and inaccessible for people living in low-resource settings. They typically cost hundreds or even thousands of dollars and often require maintenance and repair, which can be an unreasonable burden for persons living in rural areas who must invest significant time and money to travel to the nearest technician or health professional.

Prosthesis function should be easy and intuitive as well as appropriate for the daily tasks a user must perform. Size and weight are important physical characteristics that must be considered for both comfort and ease of use. The Prosthetic hybrid Hand is designed to help those with missing fingers or conditions such as Dupuytren's Contracture. It is wrist powered and requires that the wearer have enough palm to push against the device. It converts the rotation of the wrist into a linear sliding motion to activate the end gripper. When the wrist is bent down the slider pulls back, closing the hand. When the wrist is straightened the slider pushes forward and the hand opens. The Gripper heads are removable so that the user can

change them and reconfigure the device to suit their needs. I have created 2 Claw types, Tri-Claw (for picking up or catching objects) and Two-claw (for open shut grasping of objects). New claw or manipulator types can be attached with 2 screws on the hand piece. Within these you can add any flavor of gripper suitable. I have added a few grippers as extras for people to try. I recommend that you start with the Simple Claw to get the feel of the device before printing the other variants.

The multi-joint finger requires the user to tune the fingers. There is a sequence of loose and tight bolts that needs to be determined to allow

for the correct articulation of the fingers when opening and closing. I recommend first using simple or pincer claws first as the multi-joint fingers take some tuning to get working correctly.

One emerging technology that has potential for low resource settings is open-source, 3D printed prostheses. Many of these designs are body-powered, low-cost, customizable, and easy to assemble. 3D printing, or additive manufacturing, involves a three-dimensional computer model that is input into a 3D printer, which lays down layer upon layer of thermoplastic to build the model. The organization e-NABLE has created several open-source models of body-powered 3D printed prosthetic hands. This report examines e-NABLE's Raptor Reloaded, which is designed for users with a residual palm.

A few simple measurements of the residual limb are taken to determine the appropriate size and entered into the associated CAD file to scale the device, which customizes it for each specific user. The design can then be printed and assembled into a functioning prosthesis. When the prosthesis is worn, a simple forward bend of the wrist makes all of the digits bend and creates a basic grasping motion, and unbending the wrist lets the hand move back into the open position. Thermoplastics are relatively inexpensive materials, as are the additional components needed to assemble a Raptor Reloaded, so the low cost is a significant benefit of the prosthesis to the low-income user. The body-powered device, unlike an electrical device, leads to simpler maintenance; therefore, specialized repair skills and a reliable source of batteries or electricity are not necessary. The straightforward manufacturing process, easy fitting, and customizability of the device are also characteristics beneficial to the low-resource setting. We examine the performance characteristics of the 3D printed prosthesis for further validation of the appropriateness of this prosthesis for the developing world.

II. 3D PRINTING MATERIALS

The materials available for 3D printing have come a long way and its excessive weight. Similarly, participants using the since the early days of the technology. There is now a wide variety of different material types that are supplied in those same reasons. They also could not continue to hold the states (powder, filament, pellets, granules, resin etc). Specific objects for an extended period of time due to the challenge of materials are now generally developed for specific platforms keeping the wrist flexed as the participant lifted and carried the performing dedicated applications (an example would be the object. The prosthetic hand should be tested by holding different dental sector) with material properties that more precisely suit objects like water bottle, water glass, tiffin box which are our the application. However, there are now way too many basic needs and also its tested for cleaning the waste which are proprietary materials from the many different 3D print not touchable with our hand like removing waste bottles from vendors to cover them all here. Instead, this article will look at waste or from canals etc, the most popular types of material in a more generic way. And also, a couple of materials that stand out.

Table 1: Compares the main properties of PLA vs. ABS:

Properties	ABS	PLA
Tensile Strength	27 MPa	37 MPa
Elongation	3.5 - 50%	6%
Flexural Modulus	2.1 - 7.6 GPa	4 GPa
Density	1.0 - 1.4 g/cm ³	1.3 g/cm ³
Melting Point	N/A (amorphous)	173 °C
Biodegradable	No	Yes, under the correct conditions
Glass Transition Temperature	105 °C	60 °C

III. USABILITY TESTS

To provide maximum benefit to the user, the prosthesis must be user-friendly and functional in his or her daily life. Along with the tests above that are applicable for assessing the daily activities that can be completed by the prosthesis, the following tests in Table are used to determine the range of object shapes and sizes that the user is able to hold with the prosthetic hand.

Table 2:

Object to Hold	Smallest Hand Size			Largest Hand Size		
	Total No	Total Yes	Percent Yes	Total No	Total Yes	Percent Yes
Tennis Ball	3	17	85%	0	20	100%
Ping Pong Ball	0	20	100%	0	20	100%
Bottle of Water	4	16	80%	0	20	100%
Cup	0	20	100%	0	20	100%
Soup Can	20	0	0%	8	12	60%

The prosthetic hand was able to pick up several of the objects but only in a certain way. For all objects, the easiest and most applicable way was grabbing the object with the pointer finger and thumb. The contours prevented all fingers from wrapping around the objects, causing the object to drop. Using the largest hand size, all participants were able to lift the tennis ball, ping pong ball, bottle of water, and cup. Like the pouring motion mentioned before, the bottle of water and cup could not be turned over to simulate drinking because the prosthetic hand was unable to effectively grasp the objects without dropping them. When participants tried to simulate drinking, the weight of the liquid would cause the bottom of the bottle or cup to shift away from the hand's palm, causing the object to fall out of the participant's grasp. The soup can was able to be picked up by some participants using the large hand, but once it was picked up, it slipped out of the hand because of the cylindrical shape



Figure 1: Prosthetic Hybrid Hand



Figure 2: testing by holding a glass



Figure 3: Testing by Holding a water bottle



Figure 4: Testing by Holding a Tray Box

Table 2: observed readings for Prosthetic Hybrid Hand:

Properties	ABS	PLA
Tensile Strength	27 MPa	37 MPa
Elongation	3.5 - 50%	6%
Flexural Modulus	2.1 - 7.6 GPa	4 GPa
Density	1.0 - 1.4 g/cm ³	1.3 g/cm ³
Melting Point	N/A (amorphous)	173 °C
Biodegradable	No	Yes, under the correct conditions
Glass Transition Temperature	105 °C	60 °C

IV. ASSEMBLY PROCEDURE

- Slide the Tri-Claw-Slider into the Tri-Claw center hole.
- Rotate the Tri-Claw-Slider so that the shaft hole is in the orientation shown in the picture (this needs to align with the

Tendon on the final assembly – in the same orientation as the top claw bolt hole).

- Insert the pinch-finger into the slot aligning the Tri-Claw and slider. On the Pinch-Finger the SLOT must be aligned with the Slider and the Hole must be aligned with the Tri-Claw. SLOT-SLIDER & HOLE-TRI_CLAW. Insert bolts through both holes and cap with the nuts (Use the tool to tighten – Do not over tighten). Repeat for all Pinch-fingers. Align the Tri-Claw Rail holes with the Hand piece holes. Insert one bolt on each side (the Hand piece has threaded holes so there is no need for nuts). Align the Tendon Bolt hole with the Slider Bolt hole Insert a bolt and cap with a Nut.

CONCLUSION

The world is forever changing with the help of 3D printing. The use of 3D printing for medicinal purposes today is beyond astonishing but what the future holds is unknown, however it is certain that additive layer manufacturing will be a large corporate in solving our problems. 3D printing really is limitless and only the surface has been scratched, there is still much more to be uncovered. As shown in throughout the web page. 3D printing bones is still new and continuously improving and adjusting but it has already enhanced the life of many patients around the world and more specifically in Australia. It is evident that the more funding and research put into 3D printing, the further 3D printing will take us. 3D is forever unpredictable.

With the help of CATIA, design of prosthetic right hand is developed including few sub-assemblies and fabrication of right-hand components like fingers, pins palm is completed by using 3D printing machine. 3D printing technology is the most advanced manufacturing process which is trending now a day which help in printing component at high speed and reduces production cost.

In this project work, design is done by using CATIA software and then file is transformed to STL format which is used for production of the component in 3D printing machine. CURA software is used for slicing of the component produced in CATIA and it also helps in adjustment of dimensions, solidification time, material selection, printing speed and printing time. In this project ABS material is used for the production of the component in 3D printing machine. The total time was taken to print the prosthetic hand is 38 hours 3 minutes and components are successfully assembled.

REFERENCES

[1] Krebs, D. E., Edelstein, J. E., Thornby, M. A. Prosthetic management of children with limb deficiencies. *PHYS THER*, 71(12):920-934, December 1991.

[2] Ziegler-Graham, K., MacKenzie, E. J., Ephraim, P. L., Travison, T. G., Brookmeyer, R. Estimating the prevalence of limb loss in the United States: 2005 to 2050. *Archives of Physical Medicine and Rehabilitation*, 89(3):422 - 429, 2008. ISSN 0003-9993.

[3] United States Census Bureau. Resident population estimates of the United States.

[4] <http://www.census.gov/popest/data/national/totals/1990s/totals/nat-agesex.txt> accessed on 02/2014, 2001.

[5] United States Census Bureau. U.S. and world population clock <http://www.census.gov/popclock> accessed on 02/2014, 2013.

[6] Doshi, R. LeBlanc, M. The design and development of a gloveless endoskeletal prosthetic hand. *Journal of Rehabilitation Research and Development*, 35(4):388-395, October 1998.

[7] Zecca, M., Micera, S., PhD, Carrozza, M. C., Dario, P. Control of multifunctional prosthetic hands by processing the electromyographic signal. *Critical Reviews in Biomedical Engineering*, 30(4-6):27, 2002.

[8] Hu, P. X. B. Development of a Pediatric Prosthetic Hand with a Two-Degree-of-Freedom Thumb. PhD thesis, University of Toronto, 1997.

[9] Touch Bionics. The I-limb hand. <http://www.touchbionics.com/i-LIMB> accessed on 09/2011, 2011.

[10] Shida-Tokeshi, MA, J., Bagley, A., Molitor, F., Tomhave, W., Liberatore, J., Brasington, K., Mont petit, K. Predictors of continued prosthetic wear in children with upper extremity prostheses. *JPO Journal of Prosthetics & Orthotics*, 17(4):119-124, October 2005.

[11] Biddies, E. Ache, T. T. Upper limb prosthesis use and abandonment: A survey of the last 25 years. *Prosthetics and Orthotics International*, 31(3):236-257, 2007.

[12] Donovan-Hall, M., Yardley, L., Watts, R. Engagement in activities revealing the body and psychosocial adjustment in adults with a transtibial prosthesis. *Prosthetics and Orthotics International*, 26(1):15 - 22, 2002

[13] Barata, S.D.O. The alternative limb projects. <http://www.thealternativelimbproject.com/> accessed on 02/2015, 2015.

[14] Guo, G., Zhang, J., Gruver, W. A. Optimal design of a six-bar linkage with one degree of freedom for an anthropomorphic three-jointed finger mechanism. *Proceedings of the Institution of Mechanical Engineers, Part H: Journal of Engineering in Medicine*, 207(3):185 - 190, 1993.

[15] Asyali, M. H., Yilmaz, M., Tokmakc, M., Sedef, K., Aksebzec, B. H., Mittal, R. Design and implementation of a voice-controlled prosthetic hand. *Elektrik-Turkish Journal of Electrical Engineering and Computer Sciences*, 19(1):33, 2011.

Design and Fabrication of Geneva Mechanism Using 3D Printing

Shaik Nagul Meeravali, K Ravi Varma

Assistant Professor, Department of Mechanical Engineering, Narasaraopeta Engineering College, Narasaraopet, India
 IV Year Student, Department of Mechanical Engineering, Narasaraopeta Engineering College, Narasaraopet, India

Abstract—Geneva mechanism is used as a mechanism for transforming rotary motion into intermittent motion and is able to achieve a precise movement and its lock, which makes it usable in many areas, particularly in timing devices, measurement devices, feed mechanisms, positioning mechanisms, pick-up and transport machinery, textile machinery etc. from the literature review, many researchers on focuses on the kinematic study and acceleration jump of the Geneva mechanism. In this work, Design a Geneva Mechanism using 360 and analysis of mechanism with change in 3D printing properties like infill density, shapes. From the results it can be concluded that infill density of 20% and infill shape Cuboid gives an optimal time to producing Components in 3D Printer. The total time taken by the printer to print mechanism was 11 hours 9 minutes.

Keywords—Geneva Mechanism, 3D Printing, Fusion 360, Infill Density and shape.

I. INTRODUCTION

Over the last 5 years, significant development has occurred in 3D printing. All over the world people are designing and printing new devices like human upper limbs, toys, mechanical parts and Mechanisms. Scientific papers have been published regarding research in 3D Printing Components and people are printing their own images and components and large communities have established for the global community. 3D printing is the one of the additive manufacturing technique. A Geneva Mechanism were used to design and fabrication of belt drive to supply the material with in regular interval of time [1]. For both inner and outer Geneva mechanism, the kinematics coefficient of the Geneva mechanism is a stable if the groove number of the Geneva wheel is a constant. The elliptic crank using as the drive crank of the Geneva wheel is equal to the mechanism which has a variable length and speed along the elliptical moving crank. Therefore the kinematics coefficient of the Geneva mechanism is able to be changed. In this paper the analysis method of the combined Geneva mechanism is presented. The combined Geneva mechanism is put forward based upon the kinematics coefficients [2]. Kinematic study of a mechanism incorporating a Geneva wheel and a gear train to achieve intermittent motion. The goal of this mechanism is to eradicate the acceleration jump at the beginning and end of the Geneva wheel motion. An epitrochoidal path replace the circular path for the driving pin in a classical Geneva wheel drive. The epitrochoidal path is generate using a gear train and results in zero velocity, acceleration, and jerk at the beginning and end of the Geneva wheel motion. Presented a comparison of the position, velocity, acceleration, and jerk between the classical Geneva wheel mechanism and the proposed mechanism. Subsequently, the motion of the Geneva wheel is modified by introducing a non-circular gear

pair to alter the timing of the epitrochoidal path [3]. P Kali Sindhur designed a belt drive with the help of Geneva mechanism is used for giving feed and gives smooth operation and movement of the feed at required time interval. The feed from Geneva drive was cut by using slotted lever mechanism. It was designed using slider crank mechanism [4]. Han Jiguang Yu Kang, for both inner and outer Geneva mechanism, the kinematic coefficient of the Geneva mechanism is a stable if the groove number of the Geneva wheel is a constant. The elliptic crank using as the drive crank of the Geneva wheel is equal to the mechanism which has a variable length and speed along the elliptical moving crank [5]. David B Dooner studied kinematic study of a mechanism incorporating a Geneva wheel and a gear train to achieve intermittent motion. The goal of this mechanism is to eradicate the acceleration jump at the beginning and end of the Geneva wheel motion [6].

From the Literature review many researchers are studied on the Geneva Mechanism properties. This is an attempt of analyze the mechanism properties manufactured by the 3D Printer. In this work Ultimaker s5 Pro bundle 3D printer and the ABS material is used

Table 01: ABS Material properties

Properties	Metric	units
Yield Strength	1.85e7 - 5.1e7	pa
Tensile strength	2.76e7 - 5.52e7	pa
Elongation	0.015 - 1	% strain
Hardness (Vickers)	5.49e7 - 1.5e8	pa
Fracture Toughness	1.19e6 - 4.29e6	Pa·m ^{0.5}
Young's Modulus	1.19e9 - 2.9e9	pa
Max Service Temperature	61.9 - 76.9	°C
Specific Heat Capability	1.39e3 - 1.92e3	J/kg °C
Thermal Expansion Coefficient	8.46e-5 - 2.34e-4	strain/°C

II. EXPERIMENTAL WORK

Material used for this project work is ABS, short for Acrylonitrile Butadiene Styrene, is an oil-based plastic. It is a strong, sturdy material that businesses widely used for constructing things such as plastic car parts, musical instruments, and the ever-popular Lego building blocks. ABS has a high melting point, and can experience warping if cooled while printing. Because of this, ABS objects must be printed on a heated surface. ABS also requires ventilation

when in use, as the fumes can be unpleasant. The material desired properties are:

- Impact resistance
- Structural strength & Stiffness
- Chemical Resistance
- Excellent high and low temperature performance.
- Great electrical insulation properties
- Easy to pain and glue

ABS plastic attains these physical attributes through the initial creation process. By polymerizing styrene and acrylonitrile in the presence of polybutadiene, chemical “chains” attract each other and bind together to make ABS stronger. This combination of materials and plastics provides ABS with superior hardness, gloss, toughness and resistance properties, greater than that of pure polystyrene

III. METHODOLOGY

Step 1: Initially the components to be prepares are drawn using FUSION 360 software by using sketcher tool.

Step 2: Once the component is drawn as per required dimensions then the file is saved as STL file in FUSION 360software

Step 3: After completion of above procedure, STL file is loaded into cura software.

Step 4: Once the STL file is loaded, required parameters are set in cura software that is material used, layer thickness, infill density, infill shapes, fan speed, nozzle temperature, bed temperature, extrusion temperature, supports required all are selected and modified as per the requirement.

Step 5: After selection of the above parameters slicing is done by using slice option.

Step 6: Once slicing is done STL file is converted into G codes which is readable by 3D printer.

Step 7: G-code file is loaded in 3d printer by using pen drive and printing is done.

Step 8: Assembly of Printed Components.

For this research work ultimaker s5 pro bundle is used for to print the mechanism and analyzing the various print parameters. This is an attempt to establish the optimal properties for printing the objects using 3D printing technique. In this machine mainly three parts are present. Air Manager, Ultimaker s5 printer and material station. This printer has a variable nozzle diameters.

IV. MODELING OF GENEVA MECHANISM

Fusion 360 is an advanced software for shape designing, Styling, surface workflow, modeling and Simulation. This Fusion 360 is used in many companies like Tata motors, Hyundai, Ford, Honda, Suzuki, Samsung etc...

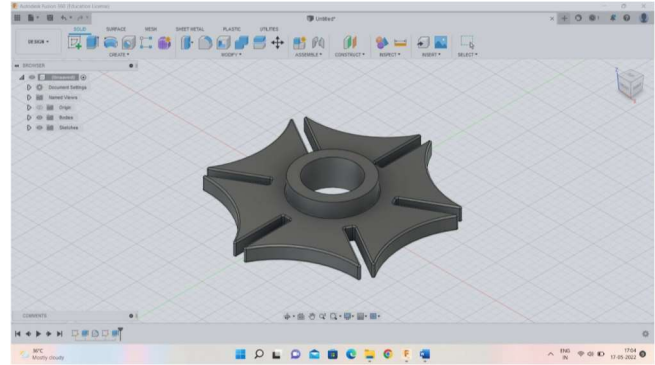


Figure 1: Design of Driven gear

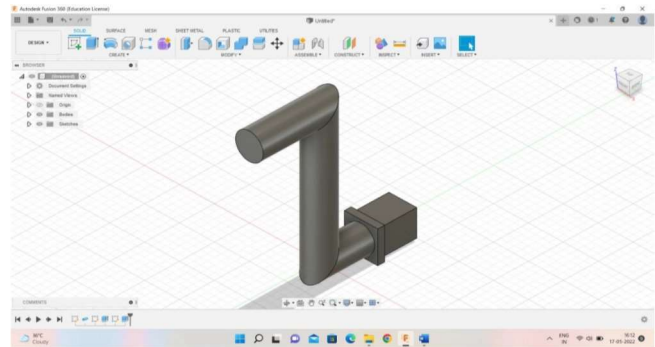


Figure 2: Design of Crank

The crank is designed in a Fusion 360 and saved in .prt file and converted this file to .stl file for preprocessing in ultimaker 3D printer software cura to analyze the properties like print time, material consumption and where supports are needed to print the components with accuracy. After completion of the preprocess convert this file into G codes and transferred to the printer.

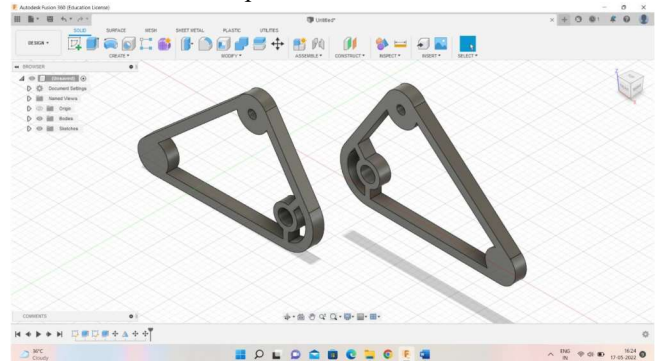


Figure 3: Design of Body Parts

Same like above steps are followed and convert this body parts into G codes and saved in .ufp format after transferred into 3D printer.

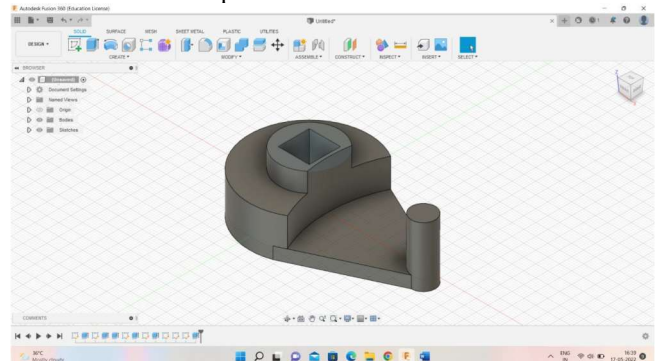


Figure 4: Design of a Drive Gear

Same like above steps are followed and convert this body parts into G codes and saved in .ufp format after transferred into 3D printer.

V. PREPROCESSING THE COMPONENTS IN CURA

Cura 3D is slicing software for 3D printers. It takes a 3D model and slices it into layers to create a file known as G-Code, which is the code that a 3D printer understands. Cura slices 3D models. It translates the 3D STL, OBJ or 3MF file into a format that the printer can understand. Fused filament fabrication (FFF) 3D printers print one layer upon another to build up the 3D object. Cura 3D takes the 3D model and works out how those layers are placed on the print bed and creates a set of instructions for the printer to follow layer on layer. Cura generates instructions for your 3D printer. They are called G-Code, a text document that ends with the file extension .ufp. Open the file and you'll actually be able to read through quite a bit of the code and understand what it's telling the printer to do. Here's a small snippet:

```
G0 F7200 X19.698 Y28.262 Z.36
G1 F1500 E0
G1 F1350 X22.467 Y26.175 E0.15654
G1 X23.338 Y25.568 E0.20447
G1 X24.246 Y25.027 E0.25218
```

Figure 5: sample G codes

As you become more adept at 3D printing you can go into this code and adjust fan speeds, layer heights and hot-end temperatures at different points. This can be handy when you need to troubleshoot some 3D print problems. As every printer has a different setup, print area, build plate and nozzle size, the slicing software needs to know these hardware details in a printer profile. Once it has the required details, you can then specify settings like layer height and thickness. Ultimaker Cura software will calculate the path the print head needs to take in order to print your model and produce a list of instructions for the printer. These instructions are saved in that G-Code file.

The G-Code be saved to an SD card or sent to the printer over wireless or cable depending on the printer directly from Ultimaker Cura software. There are many 3D slicing programs available on the market, Ultimaker Cura software is just one of many.

Ultimaker cura provides so many features and one is the infill patterns. Infill patterns affects model strength, material consumed and print time. By default, the Cura slicer prints a grid-shaped infill, printing in one diagonal direction per layer. This provides reasonable strength without eating up too much material. It is also one of the fastest patterns in terms of print time. Cura's standard infill pattern should be fine for most common applications. In some special applications though, the default pattern might not be best. In

such cases, Cura offers a range of infill patterns to choose from.

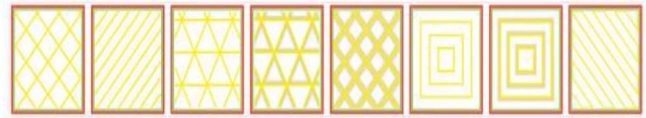


Figure 6: Ultimaker Cura infill patterns

To change Cura infill pattern, enable the Infill Pattern hidden setting and it will appear under the Infill section. You have a choice of 13 different patterns. Some of the important patterns are

- Grid: A grid-shaped infill, with lines in both diagonal directions on each layer.
- Lines: Creates a grid-shaped infill, printing in one diagonal direction per layer.
- Triangles: Creates a triangular shaped infill pattern.
- Cubic: A 3D infill of tilted cubes.
- Tetrahedral: A 3D infill of pyramid shapes.
- Concentric: The infill prints from the outside towards the centre of the model. This way infill lines won't be visible through the walls of the print.
- Concentric 3D: The infill prints from the outside towards the centre of the model, with an incline over the entire print.
- Zig Zag: A grid-shaped infill, printing continuously in one diagonal direction.

Necessity of a control the speed of the machine. If machine speed increases it decreases the printing time but it decreases the quality of the print. For the above reason need to control the speed up to 40 to 60 mm/s gives good quality results.

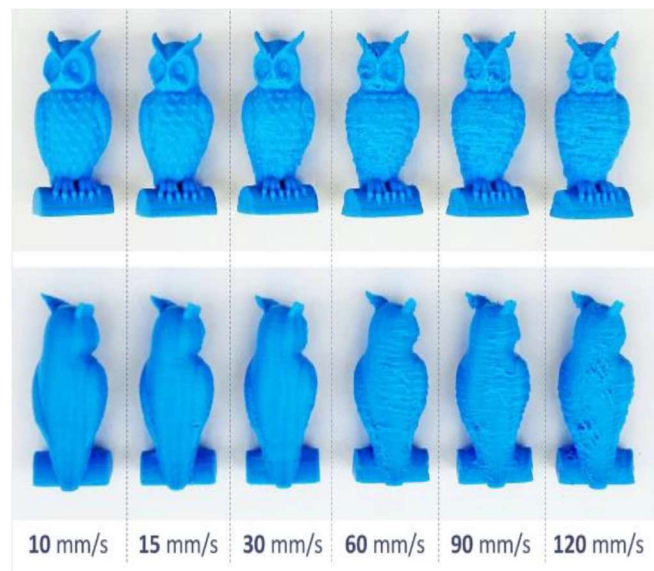


Figure 7: the quality effects by the print speed

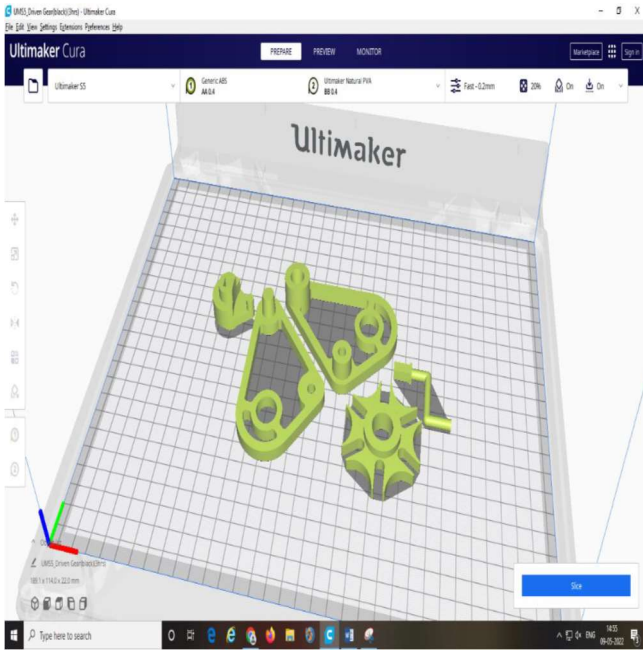


Figure 8: Geneva mechanism STL file in Cura

Table 2: Analyzed Ultimaker Cura parameters

	Fast	Normal	Fine	Extra Fine
Quality	0.2 mm	0.15mm	0.1 mm	0.06mm
Wall Thickness	1 mm	1.3 mm	1.3 mm	1.3 mm
Top Layer	6	8	12	20
Bottom Layer	6		12	20
Infill Density	20%	20%	20%	20%
Infill Pattern	Triangles	Triangles	Triangles	Triangles
Print Speed	60 mm/s	60 mm/s	55mm/s	50 mm/s
Estimated Time	9 hr 51 min	15 hr 5 min	1 day 2 hrs	1 day 19 hrs
Material Consumption	88g	95g	95g	95g
	Normal	Normal	Normal	Normal
Quality	0.16	0.17	0.18	0.19
Wall Thickness	1.3	1.3 mm	1.3 mm	1.3 mm
Top Layer	8	8	8	8
Bottom Layer	8	8	8	8
Infill Density	20%	20%	20%	20%
Infill Pattern	Triangles	Triangles	Triangles	Triangles
Print Speed	60 mm/s	60 mm/s	60 mm/s	60 mm/s
Estimated Time	14 hr 27 min	13hr 55min	12hr 54min	12hr 26min
Material Consumption	96g	97g	95g	95g

After analysing the all parameters, normal with 0.15 mm layer thickness with supports and infill density 20% was selected. Because of it gives good strength and gives optimum values.

VI. PRINTING OF OBJECTS USING 3D PRINTER

Step 1: Once the modelling is done then STL file is loaded into cura software and slicing is done. After completion of the above process the G code file loaded in to 3D printer by using SD card or Pen drive.

Step 2: In order to print the component filament is loaded into the machine

Step 3: Initially bed is prepared by cleaning it with alcohol based solvent.

Step 4: After cleaning bed is preheated to 85°C temperature.

Step 5: Before printing the component, glue stick is applied because of avoiding the warping

Step 6: Once the above procedure is done select the G code file from the SD card by using select option.

Step 7: Each and every parameter setting is visible on the machine screen. Check for any errors and parameters and do modifications if necessary.

Step 8: After checking the parameters printing is started by giving start option in the machine.

Step 9: After completion of the component wait for at least 30 minutes in order to remove the component from the machine bed.

Step 10: Post processing is done to the components by removing of excess material and component supports.

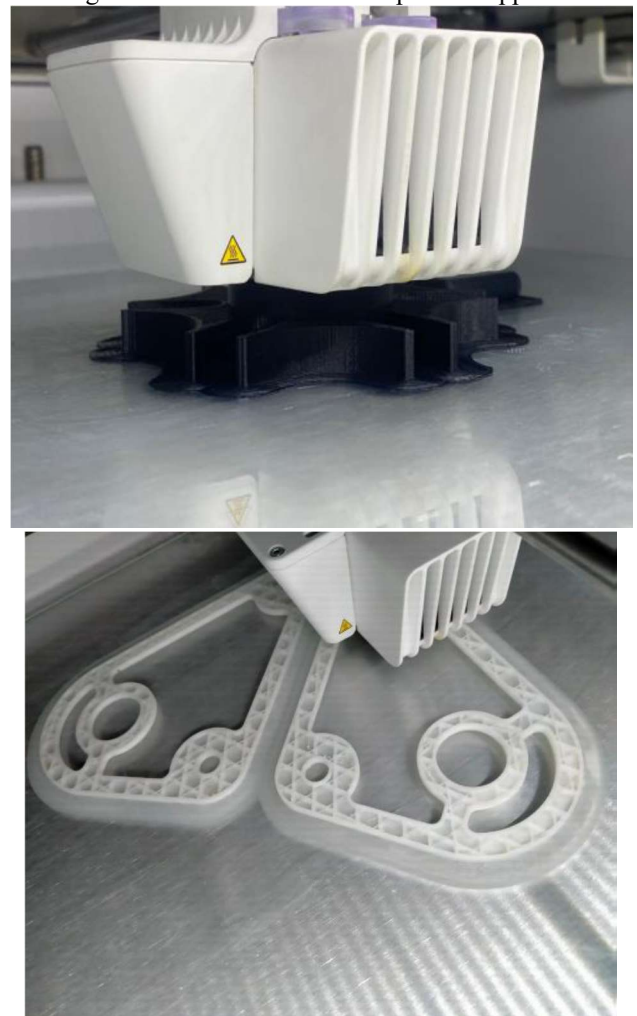


Figure 9: Components while 3D Printing



Figure 10: Finished Product

CONCLUSION

Geneva mechanism was studied and successfully realized with the help of additive technologies from ABS material. The model obtained is used as demonstration stands used in didactic applications. Of the one investigated material ABS have been proved to have properties and characteristics close to mechanical engineering applications and these results are demonstrated by graphs. ABS also has the advantage of lighter weight, which makes it suitable for applications where low mass is needed. It can also be concluded that the angular speed of the drive element is inversely proportional to the difference between the angular speeds of the Malta crosses. The latest years have brought spectacular developments to these new 3D printing technologies, which makes it possible today to find a wide variety of products manufactured by these new technologies and many in development, making them more and more competitive in wider areas. Applications of AM technologies in this area are gaining more and more importance. Challenges are related to finding and approving new materials that can be put into desirable physical forms with the most appropriate mechanical, increasing dimensional precision and surface quality, making parts from different materials with a functional gradient.

With the help of FUSION 360, design of Geneva Mechanism is developed including few sub-assemblies and fabrication gears and other components completed by using 3D printing machine. 3D printing technology is the most advanced manufacturing process which is trending now a day which help in printing component at high speed and reduces production cost.

In this project work, design is done using FUSION 360 software and then file is transformed to STL format which is used for production of the component in 3D printing machine. CURA software is used for slicing of the component produced in FUSION 360 and it also helps in adjustment of dimensions, solidification time, material selection, printing speed and printing time. In this project ABS material is used for the production of the component in 3D printing machine.

REFERENCES

[1] Bickford J.H, Geneva Mechanisms, Mechanism for Intermittent Motion, New York: Industrial Press Inc., 1972, p. 264.

[2] International Journal of Innovative Science, Engineering & Technology – [2015], Cutting Mechanism by Giving Feed through Geneva Mechanism, Vol, 2, Issue 4, pp: [1172-1175]

[3] Moraru E, Dontu O, Besnea D, Constantin V. Study and realization of prosthetic dental models by additive technologies ACME 2018, Iasi, Romania.

[4] Rizescu D, Miu S, Rizescu C.I, Complementary de mecatronică, Editura Printech, Bucuresti, 2000, p.7.

[5] Spanu A, Constantin V. The using of additive manufacturing for prototype production of moulds, International Journal of Mechatronics and Applied Mechanics, 2017(1), p.7-16

[6] P. Kali Sindhur , G. Sri Harsha “Cutting Mechanism by Giving Feed through Geneva Mechanism “4, April 2015.

DESIGN AND FABRICATION OF INDUSTRIAL TIME CONTROLLER

Dr. B. Venkata Siva¹, A Suneel Babu², G Anand Babu³, N Pedda Gopi⁴

¹Professor, Department of Mechanical Engineering, Narasaraopeta Engineering College, Narasaraopet, India

^{2,3}Student, Department of Mechanical Engineering, Narasaraopeta Engineering College, Narasaraopet, India

Abstract— Automation is basically the delegation of human control function to technical equipment for increasing productivity increasing quality reducing cost and increasing safety in working conditions. The industrial automation is very necessary for the manufacturing industry to survive in today’s globally competitive market. A programmable logic controller (PLC) is a digital computer used for automation of electromechanical processes, which is a type of computer family and they have commercial and industrial applications. The development of programmable logic controller (PLC) makes it possible to do the required changes to the program without changing the electrical circuit connections. In this project We have designed Industrial Time Controller in which using PLC create a time delay before or after the process which can be used for maintenance or machines integration or offset loss incurred due to machine failure.

A machine shop consists of 3 machines is considered, which is integrated with a PLC board. Here, every machine after completion of processing a delay time of 10 sec is given and tested successfully

Keywords— PLC, Industrial automation, Industrial Time Controller

I. INTRODUCTION

In today’s fast-moving, highly competitive industrial world, a company must be flexible, cost effective and efficient if it wishes to survive. In the process and manufacturing industries, this has resulted in a great demand for industrial control systems/ automation in order to streamline operations in terms of speed, reliability and product output. Automation plays an increasingly important role in the world economy and in daily experience. Automation is the use of control systems and information technologies to reduce the need for human work in the production of goods and services. In the scope of industrialization, automation is a step beyond mechanization. Whereas mechanization provided human operators with machinery to assist them with the muscular requirements of work, automation greatly decreases the need for human sensory and mental requirements as well.

Automation Control System - system that is able to control a process with minimal human assistance or without manual and have the ability to initiate, adjust, action show or measures the variables in the process and stop the process in order to obtain the desired output.

The main objective of Automation Control System used in the industry are:

1. To increase productivity
2. To improve quality of the product
3. Control production cost

Programmable logic controllers are small industrial computers. Their design uses modular components in a single device to automate customized control processes. They differ from most other computing devices, as they are intended for

and tolerant of severe conditions of factory settings such as dust, moisture, and extreme temperatures.

Industrial automation began long before PLCs. In the early 1900s until their invention, the only way to control machinery was through the use of complicated electro mechanical relay circuits. Each motor would need to be turned ON/OFF individually. This resulted in factories needing massive cabinets full of power relays. As industrial automation continued to grow, modern factories of the time needed dozens of motors with ON/OFF switches to control one machine, and all these relays had to be hardwired in a very specific way. PLCs were developed as a solution to have one solid control as an electronic replacement for hard-wired relay systems. The term PLC architecture refers to the design specification of the various PLC hardware and software components and the how they interact with one another to form the overall PLC system. The architecture of a PLC is based on the same principles of that used in standard computer architecture.

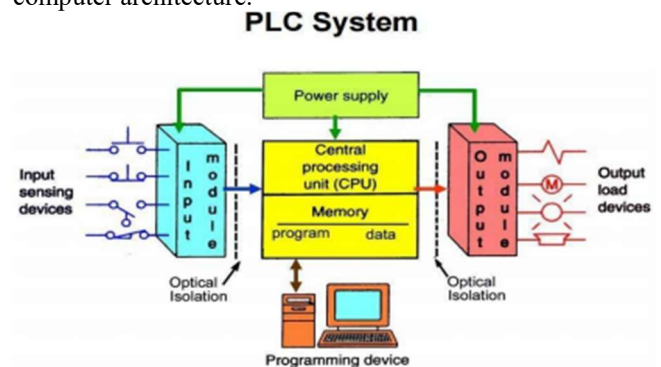


Figure 1: PLC Architecture

Automation is making the processes automatic. It is the method of using control systems to operate and control the working of industrial processing technology. Automation can be found in industries like steel factories, food and beverage industries scientific automation and so on. One of the control systems is Programmable Logic Controller, PLC, or programmable controller, using digital computer for automation of typically industrial electromechanical processes, such as control of machinery on factory assembly lines, amusement rides, or light fixtures. Process can be smooth and the process of refilling can reduce worker cost and operation cost. An investigation into the problem using simulation has been attempted here. Automatic segregation and directing of materials is controlled using PLCs. It makes use of limiting sensor, color sensor, proximity sensors for segregation and directing of the materials is controlled by using motor and the conveyer belt depending on the instructions specified in the ladder logic in PLC. In food packaging industry PLC is mainly used for automation

purpose which helps in reducing packaging time and increases the production rate as compared with manual system. The accurate weight of an object is measured through vibrator cell and load cell and has been explained in 2,3 The obtained electrical signal is passed to PLC machine which contains the ladder diagram of the circuit which holds the specified instructions of the system in internal storage. Hence the system is totally automated without manual intervention

II. COMPONENTS USED

A. *PLC Board:* A programmable logic controller (PLC) is an industrial computer control system that continuously monitors the state of input devices and makes decisions based upon a custom program to control the state of output devices

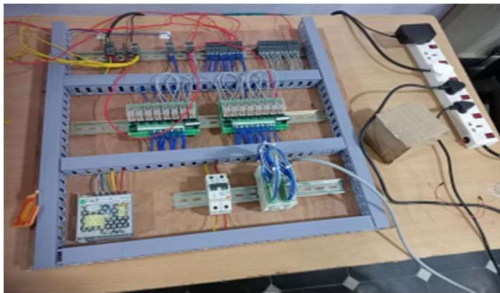


Figure 2: Programmable logic controller Board

B. *24V- DC motor:* A DC motor is any of a class of rotary electrical motors that converts direct current (DC) electrical energy into mechanical energy. The most common types rely on the forces produced by magnetic fields. Nearly all types of DC motors have some internal mechanism, either electromechanical or electronic, to periodically change the direction of current in part of the motor



Figure 3: 24V-DC Motor

C. *Indicator Lights:* Indicator lights are a type of illuminating device that is commonly used to signify that equipment is either receiving power or that there is some form of malfunction. We have all seen the red light come on when you power on a device



Figure 4 : Water Level Switch Sensor

- D. *RUBBER TAPES AND INSULATION TAPES:* Rubber tapes are designed for use in NHY6n splicing and terminating wires and cables with options rated up to 69Kv. Electrical tape is a safety tape for wires, used to cover and insulate a broad range of cables, wires and other materials that conduct electricity.
- E. *ELECTRICAL WIRES:* Stranded wire is composed of a number of small wires bundled or wrapped together to form a larger conductor. Stranded wire is more flexible than solid wire of the same total cross-sectional area.



Figure 5: Electrical wires

III. EXPERIMENTAL PROCEDURE:

We arrange the indicators separately on the top of the three Motors.

- Motor 1 will get start and the Motor associated Indicator light 1 will glow while the second and third Motors will be on off state.
- After the given delay time the Motor 2 will get start and its associated Indicator 2 light will glow and the First and third motors will be on off state.
- After the recurring delay time the third motor will get started and its associated Indicator light 3 will glow and the first and second motor will be on off state.
- This cycle runs until up to our requirement.

SCHEMATIC DIAGRAM:

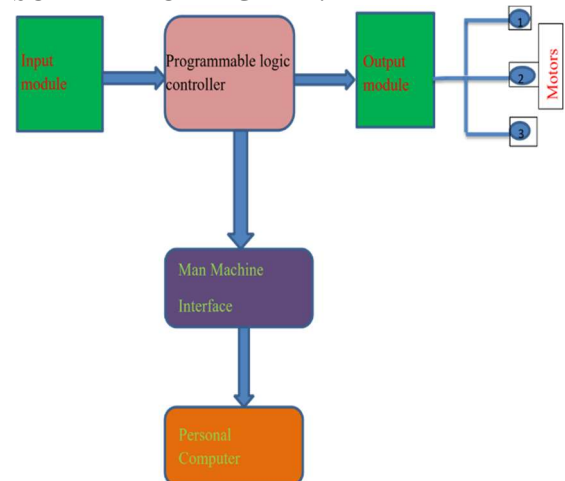


Figure 6: Schematic diagram

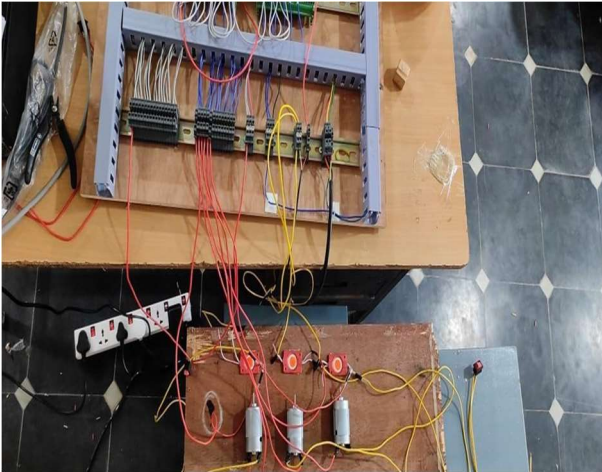


Figure 7: Industrial Time Controller connections

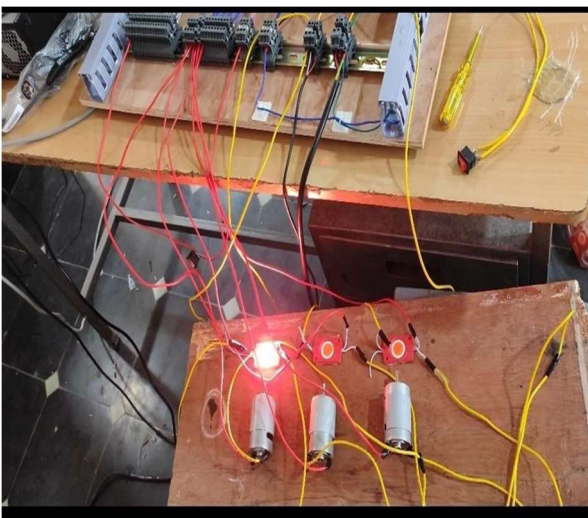


Figure 8: Industrial Time Controller execution

IV. EXPERIMENTAL RESULTS

a. Ladder diagram:

Ladder diagrams are specialized schematics commonly used to document industrial control logic systems. They are called “ladder” diagrams because they resemble a ladder, with two vertical rails (supply power) and as many “rungs” (horizontal lines) as there are control circuits to represent.

The four components of ladder diagrams are:

- ❖ Power Supply (rails).
- ❖ Input Devices (components).
- ❖ Output Devices (components).
- ❖ Conductors (rungs)

b. Ladder Logic:

Ladder logic was originally a written method to document the design and construction of relay racks as used in manufacturing and process control. Each device in the relay rack would be represented by a symbol on the ladder diagram with connections between those devices shown. In addition, other items external to the relay rack such as pumps, heaters, and so forth would also be shown on the ladder diagram. Ladder logic has evolved into a programming language that represents a program by a graphical diagram based on the

circuit diagrams of relay logic hardware. Ladder logic is used to develop software for programmable logic controllers (PLCs) used in industrial control applications. The name is based on the observation that programs in this language resemble ladders, with two vertical rails and a series of horizontal rungs between them.

c. ALGORITHM:

STEP-1

Switch ON

STEP-2

Motor 1 will get start and the motor associated indicator light will glow while the second and third motors will be on off state.

STEP-3

After the given delay time the Motor 2 will get start and it’s associated indicator light will glow and the First and third motors will be on off state.

STEP-4

After the recurring delay time the third motor will get started and It’s Associated indicator light will glow and the first and second motor will be on off state.

STEP-5

The same process will repeat again up to our requirement.

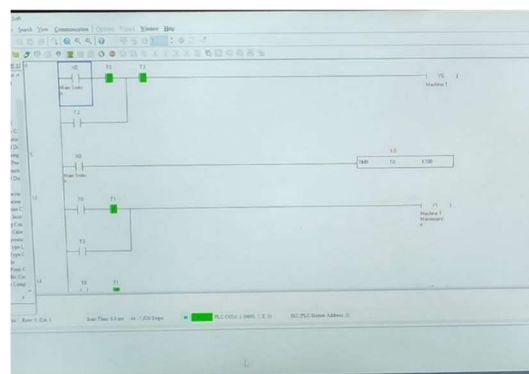
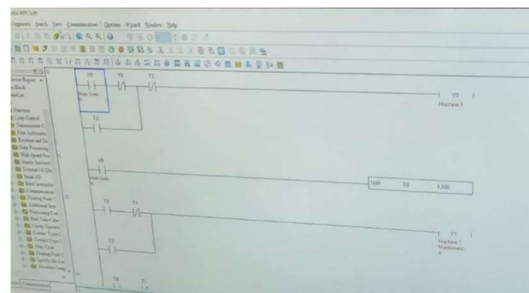


Figure 11:

Ladder diagram of Industrial Time Controller

Ladder diagram usually starts from top to bottom and left to right. Inputs placed at left side and outputs at right side of ladder diagram.

Here the,
Here the,

X0 is the main switch

The output Y0 terminal is given to connection motor-1

Y1 Terminal is given to connection of indicator light-1

Y2 Terminal is given to connection of in motor-2

Y3 Terminal is given to the connection of indicator light-2

Y4 terminal is given to the connection of motor-3
 Y5 terminal is given to the connection of indicator light-3

CONCLUSION

In industries, there would be a set of technologies that are implemented to get the desired performance or output, making the automation systems most essential for industries. In this paper we control time for multiple machines with specified Time. Through using PLC the machines are operated successfully. In this project, the Delta WPL Software has been successfully used for PLC. In this project, the monitoring and control system is designed for three phase induction motors. The system is successfully implemented and tested. After detailed experiment, it is observed that the proposed system is a feasible method for controlling of DC motor. A Machine shop consists of 3 machines is considered, which is integrated with a PLC board. Here, every machine after completion of processing a delay time of 10 sec is given and tested successfully

FUTURE SCOPE

This system is very useful in future since India is moving forward towards automated industrialization. With the help of this technology we can yield significant financial benefits which will prove beneficial for the industries as well as the country. More features can be added to this existing system which can be implemented in the future in Automation of Manufacturing at a time to improve productivity, use of sensors for the alarms which will indicate any mishandling in between the process, implementation of HMI(human-machine interface) and many more. This concept can be used in various industries like Aeronautical and Aerodynamic industries, food, medicine, chemical, and manufacturing industries

REFERENCES

[1] Albert W.L. Yao, C.H. Ku, —Developing a PC-based automated monitoring and control power systems, Electric Power Systems Research, Vol. 64, 2003, pp. 129-136.

[2] Limin Cai. —Temperature Measurement and Control System Based on Embedded Webl, Computer and Information Science, Vol.2.No.2, May.

[3] Darmstadt, —Conveyor systems, in Proceedings of the 1st IFAC-Conference on Mechatronic Systems. pp. 693-698, 2000.

[4] Shashank Lingappa M, V. Bongale, —PLC Controlled Low Cost Automatic Packing Machine, ISSN 2250-3234 Volume 4, Number 7 (2014), pp. 803-811

[5] Kevin Collins,—PLC Programming for Industrial Automation.

[6] Mohd Zulhelmi Bin Halim —The Temperature Control System using PLC.

[7].<http://ieeexplore.ieee.org/document/4603060/?reload=true>.

[8] Zhang P., Du Y., Habetler TG, Lu B., —A Survey of Condition Monitoring and Protection Methods for Medium-Voltage Induction Motors, IEEE Transactions On Industry Applications.

[9] Shwetahugar, BasavarajAmarapur —Protection of Induction Motor using MicrocontrollerIJETA5.Alberto Bellini, FiorenzoFilippetti, Carla Tasoni, And GerardAndre Capolino, —Advances in diagnostic techniques for induction motor, IEEE transaction on industrial electronics.

[10] Patrick A. Brady, —Application of AC motors with variable speed drive,IEEE. [11] Alberto Bellini, FiorenzoFilippetti, Carla Tasoni, And Gerard-Andre Capolino, —Advances in diagnostic techniques for induction motor, IEEE.

[11] A. R. Al-Ali, M. M. Negm, and M. Kassas, "A PLC based power factor controller for a 3-phase induction motor" in Proceedings of Conference Records IEEE Industry Applications.

Evaluation and Comparison of Mechanical Properties of 3D Printed PLA Material with Different Filling Patterns

N.Siva Nagaraju¹, K.John Babu²

¹ Ph.D Scholar, Department of Mechanical Engineering, Vellore Institute of Technology VIT-AP UNIVERSITY, India

² Asst.Professor, Department of Mechanical Engineering, Narasaraopeta Engineering College, Narasaraopet, India

Abstract— Now a Days, the 3D printing is the Novel and Emerging technology in all aspects, especially in the development of new product and Manufacturing. 3D printing is an Additive manufacturing technique, which produces the 3D objects directly from the CAD data base using a layer-by-layer technique. In present work, PLA (Poly Lactic Acid) has been selected as material for additive manufacturing due to its special characteristics. As per ASTM standards, specimens for tensile, fatigue and compression testing are prepared with different filling patterns, using CoLiDoX3045 printer. These specimens are characterized and the results are compared with respect to filling patterns.

I. INTRODUCTION

Polymers are made of long, repeating chains of molecules. polymers include a range of materials with a variety of properties, depending on the type of molecules being bonded and how they are bonded. Polymers touch almost every aspect of modern life. The term polymer is often used to describe plastics, which are synthetic polymers. However, natural polymers also exist. Polymers are giant molecules of high molecular weight, called macromolecules, which are build up by linking together of a large number of small molecules, called monomers. The reaction by which the monomers combine to form polymer is known as polymerization. The product is called polymer and the starting material is called monomer

CLASSIFICATION OF POLYMERS

Polymers cannot be classified under one category because of their complex structures, different behaviours, and vast applications. Therefore, we classify polymers based on the following considerations

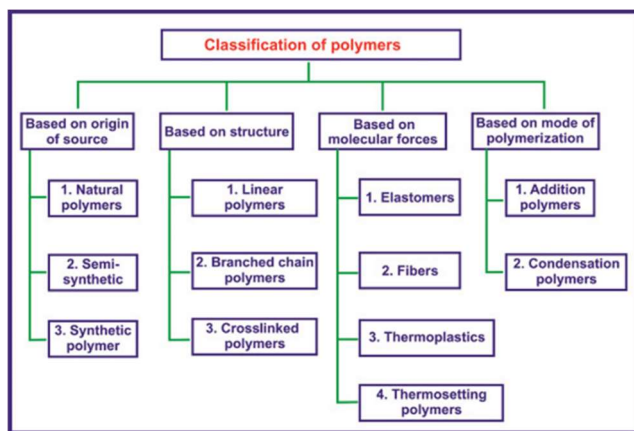


Fig. 1: Classification of polymers

CATIA V5 R21: CATIA is a multi-platform 3D software suite encompassing CAD, CAM as well as CAE Tools. Dassault is a French engineering giant active in the field of

aviation, 3D design, 3D digital mock-ups, and product lifecycle management (PLM) software. CATIA is a Rectilinear modelling tool that unites the 3D parametric features with 2D tools and also addresses every design-to-manufacturing process.

PRINT-RITE SOFTWARE: Print-Rite is a Software used for Slicing the CAD File and converting them into G-Codes, for printing the Components. It only takes the .STL File and selects the Printer for printing and starts slicing after giving the Infill Pattern and Infill Density to the software. Components can be printed directly by connecting to the computer or by saving the file in G-Code Format in SD-Card. The SD-card is connected to printer through a Pen drive. It also shows the Time for printing the Component. Print-Rite Software is used by CoLiDo Printers.

3D Printing Technology: 3D printing can create physical objects from a geometrical representation by successive addition of materials 3D printing technology has originated from the layer by layer fabrication technology of three-dimensional (3D) structures directly from computer-aided design (CAD) drawing. 3D printing technology is a truly innovative and has emerged as a versatile technology stage. It opens new opportunities and gives hope to many possibilities for companies looking to improve manufacturing efficiency. Conventional thermoplastics, ceramics, graphene-based materials, and metal are the materials that can be printed now by using 3D printing technology. 3D printing technology has the potential to revolutionize industries and change the production line. The adoption of 3D printing technology will increase the production speed while reducing costs. At the same time, the demand of the consumer will have more influence over production.

II. LITERATURE REVIEW

ShivrajYeole[1] “Tensile Testing and Evaluation of 3D Printed PLA Specimens as per ASTM D638 standard”, Fabrication of parts using additive manufacturing is proving to be an alternative to the conventional part manufacturing processes. However, achieving desired strength in such 3D printed parts using specific materials is still an area of current research. Polylactic acid (PLA), a biodegradable material, is one of the compatible materials widely used in the Fused Deposition Modelling based 3D printing process. Researchers primarily focused on strength evaluation of PLA material as per ASTM D638 Type-I standard. This paper presents evaluation of tensile strength of PLA specimens 3D printed as per ASTM D638 standard on FDM printer and its comparison with the simulated results. Process involved

preparation of ASTM specimens in Solid works software followed by printing using PLA material in a MakerBot 3D printer and then subjecting it to tensile testing in Auto Graph AG 15 universal testing machine. CAD model of the test specimens were then subjected to tensile loads in ANSYS software to obtain simulated tensile strength and maximum deformation. The experimental tensile strength values were found to be within 5% deviation of the simulated tensile strength values.

John Ryan C. Dizon[2] “Mechanical characterization of 3D-printed polymers”, It also known as Additive Manufacturing (AM), is already being adopted for rapid prototyping and soon rapid manufacturing. This review provides a brief discussion about AM and also the most employed AM technologies for polymers. The commonly-used ASTM and ISO mechanical test standards which have been used by various research groups to test the strength of the 3D-printed parts have been reported. Also, a summary of an exhaustive amount of literature regarding the mechanical properties of 3D-printed parts is included, specifically, properties under different loading types such as tensile, bending, compressive, fatigue, impact and others. Properties at low temperatures have also been discussed. Further, the effects of fillers as well as post-processing on the mechanical properties have also been discussed. Lastly, several important questions to consider in the standardization of mechanical test methods have been raised.

III. MATERIAL SELECTION

Polylactic Acid (PLA) is one of the most extensively researched 3D printing material. It has good Printability and high stiffness and Tensile Strength, besides available at cheap cost. PLA filament provides aesthetic 3D printing experience. It has better reliability and good surface quality. PLA is safe, easy to print with and it serves a wide range of applications for both novice and advanced users. easy to work with at high print speeds, user-friendly for both home and office environments, PLA allows the creation of high-resolution parts. There is a wide range of color options available. PLA is more Environmental-Friendly and Is Compositable.

Types of internal structures:

A variety of filling patterns that are used printing of components in additive manufacturing like honeycomb, rectilinear, solid, triangular, hillbert curve, Archimedean Chords, Octa gram spiral, concentric etc...Based on Filling pattern the properties of components of same material will change. . Infills play an essential role in the overall strength of an object, connecting the outer shells and supporting the upper surfaces too Our project mainly focuses on two infill patterns i.e Honey-Comb and Rectilinear with same infill densities, and comparing their mechanical properties.

Rectilinear Structure:

The rectilinear grid pattern is drawing of inclined continuous lines between the shells. Rectilinear has linear structures drawn inclined over another with different infill densities varying from 5% to 100%. It has a good strength on fatigue properties.

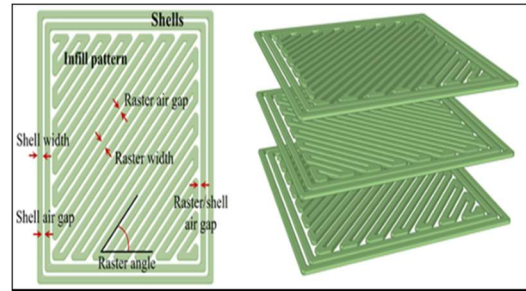


Fig 2: Rectilinear Structure

Honeycomb structure:

In 3D printing, the honeycomb is also a familiar structure, particularly for infills. 3D printed objects are typically not 100% Rectilinear and are instead held together by a lattice structure called an infill. Most 3D printed parts on FFF (FDM, Material Extrusion) 3D printers are only 20 to 30% full.

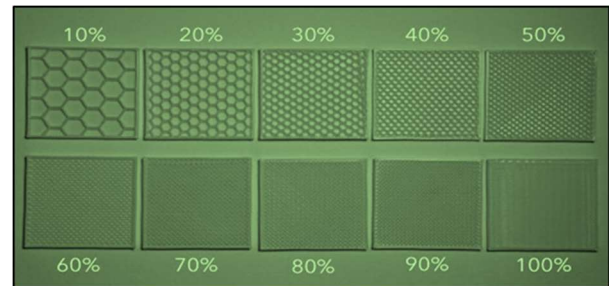


Fig. 3 : Honeycomb structure

Tensile Testing Machine:

Tensile testing is commonly used to determine the maximum load (tensile strength) that a material or a product can withstand. Tensile testing may be based on a load value or elongation value. Tensile testing is performed on a variety of materials including metals, plastics, elastomers, paper, composites, rubbers, fabrics, adhesives, films, etc.



Fig. 4: Universal tensile testing machine

Compressive Testing Machine:

Compression is a fundamental type of test used to characterize metals, composites, rock, concrete, wood,

foam, plastic and many other common materials. Compression test is conducted by applying compressive pressure to a test specimen using platens or specialized fixtures on a universal testing machine.



Fig. 4: compressive testing machine

Fatigue Testing Machine:

The fatigue life of a material is the total number of cycles that a material can be subjected to under a single loading scheme. A fatigue test is also used for the determination of the maximum load that a sample can withstand for a specified number of cycles.



Fig. 5: Fatigue test machine

Rockwell Hardness Testing Machine:

Hardness of a plastic material is most often measured by the Rockwell hardness test. It measures the resistance of the plastic toward indentation, thereby providing an empirical hardness value. These hardness values do not necessarily correlate to other properties or fundamental characteristics.



Fig. 6: Hardness Testing Machine

Modeling & Slicing

The Test Pieces were designed and drafted in CATIA V5 Software and saved the file in .STL Format. Files were loaded into PRINT-RITE software. The Specimen are sliced in 2 Different internal structures. The specimen is sliced into number of layers. Print-Rite software writes the G-codes for specimen.

Specimen Characterization:

Four different types of specimen were designed as per ASTM Standards for performing Tensile and other type of Tests. Mechanical properties of the Plastic material are carried out. The dimensions of the specimen are as follows.

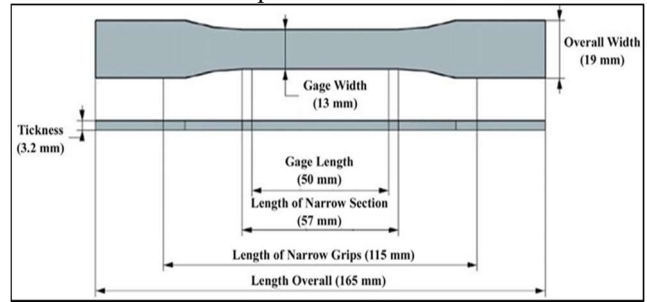


Fig 7: Tensile Test Piece Dimensions

2Modelling & Slicing of Tensile Test specimen:

A Dog Bone shaped Tensile Test specimen is designed in CATIA V5 Software in 2D model of Dimensions. The gauge length of the specimen is 57mm, width is 13mm and the thickness is 6mm. The 2D figure is extruded in 3D Modelling. The Tensile test piece is sliced by SLIC3R engine and file is converted into G-Codes.

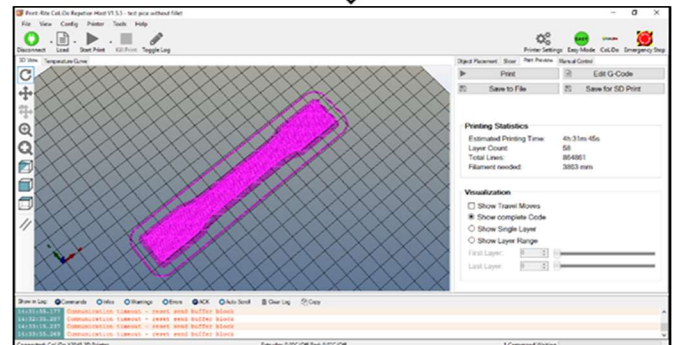
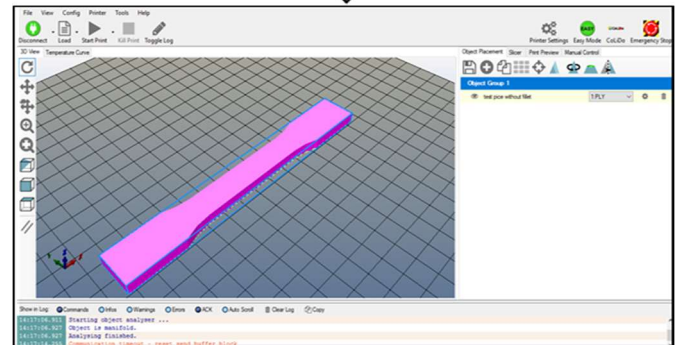
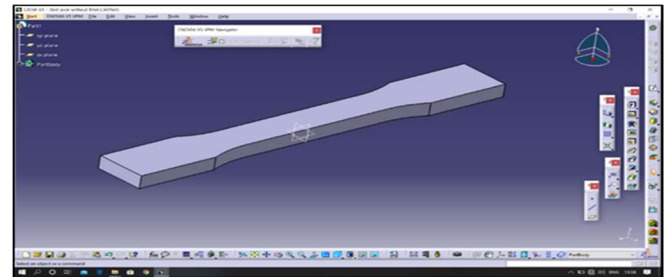


Fig. 8: Modelling, loading & Sling of Tensile test specimen

Modelling of Compressive Test Specimen:

A Compression test piece is drawn in CATIA V5 Software in 2D model. The Dimensions of the cube are Length 30mm, Width 30mm And Height 30mm. Figure is extruded in 3D Modelling. The test piece is sliced in Print-Rite Software with SLic3R engine.

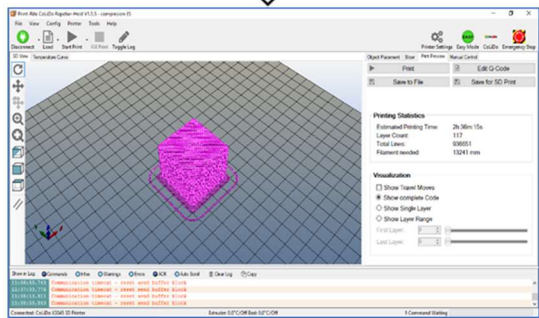
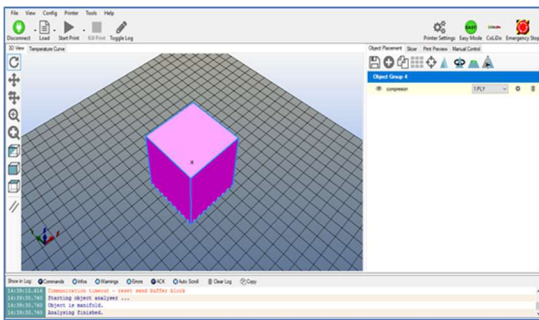
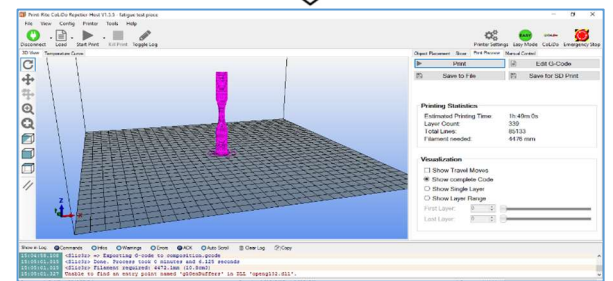
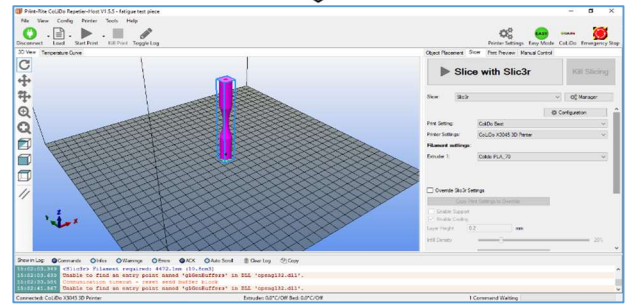
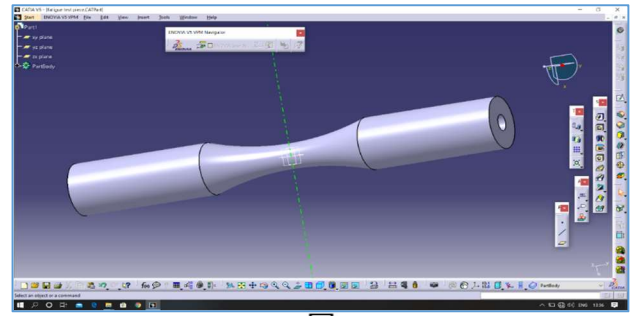
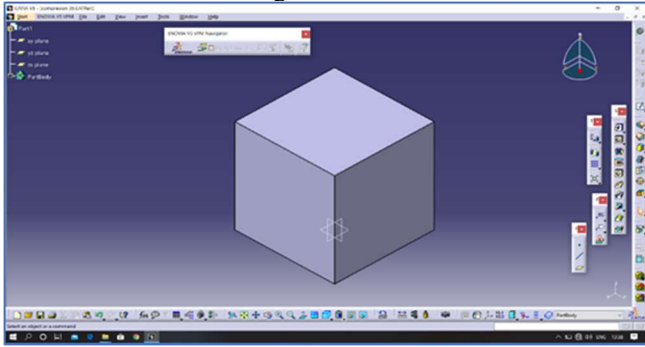


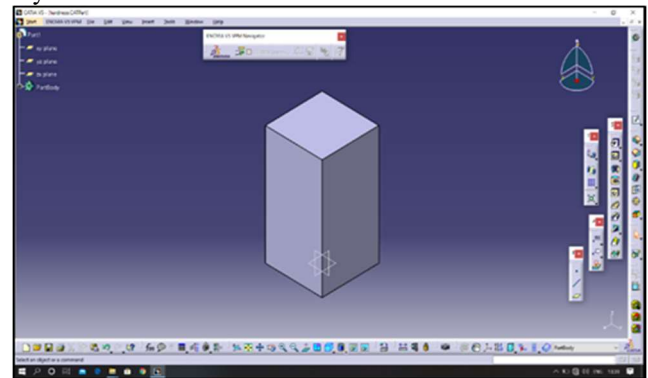
Fig. 8: modelling, loading & Sling of compressive test specimen

Fig.9: modelling, Loading & Sling of Fatigue test specimen

Modelling & Slicing of Fatigue Test specimen:

A Fatigue Test Piece had been designed and drafted in CATIA V5 software in 2D model Part Design and extruded in 3D Modelling. The specimen Dimensions are, the gauge length of the specimen is 38mm, Gauge Diameter is 6.3mm and the Total diameter is 13.6mm. The specimen is rotated and sliced by SLIC3R in PRINT-Rite Software and converted it into a G-codes file.

Modelling of Hardness Test Specimen:
 A small rectangular Bar is designed in CATIA V5 in 2D model and extruded into 3D Component. The dimensions of the cube are Length 10mm, Width 10mm And Height 20mm. In this we using SLIC3R engine to slice the specimen into layers and convert it into a G-codes file.



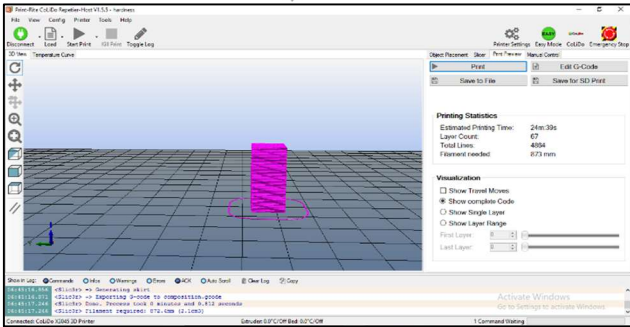
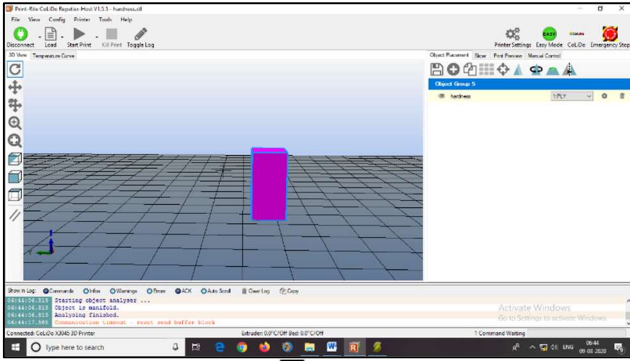


Fig.10: modelling, Loading & Sling of Hardness test specimen

Specimen were designed in CATIA V5 and are sliced in PRINT-RITE Software. Slicing Engine used is SLIC3R Engine. Two Different internal structures i.e. Honey-Comb and Rectilinear structures are selected for slicing. The files are saved in G-Codes Format in a SD-Card or LAN connection is used for connecting to a 3D printer

SPECIMEN PREPARATION

3D Printer can print any type of complex structures and have the capability to work round the clock to print objects irrespective shape and size of the object. The Specimen are Fabricated in CoLiDo X3045 Printer. Fabrication of different types of specimen are as follows.

Printing of Tensile test specimen:

A Dog-Bone shaped Tensile Test Specimen is designed, sliced and is saved in SD Card in the G-Codes Format. The file is connected to the 3D printer. The printer is loaded with the PLA filament and nozzle is heated to 210⁰C.The Bed is maintained at 80⁰C and print is given to 3Dprinter manually. Once, the print is completed the Nozzle reaches to home position and cools automatically.

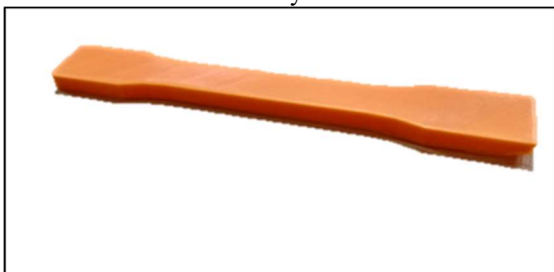


Fig.11: Printed Tensile specimen

Printing of compression test specimen:

A Cube is modelled and sliced with SLIC3R engine in Print-Rite Software. The file is saved and connected to the printer. The nozzle and bed are heated under controlled conditions by Thermocouples while printing.



Fig. 12: Printed compression specimen

Printing of Fatigue test specimen:

A Fatigue specimen is designed in Catia v5, and sliced in Print-Rite software. The STL file of the fatigue test piece is converted into G-codes, the file is saved in SD-Card or Lan Connection, and connected to printer. The 3D model of specimen is Sliced by placing specimen perpendicular to the bed. The printer starts printing automatically after the temperature of the Bed and Nozzle reaches required temperature.



Fig. 13: Printed Fatigue specimen

Printing of Hardness test specimen:

A small hardness test piece is designed and saved in .STL file. The file is sliced and saved in G-Codes format in SD-Cards or Lan Connection. SD-Cards are connected to printer and print is given by selecting the file. After reaching the required temperature print starts automatically. The Specimen are prepared in CoLiDo X3045 printer, a Biodegradable PLA filament is Used for printing the specimen. Once the printing the Specimen is completed, Bed and Nozzle starts cooling after reaching to the home position



Fig.14 Printed Fatigue specimen

IV. EXPERIMENTAL WORK

Four Specimen were printed and experiments are to be performed on these specimens for finding the mechanical properties of the PolyLactic Acid Filament with Varying in the internal structures. The tests Conducted for finding the mechanical properties are Tensile, Fatigue, Compressive and Hardness.

Tensile Test piece after testing:

Specimen is fixed to the UTM by grippers. Load is applied gradually on the specimen till the test-piece breaks. The force acting on the specimen and its displacement is continuously

monitored and plotted on a stress-strain curve until the test-piece breaks.

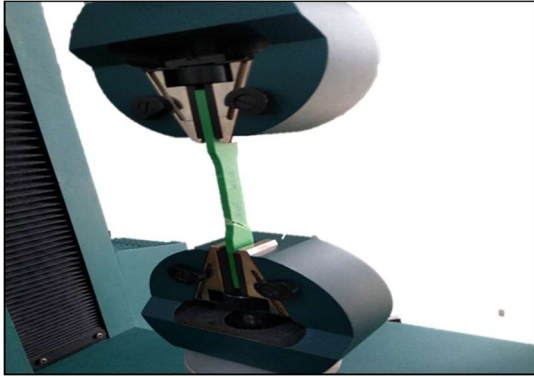


Fig 16: During the Tensile test

Compressive Test piece after testing:

To conduct the compression test on a specimen using a universal testing machine to determine ultimate compressive strength of material. When a material is subjected to compressive loading, the relationship between stress and strain is similar to that obtain for a tensile loading.



Fig.17: During the Compression test

Hardness Test piece after testing:

Rockwell hardness is generally chosen for 'harder' plastics such as polystyrene, and acetal where the resiliency or creep of the polymer is less likely to affect the results. The Standards of Ball Indentation Hardness test is (ISO 2039-1; DIN 53456).



Fig 18: During the Hardness test

Fatigue Test piece after testing:

The Fatigue test is conducted on the specimen in the rotating bending testing machine. The fatigue test determines the life and endurance limited of the material during the cyclic loads. The specimen is fixed on the both ends of the specimen. In this we can also find the bending movement of the specimen.

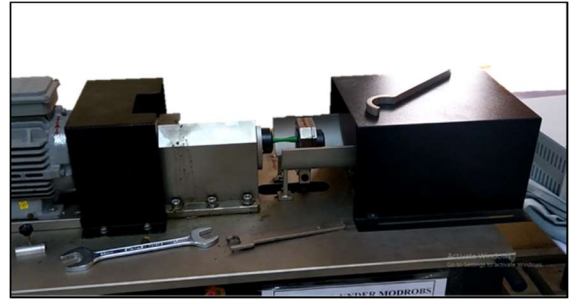


Fig.19: During the Fatigue test

RESULTS AND DISCUSSIONS

The use of plastics has been increased day due to their mechanical properties. In the present work the mechanical properties of PLA material have evaluated their properties are compared.

Tensile Test Results:

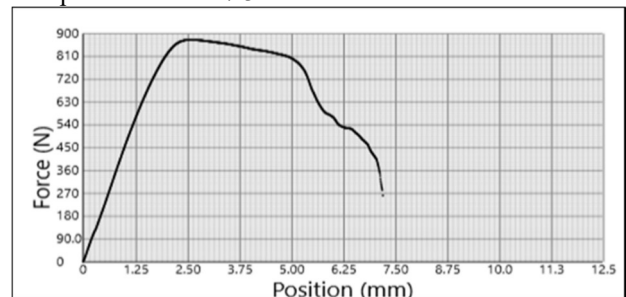
Dog-Bone Shaped Tensile Test Specimen samples of dimensions 57×13×6mm are Designed, Modelled, Sliced, Fabricated with PLA Material and Tested to calculate the mechanical properties of material with Varying Infill Patterns. Specimen is fixed to the UTM by grippers. Load is applied gradually on the specimen till the test-piece breaks. The force acting on the specimen and its displacement is continuously monitored and plotted on a stress-strain curve until failure. Load Vs displacement curve is plotted for the determination of tensile strength and elastic modulus. Calculations to be performed for finding the total elongation of the specimen and ultimate strength etc. and is plotted on a Graph.

Fatigue test piece results:

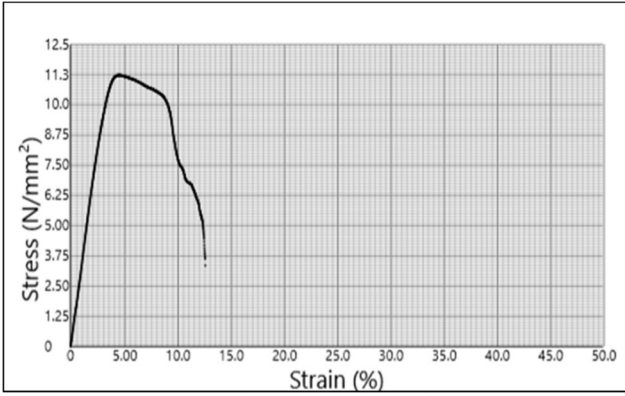
Fatigue Test-pieces of dimensions are 101mm length, Ø12mm, Ø6.35mm are Designed, modelled, sliced, Fabricated with PLA Material and are tested in rotary bending fatigue testing machine. This test is conducted to generate fatigue life and crack growth data, identify critical locations or demonstrate the safety of a structure that may be susceptible to fatigue. Cyclic loading is applied on test-pieces. Load applied, Speed, number of cycles of the rotation, etc. are monitored until the specimen breaks. Calculations were done and plotted on a Graph.

Graphs for Rectilinear Tensile test result:

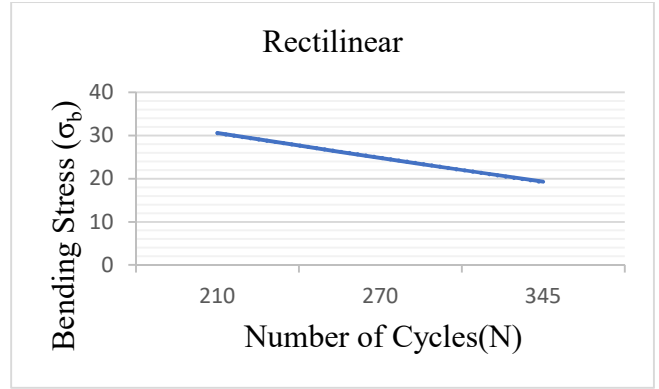
Test-Piece is fixed to UTM and Load is applied gradually on the Specimen. This entire setup is connected to a Computer for Generating Graphs of Stress-Strain & Load-Position Automatically. The ultimate strength occurs at 880N and the break point occurs at 7.3mm.



Graph: 1 force-position graph



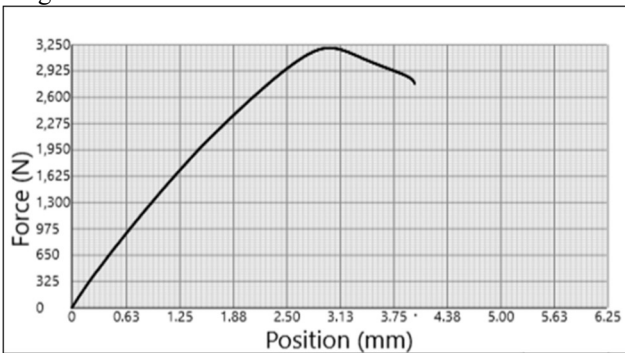
Graph: 2 stress-strain Graph



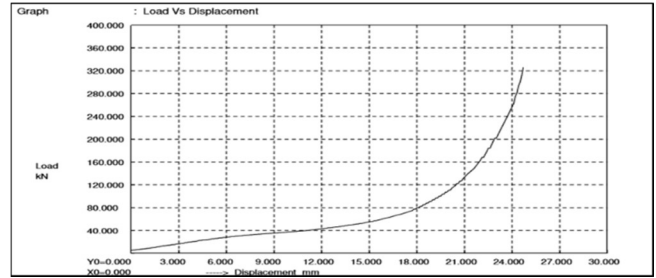
Graph: 6 Stress to No. of Cycles of Rectilinear pattern

Graphs for honeycomb Tensile test results

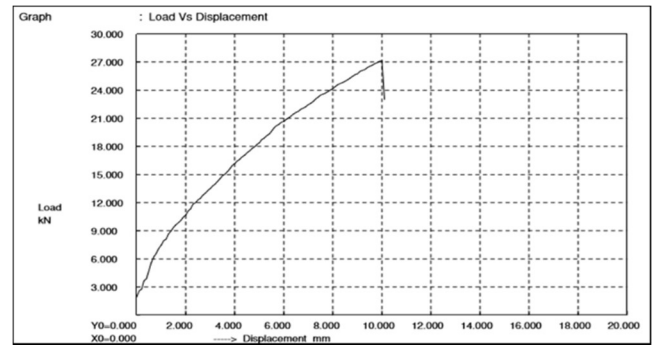
Honeycomb has better tensile strength over Rectilinear for Tensile Test-piece. It has ultimate strength at 3250 N and the Test-piece Breaks at 4mm. Stress-Strain Ratio of Honeycomb is higher than of Rectilinear.



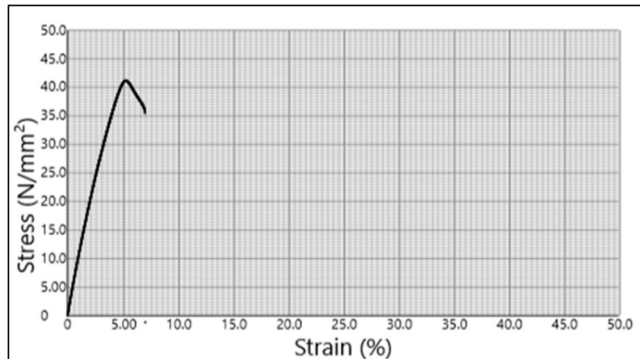
Graph: 3 force to position graph



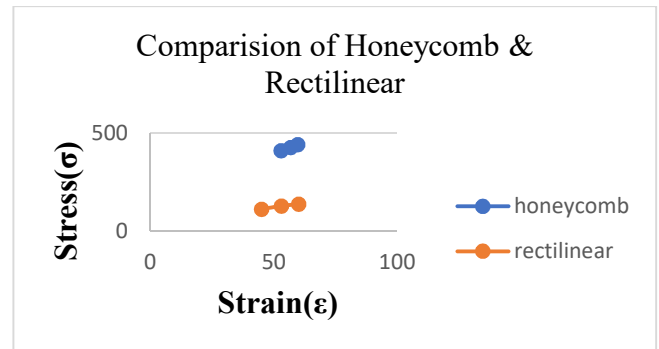
Graph:7 honeycomb Compression test piece



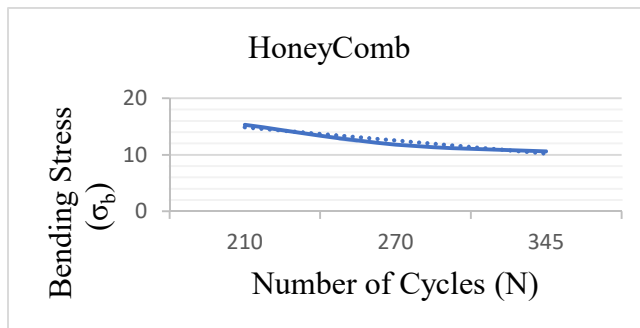
Graph: 8 Rectilinear Compression test piece



Graph: 4 stress to strain Graph



Graph: 9 Shows the graph between the Yield stress vs yield strain for three specimens



Graph: 5 Stress to No. of Cycles of Honeycomb pattern

Specimen are tested and results are tabulated, Graphs are drawn to find the mechanical properties of the polylactic acid material. Our project work discusses on the Infill pattern of the specimen and the suggesting the better applications of PLA material in industrial applications.

CONCLUSION & FUTURE SCOPE

In present work, PLA (PolyLactic Acid) has been selected a s material for additive manufacturing due to its special characteristics. As per ASTM standards, specimens for tensile, fatigue and compression testing are prepared with different filling patterns, using CoLDo X3045 printer

Four tests i.e. Tensile, compression, fatigue and Hardness are successfully carried out on PLA material. It is observed that Honeycomb material has better Ultimate tensile strength compared to Rectilinear material. compressive strength is also good for Honeycomb material when compared to Rectilinear material. It is also identified that Rectilinear material has just an edge over the honeycomb material in terms of Fatigue strength. Hence it is concluded that Honeycomb is preferred for ductile applications with moderate bending strength and hardness.

Future, different internal structures like Solid, 3D Honeycomb, Line, Concentric, Hilbert Curve, Archimedean Chords and Octa gram Spiral tested for knowing the advanced mechanical properties for each structure of PLA material.

REFERENCES

- [1] ASTM Standard D638, 2010, "Standard test methods for tensile properties of plastics," ASTM International, West Conshohocken, PA, 2010
- [2] D412 Test Methods for Vulcanized Rubber and Thermoplastic Elastomers—Tension
- [3] ASTM International takes no position respecting the validity of any patent rights asserted in connection with any item mentioned in this standard. Users of this standard are expressly advised that determination of the validity of any such patent rights, and the risk of infringement of such rights, are entirely their own responsibility
- [4] Lincoln.stl, downloaded from Smithsonian X 3D (<https://3d.si.edu/downloads/27>), educational use, 2017. Original sculptor Clark Mills, 1865.
- [6] Stephens, B., Azimi, P., El Orch, Z., Ramos, T. Ultrafine particle emissions from desktop 3D printers, Atmospheric Environment, Volume 79, November 2013, Pages 334-339
- [7] Bourell, D.L. Perspectives on Additive Manufacturing. Annu. Rev. Mater. Res. 2016, 46, 1–18. [CrossRef]
- [8] Jerez-Mesa, R., Travieso-Rodriguez, J.A., Llumà-Fuentes, J., Gomez-Gras, G., Puig, D., 2017. Fatigue lifespan study of PLA parts obtained by additive manufacturing. Procedia Manufacturing 13, 872-879.
- [9] 3ders.org. Price compare 3d printing materials. <http://www.3ders.org/pricecompare/>. (visited 4/12/2014)
- [10] Anitha, R., Arunachalam, S., Radhakrishnan, P., [2001]. Critical parameters influencing the quality of prototypes in fused deposition modeling. J. of MatProcessing Technology 118, 385–388.
- [11] B. S. Lazarov, F. Wang, and O. Sigmund, "Length scale and manufacturability in density-based topology optimization", Archive of Applied Mechanics, vol. 86, no. 1, pp. 189–218, 2016.
- [12] Averett, R.D., Realff, M.L., Jacob, K., Cakmak, M., Yalcin, B., 2011. The mechanical behavior of poly(lactic acid) unreinforced and nanocomposite films subjected to monotonic and fatigue loading conditions. J. Compos. Mater. 45(26), 2717–2726.

PHOTOLUMINESCENCE INVESTIGATIONS OF PURE AND TRANSITION METAL IONS DOPED $\text{Cd}_3(\text{BO}_3)_2$ NANOCOMPOSITES

P.N.V.V.L.Pramila Rani¹, D.Ramachandran², R.V.S.S.N.Ravi Kumar³

^{1,2}Department of Chemistry, AcharyaNagarjuna University, Guntur-522510, Andhra Pradesh

³Department of Physics, AcharyaNagarjuna University, Guntur-522510, Andhra Pradesh

Abstract: The present study reports the synthesis, structural, microstructural, photoluminescence (PL) and chromatic studies of $\text{Cd}_3(\text{BO}_3)_2$ nanocomposite (NC) and transition metal ions doped $\text{Cd}_3(\text{BO}_3)_2$ nanocomposites. The XRD studies reveals orthorhombic crystal structure, SEM and EDS studies confirms the smaller particles and composition of nanocomposite. PL data of all the prepared $\text{Cd}_3(\text{BO}_3)_2$ NCs are measured in different regions and exhibited various emission bands which correspond to different regions like UV, blue and green regions. The PL intensity is found to increase with a reduction in the particle sizes, which are in the range of 31-60nm, particle sizes are evaluated from XRD data. The PL data of all the prepared $\text{Cd}_3(\text{BO}_3)_2$ NCs, the chromaticity coordinates are calculated and plotted in chromaticity diagram. The undoped $\text{Cd}_3(\text{BO}_3)_2$ NC is located in pale blue region, whereas Cr^{3+} and Fe^{3+} doped $\text{Cd}_3(\text{BO}_3)_2$ NCs are located in dark blue region. VO^{2+} doped $\text{Cd}_3(\text{BO}_3)_2$ NCs, emitted colour is shifted to green region while Co^{2+} doped $\text{Cd}_3(\text{BO}_3)_2$ NCs exhibit whitish-blue color and these are promising to be used in lamps and display devices.

Keywords: $\text{Cd}_3(\text{BO}_3)_2$ NCs, Synthesis, Structural studies, Transition metal ions, PL studies, CIE coordinates.

1. INTRODUCTION:

Nanomaterials and nanostructures play an important role in the applications of nanoscience and nanotechnology in the fields of energy sources, environments, and health. Nanomaterials are increasingly gaining the attention of not only among the scientific community but also in the common public due to their unique properties, which lead to new and exciting applications [1, 2]. The synthesis and study of nanostructured materials have become a major interdisciplinary area of research over the past two decades. Among them semiconductor nanoparticles play a major role in several new technologies, the intense interest in this area derives from their unique chemical, physical and electronic properties, which give their potential use in the fields of displays, lighting, sensors and lasers etc. [3]. Cadmium is a component of semiconductors, such as cadmium sulfide, cadmium selenide, cadmium telluride, and cadmium oxide, which can be used for light detection and solar cells. Cadmium oxide is used in black and white television phosphors and in the blue and green phosphors for color television picture tubes [4]. The continuous attempts to develop next generation devices equipped with multi functions are now being extended to the search for materials that can combine magnetic, electronic, and photonic

responses. One example of such efforts is the quest for a ferromagnetic material that can inject spin polarized carriers into semiconductors [5].

Among the inorganic materials, metal oxides such as cadmium borate play a vital role in developing new devices as they exhibit a considerable variety of structures, stoichiometries, chemical and physical properties that can be tailored to exploit a variety of suitable synthetic techniques. There have been several reports on the photoluminescence studies of cadmium that are photoluminescence and chemically synthesized CdS nanoparticles [6]. Synthesis and characterizations of pure CdS nanocrystals using chemical precipitation method for photoluminescence applications [7]. Studies of cadmium sulfide photoluminescence in poly (methyl methacrylate)-matrix composites were reported by Smagin et al., [8]. Tuning luminescence of 3d transition-metal doped quantum particles: Ni^{2+} : CdS and Fe^{3+} : CdS reported by S. M. Taheri and M. H. Yousefimi [9].

Borate compounds are well known remarkably for their use in industries and mineralogy. Boron atom coordinates with oxygen atom in various ways, such as trigonal planar (BO_3) and tetrahedral (BO_4) structural units thus, there is considerable number of boron compounds containing also B-OH groups (hydroxyl hydrated borates) and they may also contain interstitial water [10]. Metal borates have excellent mechanical properties, good chemical inertness and high stability under high temperature.

The photoluminescence is a well-known physical phenomenon observed in many kinds of materials. In the last few years, the PL of nanocrystals has been widely investigated because of its strategic importance for the technological development of optical devices, such as light-emitting diodes, lasers, sensors, scintillators, medical diagnostics, displays, electronic panels, etc., PL studies are applied to characterize the local coordination and impurity levels of metal ions. Transition metals have good electronic properties even at low concentrations and they are easily introduced to host lattice due to their high diffusivity [11], therefore it has been the aim of many investigations to identify transition metal impurities by various measurements one of them are emission spectra. Cadmium borate is a boron-based inorganic material widely used in various fields. Cadmium borate can be isolated as crystalline

materials in various forms having different chemical compositions and structures [12].

In the present study nanocomposite (NC) samples are characterized to evaluate the structural information and nature of doped metal ions in the host $Cd_3(BO_3)_2$ lattice. The obtained nanocomposites are characterized using various techniques such as X-ray diffraction (XRD), scanning electron microscopy (SEM), Elemental dispersive (EDS), UV/vis spectroscopy and photoluminescence (PL), respectively.

2. EXPERIMENTAL DETAILS

Chemicals Required: $Cd_3(BO_3)_2$ nanocomposites were prepared by using high pure chemicals. Cadmium borate ($Cd_3(BO_3)_2$) NC was obtained by using chemical precipitation method. The Transition metal oxide doped cadmium borate NCs were produced from a solution of cadmium nitrate (0.1M), borax (0.1M) and Transition metal oxide 0.01M) by using deionized water as solvent. The uniform magnetic stirring was provided for better atomic diffusion during the length of the reaction. The resulting precipitates were centrifuged and washed several times with deionized water. The precipitates were then dried in a hot air oven at 350-400°C. The final products were then obtained by crushing the dried precipitate using pestle and mortar.



3. Characterization techniques:

The surface morphologies and elemental compositions of the prepared nanocompositions were obtained using Scanning Electron Microscopy with Elemental dispersive spectroscopy (ZEISS EVO18). PL spectrum is taken at room temperature on Horiba Jobin-Yvon Fluorolog-3 Spectrofluorimeter with Xe continuous (450 W) and pulsed (35 W) lamps as excitation sources.

3.1. Microstructure and elemental composition:

The morphology of prepared samples indicates that each of them is composed of agglomerates with irregular shape and dimension distributions. The images are taken at different magnifications showed that the prepared sample contains irregular shaped stone like particles. The grain size from SEM images does not match with the crystallite size evaluated from powder XRD studies. This can be explained by the fact that the grains seen in SEM images are the domains formed by aggregation of nanosize crystallites [13] which is shown in Fig.1.

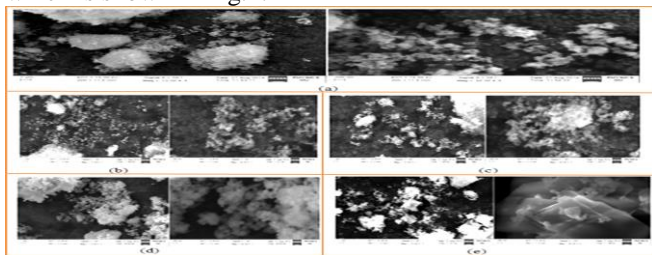


Fig.1. SEM images of $Cd_3(BO_3)_2$ NC and transition metal ion doped $Cd_3(BO_3)_2$ NCs

- (a) Undoped $Cd_3(BO_3)_2$
- (b) VO^{2+} doped $Cd_3(BO_3)_2$
- (c) Cr^{3+} doped $Cd_3(BO_3)_2$
- (d) Fe^{3+} doped $Cd_3(BO_3)_2$
- (e) Co^{2+} doped $Cd_3(BO_3)_2$

3.2. Photoluminescence Study:

Surface states are very important for the physical properties, especially for the optical properties of nanomaterials. Electrons and holes may be excited easily and escape from the ions. Many carriers trapped at the surface states or defect sites may be released by photo excitation [14,15]. So fluorescence efficiency of nanomaterials is higher than those of bulk materials. PL experiments showed a strong visible light emitting from these doped nanocomposites (NCs) having peak at 290-689 nm at room temperature. At room temperature PL spectrum of $Cd_3(BO_3)_2$ NC was excited at 325 nm, the emission peak was observed at 420 and 436 nm corresponds to blue region .

The PL spectra of $Cd_3(BO_3)_2$ NC and 3d transition metal ions (VO^{2+} , Cr^{3+} , Fe^{3+} and Co^{2+}) doped $Cd_3(BO_3)_2$ NCs exhibited various emission bands which correspond to different regions like UV, blue and green regions. The UV luminescence band belongs to the exciton recombination corresponding to near band edge (NBE) emission. UV emission centered weak band at 449 nm, weak blue emission centered at 467 nm and broad blue emission peak at 490 nm and another band at 532 nm with an excitation wavelength of 390 nm observed for Co^{2+} doped $Cd_3(BO_3)_2$ NCs .

By doping with Fe^{3+} in $Cd_3(BO_3)_2$ NC, the emission bands are exhibited a blue shifted and the quenching of visible luminescence and enhancement of UV emission was observed. In this study, a sharp and dominated UV emission at 293 nm and a suppressed blue emission at 351 nm in Fe^{3+} doped $Cd_3(BO_3)_2$ NCs indicate that the prepared samples have better quality and good optical properties. The emission bands at 293 nm and 351 nm are assigned to the transition $^4T_{2g}(D) \rightarrow ^6A_{1g}(S)$ and $^4A_{1g}(G) \rightarrow ^6A_{1g}(S)$ [16]. The emission spectrum of Cr^{3+} in $Cd_3(BO_3)_2$ NC shows three sharp emission peaks in the visible region at 462, 519 and 689 nm. PL spectrum clearly indicates that the doping of Cr^{3+} into the host material leads significant changes in PL intensity. The blue emission peak at 462 nm is a host lattice emission due to intrinsic impurities in host lattice, which was observed in undoped $Cd_3(BO_3)_2$ NC [17]. The green emission band near 519 nm is assigned to the transition $^4T_{2g}(F) \rightarrow ^4A_{2g}(F)$. The red emission band at 689 nm (R line) is a deep level emission band characteristic of Cr^{3+} ions, which is caused by the spin-forbidden $^2E_g(G) \rightarrow ^4A_{2g}(F)$ transition [18] and also the emission band results from coupling of phonon with emission photon of Cr^{3+} ions [19,20]. The emission of Cr^{3+} ions with $Cd_3(BO_3)_2$ NC can be useful in display and lighting devices.

The only emission band related to vanadium doping was observed in the emission spectrum of photoluminescence of VO^{2+} doped $Cd_3(BO_3)_2$ NC. There are two excitation bands peaking at 401 and 527 nm. Spectral features of emission and excitation spectrum are typical for photoluminescence

of ions with 3d² electron configuration in octahedral coordination [21]. The excitation wavelengths for all the prepared samples are in UV region and are given in Table.1.

Table.1. Emission peaks and excitation wavelengths of Cd₃(BO₃)₂ NC and transition metal ions doped Cd₃(BO₃)₂NCs.

Excitation wavelength (nm)	Emission peaks (nm)
Cd ₃ (BO ₃) ₂	325
	420, 436
Cd ₃ (BO ₃) ₂ :VO ²⁺	300
	401, 527
Cd ₃ (BO ₃) ₂ :Cr ³⁺	420
	462, 519, 689
Cd ₃ (BO ₃) ₂ :Fe ³⁺	250
	293, 351
Cd ₃ (BO ₃) ₂ :Co ²⁺	390
	449, 467, 490, 532

The undoped Cd₃(BO₃)₂NC is located in pale blue region, whereas Cr³⁺ and Fe³⁺ doped Cd₃(BO₃)₂NCs are located in dark blue region. VO²⁺ doped Cd₃(BO₃)₂NCs emitted colour is shifted to green region while Co²⁺ doped Cd₃(BO₃)₂NCs exhibited whitish-blue and these may be used in lamps and display devices. The PL intensity is found to increase with a reduction in the particle sizes.

The photoluminescence spectrum of nanoparticles shows a broad luminescence in green region which indicates that the nanocomposite could be used for the fabrication of photonic devices. In our samples transition metal ion doped Cd₃(BO₃)₂NCs are exhibited UV blue-green emission. Crystal quality of synthesized nanocomposite can affect the origin and the intensity of UV emission and hence enhancement in UV emission is observed for the nanocomposite with better crystal quality. Therefore, betterment in the crystal quality (less structural defects and impurities, such as oxygen vacancies and Cd interstitials) leads to the sharp and strong origination of UV emission at the room temperature of the PL spectrum [22,23]. If the concentration of oxygen vacancies is reduced in the synthesized products then it results in the appearance of a sharp and strong intensity NBE (Near band edge) emission [24].

Chromatic properties:

The Commission Internationale de l’Eclairage (CIE) chromaticity coordinates of Cd₃(BO₃)₂ NC was excited at 325 nm is shown in Fig.5(a). In Cd₃(BO₃)₂ NC, the emissions peak were calculated from the emission spectrum and location of color coordinates are represented in the CIE chromaticity diagram by solid circle (•). From this figure it is observed that the color Cd₃(BO₃)₂ NC is located in blue region and the corresponding CIE coordinates are evaluated as (x = 0.143, y = 0.057). Most lighting specifications refer to colour in terms of 1931 CIE chromatic colour coordinates which recognize that the human visual system uses three primary colours: red, green and blue [25]. The CIE coordinates are located in their specific region at different

x,y values. The comparative CIE chromatic colour coordinates of Cd₃(BO₃)₂ NC and doped Cd₃(BO₃)₂ NCs are shown in Fig. 6 along with x,y values and emitted colors given table 2.

Table 2. Chromaticity coordinates of Cd₃(BO₃)₂ and transition metal ions doped Cd₃(BO₃)₂ nanopowders

Sample	CIE Coordinates		Emitted Colour
	x	y	
Cd ₃ (BO ₃) ₂	0.143	0.057	Blue
Cd ₃ (BO ₃) ₂ :VO ²⁺	0.214	0.472	Green
Cd ₃ (BO ₃) ₂ :Cr ³⁺	0.208	0.235	Pale blue
Cd ₃ (BO ₃) ₂ :Fe ³⁺	0.155	0.022	Blue
Cd ₃ (BO ₃) ₂ :Co ²⁺	0.244	0.196	Whitish-blue

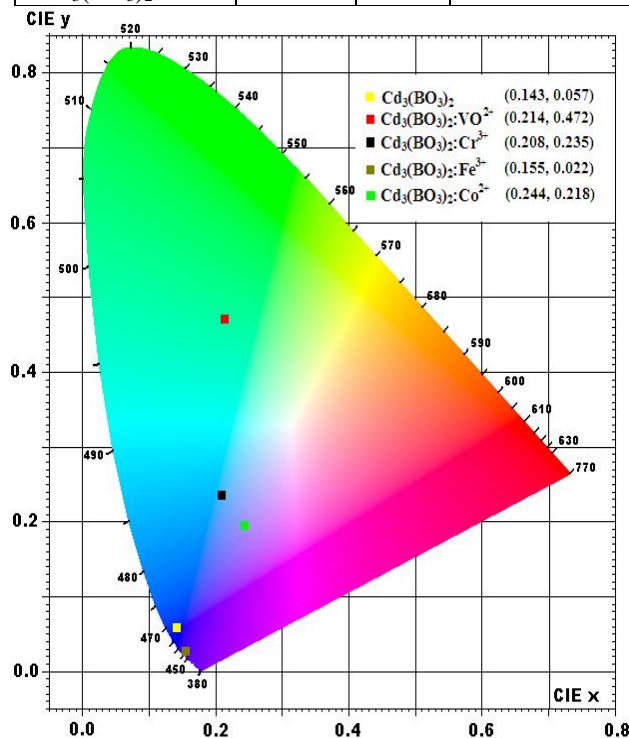


Fig. 2

Chromaticity diagram of Cd₃(BO₃)₂ and transition metal ions doped Cd₃(BO₃)₂ nanopowders

Acknowledgment:

The author P.N.V.V.L. Pramila Rani is thankful to UGC for the financial support under UGC-BSR Meritorious Fellowship, (UGC-No.F.11-67/2008) to do her research work. Authors are thankful to the Director, Central Laboratory, Acharya Nagarjuna University for providing certain laboratory facilities.

REFERENCE:

[1] K. N. Harish, H. S. BhojyaNaik, P. N. Prashanth Kumar, R. Viswanath., Catalysis Science & Technology.2, 1033(2012).

- [2] K. N. Harish, H. S. BhojyaNaik, P. N. Prashanth Kumar, R. Viswanath., ACS Sustainable Chemistry & Engineering.1(9),1143(2013).
- [3] He Hu, Weihua Zhang., Optical Materials. 28 (5), 536 (2006).
- [4] C.H. Lee, C.S. Hsi., Environ. Sci. Techn. 36, 69 (2002).
- [5] H. Ohno, Res. Inst. of Electr. Commun., Tohoku Univ., Sendai, Japan
- [6] A Srivastava , H.L. Vishwakarma., Inter. Jour. of Pure & Applied Physics.6, (3) 347 (2010).
- [7] H. L. Lee, A. M. Issam, M. Belmahi, M. B. Assouar, H. Rinnert, M. Alnot., J.ofNanomaterials. (2009) , Article ID 914501,.
- [8] V. P. Smagin,N. S. Eremina,D. A. Davydov,K. V. Nazarova,G. M. Mokrousov., Inorg. Mater.52(6), 611 (2016).
- [9] S. M. Taheri, M. H. Yousefim Brazilian., Jour.of Physics. 40(3) 2010.
- [10]R. Wahab, S.G. Ansari, Y.S. Kim, H.K. Seo, H.S. Shin., Appl. Surf. Sci. 253, 7622 (2007).
- [11]ZS Hu, JX Dong, GX Chen, JZ He, Wear, 243(1–2) 43(2000).
- [12]K Varlot, JM Martin, C Grossiord, R Vargiolu, B Vacher K Inoue, Tribology Letters 6(3) 181(1999).
- [13]N. Gomathi, S. Daniels, D.C. Cameron, L.O. Reilly, A. Mitra, P.J. McNally, O.F. Lucas, R.T. Rajendra Kumar, I. Reid, A.L. Bradley., J. Appl. Phys. 100, 033520 (2006).
- [14]M. Terauchi, H. Takahashi, N. Handa, T. Murano, M. Koike, T. Kawachi, T. Imazono, M. Koeda, T. Nagano, H. Sasai, Y. Oue, Z. Yonezawa, S. Kuramoto., J. Electron Microsc. 61, 1 (2012).
- [15]Y. Wang, N. Herron., J. Phys. Chem. 95 , 525 (1991).
- [16]W. Low, G. Rosengarten., J. Mol. Spectro. 12, 319 (1964).
- [17]T. Li, S. Yang, L. Huang, J. Zhang, B. Gu, Y. Du., J. Phys. Condens. Matter.16, 2463 (2004).
- [18]P.D. Rack, J.J. Peterson, M.D. Potter, W. Park., J. Mater. Res. 16, 1429 (2001).
- [19]B. Henderson, G.F. Imbusch., Optical Spectroscopy of Inorganic Solids. (Clarendon press, Oxford) (1896).
- [20]B. Bleaney, K.D. Bowers., Proc. Roy. Soc. London A 214 (1952) 451.
- [21]Z. Potucek,Z. Bryknar,K. Dragounova,V. Trepakov., Develop. Mat. Sci. res. Edu. 15, 8 (2014).
- [22]Y. Wang, N. Herron., J. Phys. Chem. 95, 525 (1991).
- [23]R. Wahab, S.G. Ansari, Y.S. Kim, H.K. Seo, H.S. Shin., Appl. Surf. Sci. 253, 7622 (2007).
- [24]A. Umar, Y.B. Hahn, Nanotechnology 17 (2006) 2174.
- [25]S. Koide, Phil. Mag. 4, 243 (1959).

SYNTHESIS AND CHARACTERIZATION OF STIR CASTED Al 2024-SiC METAL MATRIX COMPOSITES

Suneel Donthamsetty¹ and Penugonda Suresh Babu²

¹Vice-Principal & Professor, Department of Mechanical Engineering, Narasaraopeta Engineering College (Autonomous), Narasaraopet - 522601, Guntur District, Andhra Pradesh, India

²Associate Professor, Department of Mechanical Engineering, Narasaraopeta Engineering College (Autonomous), Narasaraopet - 522601, Guntur District, Andhra Pradesh, India.

ABSTRACT--The need of Metal Matrix Composites (MMCs) is growing day by day because of their worthy properties of light weight, more strength, corrosion resistance etc. The aim of present work is to fabricate Aluminium Metal Matrix Composites (MMCs) by reinforcing the Silicon Carbide (SiC) particles of 50 micron size with 2.5 & 5% weight percentage using stir casting method. Al 2024 alloy is well known material as a matrix material to form composite due to its strength to weight ratio and good fatigue resistance. Similarly, the silicon carbide is highly refractive material with high melting and thermal conductivity. Moreover densities of Al 2024 and SiC are close to each other which lead to uniform dispersion. Hence Al 2024 alloy & SiC are selected for the preparation of composite in present work. For synthesis of metal matrix composites, stir casting method is followed as it is a proven technique over the decades. To enhance the mechanical properties, the stir casted specimens are subjected to Heat treatment (T6) before characterization. Characterization involves microstructure analysis, Surface roughness testing, evaluation of hardness and Tensile strength. The microstructures of the specimens were tested and confirmed the presence of SiC particles. It has been observed in decrement with respect to Surface roughness after machining. Vickers Hardness testing revealed improvement in the hardness of composites compared to base Al 2024 alloy. Through tensile testing, it is found that load bearing capacity of composite material enhanced when compared with alloy material.

Keywords- Al 2024; SiC; Stir casting; Hardness; Surface roughness; tensile testing.

1. INTRODUCTION

The Metal Matrix Composites are made by scattering reinforcement material into base material or matrix which is a monolithic material and is completely continuous. The reinforcement material sometimes coated to avoid any reactions with the base material. In structural applications, matrix is generally a lighter metal such as magnesium, aluminum etc., which provides the support to the reinforcement material [1]. The composite will have combined benefits of its constituents [2].

The strength, stiffness, and density of the composite depends on its constituent materials properties, the fortifying material's size, shape, quantity & distribution and the bond between base and fortifying material. The base material shares the load among all the fibers [3]. Aluminum metal

matrix composites are getting much importance especially for aerospace, automobile, agriculture farm machinery industries etc., due to their good properties such as high strength, low density, good wear resistance compared to any other metal [4-6].

In present work, Silicon Carbide (SiC) particles are used as reinforcement material, Al 2024 as base material and synthesized by stir casting technique.

2. MATERIALS

2.1 Aluminium alloy 2024

In present work, Aluminium alloy Al 2024 is used as matrix material for which the main alloying element is copper and next is magnesium, which is predominantly added to increase the wetting between matrix and reinforcement [7]. Al 2024 alloys have high strength, good machining properties, possess low formability and corrosion resistance in the heat treated state. Composition of Al 2024 is tabulated in Table 1 and slab is shown in Fig. 1. Aluminum slabs are procured from Sri Krishna Enterprises, Secunderabad, Telangana (State), INDIA.



Fig. 1 Al 2024 Slab

2.2 Reinforcement Material (SiC)

In present work, for preparation of Al-2024-SiC metal matrix composite, Silicon Carbide (SiC) of 5% with 50 micron size used as a reinforcement material. The high thermal conductivity coupled with low thermal expansion and high strength of SiC leads to exceptional thermal shock resistant quality [9] of composite. Both Al 2024 and Silicon carbide are procured from Venuka Engineering Private Limited, Patancheru, Medak District, Telangana State, India.

3. EQUIPMENT

3.1 Stir casting machine

Stir casting machine (Make: M/s. Swam Equip, Chennai, India) used as a furnace for melting the materials and mixing with reinforcement. This is majorly accepted as a promising route, low-cost method for fabrication and also currently practicing commercially, as shown in Fig. 2. Its advantages includes more simple, flexible and can be used for high production with cost advantage [10]. The process involves heating up of Al 2024 alloy to a temperature higher than its melting point i.e., about 850°C and feeding SiC with simultaneous mixing by the rotation of stirrer.

3.1.1 Specifications of stir casting machine:

Stir casting machine used in present work is the combination of bottom pouring furnace, powder feeding mechanism, powder preheating unit, mechanical stirrer, shielding gas provision and control unit for all these elements. The Specifications of this stir casting machine are given in table 2.

Fig.2 Bottom Pouring Type Stir Casting Furnace

Fig. 3 Muffle Furnace

Table 2 Specifications of Stir Casting Machine

Sl. No.	Parameter	Value
1	Capacity of Melting Pot	2kgs (max)
2	Adjustable Melting Temperature with digital Indicator	100 – 1000° C
3	Variable Stirrer Speed arrangement with Digital Indicator	100 – 1500 RPM
4	Preheating Reinforcement Furnace with digital Indicator	100 – 500° C
5	Operating Voltage	440V AC three Phase 50 c/s.
6	Power Consumption	7.5 KW Furnace + 5 KW Motors



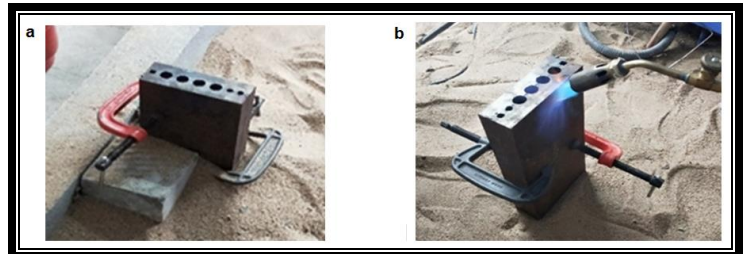
3.2 Permanent Mould



Fig. 4 Permanent Mould (Dies);

Fig. 5 Pre-Heating Equipment

The permanent dies (Fig. 4 & 6(a)) made by H12 Die steel, allows the molten metal to take final shape of component after pouring and solidifying the liquid metal into it. The two halves of dies are is as shown in Fig.4. Cooking gas operated torch (Fig. 5) used for preheating the permanent moulds (Fig. 6(b)) to 200°C to increase the die life as well reduce the tendency of die cracking.



6 (a) Dies are in clamed condition; (b) Dies are pre-heating by torch

3.3 Muffle Furnace

After solidification, the casting samples were undergone T6 heat treatment by using the muffle furnace (Fig. 3) for the purpose of improving the mechanical properties.

3.3.1 Specifications of the muffle furnace

The Specifications of the muffle furnace are given in the table 3

Table 3 Specification of Muffle Furnace

Parameter	Value
Rating	4 KW
Supply	3 Phase
Inner Size	6 x 6 x 12 inch deep
Outer Size	16 x 16 x 16 inch deep
Insulations	Ceramic board and Fiber Insulation

3.4 Microstructure Testing Equipment

For the purpose of observing the microstructure, prepared the mounting samples by using mounting press as shown in Fig. 7. After that the mounting specimens were ground by using a table top grinder and polished by using various emery papers 120, 220, 320, 400 and 600 grit sizes which meant for rough to finish polishing, as shown in Fig. 8. Disc polishing with alumina grade I, II and III in a sequence order to get mirror finishing which is needed for microscopic structure examination, as shown in Fig. 9.



Fig: 7 Hot Mounting Press ; Fig: 8 Stand with different grit emery papers



Fig: 9 Disk Polishing Machine ; Fig: 10 Electronic Microscope

The electronic microscope (Fig.10) is used to check the microstructure at various locations of the samples. All the seen microstructures were captured and recorded.

3.5 Hardness

Hardness is a characteristic of a material, not a fundamental physical property. It is defined as the resistance to scratching, machining [11], indentation and it is determined by measuring the permanent depth of the indentation mark.

3.5.1 Vickers Hardness testing:

According to ASTM Standard [12], the metallographically polished and T6 heat treated specimens of 50 mm thick and 10x10mm cross section are checked for hardness by using a Vickers micro hardness testing machine (UHL-Germany make, IMS 4.0 VMHT model). A load of 0.05 kgf is applied, on the various locations of the plane surfaces of the specimen up to 15 seconds and the indentation is observed with 100x Eye Piece Magnification. Average hardness is noted from the Vickers tester.

3.6 Portable Surface Roughness Measurement Surf test

The portable surface roughness measurement surf test machine (Mitutoyo Surf test SJ-210), as shown in Fig. 11, is a compact, portable, easy-to-use surface roughness measurement instrument equipped with extensive measurement and analysis features. The 2.4-inch color graphic LCD provides excellent readability also includes a back light for improved visibility in dark environments. The Surf test SJ-210 can be operated easily using the buttons on the front of the unit and under the sliding cover. Up to 10 measurement conditions and one measured profile can be stored in the internal memory. An optional memory card can also be used as an extended memory to store large quantities of measured profiles and conditions. Access to each feature can be password-protected, which prevents

unintended operations and allows you to protect your settings. The display interface supports 16 languages, which can be freely switched. In addition to calculation results, the SurfTest SJ-210 can display sectional calculation results and assessed profiles, load curves, and amplitude distribution curves. Surface roughness is tested before machining and after machining of specimen are compared.

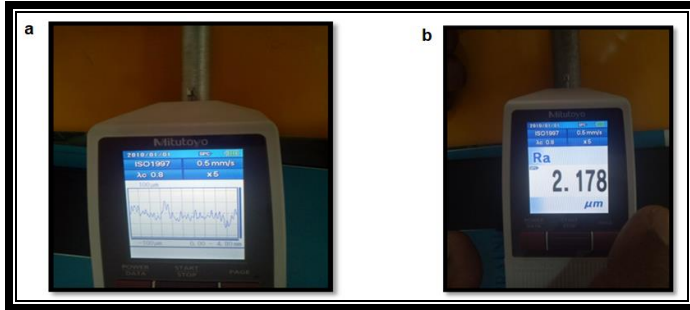


Fig.11 Surface Roughness tester with (a) Graph and (b) Value

3.7 Tensile Test

A universal testing machine (UTM), as shown in Fig. 12, also known as a universal tester, materials testing machine or materials test frame, is used to test the tensile strength and compressive strength of materials.

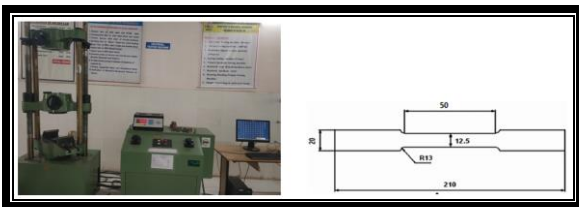


Fig. 12 Universal Testing Machine ; Fig. 13 Specimen Line Diagram

3.7.1 Specimen Preparation for tensile testing

The T6 heat treated pure and composite specimens were prepared as per ASTM E 8/E 8M-08 standard by using Automatic lathe machine to suit for tensile testing as shown in Figures 13 to 15.



Fig: 14 Tensile Specimen preparation ; Fig: 15 Finished Tensile Specimen

4. EXPERIMENTATION

4.1 Synthesis of composites

Small pieces of Al 2024 matrix material are loaded one by one in to the melting chamber of Stir casting machine and allowed the metal to heat till 790°C and simultaneously SiC of 50 μm (2.5 & 5 % by Weight) particles are preheated to 300°C to remove moisture and to enable free flow of particles through feeding unit into the furnace.

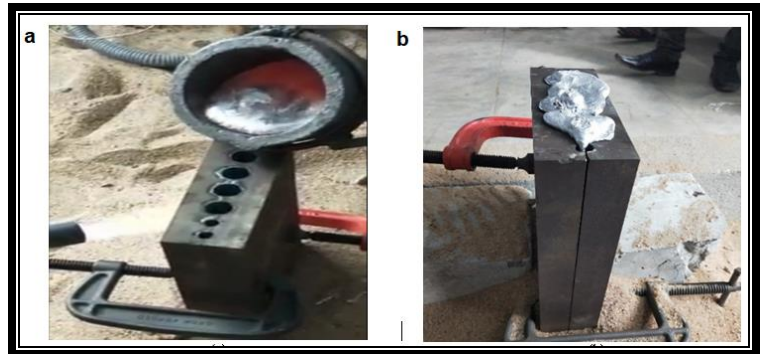


Fig.16 Al 2024-SiC Composite (a) Liquid metal pouring into dies (b) Solidified composite in the dies bars (c) Composite casting taken from the dies (d) Finished composite castings

After complete melting of Al 2024 pieces in the furnace, stirrer is allowed to rotate at a speed of 400 rpm and SiC particles are fed into it slowly. By trial and error method, experiments are conducted and stirring time is optimized to 5 minutes. Gas welding torch is used to preheat permanent mould to 200°C prior to pour molten metal into it. Preheated permanent mould is kept carefully near to the bottom opening of furnace and allowed molten metal to rush into the mould by operating control panel. The mould is then allowed to cool naturally to reach room temperature. Permanent mould is opened and specimens are verified for defects any present and on ensuring defect free specimens they are cleaned and separated from each other. The synthesized Al 2024-SiC Composite bars are as shown in Fig.16

4.2 Heat Treatment of the composite specimen

Specimens are subjected to Heat treatment (T6) to increase their mechanical properties and also to remove residual stresses present if any [13] and polished with coarse and fine grade emery papers respectively over their cross section.

5. RESULTS AND DISCUSSIONS

5.1 Hardness Analysis

To understand the affect of SiC addition to the Al 2024, the hardness is found, which is a pointer of a material’s resistance to plastic deformation. Detailed results are shown in Table 4 and Figure 17, which indicates that hardness is increasing with addition of reinforcement. The SiC particles high melting temperature, high hardness and resistance to wear and corrosion leads to increase of hardness when it is mixed with Al 2024.

Table 4. Hardness of Al 2024-SiC Composites

Sample No.	Specimen	Hardness HV
1	Al 2024 pure alloy	55
2	Al 2024 – 2.5 % SiC Composite	61
3	Al 2024 – 5 % SiC Composite	74

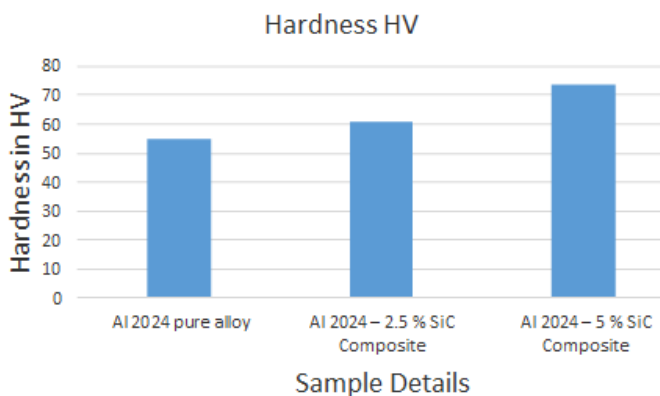


Fig. 17 Hardness of Al 2024-SiC Composites in HV

4.3 Microstructure Studies

The microstructure of fracture was carried out to make out microstructural degradations after machinability for

Al2024/SiC metal matrix composites for different percentage of reinforcements. Fractures were observed for Al2024/SiC composites, shown in Figure18. Most of the SiC particles concentrations were observed in the fractured areas for all the percentage of reinforcements.

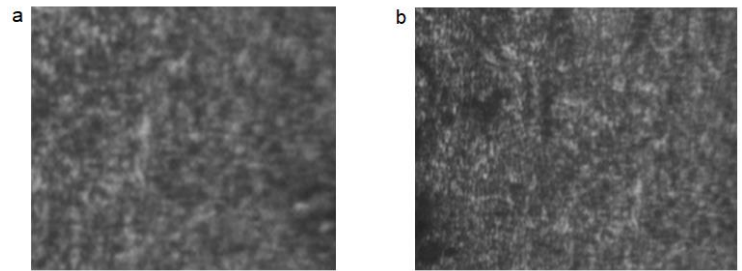


Fig. 18 Microstructure images of (a) Al 2024 (b) Al 2024 - 2.5% SiC Composite (c) Al 2024 - 5% SiC Composite

4.4 Surface Roughness

The average surface roughness of composites for 0%, 2.5% and 5% of SiC reinforcement before and after machining were shown in table 5 and Fig. 19. The values showed that the surface roughness values are decreased after machining.

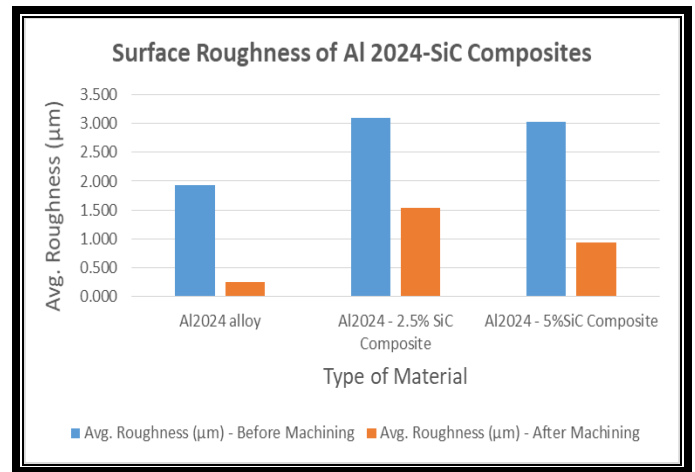


Fig. 19 Surface Roughness of Al 2024-SiC Composites

4.6 Tensile Testing

The tensile test process involves placing the test specimen in the testing machine and slowly extending it until it fractures. During this process, the elongation of the gauge section is recorded against the applied force. Repeated the procedure for other specimen of pure Al 2024, Al 2024 - 2.5% SiC, Al 2024 - 5% SiC composites. The results are shown in table 6.

Table 6. Tensile Test results of Al 2024-SiC Composites

S.No	Type of material	Initial diameter (d1) in mm	Final diameter (d2) in mm	Initial gauge length (l1) in mm	Final gauge length (l2) in mm	Initial area (a1) in mm ²	Final area (a2) in mm ²	% of Elongation	% of Reduction in area	Maximum force in KN	Tensile strength in KN/mm ²
1	Al2024 alloy	10	9.5	50	54	78.571	70.88	8	9.75	8.14	0.104
2	AL 2024 +2.5% SiC	10	9.5	50	51	78.571	70.88	2	9.75	10.32	0.131
3	AL2024 +5% sic	10	9.8	50	52	78.571	75.4296	4	3.96	7.46	0.095

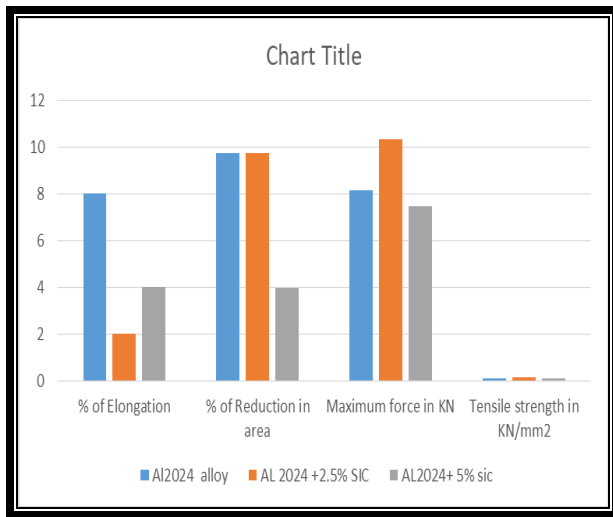


Fig. 20 Tensile testing values of Al 2024-SiC Composites

6. Conclusions

We have successfully prepared the Al 2024- SiC Metal Matrix Composites by using Stir casting technique. After proper heat treatment, machined the samples as per the standards by using lathe machine. After that we have carried out the different types of testing's and below is the summary

- The microstructure clearly reveals that uniform distribution of silicon carbide Particles throughout the composite.
- Vickers hardness are tested for Al 2024 alloy, Al 2024–2.5 % SiC and Al 2024–5% SiC composites, the average values are 55 HV, 61 74 HV HV respectively. It is found that the hardness is high for Al 2024–5% SiC composite and also it is snowing the increasing values with addition of % SiC.
- The surface roughness values of Al 2024 alloy, Al 2024–2.5 % SiC and Al 2024–5% SiC composites were found before machining are 1.935µm, 3.088µm

and 3.03 µm respectively. After machining these materials, the surface roughness found as 0.251µm, 1.538 µm and 0.936 µm respectively. It shows that the surface finish has been improved.

- Tensile testing of alloy and composite specimens were done and found that there is an increase of load in composite material with 2.5% SiC and decrease of load in composite material with 5% SiC, when compared with alloy material.

Scope for Future work

- As results shown improvement in hardness, there may be much more chances for significant change in other mechanical properties. Experimentation can be extended to establish other mechanical properties like wear, Fatigue, corrosion, Impact etc., at different wt % reinforcement of SiC.
- And other Reinforcement materials like B₄C or Carbon nanotubes may also be tested for present work.

Acknowledgment

Present work is an outcome of an undergraduate project and authors are acknowledging efforts of students for their commendable work.

REFERENCES

- [1] Deborah D. L. Chung 2010 Composite Materials Science and Applications Springer-Verlag London Limited, second edition
- [2] M Haghshenas, Metal–Matrix Composites, 2016 Elsevier Inc, Reference Module in Materials Science and Materials Engineering doi:10.1016/B978-0-12-803581-8.03950-3 <https://www.asminternational.org/documents/10192/1942084/composite.pdf/0eb5cca8-4613-482c-811c-993c58b42e92>
- [4] Rohit Sharma, Saurabh Jha P, Khushboo Kakkur, Kushal Kamboj and Pardeep Sharma 2017 A Review of the Aluminium Metal Matrix Composite and its Properties International Research Journal of Engineering and Technology (IRJET) Volume: 04 Issue: 02
- [5] Suhasini Gururaja, Mamidala Ramulu, and William Pedersen, MACHINING OF MMCs: A REVIEW, Machining Science and Technology, 17:41–73, 2013 Taylor & Francis Group, LLC, DOI: 10.1080/10910344.2012.747897
- [6] Son N. Trinh and Trinh, Son N. and Sastry, Shankar, "Processing and Properties of Metal Matrix Composites" (2016). Mechanical Engineering and

- Materials Science Independent Study. 10. <https://openscholarship.wustl.edu/mems500/10>
- [7] Atul Kumar, Sudhir Kumar and Rohit Garg, Production & Characterization of Al 2024-SiCp Metal Matrix Composite using Stir Casting, *Journal of Mechanical and Production Engineering (JMPE)*, ISSN (E): 2278-3520 Vol. 6, Issue 1, Jun 2016, 1-8
- [8] ASM Handbook, Volume 2B: Properties and Selection of Aluminum Alloys
- [9] <https://www.azom.com/article.aspx?ArticleID=6615>
- [10] S. Soltani, R. Azari Khosroshahi, R. Taherzadeh Mousavian, Stir casting process for manufacture of Al-SiC composites, Faculty of Materials Engineering, Sahand University of Technology, Tabriz 37200-000, Iran
- [11] Kevin Kurian Paul and Sijo MT, Effect of Stirrer Parameter of Stir casting on Mechanical Properties of Aluminium Silicon Carbide Composite, *International Journal Of Modern Engineering Research (IJMER)*, ISSN: 2249-6645, Vol. 5, Iss. 8, August 2015.
- [12] ASTM Standard: E 92-82, "Standard Test Method for Vickers Hardness of Metallic Materials"
- [13] Heat Treating of Aluminum Alloys, ASM Handbook, Volume 4: Heat Treating, ASM Handbook Committee, p 841-879, DOI: 10.1361/asmhba0001205

Comprehensive Review on Mechanism Accountable for Dispersion Stability of Ultra-Fine Particle Suspensions in Heat Transfer Applications

¹Vidya Chaparala ²G. Ravi Kiran Sastry ³P. Phani Prasanthi

¹Mechanical Engineering Department National Institute of Technology, Andhra Pradesh India

^{2,3}Mechanical Engineering Department P.V.P. Siddhartha Institute of Technology, Vijayawada, India

Abstract:

Dispersions of nano-sized particles in traditional heat transfer mediums in the pursuit of intensifying heat exchange rate are recognized by the research community as an emerging field. The astounding increase in the rate of heat transmission has led to this theory. Large amounts of experimental data that were published in the open literature were found to be widely dispersed and inconsistent. This fact provides a clue that it is important to comprehend the potential contributing mechanisms resulting in the improved thermal characteristics while safeguarding the dispersion stability. Therefore, this study places special emphasis on the microscopic mechanisms that contribute to the stability of nanofluid dispersion by preventing pointless agglomeration.

1. INTRODUCTION

Technological progress in renewable energy conservation techniques, heavy duty power production systems, latest electro mechanical systems and transportation sectors have led to adverse increase in thermal loads. Miniaturization of electronic systems has been demanded by the emergence of nanotechnology. Hence dealing with the heavy thermal loads in rapidly growing industrialization poses challenges to the research community. Conventional heat exchange media such as water, EG, PG, engine oil, transformer oil is failing to address the loads due to the hindrance in their thermos-physical characteristics. As part of the efforts in order to get rid of the drawbacks offered by conventional heat transfer fluids, Avtar Singh Ahuja, have proposed the technique of suspension of micro/millimeter sized metallic particles with better thermal conductivity [1]. But suspension of micro-sized particles has led to various complications such as surface erosion, flow passage clogging, particle sinking, and drop in flow pressure which ultimately declared them as inappropriate candidates for heat transfer augmentation. Stephen Masuda et al [2] proposed the dispersion of nano sized metallic particles with the purpose of enhancing thermal conductivity while keeping the pumping power lower side. Direct evaporation of metallic nanoparticles into base fluid leads to corresponding improvement in conductance capacity of nano fluids with comparatively smaller concentrations as compared to that of oxide-based coolants [3]. Succeeding research reported that the nano fluids possess improved thermal conductance capacity with very low volume concentration of particle suspension. Such enhancement majorly relies upon the geometry of the suspended particle, dimension of the particle, as well as the volume fraction of

dispersion and thermal characteristics. Dispersing a small concentration of nanoparticles increases thermal conductivity of suspension over base fluids [4,5]. Nano particles may be produced via various routes namely mechanical disintegration, gas condensation and chemical precipitation technique. Gas condensation is reported to be beneficial compared to others due clean and impure particle generation. However, the tendency of agglomeration is observed to be more by adopting this technique of nano particle synthesis [5]. Exotic application of nano fluids can be visualized in the medical sector by the way of optimal nano drug targeting and prosthetic curative devices. This signifies the role of nano fluids as the best choice in health care, thermal management and other related industrial applications.

2. PROSPECTIVE MECHANISMS CAUSING THE ENHANCEMENT OF HEAT CONDUCTION IN NANOFLUIDS:

According to the available literature, the apparent principles of exchange of heat in solid composite materials are not valid for the case of nanofluids. Based on that reasoning we attempted to look at a comprehensive list of the parameters that could be causing the theory's inadequacy. Initially, we considered the possibility that the enhancement in thermal conductivity would be caused by Brownian motion of the particles. Subsequently, we looked at how molecular stacking of the liquid at the liquid/particle interface might lead to an increase in thermal conductivity. Third, we look into the ways in which heat is transferred within nanoscale structures as well as the applicability of the macroscopic theory of diffusive heat transmission in both solid and liquid media. Finally, we examine the consequences of nanoparticle clustering both through the formation of direct solid-solid routes and through potential liquid-mediated clustering effects that may exist up to a small interparticle distance. From the present study we will be able to reduce the number of potential explanations for the exceptional improvement of heat transmission in nanofluids.

A. Brownian motion:

Brownian movement is the process in which atoms and molecules in a fluid (liquid or gas) are carried along by the fast-moving atoms or molecules in that fluid. Due to the fact that it involves the haphazard movement of suspended solid particles in a liquid or gas, it is also known as Brownian motion. [7]. As a result of the fluids' tiny particle size, motions caused by stochastic (Brownian) and inter-particle

forces can result in additional energy transport. Particle motion causes micro convection, which improves heat transfer. Most of the effective thermal conductivity models presume that the particles are immobile when the fluids are not moving in bulk, which is the case when the particle is large. Microscopic forces can be significant in nano particle fluid mixtures [8]. A nanometer-sized particle is subject to the Vander Waals force, electrostatic force brought in at the particle surface by the electric double layer, stochastic force resulting in Brownian motion of the particles, and hydrodynamic force. The combined effect of these forces causes and influences the mobility of fluids and particles. [9]. It is worth noting that the stochastic and electrostatic forces are only significant for ultra-fine particles, although the Van der Waals force is strong when the particles are close to one another. There is consequently a connection between particle size and effective heat conductivity. The chemical characteristics of the particle surface and the fluid that is hosting the particles, distribution of the particle size, as well as the arrangement of the particle system all have a significant impact on these forces, making it difficult to calculate them correctly. There hasn't been any quantitative study on the increased heat transmission brought on by the motion these forces cause at the microscopic level.[10]. Some of the forces producing the random motion of the nanoparticles suspended in a base liquid include the London-Van der Waals force, Stokes' drag force, and the Langevin force, which has a random function of time and reflects the atomic structure of the medium.[11]. It is unknown precisely how this random motion influences the energy transit through nanofluids and their morphology. The colliding suspended nanoparticles may cause particle aggregation, which may lead to cluster formation. Numerous internal forces exist between base fluid and nanoparticle contact surfaces, as well as between nanoparticles, particles, and clusters., as well as interactions between clusters, influence the cluster formation. The size of created clusters may be constrained by diffusion effects [12]. According to research by Koblinski and his team that examined a range of heat transfer mechanisms, the mechanism of heat transmission in nanofluids is significantly quicker than Brownian diffusion in the fluid, even at the limits of extremely small particles. However, it was suggested that Brownian motion would have an impact on particle clustering, which would lead to the creation of routes with lower thermal resistance and, as a result, boost heat transfer in nanofluids. Despite the fact that Brownian motion is too slow to move a significant quantity of heat, it may speed up the mixing and clustering of fluids, which might enhance thermal transport. [13].

B. Molecular layering of liquids:

In contrast, the layering of the liquid at the solid contact is an interface effect that may enhance heat conductivity due to the layer's significantly more ordered atomic structure than the bulk liquid's. Higher thermal conductivity would be anticipated as a result of such liquid layering at the interface given that liquids exhibit far worse thermal transport than clearly ordered crystalline solids, which are much more common [14]. The layering at the interface is greatly influenced by the characteristics of all other species that can inhabit that area including the co-ions, like small amounts of

leftover water. This is not just true of the counter-ions. Layering creates repulsion, and this repulsion is dependent on both the configuration and the makeup of the chemical family that each species belongs to. Thus, minute adjustments can change the interaction's balance from repellent to attractive, converting the nanoparticle structure from scattered to tiny clumps [15]. By virtue of their potential localization at the charged solid-liquid interface, the nature of counter-ions first injected into the nanoparticles—which may differ from those of the ionic liquid—is another crucial critical feature. As a result, they alter the dispersion state in the layers at the contact. Varying these localized counterions makes solids and ionic liquids compatible because it is not always simple to change the solid oxide surface's bare charge density by experimentation. When charged polymers are placed on the nanoparticles, their structural surface charge increases, adding to their repulsion and increasing their structural surface charge. Surprisingly, ionic liquid arrangement on the surface of charged nanoparticles produces a higher repulsion than the steric repulsive contribution of the polymer, which is necessary to obtain stable dispersions. All species characteristics that allow them to be found at interfaces, including the co-ions and counterions, as well as all other species that can do so, has a significant impact on the layering at the interface. This layering-induced repellency is influenced by the geometry and chemical makeup of all the species' chemical groups [15]. The thickness of the solvation layers on two particles or particle aggregates with different radii but the same temperature may be the same or smaller for the bigger radii particles or aggregates. In order to significantly improve heat conductivity and colloidal stability, the solvation layer thickness to radius ratio keeps decreasing as particle or aggregate size increases. The contributing parameters are liquid layers formed on the nanoparticle surfaces and also the solvation forces. Hydrophilic colloidal particles introduce more ordered liquid layers on the surface of the solids than those in the bulk of the solvent system. Associated with the liquid bulk, these layers have a higher thermal conductivity. This is true when water and hydrophilic nanoparticles come into contact. [16]. The hydrodynamic size of the particles gets increased when ordered layers are placed over the nanoparticles, which is expected to enhance the fluid flow resistance. Glycol molecules are stacked on the surface of metal oxide-based nanofluids, which enhances thermal conductivity, especially at lower temperatures. This qualifies metal oxide-based nanofluids as viable options for use in low temperature cooling systems. [17]. For example, the phenomenon of particle layering and the development of in-layer crystal like structures offer a novel colloid stability mechanism for macro dispersions like foams and emulsions. Particle layering in a genuine foam was reported to be produced using a solution of 20 vol. percent silica particles with a diameter of 19 nm. It is important for practical reasons that foams and emulsions with stratifying (or layering) films have a significantly longer lifespan. The dispersion is more substantial as a result.[18]. The thickness of the layering depends on how well the solid and liquid are bonded. Numerous aspects, including flow and viscosity,

are significantly impacted by these structural modifications in the liquid structure.[19].

C. Diffusive heat transport:

The particle-like characteristics of phonons have been examined, but this discussion can also be extended to the wave-like characteristics. Till date no conclusive way available to describe the regime of transfer of heat in nanostructures, not even by designating a dominant mean free path of phonons. Numerous investigations have found that low frequency phonons with lengthy mean free paths contribute significantly to phenomena because phonons can propagate over a wide range of frequency, velocity, and mean free paths [20]. The argument that ballistic phonon transport is better than diffusion phonon transport fails since both phonon transport techniques result in the similar rate of boundary conduction for heat transfer in liquids since the temperature inside the solid particle would never change.[21]. With respect to developing laminar flow of Al_2O_3 -water nanofluid with relative motion emerging from Brownian and thermophoretic diffusion, Farias Alvario et al. evaluated the effect of heat flux over heat transfer coefficient. It was discovered that the former establishes a concentration gradient, which in turn impacts the latter's ability to balance the heat flux. It was observed that the heat transfer coefficient rises whereas the thermal conductivity falls as a result of thermophoretic diffusion [22]. The particle fluxes connected to thermophoresis and Brownian diffusion possess in the order of 10^{-10} and 10^{-8} , respectively. In this way, it may be inferred that the thermophoresis, which has a greater impact on particle movement than Brownian diffusion, should not be disregarded [23]. The most significant processes of particle migration are thermophoresis and Brownian diffusion, whereas the gradient of viscosity and also non-uniform shear rate have no appreciable influence; Significantly, thermophoresis increases the nonuniformity of the concentration distribution leads to shrinking of the concentration near the walls, which alters the spatially effective thermo-physical properties of the nanofluids, particularly the thermal conductivity and viscosity because they strongly depend on particle concentrations. The boundary layer may thin close to the wall due to a reduced effective viscosity, increasing the velocity of the nanofluid there as a result. Furthermore, the movement of nanoparticles may alter the formation of the boundary layer, which may alter the flow and convective heat transfer coefficient of nanofluids [24].

D. Nanopartic clustering:

The interactions between the particles are essential for the production of nanoparticle clusters from pre-formed nanoparticles. Rapid aggregation happens when there is a very appealing interaction potential (more than 10 kT). As a result, fractal, disordered clusters with kinetically locked structures is produced. [25]. Since heat may transfer very quickly within these clusters, the effective volume fraction of the highly conductive phase (V_p in the HC theory) is greater than the solid's actual volume. The effect of clustering is the higher effective volume of highly conducting clusters caused by their greater thermal conductivity as a result of their cluster's packing fraction (ratio of the volume of the solid particles in the cluster to the

total effective volume of the cluster) [26]. The problem of magnetic nanoparticle aggregation needs to be resolved because it has a lot of negative effects. The extent of the exposed specific surface area is first abruptly reduced by the clumping of particles. As a result, another difficulty is the agglomerates' sedimentation from their suspension.[27]. In contrast to diffusive heat transfer, nanoparticles transfer heat in a ballistic fashion. Thermal conductivity enhancement suffered because of the particle clustering. Clusters that are more loosely packed have larger thermal conductivity enhancements than clusters that are more tightly packed [13]. Nanoparticle clustering may produce diminishing thermal resistance channels in the suspension. Despite that, clustering may cause solids to clump together, which in turn results in the particles settling down and reducing the suspension's conductivity [28]. After reviewing effective media theories and the conventional percolation theory, McLach et al. investigated the impact of particle clustering on the electrical conductivity of a composite medium and proposed a generalized effective medium equation combining percolation and Bruggeman's effective media theories. They came to the conclusion that a quantitative mechanism for assessing actual experimental data on electrical resistivity of composite media was provided by the general effective media equation.[29]. According to the idea of surface free energy, the level of supersaturation and the molar volume of the nucleus affect both the rate of molecular clustering and its thermodynamics. In actuality, solute molecules keep forming clusters until the Gibbs free energy is zero. The Gibbs free energy has an inverse relationship with the supersaturation level. So, when supersaturation grows, solutions become thermodynamically unstable and start to crystallize as clusters [30]. Changing the electric charges on the nanoparticle surface and in the medium can control and induce the phenomenon of clustering [31].

4. CONCLUSIONS

In this study, authors have taken into account a number of potential mechanisms that could explain the significant enhancement in stability of the nano suspensions. This study will give researchers the necessary direction to investigate the heat transport mechanisms in nanofluids because the thermal characteristics of nanofluids are a current topic of active research. Major conclusions of the survey can be presented as follows:

1. There is a connection between particle size and effective heat conductivity. Particle motion causes micro convection, which improves heat transfer. Most of the effective thermal conductivity models presume that the particles are immobile. Microscopic forces can be significant in nano particle fluid mixtures. These forces produce the random motion of nanoparticles suspended in a base fluid. This motion may speed up the mixing and clustering of fluids, which could lead to better thermal transport routes.
2. An interface phenomenon that could improve heat conductivity is layering of the liquid at the solid contact. The traits of all other species, including the co-ions, that can live there have a big impact on the layering at the interface. The configuration and constitution of each species affect the repulsion that is produced by layering. The liquid layers on

the surface of the solids that are introduced by hydrophilic colloidal particles are more organized than those in the system as a whole. The use of metal oxide-based nanofluids in low temperature cooling systems is thus made possible. For macro dispersions like emulsions, the particle stacking phenomenon offers a novel colloid stability mechanism.

3. Phonons can propagate over a wide range of frequency, velocity, and mean free paths. Most significant processes of particle migration are thermophoresis and Brownian diffusion. Gradients of viscosity and non-uniform shear rate have no appreciable influence on particle movement.

4. The effect of clustering is the higher effective volume of highly conducting clusters from pre-formed nanoparticles. Clusters that are more loosely packed have larger thermal conductivity enhancements. McLach et al. investigated the impact of particle clustering on the electrical conductivity of a composite medium.

3. FUTURE RESEARCH:

In recent years, researchers have focused on the thermophysical properties of nanofluids. There has been a lot of research done on the use of nanofluids in various applications for process optimization and energy efficiency. As stated in the previous section, very little research has been conducted on the details of the nanoparticles' molecular level interactions with the base fluid molecules, which remain unknown. These forces are also discovered to play an important role in maintaining dispersion stability. This finding opens up new directions for future research.

REFERENCES:

- [1]. Ahuja, A. S., Augmentation of Heat Transport in Laminar Flow of Polystyrene Suspension: Experiments and Results, *Journal of Applied Physics*, vol. 46, pp. 3408–3416, 1975.
- [2]. Masuda, H., Ebata, A., Teramae, K., and Hishinuma, N., Alteration of Thermal Conductivity and Viscosity of Liquid by Dispersing Ultra-Fine Particles (Dispersion of γ -Al₂O₃, SiO₂ and TiO₂ Ultra-Fine Particles), *Netsu Bussei*, vol. 4, pp. 227–233, 1993.
- [3] Eastman, J. A., Choi, S. U. S., Li, S., Thompson, L. J., and Lee, S., Enhanced Thermal Conductivity Through the Development of Nano fluids, *Proc. Nanophase and Nanocomposite Materials II*, Materials Research Society, pp. 3–11, Boston, 1997.
- [4] Wang, X., Xu, X., and Choi, S. U. S., Thermal Conductivity of Nanoparticle-Fluid Mixture, *Journal of Thermo physics and Heat Transfer*, vol. 13, pp. 474–480, 1999.
- [5] Lee, S., Choi, S. U. S., Li, S., and Eastman, J. A., Measuring Thermal Conductivity of Fluids Containing Oxide Nanoparticles, *Journal of Heat Transfer*, vol. 121, pp. 280–289, 1999.
- [6] Xinwei Wang and Xianfan Xu, Thermal Conductivity of Nano particle-Fluid Mixture, *Journal Of Thermo physics And Heat Transfer*, Vol. 13, No. 4, October–December 1999.
- [7] P. Keblinski, S.R. Phillpot, S.U.S. Choi, J.A. Eastman, Mechanisms of heat flow in suspensions of nano-sized particles (nanofluids), *International Journal of Heat and Mass Transfer*, Volume 45, Issue 4, February 2002, Pages 855–863,
- [8] Kaufui V. Wong and Michael J. Castillo, Heat Transfer Mechanisms and Clustering in Nanofluids, *Advances in Mechanical Engineering* Volume 2010, Article ID 795478, 9 pages
- [9] Manoj Venkataraman, The Effect Of Colloidal Stability On The Heat T ect Of Colloidal Stability On The Heat Transfer Characteristics Of Nanosilica Dispersed Fluids, *Electronic Theses and Dissertations*, 2004–2019. 630.
- [10] Francesco Giorgi, Diego Coglitore, Judith M. Curran, Douglas Gilliland, Peter Macko, Maurice Whelan, Andrew Worth, and Eann A. Patterson, The influence of inter-particle forces on diffusion at the nanoscale, *Scientific Reports*, 2019; 9: 12689,
- [11] Klimontovich, Y.L.: *Statistical Theory of Open Systems: Unified Approach to Kinetic Description of Processes in Active Systems* vol. 1. Kluwer Academic Publications, London (1995)
- [12] Xuan, Y., Li, Q., Hu, W.: Aggregation structure and thermal conductivity of nanofluids. *AIChE J.* 49, 1038–1043 (2003)
- [13] Keblinski, P., Phillpot, S.R., Choi, S.U.S., Eastman, J.A.: Mechanism of heat flow in suspensions of nano-sized particles (nanofluids). *Int. J. Heat Mass Transf.* 45, 855–863 (2002)
- [14] J.R. Henderson, F. Van Swol, On the interface between a fluid and a plane wall: Theory and simulations of a hard sphere fluid at a hard wall, *Molecular physics*, 51 (1984), 991–1010.
- [15] J. C. Riedl, a M. A. Akhavan Kazemi, a F. Cousin, b E. Dubois, a S. Fantini, c S. Lois, c R. Perzynski a and V. Peyre, Colloidal dispersions of oxide nanoparticles in ionic liquids: elucidating the key parameters, *Nanoscale advances*, 2020, 21560.
- [16] Kuppusamy Swaminathan Suganthi, Meera Parthasarathy, Kalpoondi Sekar Rajan, Liquid-layering induced, temperature-dependent thermal conductivity enhancement in ZnO–propylene glycol nanofluids, *Chemical Physics Letters* 561–562 (2013) 120–124.
- [17] K.S. Suganthi, K.S. Rajan, Metal oxide nanofluids: Review of formulation, thermo-physical properties, mechanisms, and heat transfer performance, *Renewable and sustainable energy reviews* 76 (2017), 226–255.
- [18] Darsh Wasan, Alex Nikolov, Brij Moudgil, Colloidal dispersions: Structure, stability and geometric confinement, *Powder Technology* 153 (2005) 135–141.
- [19] Xie, H. Q., M. Fujii, and X. Zhang. “Effect of interfacial nanolayer on the effective thermal conductivity of nanoparticle fluid mixture.” *Int. J. Heat Mass Transf.* 48, no. 14, 2005: 2926–2932.
- [20] Hu, Y., Zeng, L., Minnich, A. *et al.* Spectral mapping of thermal conductivity through nanoscale ballistic transport. *Nature Nanotech* 10, 701–706, (2015).
- [21] Angayarkanni SA, Philip John, Review on Thermal Properties of Nanofluids: Recent Developments, *Advances in Colloid and Interface Science* (2015).
- [22] Kyo Sik Hwang, Seok Pil Jang, Stephen U.S. Choi, Flow and convective heat transfer characteristics of water-based Al₂O₃ nanofluids in fully developed laminar flow regime, *International Journal of Heat and Mass Transfer*, Volume 52, Issues 1–2, 2009. Pages 193–199.
- [23] Mehdi Bahraei, Seyed Mostafa Hosseinalipour, Particle migration in nanofluids considering thermophoresis and its effect on convective heat transfer, *Thermochimica Acta*, Volume 574, 2013, Pages 47–54.
- [24] Sohn CH, Kihm KD, Non homogenous modeling of nanofluidic energy transport accounting for the thermophoretic migration of nanoparticles inside laminar pipe flows. *JKPS* 2009; 55:2200–2208.
- [25] Daphne Klotsa and Robert L. Jack, Predicting the self-assembly of a model colloidal crystal : *Soft Matter*, 2011, 7, 6294,
- [26] EASTMAN, J A; PHILLPOT, S R; CHOI, S U S; KEBLINSKI, P, THERMAL TRANSPORT IN NANOFUIDS, ANNUAL REVIEW OF MATERIALS RESEARCH; PALO ALTO VOL. 34, (2004): 219–246, DOI: 10.1146/ANNUREV.MATSCI.34.052803.090621.
- [27] YU W, XIE H, A REVIEW ON NANOFUIDS: PREPARATION, STABILITY MECHANISMS, AND APPLICATIONS. *JOURNAL OF NANOMATERIALS* 2012:1–17.
- [28] M. Bahrami, M.M. Yovanovich, J.R. Culham, Assessment of relevant physical phenomena controlling thermal performance of nanofluids, *Proceedings of IMECE* 2006.
- [29] McLachlan, D. S., Blaszkiewicz, M., and Newnham, R. E., Electrical Resistivity of Composites, *Journal of the American Ceramic Society*, vol. 73, pp. 2187–2203, 1990.

[30] Ali Ahmadi Tehrani, Mohammad Mahdi Omranpoor, Alireza Vatanara, Mohammad Seyedabadi, Vahid Ramezani, Formation of nanosuspensions in bottom-up approach: theories and optimization, DARU Journal of Pharmaceutical Sciences

[31] Vanessa Pilati, Guilherme Gomide, Rafael Cabreira Gomes, Gerardo F. Goya, and Jerome Depeyrot, Colloidal Stability and Concentration Effects on Nanoparticle Heat Delivery for Magnetic Fluid Hyperthermia, Langmuir 2021, 37, 1129–1140

Fracture, Fatigue Growth Rate and Vibration Analysis of Cam Shafts used in Railways

Nelaturi Vijaya Sekhar

Department of Mechanical Engineering, Narasaraopeta Engineering College (A), Narasaraopeta, A.P.

ABSTRACT:

The cam shaft and its associated parts control the opening and closing of the two valves. The associated parts are push rods, rocker arms, valve springs and tappets. It consists of a cylindrical rod running over the length of the cylinder bank with a number of oblong lobes protruding from it, one for each valve. The cam lobes force the valves open by pressing on the valve, or on some intermediate mechanism as they rotate. This shaft also provides the drive to the ignition system.

The camshaft is driven by the crankshaft through timing gears. Cams are made as integral parts of the camshaft and are designed in such a way to open and close the valves at the correct timing and to keep them open for the necessary duration. A common example is the camshaft of an automobile, which takes the rotary motion of the engine and translates it into the reciprocating motion necessary to operate the intake and exhaust valves of the cylinders.

In this work, a camshaft is designed for multi cylinder engine and 3D-model of the camshaft is created using modeling software pro/Engineer. The modeled in creo is imported into ANSYS. After completing the element properties, meshing and constraints the loads are applied on camshaft for three different materials namely aluminium alloy, forged steel and cast iron to determine the displacement, equivalent stress of the cam shaft. After taking the results of static analysis, the model analysis and harmonic analysis are done one by one.

1. INTRODUCTION

A **cam** is a rotating or sliding piece in a mechanical linkage used especially in transforming rotary motion into linear motion or vice versa. It is often a part of a rotating wheel (e.g. an eccentric wheel) or shaft (e.g. a cylinder with an irregular shape) that strikes a lever at one or more points on its circular path. The cam can be a simple tooth, as is used to deliver pulses of power to a steam hammer, for example, or an eccentric disc or other shape that produces a smooth reciprocating (back and forth) motion in the *follower*, which is a lever making contact with the cam.

OVERVIEW

The cam can be seen as a device that translates from circular to reciprocating (or sometimes oscillating) motion. A common example is the camshaft of an automobile, which takes the rotary motion of the engine and translates it into the reciprocating motion necessary to operate the intake and exhaust valves of the cylinders.

The opposite operation, translation of reciprocating motion to circular motion, is done by a crank. An example is the crankshaft of a car, which takes the reciprocating motion of

the pistons and translates it into the rotary motion necessary to operate the wheels.

Cams can also be viewed as information-storing and -transmitting devices. Examples are the cam-drums that direct the notes of a music box or the movements of a screw machine's various tools and chucks. The information stored and transmitted by the cam is the answer to the question, "What actions should happen, and when?" (Even an automotive camshaft essentially answers that question, although the music box cam is a still-better example in illustrating this concept.)

Certain cams can be characterized by their displacement diagrams, which reflect the changing position a roller follower would make as the cam rotates about an axis. These diagrams relate angular position to the radial displacement experienced at that position. Several key terms are relevant in such a construction of plate cams: base circle, prime circle (with radius equal to the sum of the follower radius and the base circle radius), pitch curve which is the radial curve traced out by applying the radial displacements away from the prime circle across all angles, and the lobe separation angle (LSA - the angle between two adjacent intake and exhaust cam lobes). Displacement diagrams are traditionally presented as graphs with non-negative values. A **camshaft** is a shaft to which a cam is fastened or of which a cam forms an integral part.



2. LITERATURE SURVEY

CAMSHAFT CONFIGURATION

Single Overhead Cam

This arrangement denotes an engine with **one cam per head**. So if it is an inline 4-cylinder or inline 6-cylinder engine, it

will have one cam; if it is a V-6 or V-8, it will have two cams (one for each head).

The cam actuates rocker arms that press down on the valves, opening them. **Springs** return the valves to their closed position. These springs have to be very strong because at high engine speeds, the valves are pushed down very quickly, and it is the springs that keep the valves in contact with the rocker arms. If the springs were not strong enough, the valves might come away from the rocker arms and snap back. This is an undesirable situation that would result in extra wear on the cams and rocker arms.

On single and double overhead cam engines, the cams are driven by the crankshaft, via either a belt or chain called the **timing belt** or **timing chain**. These belts and chains need to be replaced or adjusted at regular intervals. If a timing belt breaks, the cam will stop spinning and the piston could hit the open valves.



Double Overhead Cam



A double overhead cam engine has **two cams per head**. So inline engines have two cams, and V engines have four. Usually, double overhead cams are used on engines with four or more valves per cylinder -- a single camshaft simply cannot fit enough cam lobes to actuate all of those valves.

The main reason to use double overhead cams is to allow for more intake and exhaust valves. More valves means that intake and exhaust gases can flow more freely because there are more openings for them to flow through. This increases the power of the engine.

The final configuration we'll go into in this article is the pushrod engine.

Pushrod Engines

Like SOHC and DOHC engines, the valves in a pushrod engine are located in the head, above the cylinder. The key

difference is that **the camshaft on a pushrod engine is inside the engine block**, rather than in the head.



The cam actuates long rods that go up through the block and into the head to move the rockers. These long rods add mass to the system, which increases the load on the valve springs. This can limit the speed of pushrod engines; the overhead camshaft, which eliminates the pushrod from the system, is one of the engine technologies that made higher engine speeds possible.

The camshaft in a pushrod engine is often driven by gears or a short chain. Gear-drives are generally less prone to breakage than belt drives, which are often found in overhead cam engines.

DESIGN CALCULATIONS

PRESSURE CALCULATIONS

Bore \times stroke(mm) = 57 \times 58.6

Displacement = 149.5CC

Maximum power = 13.8bhp @ 8500rpm

Maximum torque = 13.4Nm @ 6000 rpm

Compression ratio = 9.35/1

Density of petrol $C_8H_{18} = 737.22 \frac{kg}{m^3}$ at 60F
 = 0.00073722 kg/cm³

= 0.0000073722 kg/mm³

T = 60F = 288.855K = 15.55⁰C

Mass = density \times volume

m = 0.0000073722 \times 149500

m = 0.11kg

Molecular cut for petrol 144.2285 g/mole

PV = mRT

$P = \frac{mRT}{V} = \frac{0.11 \times 8.3143 \times 288.555}{0.11422 \times 0.0001495} = \frac{263.9}{0.00001707}$

P = 15454538.533 j/m³ = n/m²

P = 15.454 N/mm²

DESIGN OF CAMSHAFT

The cam is forged as one piece with the camshaft

The diameter of camshaft

$D^1 = 0.16 \times \text{cylinder bore} + 12.7$ $D^1 = 0.16 \times 57 + 12.7 = 21.82\text{mm}$

The base circle diameter is about 4mm greater than camshaft diameter

Base circle diameter = 21.82 + 3 = 24.82mm = 25mm

Width of camshaft

$$w^1 = 0.09 \times \text{cylinder bore} + 6$$

$$W^1 = 0.09 \times 57 + 6 = 11.13 \text{mm}$$

$$\begin{aligned} \text{OA} &= \text{minimum radius of camshaft} + (1/2 \times \text{diameter of roller}) \\ &= 12.5 + (1/2 \times 41) = 33 \text{mm} \end{aligned}$$

2. MATERIALS AND METHODS

- Forged steel
- Cast iron
- Aluminum alloy

INTRODUCTION TO CAD

Computer-aided design (CAD) is the use of computer systems (or workstations) to aid in the creation, modification, analysis, or optimization of a design. CAD software is used to increase the productivity of the designer, improve the quality of design, improve communications through documentation, and to create a database for manufacturing. CAD output is often in the form of electronic files for print, machining, or other manufacturing operations. The term CADD (for Computer Aided Design and Drafting) is also used.

Its use in designing electronic systems is known as electronic design automation, or EDA. In mechanical design it is known as mechanical design automation (MDA) or computer-aided drafting (CAD), which includes the process of creating a technical drawing with the use of computer software. CAD may be used to design curves and figures in two-dimensional (2D) space; or curves, surfaces, and solids in three-dimensional (3D) space.

CAD is an important industrial art extensively used in many applications, including automotive, shipbuilding, and aerospace industries, industrial and architectural design, prosthetics, and many more. CAD is also widely used to produce computer animation for special effects in movies, advertising and technical manuals, often called DCC digital content creation. The modern ubiquity and power of computers means that even perfume bottles and shampoo dispensers are designed using techniques unheard of by engineers of the 1960s. Because of its enormous economic importance, CAD has been a major driving force for research in computational geometry, computer graphics (both hardware and software), and discrete differential geometry.

INTRODUCTION TO CREO

PTC CREO, formerly known as Pro/ENGINEER, is 3D modeling software used in mechanical engineering, design, manufacturing, and in CAD drafting service firms. It was one of the first 3D CAD modeling applications that used a rule-based parametric system. Using parameters, dimensions and features to capture the behavior of the product, it can optimize the development product as well as the design itself.

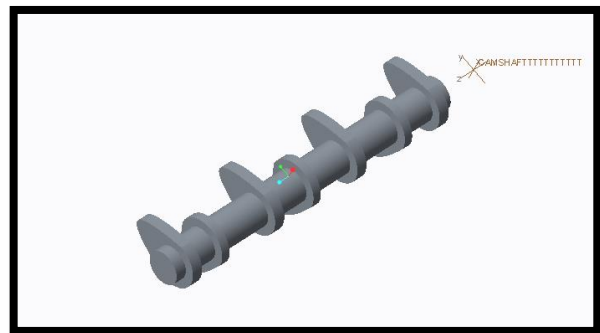
The name was changed in 2010 from Pro/ENGINEER Wildfire to CREO. It was announced by the company who developed it, Parametric Technology Company (PTC), during the launch of its suite of design products that includes applications such as assembly modeling, 2D orthographic views for technical drawing, finite element analysis and more.

PTC CREO says it can offer a more efficient design experience than other modeling software because of its unique features including the integration of parametric and direct modeling in one platform. The complete suite of applications spans the spectrum of product development, giving designers options to use in each step of the process. The software also has a more user friendly interface that provides a better experience for designers. It also has collaborative capacities that make it easy to share designs and make changes.

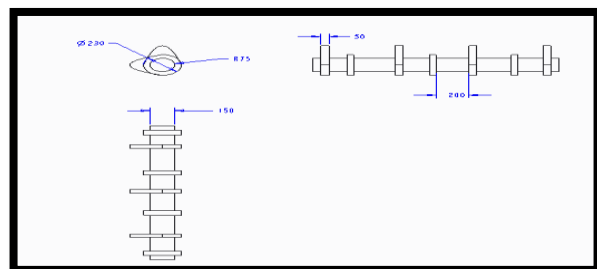
PTC also offers comprehensive training on how to use the software. This can save businesses by eliminating the need to hire new employees. Their training program is available online and in-person, but materials are available to access anytime.

A unique feature is that the software is available in 10 languages. PTC knows they have people from all over the world using their software, so they offer it in multiple languages so nearly anyone who wants to use it is able to do so.

3D MODEL OF CAM SHAFT



2D MODEL



INTRODUCTION TO FEA

Finite element analysis is a method of solving, usually approximately, certain problems in engineering and science. It is used mainly for problems for which no exact solution, expressible in some mathematical form, is available. As such, it is a numerical rather than an analytical method. Methods of this type are needed because analytical methods cannot cope with the real, complicated problems that are met with in engineering. For example, engineering strength of materials or the mathematical theory of elasticity can be used to calculate analytically the stresses and strains in a bent beam, but neither

will be very successful in finding out what is happening in part of a car suspension system during cornering. One of the first applications of FEA was, indeed, to find the stresses and strains in engineering components under load. FEA, when applied to any realistic model of an engineering component, requires an enormous amount of computation and the development of the method has depended on the availability of suitable digital computers for it to run on. The method is now applied to problems involving a wide range of phenomena, including vibrations, heat conduction, fluid mechanics and electrostatics, and a wide range of material properties, such as linear-elastic (Hookean) behavior and behavior involving deviation from Hooke's law (for example, plasticity or rubber-elasticity).

INTRODUCTION TO ANSYS

Structural Analysis

ANSYS Autodyn is computer simulation tool for simulating the response of materials to short duration severe loadings from impact, high pressure or explosions.

ANSYS Mechanical

ANSYS Mechanical is a finite element analysis tool for structural analysis, including linear, nonlinear and dynamic studies. This computer simulation product provides finite elements to model behavior, and supports material models and equation solvers for a wide range of mechanical design problems. ANSYS Mechanical also includes thermal analysis and coupled-physics capabilities involving acoustics, piezoelectric, thermal-structural and thermo-electric analysis.

FLUID FLOW

The ANSYS/FLOTRAN CFD (Computational Fluid Dynamics) offers comprehensive equipment for studying - dimensional and 3-dimensional fluid go with the flow fields. ANSYS is able to modeling a sizable variety of analysis sorts such as: airfoils for pressure analysis of plane wings (elevate and drag), drift in supersonic nozzles, and complicated, three-dimensional waft styles in a pipe bend. In addition, ANSYS/FLOTRAN may be used to carry out obligations together with:

- Calculating the gasoline pressure and temperature distributions in an engine exhaust manifold
- Studying the thermal stratification and breakup in piping systems
- Using drift blending research to evaluate ability for thermal surprise
- Doing herbal convection analyses to evaluate the thermal performance of chips in digital enclosures
- Conducting warmness exchanger research related to exceptional fluids separated by using strong regions

INTRODUCTION TO CFD

Computational fluid dynamics, commonly abbreviated as CFD, is a department of fluid mechanics that makes use of numerical strategies and algorithms to clear up and analyze problems that involve fluid flows. Computers are used to

carry out the calculations required to simulate the interplay of beverages and gases with surfaces described by boundary conditions. With high-pace supercomputers, higher solutions can be performed. Ongoing research yields software that improves the accuracy and speed of complex simulation scenarios together with transonic or turbulent flows. Initial experimental validation of such software program is executed using a wind tunnel with the very last validation coming in complete-scale testing, e.g. Flight assessments.

**STATIC ANALYSIS OF CAM SHAFT
MATERIALS - FORGED STEEL**

Young's modulus = 205000mpa

Poisson's ratio = 0.3

Density = 7850kg/mm³

Save creo Model as .iges format

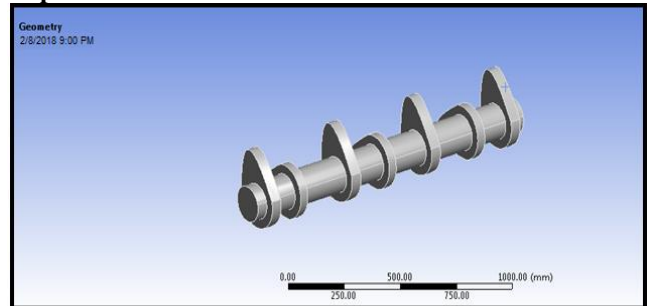
→→Ansys → Workbench→ Select analysis system → static structural → double click

→→Select geometry → right click → import geometry → select browse →open part → ok

→→ Select mesh on work bench → right click →edit

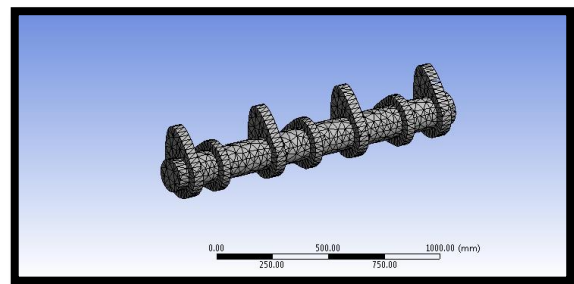
Double click on geometry → select MSBR → edit material →

Imported Model from CREO

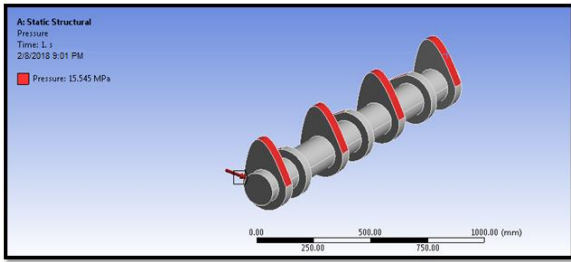


Select mesh on left side part tree → right click → generate mesh →

Meshed Model



Select static structural right click → insert → select rotational velocity and fixed support → Select displacement → select required area → click on apply → put X,Y,Z component zero →



Select force → select required area → click on apply → enter rotational velocity

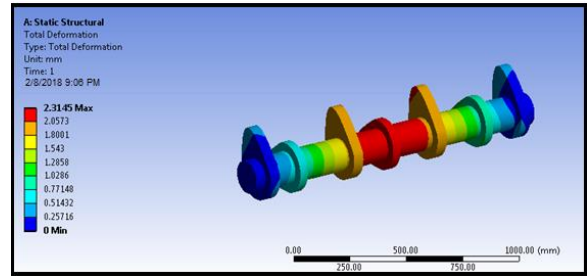
Select solution right click → solve →

Solution right click → insert → deformation → total →

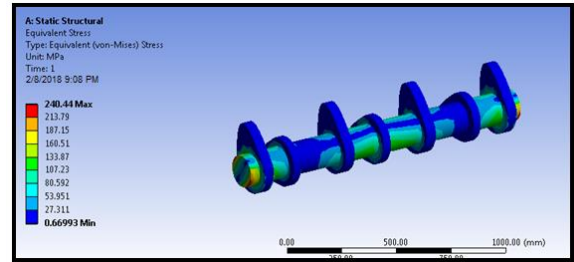
Solution right click → insert → strain → equivalent (von-mises) →

Solution right click → insert → stress → equivalent (von-mises) →

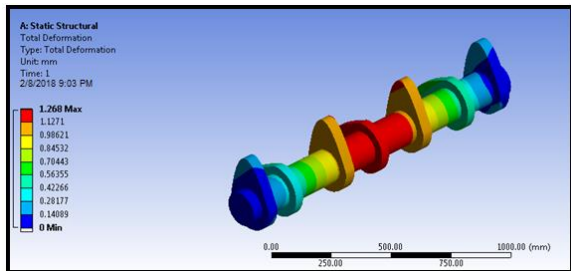
Right click on deformation → evaluate all result



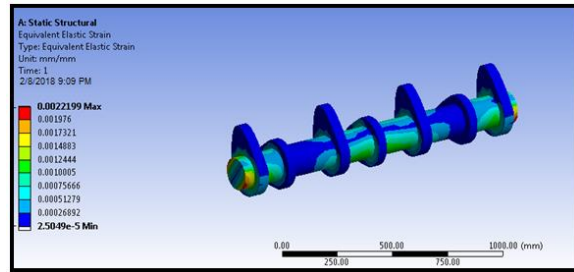
VON-MISES STRESS



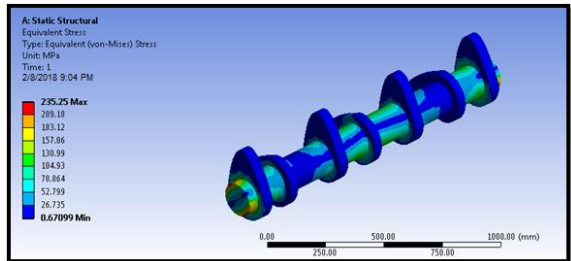
TOTAL DEFORMATION



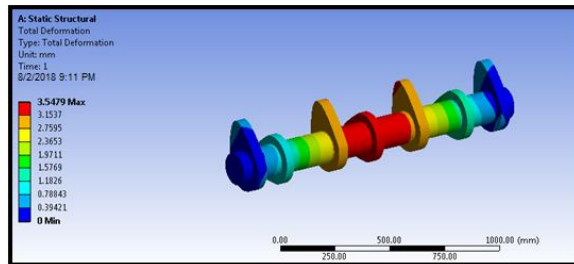
VON-MISES STRAIN



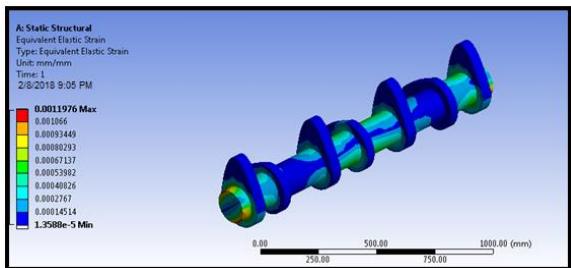
VON-MISES STRESS



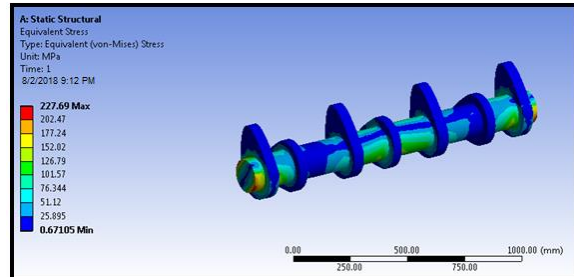
**MATERIALS - ALUMINUM ALLOY
TOTAL DEFORMATION**



VON-MISES STRAIN

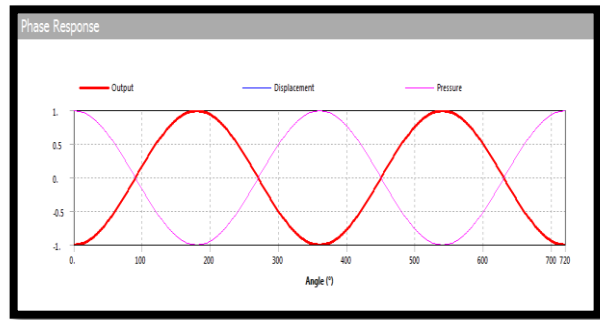
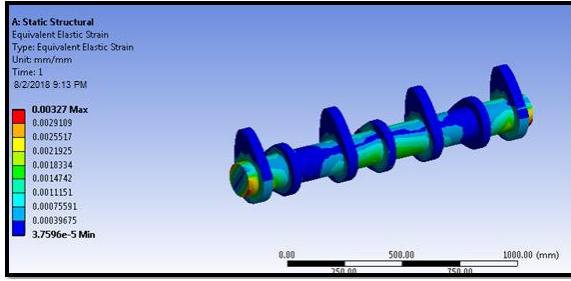


VON-MISES STRESS

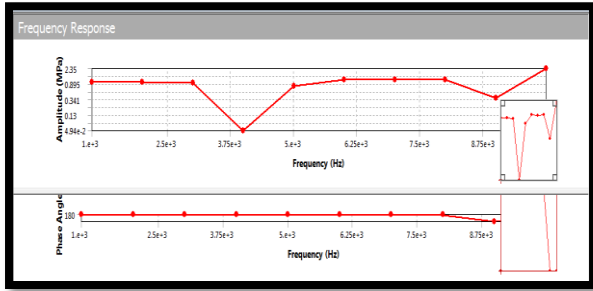


**MATERIALS - CAST IRON
TOTAL DEFORMATION**

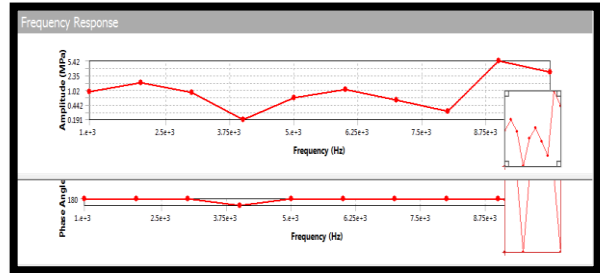
VON-MISES STRAIN



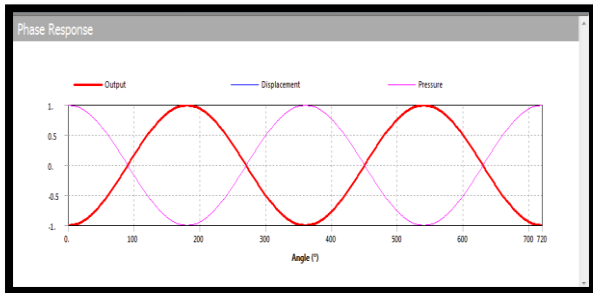
HARMONIC ANALYSIS OF CAMSHAFT MATERIALS - FORGED STEEL STRESS FREQUENCY RESPONSE



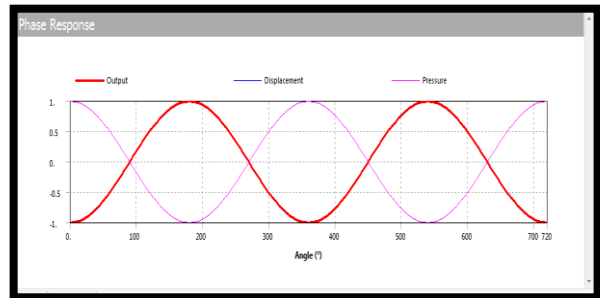
MATERIALS - ALUMINUM ALLOY STRESS FREQUENCY RESPONSE



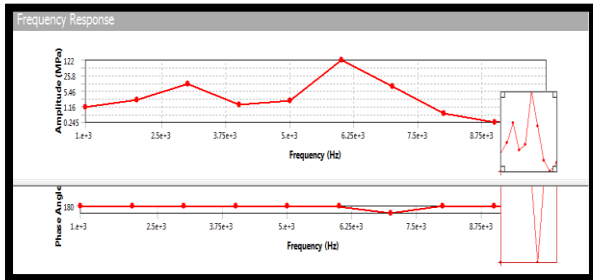
PHASE RESPONSE



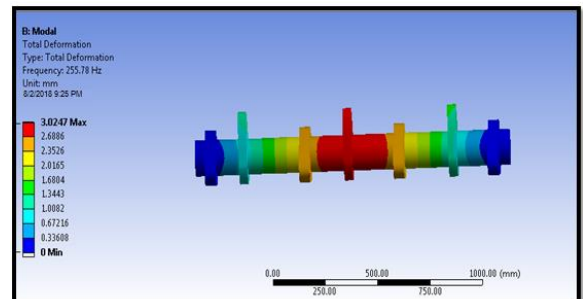
PHASE RESPONSE



MATERIALS - CAST IRON STRESS FREQUENCY RESPONSE

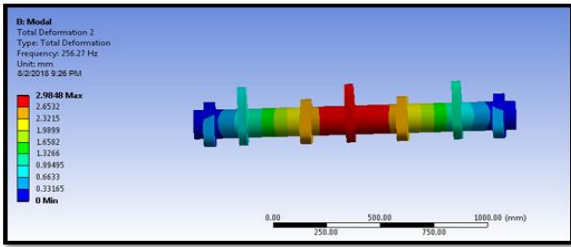


MODAL ANALYSIS OF CAM SHAFT TOTAL DEFORMATION 1

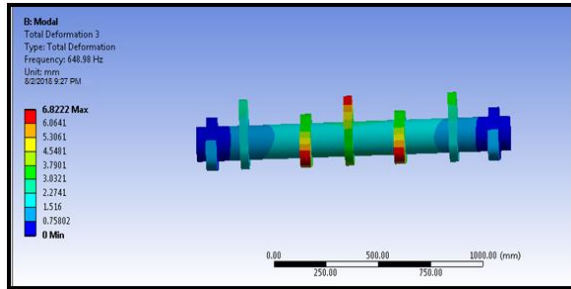


PHASE RESPONSE

TOTAL DEFORMATION 2

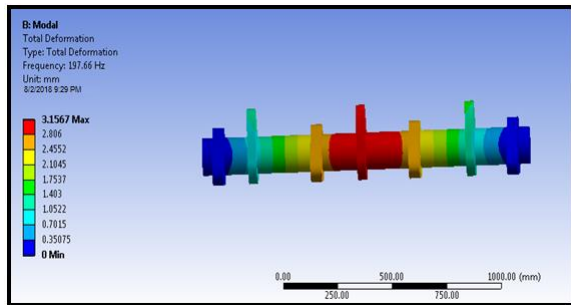


TOTAL DEFORMATION 3

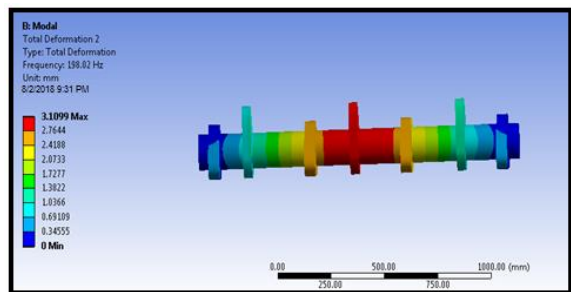


MATERIALS - CAST IRON

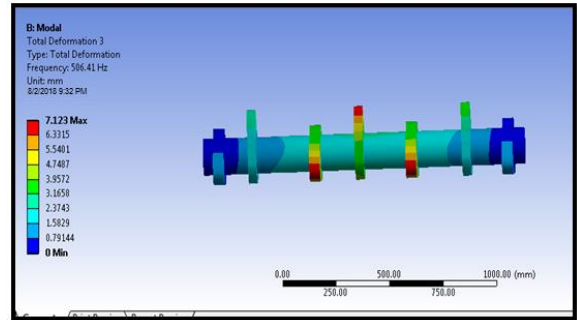
TOTAL DEFORMATION 1



TOTAL DEFORMATION 2

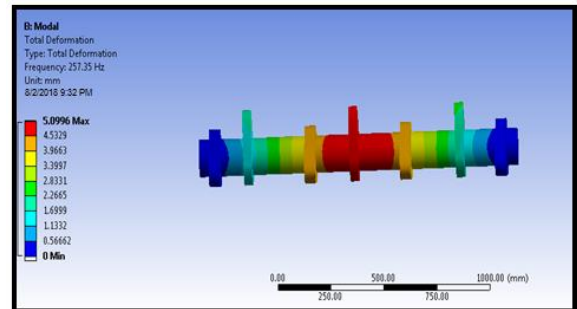


TOTAL DEFORMATION 3

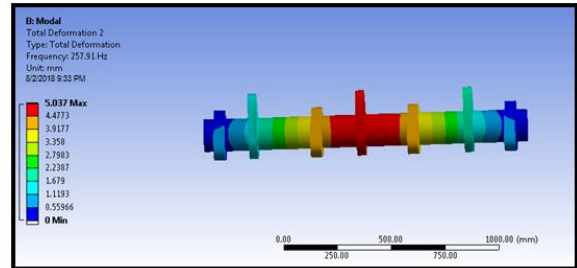


MATERIALS - ALUMINUM ALLOY

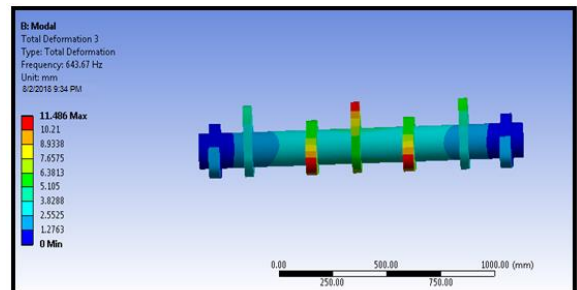
TOTAL DEFORMATION 1



TOTAL DEFORMATION 2



TOTAL DEFORMATION 3



RESULTS TABLE

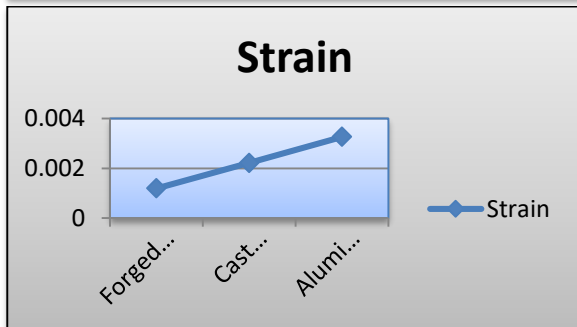
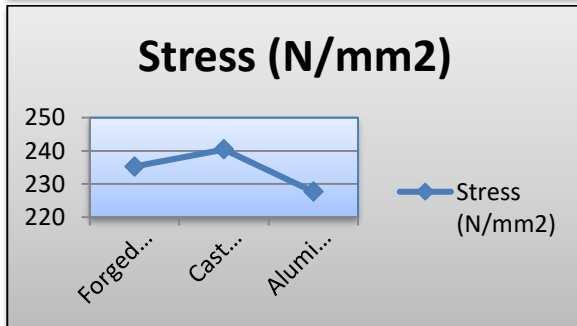
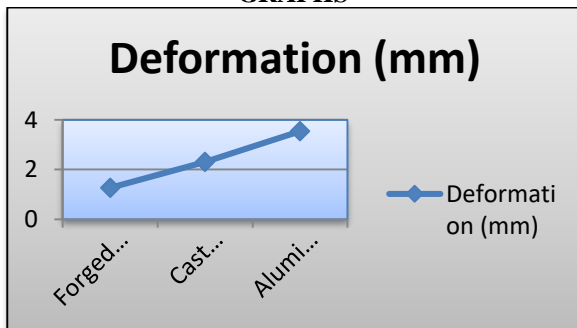
STATIC ANALYSIS RESULTS

Material	Deformation (mm)	Stress (N/mm ²)	Strain
Forged steel	1.268	235.25	0.0011976
Cast iron	2.3145	240.44	0.002219
Aluminum alloy	3.5479	227.69	0.00327

MODEL ANALYSIS RESULTS

Material	Deformation1 (mm)	Frequency (Hz)	Deformation 2 (mm)	Frequency (Hz)	Deformation 3 (mm)	Frequency (Hz)
Forged steel	3.0247	255.78	2.9848	256.27	6.8222	648.98
Cast iron	3.1567	197.66	3.1099	198.02	7.123	506.41
Aluminum alloy	5.0966	257.35	5.037	257.91	11.486	643.67

GRAPHS



3. CONCLUSION

The camshaft is driven by the crankshaft through timing gears cams are made as integral parts of the camshaft and are designed in such a way to open and close the valves at the correct timing and to keep them open for the necessary duration. A common example is the camshaft of an automobile, which takes the rotary motion of the engine and

translates it in to the reciprocating motion necessary to operate the intake and exhaust valves of the cylinders.

By observing the static analysis the stress values are less for aluminum alloy compare with forged steel and cast iron.

By observing the modal analysis the deformation and frequency values are more for aluminum alloy.

So it can be conclude the aluminum alloy is better material for cam shaft.

REFERENCES

1. H. Tada, P. C. Paris and G.R. Irwin, "The Stress Analysis of Cracks Handbook", Del Research Corporation, Hellertown, Penna. (1973).
2. D.E Rooke and D.J. Cartwright, "Compendium of Stress Intensity Factors", Her Majesty's Stationery Office, London (1976).
3. G.C. Sih, "Handbook of Stress Intensity Factors", Institute of Fracture and Solid Mechanics, Lehigh University (1973).
4. E.E. Gdoutos, "Fracture Mechanics: An Introduction", Springer, 2005.
5. Gdoutos, E.E., "Fracture Mechanics Criteria and Applications", Kluwer Academic Publishers, (1990).
6. Murakami, Y. (ed.) , "Stress Intemity Factors Handbook", Pergamon Press. (1987).
7. Majid Mirzaei, "Fracture Mechanics: Theory and Applications", Dept. of Mechanical Eng., TMU, <http://www.modares.ac.ir/eng/mmirzaei>.
8. W.D. Pilkey, "Formulas for Stress, Strain, and Structural Matrices", John Wiley and Sons, 2005.

Design and Fabrication of Multi-Purpose Operations Machine of Drilling, sawing, grinding and Cutting

Vijay Kumar.N, Kiran Chand Kopila

Assistant Professor, Department of Mechanical Engineering, Pace Institute of Technology and Sciences (A), Ongole, A.P.India
Assistant Professor, Department of Mechanical Engineering, Narasaraopeta Engineering College (A), Narasaraopet,A.P. India

Abstract— In an industry a considerable portion of investment is being made for machinery Installation , So in this project we have a proposed a machine which can perform operations like Drilling, Sawing, Grinding and cutting ,these are some operations at different working centres simultaneously, which implies that industrialist has not to pay for machine performing above tasks individually for operation. Multi- Purpose Machine as we call it is a machine that is made especially for the small scale industries, where there is lack of high investment. This Project present the concept of Multi-Function Operating Machine mainly carried out for production based industries. We have developed a conceptual model of a machine which would be machined, we are actually giving drive by using robust high capacity motor to the main shaft, On the main shaft a bevel gear system is used for power transmission along with four shafts to which “scotch yoke mechanism” is directly attached for one shaft, scotch yoke mechanism is used for sawing operation. Before starting our work we have undergone through many research papers which indicates that for a production based industries machine installation is a tricky task as many factor being associated with it such as power consumption (electricity bill per machine), maintenance cost, no. of units produced per machine i.e. capacity of machine, time consumption and many more.

Keywords: Drilling, Sawing, Grinding and cutting, bevel gear system, scotch yoke mechanism.

INTRODUCTION

Multi-operation machine as a research area is motivated by questions that arise in industrial Manufacturing, production planning, and computer control. Consider a large automotive garage with specialized shops. A car may require the following work like replace exhaust system, align wheels and tune up. These three tasks may be carried out in any order. However, since the exhaust system, alignment and tune-up shops are in different buildings, it is impossible to perform two tasks for a car simultaneously. When there are many cars requiring services at the three shops, it is desirable to construct a service schedule that takes the least amount of total time.

Industries are basically meant for Production of useful goods and services at low production cost, machinery cost and low inventory cost. Today in this world every task have been made quicker and fast due to technology advancement but this advancement also demands huge investments and expenditure, every industry desires to make high productivity rate maintaining the quality and standard of the product at low average cost.

Economics of manufacturing: According to some economists, manufacturing is a wealth-producing sector of an economy, whereas a service sector tends to be wealth-

consuming. Emerging technologies have provided some new growth in advanced manufacturing employment opportunities in the Manufacturing Belt in the United States. Manufacturing provides important material support for national infrastructure and for national defence.

Before starting our work we have undergone through many research papers which indicates that for a production based industries machine installation is a tricky task as many factor being associated with it such as power consumption (electricity bill per machine), maintenance cost, no of units produced per machine i.e. capacity of machine, time consumption and many more.

Model of The Machine:

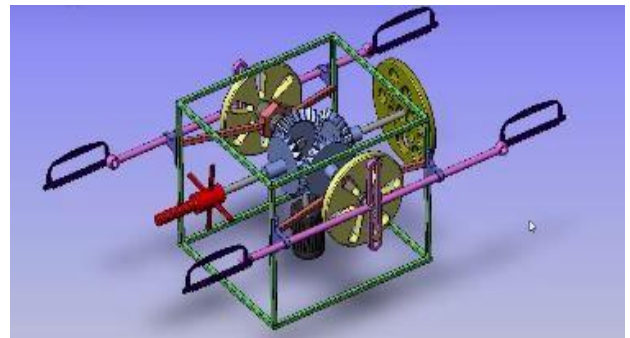


Fig:1 Example of model of the machine

Actual model:



Figure 2: Actual model

Operations Performed by the Machine:
Drilling, Hack saw cutting, Grinding, Wheel cutting

LITERATURE SURVEY

Rather long re-investment cycles of about 15 years have created the notion that innovation in the machine tool industry happens incrementally. But looking at its recent history, the integration of digital controls technology and computers into machine tools has hit the industry in three waves of technology shocks. Most companies underestimated the impact of this new technology. This article gives an overview of the history of the machine tool

industry since numerical controls were invented and introduced and analyzes the disruptive character of this new technology on the market. About 100 interviews were conducted with decision-makers and industry experts who witnessed the development of the industry over the last forty years. The study establishes a connection between radical technological change, industry structure, and competitive environment. It reveals a number of important occurrences and interrelations that have so far gone unnoticed. Recent trends in the machine tool technologies are surveyed from the viewpoints of high speed and high performance machine tools, combined multifunctional machine tools, ultra precision machine tools and advanced and intelligent control technologies.

The crisis is over, but selling machinery remains a tough business. Machine tools nowadays have to be veritable “jack of all trades”, able to handle all kinds of materials, to manage without any process materials as far as possible, and be capable of adapting to new job profiles with maximized flexibility. Two highly respected experts on machining and forming from Dortmund and Chemnitz report on what’s in store for machine tool manufacturers and users.

MODEL & DESIGNING

COMPONENTS DESIGNED FOR THIS MACHINE:

Frame, Scotch yoke mechanism, Bevel gears, Motor, Radial bearings and cups, Shafts, Grinding wheel, Wheel cutter, Drill chuck and bit, Clamp.

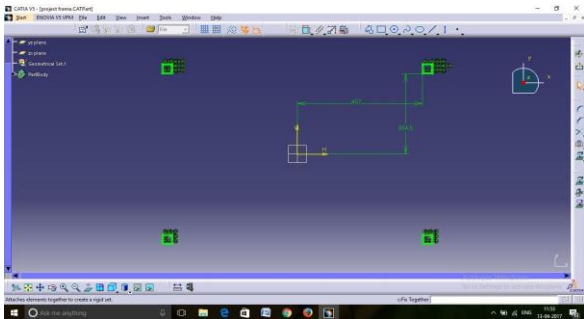


Fig 3: Indicates length =3 ft and width =2ft

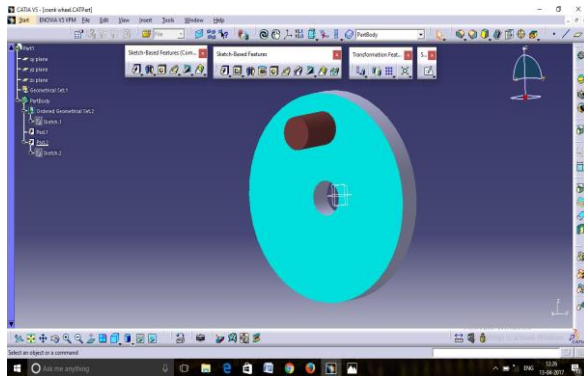


Fig 7: Designed part of crank and stud of scotch yoke mechanism

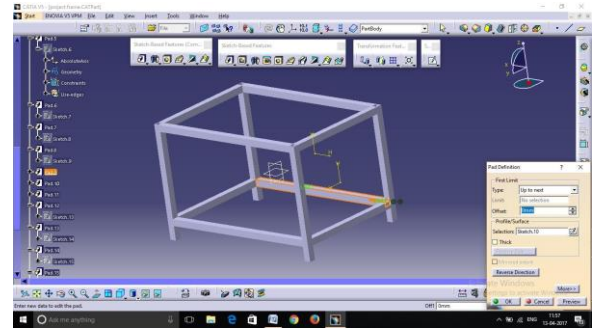


Fig 4: Indicates Height of the frame: 2 feet 10inches

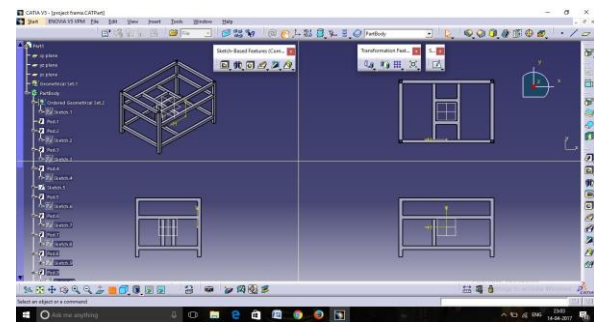
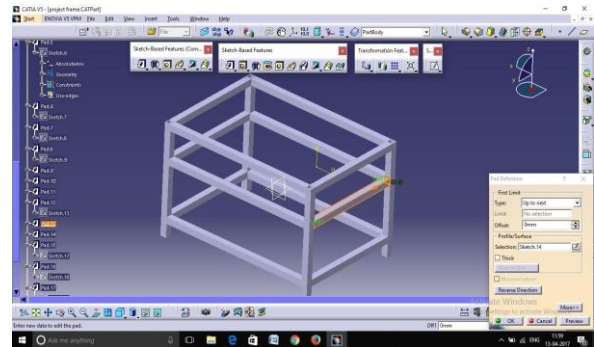


Fig 6: Final structure of frame

Design of scotch yoke mechanism:

- Outside Diameter of crank : 150mm
- Inside diameter of Crank : 25mm
- Thickness of the crank : 20mm
- Diameter of the stud : 24mm
- Height of the stud : 40mm

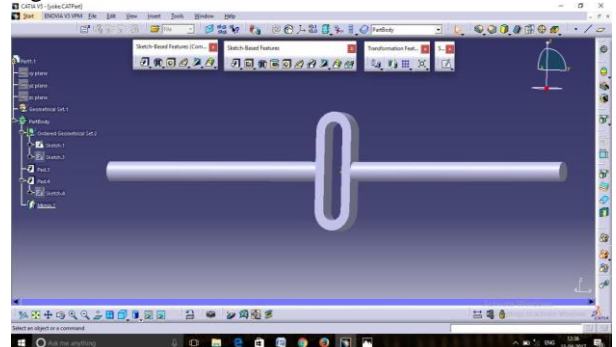


Fig 8: Designed part of yoke and connecting rod of scotch yoke mechanism

Inner diameter of yoke : 25mm

Outer diameter of yoke : 50mm
 Thickness of yoke : 12.5mm0
 Height of yoke : 25mm
 Diameter of shaft at yoke : 25mm
 Length of the shaft at yoke :2.5 feet or 762mm at both sides

Design of main bevel gear

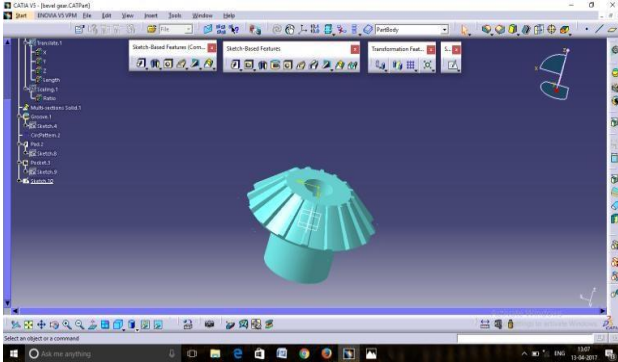


Fig 9: Designed part of main bevel gear

Outside diameter of the gear: 90mm
 Inside diameter of the gear: 55mm
 Height of gear : 18 mm
 Height of the hub : 40mm
 No of teeth 16

Design of sub bevel gears:

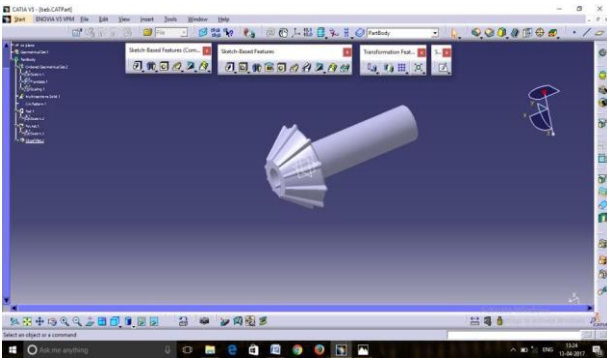


Fig 10: Designed part of sub bevel gear

Outside diameter of the gear: 56mm
 Inside diameter of the gear: 35mm
 Height of gear : 18 mm
 Height of the hub : 40mm
 No of teeth 10

Design of motor:

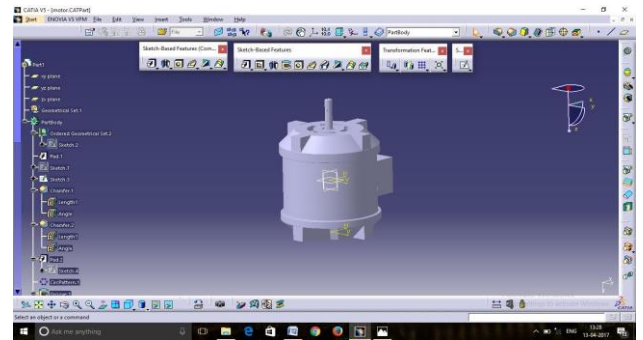
Height of the body : 177mm
 Outside diameter of body : 160mm
 Length of the motor shaft : 60mm

Fig 11: Design of motor:

Design of radial bearing and cup:

Length of the radial bearing: 13mm
 Internal diameter of radial bearing: 30mm

External diameter of radial bearing: 55mm



Distance of ball from the centre: 21.25mm
 Diameter of the ball in the bearing: 8mm
 Internal diameter of cup : 55mm
 External diameter of cup: 60mm

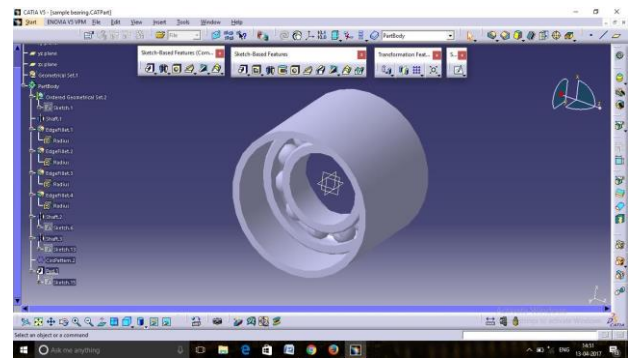


Fig 12: Designed part of radial bearing and cup

Design of shaft:

Diameter of the shaft: 24mm
 Length of the shaft1 and3 :600mm
 Length of the shaft2 and4:350mm

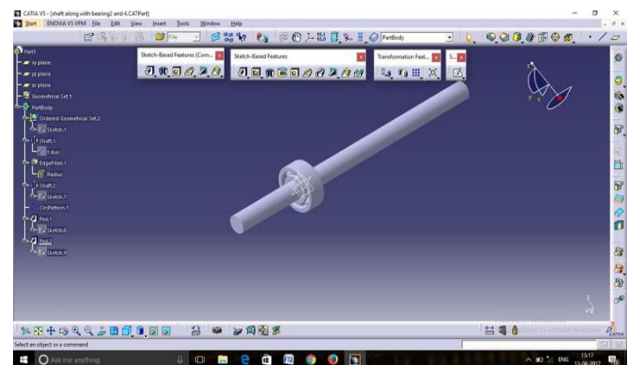


Fig 13: Designed part of second and fourth shaft

Design of the grinding wheel:

Internal diameter of grinding wheel : 22mm
 External diameter of grinding wheel: 150mm

Thickness of grinding wheel : 20mm

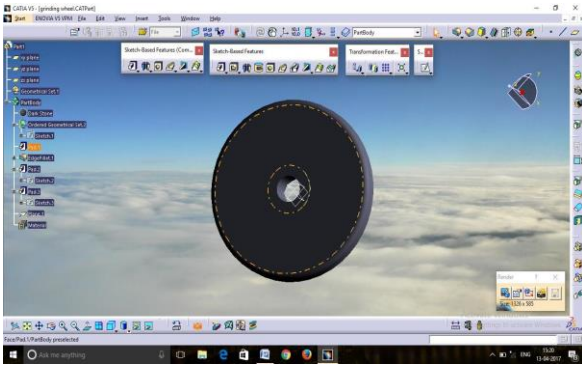


Fig 14: Designed part of grinding wheel

Design of wheel cutter:

Diameter of the wheel: 150mm
 Thickness of the wheel: 5mm
 No of teeth: 60

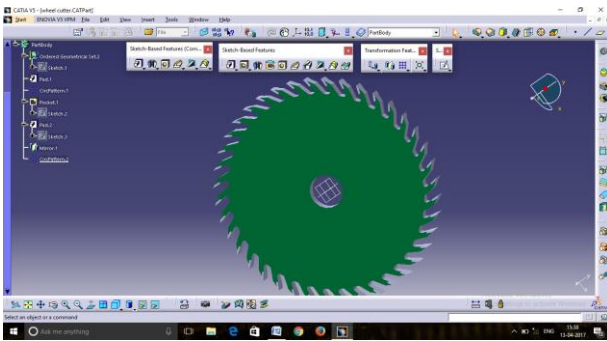


Fig 15: Designed part wheel cutter

Design of drill chuck:

Length of the drill chuck: 150mm
 Length of the drill bit: 50mm
 Outer diameter of drill chuck: 80mm
 No of teeth on the chuck: 25
 No of jaws: 3

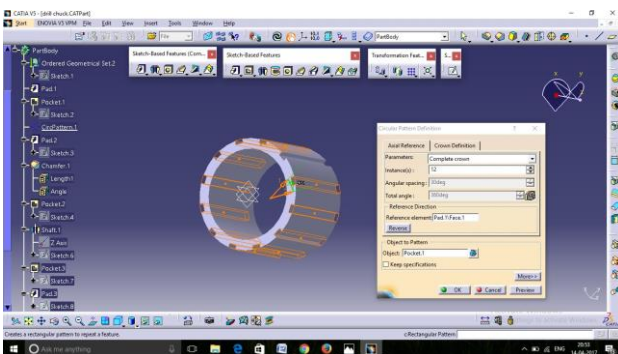


Fig 16: Outer shell of drill chuck

Drill chuck and Bit:

Length of the drill chuck : 150mm
 Length of the drill bit: 50mm

Outer diameter of drill chuck: 80mm
 No of teeth on the chuck: 25
 No of jaws: 3

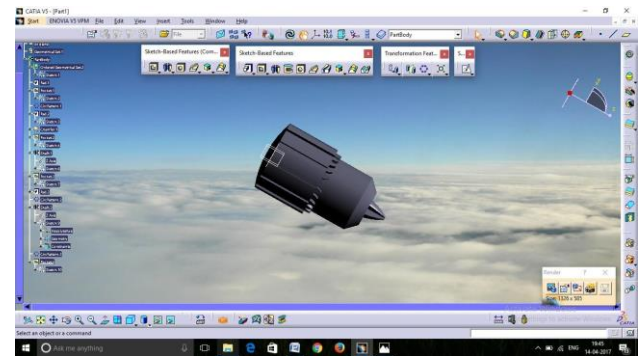
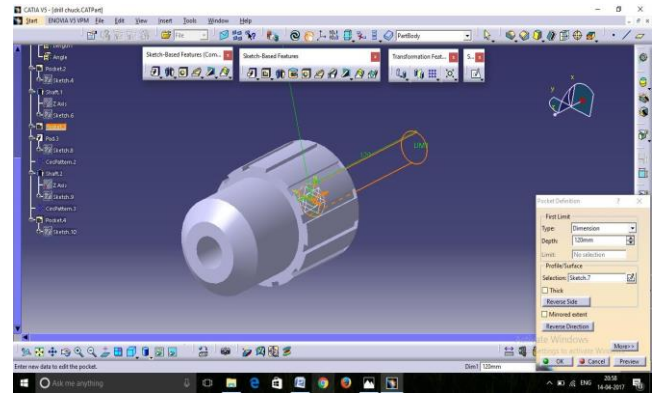


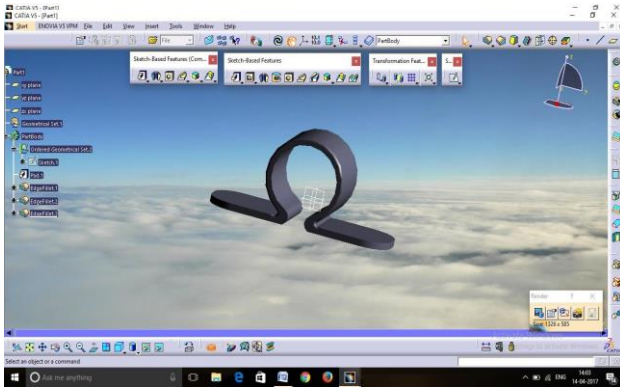
Fig 19: Designed part of drill chuck

Design of hack saw fitted to yoke:

Length of hack saw: 300mm
 Height hack saw : 150mm
 Diameter of inner ring: 45mm
 Diameter of outer ring: 50mm
 Blade length : 140mm
 No blade teeth 130
 Thickness of blade: 3mm

Design of clamp:

Internal diameter of the clamp : 25mm
 External diameter of the clamp : 30mm
 Total height of the clamp : 27mm
 Length of the clamp : 70mm



RESULT

By using this machine we can do operation at one place we can reduce the time consumption as well as power this is well suited for the small scale industries as well as large scale industries. And another advantage that this machine have is, it can perform single operation as well as multi operation at one time.

Photos taken during the operation:



Fig 27: Drilling operation on wood

CONCLUSION

We can see that all the production based industries wanted low production cost and high work rate which is possible through the utilization of multi-function operating machine which will less power as well as less time, since this machine provides working at different centre it really reduced the time consumption up to appreciable limit.

In an industry a considerable portion of investment is being made for machinery installation. So in this paper we have proposed a machine which can perform operations like drilling, sawing, grinding at different working centers simultaneously which implies that industrialist have not to pay for machine performing above tasks individually for operating operation simultaneously.

This project has wide range of scope in the small scale industries. In coming future, this type of lightweight and potable machine will be implemented in every small and large scale industries. This type of machine can be used anyone due to its simplicity of working and doing wide range of operation. n be used by anyone due to its simplicity of working anddoing wide range of operations

REFERENCES

[1].Heinrich Arnold1”The recent history of the machine tool industry and the effects of technological change “University of Munich, Institute for Innovation Research and Technology Management, November 2001.
 [2].Dr. Toshimichi Moriwaki “Trends in Recent Machine Tool Technologies” Professor Department f Mechanical Engineering Kobe University ,NTN Technical Review No.74(2006).
 [3].T. Moriwaki “Multi-functional machine tool” ,Department of Industrial and Systems Engineering, Setsunan University, Neyagawa, Japan CIRP Annals - Manufacturing Technology
 DOI:10.1016/j.cirp.2008.09.004.
 [4]. Frankfurt am Main “Multi-purpose machines ensure enhanced “, 1 January 11. [5]. “Selecting and Planning the Process of Manufacture: Dr. Pulak Pandey.
 [6]. Dharwa Chaithanya Kirthikumar, “A Research on Multi-Purpose Machine”, International Journal for Technological Research in Engineering (Vol.1, Issue.1, ISSN: 2347-4718) (2013).
 [7]. S.G.Bahaley, Dr.A.U.Awate, S.V.Saharkar, “Performance Analysis of Pedal Powered Multipurpose Machine”, International Journal of Engineering Research and Development (IJERD) (Vol.1, Issue.5, eISSN: 2278-0181) (2012).

Preparation of Al/Brass Composite (MMC) By Using Stir Casting Technique and Its Characterization

K.Krishna kishore, C.Sai Ram Kumar

Department of Mechanical Engineering, Gudlavalleru Engineering College, Gudlavalleru, A.P. India

Abstract— A new composite material is prepared with aluminum as base metal and Brass as reinforcement which is particulate reinforced composite type material. Aluminum composite has been prepared in a view to enhance strength, ductility, effective transfer of load. Al-Brass composite is prepared through stir casting technique at 2, 4 & 6 wt % .The mechanical behaviour of composite is studied in terms of hardness and the microstructure was observed with optical metallurgical microscope. The mechanical properties of the composites are examined by conducting tests like compression test, tensile test and hardness test to understand the relationship between the weight percentages of reinforcement on the mechanical characteristics of the manufactured AMCs. This work divulges that the addition of reinforcement increases the mechanical properties like tensile strength, Vickers hardness and decrease in compressive strength.

1. Introduction

Composite materials are widely accepted all over the world due to the excellent properties such as wear resistance, specific strength & stiffness. Metal Matrix Composites (MMCs) have been used in many applications due to its modulus, hardness properties and high strength .Various engine parts can be made of MMCs with aluminum as a base metal due to its chemical composition of Al matrix different mechanical properties can be obtained. Aluminum matrix composites (AMC) are considered to meet the requirements of various industries. General reinforcing elements used in AMCs are silicon carbide, Al₂O₃ etc. Metal matrix composites (MMC) refer to materials consisting of a ductile metal or alloy matrix in which some sized reinforcement material is implanted. These materials combine metal and ceramic features, i.e., ductility and toughness with high strength and modulus. Thus, metal matrix composites are suitable for production of materials with high strength in shear/compression processes and high service temperature capabilities. They show an extraordinary potential for application in many areas, such as aerospace, automotive industries and other Metal Matrix composites include Al/ Al₂O₃, Al/SiC, Fe-Cr/ Al₂O₃, Ni/ Al₂O₃, Co/Cr, Fe/MgO, Al/CNT, Mg/CNT etc.. They have been developed in recent years. Metal Matrix Composites have emerged as a class of material capable of advanced structural, aerospace, automotive, electronic, thermal management and wear applications. A composite material is a material consisting of two or more physically and or chemically distinct phases. The composite generally has superior characteristics than those of each of the individual components. Usually, the reinforcing component is distributed in the continuous or matrix component. When the matrix is a metal, the composite is termed a metal matrix composite (MMC).

Stir casting is currently the most popular commercial method of producing aluminium based composites. Fabrication of aluminum and its alloys based casting composite materials via stir casting is one of the prominent and economical technique for development and processing of MMCs and widely used for applications that require high production volumes and low cost. Stir casting is suitable for manufacturing composites with up to 30% volume fractions of reinforcement allows for the use of conventional metal processing methods with the addition of an appropriate stirring system such as mechanical stirring; ultrasonic or electromagnetic stirring; or centrifugal force stirring, to achieve proper mixing of reinforcement into melt which depends on material properties and process parameters

2. Materials and Methods

In the present investigation Aluminium was used as a matrix material. The main application of Aluminium is in aircraft industry in producing numerous elements in the construction of aircrafts, and to make intricate shapes and patterns of aircraft industry. Aluminium is most widely used due its low weight, density, machinability, workability and can be rolled, forged and extruded easily. Individually Aluminium shows poor stiffness and tribological properties. Hence if the Aluminium matrix is combined with other elements, required properties can be obtained. The chemical composition of the matrix material is as follows. Al-99.77; Cu-0.005; Fe-0.095; Mg-0.005; Mn-0.011; Si-0.083; Ni-0.015; Zn-0.013;

Reinforcement material

The brass is used as reinforcement in this project due to its applications includes its excellent corrosive resistance, and its joining, polishing and finishing characteristics. The presence of Aluminum makes brass extremely resistance to many kinds of moisture such as heat exchangers and condensers.

3. Experimental Details

In this project composites are prepared using stir casting technique. In this technique reinforcement (Brass) particulates were dispersed in pure aluminum matrix with 2%, 4% and 6% weight fractions. The aluminum was melted in vertical melt furnace at 660C. By using rotating impeller which runs at 400rpm at good vortex is created at the middle of the melt. Mean while the brass reinforcement is preheated to 3000C. when the melt reaches to 7000C preheated particles are added at good vortex. After 90 seconds of stirring time, melt was poured into the preheated mould. These ingots are homogenized by keeping them in heat treatment furnace at 1000C for 24 hours.



Fig 1: Stir Casting Equipment



Fig 2: Muffle furnace



Fig 3: Ingots in die

Hardness test

Hardness test were carried on Vickers hardness test by taking 0.5 kg load. Hardness value was finalized by taking average of six reading for each sample.

Table: 1 Vickers Hardness values of different weight fractions.

S.no	Percentage of Reinforcement	Hardness value
1	0	21
2	2	76
3	4	89

Tensile test

A tensile test, otherwise known as strain test, exposes the specimen to a controlled strain until the scientific investigation of the materials fails. The results from the experiments are often used to select material applications, quality control and foresee how the material will respond under different loads.

Tensile strength of composites at room temperature was determined using computerized Universal test machine (400KN) with an electronic extensive meter as per ASTM standards online plotting of load Vs extension was done continuously through a data acquisition system.

Table: 2 Tensile testing machine parameters

S.No	Item	Description
1	Make	Mechatronic control system
2	Model	MECH C.S/UTE 40
3	Maximum Capacity	400KN
4	Clearance for tensile test at fully descended working piston	50 – 700 mm

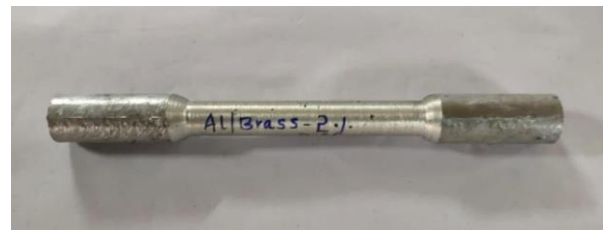


Fig 4: Al-Brass - 2%



Fig 5: Al-Brass - 4%



Fig 6: Al-Brass - 6%

4. RESULTS AND DISCUSSIONS

Metallographic studies

Optical metallurgical microscope was taken to observe the microstructures of the various samples used in this investigation. The optical microstructures of the fabricated aluminum matrix composites with different weight % of brass reinforcement are shown in fig 7 a, b and c. The microstructures reveal that brass particles are uniformly distributed in the aluminum matrix for 4 and 6 wt %. This behaviour can be attributed to the effective stirring action and the use of appropriate process parameters, in addition to the greater wettability of the brass particles with the aluminum composite. Figures 7a (100X), b (200X) shows the microstructural images of composite material at 2% reinforcement at various magnification.

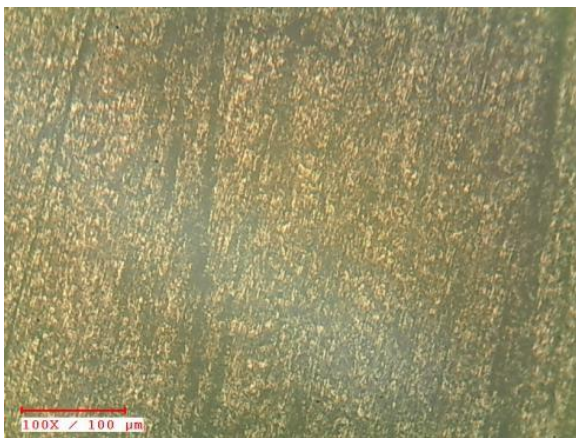


Fig7.a 100X

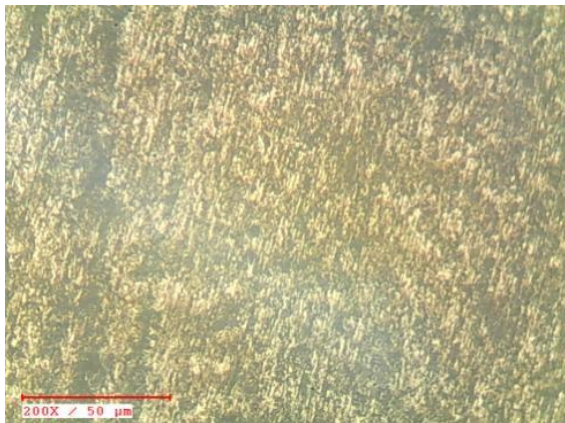
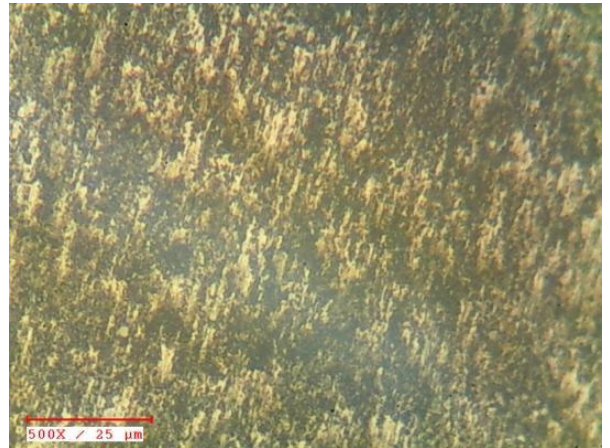
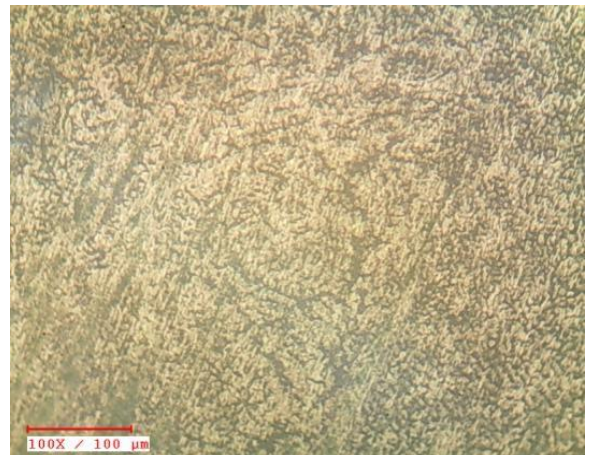


Fig.7b 200X



Figures 8a (100X), b (200X), c (500X) shows the



microstructural images of composite material at 4% reinforcement.

Fig8.a 100X

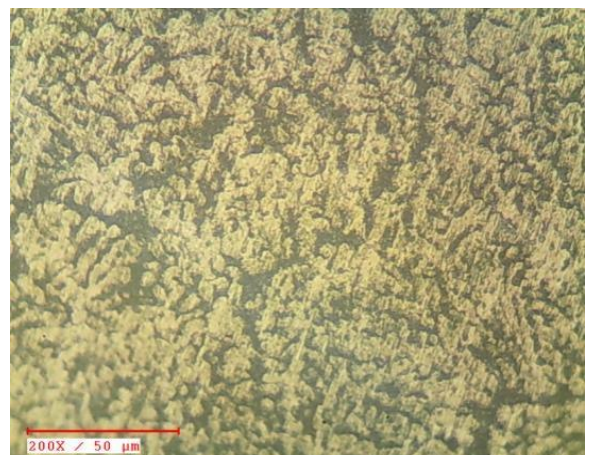


Fig.8b 200X

The following figure 10 shows the effect of reinforcement content on hardness of the composites. Hardness increases with increase of amount of reinforcement contents.

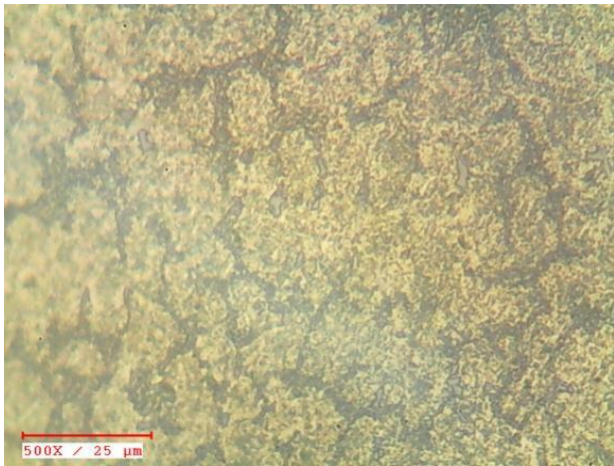


Fig.8b 500X

Figures 9 a (100X), b (200X), c (500X) shows the microstructural images of composite material at 6 % reinforcement

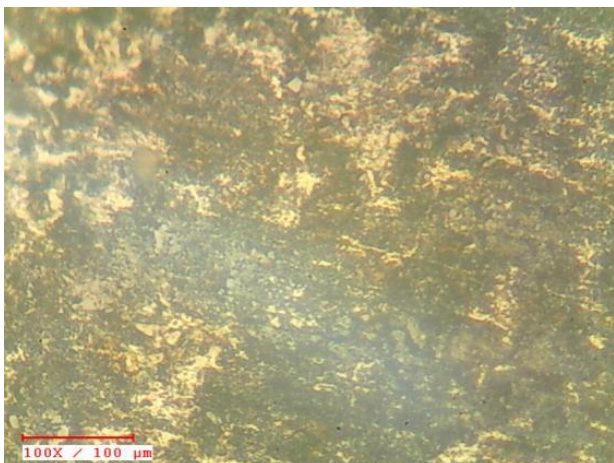


Fig9.a 100X

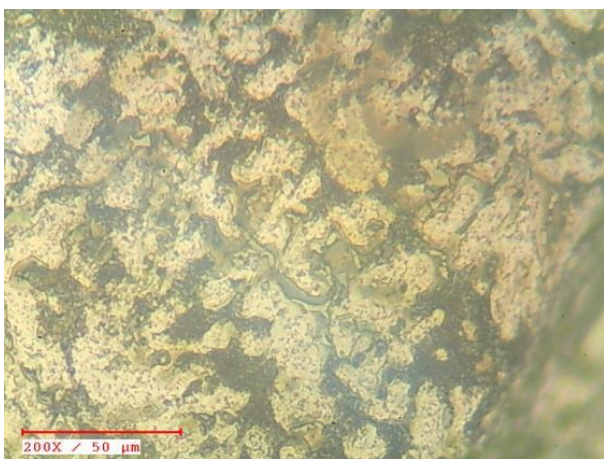


Fig9.b 100X

Hardness studies

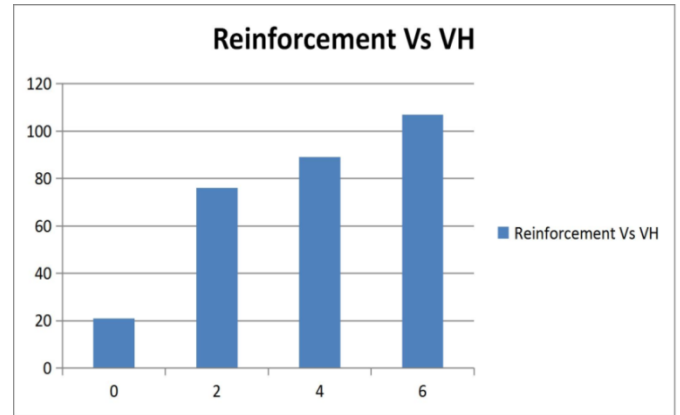


Fig 10. Hardness variation of composites

Tensile studies

The tensile strength results of the Al-Brass composites of reinforcement as 2%, 4% & 6% shown in figure. It is observed that ultimate strength is increased by increasing the percentage of brass particles in the composite. This is due to better interfacial bonding between the matrix and reinforcement which transverse and distributes the load from the matrix to the reinforcement. Therefore the reinforcement particle tends to bear the entire load that has acted upon the matrix. The addition of brass particles in the matrix induces much strength to matrix composite by offering more resistance to tensile stresses.

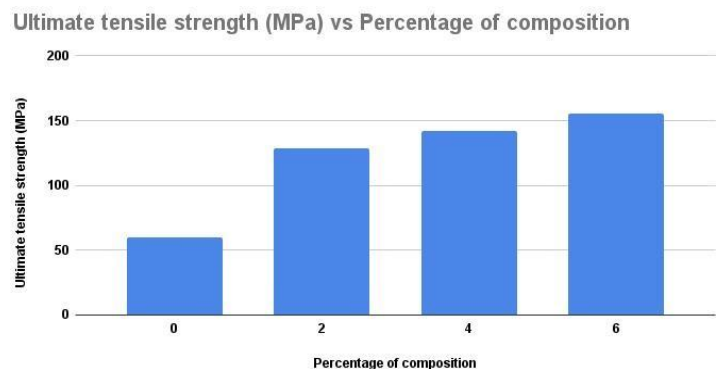


Fig:11 Comparison between Ultimate tensile strength & Percentage of composition

Pure aluminium had ultimate tensile strength of 60MPa and elongation percentage of 30% during increase in weight percentage of reinforcement as 2%, 4% & 6%. Ultimate strength was increase but elongation percentage had increased.

5. CONCLUSIONS

In the present study the aim is to prepare MMC with help of stir casting process and its characterization. For this pure Al is selected as matrix phase while brass particles (2, 4 and 6 wt. %) act as reinforcement with help of stir casting process. We had successfully manufactured composites and the following results were observed.

- In Vickers hardness test, the hardness of the composites increases with increase in brass content compared with the matrix. The maximum hardness attained at 6% in the fabricated composites.
- The tensile strength of the composites increases with increase in reinforcement content compared with the matrix. The maximum compressive strength attained at 6% brass in the fabricated composites.
- The micro structures reveal that brass particles are uniformly distributed in the aluminum matrix for 4 and 6 wt %. This behaviour can be attributed to the effective stirring action and the use of appropriate process parameters, in addition to the greater wettability of the brass particles with the aluminum composite.

REFERENCES

1. D. Sujan, Z. Oo, M. E. Rahman, M. A. Maleque, C. K. Tan "World Academy of Science, Engineering and Technology International Journal of Chemical, Molecular, Nuclear, Materials and Metallurgical Engineering Vol:6, No:8, 2012, "Physio-mechanical Properties of Aluminium Metal Matrix Composites Reinforced with Al₂O₃ and SiC "
2. Vencl A, Bobic I, Arostegui S, Bobic B. "Structural, mechanical and tribological properties of A356 aluminium alloy reinforced with Al₂O₃, SiC and SiC + graphite particles". J Alloys Compd 2010; 506:631–9.
3. Luan BF, Hansen N, Godfrey A, Wu GH, Liu Q. "High strength Al– Al₂O₃p composites: Optimization of extrusion parameters". Materials Design, 2011; 32: 3810–3817.
4. Manoj Singla, D. Deepak Dwivedi, Lakhvir Singh, Vikas Chawla, "Development of Aluminium Based Silicon Carbide Particulate Metal Matrix Composite" Journal of Minerals & Materials Characterization & Engineering, Vol. 8, No.6, pp 455-467, 2009
5. Tjong SC. "Recent Advances in Discontinuously Reinforced Aluminum Based Metal Matrix Nano composites", Composite Materials Research Progress (ISBN: 1-60021-994-2), Editor: Lucas P. Durand, Nova Science Publishers, Inc, 2008; pp 275-296.
6. Law E, Pang SD, Quek ST. "Discrete dislocation analysis of the mechanical response of silicon carbide reinforced aluminum nano composites". Composites, 2011; Part B 42: 92–98.
7. Senthilkumar V, Omprakash BU. "Effect of Titanium Carbide particle addition in the aluminium composite on EDM process parameters". J Manufact Processes, 2011; 13: 60–66.
8. Kumar BA, Murugan N. "Metallurgical and mechanical characterization of stir cast AA6061-T6–AlNp." Composite Materials Design, 2012; 40: 52–58.

Multi Optimization of Process Parameters using Grey Relational Analysis

¹Gopalakrishnaiah Peteti, ²Venkaiiah Mandula and ³Bharathi Penumalla

¹Department of mechanical engineering, PVP Siddhartha Institute of Technology, Kanuru, Krishna, A.P. India

²Department of mechanical engineering, Narasarao peta engineering college narasaraopet, Guntur, A.P. India

³Department of mechanical engineering, Acharya Nagurjuna University Guntur, A.P. India

Abstract: This project reports on the optimization of turning process on all geared lathe by the effects of machining parameters applying Taguchi methods to improve the quality of manufactured goods, and engineering development of designs for studying variations. The main objective of today's manufacturing industries is to produce the products with low cost and high quality. In order to change the quality of machining products selection of optimal machining parameters plays an important role. Aluminum 8011 alloy is used as the work piece material and digital Lathe tool dynamometer with computer interface via LAB VIEW based software for calculating cutting forces in three directions for carrying out the experimentation to optimize the Material Removal Rate and the Surface Roughness. There are three machining parameters i.e., Spindle speed, Feed rate, Depth of cut. Nine experiments are done by varying all the parameters.

Taguchi method forces are the importance of studying in minimization of quality characteristic variation due to uncontrollable parameter. The surface roughness was considered as the quality Optimum value of each parameter will be obtained. The analysis also shows that the predicted values and calculated values are very close. This indicates that the developed model can be used to predict the surface roughness in the turning operation of Aluminum 8011 alloy. Or Abstract. (Abstract)

1. INTRODUCTION

Aluminium resists the kind of progressive oxidization that causes steel to rust away. The exposed surface of aluminum combines with oxygen to form an inert aluminum oxide film only a few ten-millionths of an inch thick, which blocks further oxidation. And, unlike iron rust, the aluminum oxide film does not flake off to expose a fresh surface to further oxidation. If the protective layer of aluminum is scratched, it will instantly reseal itself.

Cast and wrought alloy nomenclatures have been developed. The Aluminum Association system is most widely recognized in the United States. Their alloy identification system employs different nomenclatures for wrought and cast alloys, but divides alloys into families for simplification. For wrought alloys a four-digit system is used to produce a list of wrought composition families as follows: The thin oxide layer itself clings tightly to the metal and is colorless and transparent—invisible to the naked eye. The discoloration and flaking of iron and steel rust do not occur on aluminum

It is convenient to divide aluminum alloys into two major categories: wrought compositions and cast compositions. A further differentiation for each category is based on the primary mechanism of property development. Many alloys respond to thermal treatment based on phase

solubilities. These treatments include solution heat treatment, quenching, and precipitation, or age, hardening. For either casting or wrought alloys, such alloys are described as heat treatable. A large number of other wrought compositions rely instead on work hardening through mechanical reduction, usually in combination with various annealing procedures for property development. These alloys are referred to as work hardening. Some casting alloys are essentially not heat treatable and are used only in as-cast or in thermally modified conditions unrelated to solution or precipitation effects..

S. S Abhutakeer P. V Mohanram G. Mohan Kumar [1] In this paper, Experiments were conducted on CNC lathe using CCGT-0930FL carbide turning insert, machining variables such as cutting tool vibration in tangential and axial direction were measured in CNC machining processes based on the vibration signal collected through a Lab VIEW data acquisition system and controlled by using Viscoelastic material (VEM) neoprene. The effect of cutting parameters such as cutting speed, depth of cut and feed rate on machining variables is evaluated. The testing result showed that the developed method was successful.

Julie and Joseph [2] have been trying to demonstrate tool condition monitoring approach in an end-milling operation based on the vibration signal collected through a low-cost, microcontroller-based data acquisition system.

Marlon C. Battery and Hamid R. Hamidzadeh [3] has done analytical and experimental vibration analyses for a lathe system to detect the possibility of faults and to develop an accurate cutting process. The vibration signatures were analyzed to determine cause of inaccuracy in the manufacturing process and faulty components. Problem causing components for several case studies (different speeds feed rate and tool lengths) were identified.

Kirby and Chen [4] the researchers determine mean amplitude of vibration using accelerations in both directions along the axis. There have been many investigations on vibration prediction and controlling based on periodic measurements of various machining conditions using accelerometer and active vibration controller.

S. Saravanan, G.S. Yadava and P.V. Rao [5] In this study, critical subsystems and components have been identified for lathes using failure data. The application of condition monitoring techniques like vibration, acoustic emission (AE) and surface roughness monitoring have been successfully implemented for diagnosing faulty bearings in a lathe. they were concluded that Headstock subsystem is critical because it faces a longer downtime and frequent failures of components like spindle bearings and gears for

defective bearing conditions, overall vibration levels at headstock spindle beatings are higher than those in defect free lathes. This increase in vibration level is much greater at higher feed and depth of cut values. For defective beating conditions, significant peaks at the beating fault frequencies are observed. Larger sized contamination particles increase surface waviness considerably. As a result, the vibration level increased considerably at larger particle sizes. AE levels show an increasing trend with an increase in feed rate and depth of cut. For defective bearing conditions, AE levels are higher than those measured under healthy conditions. The increase in AE levels is much greater for higher values of feed and depth of cut. For defective bearing condition, surface roughness value increases sharply.

Robert X. Gao [6] Extensive research over the past decade has turned neural networks into an indispensable tool for solving a wide range of problems in both scientific labs and on the factory floor. In the specific areas of machine condition monitoring, fault diagnosis, and remaining service life prognosis, neural networks will play an increasingly important role, and its ability will be continually enhanced through other innovative and complementary technologies. Research is continuing in the author's group, with the ultimate goal to develop effective and efficient bearing condition monitoring and diagnostic techniques that can be applied to solving real world problems.

Amit R Patel [7] in this paper Test rig for vibration monitoring of bearing have been designed. The design of test rig includes design of Shaft, Bearing selection, pedestal selection, motor selection, and base preparation. A 3-D model have been developed using Pro-engineer modeling software. The vibration signals generated by the healthy/faulty bearing can be captured by the accelerometer mounted on the test bearing. The analysis of the vibration signal is useful for the condition monitoring of rolling Element bearings.

Surt Reddy Dr. S. P. Gupta, Dr. Vinod Kumar [8], in this paper a remote condition monitoring system has been developed using Lab VIEW. This developed system enables the transfer of the digital data simultaneously from the plant location to the several remotely placed control stations through internet or any other transmission networks like LAN, WAN e.tc. Particular attention has been paid to the wavelet analysis of the vibration signal for demonstrating the condition monitoring of the induction motor. The developed system has been tested for the bearing fault identification of the Laboratory test motor. A key feature of this work is the development of the sophisticated GUI at the server and the client locations thus facilitating the operators at both the ends with not only customized and user friendly but also efficient remote condition monitoring system.

Grey relational method extensively used in multiple objective optimization problems [8 &9]. The detailed procedure of the GRA optimization is discussed here. The foremost step is the evaluation of S/N ratio from the experimental data starting from 0 to 1.

2. GRE RELATIONAL ANALYSIS APPROACH

Then after Grey relation Normalization, Grey relational coefficient (GRC) and resolve of Grey relational grade (GRG) are to be evaluated. The experimental data is used to

estimate the grey relation normalization smaller-is-better criterion is given by equation (1).

$$x_i(k) = \frac{y_i(k) - \min y_i(k)}{(\max y_i(k) - \min y_i(k))}$$

S/N ratio larger-is-better criterion is applied for work piece displacement by equation (2)

$$x_i(k) = \frac{\max y_i(k) - y_i(k)}{(\max y_i(k) - \min y_i(k))} \quad (2)$$

where $x_{-i}(k)$ is the value after Grey relational generation, $\min y_{-i}(k)$ is the smallest value of $y_{-i}(k)$ for the k th response, and $\max [y]_{-i}(k)$ is the largest value of $y_{-i}(k)$ for the k th response. After normalizing the new order, the resulting step is to find out the Grey relational coefficients $\epsilon_{-i}(k)$.

$$\epsilon_{-i}(k) = \frac{\Delta_{\min} + \phi \Delta_{\max}}{\Delta_{oi}(k) + \phi \Delta_{\max}} \quad (3)$$

where $\Delta_{oi} = |x_{oi}(k) - x_{-i}(k)|$ = change of entire value $x_{oi}(k)$ and $x_{-i}(k)$; ϕ is individual coefficient. Grey relational is the average response of each grey relational coefficient. Grey relational grade γ_i can be estimated by eq (4) and is given below.

$$\gamma_i = \frac{1}{n} \sum_{k=1}^n \epsilon_{-i}(k) \quad (4)$$

n stands for the number of process response.

D.Vishnu Vardhan Reddy (2016) [9], The Taguchi technique and Genetic algorithm (GA) for predicting the responses of turning operation on CNC lathe machine for EN19steel. The number of experiments has been carried out using Taguchi's orthogonal array in the design of experiments (DOE). The cutting parameters are spindle speed, feed rate and depth of cut. The Analysis of Variance (ANOVA) and Signal-to-Noise ratio were used to study the performance characteristics in turning operation. The accurate mathematical model has been developed using genetic algorithm. The research showed acceptable prediction results for the developed model.

TABLE I. input Process parameters values

S.NO.	input			Output		
	SPEED	FEED	DOF	CF	MRR	SR
1	315	0.002	0.2	2.4237	0.0134	2.2880
2	315	0.003	0.4	4.2137	0.0285	2.2856
3	315	0.004	0.6	8.0463	0.0663	2.9063
4	775	0.002	0.4	3.0622	0.0663	1.5346
5	775	0.003	0.6	6.9265	0.2101	3.5620
6	775	0.004	0.2	4.2646	0.0750	4.3636
7	1200	0.002	0.6	15.0742	0.3875	2.8330
8	1200	0.003	0.2	4.3426	0.1851	1.7216
9	1200	0.004	0.4	13.3500	0.4415	2.1740

TABLE II. S/N Ratio values

S.NO.	S/N RATIO		
	CF	MRR	SR
1	7.689	-37.458	-7.189
2	12.493	-30.903	-7.180
3	18.112	-23.570	-9.267

4	9.721	-23.570	-3.720
5	16.810	-13.551	-11.034
6	12.598	-22.499	-12.797
7	23.565	-8.235	-9.045
8	12.755	-14.652	-4.719
9	22.510	-7.101	-6.745

TABLE III. Grey relational coefficient values

CF	GRC		GRG	Rank
	MRR	SR		
1.000	1.000	0.447	0.816	1
0.623	0.698	0.447	0.589	3
0.432	0.522	0.562	0.506	6
0.796	0.522	0.333	0.551	4
0.465	0.388	0.720	0.525	5
0.618	0.504	1.000	0.707	2
0.333	0.342	0.547	0.408	8
0.610	0.400	0.360	0.457	7
0.349	0.333	0.429	0.370	9

TABLE IV ANOVA ANALYSIS

Source	DF	Adj SS	Adj MS	F-Value	P-Value	% Contribution
SPEED	2	1.328	0.6638	0.72	0.582	20.550
FEED	2	1.347	0.6735	0.73	0.578	20.850
DOF	2	1.94	0.9699	1.05	0.488	30.026
Error	2	1.846	0.9229			28.571
Total	8	6.46	3.2301			100

3. CONCLUSIONS

The influence of process parameters (speed, feed and depth of cut) on the plain turning process is numerically analyzed in this work. The AA 8011 material is machined, and the responses are cutting force, material removal rate, surface roughness and amplitude. Initially, the influence of process parameters is investigated separately. Then, using Grey relation analysis, multi objective optimization is performed. The proposed ANOVA model describes the effect of plain turning process parameters on output responses. In this present work it was observed that vibration of amplitude increases in speed and feed rate. The material removal rate increases when the amplitude of tool increases. Cutting force and material removal rate increase as process parameters are increased and surface roughness and amplitude decreases with the increase of process parameters The productivity (MRR) is highly influenced by speed followed by feed and depth of cut in pure Aluminum composition. Speed is most significant factor for quality of the surface (SR) as well as the power consumption(CF) in pure Aluminum alloy

ACKNOWLEDGMENT

The authors gratefully acknowledge Siddhartha Academy of General and Technical Education, Vijayawada, Andhra Pradesh, India for their continuous support in completing this work

REFERENCES

[1] S.S.abuthakeer,P.v mohnram,G.mohnkumar (june 2011)“Prediction and control of cutting tool vibration in cnc lathe with anova and ann”international journal of lean thinking vol.2 issue1

[2] Julie Z.Z. and Joseph C.C. Tool condition monitoring in an end-milling operation based on the vibration signal collected through a microcontroller- based data acquisition system. International Journal of AdvancJoed Manufacturing Technology, 2008; 39: 118-128.

[3] Marlon C.Batery,Hamid R Zadekh(2007) “Enhancement of Turning Process using Vibration Signature Analysis Journal of Vibration and Control”Vol 13 No .5 pp.527-536.

[4] Kirby and Chen, “Predictive monitoring and control of the cold extrusion process”, Annals of CIRP 49 (1) (2000) 383–386.

[5] Nidhi gupta,sawan arya,nitin rai(Nov2012) “a real time tool condition monitoring of central lathe machine” International journal of engineering tred in engineering and development issue2,Vol.7

[6] Dr. Pratesh Jayaswal, Nidhi Gupta(Aug2012) “An investigation of tool condition monitoring” International Journal of Engineering Science and Technology (IJEST) Vol. 4

[7] Jagdish.M.S,H.Vravindra “Monitoring The Machine Elements In Lathe Using Vibration Signals”

[8] Dadaso D. Mohite "An Investigation of Effect of Dressing Parameters for Minimum Surface Roughness using CNC Cylindrical Grinding Machine "International Journal of Research in Engineering and Applied Sciences (ISSN 2249-3905) VOLUME 6, ISSUE 6 (June, 2016)

[9] D.Vishnu Vardhan Reddy, N. Jaya Krishna, N.Bhaskar,"Optimization of Cutting Parameters in Turning of En-19 by using Taguchi and Genetic Algorithm" International Journal of Engineering Research & Technology (IJERT) ISSN: 2278-0181 Vol. 5 Issue 01, January-2016.

Optimization of Wear behaviour of A7075-Flyash-Silicon Carbide metal matrix composite using Taguchi Method

I Veeranjanyulu¹, Sekhar chinthamreddy², Sandip Kumar³, Devarapalli Raviteja⁴

^{1, 3, 4} Department of Mechanical Engineering (A), Aditya Engineering College (A), Surampalem, India
² Department of Mechanical Engineering, Narasaraopeta Engineering College (A), Narasaraopet, India

Abstract—Hybrid composites were synthesized using A7075 reinforced with Fly ash (FA), and Silicon Carbide (SiC) with weight fractions of 1%, 3%, and 5% by the process of stir casting technique. Further, the developed 3% of metal matrix hybrid composite was performed under dry conditions by using a pin on the disc tribometer (TR-201). Experiments were conducted based on the plan of experiments generated through Taguchi’s technique. A L9 Orthogonal array was selected for analysis of the data. The investigation is to find the effect of applied load, sliding speed and sliding distance on wear rate and Coefficient of Friction (CoF) of the hybrid A7075-FA-Sic composite and to determine the optimal parameters for obtaining minimum wear rate and CoF. In the present work wear parameters have been optimized using Taguchi technique to obtain better tribological properties in the produced A7075- FA- SiC hybrid metal matrix composite and generated the regression equation for wear rate and CoF.

1. INTRODUCTION

Composites have wide variety of application in aerospace, defense and it in automotive industries because of its unique properties such as high specific strength, wear resistance, strength-to-weight, strength-to-cost, etc. [1-3]. As a result, many of the current applications for HMMCs are widely in the field of aerospace and automobile components. Aluminium matrix is reinforced with ceramic particles like Al₂O₃, B₄C, SiC, TiB₂, etc, which increases the mechanical properties of the resulting composite materials by dispersion strengthening mechanism. Arunkumar and Swamy [4] reinforced the Al6061 matrix with varying percentage of fly ash and e-glass fibers, and concluded that the tensile properties, compressive strength and hardness of hybrid metal matrix composite increased with increasing fly ash content. Dhanalakshmi et al. [5] have found that the increasing the reinforcement percentage in the hybrid Al7075- Al₂O₃- B₄C composite increases the tensile strength and hardness of matrix. S Dhanalakshmi et al [6] made an attempt to study the influence of wear parameters using L27 orthogonal array. Al7075 alloy was reinforced with Al₂O₃ and B₄C particle reinforcement varied from 3 to 15 wt% in steps of 3. ANOVA results show that load has the highest influence followed by sliding speed and distance, both on wear rate and coefficient of friction. R Ranjith et al [7] outcomes exposed that the coefficient of friction decreases with upsurge in percentage reinforcement and increases with applied load, and

sliding distance. Liu [8] studied the arrangement of the Al₄C₃ stage was effectively maintained a strategic distance by the inclusion of the FA in SiCp. The composites strengthened with rice husk debris displays better tribological properties [9–10].

2. METHODS AND MATERIALS

The Hybrid Aluminium Metal Matrix Composites (HAMMCs) are produced through Stir casting method. Aluminium alloy A7075 is used as the matrix material and its chemical composition is shown in Table 1. Fly ash (FA) and Silicon Carbide (Sic) particles of 53µm and 3% weight was used as reinforcement fabricated by the stir casting process.

Table01: Chemical composition of A7075 in wt %

Elements	Zn	Cu	Mg	Si	Cr	Mn	Fe	Pb	Sn	Ti	Al
Wt%	5.1	1.2	2.1	0.4	0.18	0.3	0.5	0.03	0.01	0.2	Rest

The composite was produced by stir casting as shown in Figure 1. Small sized ingots are loaded into a crucible made of graphite and placed in an electric furnace in which the melting was performed. The melt temperature is maintained above 770°C to compensate the heat loss during the pouring operation. The reinforcement materials are preheated to more than 200°C and the mold is preheated to 300°C to reduce the temperature gradient. To ensure continuous and smooth flow of the particles proper care should be taken to avoid the agglomeration. The inert gas shielding should be maintained throughout to avoid the oxidation as the casting is exposed to the atmosphere during the stirring time approximately 2 to 3 minutes.



Figure 1: Stir casting

3. DRY SLIDING WEAR TEST

Pin-on-disc wear test machine was used to study the wear behavior of the specimen according to ASTM standard. The

EN31 steel was used as the counter disc. The wear test pin having dimension of 12 mm diameter and 25 mm long is prepared from the composites and held against the rotating steel counter disc during the test. Between each tests, the counter disc and the samples are thoroughly cleaned to remove any wear debris attached to the disc or sample. The weight of the sample before and after the test is measured using weighing balance. Design of experiments technique enables us to carry out modeling and analysis of the influence of process variables on the response variables. The wear parameters chosen for the experiment are Load (L), speed (S) and distance (D). The process parameters and their levels are shown in Table 2.

4. PLAN OF EXPERIMENTS

In the present investigation L9 orthogonal array was chosen. The selection of Orthogonal array depends on three items in order of priority, viz., the number of factors and their interactions, number of levels for the factors and the desired experimental resolution or cost limitations.

A total of 9 experiments were performed based on the run order generated by the Taguchi model. The objective of model is to minimize wear rate and coefficient of friction. The responses were tabulated and results were subjected to Analysis of Variance (ANOVA).

The Signal to Noise (S/N) ratio, which condenses the multiple data points within a trial, depends on the type of characteristic being evaluated. The S/N ratio for wear rate and coefficient of friction is analyzed using ‘smaller the better’ characteristic. The experimental observations are further transformed into Signal to Noise ratio. The response to be studied was the wear rate and coefficient of friction with the objective as smaller the better, which is calculated as logarithmic transformation of loss function as shown below,

$$S/N = -10 \log \frac{1}{n} \sum (y_i^2) \tag{1}$$

Table02: Input process parameters and their Levels

Parameter	Notation	Levels		
		1	2	3
Load (N)	A	20	30	40
Velocity (m/s)	B	0.5	1.0	1.5
Distance (m)	C	150	300	450

$$\text{Wear rate (mm}^3\text{)} = \frac{\text{Weight loss in g}}{\text{density in g/mm}^3} \tag{2}$$

$$\text{Coefficient of friction (CoF)} = \frac{\text{Frictional force in N}}{\text{Normal force in N}} \tag{3}$$

5. RESULTS AND DISCUSSIONS

Experiment was conducted to estimate the most influencing parameters on wear and CoF at different levels. Table03: Experiments and S/N ratios

S. No.	L (N)	V (m/s)	D (m)	Wear rate (µm)		CoF	
				M V	S/N	M.V	S/N
1	20	0.5	150	126	-42.0074	0.18	14.8945
2	20	1	300	92	-39.2758	0.125	18.0618
3	20	1.5	450	118	-41.4376	0.293	10.6626
4	30	0.5	300	88	-38.8897	0.26	11.7005
5	30	1	450	84	-38.4856	0.29	10.752
6	30	1.5	150	285	-49.0969	0.296	10.5742
7	40	0.5	450	182	-45.2014	0.31	10.1728
8	40	1	150	436	-52.7897	0.262	11.634
9	40	1.5	300	287	-49.1576	0.27	11.3727

Main effects plot and residual plot for wear and CoF were drawn using MINITAB software. Table 3 shows the measured (MV) and S/N values for Wear rate and CoF. Table 4 displays the mean S/N ratio response for the wear rate. The wear rate was most significantly influenced by the load, which is placed first, followed by distance and velocity. Figure 2 represents the mean S/N ratio graph obtained in Minitab. From this graph noticed that the highest value was obtained load at 20 N, velocity at 0.5 m/s, and sliding distance 450 m. Thus, it can be said the optimum process parameters were setup as L=20N, V=0.5m/s and D=450m and values were marked in Table 4. The optimum setup was marked as L1 - V1 – D3 for wear rate.

The S/N ratio response table for the CoF is shown in Table 5. The CoF was most significantly influenced by the applied load, which is ranked first, followed by distance and velocity. Figure 3 represents the mean S/N ratio graph, noticed that the highest value was obtained load at 20 N, sliding velocity at 1 m/s, and sliding distance 300 m. Finally, concluded that the optimum process parameters were setup as L=20 N, V=1 m/s and D=300 m and values were marked in Table 5.

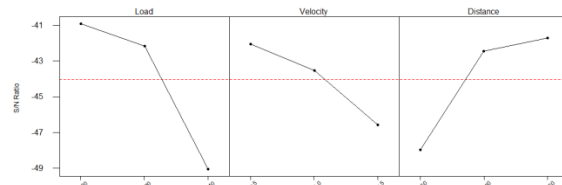
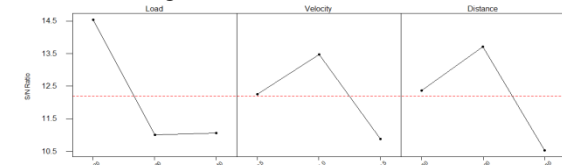


Figure2: Mean S/N ratio of wear rate



Mean S/N ratio of CoF

Table04: Mean S/N ratio response table for wear rate

Level	Load;L(N)	Sliding Velocity;V(m/s)	Sliding Distance;D(m)
-------	-----------	-------------------------	-----------------------

1	-40.91	-42.03	-47.97
2	-42.16	-43.52	-42.44
3	-49.05	-46.56	-41.71
Delta	8.14	4.53	6.26
Rank	1	3	2

Table05: Mean S/N ratio response table for CoF

Level	Load;L(N)	Sliding Velocity;V(m/s)	Sliding Distance;D(m)
1	14.54	12.26	12.37
2	11.01	13.48	13.71
3	11.06	10.87	10.53
Delta	3.53	2.61	3.18
Rank	1	3	2

ANOVA is a statistical technique used to analyze the outcomes of experiments. It was conducted for level of confidence at 95%. ANOVA investigated order of influencing parameters on wear rate and CoF. The results of wear rate listed in Table 6 where as CoF listed in Table 7. From Table 6, observed that the load had the greatest influence on the wear rate with value of P=0.009. From Table 7, observed that the velocity had the greatest influence on the CoF with value of P=0.443. ANOVA recognize that the load and velocity was the outstanding parameter to influencing wear rate and CoF respectively.

Table06: ANOVA for wear rate

Source	T-Value	P-Value
Load (N)	4.18	0.009
Sliding Velocity (m/s)	2.16	0.083
Sliding Distance (m)	-3.40	0.019

S = 55.55 R-Sq = 87.1% R-Sq(adj) = 79.3%

Table07: ANOVA for wear rate

Source	T-Value	P-Value
Load (N)	1.86	0.121
Sliding Velocity (m/s)	0.83	0.443
Sliding Distance (m)	1.18	0.290

S = 0.05345 R-Sq = 52.7% R-Sq(adj) = 24.3%

To create the predictive model equation for the wear rate and CoF in the current study, linear regression analysis was done using Minitab software. The dependent variables are wear rate, and CoF and it has a function of load, velocity, and distance respectively. The linear regression equation was as shown in the Eqn. (4) for wear rate and Eqn. (5) for CoF of hybrid composite respectively.

$$\text{Wear rate } (\mu\text{m}) = -39.5 + 9.48 \text{ Load} + 98.0 \text{ Velocity} - 0.514 \text{ Distance} \text{ ---- (4)}$$

$$\text{COF} = 0.0440 + 0.00407 \text{ Load} + 0.0363 \text{ Velocity} + 0.000172 \text{ Distance} \text{ ---- (5)}$$

The developed models were checked by using R² value. Usually, it varies from zero to 100%. If this value is close to 100%, it gives a good fit between the variables. Therefore, the developed linear regression model for wear rate has moderate R²=87.1%, and for CoF has 52.7%.

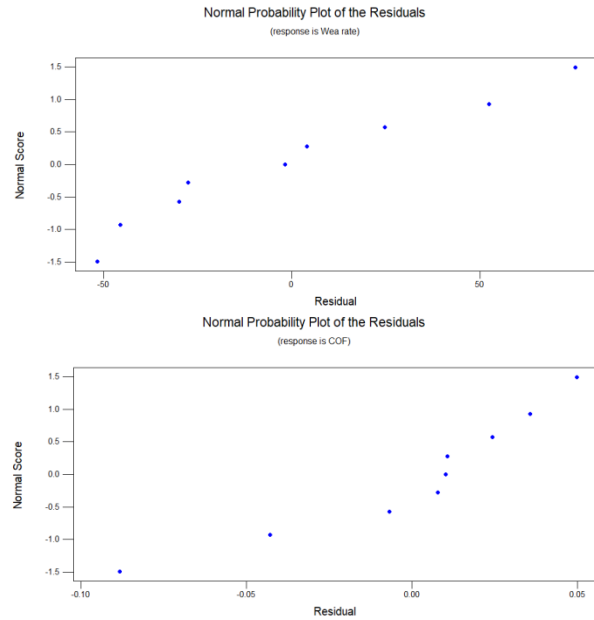


Figure4: Residual plots for wear rate and CoF

The coefficients in the projected model were checked for significance using the residual plot. If the residual plot is a straight line, the model's residual errors are normally distributed and the coefficients are significant. Figure 4 shown the residual plots for wear rate and CoF and noticed that the residuals shown around the straight line, which gives the developed model was appreciable.

5. Conclusions

A7075 alloy reinforced with 3% wt. of FA and 3% wt. of SiC particles was successfully fabricated by stir casting process and tested for wear behaviour. The tribological results indicated the following conclusions:

- Taguchi method determined that, the optimum combination of parameters to obtain the best tribological characteristics were load, distance and velocity.
- ANOVA results indicated that the load was the most influencing parameter with a contribution of P=0.009 on wear rate and P=0.443 on CoF.
- A linear regression analysis developed the predictive model equation for the wear rate and CoF of the hybrid metal matrix composites.

REFERENCES

[1] S. Jayasathyakawin, M. Ravichandran, N. Baskar, C. Anand Chairman, R. Balasundaram, Mechanical properties and applications of Magnesium alloy – Review. Materials Today: Proceedings2020.01.255.
 [2] S. Das, 2004. Development of Aluminium Alloy Composite for Engineering Applications, Indian Institute of Materials, 27 (4), pp. 325-334.

- [3] Clyne T W 2000 An Introductory Overview of MMC Systems, Types, and Developments, Comprehensive Composite Materials Vol 3,ed-Clyne T W (Elsevier) pp.1-26.
- [4] Arunkumar M B and Swamy R P 2011 Evaluation of mechanical properties of Al6061, flyash and e-glass fiber reinforced hybrid metal matrix composites, ARPN Journal of Engineering and Applied Sciences 6 5 40-44.
- [5] Dhanalakshmi S, Mohanasundararaju N and Venkatakrishnan P G 2014 Preparation and mechanical Characterization of stir cast hybrid Al7075-Al₂O₃-B₄C Metal Matrix Composites, Applied Mechanics and Materials 592-594, 705-10.
- [6] S Dhanalakshmi, N Mohanasundararaju, Optimization of friction and wear behaviour of Al7075-Al₂O₃- B₄C metal matrix composites using Taguchi method. Materials Science and Engineering 314 (2018) 012025.
- [7] R Ranjith, S Venkatesan, N S Sivakumar and P Naresh Kumar, Frictional behaviour of AA7050/7.5B₄Cp/Gr hybrid composites fabricated through stir casting. Materials Science and Engineering 1070 (2021) 012135.
- [8] Liu, H., Falzon, B. G., & Dear, J. P. An experimental and numerical study on the crush behaviour of hybrid unidirectional/woven carbon-fibre reinforced composite laminates. International Journal of Mechanical Sciences, (2019). 164, 105160.
- [9] Akbarpour, M. R., Alipour, S., Safarzadeh, A., & Kim, H. S. (2019). Wear and friction behavior of self-lubricating hybrid Cu-(SiC+ x CNT) composites. Composites Part B: Engineering, 158, 92-101.
- [10] Turan, M. E., Zengin, H., & Sun, Y. (2019). Dry sliding wear behavior of (MWCNT+ GNPs) reinforced AZ91 magnesium matrix hybrid composites. Metals and Materials International, 1- 10.

Optical and Luminescence Features of PbO-Al₂O₃-B₂O₃ Glasses Doped with Rare Earth Oxides

¹K. Neeraja, ²K.Ephreme Babu and ³G.S. John

^{1,3} Department of Physics, Narasaraopeta Engineering College, Narasaraopeta, A.P., India

² Department of Physics, Adikavi Nannaya University Campus, Tadepalligudem, West Godavari (Dist.), A.P, India

Abstract: PbO-Al₂O₃-B₂O₃ glasses were prepared by melt quenching method to study the optical and luminescence properties. The analysis of optical intensities based on absorption and luminescence spectra has been performed under different constraints using Judd-Ofelt (JO) theory. The JO intensity parameter has been used to predict the radiative properties. Luminescence properties of Pr³⁺ ions exhibit significant intensities of two emission transitions ³P₀ → ³H₅, ³F₃, Nd³⁺ doped glasses are expected to exhibit an emission transition ⁴F_{3/2} → ⁴I_{11/2}, emission spectra of Sm³⁺ ion, the transitions, ⁴G_{5/2} → ⁶F_{9/2} and ⁴G_{5/2} → ⁶H_{9/2} occurring in the near infrared and visible region respectively are also identified as hypersensitive, these data reveals that the present glasses are useful for developing visible red lasers as well as optical display devices.

1. INTRODUCTION

The rare earth elements are f-block elements with 4fⁿ5s²5p⁶ as the outer most electronic configuration when they are in the trivalent states. As mentioned earlier the volume of the rare earth ions shrinks as we go from the starting ion Ce³⁺ to ending ion Yb³⁺; this shrinkage is due to the imperfect shielding from the nuclear charge of f-electrons. This shielding makes these ions to serve as active centers for laser emission and have strong bearing over the optical, electrical and mechanical properties. A vast number of studies especially on optical properties of various rare earth ions doped glasses are available in the literature [1-10]. For the present study nine rare earth ions viz., Pr³⁺, Nd³⁺ and Sm³⁺ have been chosen for the doping in PbO-Al₂O₃-B₂O₃ glass matrix.

The optical characterization of the glasses, i.e., the study of glass transparency, IR transmission performance and their ability to accept rare earth ions as the luminescent centers is essential for their use in glass laser technology. During the last few years, a large variety of new inorganic glasses have been developed and characterized [14-18]. However, most of these studies are restricted to alkali oxy borate, alkali phosphate and silicate glasses. Lead alumino borate glasses based B₂O₃ glasses in particular are advantageous as laser hosts in view of their optical transparency over a wide range of wavelength; transparency at shorter wavelengths of these glasses helps in getting the optimum efficiency of optical pumping of lasing ions whereas transparency in the high wavelength region causes to give the maximum output intensity of the laser radiation from these glasses. In addition, these glasses possess a very lower rate of crystallization, high transparency, non-toxicity and resistant to moisture. It is therefore felt worth to investigate their optical properties after incorporating certain rare earth ions in them.

This paper reports about the systematic investigation of PbO-Al₂O₃-B₂O₃ glasses doped with rare earth oxides (where Ln³⁺ = Pr³⁺, Nd³⁺, Sm³⁺) have been carried out on these glasses for optical properties such as absorption and photoluminescence at room temperature.

2. EXPERIMENTAL METHOD:

The composition of present study is 19 PbO-5Al₂O₃-75 B₂O₃-1 Ln₂O₃ (where Ln³⁺ = Pr³⁺, Nd³⁺, Sm³⁺) were prepared by melt quenching method, the chemicals PbO, Al₂O₃, B₂O₃, Pr₂O₃, Nd₂O₃ and Sm₂O₃ with high purity was totally weighted to 100g and were mixed thoroughly in a silica crucible and melted at 1420°C for half hour in an electrical furnace. After melting, glassy liquid was quenched in preheated brass moulds. The obtained glasses were annealed at 550°C for 6 hours in order to remove the thermal stress and then samples are cut into shapes and polished for the dimensions of 1.0x1.5x0.3 cm³.

3. RESULT AND DISCUSSIONS:

Praseodymium Doped Glasses:

Pr³⁺ has the 4f² electronic configuration with ³H₄ ground state. The transition ³H₄ → ³P₂ of Pr³⁺ in the absorption spectra is the characteristic of coordination of the Pr³⁺ ion in the crystalline and glassy host matrices. The effective coordination number of this ion in aqueous solutions is about 11.2 where as in certain praseodymium salts the coordination number is observed to be 9.8. The difference in the coordination leads to the variation in the energy of the above transition. The concentration dependence of this ion transitions has been investigated in detail recently in various single crystals and powder samples, for example lanthanum oxides, oxy chlorides and certain phosphate crystals [19 – 23]. The increase in the concentration of this ion is found to enhance ³H₄ → ³P_{1,2}, ¹D₂ electronic absorption and vibrational absorption lines' intensity and these were attributed to essentially cooperative due to exchange of virtual phonons between the coupled Pr³⁺ ion pair [24]. Among various transitions, the transition ³H₄ → ³F₄ is found to be hyper sensitive due to quadrupole selection rules whereas the hypersensitiveness of the two other transitions, ³H₄ → ³P₂, ¹D₂ is due to the influence of ligand environments [25]. The application of Judd-Ofelt theory to the Pr³⁺ ion works less in general when compared with the other lanthanide ion since out of seven expected transitions three are hypersensitive.

Optical Absorption:

The optical absorption spectrum of Pr³⁺ doped PbO- Al₂O₃ -B₂O₃ glasses recorded at room temperature in the visible and near infrared regions has exhibited six absorption levels (Fig 1 a & b). These levels are assigned to the appropriate electronic transitions as mentioned below:

$$^3H_4 \rightarrow ^1D_2, ^3P_0, ^3P_1, ^3P_2, ^3F_2 \text{ and } ^3F_3.$$

Spectral intensities of these bands have been used in the least square fitting procedure to determine the Judd – Ofelt intensity parameter viz., $\Omega_2, \Omega_4,$ and Ω_6 using unit tensor operators $||U \lambda ||^2$ and are presented in the Table 4. 8 along with the other pertinent data. The values of Ω_λ are found to be in the following order:

$$\Omega_6 > \Omega_2 > \Omega_4.$$

Using these values of Ω_λ the magnitudes of electric dipole line strength Sed are calculated for each transition and presented in Table 1.

Transition from ⁴ I _{9/2}	Energy (Cm ⁻¹)	f _{exp} × 10 ⁻⁶	f _{calc} × 10 ⁻⁶	J-O Parameters (Cm ⁻¹)
⁴ F _{3/2}	11529	15.9	24.8	Ω ₂ =13.7
⁴ F _{5/2}	12500	29.0	77.96	
⁴ F _{7/2}	13513	8.8	21.75	
⁴ F _{9/2}	14706	2.2	27.15	Ω ₄ =6.1
⁴ G _{5/2}	17216	150.0	35.3	Ω ₆ =3.65
⁴ G _{7/2}	19183	18.5	16.5	
⁴ G _{9/2}	19608	5.8	16.4	
				Ω ₄ / Ω ₆ = 1.67

Table-1:The absorption band energies, the electric dipole line strength Sed, the oscillatory strength fexp for some of the transitions and Judd – Ofelt intensity parameters and spectroscopic quality factor (Ω₄/Ω₆) of Pr³⁺: PbO- Al₂O₃ -B₂O₃ glasses.

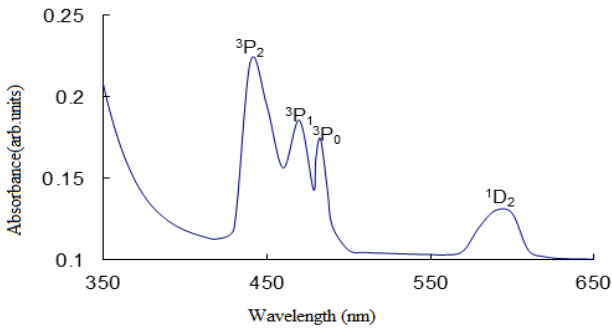


Fig.1(a) Optical absorption spectrum of PbO-Al₂O₃-B₂O₃ doped glasses doped with Pr³⁺ ions recorded at room temperature in the visible region. All the transitions are from the ground state ³H₄

Fig-1(b). Optical absorption spectrum PbO-Al₂O₃-B₂O₃ glasses doped with Pr³⁺ ions recorded at room temperature in the NIR region. All the transitions are from the ground state ³H₄.

The emission spectrum of Pr³⁺ ion is also well studied in number of glasses like fluoro zirconate, TeO₂ glasses etc., [26,27]. Among various emission transitions the two transitions ³P₀ → ³H₅, ³F₃ are found to exhibit significant intensities due to J mixing. The terms corresponding to even values do not contribute to these transitions since the reduced matrix elements U₂, U₄, U₆ are zeros for these transitions [28].

Photoluminescence:

The photoluminescence (PL) spectrum recorded at room temperature for Pr³⁺: PbO-Al₂O₃-B₂O₃ glasses is shown in Fig 2; the spectrum gives out the following emission transitions:

$$^3P_0 \rightarrow ^3F_2, ^3H_4, ^3H_5, ^3H_6;$$

$$^3P_1 \rightarrow ^3F_4, ^3H_5 \text{ and } ^1D_2 \rightarrow ^3H_4$$

The Judd – Ofelt theory has been applied to characterize the photoluminescence spectrum of these glasses. The transition probability A (Ψ J ' , Ψ J), the total transition probability A T (Ψ J ') , and the fluorescence branching ratio Ψr have been determined using the expressions 1.24 to 1.26 for some of the transitions and presented in Table 2. Among different transitions from ³P₀ state, ³P₀ → ³H₄, has been found to have the highest transition probability and hence the stimulated emission cross section Ψ EP (Eqn. 1.27).

The other important laser characteristic parameter , has been calculated for this level and it is found to be 4.2 x 10⁻²⁰ cm² (Table 2) , which is slightly high when compared with the conventional metallic fluoride glass hosts of Pr³⁺ ion for this transition. These parameters have also been computed for other observed levels and are furnished in the same Table.

Table 2. Radiative properties of Pr³⁺ doped PbO-Al₂O₃-B₂O₃ glasses

Transition from ⁴ I _{9/2}	Energy (Cm ⁻¹)	f _{exp} × 10 ⁻⁶	f _{calc} × 10 ⁻⁶	J-O Parameters (Cm ⁻¹)
⁴ F _{3/2}	11529	15.9	24.8	Ω ₂ =13.7
⁴ F _{5/2}	12500	29.0	77.96	
⁴ F _{7/2}	13513	8.8	21.75	
⁴ F _{9/2}	14706	2.2	27.15	Ω ₄ =6.1
⁴ G _{5/2}	17216	150.0	35.3	Ω ₆ =3.65
⁴ G _{7/2}	19183	18.5	16.5	
⁴ G _{9/2}	19608	5.8	16.4	
				Ω ₄ / Ω ₆ = 1.67

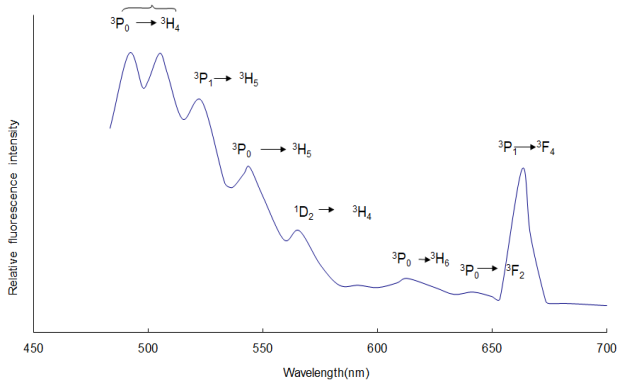


Fig 2 Luminescence spectrum of Pr³⁺ doped PbO-B₂O₃-Al₂O₃ glasses (λ_{exc} = 440 nm).

Neodymium Doped Glasses

Nd³⁺ ion has 4f² electronic configuration with ⁴I_{9/2} ground state. The absorption and emission of this ion has been reported in a number of crystalline materials and glasses because of its potential applications in laser technology [29,30]. The transition ⁴I_{9/2} → ²P_{1/2} of Nd³⁺ ion in the absorption spectra is a characteristic of coordination of this ion. The effective coordination of this ion is found to be varying between 6 and 9 with the variations in the transition energy from 23,200-23,400 cm⁻¹ [31]. The J-O theory works very well for this ion and the radiative parameters can therefore be conveniently evaluated from J-O parameters.

In the emission spectrum, the focus in general is mainly on ⁴F_{3/2} → ⁴I_{11/2} which is identified as the lasing transition. However, in the present study the emission spectrum for this ion in the present host glass could not be carried out due to the lack of a laser excitation source.

Optical Absorption:

The optical absorption spectrum recorded at room temperature for Nd³⁺ doped glasses has exhibited the following absorption bands (Fig 3):

- ⁴I_{9/2} → ⁴F_{3/2}, ⁵/₂, ⁷/₂, ⁹/₂,
- ⁴I_{9/2} → ⁴G_{5/2}, ⁷/₂, ⁹/₂, ¹¹/₂, ²P_{1/2}, ⁴D_{5/2}

Among these observed bands, only seven clearly resolved bands are considered for applying the Judd – Ofelt theory to characterize the spectral intensities of the absorption bands of these glasses. The electric dipole line strength Sed, oscillator strength f_{exp} and the best fit Judd – Ofelt intensity parameters Ω_λ of Nd³⁺ doped PbO-Al₂O₃-B₂O₃ glasses are reported in Table 3. From this absorption spectral profiles, it is observed that a particular transition ⁴I_{9/2} → ⁴G_{5/2} is more intense than any other transition. This is obviously because of better validity of the selection rules:

Δ J < 2, Δ L < and Δ S = 0

for this transition . In addition, the magnitude of || U λ | | 2 of this level is also considered as an important value for the hypersensitivity nature of this level.

The spectroscopic quality factor (Ω₄/ Ω₆) for these glasses has also been calculated and presented in

Table 3. The J- O intensity parameters obtained for these glasses show the following trend:

Ω₂ > Ω₄ > Ω₆.

Table: 3-The absorption band energies, the electric dipole line strength (Sed), the oscillator strength f for some transitions and Judd – Ofelt intensity parameters(Ωλ) and spectroscopic quality factor (Ω₄/Ω₆) of Nd³⁺: PbO-Al₂O₃-B₂O₃ glasses.

Emission Transition	λ(nm)	Δλ (nm)	A(s ⁻¹)x10 ⁴	AT(s ⁻¹)x10 ⁴	B _λ (%)	Emission Cross Section σ _e ^λ (10 ⁻²⁰ , cm ²)
P ₁ → F ₄	663	8.33	1.76	52.34	33.66	0.23
P ₀ → F ₂	643	16.66	3.66	18.13	20.18	21.70
P ₀ → H ₆	613	23.33	0.73	18.13	4.03	2.56
P ₀ → H ₅	543	29.16	2.70	18.13	14.93	4.65
P ₀ → H ₄	493	33.33	11.03	18.13	60.83	11.29
P ₁ → H ₅	523	30.00	2.82	52.34	53.90	4.06

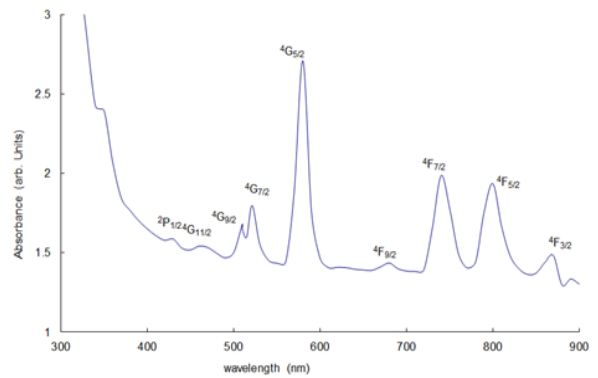


Fig 3 Optical absorption spectrum PbO-Al₂O₃-B₂O₃ glasses doped with Nd³⁺ ions recorded at room temperature. All the transitions are from the ground state ⁴I_{9/2}.

Samarium Doped Glasses

Samarium ion exists in Sm³⁺ and Sm²⁺ states but between these two states, Sm³⁺ is found to be more stable. This ion has 4f⁵ electronic configuration with ⁶H_{5/2} ground state. Earlier it was shown that the oscillator strengths of Sm³⁺ ions may be arranged in two groups, one referring to transitions up to 10,700 cm⁻¹ and the second to transitions in the range 17,600-32,800 cm⁻¹ and the Judd-Ofelt parameters can be calculated separately for these two regions [31]. Such separation was attributed to the splitting of f_N configuration being smaller than the f-d energy gap[32]. In such a case it is incorrect to use the oscillator strengths of transitions which are about 10,000 cm⁻¹ for calculations of Ω_λ parameters by means of the Judd-Ofelt theory. The transitions ⁶H_{5/2} → ⁴F_{3/2}, ⁴F_{3/2} of Sm³⁺ occurring in the absorption spectrum in the near infrared region are hypersensitive [33-34]. In the emission spectra of Sm³⁺ ion, the transitions, ⁴G_{5/2} → ⁶F_{9/2} and ⁴G_{5/2} → ⁶H_{9/2} occurring in the near infrared and visible region respectively are also identified as hypersensitive [35].

Optical Absorption:

The optical absorption spectrum recorded at room temperature in the visible region for Sm³⁺ doped glasses has exhibited the following nine absorption bands (Fig 4):



The oscillator strength f_{exp} , electric dipole line strength S_{ed} and the best fit Judd –Ofelt intensity parameters Ω_λ of Sm³⁺ doped PbO-Al₂O₃-B₂O₃ glasses are reported in Table 4 . From these absorption spectral profiles, it is observed that a particular transition ${}^6H_{5/2} \rightarrow {}^4F_{7/2}$, is more intense than any other transition.

Transition from ${}^4I_{9/2}$	Energy (Cm ⁻¹)	$f_{exp} \times 10^{-6}$	$f_{cal} \times 10^{-6}$	J-O Parameters (Cm ⁻¹)
${}^4I_{11/2}$	20833	3.94	0.012	$\Omega_2 = 28$ $\Omega_4 = 3.52$ $\Omega_6 = 3.31$ $\Omega_4 / \Omega_6 = 1.06$
${}^4I_{13/2}$	21739	9.50	0.518	
${}^4G_{9/2}$	22727	1.38	0.092	
${}^6P_{5/2}$	23810	8.24	0.091	
${}^4F_{7/2}$	25000	0.60	0.951	
${}^6P_{7/2}$	26824	21.78	1.014	
${}^4D_{5/2}$	27670	11.76	0.348	

The spectroscopic quality factor (Ω_4/Ω_6) for these glasses has also been calculated and presented in Table 4, the J- O intensity parameters obtained for these glasses show the following trend:

$$\Omega_2 > \Omega_4 > \Omega_6.$$

Table: 4- The absorption band energies, the electric dipole line strength (Sed), the oscillatory strength f for some transitions and Judd – Ofelt intensity parameters(Ω_λ) and spectroscopic quality factor (Ω_4/Ω_6) of Sm³⁺: PbO-Al₂O₃-B₂O₃ glasses.

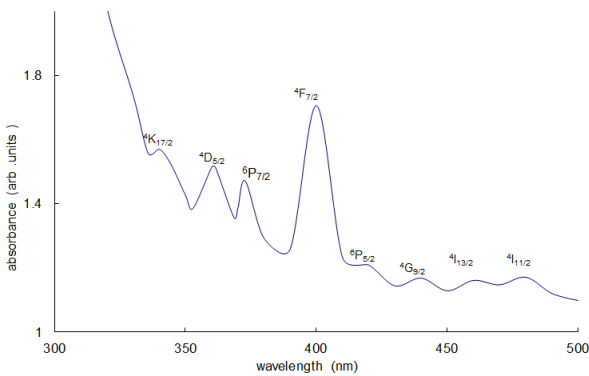
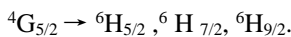


Fig. 4 Optical absorption spectrum PbO-Al₂O₃-B₂O₃ glasses doped with Sm³⁺ ions recorded at room temperature. All the transitions are from the ground state ${}^6H_{5/2}$.

Photoluminescence:

The photoluminescence (PL) spectrum has been recorded at room temperature for Sm³⁺: PbO-Al₂O₃-B₂O₃ glasses. The luminescence spectrum (excited at 400 nm) shown in Fig 5 for these glasses gives out the following emission transitions:



The Judd – Ofelt theory could successfully be applied to characterize the photoluminescence spectrum of these glasses. The transition probability A ($\Psi J', \Psi J$), the total transition probability AT ($\Psi J'$), and the fluorescence branching ratio β_f have been determined using the usual procedure for these transitions and are presented in Table 5.

Among different transitions from ${}^4G_{5/2}$ state, ${}^4G_{5/2} \rightarrow {}^6H_{9/2}$, has been found to have the highest transition probability. The stimulated emission cross section σ_{EP} for all the three observed levels have been calculated and are presented in Table 5.

Table 5: Radiative properties of Sm³⁺ doped PbO-Al₂O₃-B₂O₃ glasses

Emission Transition	λ (nm)	$\Delta\lambda$ (nm)	A(s ⁻¹)x10 ⁴	AT(s ⁻¹)x10 ⁴	β_f (%)	Emission Cross Section σ_{EP}^i (10 ⁻²⁰ , cm ²)
${}^4G_{5/2} \rightarrow {}^6H_{9/2}$	645	12.1	3.27	4.82	67.84	0.121
${}^4G_{5/2} \rightarrow {}^6H_{7/2}$	598	13.4	0.42	4.82	8.71	0.254
${}^4G_{5/2} \rightarrow {}^6H_{5/2}$	562	16.2	0.11	4.82	2.28	0.035

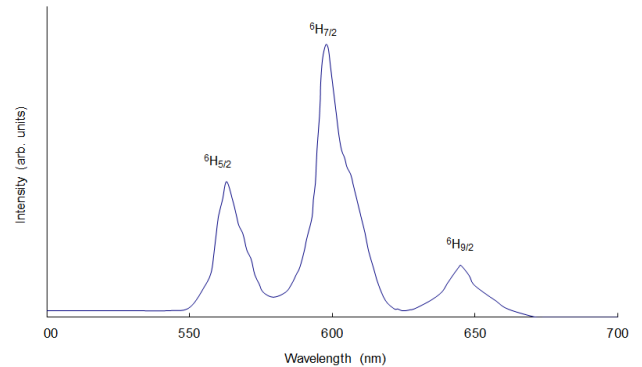


Fig. 5 Photoluminescence spectrum of Sm³⁺ doped PbO-Al₂O₃-B₂O₃ glasses ($\lambda_{exc} = 400$ nm) recorded at room temperature. All the transitions are from the upper state ${}^4G_{5/2}$.

4. Conclusion:

For Pr³⁺ doped glasses the ${}^3H_4 \rightarrow {}^3P_2$ transition is found to be higher sensitive whose intensity vary significantly with environment due to strong 4f – 5d mixing and due to significant contributions by the terms corresponding to the odd values of U_λ in the expression for oscillator strength f ; similarly, in the Nd³⁺ doped sample the transition ${}^4I_{9/2} \rightarrow {}^4G_{5/2}$ is found to be more intense than any other state. Spectral studies of vibronic transitions for rare earth systems show that they are most intense at the beginning and the end of the series with Sm³⁺ exhibiting a minimum vibrational structure. Contributions due to vibrational interactions by turns common to Ω_4 and Ω_6 can qualitatively account for the observed trends in the present cases.

REFERENCES:

- [1].D. Lezal, M.Poulain and J. Zavadil, *Ceramics Silikaty*, 45 (2001) 105.
- [2].H. Hefang and Z. Long, *Journal- Chinese Ceramic Society*, 29 (2001) 460.
- [3].Y. C. Ratnakaram and A.V. Reddy, *Bulletin of Materials Science*, 24 (2001) 539.
- [4].D. Thomazini, F. Lanciotti and A.S.B. Sombra, *Ceramica*, 47 (2001) 88.
- [5].W. J. Miniscalco, *Optical Engineering*, 71 (2001) 17.
- [6].J. M. Cole, E. van Eck and G.A. Saunders, *J. Phys: Condensed Matter*, 13 (2001) 4105.
- [7].E. A. Gouveia, M.T. de Araujo and A.S. Gouveia-Neto, *Braz. J. Phys.*, 31 (2001) 89.
- [8].L. Huang, X. Wang, H. Lin and X. Liu, *J. Alloys. Comp.*, 316 (2001) 256.
- [9].Y. Menke, V. Peltier-Baron and S. Hampshire, *J. Non-Cryst. Solids*, 276 (2000)145.
- [10]. T. Brennan, J. C. Knight and G.A. Saunders, 40 (1999) 113.
- [11]. B. Sridhar, B. Indira and K. Bhatnagar, *Ind. J. Pure Appl. Phys.* 33 (1995) 153.
- [12]. J E Shelby *Key Eng. Mater.* 94 (1994) 43.
- [13]. B.B.Laud, *Lasers and Non -Linear Optics* (New Age Int. Pvt. Ltd., New Delhi (1996).
- [14]. C.K. Jayasankar, E. Rukmini, *Optical Materials* 8 (1997) 193.
- [15]. A.Renuka Devi, C.K. Jayasankar, *J. Non-Cryst. Solids*, 197 (1996) 111.
- [16]. N. Sooraj Hussain, Y. Prabhakara Reddy, S. Buddhudu, *Mater.Letts.*48 (2001)303.
- [17]. V.Ravi Kumar, N.Veeraiah, *J. Mat. Science* 33 (1998) 2659.
- [18]. P.K.D. Sagar, P. Kistaiah, N. Veeraiah, *J. Mat. Science Lett.* 18 (1999) 55.
- [19]. J.M. Hickmann, E.A. Gouveia, A.S. Gouveia-Neto, D.C. Dini, *Opt. Lett.* 19 (1994) 1726.
- [20]. K.B.Yatsimirskii and N.K. Davidenko, *Coord. Chem. Rev.* 27 (1979) 223
- [21]. M. Galczynski, M.Blazej and W. Strek, *Mat. Chem. Phys.* 31 (1992) 175.
- [22]. M. Galczynski, M.Blazej and W. Strek, *Mat. Chem. Phys.* 31 (1992) 175. 60
- [23]. A. Meijerink, C. de Mello Donega, and G.Blasse, *J. Lumin.*58 (1994) 26.
- [24]. M. Galczynski, M.Blazej and W. Strek, *Mat. Chem. Phys.* 31 (1992) 175.
- [25]. C. de Mello Donega, A. Meijerink and G. Blasse, *J.Lumin.* 62 (1994) 189.
- [26]. S.T. Lai, S. Haung and W.M. Yen, *Phys.Rev.B* 26 (1982) 2349.
- [27]. V.Ravi Kumar and N.Veeraiah, *J. Lumin* 75 (1997) 57.
- [28]. M. Eyal, E. Greenberg and R. Reisfeld, *Chem. Phys. Lett.* 117 (1985) 108.
- [29]. R. Reisfeld and C.K. Jorgensen, *Lasers and Excited states of Rare Earths*
- [30]. R.Reisfeld and C.K. Jorgensen, *Hand Boo9k on the Physics and Chemistry of Rare Earths*, (Eds.) 9 (North-Holland, New York, 1987) chap.58.
- [31]. K.B.Yatsimirskii and N.K. Davidenko, *Coord. Chem. Rev.* 27 (1979) 223.
- [32]. R.Reisfeld, *Structure and Bonding* 22 (Springer-verlag, New York, 1975) 123
- [33]. D.E. Henrie, R.L. Fellows and G.R. Choppin, *Coord. Chem. Rev.* 18 (1976) 199.
- [34]. R.D. Peacock, *Structure and Bonding* 22 (Springer-Verlag, New York,1975) 83.
- [35]. W.D. Horrocks, Jr. and M. Albin, *Prog. Inorg. Chem.* 31 (An Interscience Publication, New York, 1984)1.

Finite Element Analysis of Sheet Moulding Compound Panels

M Gangaraju, S.Praveen Kumar and D.Raghuramireddy,
 Department of Mechanical Engineering,
 Sree Vidyanikethan Engineering College, Tirupati, INDIA

ABSTRACT- Now a days the growing technology in all fields of engineering demands improved material properties. One of the alternative materials found is composite materials, combining two or more than two materials on macroscopic scale results a material having superior mechanical properties. Sheet moulding compound (SMC) is one type of the composite material. The panels made by SMC provide low light transmittance thus low light intensity on the inner surface of the panel thus it prevents the growth of the algae, thus hygienic quality is maintained. In this work the panels of different configurations have been modelled by using PRO-E software as per the geometrical details and analysed by using FEA software package ANSYS at a specified pressure. During the analysis the bottom panel is subjected to uniform pressure and side panel is subjected varying pressure. A comparison is made between panels of different configurations for normal displacement, Von misses stress, and Von misses strain. Based on the results, the best panel configuration is recommended for the water tank.

Key words: Composite plate, SMC panels, Composite Design, Finite element method, Fibre length.

I. INTRODUCTION

1.1 SMC Composites:

Advanced composite materials, particularly continuous fibre-reinforced composites are currently being used in a wide variety of structural applications. These materials have now emerged as engineering materials, due to a number of attributes like low weight, high stiffens, large ultimate strength, excellent fatigue and corrosion resistance, ease in fabrication and so on. Sheet moulding compound (SMC) is a fibre composite material which contains 30% of organic ingredients and 70% of inorganic ingredients which curves by curing process by cross linking reaction. Sheet moulding compound is the most commonly used composite material for manufacturing of water tanks. It is fibre reinforced material which primarily consists of inorganic ingredients.

1.2 Manufacturing of SMC materials:

SMC is usually manufactured by a highly automated continuous flow process by compression moulding process. Continuous fibre glass is chopped into length of 20 to 50 mm length and deposited on a layer of resin filler paste which is travelling on a polyethylene film. Another layer of resin filler paste is deposited over the layer to form a continuous sandwich of fibre glass and resin filler. The sandwich with top and bottom covers of polyethylene is compacted and rolled in to a package sized rolls. The rolled up SMC is stored and then SMC rolls are moved to near the press and cut in to the proper charge pattern for the specific part and placed in a matched metal mould which is hot.

Under the pressure of the press the system will flow to fill the complete mould. In parallel the cutting process is started and after a short time the curved part will be remoulded. This process is atomized and can be used for mass production i.e. automotive industry. For series production the moulds are metal dies which are heated with steam to temperature around 120 °C to reduce the curing time.

1.3 Material properties of SMC Materials:

All the properties of SMC material are taken from the Devi polymers Limited, Chennai; the properties are given as shown in table1.

Table 1: SMC material properties

Sl.no	Material property	Value
1	Fibre Strength	20-50mm
2	Tensile strength	100-200gpa
3	Tensile Modulus	8-25gpa
4	Flexural Strength	200-600mpa 60-
5	Impact Strength	300kj/mm ²
6	Density	1.9gm/cm ²
7	Young's modulus	10gpa
8	Possion's ratio	0.4990.449

1.4 Comparison table of the SMC material:

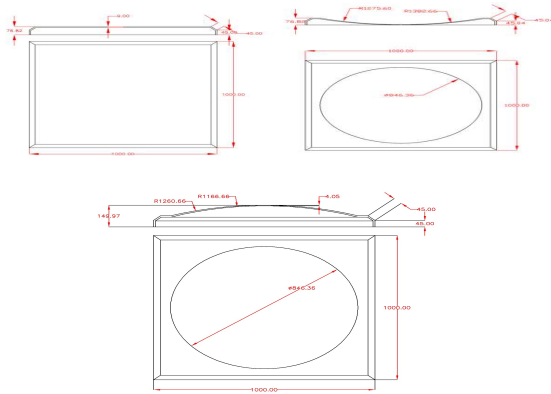
Table2: Water tank with other material water tanks

Kind of tank	Water quality	Leak Proof	durability	Transporta tion and assembly	maintenance	Adaptabil ity of design and size	Corrosion resistance
S.M.C.TANKS	⊙	⊙	⊙	⊙	⊙	⊙	⊙
CONCRETE TANKS	✦	△	△	✦	✦	△	⊙
STEEL TANKS	△	✦	△	△	✦	⊙	✦
STAINLESS STEEL TANKS	⊙	⊙	⊙	△	△	⊙	△
PVC TANKS	⊙	⊙	⊙	⊙	✦	✦	⊙

⊙ EXCELLENT ○ GOOD ✦ POOR △ FAIR

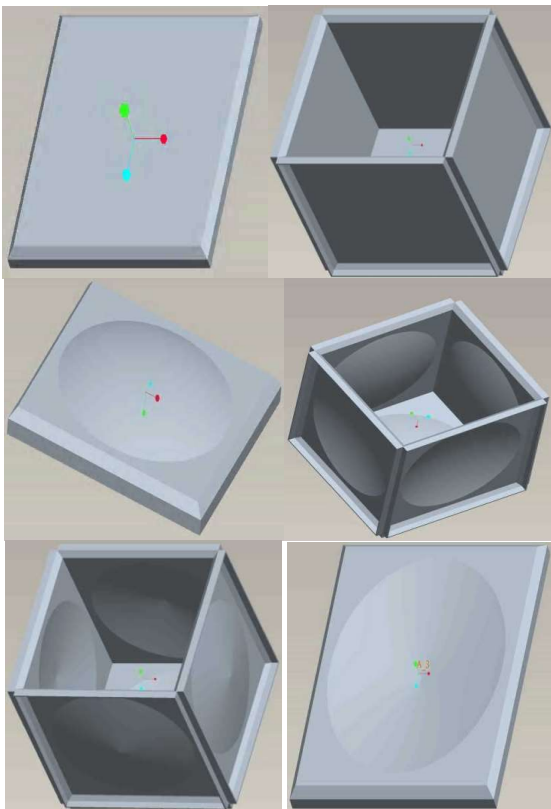
II. MODELING OF SMC PANELS

To have the realistic view of any component the solid model is essential. So the solid models of SMC water tank panels are modelled in special CAD software package like PRO/E. The SMC water tank panels are of different configurations. We have selected the panels of three different configurations. They are a) flat panel b) Concave panel c) Convex panel. Two dimensional drawings of different configurations are given as follows.



- a) Flat SMC Panel
- b) Concave SMC Panel
- c) Convex SMC Panel

2.1 Modelled views



III. FINITE ELEMENT METHOD

The Finite Element Method has become a powerful tool for the numerical solution of a wide range of engineering problems. With the advance in computer technology and CAD system, complex problems can be modelled with relative ease. Several alternative configurations can be tried out on a computer before the first prototype is built. All of this suggests that we need to keep pace with these developments by understanding the basic theory, modelling technique and computational aspects of the Finite Element Method. In this method of analysis, a complex region defining a continuum is discretized into simple geometric shapes called finite Elements. The material properties and the governing relationships are considered over these elements and expressed in terms of unknown values at element corners. An assembly process, duly considering the loading and constraints, results in a set of equations.

3.1 Shell theory

Thin shell theories are based on Love-Kirchhoff assumption that as the shell deforms and the mid-surface stretches and bends the fibres of the shell initially straight and normal to the mid surface remain straight and normal to the mid-surface. Also it is usually assumed that the normal stress is zero. These assumptions permit to define the displacement of every point in terms of the displacement of the mid-surface of the shell. This in effect represent the reduction of a problem from a three dimensional to a two dimensional case. A shell may thus be thought of as the material form taken by enclosure of a volume bounded by curved surfaces. To analyse the internal forces, a small shell element is considered whose thickness is small in comparison with the other dimension of the shell and with its radii of curvature.

3.2 Overview of ANSYS

The ANSYS computer program is a large scale multipurpose finite element program which may be used for solving several classes of engineering analyses? The analysis capabilities of ANSYS include the ability to solve static and dynamic structural analyses, steady state and transient heat transfer problems, mode frequency and buckling, Eigen value problems, static or time varying magnetic analyses and various types of field and coupled field applications. The program contains main special features which allow nonlinearities or secondary effects to be include in the solution such as plasticity large strain, hyper-elasticity, creep, swelling, large deflections, contact, stress stiffening, temperature dependency, material anisotropy and radiation. ANSYS has been developed. Other capabilities ,sub structuring, sub modelling, random vibration, kineto statics, kineto dynamics, free convection, fluid analysis, acoustics, magnetic, piezoelectric, coupled field analysis and design analysis and, design optimization have been added to the program. These capabilities contribute further to making ANSYS a multipurpose analysis tool for varied engineering disciplines. The ANSYS program has been in commercial use since 1970, and has been used

extensively in the aerospace, automotive, construction, electronic, energy services, manufacturing, nuclear, plastics, oil, and steel industries.

IV. FINITE ELEMENT ANALYSIS OF SMC PANELS OF DIFFERENT CONFIGURATIONS

Sheet Moulding Compound (SMC) panels of different configurations for a water tank have been analysed by FEA software package ANSYS 10.0 at a specified pressure of 0.04905 N/mm². The finite element idealization of the panel 1 is as shown in the figure. The side panel is subjected to simulated variable pressure and the bottom panel is subjected to simulated uniform pressure. The clamped edge conditions are simulated at the bolt hole locations. The material properties used are as follows
 Young's modulus – 10e3 N/mm²
 Poison's ration – 0.499
 Density – 1.9e-9 kg/mm³
 Element edge length – 50 mm
 Added mass per unit area – 10-3kg/mm²
 Average shell thickness – 9 mm

Results	Normal displacement(mm)	on misses stress(N)	Von misses strain
Flat bottom panel	66.815	138.219	0.013822
Flat side panel	42.797	91.429	0.009143
Concave bottom panel	13.947	106.623	0.0010662
Concave side panel	5.888	45.41	0.004541
Convex bottom panel	9.358	75.507	0.007551
Convex side panel	4.309	70.963	0.007092

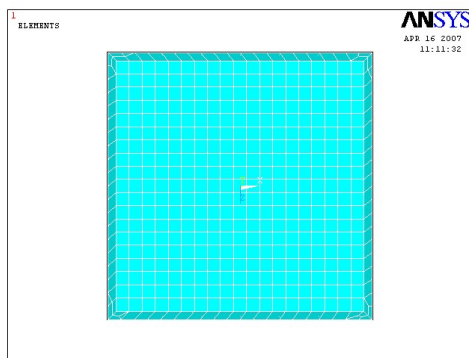


Fig-1.Flat Panel Geometry with Mesh

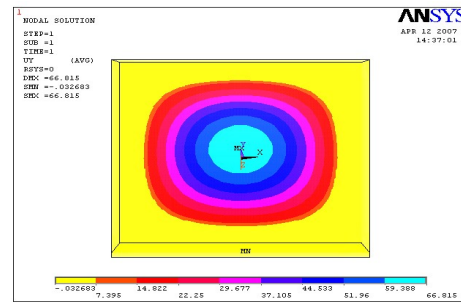


Fig-2 : Deflection Plot for A Bottom Flat SMC Panel

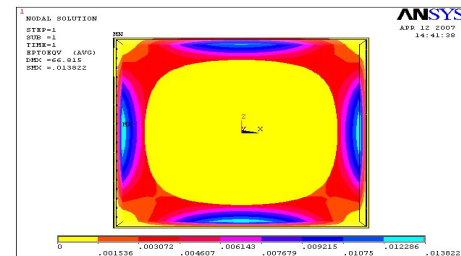


Fig-3: stress plot for a bottom flat SMC panel

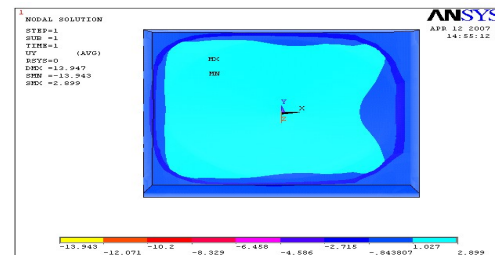


Fig-4: Strain plot for bottom flat SMC panel

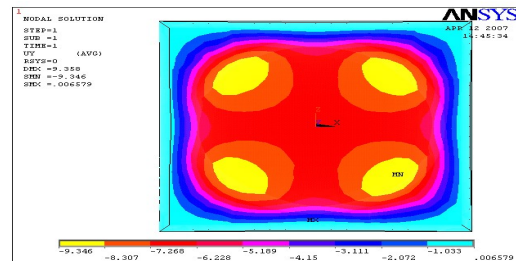


Fig-5: Deflection plot for a bottom SMC convex panel

V. RESULTS AND DISCUSSION

A SMC material flat panel 1000 mm square, 76.82 mm height and uniform thickness of 9 mm over the entire panel when subjected to uniform pressure of 0.04905N/mm^2 yields to a central deflection of 66.815 mm at the midpoint of the panel, and stress of 138.219N/mm^2 and when subjected to varying pressure from 0.01635N/mm^2 to 0.04905N/mm^2 yields to a deflection of 42.797 mm and stress of 91.429N/mm^2 using FEA solution package ANSYS 10.0. Next SMC material concave panel 1000mm square, 76.82 mm height including concave dome shape with a thickness varying from 4 mm at the centre to 9 mm thickness at the edge of concave profile when subjected to uniform pressure of 0.04905N/mm^2 yields to a deflection of 13.947 mm and stress of 106.623N/mm^2 and when subjected to varying pressure from 0.01635N/mm^2 to 0.04905N/mm^2 yields to a deflection of 5.888 mm and stress of 45.41N/mm^2 using FEA solution package ANSYS 10.0

Another SMC material convex panel 1000 mm square, 150 mm height including convex dome shape with a thickness varying from 4mm at the centre to 9 mm thickness at the edge of convex profile when subjected to uniform pressure of 0.04905N/mm^2 yields to a deflection of 9.358 mm and stress of 75.507N/mm^2 and when subjected to varying pressure from 0.01635N/mm^2 to 0.04905N/mm^2 yields to a deflection of 4.309 mm and stress of 70.963N/mm^2 using FEA solution package ANSYS 10.0

The thickness of flat panel is 9 mm. But the deflection of flat panel at factor of safety 5 is 66.815 mm and 42.797 mm. At factor of safety 1 its value will be 13.33 mm and 8.4 mm. so that flat panel is not recommendable. The thickness of the concave panel at the centre is 4 mm. But the deflection of concave panel at factor of safety 5 is 13.947 mm and 5.888 mm. At factor of safety 1 it will be 2.79mm and 1.18mm which is less than 4mm thickness at the centre and the maximum stress value is 106.623N/mm^2 and 45.41N/mm^2 this is within the range of 100 – 200 MPa i.e actual tensile strength of the SMC material. The thickness of the convex panel at the centre is 4mm. But the deflection of concave panel at Factor of safety 5 is 9.358 mm and 4.309 mm. At factor of safety 1 it will be 1.87 mm and 0.86 mm which is less than 4mm thickness at the centre and maximum stress value is 75.507N/mm^2 and 70.963N/mm^2 . This is within the range of 100 – 200 MPa i.e actual tensile strength of the SMC material.

VI. CONCLUSTIONS

From the displacement consideration panel 1 (Flat Panel) is not at all recommendable for the water tank. For a water tank capacity of 1m³, panel 2 or panel 3 can be recommended for side and bottom panels by increasing its thickness at the crown section. Panel 3 (convex panel) is placed as a bottom panel eliminates the possibility of separation and leakage of the tank. The combination of concave and convex panels ensures complete and faster

drainage. Using washers and stiffeners in bolt location will control the stresses.

VII. SCOPE OF THE WORK

There are still many areas on which we can extend our analyses work on different configurations of SMC panels based on day to day requirement. As the SMC material has got its applications in the field of automobile industry, which are traveling with high speeds, the air resistance on the body and other parts of the automobile may cause to temperature. So the thermal analysis of the composite structure should also be carried out and the thermal distribution can be analysed for the thermal stability and safety. Depending on the fibre length from 20 to 50 mm length, the properties of SMC material varies, so we can apt different fibre lengths and checks the results and compare them. Depending on the fibre orientation i.e., Random fibres and continuous fibres, the properties of SMC material varies, so we can apt different orientation fibres and compare the results. Depending on the type of fibre i.e., longitudinal fibre, transverse fibres, the properties of SMC material varies, so consider different type of fibres and apply the load and compare the results among them. Not only above still, we can extend our analyses work by comparing the results obtained manually using displacement matrices, stiffness matrices, strain transformation matrices with the values obtained using FEA solution package.

REFERENCES

1. C.S. Krishna Murthy, Finite element Analysis, Tata Mc Graph Hill Ltd. New Delhi 1986.
2. Martin Fisk, Damage level calculation in SMC composite structures, master's thesis, Lulea University of Technology, Gothenburg, Sweden, 2006
3. Jones, R. M., Mechanics of Composite Materials, McGraw Hill, 1975.
4. Lagace, P. A., Jensen, D. W., and Finch, D. C., "Buckling of Unsymmetric Composite Laminates," Composite Structures, Vol. 5, 1986, pp. 101-123
5. Ashton, J.E., J.C. Halpin and P.H. Petit, Primer on Composite Materials: Analysis, Technomic Press, Westport, CT, 1969.
6. Noor, A. et al. (eds.) (1989), "Analytical and Computational Models of Shells", ASME Special Publication, CED-3.
7. Bathe, K.J. and Dvorkin, E. (1986), "A Formulation of General Shell Elements | the Use of Mixed Interpolation of Tensorial Components", International Journal for Numerical Methods in Engineering, 22, pp. 697-722.
8. Koiter, W.T. (1959), "A Consistent First Approximation in General Theory of Thin Elastic Shells", In Proc. IUTAM Symposium on the Theory of Thin Elastic Shells, Delft, pp. 12-33.
9. R. F. Gibson, Principles of Composite Material Mechanics, McGraw-Hill, New York, 1994.
10. Z. Vnućec, Engineering Properties and Applications of the Laminated Composite Materials, RIM'99 – Revitalization and Modernization of Production, Proceedings, pp 71- 78, Bihac, 1999.

Design and fabrication of agriculture cutting machine using crank and slotted lever mechanism

Mr. M Gangaraju, Mr. K.Ravi Prasad and Mr. Shaik Fahad,

Department of Mechanical Engineering, Sree Vidyanikethan Engineering College, Tirupati, INDIA.

ABSTRACT: Agriculture is one of the oldest professions but the development and use of machinery has made the job title of farmer a rarity. The basic technology of agricultural machines has changed little in the last century with the coming of the Industrial Revolution and the development of more complicated machines. In this work design and fabricate the automatic mechanical cutter by using crank and slotted lever mechanism, for cutting agricultural products like sugarcane, long grasses, etc for cultivation. The present work to fabricate a machine which is simple in construction than the existing machines. The equipment make the use of crank and slotted lever mechanism with one slider to couple with an electric motor or manually operated by hand using pulley and belt. **Key words:** Composite plate, SMC panels, Composite Design, Finite element method, Fibre length.

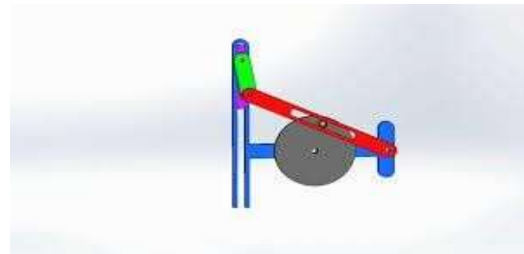
I. INTRODUCTION

The working principle behind the operation of simple mechanical cutting machine is four bar chain mechanism particularly crank and slotted lever mechanism. The crank wheel is rotated by the motor through the pulley belt assembly. The rotating motion of the crank wheel is converted into oscillating motion by the coupling link by using the slider. The oscillating motion at the other end of the coupling link is converted into reciprocating motion to the blade by using guide hole. Therefore the rotating motion of the crank wheel is converted into reciprocating motion to the blade through the coupling link. The object to be cut is place on the platform. Due to the reciprocating motion of the blade, the object placed on the platform is cutter for successfully transmitting the rotational motion from the motor to the crank with minimum slip v-belt drive is used. The bearing which supports the shaft is rolling ball bearing for smooth operation. by using 110 watt power single phase a.c induction motor, this machine can able to reciprocates approximately 250 times per minute.

II. MATERIALS AND METHODS

If a number of bodies are assembled in such a way that the motion of one causes constrained and predictable motion to the others, it is known as a mechanism. A mechanism is a simplified model, usually in the form of a line diagram, which is used to reproduce the motion occurring in a machine. The purpose of this reproduction is to enable the nature of the machine. The purpose of this reproduction is to enable the nature of the motion to be investigated without the encumbrance of the various solid bodies which form the machine elements. The various parts of the mechanism are called links or elements. Where two links are in contact and a relative motion is possible, then they are known as a pair. An arbitrary set of a links which form

a closed chain that is capable of relative motion, and that can be made into a rigid structure by the addition of a single link, is known as a kinematics chain. To form a mechanism from a kinematics chain one of the links must be fixed. However as any of the links can be fixed, it follows that there are as many mechanism as there are links in the chain. The technique obtaining



different mechanism by fixing the various links in turn is known as inversion.

Fig-1. Crank and Slotted lever

Material Used:

Blade:



Motor:

Motor is used to produce high torque with low speed motor used has specifications as single phase 220V, 15A which produces power of 0.35 HP and frequency of 50 Hz and the shaft speed is 75 rpm



Shaft:

Shaft made up of mild steel of diameter 15mm is used to transmit rotary motion from motor to the four bar

linkage. Holes provided on the shaft, adjust the four bar linkage according to the diameter of the tank



Bolt and Nut:

When selecting fasteners that are to be assembled together, it is important to consider their strength compatibility. The nut should always be stronger than the bolt, so when using higher strength bolts, such as metric class 10.9, make sure to use the correct, corresponding nut. In this case, a class 10 nut would be correct. Stronger nuts may be used with lower strength bolts without any problems. Strength of washers should also be considered, but are often overlooked. Using non-heat treated washers with heat treated hex head cap screws can cause joint settling as the relatively small bearing surface of the cap screw can embed itself into the soft washer over time, causing a loss of clamp load. Standard metric flat washers have class designations that can be paired with heat treated bolts. Below is a compatibility chart that will help you make the right choice.

III. MECHANISM USED

Common to most reciprocating engines is a linkage known as a crank-slider mechanism. Diagrammed in Figure.5, this mechanism is one of several capable of producing the straight-line, backward-and-forward motion known as reciprocating. Fundamentally, the crank-slider converts rotational motion into linear motion, or vice versa.

The position of the piston with respect to the crank center line problem for the control is given by

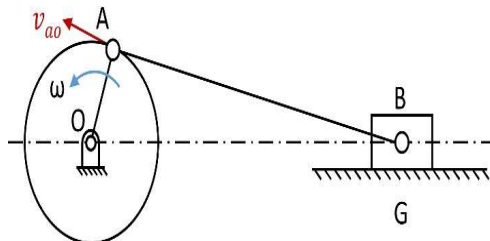
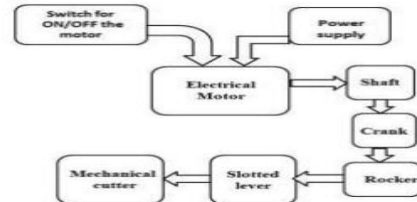


Fig-2. Slider mechanism

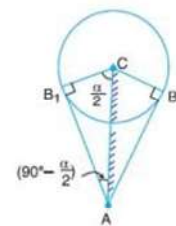
IV. CRANK ROCKER MECHANISM

The four bar linkage is the simplest and often times, the most useful mechanism. As we mentioned before, a mechanism composed of rigid bodies and lower pairs is called a linkage (Hunt 78). In planar mechanisms, there are only two kinds of lower pair sand revolute pairs and prismatic pairs. The simplest closed-loop linkage is the four bar linkage which has

four members, three moving links, one fixed link and four pin joints. A linkage that has at least one fixed link is a mechanism. This mechanism has four moving links.



V. DETERMINATION OF LENGTH OF STROE AND TIME RATIO:



We know that $\sin \angle CAB_1 = \sin (90^\circ - \frac{\alpha}{2})$

$$= \frac{B_1 C}{AC} = \frac{100}{250} = 0.4$$

$$\angle CAB_1 = (90^\circ - \frac{\alpha}{2}) = 23.58^\circ$$

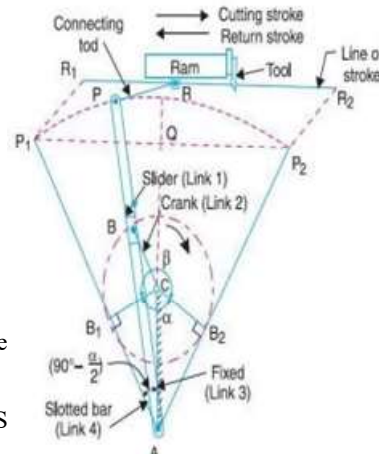
Again,

$$\angle CAB_1 = (90^\circ - \frac{\alpha}{2})$$

$$\alpha = 132.84^\circ$$

$$\text{Time ratio} = \frac{\text{Time of cutting stroke}}{\text{Time of return stroke}} = \frac{360 - \alpha}{\alpha} = 1.71$$

$$\text{Length of stroke} = R_1 R_2 = P_1 P_2 = 2 P_1 Q = 2 AP_1 \sin (90^\circ - \frac{\alpha}{2}) = 520 \text{ mm}$$



where

$$x = (S$$

$y_A = (S/2) \sin \theta = L \sin \theta$ can be used to eliminate θ to obtain

$$X/L = (S/2L) \cos \theta + [1 - (S/2L) \sin \theta]^2$$

VI. CRANK AND SLOTTED LEVER QUICK RETURN MOTION MECHANISM:

In this mechanism, the link AC (i.e. link 3) forming the turning pair is fixed, as shown in Fig. The link 3 corresponds to the connecting rod of a reciprocating steam engine. The driving crank CB revolves with uniform angular speed about the fixed centre C. A sliding block is attached to the crank pin at B slides along the slotted bar AP and thus causes AP to oscillate about the pivoted point A. A short link PR transmits the motion from AP to the ram which carries the tool and reciprocates along the line of stroke R1R2. The line of stroke of the ram (i.e. R1R2) is perpendicular to AC produced. In the extreme positions, AP1 and AP2 are tangential to the circle and the cutting tool is at the end of the stroke. The forward or cutting stroke occurs when the crank rotates from the position CB1 to CB2 (or through an angle β) in the clockwise direction. The return stroke occurs when the crank rotates from the position CB2 to CB1 (or through angle α) in the clockwise direction.

The time ratio is given by-

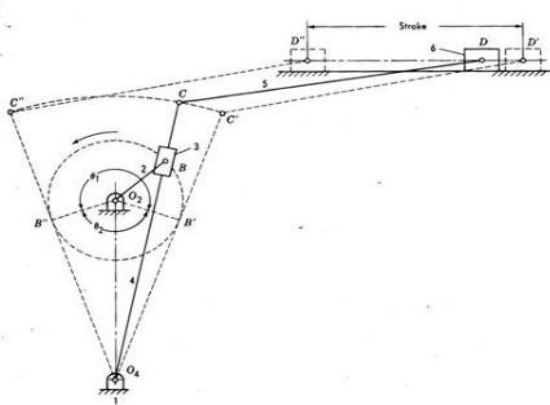
$$\text{Time ratio} = \frac{\text{time of cutting stroke}}{\text{time of return stroke}} = \frac{360 - \alpha}{\alpha}$$

From figure-

$$\sin \angle CAB_1 = \sin \left(90^\circ - \frac{\alpha}{2} \right) = \frac{B_1C}{AC}$$

distance between pivot centres

We have used these two formulas for determining various time ratios and angle turned by crank during return stroke for constant distance between pivots.



I. Fig-3 Quick return mechanism

VII. EXPERIMENTAL SETUP:

All the components of the fabrication of mechanical cutter such as rotor, crank, cutter, slotted lever, four bar mechanism are placed very carefully set on the frame stand. The existing model presents an Integrating feature of all the hardware components which has been used and developed in it. The presence of each and every module has been reasoned out and placed very carefully experimental setup represents the fabrication of mechanical cutter for agriculture purpose. For doing experiment or to check the ability of the work is created with the crank and slotted lever mechanism and all the required components are carefully connected. In the four bar mechanism having four bars called four bar linkage. As same in the four bar linkage, present work is setup in the same order wise. The electrical motor clamped on the frame. Firstly the rotor shaft is connected with the crank. The first edge of the rocker is connected with crank and the second edge of the rocker is pinned with the slotted lever, it moves along the parallel motion. Finally the slotted lever is joined with the working blade. The working blade is fixed at the bottom side of the stand the working procedure of design and fabrication of mechanical cutter is to check the ability of the work, an experimental setup is created with four bar mechanism and all required components are carefully connected.

In the four bar mechanism having four bar called four bar linkage. As same in the four bar linkage, the present work is setup in the order wise.

Figure: The parts or linkages of four bar linkage are crank, rocker, slotted lever and frame. The whole setup of the work is placed on a frame. The motor is working with the help of electric power supply, on the motor shaft fixing the arrangement of crank. When switch ON power button, the motor start to rotate and the total arrangements. Here the rotary motion is converted in to the reciprocating motion by using simple mechanisms. The reciprocating motion ram is connected to the cutters as shown in figure 4.1, so that the cutter moves upward and downward direction the cutting process is carrying out through this machine. At that situation the work means sugar cane or required size of boiler sticks is placed under the knife-edge cutter after that it will be separated and obtain require size. The separated work will fall down under the frame.

Then sugarcane pieces will be collected and the process of work will be continuously repeated. Rocker, slotted lever, frame. The whole setup of the work is placed on a frame. The motor is working with the help of electric power supply, on the motor shaft fixing the arrangement of crank. When switch ON power button, the motor start to rotate and the total arrangements. Here the rotary motion is converted in to the reciprocating motion by using simple mechanisms. The reciprocating motion ram is connected to the cutters as shown in figure 4.1, so that the cutter moves upward and downward direction the cutting process is carrying out through this machine. At that situation the work means sugar cane or required size of boiler sticks is placed under the knife-edge cutter after that it will be separated and obtain require size. The

separated work will fall down under the frame. Then sugarcane pieces will be collected and the process of work will be continuously repeated.

IX SOFTWARE USED

Creo parametric 2.0

What is CREO PARAMETRIC 2.0 all about



Creo Parametric provides the broadest range of powerful yet flexible CAD 3D modeling software capabilities to accelerate the design of parts and assemblies.

Creo Elements is a software application within the CAID/CAD/CAM/CAE category. Creo Elements is a parametric, feature-based modeling architecture incorporated into a single database philosophy with rule-based design capabilities. It provides in-depth control of complex geometry. The capabilities of the product can be split into the three main headings of Engineering Design, Analysis and Manufacturing. This data is then documented in a standard 2D production drawing or the 3D drawing standard [ASME Y14.41-2003](#)

- Product Design

Creo Elements offers a range of tools to enable the generation of a complete digital representation of the product being designed. In addition to the general geometry tools there is also the ability to generate geometry of other integrated design disciplines such as industrial and standard pipe work and complete wiring definitions. Tools are also available to support collaborative development.

A number of concept design tools that provide up-front Industrial Design concepts can then be used in the downstream process of engineering the product. These range from conceptual Industrial design sketches, reverse engineering with point cloud data and comprehensive free-form surface.

- Analysis

Creo Elements has numerous analysis tools available and covers thermal, static, dynamic and fatigue finite element analysis along with other tools all designed to help with the development of the product. These tools include human factors, manufacturing tolerance, mould flow and design optimization. The design optimization can be used at a geometry level to obtain the optimum design

dimensions and in conjunction with the finite element analysis.

- Surface Modelling

Creo has a good surface modeling capabilities also. Using commands like Boundary blend and Sweep we can create surface models. Advance options like Style (Interactive Surface Design Extension - ISDX) and Freestyle [\[3\]](#) provide more capabilities to designer to create complicated models with ease.

- Manufacturing

By using the fundamental abilities of the software with regards to the single data source principle, it provides a rich set of tools in the manufacturing environment in the form of tooling design and simulated CNC machining and output.

Tooling options cover specialty tools for molding, die-casting and progressive tooling design.

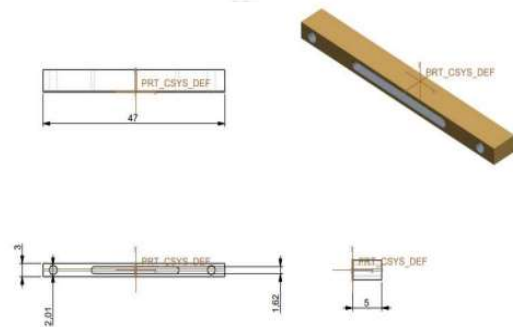


Figure-4 Slotted lever

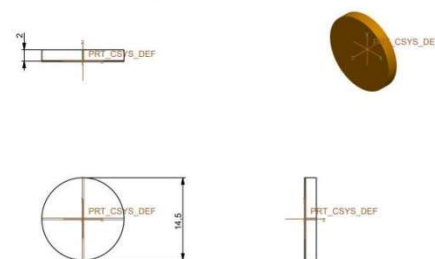


Figure-6 Crank

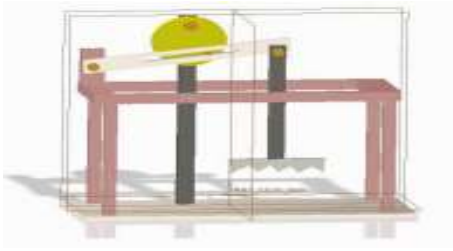


Fig-7 Assembly of components in zero parametric 2.0

CONCLUSION

The existing model presents an Integrating feature of all the hardware components used have been developed in it. The mechanical cutter system helps to the agriculture products cutting and also used to decrease human assistance. The presence of each and every module has been reasoned out and placed very carefully. Hence the contributing to the best working unit for “Design and development of mechanical cutter” has been designed and fabricated perfectly. Thus, the work has been successfully fabricated and tested.

REFERENCES

1. Hajrachoudhury S.K., Hajrachoudhury, A.K. Nirjharroy, Elements of workshop technology volume II –twelfth edition Media promoters and publishers pvt .Ltd, 2007.
2. Rattan .S.S Theory of machines third edition. Tata McGraw Hill publications, New Delhi ,1988. 3.
3. Roa .J.S. and Dukkipatti T.V, Mechanism and machine theory” Wiley eastern ltd, New Delhi 1992
4. Bansal, R.K. Strength of materials”. Lakshmi Publishers. Joseph Edward Shigleyand Charles R. Mschke Mechanical EGINEERING Design ” McGraw Hill Publications, 1989
5. Wen-Hsiang Hsieh and Chia-Heng Tsai, —A Study On A Novel Quick Return Mechanisml, Vol. No. 08-CSME-13, E.I.C. Accession 3051, September 2009.
6. Matt Campbell Stephen S. Nestinger, Department of Mechanical and Aeronautical Engineering, University of California Davis, CA 95616,—ComputerAided Design and Analysis Of the Whitworth Quick Return Mechanism.
7. Dr. Harry H. Cheng, —Computer-Aided Mechanism Designl in journal of Mechanical Engineering Sc

DESIGN AND ANALYSIS OF HELICAL COIL SPRING IN TWO WHEELER SUSPENSION SYSTEM

K. John Babu, K. Maria Arun Kumar and E. Ramu

Department of Mechanical Engineering, Narasaraopeta Engineering College, Narasaraopeta, India

Abstract— In vehicles problem happens while driving on bumping road condition. The objective of this project is to design and analyze the performance of Shock absorber by varying the wire diameter of the coil spring. The Shock absorber which is one of the Suspension systems is designed mechanically to handle shock impulse and dissipate kinetic energy. It reduces the amplitude of disturbances leading to increase in comfort and improved ride quality. The spring is compressed quickly when the wheel strikes the bump.

The compressed spring rebound to its normal dimension or normal loaded length which causes the body to be lifted. The spring goes down below its normal height when the weight of the vehicle pushes the spring down. This, in turn, causes the spring to rebound again. The spring bouncing process occurs over and over every less each time, until the up-and- down movement finally stops. The vehicle handling becomes very difficult and leads to uncomfortable ride when bouncing is allowed uncontrolled. Hence, the designing of spring in a suspension system is very crucial. The analysis is done by considering bike mass, loads, and no of persons seated on bike. Comparison is done by varying the wire diameter of the coil spring to verify the best dimension for the spring in shock absorber.

Modelling and Analysis is done using CATIA and ANSYS respectively. Shock absorber are made with Structural steel, Titanium alloy, Beryllium copper. Modelling of the components are done by CATIA. Parameters such as Stress, Deformation, and Shear stress are tested using ANSYS. Based on the full results Structural steel is best suitable for shock absorber system.

Keywords: Spring, Stress, Ansys, Catia

I. INTRODUCTION

The suspension system is the main part of the vehicle, where the spring is designed to handle shock impulse and dissipate kinetic energy. In a vehicle, shock absorbers reduce the effect of traveling over rough ground, leading to improved ride quality and vehicle handling. The limiting excessive suspension movement is served by the spring. Hysteresis is the tendency for elastic materials to rebound with less force. Hence, the designing of suspension system is very crucial. In modelling, the time is spent in drawing the helical coil spring model and the front suspension system, where the risk involved in design and manufacturing process can be easily reduced. So the

modeling of the coil spring is made by using CATIA. Later the model is imported to ANSYS for the analysis work.

II. LITERATURE SURVEY

For providing the best design of spring coil to the suspension system of two wheeler vehicles, a lot of technical papers and review processes is studied before deciding the most feasible process for the work. The following list presents a gist of the main papers referred throughout the: [1] Dr A.Gopichand, In this a shock absorber is designed and a 3D model was developed in PROE. Later structural and static analysis was done by varying the materials as structural steel, chrome vanadium and AISI 1050 steel. Comparison is made by between the simulation, analytical and experimental values for deflection and maximum shear stress. [2] N.Lavanya, The present work is optimum design and analysis of a suspension spring for motor vehicle subjected to static analysis of helical spring the work shows the strain and strain response of spring behavior will be observed under prescribed or expected loads and the induced stress and strains values for low carbon structural steel is less compared to chrome vanadium material also it enhances the cyclic fatigue of helical spring.[3] Kommalapati. Rameshbabu, In this project they have designed a shock absorber used in a 150CC bike and modeled the shock absorber by using 3D parametric software Pro/Engineer.

Applications Shock absorbers are an important part of automobile and motorcycle suspensions, aircraft landing gear, and the supports for many industrial machines. Large shock absorbers have also been used in structural engineering to reduce the susceptibility of structures to earthquake damage and resonance. A transverse mounted shock absorber, called a yaw damper, helps keep railcars from swaying excessively from side to side and are important in passenger railroads, commuter rail and rapid transit systems because they prevent railcars from damaging station platforms

MATERIAL USED FOR HELICAL SPRING:

The following materials used for this work: Structural Steel, Beryllium Copper, Titanium Alloy

SOFTWARE (CATIA and ANSYS WORKBENCH)
CATIA is a multi-platform software suite for computer-

aided design, computer-aided manufacturing, computer-aided engineering, PLM and 3D. With the use of CATIA software, suspension system has designed a helical spring with accurate dimensions which is taken from motor bike. The designed helical spring is imported to Ansys software for finding maximum shear stress and total deformation. Ansys is analysis software which develops finite element analysis software used to simulate engineering problems. Ansys software is analyzed a maximum shear stress and Total deformation for three materials (Structural Steel, Beryllium Copper, Titanium Alloy). The analytical results conform to the simulation results from the ANSYS

HELICAL SPRING DESIGN: The following are the factors are considered for design and explain in this section.

- Spring wire diameter (d) = 7 mm,
- Coil mean diameter (D) = 42 mm,
- Coil free height (h) = 100 mm,
- No. of active coils (n) = 14,
- Pitch (P) = 10 mm.

DESIGN SPECIFICATIONS OF HELICAL COIL SPRING: Consider, Assume the bike 100cc splendour plus assume the only bike weight without any weight on this is 112kg,

1. Bike load (assume) = 112kg
2. Bike load + 1 person = 112 + 60 = 172kg
3. Bike load + 2 person = 172 + 60 = 192kg
4. Bike load + 3 person = 192 + 60 = 252kg.

Spring Index: $k = D/d = 42.5/7 = 6$

Inner Diameter of spring: $= D - d = 42.5 - 7 = 35$

Outer Diameter of a spring: $= D + d = 42.5 + 7 = 49$.

Spring Index: $C = D/d = 42.5/7 = 6$

Shear Stress: $\tau = K(8PD/\pi d^3)$

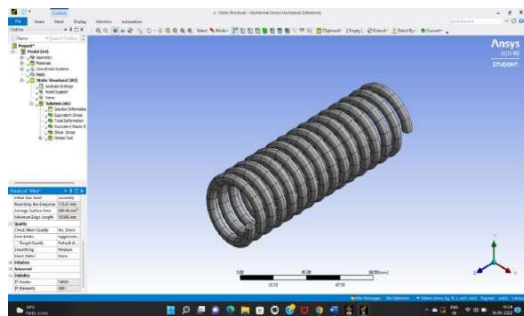


Figure 1: Meshing the model

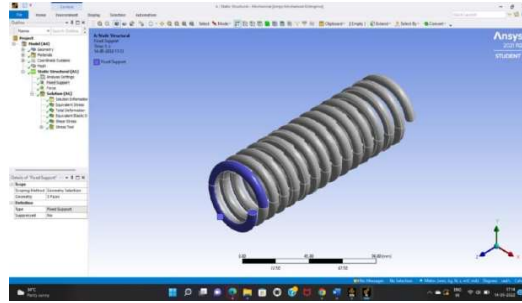


Figure 2: Apply the force to the spring

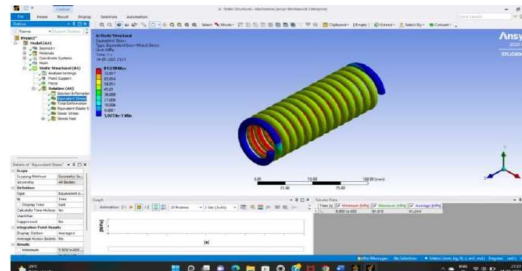


Figure 3: Pictorial view of equivalent stress at 112N

The analysis has based on the boundary condition. The pictorial view of equivalent Minimum stress is $5.905e-005$ and maximum stress is 81.019(MPA).

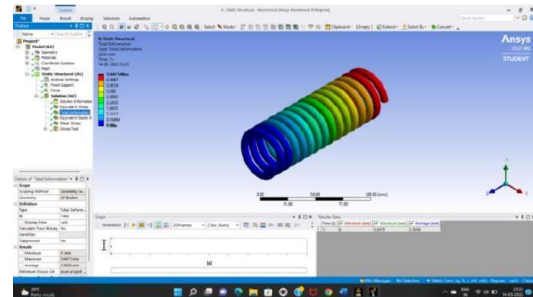


Figure 4: Pictorial view of deformation at load 112N

The analysis has based on the boundary condition. Pictorial view of minimum Deformation is 0, and maximum deformation is 5.0475(MPA).

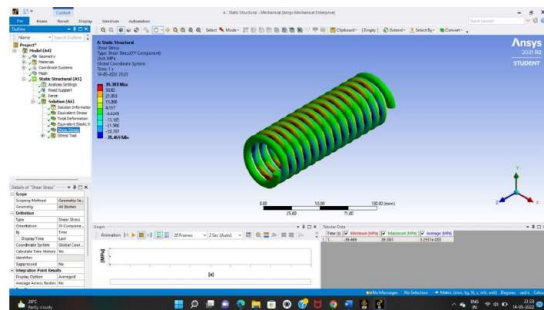


Figure 5: Pictorial view of shear stress at 112N

The analysis has based on the boundary condition. The pictorial view of minimum Shear stress is 39.469(MPA), and maximum shear stress is 39.381(MPA).

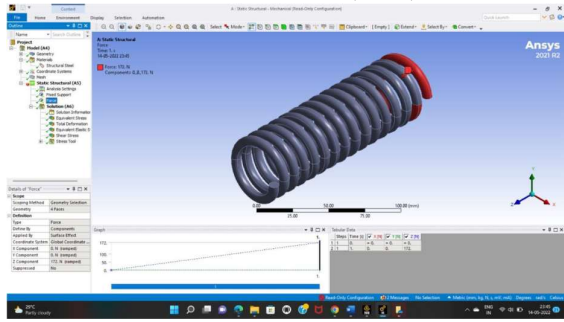


Figure 6: Pictorial view of load applied on the spring

The analysis has based on the boundary condition. Pictorial view of load On the spring is 112N

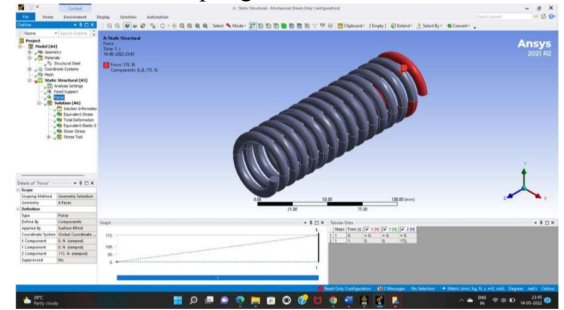


Figure 7: Pictorial view of load applied on the spring

The analysis has based on the boundary condition. Pictorial view of load on the spring is 172N

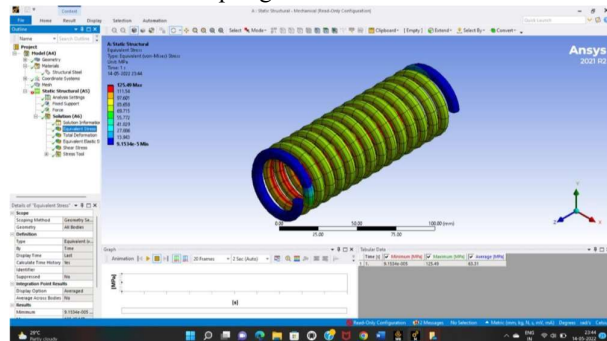


Figure 8: Pictorial view of stress at load 172N

The analysis has based on the boundary condition. The Pictorial view of equivalent Minimum stress is 9.1534e-005 and maximum stress is 125.49(MPA).

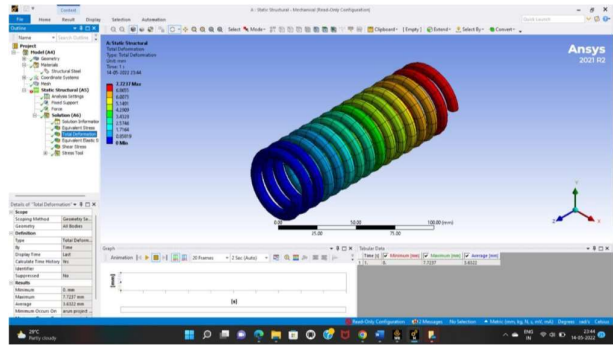


Figure 9: Pictorial view of deformation at 172N
The analysis has based on the boundary condition. Pictorial view of minimum. Deformation is 0, and maximum deformation is 7.723(MPA).

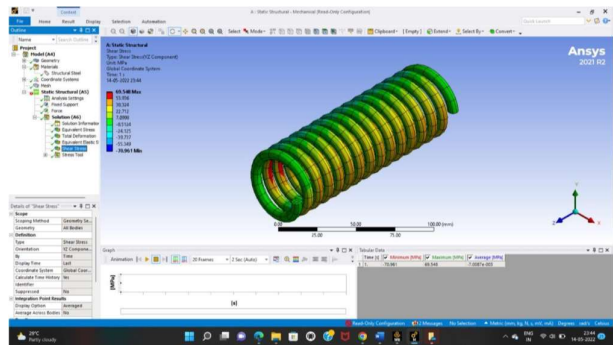


Figure 10: Pictorial view of shear stress at load 172N

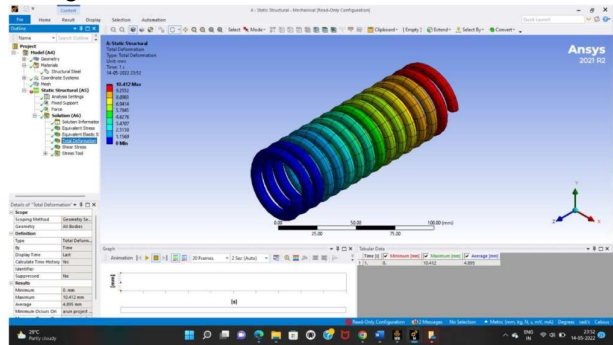


Figure 11: Pictorial view of deformation at 172N
The analysis is based on the boundary condition. The pictorial view of minimum Shear stress is -70.961(MPA), and maximum shear stress is 69.548(MPA)

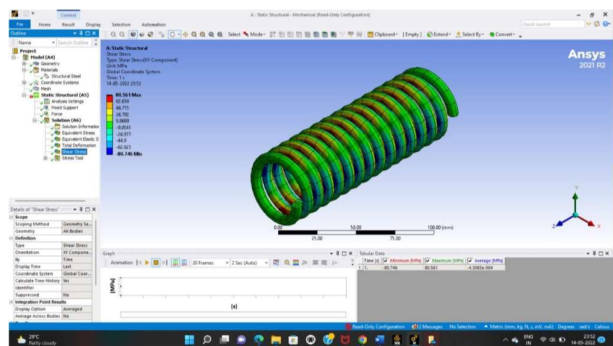


Figure 12: Pictorial view of shear stress at load 232N

The analysis is based on the boundary condition. The pictorial view of minimum shear stress is -80.746(MPA), and the maximum shear stress is 80.561(MPA).

III. RESULTS AND DISCUSSION

The analysis has been done based on boundary conditions. The results obtained from the analysis are shown in tabular form in the below sections. Structural FEA analyses in ANSYS Mechanical, you can be curious about the deformation results. ANSYS provides a very useful deformation result tool that you can easily add to your solutions. Here, we show how to see the deformation results in ANSYS Mechanical, and we will show you the most important options for the deformation results in ANSYS Mechanical. In the ‘Results’ and ‘Information’ sections, you can see all the required information about the maximum, minimum, and average deformation results

Observation:

In this project was done by a helical compression spring is designed as CATIA structural and finite element analysis on the helical spring and it is analysed by different materials. In this suspension spring, four different materials like structural steel, Beryllium copper, Titanium alloy were used and applied a constant load of 112N, 172N, 232N, and 292N, based on the theoretical calculations obtained. The boundary conditions considered are the bottom portion of the part is fixed and the load is applied at the top position. Because of the applied load the stresses will be developed in the spring. Here stress values are compared for different materials.

After analysing and comparing the results, the spring made with structural steel has less stress value that is 81Mpa at load of 112N and 252.08Mpa at 292N load ,when completed to other materials out of all materials are Berllium Copper on the applied load is 232N that time measured the values are equivalent stress maximum (1.4203e-004Mpa) and minimum (125.17Mpa)stress, at the position of the total deflection minimum is 0 mm and maximum 26.712mm ,and minimum shear stress is -95.241(Mpa) the maximum shear stress

95.567Mpa.and the last material is Titanium Alloy on the applied load is 292N that time measured the values are equivalent stress maximum(4.7859e-005Mpa) and minimum (209.65Mpa)stress,the total deflection minimum is 0 and maximum 34.417 mm and minimum shear stress is -122.5Mpa and maximum shear sress is 122.26Mpa.

Graphical Representation of Static Analysis of a Different Materials

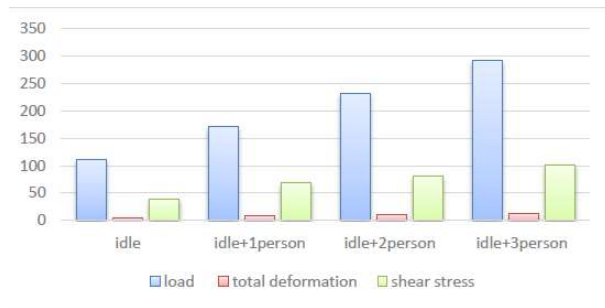


Fig 12: Graph representation of a maximum Structural Steel

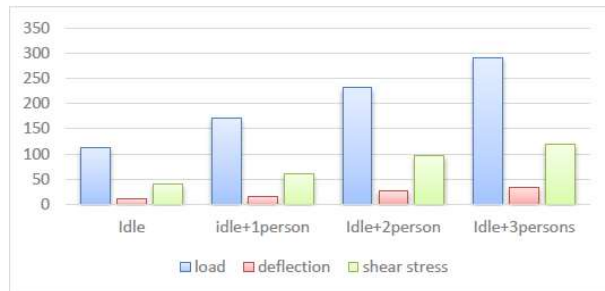


Fig 13: Graph representation of a maximum beryllium copper

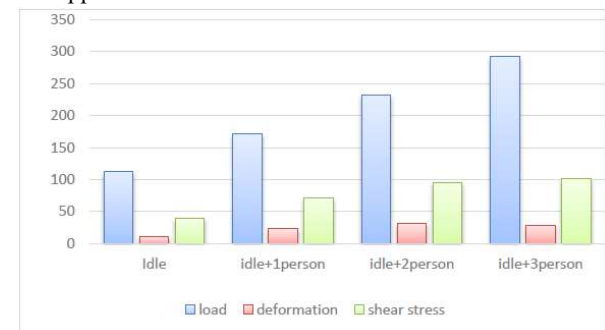


Fig 14: Graph representation of a maximum Titanium Alloy

IV. CONCLUSION

This project was done by a helical compression spring is designed as CATIA structural and finite element analysis on the helical spring and it is analyzed by different materials. In this suspension system, four different materials like structural steel, Beryllium Copper, and Titanium alloy were used and applied a constant load of 112N, 172N, 232N and 292N, based on the theoretical calculations obtained. The boundary conditions considered are the bottom portion of the part is fixed and the load is applied at the top position. Because of the applied load the stresses will be developed in the spring. Here stress values are compared for different materials.

After analysing and comparing the results, the spring made with structural steel has less stress value that is 81MPa at a load of 112N and 252.08 MPA at 292N load, when completed to other materials out of all materials are Beryllium Copper on the applied load is 232N that time measured the values are equivalent stress maximum

(1.4203e-004MPa) and minimum (125.17MPa) stress, at the position of the total deflection minimum is 0 mm and maximum 26.712mm, and minimum shear stress is -95.241(MPa) the maximum shear stress 95.567MPa. and the last material is Titanium Alloy on the applied load is 292N that time measured the values are equivalent stress maximum(4.7859e-005MPa) and minimum (209.65MPa) stress, the total deflection is zero at minimum and maximum at 34.417 mm and minimum shear stress is -122.5MPa and maximum shear stress is 122.26MPa. Fig 6.5.16: Pictorial view of shear stress at load 292N

The least stress value material is Structural steel and its stress value is 252.68MPa. Finally after comparing the analysed stress values Structural steel having the less stress value. So we conclude that Structural steel is the best suitable material for the spring

FACTURE SCOPE

Analysis of helical spring can be performed and tested in Finite Element Analysis (FEA), Dynamic analysis of spring can also be performed on ANSYS software to get better Results. Analysis of different spring either for heavy duty vehicle or light duty vehicle can also be analysed. There is a growing opportunity of a spring with the steel material and use of composite materials for helical spring in the future many.

REFERENCES

1. Chavhan.G.R, Burande.S.W, Dhole.L.P (December 2014) "Analysis of shock absorber using different material of spring" IJAET, Vol .8.
2. Singh Pankaj, Amilkanthwar Rushikesh, Walli Sanket, Jasoliya Viraj, Patel Kaushal (2017) "Design and analysis of helical compression spring used in suspension system by finite element analysis method" IRJET, Vol.6.
3. Prince Jerome Christopher.J., Pavendhan.R (2012)"Design and Analysis of Two Wheeler Shock Absorber Coil Spring"IJMER,Vol.12.
4. Pawar.H.B, Desale.D.D (2018) "optimization of three wheeler front suspension coil spring" ELSEVIER , Vol.7.
5. Vijayeshwar BV, Preetham B M, Bhaskar U (2017) "Design and Static Analysis of Helical Suspension Spring with Different Materials", IARJSET,Vol.4.
6. Atul.M, Pungal, Prof.Bhosale.K.C(2018) "Comparative analysis of two wheeler suspension helical compression spring for steel and composite material at different loading conditions, IRJET,Vol.5"
7. Akshat Jain,SheelamMisra, Arun Jindal, Prateek Lakhian (2017) "Structural Analysis of Compression Helical Spring Used in Suspension System, AIP,Vol.3"
8. Robert L. Norton, "Machine design an integrated approach" Fourth edition, 2010, Pearson publication, pp. 785-806.
9. Michael F.Ashby, "Material selection in mechanical design" Fourth edition, 2011, Elsevier ltd, pp. 31-55.

FE ANALYSIS KNUCKLE JOINT USED IN TRACTOR TRAILER

¹Dr.K.L.N.Murthy and ²N.Vijaya Sekhar

¹AM Reddy College of engineering, Narasaraopet, Andhra Pradesh, India

²Narasaraopeta engineering college, Narasaraopet, Andhra Pradesh, India

ABSTRACT: A knuckle joint is used to connect two rods under tensile load. This joint permits angular misalignment of the rods and may take compressive load if it is guided. These joints are used for different types of connections e.g. tie rods, tension links in bridge structure. In this, one of the rods has an eye at the rod end and the other one is forked with eyes at both the legs. A pin is inserted through the rod end eye and fork-end eyes and is secured by a collar and a split pin. Screwed connections often play an important part in the transmission of load through machine assemblies. In large circuit breakers they are subjected intermittently to high impulsive loads transmitted through large-scale linkages. The paper reports on design and analysis of a knuckle joint which is used in power transmission.

In this study, modelling and analysis of a knuckle joint was performed by using Finite Element Method. The knuckle joint takes compressive loads often, thus there is a need for quality design tools. The modelling of the knuckle joint is done using 3D software. Here we will be using Creo for modelling. These joints are used for different types of connections e.g. tie rods, tension links in bridge structure. In this project, static analysis done at different loads (100N and 110N) with different materials (steel and cast iron) analysis done in ANSYS.

I.INTRODUCTION

In mechanical & automobile domain the joints play very crucial role, depending upon the application the joints are used may be temporary or permanent. For power transmission or motion transfer application we generally uses temporary joints like screwed joint, cotter joint, sleeve cotter joint, universal joint or knuckle joint.

The Knuckle joint is a type of joint which is used in steering system in between the steering rod and pinion of the steering gear, as the line of the action/axis of both the mechanical parts are intersecting and lies in different planes, so it is the only joint that we can employ here In order to gain the maximum productivity for the plant, the manufacturing technology must not be stiff; it must have an option of customizability of manufacturing system to gain the agility. For this a term FMS, i.e., Flexible Manufacturing System is used in order to gain the advantage over simple manufacturing system.

FMS consists of a group of a processing work stations interconnected by means of an automated material handling and storage system and controlled by integrated computer controlled system. FMS is an arrangement of machines interconnected by a transport system which is accurate, rapid and automatic.

The manufacturing plant is located in Gwalior which is a new and developing industry, having a small set up of six milling centers, two turning centers, one drill and a hacksaw machine, with a total employee staff of twenty-five. A small scale industry is manufacturing knuckle joint for automotive applications for his clients in batch

production of fifty pieces. A mechanical joint is a part of machine which are used to connect the other mechanical part or mechanism. Mechanical joints may be temporary or permanent. Most types are designed to be disassembling when required.

KNUCKLE JOINT

Knuckle joint is a joint between two parts allowing movement in one plane only. It is a kind of hinged joint between two rods, often like a ball and socket joint. There are many situations where two parts of machines are required to be restrained, for example two rods may be joined coaxially and when these rods are pulled apart they should not separate i.e. should not have relative motion and continue to transmit force. Similarly if a cylindrical part is fitted on another cylinder (the internal surface of one contacting the external surface of the other) then there should be no slip along the circle of contact. Such situations of no slip or no displacements are achieved through placing a third part or two parts at the jointing regions. Such parts create positive interference with the jointing parts and thus prevent any relative motion and thus help transmit the force. One should remember that the rivets in a riveted joint had exactly the same role as it prevents the slipping of one plate over the other (in lap joint) and moving away of one plate from other (in butt joint). The rivets provided positive interference against the relative motion of the plate. Knuckle joint is another promising joint to join rods and carry axial force. It is named so because of its freedom to move or rotate around the pin which joins two rods. A knuckle joint is understood to be a hinged joint in which projection in one part enters the recess of the other part and two are held together by passing a pin through coaxial holes in two parts. This joint cannot sustain compressive force because of possible rotation about the pin. There are most common in steering and drive train applications where it needs to move something but also need to allow for offset angles. A knuckle joint is used when two or more rods subjected to tensile and compressive forces are fastened together such that their axes are not in alignment but meet in a point.

DESIGN OF KNUCKLE JOINT

The assembly diagram of knuckle joint is as shown in fig.

The dimension of knuckle joints are

Diameter of rod = **d**

Diameter of knuckle pin = **d_p**

Outside diameter of single eye = **d_{oe}**

Outside diameter of double eye = **d_{od}**

Thickness of single eye = **t**

Thickness of fork = **t₁**

Axial tensile force on rod = **P**

(1) Diameter of rod

Consider the rod is subjected to a direct tensile stress

$$\zeta = P / \pi d^2$$

From above equation, diameter of rod 'd' is obtained.

(2) Design of pin (d_p)

(a) Consider the failure of pin under double shear due to tensile force.

Therefore, direct shear stress induced in knuckle pin is given by Equation

$$\zeta = P / 2A = (P/2) / (\pi/4)d_p^2 = 2P / \pi d_p^2$$

(b) Failure of knuckle pin in bending

Assume there is no clearance or slack but in actual, knuckle pin is loose in forks to permit angular moment of one with respect to other, so it is subjected to bending moment in addition to shear, consider uniformly distributed load along the portion of pin.

Taking moment about axis XX

$$M = [(-P/2) \times (t/4)] + \{ (P/2) \times [(t/2)+(t_1/3)] \}$$

$$= P/2 [(t_1/3)+(t/2)-(t/4)]$$

$$= P/2 [(t_1/3)+(t/4)]$$

Section modulus,

$$Z = (\pi / 32) d_p^3$$

Maximum bending stress, σ_b

$$\sigma_b = M/Z = \{ P/2 [(t_1/3)+(t/4)] \} / \{ (\pi / 32) d_p^3 \}$$

Here, we check the pin in bending and find the value of d_p

(3) Design of single eye:

(a) To find the outside diameter of single eye (d_{oe}) the single eye is subjected to a direct tensile stress, due to this single eye under tear.

$$\sigma_t = P/A = P / (d_{oe}-d_p) \times t$$

(b) Due to direct tensile strength, the single eye is subjected to double shear.

$$\text{Resisting shearing area} = 2(d_{oe}-d_p) \times (t/2)$$

The direct shear stress induced is

$$\zeta = P / (d_{oe}-d_p) \times t$$

From this equation the outside diameter of single eye d_{oe} is obtained.

(C) Failure of single eye or pin due to tensile load in crushing

$$\text{Resisting crushing area} = d_p \times t$$

$$\sigma_c = P / (d_p \times t)$$

Form this equation crushing stress checked if fail, increase the thickness of eye (t).

(4) Design of fork (double eye):

(a) The tearing of the double eye at weakest section due to tension

$$\text{Area resisting tear} = (d_{of} - d_p) \times 2 t_1$$

$$\sigma_t = p / [(d_{of} - d_p) \times 2 t_1]$$

From this equation, find the outside diameter of fork (**dof**).

(b) Failure of double eye (fork) in double shear due to tensile load.

$$\text{Area resisting shear} = 4 \times [(d_{of} - d_p) / 2] \times t_1$$

$$= 2 \times (d_{of} - d_p) t_1$$

The shear stress is given by,

$$\zeta = p / [(d_{of} - d_p) \times 2 t_1]$$

From this equation, check shear stress if less than design, increase thickness of fork t_1 .

(c) Failure double eye in crushing (thickness of fork)

Double eye may fail in crushing due to tensile load

The crushing stress is given by,

$$\sigma_c = P / (2 \times d_p \times t_1)$$

Check crushing stress or find t_1

ANALYTICAL DESIGN:

Assumptions:

1. Rod diameter $d = 40\text{mm}$
2. Load applied $P = 9810\text{ N (1Ton)}$
3. Diameter of knuckle pin (d_p) = d
 $d_p = 40\text{mm}$
4. Thickness of single eye (t) = $1.25d$
 $= 1.25 \times 40\text{ t} = 50\text{mm}$
5. Thickness of fork (t_1) = $0.75d$
 $= 0.75 \times 40\text{ t}_1 = 30\text{mm}$
6. Outer diameter of eye (D) = $2d$
 $= 2 \times 40\text{ D} = 80\text{mm}$
7. Failure of fork end in tension (σ_t)
 $\sigma_t = 4.0875\text{ N/mm}^2$
8. Failure of fork end in shear (τ)
 $\tau = 4.0875\text{ N/mm}^2$

I. MATERIALS AND METHODOLOGY

MATERIAL SELECTION

There are several materials used for manufacturing of knuckle joint such as S.G. iron (ductile iron), white cast iron and grey cast iron. But grey cast iron mostly used. Forged steel are most demanding material for this application. For this Structural steel is used Structural Steel

- Modulus of Elasticity: $2.0 \times 10^5\text{ MPa}$
- Poisson's ratio: 0.30
- Density: $7.85 \times 10^{-6}\text{ kg/mm}^3$
- Yield Strength: 250 MPa

CALCULATIONS OF KNUCKLE JOINT

PROBLEM: Two mild steel rods are connected by a knuckle joint to transmit an axial force of 50kN . Design the joint completely assuming the working stresses for both the pin and rod materials to be 100 MPa in tension, 65MPa in shear and 150 MPa in crushing. Refer to figure For failure of rod in tension, $P = \pi d^2 \sigma_y$. On substituting $P=50\text{ kN}$,

$\sigma_y = 100 \text{ MPa}$ we have $d = 25 \text{ mm}$. Let us choose the rod diameter $d = 25 \text{ mm}$ which is the next standard size. We may now use the empirical relations to find the necessary dimensions and then check the failure criteria. $d_1 = 25 \text{ mm}$, $t = 32 \text{ mm}$, $d_2 = 50 \text{ mm}$, $t_1 = 19 \text{ mm}$; $d_3 = 38 \text{ mm}$, $t_2 = 13 \text{ mm}$; Split pin diameter = $0.25d_1 = 10 \text{ mm}$

INTRODUCTION TO CAD

Computer-aided design (CAD) is the use of computer systems (or workstations) to aid in the creation, modification, analysis, or optimization of a design. CAD software is used to increase the productivity of the designer, improve the quality of design, improve communications through documentation, and to create a database for manufacturing. CAD output is often in the form of electronic files for print, machining, or other manufacturing operations. The term CADD (for Computer Aided Design and Drafting) is also used.

Its use in designing electronic systems is known as electronic design automation, or EDA. In mechanical design it is known as mechanical design automation (MDA) or computer-aided drafting (CAD), which includes the process of creating a technical drawing with the use of computer software. CAD may be used to design curves and figures in two-dimensional (2D) space; or curves, surfaces, and solids in three-dimensional (3D) space.

CAD is an important industrial art extensively used in many applications, including automotive, shipbuilding, and aerospace industries, industrial and architectural design, prosthetics, and many more. CAD is also widely used to produce computer animation for special effects in movies, advertising and technical manuals, often called DCC digital content creation. The modern ubiquity and power of computers means that even perfume bottles and shampoo dispensers are designed using techniques unheard of by engineers of the 1960s. Because of its enormous economic importance, CAD has been a major driving force for research in computational geometry, computer graphics (both hardware and software), and discrete differential geometry.

II. INTRODUCTION TO CREO

PTC CREO, formerly known as Pro/ENGINEER, is 3D modeling software used in mechanical engineering, design, manufacturing, and in CAD drafting service firms. It was one of the first 3D CAD modeling applications that used a rule-based parametric system. Using parameters, dimensions and features to capture the behavior of the product, it can optimize the development product as well as the design itself.

The name was changed in 2010 from Pro/ENGINEER Wildfire to CREO. It was announced by the company who developed it, Parametric Technology Company (PTC), during the launch of its suite of design products that includes applications such as assembly modeling, 2D orthographic views for technical drawing, finite element analysis and more.

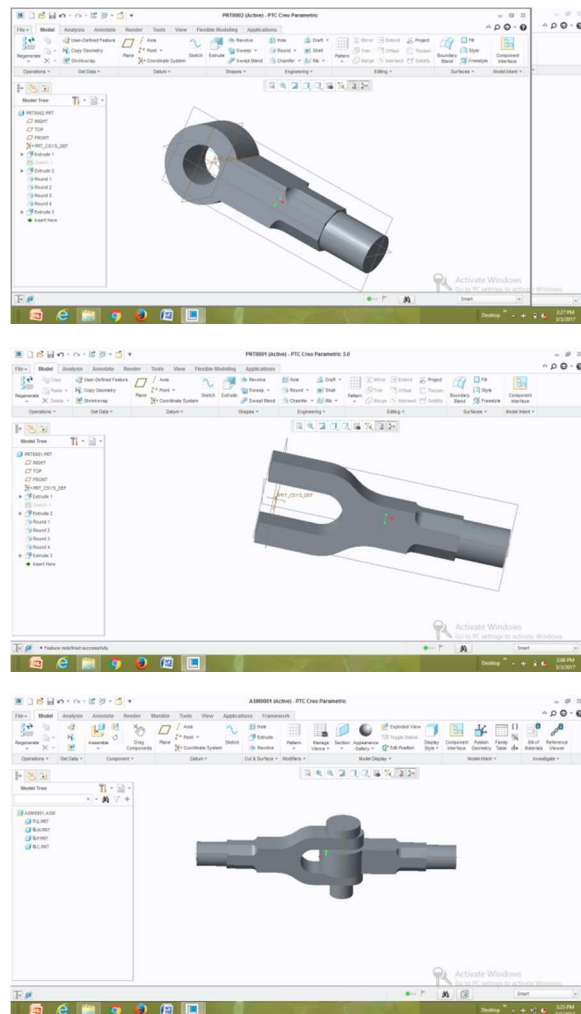
PTC CREO says it can offer a more efficient design experience than other modeling software because of its unique features including the integration of parametric and direct modeling in one platform. The complete suite of applications spans the spectrum of product development, giving designers options to use in each step of the process. The software also has a more user friendly interface that provides a better experience for designers. It also has

collaborative capacities that make it easy to share designs and make changes.

PTC also offers comprehensive training on how to use the software. This can save businesses by eliminating the need to hire new employees. Their training program is available online and in-person, but materials are available to access anytime.

A unique feature is that the software is available in 10 languages. PTC knows they have people from all over the world using their software, so they offer it in multiple languages so nearly anyone who wants to use it is able to do so.

3D MODEL



III. INTRODUCTION TO FEA

Finite element analysis is a method of solving, usually approximately, certain problems in engineering and science. It is used mainly for problems for which no exact solution, expressible in some mathematical form, is available. As such, it is a numerical rather than an analytical method. Methods of this type are needed because analytical methods cannot cope with the real, complicated problems that are met with in engineering. For example, engineering strength of materials or the mathematical theory of elasticity can be used to calculate analytically the stresses and strains in a bent beam, but neither will be very successful in finding out what is happening in part of a car suspension system during cornering.

One of the first applications of FEA was, indeed, to find the stresses and strains in engineering components under load. FEA, when applied to any realistic model of an engineering component, requires an enormous amount of computation

and the development of the method has depended on the availability of suitable digital computers for it to run on. The method is now applied to problems involving a wide range of phenomena, including vibrations, heat conduction, fluid mechanics and electrostatics, and a wide range of material properties, such as linear-elastic (Hookean) behavior and behavior involving deviation from Hooke's law (for example, plasticity or rubber-elasticity).

IV. INTRODUCTION TO ANSYS

Structural Analysis

ANSYS Autodyn is computer simulation tool for simulating the response of materials to short duration severe loadings from impact, high pressure or explosions.

ANSYS Mechanical

ANSYS Mechanical is a finite element analysis tool for structural analysis, including linear, nonlinear and dynamic studies. This computer simulation product provides finite elements to model behavior, and supports material models and equation solvers for a wide range of mechanical design problems. ANSYS Mechanical also includes thermal analysis and coupled-physics capabilities involving acoustics, piezoelectric, thermal-structural and thermo-electric analysis.

Fluid Dynamics

ANSYS Fluent, CFD, CFX, FENSAP-ICE and related software are Computational Fluid Dynamics software tools used by engineers for design and analysis. These tools can simulate fluid flows in a virtual environment — for example, the fluid dynamics of ship hulls; gas turbine engines (including the compressors, combustion chamber, turbines and afterburners); aircraft aerodynamics; pumps, fans, HVAC systems, mixing vessels, hydro cyclones, vacuum cleaners, etc.

V. STATIC ANALYSIS OF KNUCKLE JOINT MATERIAL-STEEL AT LOAD-100N

Save CREO Model as .iges format

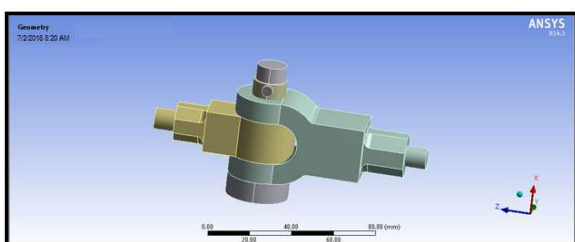
→→Ansys → Workbench→ Select analysis system → static structural → double click

→→Select geometry → right click → import geometry → select browse →open part → ok

→→ Select mesh on work bench → right click →edit

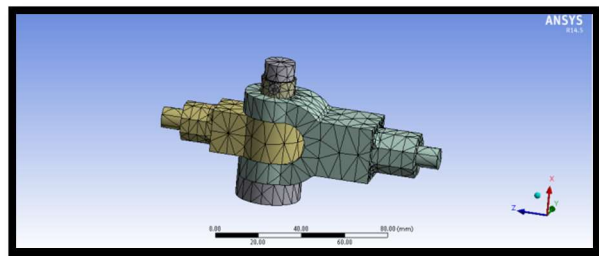
Double click on geometry → select MSBR → edit material →

Imported Model from CREO

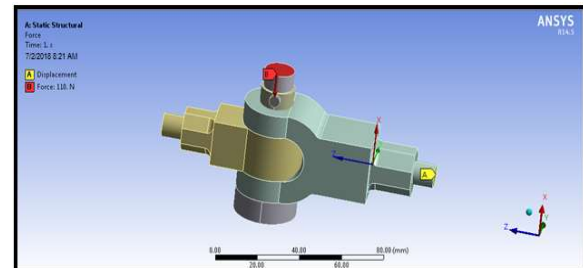


Select mesh on left side part tree → right click → generate mesh →

Meshed Model



Select static structural right click → insert → select rotational velocity and fixed support → Select displacement → select required area → click on apply → put X,Y,Z component zero →



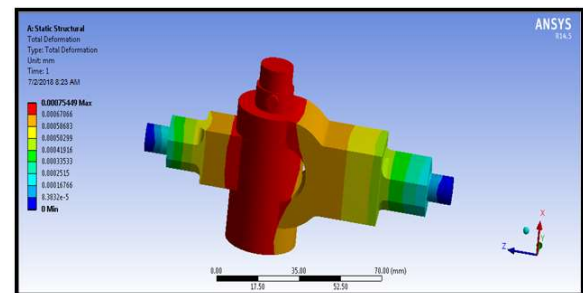
Select force → select required area → click on apply → pressure

Select solution right click → solve →

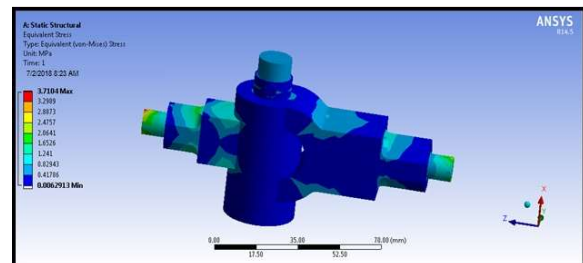
Solution right click → insert → deformation → total → Solution right click → insert → strain → equivalent (von-mises) → Solution right click → insert → stress → equivalent (von-mises) →

Right click on deformation → evaluate all result

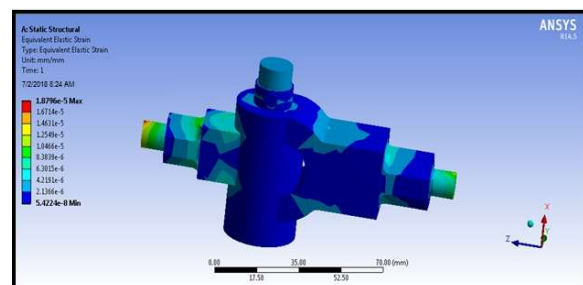
TOTAL DEFORMATION



VON-MISES STRESS

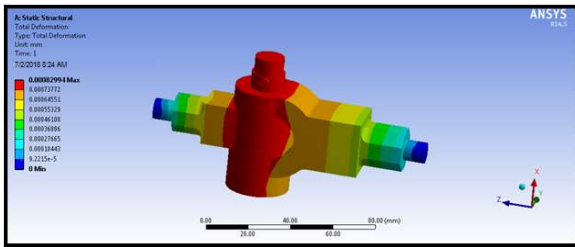


VON-MISES STRAIN

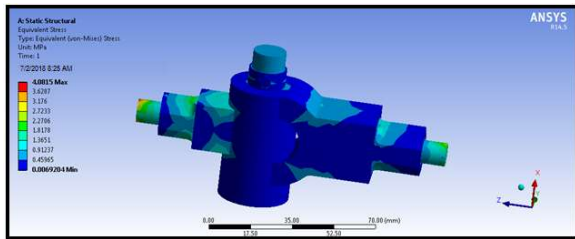


AT LOAD-110N

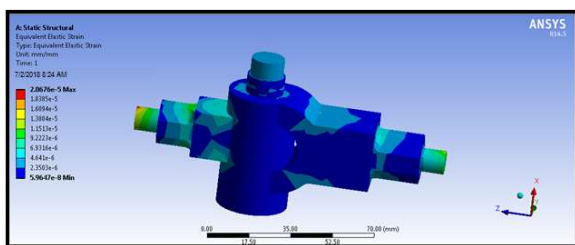
TOTAL DEFORMATION



VON-MISES STRESS



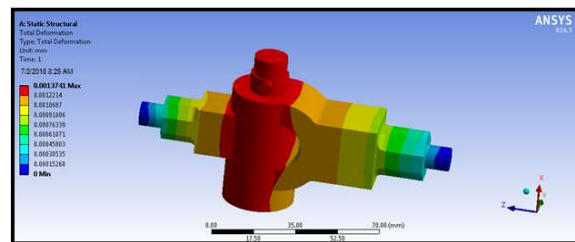
VON-MISES STRAIN



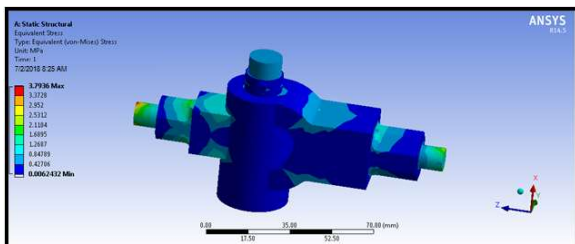
MATERIAL-CASTIRON

AT LOAD-100N

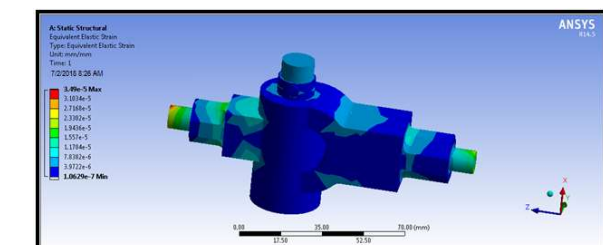
TOTAL DEFORMATION



VON-MISES STRESS

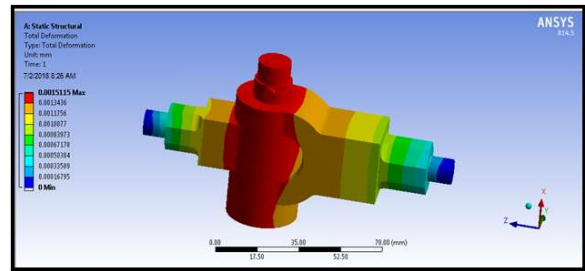


VON-MISES STRAIN

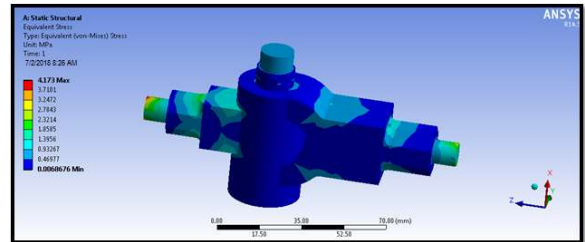


AT LOAD-110N

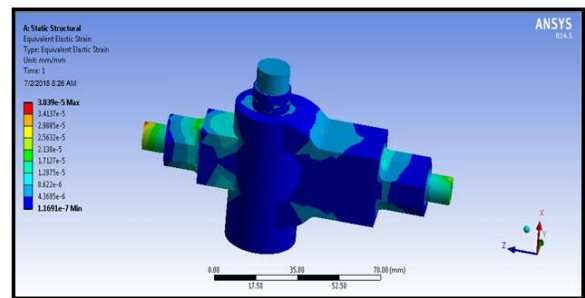
TOTAL DEFORMATION



VON-MISES STRESS



VON-MISES STRAIN



RESULT TABLES

Material	Load (N)	Deformation (mm)	Stress (N/mm ²)	Strain
Steel	100	0.00075499	3.7014	1.87e-5
	110	0.00082994	4.0815	2.06e-5
Cast iron	100	0.0013741	3.7936	3.49e-5
	110	0.0015115	4.173	3.839e-5

VI. CONCLUSION

From the above results and discussion, Knuckle joint was design for 100N and 110N axial load by theoretical calculation. Final dimensions from theoretical calculation, model of Knuckle joint is made in CREO. In this project, static analysis done at different loads (100N and 110N) with different materials (steel and cast iron) in static analysis, observed the stress values are less steel compared with cast iron at 100N load. So it can be concluded that the better material for steel.

REFERENCES

1. Gupta, R.S. Khurmi, J.K. (2008). A textbook of machine design (S.I. units) : [a textbook for the students of B.E. / B.Tech., U.P.S.C. (Engg. Services); Section 'B' of A.M.I.E. (1)] (14th ed.). Ram Nagar, New Delhi: Eurasia Publishing House.
2. R.J. Crawford, BSc, PhD, DSc, FEng, FIMechE, FIM Butterworth Heinemann. PLASTICS ENGINEERING_ Third Edition
3. K.I.Narayan, P,kannaiah, K.Venkata reddy, Machine drawing
4. H. Gradin Jr. Macmillan, Newyork, Xvi + 528pp, 1986, Fundamental of FEM,
5. Irvin L. Rubin (1990).Dry-as Molded/Moisturized, Adapted from: Handbook of Plastic Materials and Technology.

THE AERODYNAMIC ANALYSIS ON CAR BODY AND DRAG REDUCTION BY MODIFYING THE DESIGN

Shaik. Chand Mabhu Subhani and P. Sravani,

Department of Mechanical Engineering, Eswar college of Engineering, Narasaraopet, India.
Department of Mechanical Engineering, Narasaraopeta Engineering College, Narasaraopet, India.

Abstract— This is a case study on the influence of CAR on the global drag characteristics. Reducing overall drag by redesigning the CAR has a potential of almost 20% in the overall drag breakdown, mainly due to the viscous effects and the fluidic interaction of the flow under the car with the typical bluff body flow pattern behind the vehicle. A special parameterization is proposed for the global shape of the sedan car, taking into account most of the specificities of the system. For such a complex interaction, CFD analysis is probably the only efficient tool in order to assess specific design parameterization of a generic car shape. Based on the CFD results, possible strategies to be used in order to reduce viscous drag and global drag characteristics are proposed.

Aerodynamic drag is one of the main obstacles to accelerate a solid body when it moves in the air. Firstly we analyzed the Sedan car using at a definite velocity to note down the Drag coefficient. We also noted the velocity, pressure and Vortex generation around the car body at a certain velocity. Then we validated our Results with the Issued Research Paper and we were almost nearer to the value of Drag coefficient. Further, we tried to reduce the Drag coefficient by attaching the Vortex generator at the rear end of the roof of the Car body.

I. INTRODUCTION

Aerodynamics is a branch of fluid dynamics concerned with studying the motion of air, particularly when it interacts with a moving object. Automotive aerodynamics is a sub branch dealing with the aerodynamics of road vehicles. Its main goals are reducing drag and wind noise, minimizing noise emission, and preventing undesired lift forces and other causes of aerodynamic instability at high speeds. Air is also considered a working fluid in this case. For some classes of racing vehicles, it may also be important to produce downforce to improve traction and thus cornering abilities by understanding the motion of air around an object.

Aerodynamic drag of racing cars has probably received highest attention over last five decades in using the experimental and practical field of fluid dynamics. Many researchers and authors have described different forms of drag, possible reasons behind them and several ways of minimizing the drag to improve the fuel efficiency of the vehicle.

By defining a control volume around the flow field, equations for the conservation of mass, momentum, and energy can be defined and used to solve for the properties. The use of aerodynamics through mathematical analysis, empirical approximation and wind tunnel experimentation form the scientific basis. External aerodynamics is the study of flow around solid objects of various shapes. Evaluating the lift and drag on an airplane, the shock waves that form in front of the nose of a rocket, or the flow of air over a wind turbine blade are examples of external aerodynamics. On the other hand, internal aerodynamics is the study of flow through passages in solid objects. For instance, internal aerodynamics encompasses the study of the airflow through a jet engine or through an air conditioning pipe and other internal flow

conditions.

The vehicle aerodynamic flow process is fall into three types

- (i) Flow of air around the vehicle
- (ii) Flow of air through the vehicle body
- (iii) Flow of air within the vehicle machinery. Today's fast-moving, highly competitive industrial world, a company must be flexible, cost effective and efficient if it wishes to survive. In the process and manufacturing industries, this has resulted in a great demand for industrial control systems/ automation in order to streamline operations in terms of speed, reliability and product output. Automation plays an increasingly important role in the world economy and in daily experience. Automation is the use of control systems and information technologies to reduce the need for human work in the production of goods and services. In the scope of industrialization, automation is a step beyond mechanization. Whereas mechanization provided human operators with machinery to assist them with the muscular requirements of work, automation greatly decreases the need for human sensory and mental requirements as well.

Automation Control System - system that is able to control a process with minimal human assistance or without manual and have the ability to initiate, adjust, action show or measures the variables in the process and stop the process in order to obtain the desired output.

The main objective of Automation Control System used in the industry are:

1. To increase productivity
2. To improve quality of the product
3. Control production cost

1.1 Drag Force

A drag force is the resistance force caused by the motion of a body through a fluid, such as water or air. A drag force acts opposite to the direction of the oncoming flow velocity.

This is the relative velocity between the body and the fluid.

$$D = \frac{1}{2} C \rho A v^2$$

The drag force D exerted on a body traveling through a fluid is given by

Where:

C is the drag coefficient, which can vary along with the speed of the body.

ρ is the density of the fluid through which the body is moving

v is the speed of the body relative to the fluid

A is the projected cross-sectional area of the body perpendicular to the flow direction.

1.2 Vortex Generator

While designing a car, one should consider many factors in mind like fuel efficiency, aerodynamic properties, aesthetic considerations etc. In recent year designers are trying to reduce the drag of the vehicle by using different techniques. Reason behind the reduction in drag is to increase the fuel efficiency. Vortex generator is one of the techniques used to reduce drag of the vehicle by controlling flow separation at the rear roof end of a car. The purpose of using Vortex Generators in car is similar to the aircraft Vortex Generators.

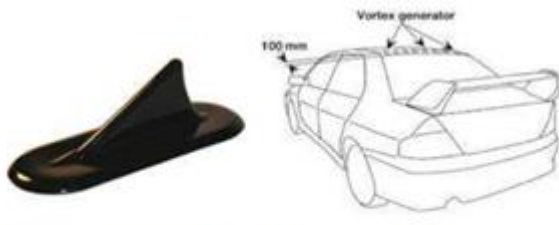


Figure 1.2: Vortex generator and location of vortex generators

II. MODELLING & CFD ANALYSIS ON CAR

CFD is one of the branches of fluid mechanics that uses numerical methods and algorithms to solve and analyse problems that involve fluid flows. Computers are used to

perform the millions of calculations required to simulate the interaction of fluids and gases with the complex surfaces used in engineering. However, even with simplified equations and high speed supercomputers, only approximate solutions can be achieved in many cases. More accurate codes that can accurately and quickly simulate even complex scenarios such as supersonic or turbulent flows are an ongoing area of research.

The physical aspects of any fluid flow are governed by three fundamental principles:

- 1) Conservation of Mass (i.e. Continuity Equation)
- 2) Newton's second law (force = rate of change of momentum)
- 3) Conservation of Energy (Energy equation)

These fundamental principles are expressed in terms of basic mathematical equations, which

Generally are either integral equations or partial differential equations. CFD is the art of replacing the integrals or the partial derivatives in these equations with discretized algebraic forms, which in turn are solved to obtain numerical values for the flow field at discrete points in time and/or space.

There are two principles used to identify an optimum shape for the sedan car when we consider drag reduction as a main objective:

- the car needs to perform its basic functions.

$$\int_S (\vec{U} - \vec{U}_r) \cdot d\vec{S} = 0$$

$$\rho \left(\frac{d}{dt} \int_V \vec{U} dV + \int_S \vec{U} (\vec{U} - \vec{U}_r) \cdot \vec{n} dS \right) = - \int_S p \vec{n} dS + \int_S \vec{\tau} dS + \rho \int_V \vec{f} dV$$

Therefore, shape optimization is performed with constraints, coming from this basic parameters of the basic functionality. This includes the total volume, a fixed geometry for the interior, frozen geometry for the wheels track.

- the optimization with respect to drag reduction is based on the need to improve cruise drag, without affecting other dynamic characteristics. This includes the need for a specific correlation between a down force to be obtained at a specific cruise speed, without introducing additional elements (e.g. wings) in order to achieve this.

Therefore, an interesting analysis for the sedan car would be to identify tools and a methodology for global drag reduction, by re-designing the lower part of the car, mainly the floor.

For this geometry, based on detailed CFD analysis, we consider a set of global data as basic reference:

- Reference speed $V = 25 \text{ m/s (90 Km/h)}$
- Reference Reynolds number $Re = 2.5 \times 10^6$
- Length $b = 1.5 \text{ m}$
- Reference total drag $CD = 0.2411$

Reference lift $CL = 0.5662$

The lift and drag calculated values are for a "clean" surface configuration, without all the additional elements existing on the real car. From experience, if we add all additional elements, the total drag value for this configuration is in the range of $CD=0.28 - 0.3$.

In order to identify a new shape with lower drag, by only changing the lower part of the body, a parameterization of the shape is proposed

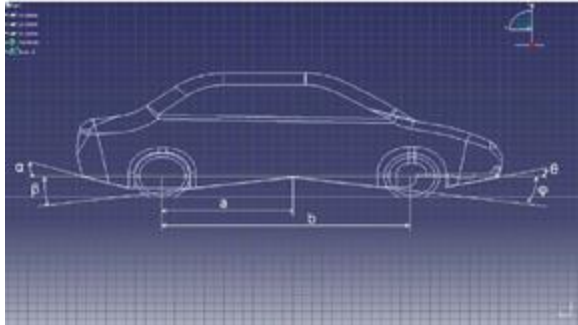


Fig: 2 modelling of car

This parameterization takes into account realistic elements possible to be changed without violating other global functional constraints.

Using this parameterization, we look for a new lower car shape so that the global drag is lower, using independent variation of this parameters. Main interest is for the variation of the angular parameters $\alpha, \beta, \phi, \theta$ (Figure 5).

The CFD analysis is performed based on a discretisation of the model in tetrahedral CFD code used based on unstructured domains, with additional option for grid refinement close to the solid surfaces.

III. NAVIER STOKES EQUATION

The computational flow model is based on the finite volume formulation of unsteady incompressible Navier-Stokes equations, outlined in Versteeg and Malalasekara and implemented in the multi-physics suite of CFD software. For low Reynolds number flight of typical low aspect ratio paper airplane models, the flow can be assumed to be laminar as a first approximation and modelled as follows:

Where;

U is the absolute local velocity relative to the stationary (inertial) frame,

$r U$ is the total velocity of the meshed control volume fixed to a moving body (which consists of the translational velocity of the body $b U$ and the rotational velocity of the body where r is relative to the origin of the mesh fixed to the moving body) which is overset on the stationary background mesh,

p is the pressure,

f contains all the body force terms

3.1 Geometry

For the validation, solid model to do analysis in CFD software to know the different results like Velocity, Pressure, Coefficient of Drag (Cd) etc.

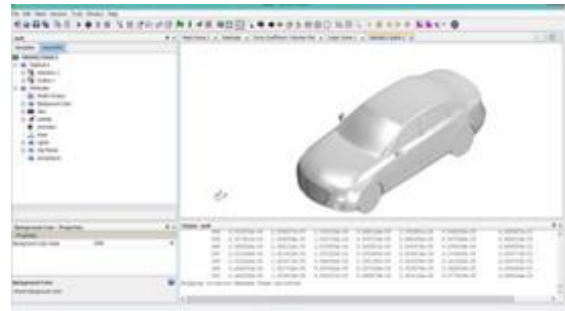


Fig3: Geometry of Audi A4 without vortex generators.

3.2 Boundary Conditions

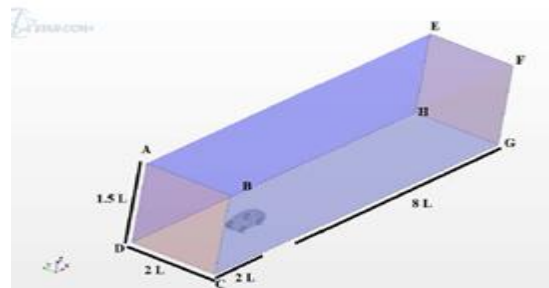


Fig 4: Boundary condition of CAR without vortex generators

Where;

ABCD– Velocity Inlet. (U_i)

EFGH– Pressure outlet.

AEHD, BFGC, AEFB– Far Field.

CDHG– Tangential Velocity. (U_t)

$U_i = U_t$.

$L = 4726 \text{ mm}$.

3.3 Meshing

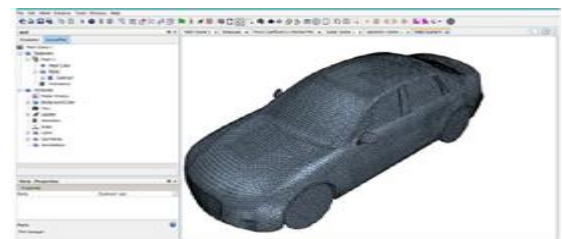


Fig5: Meshing of Audi A4 without vortex generators

Model no. 2: Audi A4 (with vortex generator).

3.4 Geometry.

After the validation, our aim is to reduce the Coefficient of drag (Cd). So we considered different parameters like vortex generator and spoilers. We can't put spoiler because it increases the coefficient of drag (Cd) and it contradicts our aim. So we put 7 vortex

generators, each of length 80mm, width 20mm, height 90mm and radius 60mm. we placed them 100mm from the rear end at the top.



Fig 6: Geometry of Audi A4 with vortex generators

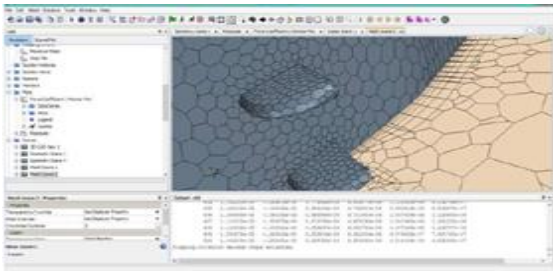


Fig 7: Meshing of Audi A4 with vortex generators in STAR CCM+.

IV. RESULTS

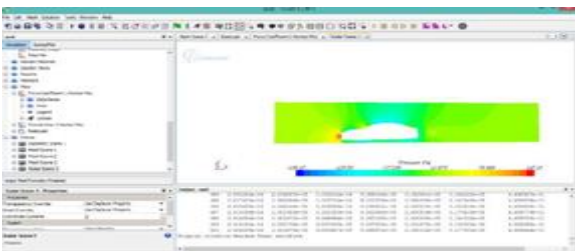


Fig 8: Pressure Contour of Audi A4 without vortex generator in STAR CCM+

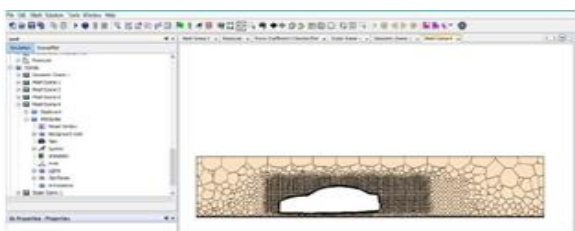


Fig 9: Velocity Contour of Audi A4 without vortex generator

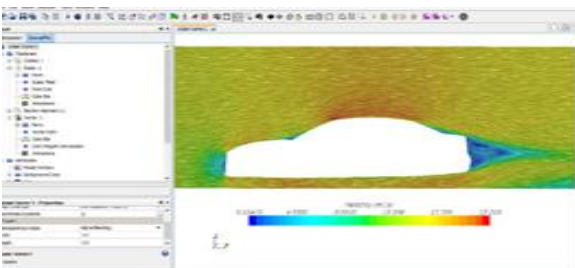


Fig10: Vortex Contour of Audi A4 without vortex generator

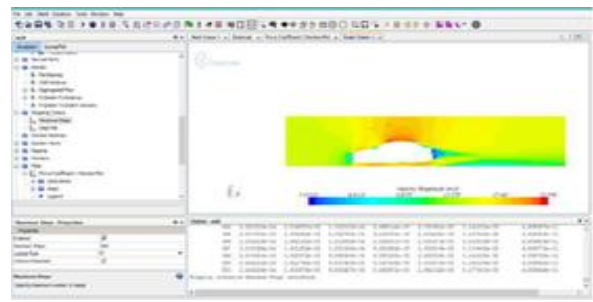


Fig11: Pressure Contour of Audi A4 with vortex generator in STAR CCM+.

CONCLUSION

The objective of this analysis was to demonstrate the importance of the CFD analysis in car optimization, taking into account the flow under the car. This is the only available tool for this type of analysis with the potential to introduce important changes mainly to the optimization strategy in car industry.

From the results and comparison of simulations, it is clear that after installing vortex generators, drag and boundary layer separation is reduced.

Therefore, finally we can conclude that designed vortex generators have met their purpose of increasing fuel efficiency and improving aerodynamics stability of vehicle by reducing the drag.

REFERENCES

- [1] W. H.Hucho, “Aerodynamik des Automobils”, VDI Verlag, 1994
- [2] T. Kobayashi, K. Kitoh, “A Review of CFD Methods and Their Application to Automobile Aerodynamics”, SAE Paper 920338.
- [3] C. Nae, “Flow Solver and Anisotropic Mesh Adaptation using a Change of Metric based on Flow Variables”, AIAA Paper 2000-2250.
- [4] D. C. Wilcox, Turbulence Modeling for CFD, ISBN 1-928729-10-X, 2nd Ed., DCW Industries, Inc., 2004.
- [5] P.N.Selvaraju et al (2015), “Analysis of Drag and Lift Performance in Sedan car model using CFD”, Proceeding of National conference on recent trends and developments in sustainable green technologies, pp 429-435.
- [6] Dan barbut, Euget Mihai Negrus CFD “Analysis of road vehicles-case study”, Inca bulletin, 3(2011) 15-22.
- [7] Jaspinder Singh review on Aerodynamic Drag Reduction of Automobile Car”, International Journal of Scientific Research vol3.

DESIGN AND ANALYSIS OF BUMPER ASSEMBLY TO IMPROVE THE DESIGN FOR IMPACT

Bachali Rambabu

Department of Mechanical Engineering, Narasaraopeta Engineering College, Narasaraopet, India

Abstract—Now a day's bumper beam plays a vital role for accidental prevention in low speed collisions. The main purpose of this paper is to increase the crashworthiness of the bumper, lessen the weight, and enhance the cost of the component. Designing a heavy vehicle bumper beam and sequential analysis on how it affects the parameters such as shape, thickness and materials will help in increase the beam strength and reduction in weight. This also provides a way of using materials that are recyclable and biodegradable which help in controlling environmental pollution. The bumper beam of a heavy vehicle is modelled and analysed with the steel materials and then the design is modified and improvised by using a shape optimization tool in the Ansys. Based on the shape optimization results, the shape of the model is modified and analysed with aluminium and composites (composite material). In this paper the main parameters that are considered in this analysis are material, thickness and the shape of the bumper beam are premeditated for the analysis on an automotive bumper beam to enhance the properties of the beam particularly to stand against the impact forces of crash, ranging from medium speed to high speed impact collisions. In this project work conventional materials like steel, magnesium and aluminum were studied and their impact behaviour is discussed. **Keywords**—Selective catalytic reactor, honeycomb, catalyst, space velocity, Nox conversion efficiency, ammonia slip.

I. INTRODUCTION

Car accidents are happening every day. We must take into account the statistics – ten thousand dead and hundreds of thousands to million wounded each year. These numbers call for the necessity to improve the safety of automobiles during accidents. Automotive bumper system is one of the key systems in passenger cars which helps to protect the vehicle during impacts. A bumper is a shield made of steel, aluminum, rubber, or plastic that is mounted on the front and rear of a passenger car. When a low speed collision occurs, the bumper system absorbs the shock to prevent or reduce damage to the car. The car bumper is designed to prevent or reduce physical damage to the front and rear ends of passenger motor vehicles in low -speed collisions. Bumper beams are one of the key structures in passenger cars for which careful design and manufacturing should be considered in order to achieve good impact behaviour. The bumper beam is the main structure for absorbing the energy of collisions. India has a high number of deaths due to road accidents. India has the world's sixth-largest car market, but is still the only country among the global top ten car markets without proper new car safety regulation or

testing programs. Passenger cars are a major mode of transport in the developed as well as in the developing countries. Therefore the accidents caused due to passenger cars are also significantly on the rise. In all types of crash accidents, about 30 % of the total numbers of accidents are frontal crash case. Therefore, measures to improve passenger vehicle passive safety performance in crash to reduce injury and death of passengers during a crash to the maximum has become an important subject of research. Automotive bumper system is one of the key systems in passenger cars. Bumper systems are designed to prevent or reduce physical damage to the front or rear ends of passenger motor vehicles in collision condition

II. BUMPER DESIGN

A bumper is a structure attached to or integrated with the front and rear ends of a motor vehicle, to absorb impact in a minor collision, ideally minimizing repair costs. [1] Invented by Briton Frederick Simms in 1901, bumpers ideally minimize height mismatches between vehicles and protect pedestrians from injury. Regulatory measures have been enacted to reduce vehicle repair costs, and more recently impact on pedestrians.

2.1. International standards International safety regulations, originally devised as European standards under the auspices of the United Nations, have now been adopted by most countries outside North America. These specify that a car's safety systems must still function normally after a straight-on pendulum or moving-barrier impact of 4 km/h (2.5 mph) to the front and the rear, and to the front and rear corners of 2.5 km/h (1.6 mph) at 45.5 cm (18 in) above the ground with the vehicle loaded or unloaded.

2.2 Pedestrian safety European countries have implemented regulations to address the issue of 270,000 deaths annually in worldwide pedestrian/auto accidents.

2.3 Bull bars specialized bumpers, known as "bull bars" or "Roo bars", protect vehicles in rural environments from collisions with large animals. However, studies have shown that such bars increase the threat of death and serious injury to pedestrians in urban environments, because the bull bar is rigid and transmits all force of a collision to the pedestrian, unlike a bumper which absorbs some force and crumples. In the European Union, the sale of rigid metal bull bars which do not comply with the relevant pedestrian protection safety standards has been banned.

2.4 Off-road bumpers Off-road vehicles often utilize aftermarket off-road bumpers made of heavy gauge metal to improve the road clearance, maximize departure angles, clear larger tires and ensure additional protection from the elements. The same as bull bars off-road bumpers feature a rigid construction and transmit all force of a collision to the object that they bump on, which is more dangerous for pedestrians than factory plastic bumpers. The legality of the aftermarket off-road bumpers varies significantly from country to country (from state to state in the USA).

United States the United States has focused on protecting consumers from repair costs, using government legislation.

FIRST STANDARDS 1971



In 1971, the US National Highway Traffic Safety Administration (NHTSA) issued the country's first regulation applicable to passenger car bumpers. Federal Motor Vehicle Safety Standard No. 215 (FMVSS 215), "Exterior Protection," took effect on 1 September 1972—when most automakers would begin producing their model year 1973 vehicles. The standard prohibited functional damage to specified safety-related components such as headlamps and fuel system components when the vehicle is subjected to barrier crash tests at 5 miles per hour (8 km/h) for front and 2.5 mph (4 km/h) for rear bumper systems. The requirements effectively eliminated automobile bumper designs that featured integral automotive lighting components such as tail lamps.

In October 1972, the US Congress enacted the Motor Vehicle Information and Cost Saving Act (MVICSA), which required NHTSA to issue a bumper standard that yields the "maximum feasible reduction of cost to the public and to the consumer". Factors considered included the costs and benefits of implementation, the standard's effect on insurance costs and legal fees, savings in consumer time and inconvenience, as well as health and safety considerations. The 1973 model year passenger cars sold in the US used a variety design. They ranged from no dynamic versions with solid rubber guards, to "recoverable" designs with oil and nitrogen filled telescoping shock-absorbers.[35] The standards were further tightened for the 1974 model year passenger cars, with standardized height front and rear bumpers that could take angle impacts at 5-mile-per-hour (8 km/h) with no damage to the car's lights, safety equipment, and engine. There was no provision in the law for consumers to 'opt-out' of this protection.

2.6 Regulatory effect on design Cars for the US market were equipped with bulky, massive, heavy, protruding bumpers to comply with the 5-mile-per-hour bumper standard in effect from 1973 to 1982. [36] This often-meant additional overall vehicle length, as well as new front and rear designs to incorporate the stronger energy absorbing bumpers.[37] Passenger cars featured gap-concealing flexible filler panels between the bumpers and the car's bodywork causing them to have a "massive, blockish look". [38] A notable exception that year was the new AMC Matador coupe that featured "free standing" bumpers with

rubber gaiters alone to conceal the retractable shock absorbers.

III. LITERATURE REVIEW

Modelling and Analysis of an Automotive Bumper Used for a Low Passenger Vehicle: Automotive design with economy, safety and aesthetics has been a great challenge to design engineers. Augmenting to these factors today environment impact is an upcoming research area. The safety of the passengers during vehicle crashes can be ensured to a certain limit by using good bumpers. At the same time these automotive parts should not be massive in terms of weight contributing to the increase in total the weight of the vehicle. In this work, a bumper used for low passenger vehicle, Ambassador car is modelled by using the software CATIA V5R18. Then this model is imported into FEM package of ABAQUS 6.10 impact as well as static analysis. Again, modal analysis and analysis under dynamic loading done for the same model using ANSYS Workbench 11.0. The materials used for these analyses are Aluminum B390 alloy, Chromium coated mild steel and carbon composite. During static analysis, Carbon composite shows the lowest deformation and maximum von misses stress value. After the impact analysis, the composite shows the highest stress value, lowest deformation and the lowest strain value on compared with above materials. The analysis under the dynamic loading shows this carbon composite has the maximum stress value and it having the highest strength to weight ratio and producing low deformation. From all these analyses, it can conclude that carbon composite is the best material which can use as the bumper material among all the other materials used here.

3.1 Impact: Analysis of Front Frame Car Bumper Bumpers play an important role in preventing the impact energy from being transferred to the automotive and a passenger, saving impact energy on the bumper to be released in the environment reduces the damages of the automotive and passengers. The new design considers on reducing the amount of material use and also eliminating the process involve in manufacture the bumper for example eliminating the grille attachment. The goal of this project is to design a bumper with minimum weight by employing the composite materials (just like glass fibre epoxy materials). This bumper either absorbs deformation or transfers it perpendicular to the impact direction. To reach this aim, a mechanism is designed to convert above 80% of kinetic impact energy is to the spring potential energy. In addition, since the residual kinetic energy will be damped with infinitesimal elastic deformation of the bumper elements, the passengers will not sense any impact, it should be noted in this project modelling, solving and results are analysis are done in a ANSYS software respectively. The suitable material that can be used as the bumper in terms of economical but still maintaining the

toughness is Carbon Fibre composite which is not expensive compare to the best material from the analysis Aluminium alloy, Mild steel (chromium Coated)

IV. INTRODUCTION TO CAD

Computer-aided design (CAD), also known as computer-aided design and drafting (CADD), is the use of computer technology for the process of design and design-documentation. Computer Aided Drafting describes the process of drafting with a computer. CADD software, or environments, provide the user with input-tools for the purpose of streamlining design processes; drafting, documentation, and manufacturing processes. CADD output is often in the form of electronic files for print or machining operations. The development of CADD-based software is in direct correlation with the processes it seeks to economize; industry-based software (construction, manufacturing, etc.) typically uses vector-based (linear) environments whereas graphic-based software utilizes raster-based (pixilated) environments. CADD environments often involve more than just shapes. As in the manual drafting of technical and engineering drawings, the output of CAD must convey information, such as materials, processes, dimensions, and tolerances, according to application-specific conventions. CAD may be used to design curves and figures in two-dimensional (2D) space; or curves, surfaces, and solids in three-dimensional (3D) objects. CAD is an important industrial art extensively used in many applications, including automotive, shipbuilding, and aerospace industries, industrial and architectural design, prosthetics, and many more. CAD is also widely used to produce computer animation for special effects in movies, advertising and technical manuals. The modern ubiquity and power of computers means that even perfume bottles and shampoo dispensers are designed using techniques unheard of by engineers of the 1960s. Because of its enormous economic importance, CAD has been a major driving force for research in computational geometry, computer graphics (both hardware and software), and discrete differential geometry. The design of geometric models for object shapes, in particular, is often called computer-aided geometric design (CAGD). 11 Current computer-aided design software packages range from 2D vector-based drafting systems to 3D solid and surface modellers. Modern CAD packages can also frequently allow rotations in three dimensions, allowing viewing of a designed object from any desired angle, even from the inside looking out. Some CAD software is capable of dynamic mathematic modelling, in which case it may be marketed as CADD — computer-aided design and drafting. CAD is used in the design of tools and machinery and in the drafting and design of all types of buildings, from small residential types (houses) to the largest commercial and industrial structures (hospitals and factories). CAD is mainly used for detailed engineering of 3D models and/or 2D

drawings of physical components, but it is also used throughout the engineering process from conceptual design and layout of products, through strength and dynamic analysis of assemblies to definition of manufacturing methods of components. It can also be used to design objects. CAD has become an especially important technology within the scope of computer-aided technologies, with benefits such as lower product development costs and a greatly shortened design cycle. CAD enables designers to lay out and develop work on screen, print it out and save it for future editing, saving.

4.1 Types of CAD Software

4.1.1 2D CAD Two-dimensional, or 2D, CAD is used to create flat drawings of products and structures. Objects created in 2D CAD are made up of lines, circles, ovals, slots and curves. 2D CAD programs usually include a library of geometric images; the ability to create Bezier curves, splines and poly lines; the ability to define hatching patterns; and the ability to provide a bill of materials generation. Among the most popular 2D CAD programs are AutoCAD, CAD key, CADD5, and Medusa.

4.1.2 3D CAD Three-dimensional (3D): CAD programs come in a wide variety of types, intended for different applications and levels of detail. Overall, 3D CAD programs create a realistic model of what the 1;2 design object will look like, allowing designers to solve potential problems earlier and with lower production costs. Some 3D CAD programs include Autodesk Inventor, Co Create Solid Designer, Pro/Engineer Solid Edge, Solid Works, Unigraphics NX and VX CAD, CATIA V5.

4.1.3 3D Wireframe and Surface Modelling CAD programs that feature 3D wireframe and surface modelling create a skeleton-like inner structure of the object being modelled. A surface is added on later. These types of CAD models are difficult to translate into other software and are therefore rarely used anymore.

4.1.4 Solid Modelling solid modelling in general is useful because the program is often able to calculate the dimensions of the object it is creating. Many sub-types of this exist. Constructive Solid Geometry (CSG) CAD uses the same basic logic as 2D CAD, that is, it uses prepared solid geometric objects to create an object. However, these types of CAD software often cannot be adjusted once they are created. Boundary Representation (Brep) solid modelling takes CSG images and links them together. Hybrid systems mix CSG and Brep to achieve desired designs

**V. INTRODUCTION TO PRO/ENGINEER
Pro/ENGINEER**

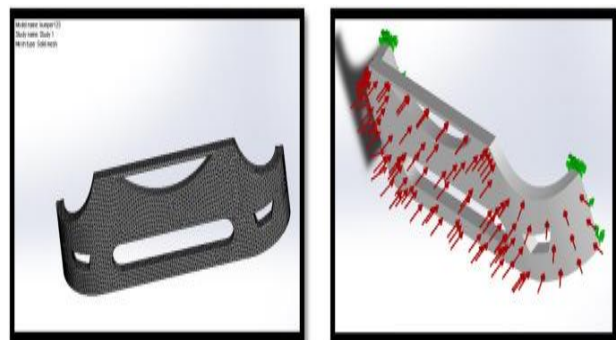
Wildfire is the standard in 3D product design, featuring industry-leading productivity tools that promote best practices in design while ensuring compliance with your industry and company standards. Integrated Pro/ENGINEER CAD/CAM/CAE solutions allow you to design faster than ever, while maximizing innovation and quality to ultimately create exceptional products. Customer requirements may change and time pressures may continue to mount, but your product design needs remain the same - regardless of your project's scope, you need the powerful, easy to use, affordable solution that Pro/ENGINEER provides

5.1 Different Modules in Pro E

- PART DESIGN
- ASSEMBLY
- DRAWING
- SHEETMETAL

1.2 Types of Engineering Analysis

Structural analysis consists of linear and non-linear models. Linear models use simple parameters and assume that the material is not plastically deformed. Non-linear models consist of stressing the material past its elastic capabilities. The stresses in the material then vary with the amount of deformation as in. Vibrational analysis is used to test a material against random vibrations, shock, and impact. Each of these incidences may act on the natural vibrational frequency of the material which, in turn, may cause resonance and subsequent failure. Fatigue analysis helps designers to predict the life of a material or structure by showing the effects of cyclic loading on the specimen. Such analysis can show the areas where crack propagation is most likely to occur. Failure due to fatigue may also show the damage tolerance of the material. Heat Transfer analysis models the conductivity or thermal fluid dynamics of the material or structure. This may consist of a steady-state or transient transfer. Steady-state transfer refers to constant thermo properties in the material that yield linear heat diffusion.



a) Meshed bumper model

b) Boundary conditions applied for the model

CONCLUSION

In this work, a bumper used for low passenger vehicle, Benz car. This bumper either absorbs the impact energy with its deformation or transfers it perpendicular to the impact direction at different speeds (40, & 60, km/hr). The materials used for these analyses are Aluminum B390 alloy, Chromium coated mild steel and Glass Mat Thermoplastic (GMT) materials. By observing the static analysis, the deformation and stresses increases by increasing the car speed. Stress values are more for glass mat thermoplastic material when compare the mild steel and aluminum alloy B390. By observing the modal analysis the deformation increase for glass mat thermoplastic material than mild steel and aluminum alloy B390. By observing the impact analysis, the deformation increases by increasing the car speed and decreased for glass mat thermoplastic material when compare the mild steel and aluminum alloy B390. So it can conclude the glass mat thermo plastic material is better for car bumper.

CONVERTIBLE FOUR WHEEL STEERING MECHANISM

¹Chavali Meenakshi Devi and ²Kiran Chand Kopila

¹Department of Mechanical Engineering, Pace Institute of Technology and Sciences (A), Ongole, A.P.India

²Department of Mechanical Engineering, Narasaraopeta Engineering College (A), Narasaraopet, A.P. India

Abstract— The most conventional and general steering arrangement is to turn the front wheels using a hand operated steering wheel which is positioned in front of the Driver. The steering column, which contain a universal joint which is part of the collapsible steering column which is designed to allow it to deviate from a straight line according to the Roadmap. In convertible four wheel steering with three mode operation three steering modes can be changed as needed which assists in parking at heavy traffic conditions, when negotiating areas where short turning radius is needed and in off road Driving.

Keywords: Hand operated steering, front wheel, heavy traffic, driving.

I. INTRODUCTION

An Automobile is a self-propelled vehicle which is used for the transportation of passengers and goods upon the ground. A vehicle is a machine which is used for the transportation of passengers and goods. A self-propelled vehicle is that in which power required for the propulsion is produced from within. Aeroplane, ship, motor boat, locomotive, car, bus, truck, jeep, tractor, scooter, motor cycle is the example of self-propelled vehicles. Motor vehicle is another name for the self-propelled and used for the transportation purposes upon the ground, so it differs from other types of self-propelled vehicles. Like aeroplane, helicopter, rocket, ship, motor boat, locomotive.

Mobile or motive means one which can move. Automobile or automotive means one which itself can move. A railway wagon cannot move itself on the rails if it is not pushed or pulled by external force. A trolley cannot move itself on the road if it is not pulled by external force. The railway wagon is pulled on the rails by a locomotive. The trolley is pulled on the road by an automobile which may be a jeep or tractor. In automobile engineering we study about the self-propelled vehicles like car, bus, jeep, truck, tractor, scooter, motorcycle. Aeronautical engineering deals with aeroplane, helicopter, rocket, etc., which fly in air. Marine engineering deals with ship, motor, etc which sail in water.

STEERING SYSTEM:

The steering of a four wheel vehicle is, as far as possible, arranged so that the front wheels will roll truly without any lateral slip. The front wheels are supported on front axle so that they can swing to the left or right for steering. This movement is produced by gearing and linkage between the steering wheel in front of the driver and the steering knuckle or wheel. The complete arrangement is called the steering

system. The steering system essentially consists of two elements- a steering gear at the lower end of the steering knuckles and steering linkage shows a simplified diagram of a steering system.

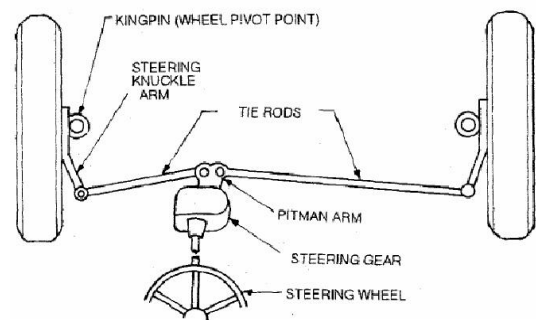


Fig: 1 Steering System

The function of the steering system is to convert the rotary movement of the steering wheel into angular turn of the front wheels. The steering systems also absorb a large part of the road shocks, thus preventing them from being transmitted to the driver. Figure 1.1 shows a late model of steering system. It has worm and roller type steering gear and relay type steering linkage. When the driver turns the steering wheel, the resulting motion is transmitted down a steering tube to a steering gear set at the end of the steering tube. The gear set changes the direction of motion, and multiplies the twisting force according to the gear ratio. Its output shaft rotates to move the pinion arm which transmits the motion of the steering knuckles through the relay road, idler arm, two tie rods, two steering arm and the two front wheels. Thus as soon as the driver puts his hands on the steering wheel the motion of the front wheels is in his hands. If he wants to turns the vehicle to the left, he turns the steering wheel to the left, and if he wants to turn the vehicle to the right, he turns steering wheel to the right, otherwise the steering wheel is in its middle position and the vehicle is going in a straight line.

REQUIREMENTS OF STEERING SYSTEM:

1. It should multiply the turning effort applied on the steering wheel by the driver.

2. It should be to a certain degree irreversible so that the shocks of the road surface encountered by the wheels are not transmitted to the driver's hand.

3. The mechanism should have self – tightening effect so that when the driver release the steering wheel after negotiating the turn , the wheel should try to achieve straight ahead position .The readers may bear in mind that the requirements of any system may vary but they should have some kind of average compromise.

FUNCTIONS OF THE STEERING SYSTEM

1. To control the angular motion the wheels and thus the direction of motion of the vehicle.
2. To provide directional stability of the vehicle while going straight ahead.
3. To facilitate straight ahead condition of the vehicle after completing a turn.
4. The road irregularities must be damped to the maximum possible extent.

II. TYPES OF STEERING

FRONT WHEEL STEERING:

The most commonly used type of steering, only the two front wheels of the vehicle are used to steer the vehicle. This type of steering suffers from the comparatively larger turning circle and the extra effort required by the driver to negotiate the turn. A typical front wheel steering mechanism layout is given in below



Figure: 2 Conventional Front Wheel Steering System

REAR WHEEL STEERING:

Some types of industry battery trucks and backhoe loaders use this type, where only the two rear wheels control the steering. It can produced smaller turning circles, but is unsuitable for high speed purposes and for ease of use.

FOUR WHEEL STEERING:

In a typical front wheel steering system, the rear wheels do not turn in the direction of the curve, and thus curb on the efficiency of the steering. Normally, this system has not been the preferred choice due to the complexity of conventional mechanical four wheel steering systems. However, a few cars like the Honda Prelude, Nissan Skyline GT-R have been available with four wheel steering systems, where the rear wheels turn by a small angle to aid the front wheels in steering. However, these systems had

the rear wheels steered by only 2 or 3 degrees, as their main aim was to assist the front wheels rather than steer by themselves.

III. LITERATURE SURVEY

Jaishnu Moudgil, Shubhankar Mengi, Mudit Chopra, Dr. Jaswinder Singh [1] in their study focused on a steering mechanism which offers feasible solutions to a number of current maneuvering limitations. A prototype for the proposed approach was developed by introducing separate mechanism for normal steering purpose and 360 steering purpose. This prototype was found to be able to be maneuvered very easily in tight spaces, also making 360° steering possible.

K. Lohith, Dr. S. R. Shankapal, M. H. Monish [2] they were studied and analyzed that four wheel steering concept can be generated and the four wheel concept was simulated in ADAMS to check for functionality of Mechanism Working prototype was built to carry out CRC tests and to find the reduction in turning radius with four wheel steering when compared to two wheel steering.

Sachin Saxena¹, Vinay Kumar, Sarabjeet Singh Luthra and Alok Kumar¹ in their study it is all about 4-wheel steering system rather than 2-wheel steering as in conventional vehicles running in INDIA. A 4-wheel steering is completely different from a 4-wheel drive (in which each wheel is given power rather than to 2 wheels). A 4-wheel steering system is superior to a 2- wheel steering system. It reduces the turning radius as well as the space required for turning. It also enables to change road lane while driving even at high speed. This paper is under research in a university of Egypt. In this project we want to develop an electric car with the wheel rotation up to 90° for the cause –the parking problem faced in metro cities. This car will be a special utility vehicle which can run on 2-wheel steering as well as on 4-wheel steering.

IV. TYPES OF STEERING MECHANISMS

ACKERMAN STEERING MECHANISM:

Ackermann steering geometry is a geometric arrangement of linkages in the designed to solve the problem of wheels on the inside and outside of a turn needing to trace out circles of different radius. It was invented by the German Carriage Builder Georg Lankensperger in Munich in 1817, then patent by his agent in England Rudolph Ackermann (1764-1834) in 1818 for horse drawn carriage. The intention of Ackermann geometry is to avoid the need for tyres to slip sideways when following the path around a curve. The geometrical solution to this is for all wheels to have their axles arranged as radii of a circle with a common center point. As the rear wheels are fixed, this center point must be on a line extended from the rear axle. Intersecting the axes of the front wheels on this line as well requires that the inside front wheel is turned, when steering, through a greater angle than the outside wheel.

MORE, LESS & TRUE ACKERMAN STEERING:

These are often terms in model car racing and refer to the amount of inequality of the angles of the wheels relative to true Ackerman steering geometry.

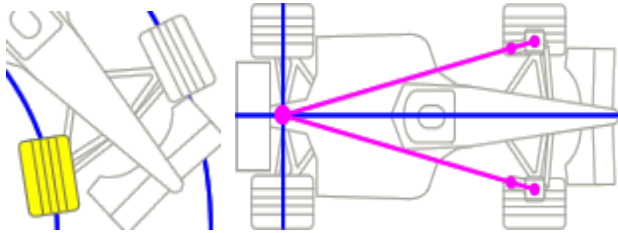


Figure: 3 True Ackerman Angle - Zero Toe on Turn In

True Ackerman steering geometry is shown in the image to the right. This is defined by angling the steering arms so that a line drawn between both the kings pin and steering arm pivot points intersects with the center line of the rear axle.

As this gives true Ackerman steering geometry, there is no Toe Angle change on the inside wheel (the wheel is aligned with the circumference of the circle), which can be seen in the image above left.

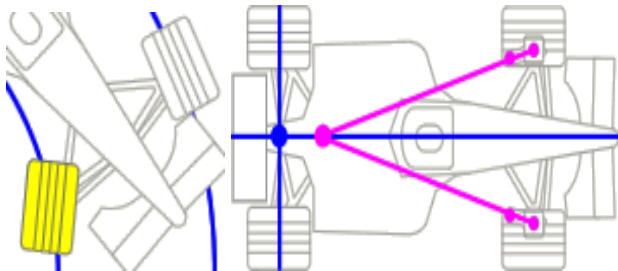


Figure4: More Ackerman Angle - Toe Out On Turn In

More Ackerman angle can be added to a steering set-up, which involves adjusting the angle of the pivot points on the steering arms so that the point of intersection is *forward* of the centre line of the rear axle. Please refer to the image on the right.

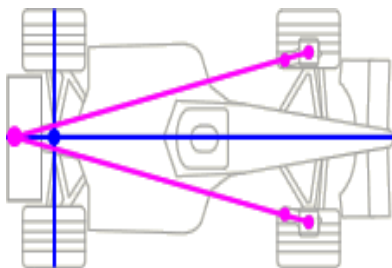


Figure5: Less Ackerman Angle - Toe In On Turn In

Less Ackerman angle can be set on a steering set-up, which involves adjusting the angle of the pivot points on the

steering arms so that the point of intersection is *behind* the center line of the rear axle. Please refer to the image on the right.

KING PIN AND KING PIN AXIS:

The imaginary axis about which the steer wheels are swivelled. In older models a solid structural component is used as a king pin and its centre line is the king pin axis. In present day models the solid component is absent .instead ball joints are used. The imaginary line joining upper and lower ball joint acts as king pin axis.

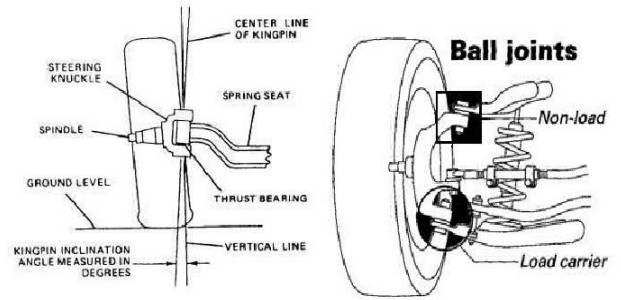


Figure6: Kingpin axis

KING-PIN INCLINATION OR STEERING AXLE INCLINATION:

The angle between the vertical line and center of the king pin or steering axle, when viewed from the front of the vehicle is known as king pin clinationor steering axle inclination. The king pin inclination, in combination with caster, is used to provide directional stability in modern cars, by tending to return the wheels to the straight – ahead position after any turn. It also reduces steering effort particularly when the vehicle is stationary. It reduces tyre wear also. Thanking pin inclination in modern vehicle range from 4 to 8 degree .It must be equal on both the sides. If it is greater on one side than the other, the vehicle will tend to pull to the side having the greater angle. Also, if the angle is to large, the steering will become exceedingly difficult. The king-pin inclination is made adjustable only by bending

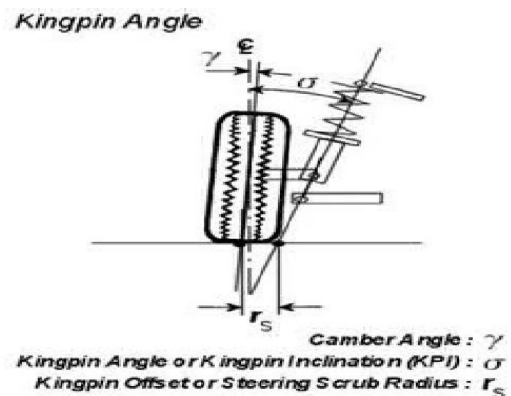


Figure7: Kingpin Angle

CASTOR:

In addition to being tilted inward toward the center of the vehicle, the kingpin axis may also be tilted forward or backward from the vertical line. This tilt is known as caster. Thus the angle between the vertical line and the kingpin Centre line in the plane of the wheel (when viewed from the side) is called caster angle. When the top of the king pin is backward, the caster angle is positive, and when it is forward the caster angle is negative .the caster angle in modern vehicles ranges from 2 to 8 degree .Tilt of the king pin axis from the vertical either towards the front(negative castor) or towards the rear (positive Castor gives directional stability: The force acting at the pivot (steering axis)and the resistance at the surface constitute a couple so that the wheel follows the line of thrust.

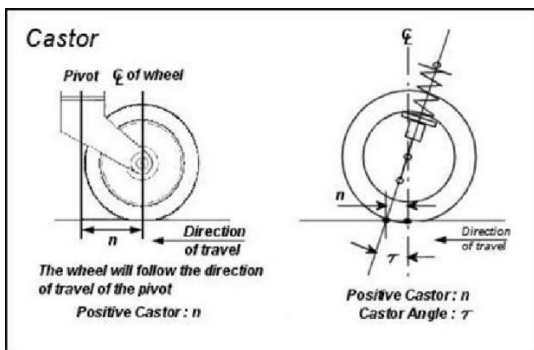


Figure8: Castor Angle

CAMBER:

The angle between the center line of the tyre and the vertical line when viewed from the front of the vehicle is known as camber. When the angle is outward, so that the wheels are farther apart at the top than at the bottom, the camber is positive. When the angle is inward, so that the wheels are closer together at the top than at the bottom, positive or negative, tends to cause uneven or move tire wear on side than on the other side. Camber should not exceed to 2°.

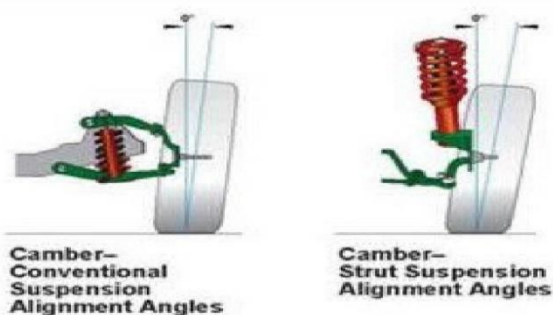


Figure9: Chamber Angle

TOE IN:

Toe In the front wheels are usually turned in slightly in front so that the distance between the front ends (a) is slightly less than the distance between the back ends (b), when viewed from the top. The difference between these distances is called toe in. On a car with toe – in, the distance between the front wheels is less at the front (a) than at the rear (b), when

viewed from the top. The amount of toe-in is usually 3 to 5 mm.

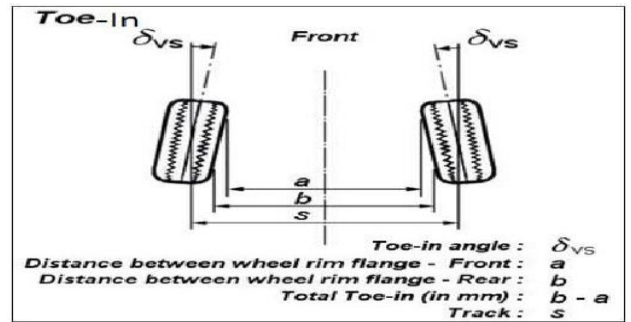


Figure10: Toe In

TOE OUT:

Toe-out is the difference in angles between the two front wheels and theca frame during turns. The steering system is designed to turn the inside wheel through a larger angle than the outside wheel when making a turn. This condition causes the wheels to toe-out on turns, due to the difference in their turning angles. When the car is taking turn, the outer wheels rolls on a larger radius than the inner wheel, and the circles on which the two front wheels must roll are concentric.

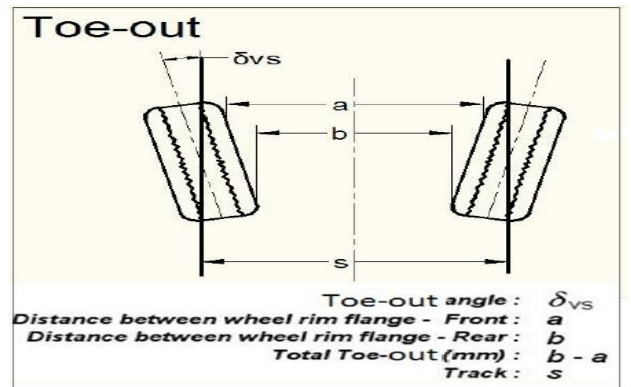


Figure11: Toe Out

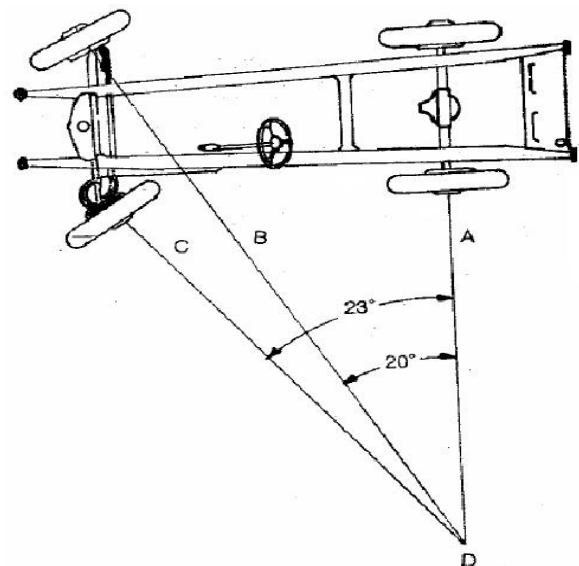


Figure12: Toe-Out (Detailed)

REASON FOR TOE IN AND TOE OUT:

- Compensate for movement within steering ball joints, suspension linkages, etc.
- In motion the toe in / toe out leads to parallel tires.
- Toe – in neutralizes cone running due to camber and hence dependent on camber.

DAVIS STEERING MECHANISM:

In Davis steering gear, it is in the front of the front wheels. Davis steering gear consists of sliding members.

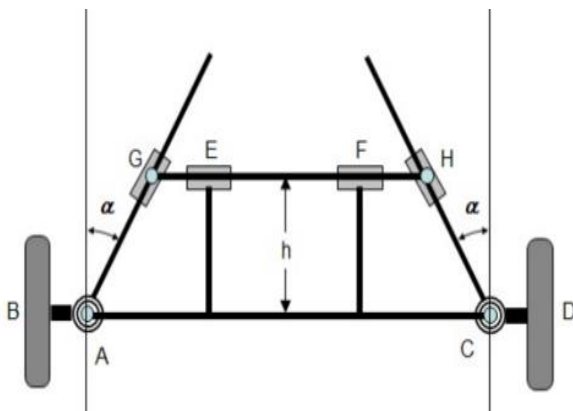


Figure13: Davis Steering Gear Mechanism

The Davis Steering gear has sliding pair; it has more friction than the turning pair, therefore the Davis Steering Gear wear out earlier and become inaccurate after certain time. This type is mathematically Accurate. The Davis gear mechanism consists of cross link KL sliding parallel to another link AB and is connected to the stub axle of the two front wheel by levers ACK and DBK pivoted at A and B respectively.

The cross link KL slides in the bearing and cross pins at its ends K and L. The slide blocks are pivoted on these pins and move with the turning of bell crank levers as the steering wheel is operated. When the vehicle is running straight the gear is said to be in its mid-position. The short arms AK and BL are inclined an angle $90^\circ - \alpha$ to their stub axles AC and BD respectively. The correct steering depends upon the suitable selection of cross arm angle α , and is given by

$$\tan \alpha = \frac{b}{2l}$$
 Where $b = AB =$ distance between the pivots of front axle.

$$l = \text{wheel base}$$

V. VEHICLE DYNAMICS AND STEERING

UNDER STEER:

Under steer is so called because when the slip angle of front wheels is greater than slip angle of rear wheels. Under steer can be brought on by all manner of chassis, suspension and speed issues but essentially it means that the car is losing grip on the front wheels. Typically it happens as you brake and the weight is transferred to the front of the car. At this point the mechanical grip of the front tyres can simply be overpowered and they start to lose grip (for example on a wet or greasy road surface). The end result is that the car will start to take the corner very wide. In racing, that normally involves going off the outside of the corner into a catch area or on to the grass.

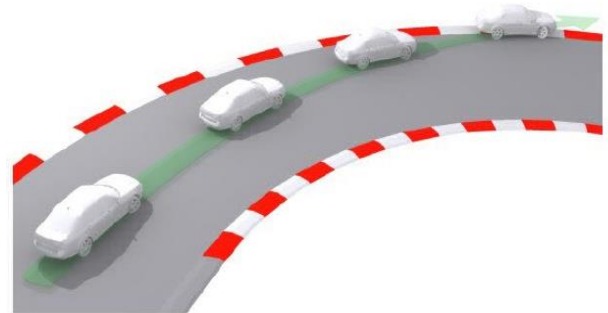


Figure14: Under Steer

OVER STEER:

Over steer is defined when the slip angle of front wheels lesser than the slip angle of rear wheels. With oversteer, the car goes where it's pointed far too efficiently and you end up diving into the corner much more quickly than you had expected. Oversteer is brought on by the car losing grip on the rear wheels as the weight is transferred off them under braking, resulting in the rear kicking out in the corner.

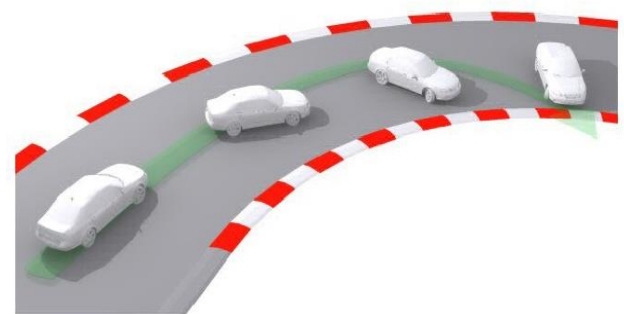


Figure15: Over Steer

NEUTRAL STEER OR COUNTER STEERING:

Counter-steering can be defined as when the slip angle of front wheels is equal to slip angle of rear wheels. It is what you need to do when you start to experience oversteer. If you get into a situation where the back end of the car loses grip and starts to swing out, steering opposite to the

direction of the corner can often 'catch' the over steer by directing the nose of the car out of the corner.

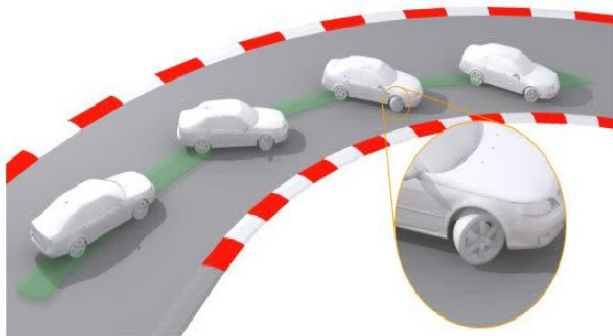


Figure16: Neutral Steer

VI. DESIGN OF STEERING SYSTEM

It is to be remembered that both the steered wheels do not turn in the same direction, since the inner wheels travel by a longer distance than the outer wheels, as described in FIG.

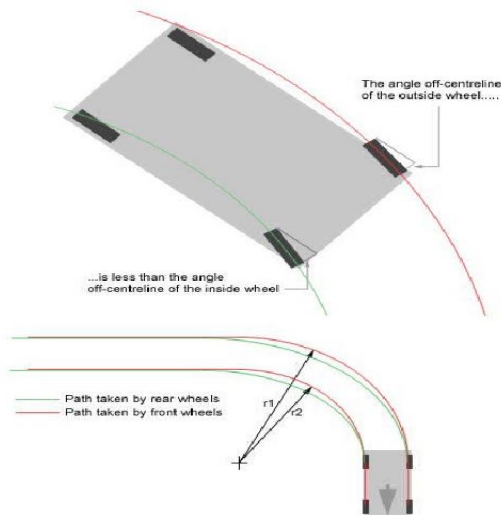


Figure17: Relative angles of the tires to the car

FUNDAMENTAL EQUATION FOR CORRECT STEERING:

When the vehicle takes a turn, the outer wheels moves faster than the inner wheels. The four wheels must roll on the road so that there is a line contact between road surface and tyres. This is essential to prevent tyre wear. The rolling motion of the wheels on the road surface is possible only if these describe concentric circles on the road at an instantaneous centre, when the vehicle is taking a turn. In order for turning the vehicle to the left or right, its two front wheels are mounted on short axles, known as stub axles, pivoted to the chassis of the vehicle. The axes of these axles, when produced meet at an instantaneous centre which lies on the

common axis of the rear wheels. The axis of the inner wheel makes a larger turning angle θ than angle ϕ made by the axis of outer wheel.

Let $a = CD$ wheel track

$b = AB =$ distance between the points of front axles

$L = AE$ wheel base $I =$ common instantaneous centre of all four wheels.

Draw IP perpendicular from I to AB produced meeting at P .

Then, $b = AP - BP = l \cot \phi - l \cot \theta = l (\cot \phi - \cot \theta)$ Or $\cot \phi - \cot \theta = b/L$

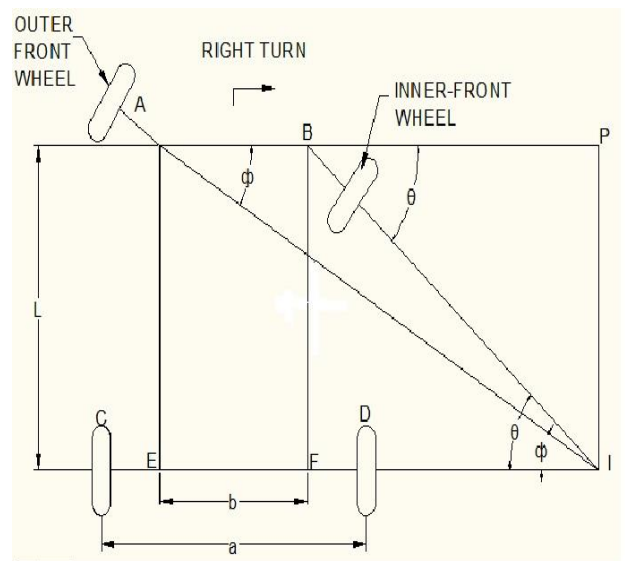


Figure18: Steering Angles

TURNING CIRCLES:

The turning circle of a car is the diameter of the circle described by the outside wheels when turning on full lock. There is no hard and fast formula to calculate the turning circle but you can get close by using this:

$$\text{TURNING CIRCLE RADIUS} = (\text{TRACK}/2) + (\text{WHEELBASE}/\text{SIN} (\text{AVERAGE STEER ANGLE}))$$

The numbers required to calculate the turning circle explain why a classic black London taxi has a tiny 8m turning circle to allow it to do U-turns in the narrow London streets any other car, but the average steering angle is huge. For comparison, a typical passenger car turning circle is normally between 11m and 13m with SUV turning circles going out as much as 15m to 17m. No Company Name Steering wheel radius in cm 1 Ambassador 43.22 Willy Jeep 43.83 Premier car 43.4 Standard - 10 car 39.5 Maruti - 800 car 37 Table: 3.2 Steering wheel radius of some of the light vehicles manufactured in India.

VII. METHODOLOGY

Modification was made in the rear wheel assembly and addition of one more rack and pinion steering gear box for steering the rear wheels. Then a transfer rod is placed between the front and rear steering gear box to transfer the motion to rear steering gear box. As the vehicle Maruti 800 is front wheel drive as shown in fig 10.1 there will be no difficulty in transferring the power from the Engine through Gear box, only a rear wheel assembly with steering gear box is required.

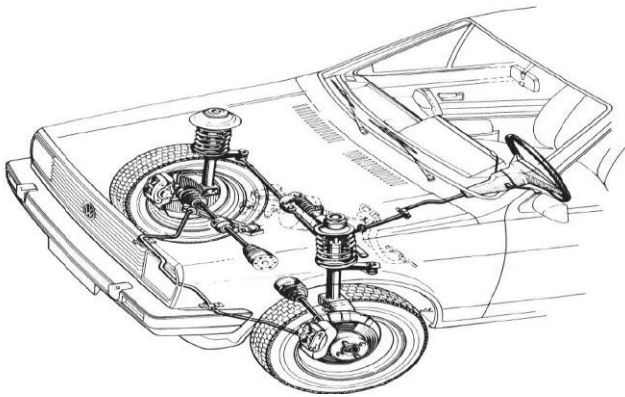


Figure19: Maruti 800 Front Wheel Drive

Maruti 800 Uniq Steering

Table 1 shows the Maruthi 800 steering details

Steering Type	Power
Steering Column	collapsible
Steering Gear Type	Rack and Pinion
Turning Radius (wheel base)	4.4 m

Maruti 800 Uniq Dimensions

Table 2 shows the Maruthi 800 Dimension

Length (mm)	3335
Width (mm)	1440
Height (mm)	1405
Wheelbase (mm)	2175
Ground Clearance (mm)	170
Weight (Kgs.)	72

Specifications of prototype:

Table 3 shows the prototype Specifications

Length (cm)	111.8
Width (cm)	65.5
Height (cm)	25
Wheelbase (mm)	2175
Ground Clearance (mm)	170

DESIGN OF PROTOTYPE:

For building of prototype model, the designed model is considered along with that a frame is built to support the steering and gear mechanism.

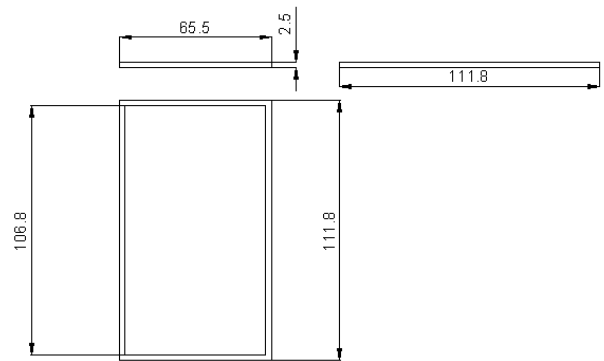


Figure20: Design of the frame

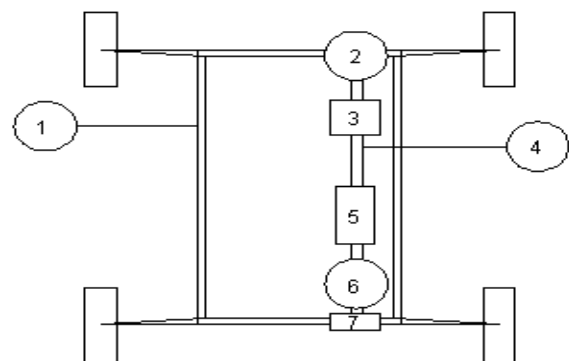


Figure21: Components of Prototype

RACK AND PINION: A rack and pinion is a pair of gears which convert rotational motion into linear motion.

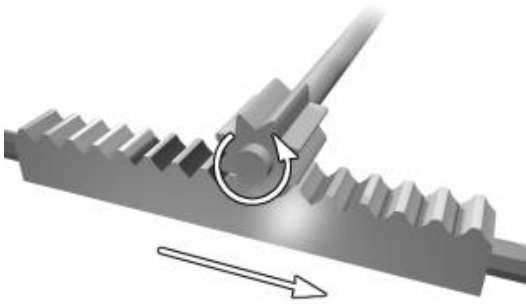


Figure22: Rack and pinion

BEVEL GEARS: Bevel gears are gears where the axes of the two shafts intersect and the tooth-bearing faces of the gears themselves are conically shaped.



Figure23: Bevel Gears

UNIVERSAL JOINT:

This is used in pairs so that fluctuation of one is nullified by the other.



Figure24: Universal Joint



SPUR GEAR :

They have straight teeth whose axis is parallel to the axis of the gear.

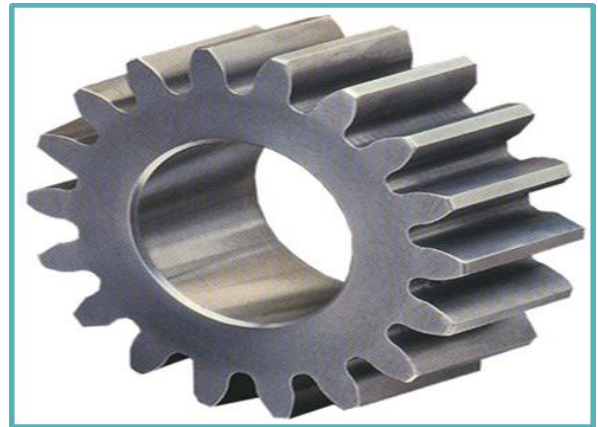


Figure25: Spur Gear

STEERING WHEEL:

Steering wheel is a type of wheel used to control the vehicle and give direction to vehicle.



Figure26: Steering wheel



Figure27: Two Wheel Steering System



Figure28: Four Wheel Steering System



Figure29: Front Wheel Gearing System

VIII. RESULTS AND DISCUSSION

The results of steering systems are shown in Table 4 shows Comparison of turning radius

	TWO WHEEL STEERING SYSTEM	FOURWHEEL STEERING SYSTEM
Turning radius	R _{if} =56 R _{of} =109 R _{ir} =46 R _{or} =104	R _{if} =46 R _{of} =104 R _{ir} =40 R _{or} =95s
By calculation	4.4 m	2.59 m
By experiment	5.75 m	2.85 m

Table 5 Comparison of two wheel steering and four wheel steering system

Steering wheel Angle	40°	20°
Stability	Low	High
Handling	Comparatively low	High

CORRECT STEERING MECHANISM:

$Cot\theta - cot\alpha = a/b$

1.1=1.1

CONCLUSIONS AND FUTURE SCOPE

On comparing our four wheel steering mechanism with two wheel steering mechanism the following conclusions were made

1. Four wheel steering concept was generated
2. Four wheel steering is a relatively new technology that imposes manoeuvrability in cars, trucks and trailers.
3. Turning radius was reduced.
4. Stability of the vehicle is improved highly.

FUTURE SCOPE:

1. This mechanism implements 360° Rotation for a vehicle.
2. Facilitates parallel parking.
3. Optimal palletizing of vehicles.
4. Aerodynamic turning property of a vehicle can be improved without any change in design
5. Can be best applied to Jassi –Jeepers

REFERENCES

[1] Jaishnu Moudgil, Shubhankar Mengi, Mudit Chopra, Dr. Jaswinder, 360° Rotating Vehicle to Overcome the Problem of Parking Space, IJRMET Vol. 5, Issue 2, May - Oct 2015

[2] K. Lohith¹, Dr. S. R. Shankapal², M. H. Monish Gowda, development of four wheel steering system for a car, Volume 12, Issue 1, April 2013.

[3] Sachin Saxena¹, Vinay Kumar, Sarabjeet Singh Luthra and Alok Kumar, 4 wheel steering systems (4was), Int. J. Mech. Eng. & Rob. Res. 2014

[4] Shijin T. G , Sooraj V. T , Shuaib A. V, Shirin P. R , M. Dinesh, international journal of research in aeronautical and mechanical engineering four wheel steering control with 3 mode operations, Vol.2 Issue.3, March 2014.

[5] Arun Singh , Abhishek Kumar, Rajiv Chaudhary, R. C. Singh, Study of 4 Wheel Steering Systems to Reduce Turning Radius and Increase Stability, International Conference of Advance Research and Innovation (ICARI-2014).

[6] Saket Bhishikar, Vatsal Gudhka, Neel Dalal, Paarth Mehta, Sunil Bhil, A.C, Design and Simulation of 4 Wheel Steering System, International Journal of Engineering and Innovative Technology (IJEIT) Volume 3, Issue 12, June 2014.

[7] PSG College of Technology, Design Data, DVP Printers Publication revised edition (1978).

DESIGN AND ANALYSIS OF CONNECTING ROD USING GENERATIVE DESIGN

Mr. M. Balaji Naik¹, Sk. Begam Khaleeda Hafeez², K. Meher Sai Tejaswini³

¹Asst. Professor, Department of Mechanical Engineering, University College of Engineering Narasaraopet-Jntuk, India

²Department of Mechanical Engineering, University College of Engineering Narasaraopet-Jntuk, Narasaraopet, India

Abstract— The following paper focuses on the mass reduction of the connecting rod. Connecting rod is a component that converts the reciprocating motion of the piston to the rotary motion of the crankshaft. Due to the brake power generated, it is subjected to axial and bending stresses. During each crankshaft rotation, the connecting rod is often subjected to large and repetitive compressive forces as the piston moves downwards, and tensile forces as the piston moving upwards. As the connecting rod carries the power thrust from the piston to the crankpin it must be firm, rigid, and as light as possible. The lighter the connecting rod and the piston, the greater the resulting power and the lesser the vibrations because the reciprocating weight is less. So by using generative design and re-designing of connecting rod mass can be reduced with consideration of permissible limit for manufacturing of better connecting rod is performed with the CATIA and imported into Ansys workbench for analysis. Modal analysis of connecting rod is also carried out to determine the natural frequencies and mode shapes.

Keywords—Connecting rod, CATIA, Ansys, modal analysis, natural frequencies.

I. INTRODUCTION

The connecting rod is a critical component of the engine. It connects the piston and crankshaft.

The small end of the connecting rod is connected to the piston through piston pin and the big end is connected to the crankshaft through crankpin.

It is the main part in converting the chemical energy at the piston to mechanical energy at the crankshaft. The reciprocating motion of the piston is converted to rotary motion. The connecting rod is subjected to high shear, compressive and tensile stresses. Therefore, it must be of high strength. The weight of the connecting rod should be least in order to reduce the vibrations from developing. The connecting rod is shown in the below figure 1.

Reduction in vibrations leads to increase in efficiency of the engine. Nowadays every component is made light weight in order to reduce the material costs and manufacturing costs of the products.

This research paper aims to explore opportunities for weight and cost reduction in the design and development of connecting rods. A connecting rod was designed and subjected to generative design for additive manufacturing, in order to reduce its weight, optimize the shape, and provide the most efficient 3d printable connecting rod. Ti-6Al4V and 17-4Ph stainless steel are some 3d printable materials that are easily available.

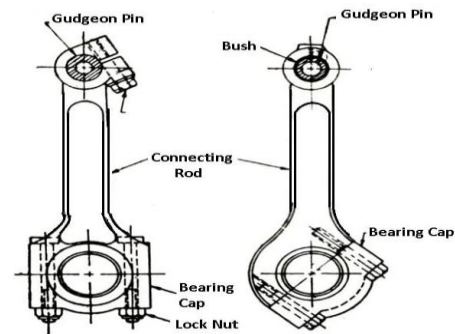


Figure a

They were applied to the connecting rod in the analyses carried out by Finite element method through ANSYS, which resulted in a few important computations such as deformation; equivalent (von Mises) stress and shear elastic strain values for both. On examination, the results concluded that both Ti-6Al4V and 17-4Ph stainless steel possessed the required level of properties but 17-4Ph stainless steel exhibited superior strength and also proved to be a cheaper alternative [1]. In this paper, Finite Element Method (FEM) using ANSYS workbench was used to carry out the weight optimization of the connection rod with target weight reduction of 20%, 30%, 40%, 50%, and 60% under a loading force of 30KN to determine the mass that needs to be removed to minimize both weight and cost. Structural optimization is done to determine an optimized structure with new deformation, Von-misses stress, and equivalent elastic strain values followed by the comparison of these values before and after the structural optimization to verify the effect of the analysis. The result obtained shows that the initial structure before optimization experience a relatively high deformation, stress and strain values respectively. Hence, reduces material cost and wastages to the production industry [2]. The primary goal of this project is performing the static and dynamic load analysis, and to explore the weight reduction opportunity of connecting rod. The maximum stress, strain, and deformation in the connecting rod were estimated using linear static structural analysis. Peak stress of 143.88 Mpa and total deformation of 0.088329 mm are achieved. Weight of 0.72154 kg in connecting rod, which is optimized to improve efficiency and longevity the optimization of connecting rod, is improved significantly [3]. This paper illustrate a general study on three designs of connecting rod along with modern structure. The primary goal of this project is to reduce the weight and this further analysis move towards von misses stresses for 10 Mpa to 50 Mpa, the vertical cut connecting rod is used instead of solid connecting rod if permissible limit is consider up to 10%. e, if permissible limit is considered up to 15% the horizontal cut center section connecting rod of

Al7068 can be used in the place of solid connecting rod of Al7068 [4]. This paper talks about the analysis of connecting rod by applying various load conditions compression and tension in crank end and piston end. Design of connecting rod is designed by machine design approach is compared with actual production drawing of connecting rod.

In this paper, the shape of the connecting rod is designed through CATIA V5 software and analysis is done through Ansys.

II. METHODS AND MATERIALS

Table.1 Mechanical properties of structural steel

S.NO	Material Property	Structural steel
1	Density	7850Kg/m ³
2	Young's Modulus	200000MPa
3	Poisson's ratio	0.3
4	Tensile strength	250MPa
5	Ultimate strength	460MPa

ANSYS is a general-purpose, finite-element modeling package for numerically solving a wide variety of mechanical problems. These problems include static/dynamic, structural analysis, heat transfer, and fluid problems, as well as acoustic and electromagnetic problems. Most Ansys simulations are performed using the Ansys Workbench system, which is one of the company's main products. Typically, Ansys users break down larger structures into small components that are each modeled and tested individually. A user may start by defining the dimensions of an object, and then adding weight, pressure, temperature and other physical properties. Finally, the Ansys software simulates and analyses movement, fatigue, fractures, fluid flow, temperature distribution, electromagnetic efficiency and other effects over time.

CATIA (an acronym for computer-aided three-dimensional interactive application) is a multi-platform software suite for computer-aided design (CAD), computer-aided manufacturing (CAM), computer-aided engineering (CAE), and 3D modeling and Product lifecycle management (PLM), developed by the French company Dassault Systems.

The aim of this paper is to perform optimization of connecting rod by reducing weight up to 40% by applying the forces acting on it in the range of 10-20KN. This paper also consists of structural analysis, von-misses stress analysis and modal analysis of both existing and optimized models. Both are compared and the optimized structure is identified by comparing the values.

III. DESIGN SPECIFICATIONS

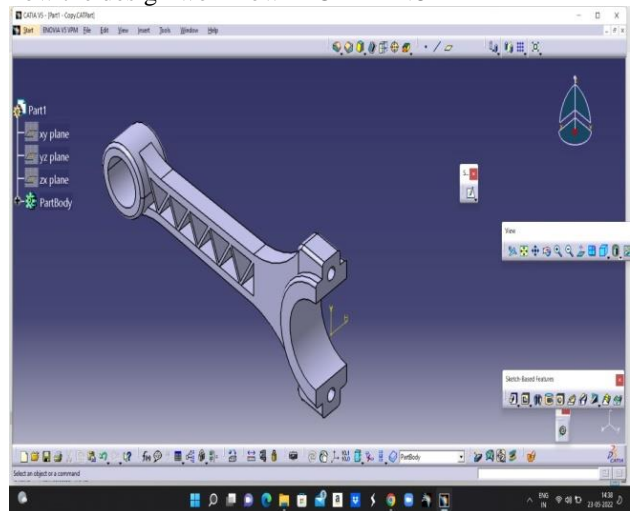
Being among one of the most essential components in an IC engines layout, the connecting rod should be able to endure a remarkable amount of load and also send a lot of power. The failure in a connecting rod can be one of the most damaging and costly failures in an engine.

The present work involves the modification in the design of YAMAHA R15 V4 bike engines' connecting rod which is 4 stroke 4 cylinder petrol engine.

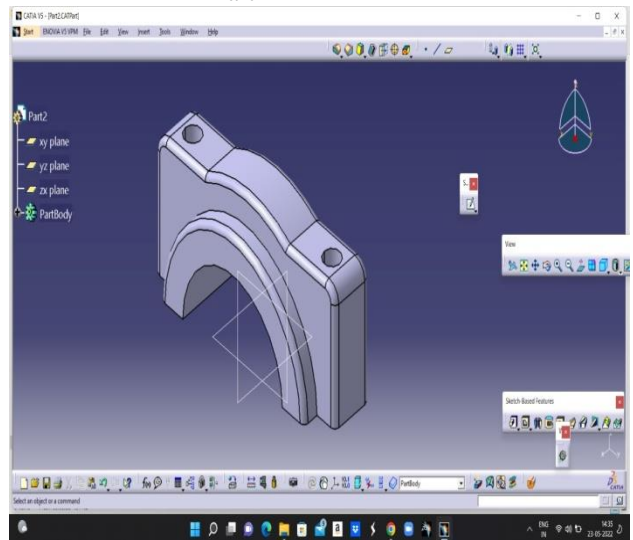
ENGINE TYPE	LIQUID-COOLED, 4-STROKE, SOHC, 4-VALVE
DISPLACEMENT	155 CC
BORE &STROKE	58.0 MM X 58.7 MM
COMPRESSION RATIO	11.6:1
MAXIMUM HORSE POWER	13.5 kW(18.4 PS)/10000 RPM
STARTING SYSTEM TYPE	ELECTRIC STARTER
CLUTCH TYPE	WET, MULTIPLE-DISC
FUEL SYSTEM	FUEL INJECTION
MAXIMUM TORQUE	14.2 NM(1.4KGF M) @7500 RPM
TRANSMISSION TYPE	CONSTANT MESH, 6-SPEED

TABLE 2: FUNCTIONAL SPECIFICATIONS OF YAMAHA V4 R15 ENGINE

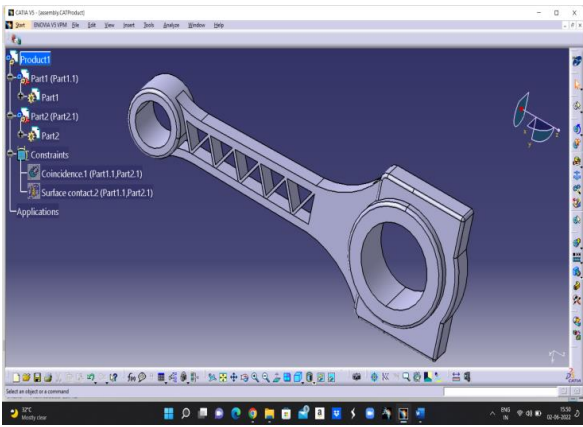
The original design of the connecting rod is optimized based on the calculations. Below diagram depicts how the design workflow in CATIA v5



Part 1



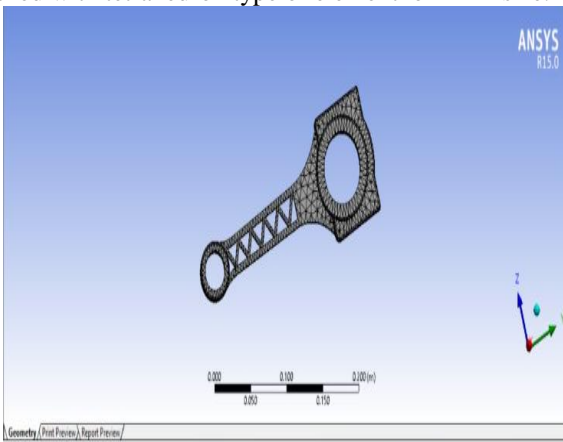
Part 2



Assembled Design

IV. EXPERIMENTAL SYSTEM DESCRIPTION

After the new design of the component is designed, then it is meshed with tetrahedron type of element of 2mm size.



Meshed connecting rod

Establishing boundary condition is an important factor to consider in FEA. The first key action required prior to the start of an analysis is the setting of boundary conditions. Constraints that include fixed support, forces, and pressure applied to the model after meshing process are embedded in a way that adapt to the practical real life situation, which is an important and main action needed in analysis. The deformation, stress and strain values of the connecting rod are based on an acceptable design constraint using static structural analysis. The static and dynamic analysis using ANSYS software of connecting rod using steel is done. The deformation, stress, and strain values under a compression load of 10-20KN were determined for the static structural analysis. The boundary conditions on the connecting rod include supports and loads; the smaller end is subjected to the loading while the big end is fixed of the connecting rod.

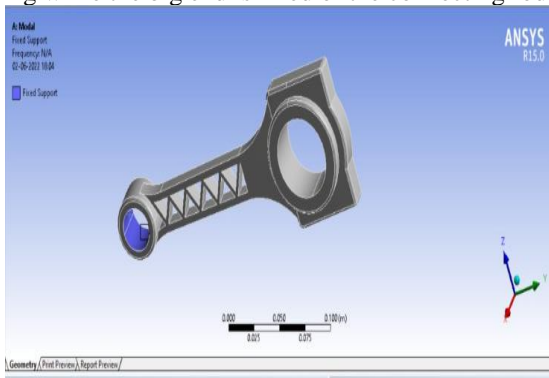
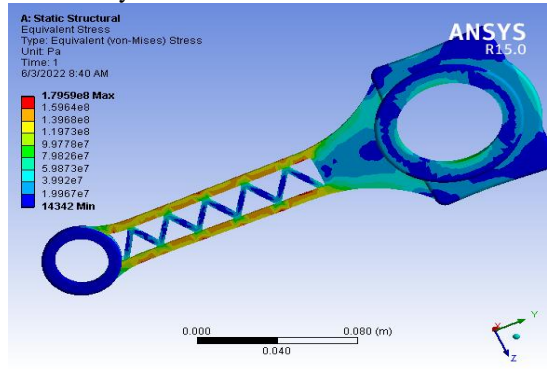


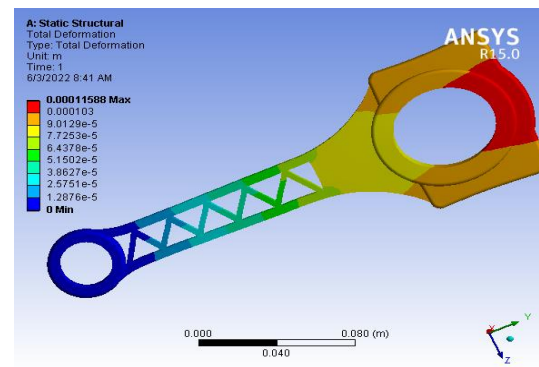
Fig Represents the fixed support at small end

V. EXPERIMENTAL PROCEDURE

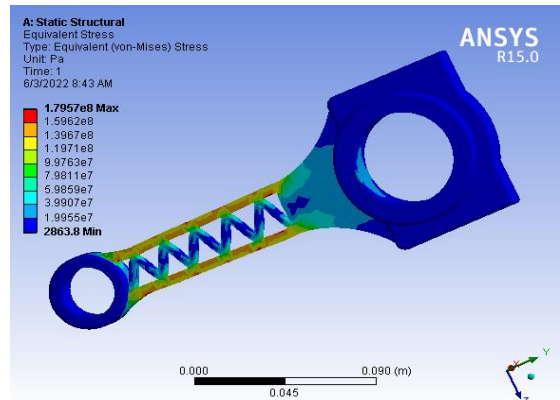
Structural Analysis:



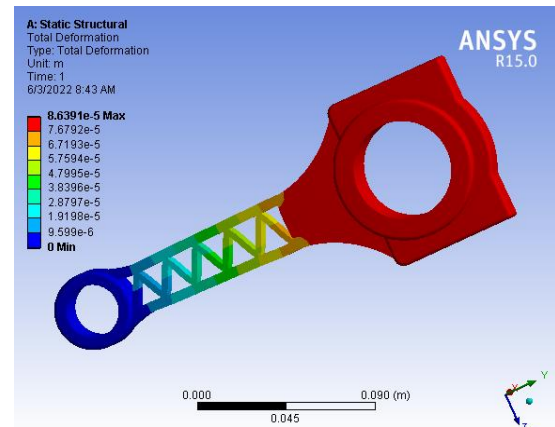
Stress due to tension when small end is fixed



Deformation due to tension when small end is fixed



Stress due to compression when small end is fixed

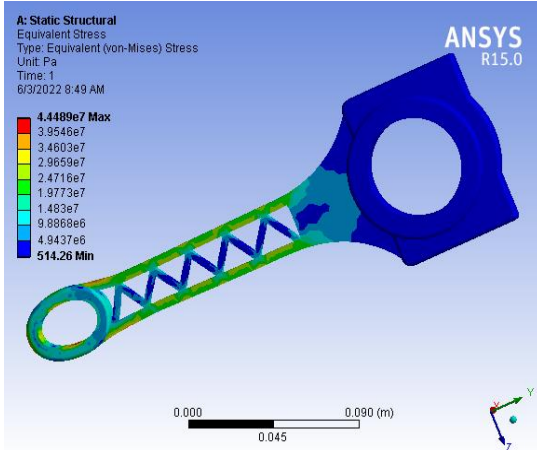


Deformation due to compression when small end is fixed

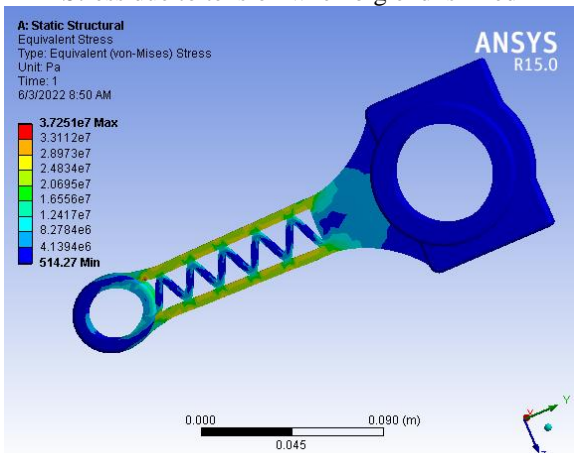
$$= 500/129.2$$

$$= 1.12$$

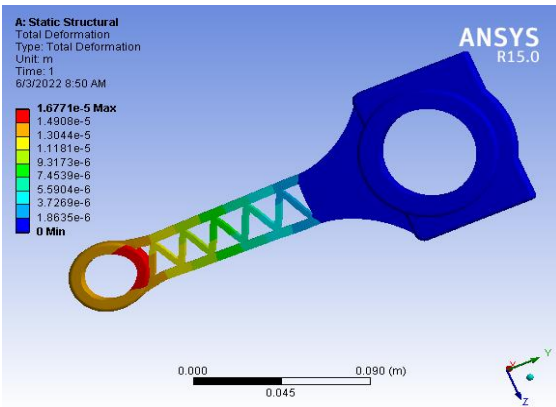
a) MODAL ANALYSIS OF OPTIMIZING MODEL



Stress due to tension when big end is fixed



Stress due to compression when big end is fixed



Deformation due to tension when big end is fixed

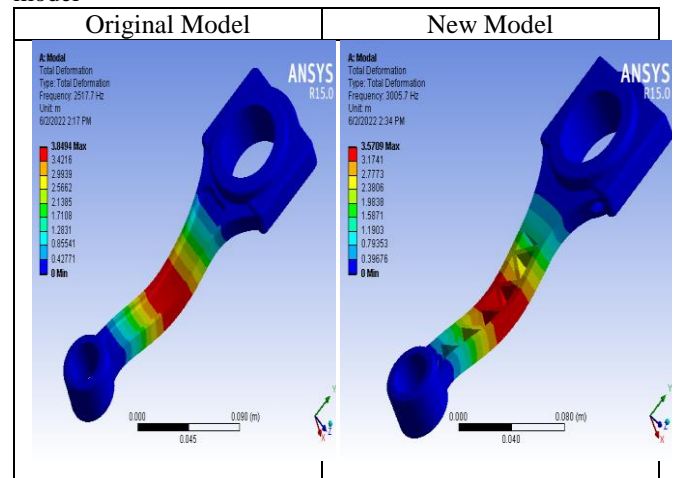
	Max. stress(MPa)	Total deformation(mm)
Big end compression	129.2	0.07
Small end compression	22.58	0.013
Big end tensile	129.03	0.0105
Small end tensile	44.35	0.02

Factor of Safety = Ultimate stress/ Maximum stress

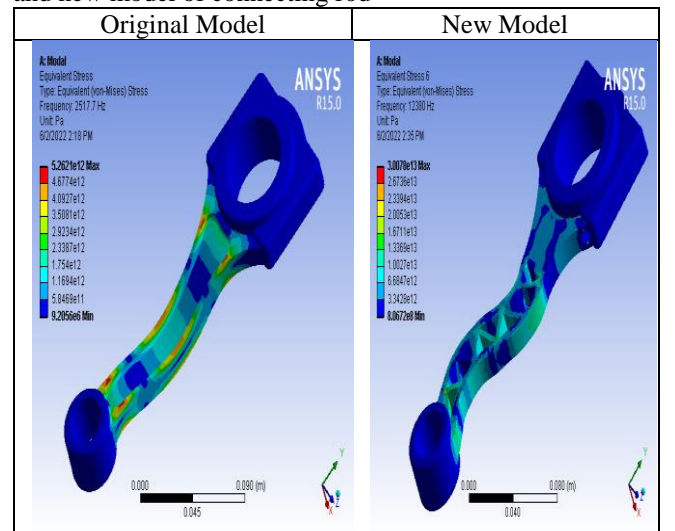
A mode shape is a deformation that the component would show when vibrating at the natural frequency. However, the vibration and deformation do not occur until there is an excitation. Depending on this excitation, the result is the total vibration of a structural component, which is basically comprised of the individual vibration shapes.

The modal analysis comprises two cases. The modal analysis of the existing connecting rod model and the optimized design connecting rod has been done by considering six modes. The total deformation and the equivalent stress (Von mises stress) of the original and the optimized connecting rod has been compared.

Comparison for total deformation of original model and new model



Comparison table for Von mises stress of Original model and new model of connecting rod



b) NATURAL FREQUENCIES FOR TENSILE AND COMPRESSIVE LOADS

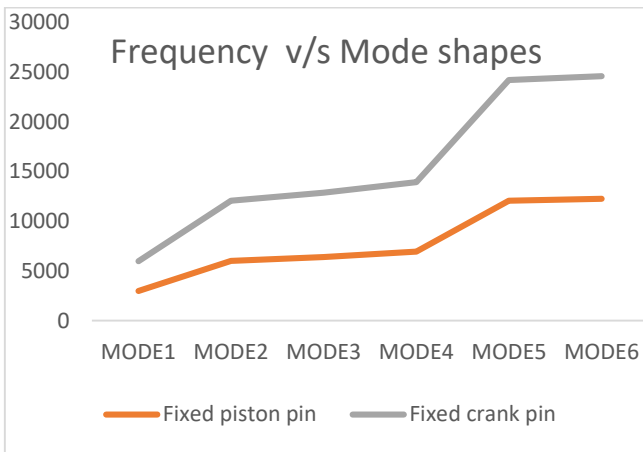
The natural frequency of the connecting rod shows limited free vibration up to which its vibration will not produce severe destruction, but when the loading the vibration gets closer to the natural frequency of the

connecting rod then, resonance will occur. This can produce the destruction of the connecting rod as well as the components that connect with it such as the piston and crank rod.

The natural frequency of the connecting rod when it is fixed at the piston pin once and fixed at the crank pin once have been plotted in the graph. The mesh size of the connecting rod is fixed to 2mm.

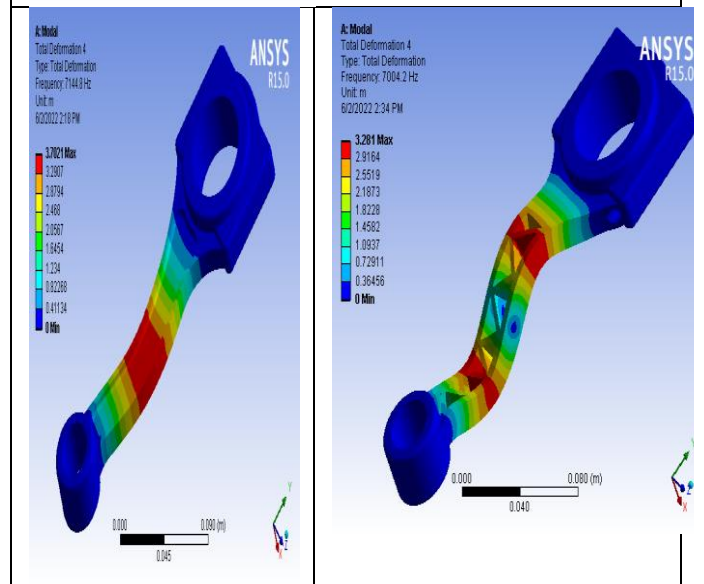
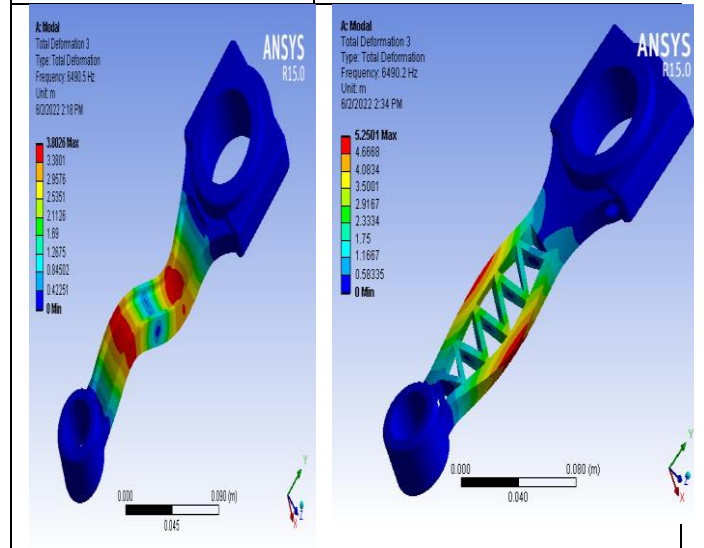
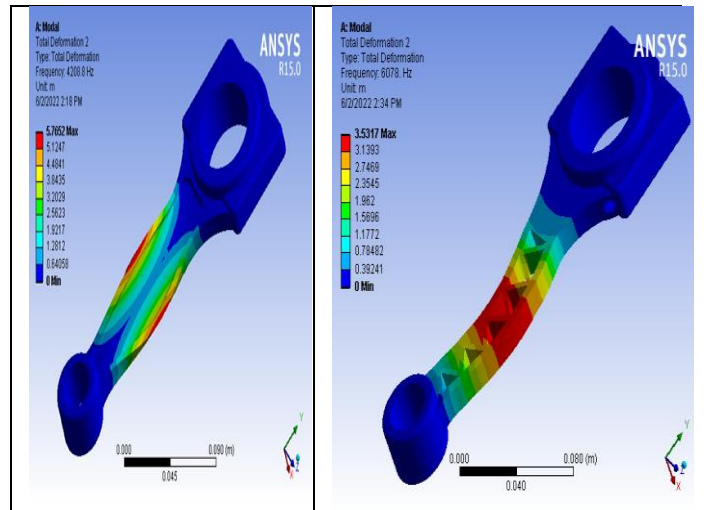
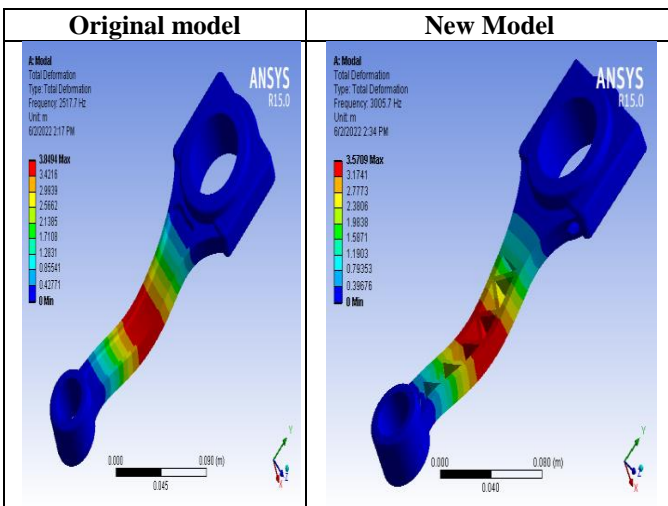
Thus the graphs have been plotted against Mode shapes on the positive X-Axis and Frequency on the positive Y-Axis as shown below in the graph.

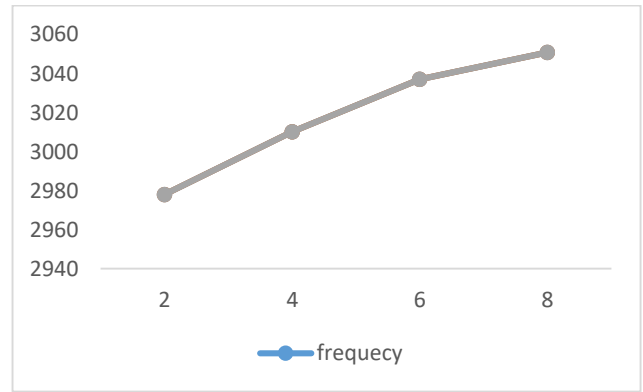
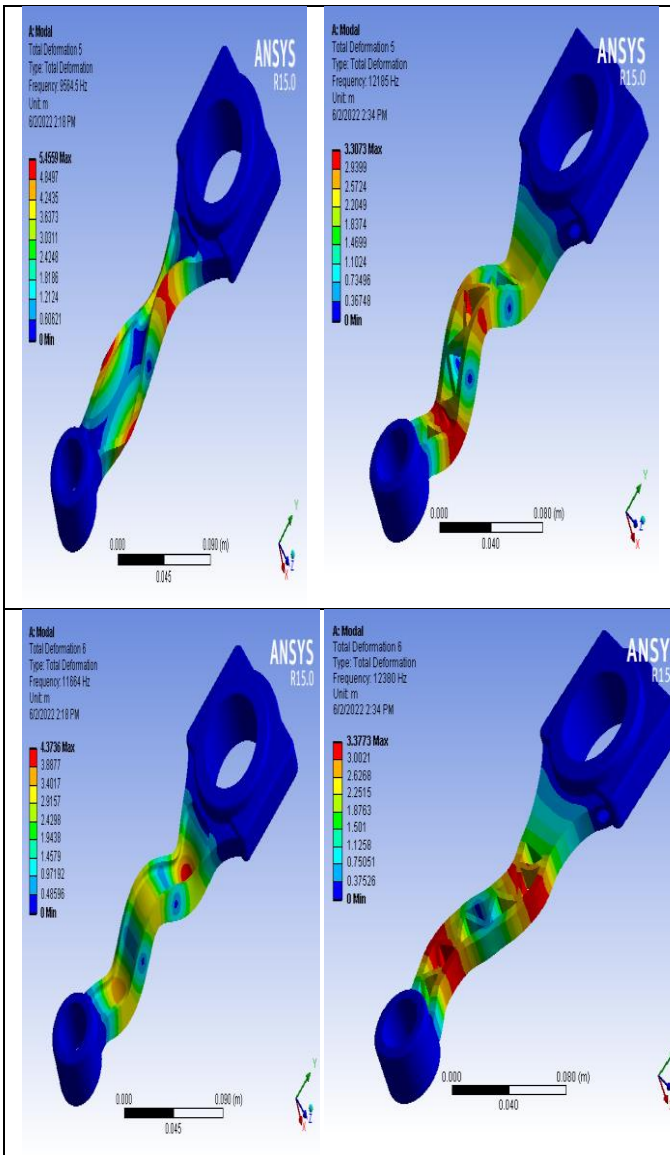
The natural frequency of the connecting rod when it is fixed at the piston pin and free at the crankpin is less than when it is fixed at the crankpin.



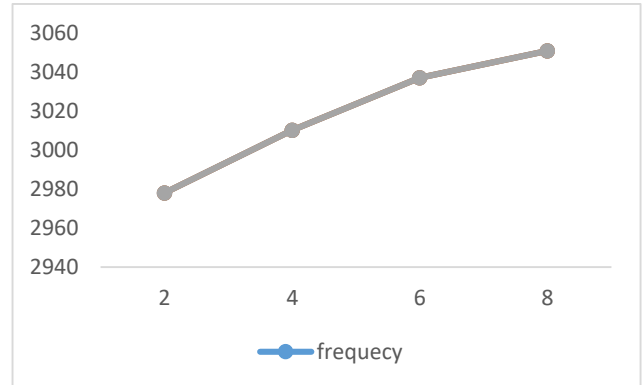
This indicates that the loading frequency, which means the number of cycles of the piston per unit time, should be less than the natural frequency of the connecting rod when it is fixed at the piston pin.

Comparison table for total deformation of original model and new model

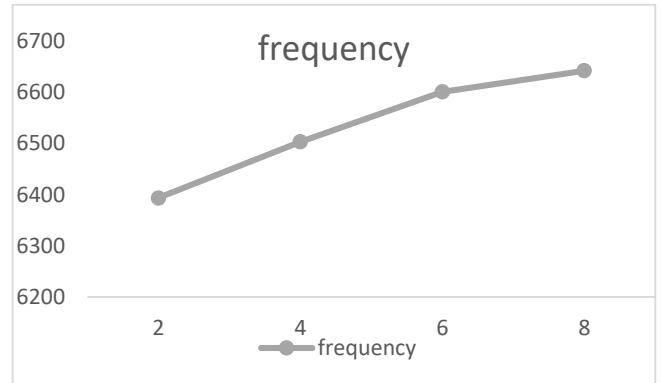




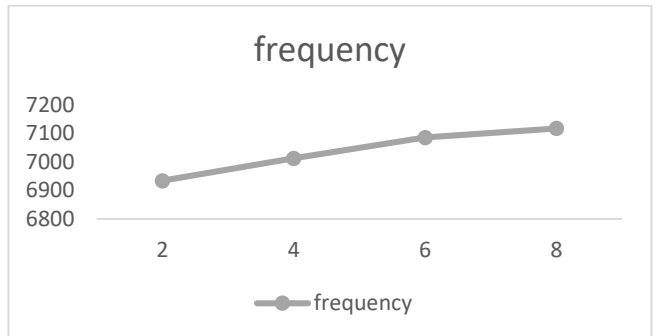
Mode 2



Mode 3



Mode 4

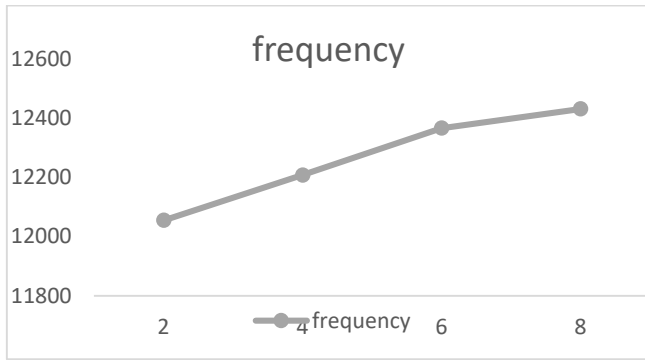


Mode 5

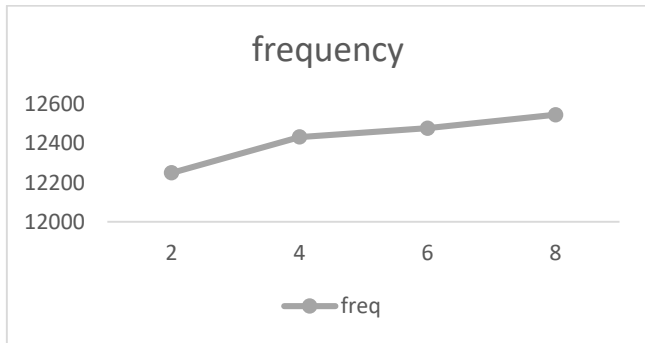
c) THE EFFECT OF MESH DENSITY ON NATURAL FREQUENCY

The effect of the mesh density on the modal frequency of connecting rod is analyzed for a fixed crankpin and the frequencies with mesh size. The mesh size begins with 2 mm and it is incremented by 2 up to 8mm. The mesh density affects the modal frequencies.

Model



Mode 6



The mesh size density slightly affects the modal frequencies. The frequency difference between lower and higher mesh density for the six modes are:-

- Mode 1 = 72.9 Hz
- Mode 2 = 137.9 Hz
- Mode 3 = 248.8 Hz
- Mode 4 = 183.4 Hz
- Mode 5 = 376 Hz
- Mode 6 = 298 Hz

The maximum frequency difference is found in the fifth-order mode.

VI. RESULTS AND DISCUSSIONS

S.NO	Properties	Existing rod	Optimized rod
1	Mass	1222.04gm	1197.81gm
2	Volume	158706.67mm ³	155559.58mm ³
3	Maximum deformation	0.0105mm	0.016mm
4	Maximum stress	129.03MPa	179.59MPa
5	Minimum stress safety factor	3.10	2.22

By the above analysis done in the Ansys software, we can say that according to the structural analysis carried out the strength and load-carrying capacity of the connecting rod remain the same, but the material that is used in the production is reduced and as it is a material addition manufacturing process the material wastage is untraceable. As of its design, we can conclude from the product weight analysis that the weight is also reduced by a considerable quantity. Thus the material usage decreases and mass production costs also get reduced.

VII. CONCLUSION

In this paper, the shape is optimized and the weight is reduced. Modal analysis of connecting rod is done by considering two cases those are fixed piston pin and fixed crank pin. The natural frequency of the fixed piston pin is lower than the fixed crankpin. The structural analysis is done which showed same strength and stress values with reduced weight, which in turn results in low material usage.

VIII. REFERENCES

[1] R Nishanth et al 2021, “Generative Design Optimization and Analysis of Connecting Rod for Weight Reduction and Performance Enhancement” in J. Phys.: Conf. Ser. 1969

[2] Aisha Muhammad, Ibrahim Haruna Shanono “Static Analysis and Optimization of a Connecting Rod”. In International Journal of Engineering Technology and Sciences (IJETS), Vol.6 (1) June 2019, University Malaysia Pahang.

[3] Asimuddin Patel, Aswatha, “Design Optimization of Connecting Rod for Static Loading Condition”. In International Research Journal of Engineering and Technology (IRJET) Volume: 08 Aug 2021.

[4]. Naman Gupta, Manas Purohit, Kartik Choubey, “Modern Optimized Design Analysis of Connecting Rod of an Engine” in International Research Journal of Engineering and Technology (IRJET) Volume: 05 Feb-2018.

[5]. Prof.N.P.Doshi, Prof.N.K.Ingole “Analysis of connecting rod using analytical and finite element method” in International Journal of Multidisciplinary Educational Research (IJMER) Volume.3, 2013.

[6]. Adnan Ali Haider, Akash Kumar, Ajinkya Chowdhury, Moin Khan, P. Suresh, “Design and Structural Analysis of Connecting Rod” in International Research Journal of Engineering and Technology (IRJET) Volume 5, 2018.

[7] Getachew Admassie Ambaye, “Numerical Comparative Modal Analysis of Connecting Rod between Fixed Crankpin and Fixed Piston Pin” in 8th International Conference on Innovation Science and Technology in 2021.

STRUCTURAL ANALYSIS OF CAM MECHANISM WITH DIFFERENT LOAD APPLICATIONS

Prakash Babu Kasukurthi¹, Venkannababu Mendi²

Associate Professor, Department of Mechanical Engineering, Azad College of Engineering and Technology, Hyderabad.
Associate Professor, Department of Mechanical Engineering, Narasaraopeta Engineering College (Autonomous), Narasaraopet.

Abstract- This thesis introduces a theoretical idea and detailed explanation of the PSO algorithm, the advantages and disadvantages, the effects and judicious selection of the various parameters. Moreover, this thesis discusses a study of boundary conditions with the invisible wall technique, controlling the convergence behaviors of PSO, discrete-valued problems, multi-objective PSO, and applications of PSO. Finally, this paper presents some kinds of improved versions as well as recent progress in the development of the PSO, and the future research issues are also given. Particle Swarm Optimization (PSO) is a metaheuristic global optimization paradigm that has gained prominence in the last two decades due to its ease of application in unsupervised, complex multidimensional problems which cannot be solved using traditional deterministic algorithms.

The canonical particle swarm optimizer is based on the flocking behavior and social cooperation of birds and fish schools and draws heavily from the evolutionary behavior of these organisms. This paper serves to provide a thorough survey of the PSO algorithm with special emphasis on the development, deployment and improvements of its most basic as well as some of the very recent state-of-the-art implementations. Concepts and directions on choosing the inertia weight, constriction factor, cognition and social weights and perspectives on convergence, parallelization, elitism, niching and discrete optimization as well as neighborhood topologies are outlined.

I. INTRODUCTION

Cam to Lever Mechanism

A cam is mechanical component capable of transmitting motion to follower by direct contact. In cam mechanism, cam is driver driven member is called the follower.

The follower can sit, oscillate or rotate stationary. The general shape of the camera system is seen in cinematic diagram Fig. It consists of two rounded A and B components with touch surfs attached to a third C body, smooth, round or extended. Bodies A or B will be driver, while the other body is driver. These bodies may be supplemented by a system of equivalency. Points 1 and 2 are joined by the pin at centers of the touch surfaces curvature. When the relative locations of bodies A and B change, paragraphs 1 and 2 are changed and the relations equivalent systems are of varying lengths.

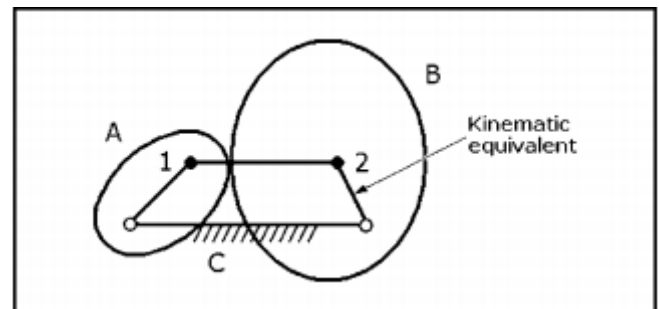


Figure: Basic cam mechanism and its kinematic equivalent. Points 1 and 2 are centers of curvature of the contact point.

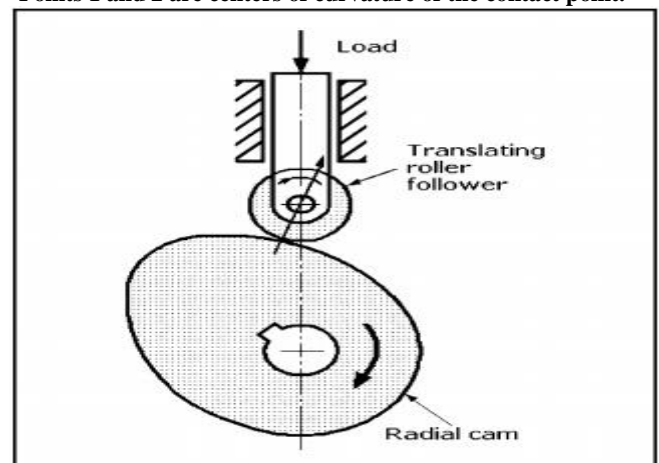


Figure: Radial open cam with a translating roller follower. The roller is kept in contact with the cam by the mass of the load.

Figure indicates a commonly used mechanism in open radial cameras. In these mechanisms, the roller follower is the most frequent user, as it can effectively pass power between the cam and the follower by decreasing friction and reducing wear throughout. The system seen here is called a gravity limit cam. It is simple and efficient and can be used for spinning disc or end cams if the weight of the system is adequate to maintain the cam profile in constant relation. In most practical cam mechanisms, however, pre-loaded compression springs limit cam and follower at all operating speeds. Cams can be developed.

- Shaping the cam body into a well-known spiral, parabola, or circular arc
- Mathematical cameras to assess followers' motions and then to draw the tabulated details into the cameras
- Draw the cam profile through free use of different draught curves

Classification of Cam Mechanisms

Input/output movements, the layout, the structure of the follower, and the form of the cam mechanisms can be classified. Often, cams can be grouped according to the following types of movements and the cam profile characteristics. In the figures 3a to e, there are examples of the potential input/output movements in cam mechanisms which are the most common disc-cams. Fig. 3f instead shows a follower arm with a roll which swings in the circular arc or oscillates in following arc as the cam rotates. Figs 3a configurations of the following: knife tip, b, e and f roller, c flat faced and d spherical face, to be named according to their characteristics. With regard to cam, even profile flat follower is oblique. The follower is entity which moves up, down, or side by side following the cam's contour.

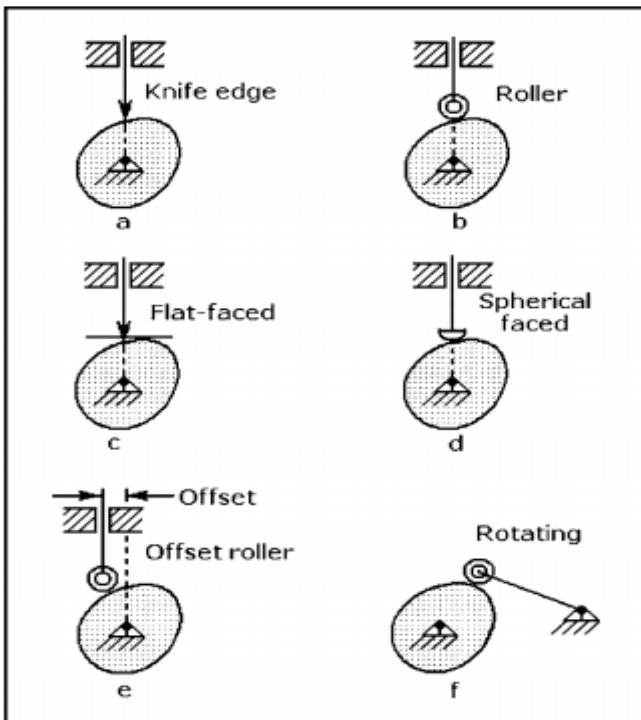


Figure: Cam configurations: Six different configurations of radial open cams and their followers

II. WORKING OF CAM

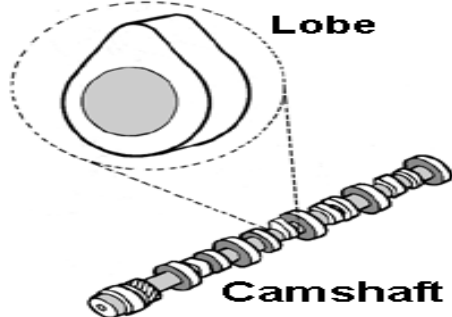


Figure: Showing Cam Shaft & Lobe

The lobes are fundamental components cam shaft. The lobes open shut intake exhaust valves with piston's movement as the came-shaft rotates. The results show that form cam lobes manner motor runs in various speed ranges is directly related. The intake valve would open when the piston begins to move downwards in intake

stroke (TDC). When the piston bottoms out, intake valve would shut down. At the conclusion stroke and when column finish completes the exhaust stroke, exhaust valve would open. When the valve is opened piston begins its intake stroke, combination air and fuel in in taken runner begins to speed up into cylinders. The air/fuel moves at rather high speed when piston hits bottom its intake stroke. If we shut down intake valve, all air/fuel stops and does not enter cylinder. With the input vanner opened little longer, when piston starts compression stroke, momentum fast flowing air/fuel continues to drive air/fuel in cylinder. The quicker engine is going, faster air/fuel travels larger we want to keep intake valve open

III. CREATING THE CAM FOLLOWER MECHANISM



Figure: The cam, cam tappet, valve, and valve springs

A cutout image cam-following mechanism in direct action is displayed, in shape bucket tappet working on valve with spring valve. This mechanism, like other cam followers devices, must during the planned work cycle in order to "trustfully" produce planned valve lift profile. This service may vary from 1000 hours of Joe Bloggs urban travel in his road vehicle to whole one race scenario before whole valve train is replaced for following race. In any instance, designer should identify allowable stress levels between movement surfaces and all components of the mechanism.

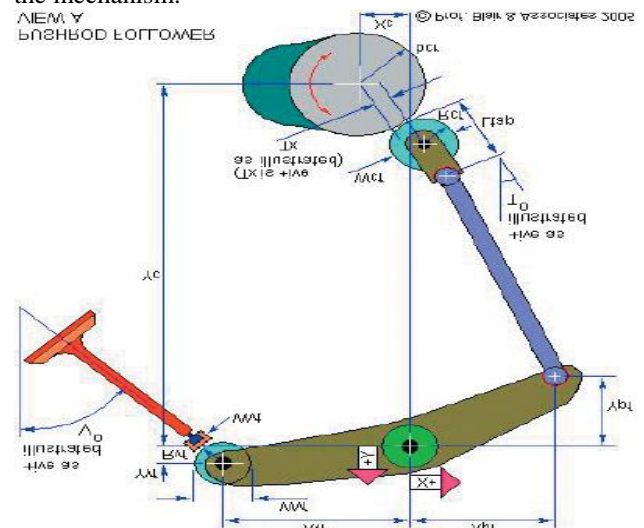


Fig. Geometrical data for a pushrod cam follower mechanism

The choice of whatever sort cam follow mechanism is not always designer's free option. Regulations such as NASCAR pushrod system or production vehicle may be required to comply with same requirements if Le Mans

GT car is installed. In any case, for pushrod system or likewise for finger followers, rockers or seemingly simple pocket tappets, geometry cam follower's mechanism must be constructed and numbered. The following cam tappet lift and came profile cannot be estimated without knowing that geometry to create correct valve lift diagram.

IV. METHODOLOGY

Process of optimization:

- Methods of improvement utilizing Taguchi execution
- Practical improvement of the component
- Analyze range once machine vibration ID and assortment is finished, the way toward breaking down the range can be led. Examination generally follows a cycle of disposal.
- Exaggeration of Repeatability, backfire examination and symmetrical cluster development

Simulation conditions:

- The systematic methodology is led dependent on the yields got during cycle of pragmatic upgrade
- The all-out usage utilizing Freudenstein's condition, Mat lab.
- Output interface relies upon length of each connections. Subsequently, expectations exchange capacities of linkage instruments are troublesome. Way age of yield interface is determined with help of Freudenstein's condition.
- The interface proportions acquired from Matlab is recreated in Adams. Information point is contacted from zero to 120° and relating yield edge is planned.

Analysis of variants:

- Parameter contrasts
- Thickness – 8,10,12 mm
- Width - 38,40,42 mm
- Displacement, stress, strain examination for every one of the 3 joints to get ideal outcomes for additional thought.
- Material streamlining carbon steel, SS and MS

Motor definitions for motion study:

- Motor speed-600 rpm,
- Force got at fixed connection 10N
- Angle of tendency 3°
- Standard 4-bar plan
- Material considered-SS304 compound steel
- Modelling of 4-bar instrument in strong works

Case Study Approach:

- By watching the cycle, variations are investigated to limit reasonable material expense by utilizing strong works recreation.
- The results are contrasted with get ideal measurements for pragmatic commencement.

Materials and Mechanisms:

- Mechanism at present-wrench based switch to switch instrument
- Materials: switch based focuses and switches with SS304 joins.
- Crank working distance across 300mm.

- Analysis completed for various thickness and width.

Case study-2

Plan details

The cam profile has arched and level segments.

r1= base circle radius= 70 mm

rr = range of the roller= 60mm

Lift = 70 mm

Engine rpm to equip box at 1440 rpm, cam one turn time is 3.75 seconds cam pivot at 16 rpm.

Edge of outward = (outward stroke time/all out time)

x360= (1.16/3.75)x360= 1110

Edge of abide at close= (0.856/3.75)x 360= 830

Edge of return= (return stroke time/complete time) x360= (1.16/3.75)x360= 1110

Abide at open= (0.573/3.75)x 360= 550

During the return stroke is as same as forward the speeding up viewed as uniform.

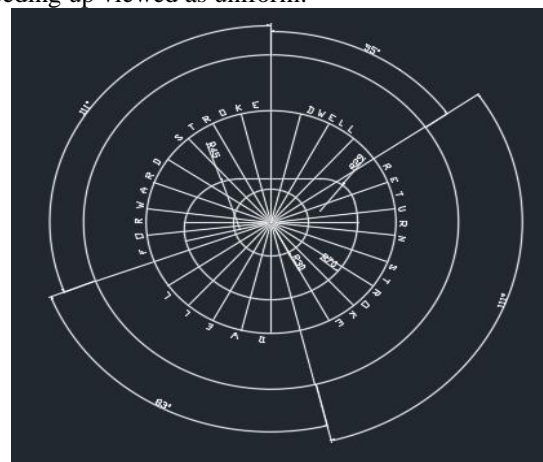


Figure: shows the cam peripheral design for stroke and return with dwell

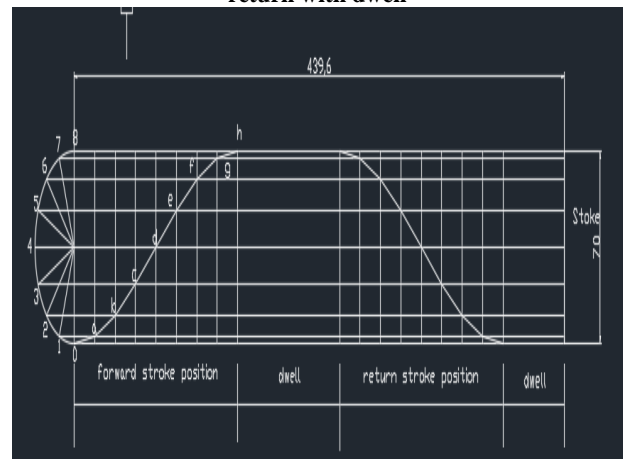


Figure: shows the simple harmonic motion diagram of lift vs crank angle

The path curve plotted with contact intersections shows lift and return with dwell for present used cam.

sent out to ANSYS programming as an IGES records as appeared in figure

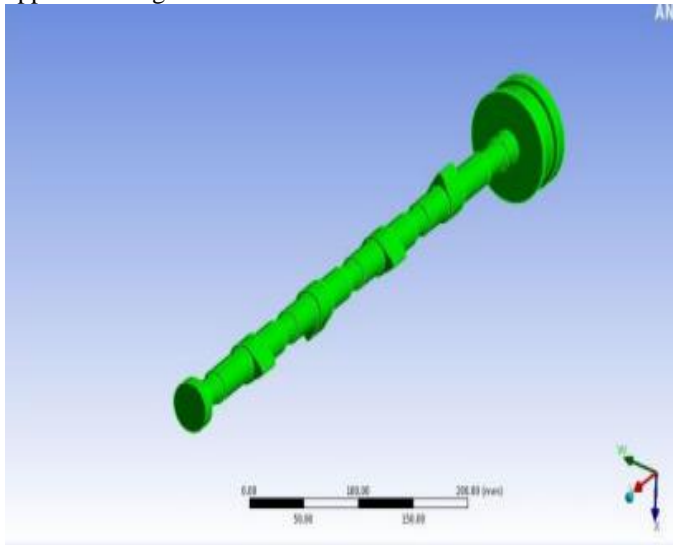


Figure: structural analysis Cam Follower

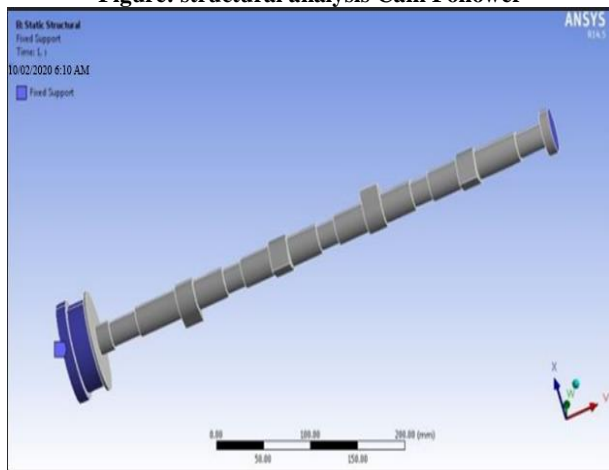


Figure: Fixed support Cam Follower

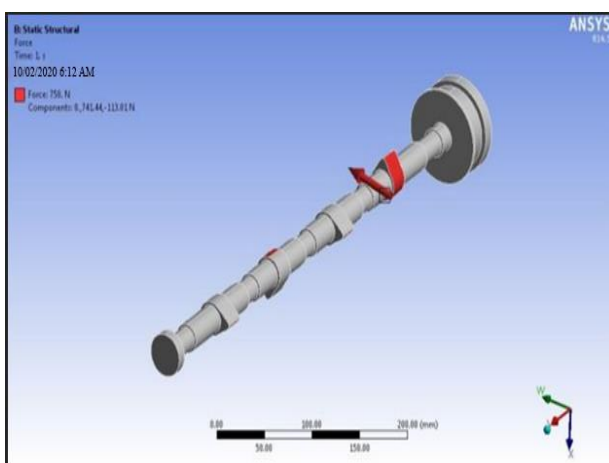


Figure: Cam Follower load 750N

CONCLUSION

In this project Design and Modal Analysis of camshaft is done by using CATIA and ANSYS software. By using ANSYS the modal analysis is done to find out the natural frequencies of Cam. The displacement and stress are calculated. The design of the cam is done by using CATIA software. The design is done by using cam profile at inlet and outlet (exhaust). The Cam have knife edge

follower. The structural analysis is used to find the stress and displacement values in Cam. The modal analysis is used to find the natural frequencies of the camshaft and the safety of factor is also considered. In this project the preferred material for Cam is selected at it's working environment. The material selection is done by considering stress, displacement and natural frequencies of the materials. The material selection for Cam is done by using ANSYS software. In this the two materials are compared. The stress and displacements are calculated at inlet and outlet of Cam. Finally the nickel chromium molybdenum steel is preferred.

REFERENCES

[1] Mendes, R., Kennedy, J., Neves, J., "Watch thy Neighbour or How the Swarm can Learn from its Environment", *Proceedings of the IEEE Swarm Intelligence Symposium*, pp. 88-94, Apr. 2003.

[2] Metropolis, N. et al. "Equations of state calculations by fast computing machines", *J. Chem. Phys.* 21 (1953) 1087-1092.

[3] Mohammadi, A., Jazaeri, M., "A hybrid particle swarm optimization-genetic algorithm for optimal location of SVC devices in power system planning", *Proceedings of 42nd International Universities Power Engineering Conference*, 2007, pp.1175-1181.

[4] Moussa, R., Azar, D., "A PSO-GA approach targeting fault-prone software modules", *The Journal of Systems and Software*, 132 (2017) 41-49.

[5] Naka, S., Genji, T., Yura, T., Fukuyama, Y., "Practical Distribution State Estimation using Hybrid Particle Swarm Optimization", *IEEE Power Engineering Society Winter Meeting*, vol. 2, pp. 815-820, Jan. 2001.

[6] Nik, A. A., Nejad, F. M., Zakeri, H., "Hybrid PSO and GA approach for optimizing surveyed asphalt pavement inspection units in massive network", *Automation in Construction* 71 (2016) 325-345.

[7] Niknam, T., Amiri, B., An efficient hybrid approach based on PSO, ACO and k-means for cluster analysis, *Applied Soft Computing*, Volume 10, Issue 1, 2010, Pages 183-197.

[8] P. C. Ma, F. Tao, Y. L. Liu, L. Zhang, H. X. Lu and Z. Ding, "A hybrid particle swarm optimization and simulated annealing algorithm for job-shop scheduling," *2014 IEEE International Conference on Automation Science and Engineering (CASE)*, Taipei, 2014, pp. 125-130.

[9] P. Li, N. Cui, Z. Kong and C. Zhang, "Energy management of a parallel plug-in hybrid electric vehicle based on SA-PSO algorithm", *2017 36th Chinese Control Conference (CCC)*, Dalian, 2017, pp. 9220-9225.

[10] Premalatha, K., Natarajan, A.M., "Discrete PSO with GA operators for document clustering", *International Journal of Recent Trends in Engineering I* (2009) 20-24.

[11] Price, K., Storn, R., "Differential evolution – a simple and efficient adaptive scheme for global optimization over continuous spaces", *Technical Report, International Computer Science Institute, Berkeley*, 1995.

Traffic Signal Control Using Programmable Logic Controller (PLC)

P. Sravani¹, M. Shabran Baig², P. Prem Kumar³, U. Ramu⁴

¹Asst.Professor, Department of Mechanical Engineering, Narasaraopeta Engineering College, Narasaraopet, India

^{2,3,4} Student, Department of Mechanical Engineering, Narasaraopeta Engineering College, Narasaraopet, India

Abstract—Traffic signal control system is used to control flow of automobiles through intersection of many roads. This paper presents feasible approach of Programmable Logic Controller (PLC) for controlling traffic signal lights using eddy current displacement sensors and for traffic intersection a proportionate signaling is designed. In this system, piezoelectric material is used to generate power from load of vehicles when the vehicles is in idle situation in traffic signal junction and load of people who usually use pathways across traffic road. This paper also represents that manual traffic signal control system can be replaced by using PLC automatic control system. For this work DELTA PLC, monitor is used and this idea which is implemented in traffic control system is feasible and affordable in any situation of traffic congestion all over the world. **Keywords**—Programmable Logic Controller (PLC), traffic signal, Relay card.

I. INTRODUCTION

In today’s fast-moving, highly competitive industrial world, a company must be flexible, cost effective and efficient if it wishes to survive. In the process and manufacturing industries, this has resulted in a great demand for industrial control systems/ automation in order to streamline operations in terms of speed, reliability and product output. Automation plays an increasingly important role in the world economy and in daily experience. Automation is the use of control systems and information technologies to reduce the need for human work in the production of goods and services. In the scope of industrialization, automation is a step beyond mechanization. Whereas mechanization provided human operators with machinery to assist them with the muscular requirements of work, automation greatly decreases the need for human sensory and mental requirements as well.

Automation Control System - system that is able to control a process with minimal human assistance or without manual and have the ability to initiate, adjust, action show or measures the variables in the process and stop the process in order to obtain the desired output.

The main objective of Automation Control System used in the industry are:

1. To increase productivity
2. To improve quality of the product
3. Control production cost

Programmable logic controllers are small industrial computers. Their design uses modular components in a single device to automate customized control processes. They differ from most other computing devices, as they are intended for and tolerant of severe conditions of factory settings such as dust, moisture, and extreme temperatures.

Industrial automation began long before PLCs. In the early 1900s until their invention, the only way to control machinery was through the use of complicated electro mechanical relay circuits. Each motor would need to be turned ON/OFF individually. This resulted in factories

needing massive cabinets full of power relays. As industrial automation continued to grow, modern factories of the time needed dozens of motors with ON/OFF switches to control one machine, and all these relays had to be hardwired in a very specific way. PLCs were developed as a solution to have one solid control as an electronic replacement for hard-wired relay systems.

Traffic light which is one of the vital public facilities plays an important role to the road users. It will help to curb from accidents and gridlocks. This research exposed the operational of traffic light such as understanding the flow of the traffic system and the program itself. Traffic signal light is used to control the movement of vehicles and passengers, so that traffic can flow smoothly and safely. Traffic signal lights have been around for years and are used to efficiently control traffic through intersections. Although traffic signal lights are relatively simple and commonplace, they are critical for ensuring the safety of the driving area. The growing use of traffic lights attests to their effectiveness in directing traffic flow, reducing the number of accidents, and the most recently to their utility in controlling the flow of traffic through metropolitan areas when have been used together with computer systems.

The transition of the light is controlled by PLC to help the traffic movement run smooth from one direction to the other. PLC reduces traffic congestion especially in the morning and evening. Besides, it also helps to reduce the accident rate especially in town.

This paper presents an automatic traffic systems which are implemented with PLC which are fixed and don’t depend on real time traffic flow and it does not consider roadwork’s, accidents, breakdown of cars that affects the traffic jam. So the main aim is to design a traffic control system which controls the traffic according to the real time data, reducing the delay time of vehicles in each lane, optimizing cars safety and expanding the benefits in environment, economic and health sectors.

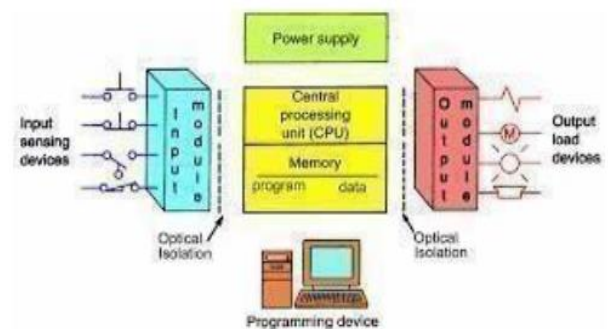


Figure 1: PLC Block Diagram

II. METHODOLOGY

The procedure for the implementation of the proposed project is as follows. Tools & materials used

1. Plywood 3.5 * 3.5 m.
 2. Wires 2m.
 3. Soldering device
 4. LED lights set 4*3(Red, Green, Yellow)
- First prepare the four-road junction 1.5*1.5 by using plywood and sticker.
 - After that, fix or attach the LED lights at the each 3*4 sides remove the sleeves (insulations) of led terminal wires for connecting PLC.
 - Join the wires with LED terminal wires of certain length for our requirement and those wires connect by the help of soldering device and place the sleeve at soldering portion.



Figure 2: Prototype of Traffic Signal Controlling System

III. EXPERIMENTAL SYSTEM DESCRIPTION

Ladder logic is a graphical programming language with simple contacts that simulate the opening and closing of the relays. Making ladder logic of working of traffic light. PLC mainly operates by continues scanning of instruction in the logic, one at a time to switch on or off the various outputs. The program is written for different conditions. The program is written on real time basis. After making the ladder logic the program was saved and simulates to check if there was any error in the program. Running the program was done after checking it. The model and sensors are connected with PLC by wire. According to the input the traffic control system is operated.

a) Connections:

- In our PLC kit there are 12 inputs and 4(2) outputs used, those are in red colour wires as inputs and yellow colour wires are as outputs.
- And we are assume that red colour wires are as positive terminal and yellow colour are negative terminals.
- Here we have 4 signal points/spots each one has to form a closed loop of negative terminal connections.
- First we have to connect red light negative terminal to with other negative terminal that successive to green and same as red also to get a loop which is used by yellow wires and another long wire is taken as output.
- Remain three are connected similarly and then wires are twelfth inputs are as connected to PLC of Y series bus system sequentially with each colour and same as after one colour like green is screwed with first four ports after yellow and finally red.

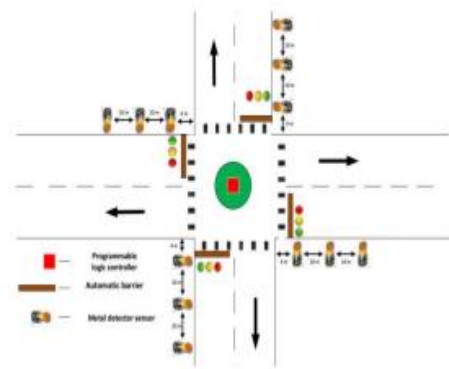


Figure 3: Layout of Traffic Signal Controlling System

b) ladder diagram

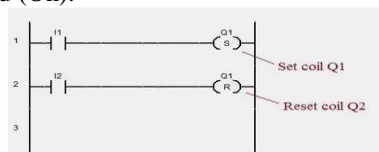
The ladder diagram is the universal programming language of PLC. It has a short abbreviation as LD and also known as Ladder Logic. It is one of the oldest programming languages for PLC. In the ladder diagram, the programming language that used to create the program to control the PLC system is known as Ladder Diagram Language or Ladder Logic Language. It has signified by the graphical representation, just like electrical wiring for logic control.

c) Rules of Ladder Diagram Programming

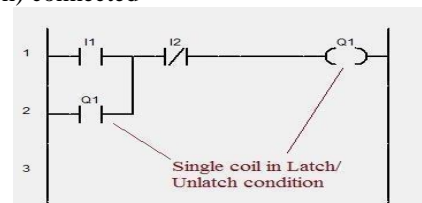
- Inputs can be used in Series as well as Parallel to form a connection
The number of inputs (I1, I2, I3, I4,In) can link with different outputs (Q1, Q2...Qn) by using series or parallel connection.



- Outputs (or coil) can be used only in Parallel
According to the second rule, outputs (Q1, Q2, Q3, and Q4 ...Qn) are connected in parallel along with the single input (I1). If the single input (I1) is normally closed (NC contact) then all outputs (Q1, Q2, Q3, Q4.... Qn) will be activated (On).



- One Input can be used in multiple times in one program
As per the third rule, a single input can be used to repeatedly in the different rungs. From the below image, the program has different outputs but the same input (switch) connected

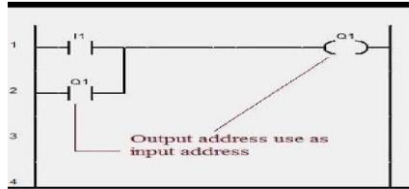


- Input Address cannot be used as an Output Address

The same input address can be used as multiple inputs. And it cannot be used as output.



- Outputs Address can be used as Inputs Address
The last rule is for the cycling process (i.e. process continuous from start to end).



IV. EXPERIMENTAL RESULTS

a) The implementation of ladder-diagrams

- Enumeration at each stage
1. Below figure shows that GREEN glows and remaining 3 are in RED colour for road (N). Green terminal has switched on and other lights are in red terminal where those 4 are simultaneously on but colour differentiate.



2. Here after the GREEN light time (30sec) over then YELLOW will turns ON. Yellow replaces green which is in switched on condition.



3. After road(N) cleared RED replaces YELLOW and next road will open it means GREEN turn ON for few seconds.



4. Here the road(S) traffic cleared, YELLOW light will glow, remain three are in RED colour.



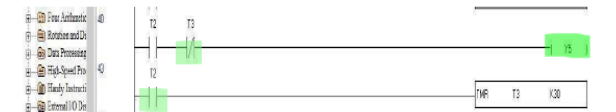
5. After few seconds road (N&S) are closed for (60sec) and road (E) will call to clear that traffic.



6. After 30 sec the GREEN time overs then the road will be closing soon when yellow comes.



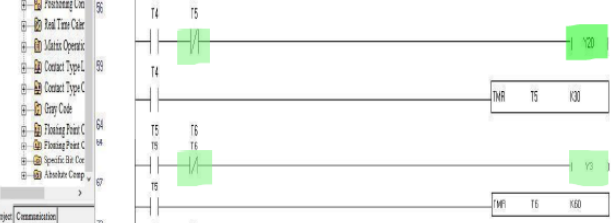
7. Here the roads (N,S&E) are in closed then road (W) is for clearance of that traffic.



8. Remain three are still be wait for next fifteen seconds it means input Y2 stays for fifteen second.



9. Here the YEELOW comes and after road(W) cleared, it will turns off it means that road is being closed for next 45 second, similarly the same phenomena happens again and again and we will change that timing in some emergency situations also.



The Total Ladder Diagram for this system is given below.

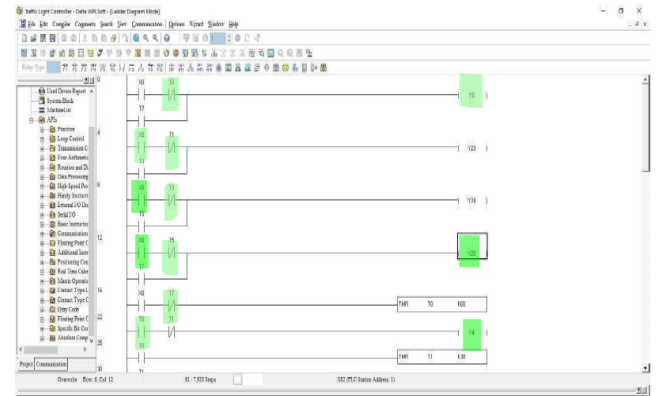


Figure 4: Ladder Diagram for Traffic Signal Controlling System

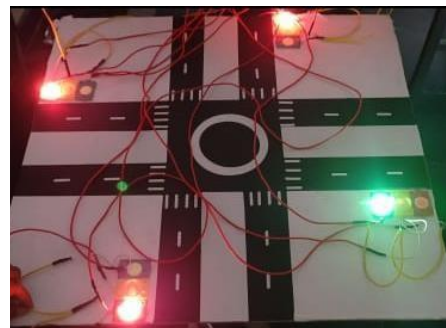


Figure 5: Execution of Traffic Signal Controlling System through PLC

Table 1: Overall Execution Results

S.No.	Road	Signal	Gate and Time
1	Road N	Green	Open 30sec
	Road S	Red	Close
	Road E	Red	Close
	Road W	Red	Close
2	Road N	Red	Close
	Road S	Green	Open 30sec
	Road E	Red	Close
	Road W	Red	Close
3	Road N	Red	Close
	Road S	Red	Close
	Road E	Green	Open 30sec
	Road W	Red	Close

CONCLUSIONS

Traffic signal problem is obviously one of the biggest concerns for the citizens and government. A model has been developed using PLC. This model of traffic control system will reduce traffic congestion and it would reduce accidental rate as this system properly control the vehicles. Thus this system would make our roads safer place to travel. This model has been successfully implemented with the PLC Module. This interface is synchronized with the whole process of the traffic system. This prototype can easily implement in real road.

This method will help reduce congestion on roads and would help in coping with accidents. Resultantly, a solution to a much critical problem of traffic congestion and fatal accidents is possible using this system. Thus the proposed system would make our roads a safer place to travel. By using PLC Board (model) the Automatic traffic signal controlling for a four road junction had successfully been designed and developed by using ladder diagram programming. The delay time is taken as 30 seconds and the delay time can be changed by using Timer controller with respect to Traffic density.

In this project a four-road junction was taken for automation by using DELTA PLC with delay time for each junction was 30 seconds. With this project the traffic signal can be controlled automatically without human effort.

FUTURE SCOPE

In future scope the sensors were interfaced with PLC Module. This interface is synchronized with the whole process of the traffic system. This prototype can easily be implemented in real life situations. Increasing the number of sensors to detect the presence of vehicles can further enhance the design of the traffic light system. Another room of improvement is to have the infrared sensors and imaging system/camera system so that it has a wide range of detection capabilities, which can be enhanced and ventured into a perfect traffic system.

REFERENCES

- [1] AHMAD, A. B. (n.d.). UMP@ INSTITUTIONAL REPOSITORY (UMP IR) Open Access Repository of UMP Resear. Retrieved from <http://umpir.ump.edu.my/75/1/cd2636.pdf>
- [2] Angelfire.(n.d.). Retrieved from http://www.angelfire.com: http://www.angelfire.com/planet/mandy88/Topic_8_PLC.pdf
- [3] (April 2005, April). (Traffic Engineering Division Colorado Springs, Colorado) Retrieved from https://permits.springsgov.com https://permits.springsgov.com/units/traffic/Signal_Coordination_Plan.pdf
- [4] B, Z. B. (2008, MAY). uTeM PERPUSTAKAAN. Retrieved MARCH 2016, from
- [5] http://library.utem.edu.my/index2.php?option=com_docman&task=doc_view&g id=5 128&It emid=342
- [6] Dr. Tom V. Mathew, I. B. (2014, February 19). (Transportation Systems Engineering) Retrieved march2016,fromhttp://nptel.ac.in: http://nptel.ac.in/courses/105101008/downloads/cete_39.pdf
- [7] Hudedmani, Mallikarjun G., R. M. Umayal, Shiva Kumar Kabberalli, and Raghavendra Hittalamani. "Programmable Logic Controller (PLC) in Automation." *Advanced Journal of Graduate Research* 2
- [8] L. Yang, and C. XianFeng, (2009), Design of Traffic Lights Controlling System Based on PLC and Configuration Technology.
- [9] Ovidiu TOMESCU, Ilona Madalina MOISE, Alina Elena STANCIU, Iulian BĂȚROȘ "Adaptive Traffic Light Control we consider an urban arterial road and investigate the problem of adaptive traffic light control using real-time traffic information.
- [10] C. M. Mwangi, S. M. Kang'ethe and G. N. Nyakoe "Design and simulation of a fuzzy logic traffic signal controller for asignalized intersection"
- [11] Monica Voinescu, Andreea Udrea, Simona Caramihal "On Urban Traffic Modelling and Control"
- [12] Azura Che Soh/Lai Guan Rhung "MATLAB Simulation of Fuzzy Traffic Controller for Multilane Isolated Intersection" Institute of Clean Air Companies (ICAC). White Paper. Selective Catalytic Reduction (SCR) Control of NOx Emissions from Fossil Fuel-Fired Electric Power Plants. May 2009.

PLC BASED AUTOMATIC LIQUID FILLING AND MIXING SYSTEM

A. PAVAN kumar¹, M.Bhupathi², T.Chaitanya Krishna³

¹ Assistant .Professor, Department of Mechanical Engineering, Narasaraopeta Engineering College,Narasaraopet, India

^{2,3} Student, Department of Mechanical Engineering, Narasaraopeta Engineering College, Narasaraopet, India

Abstract- In a present world of industrialization with modernization of societies, it has now become a challenging problem to meet the demand of the people. Presently the task to obtain the output and to meet the demand is one of the adversaries in a present scenario that we need to do something to improve and to be a part of this modernization. In this project, we are implementing an “Automatic Bottle Filling and Capping” and are dedicating to the industries. In this project we are using PLC which is a brain of this entire project. The main work it will do is the filling and capping of the bottles used in industries for the various purpose such as pouring fluids (such as milk, water etc.) in a packing bottles, toxic chemical containers storing in bottles without any injuries.

Keywords—PLCboard,24V-DC Pump motor, 24v DC motor, Containers, Water Tube, Insulation Tape, Rubber Tape, Indicators, Stirrer Fan, Electrical Wires

I. INTRODUCTION

Automation is the use of control system such as computers to control industrial machinery & process, reducing for need for human intervention. In the scope of industrialization, Automation is a step beyond mechanization, whereas mechanization provided human operators with machinery assist them with physical requirement of work, automation greatly reduces the need for human sensory and mental requirements as well. Process and system can also be automated. In other words, Automation is a delegation of human control function to technical equipment for increasing productivity, to better quality, to reduce cost & increase in safety working condition, to reduce man power. Example of automation are Automatic machine tools to process parts-CNC m/c, Industrial robots, Automatic material handling ,and Feed-back control system.

Automation Control System - system that is able to control a process with minimal human assistance or without manual and have the ability to initiate, adjust, action show or measures the variables in the process and stop the process in order to obtain the desired output.

The main objective of Automation Control System used in the industry are:

1. To increase productivity
2. To improve quality of the product
3. Control production cost

TYPES OF AUTOMATION

a) Fixed automation: Fixed automation refers to the use of custom-engineered (special purpose) equipment to automated a fixed sequence of processing or assembly operations. This is also called hard automation. The primary drawbacks are the large initial investment in requirement and the relative flexibility

b) Programmable automation

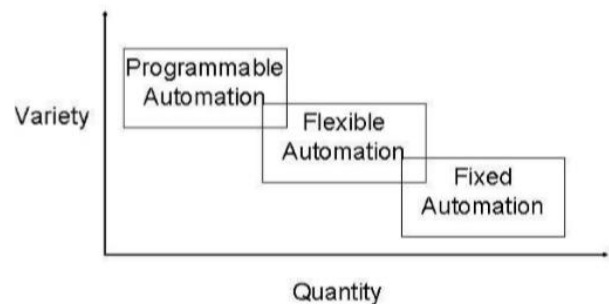
In programmable automation, the equipment is designed to accommodate a specific class of product changes and the processing or assembly operation can be changed by modifying the

c) Flexible automation In flexible automation the equipment is designed to manufacture a variety of products or parts and very little time is spend on changing from one product to

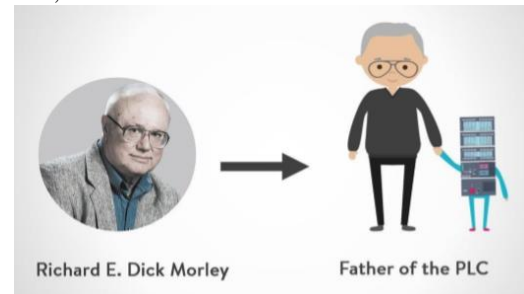
another . A flexible manufacture various combination of products according to any specified schedule.

Examples of fixed automation: machining transfer lines found in the automotive industry, automatic assembly machines, and certain chemical processes.

Programmable automation: is a form of automation for producing products in batches



FATHER OF PLC: Richard E. Morley (December 1, 1932 – October 17, 2017) was an American mechanical engineer who was considered one of the "fathers" of the programmable logic controller (PLC) since he was involved with the production of the first PLC for General Motors, the Mod icon, at Bedford and Associates in 1968.



Father of Plc

First Automotive PLCs:

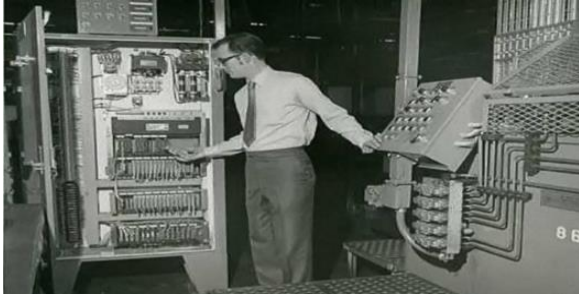
In 1968, the invention of the first PLC revolutionized the automation industry. First adopted by the automotive sector, General Motors began to deploy PLCs into their operations in 1969. Today, PLCs have broadly been accepted as the standard automated control system in manufacturing industries.

Known as “The Father of the PLC,” Dick Morely first came up with the vision of a programmable controller which could work for every job. He put the proposal together on January 1, 1968. Along with the team at his company (Bedford and Associate) they created a design for a unit which would be modular and rugged while using no interrupts .They called it the 084, which was named after their 84th project.

At the same time as the 084, Bill Stone with GM Hydromatic (automatic transmission division of General Motors) was having the same issue: problems with reliability and documentation for the machines in his plant. His solution proposed a solid-state controller as an electronic replacement for hard-wired relay systems.

For this reason, Morely insists he is not the inventor of the PLC. Morley stated: “the programmable controller’s time was right.

PLCs were designed so that they could easily be understood and used by plant engineers and maintenance electricians, using a software called Ladder Logic. Widely used in PLCs today, Ladder Logic is a programming language which uses ladder.

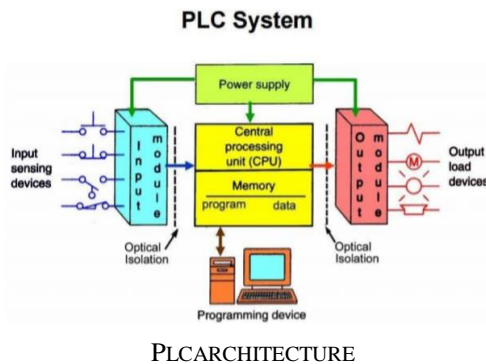


First automotive PLC in Past

II. PROGRAMMABLE LOGICAL CONTROLLER

PLC Architecture:

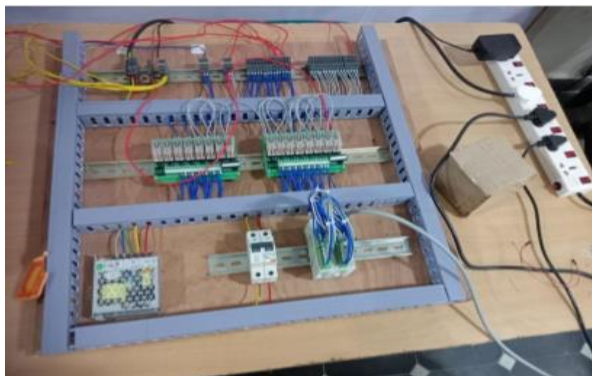
The term PLC architecture refers to the design specification of the various PLC hardware and software components and the how they interact with one another to form the overall PLC system. The architecture of a PLC is based on the same principles of that used in standard computer architecture.



PLCARCHITECTURE

Programmable logic controller :

A programmable logic controller (PLC) is an industrial computer control system that continuously monitors the state of input devices and makes decisions based upon a custom program to control the state of output devices. Plcs were first developed in the automobile manufacturing industry to provide flexible, rugged and easily programmable controllers to replace hard-wired relays. Since then, they have been widely adopted as high reliability automation controllers suitable for harsh environments.



PLC BOARD

Magnetic relays:

Relay works on the principle of electromagnetic induction. When the electromagnet is applied with some current, it induces a magnetic field around it .Above image shows working of the relay. A switch is used to apply DC current to the load.

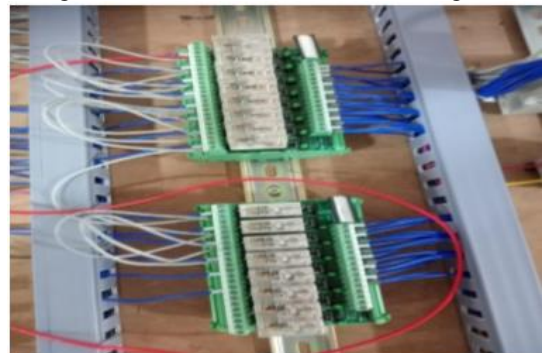
On the logic module market, the PLC logic relay system is the first to combine logic, interface, and field connection level single solution. This means that you can switch and control I/O signals using a single compact system.

Types of Relays

- Electromagnetic Relays.
- Latching Relays.
- Electronic Relays.
- Non-Latching Relays.
- Reed Relays.
- High-Voltage Relays.
- Small Signal Relays.
- Time Delay Relays.

On the logic module market ,the PLC logic relay system is the first to combine logic, interface, and field connection levels in a single solution. This means that youc ans witc hand control I/O signals using a single compact system.

Relays are electric switches that use electromagnetism to convert small electrical stimuli into larger currents. These conversions occur when electrical inputs activate electromagnets to either form or break existing circuits.



Relay switches

III. PLC PROCESSOR

The processor, or the brain of the PLC system, is a solid-state device designed to perform a wide variety of production, machine tool, and process-control functions. Conventional electromechanical devices, relays and their associated wiring formerly performed these functions.

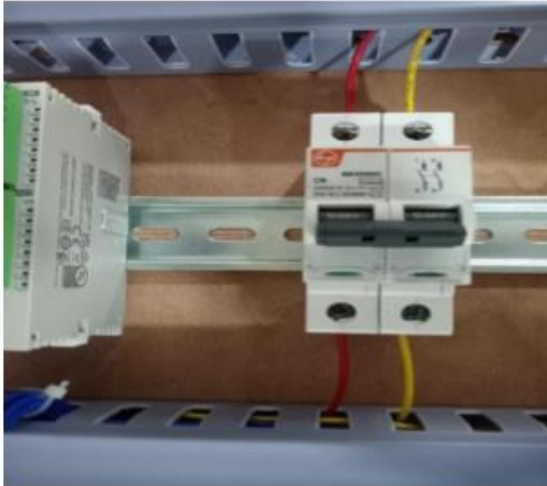


PLC processor

A programmable logic controller is a type of tiny computer that can receive data through its inputs and send operating instructions through its outputs. Fundamentally, a PLC's job is to control a system's function using the internal logic programmed into it.

MCB–MiniatureCircuitBreaker

When the over flow of current takes place through MCB– Miniature Circuit Breaker, the bimetallic strip gets heated and it deflects by bending. The deflection of the bi-metallic strip releases a latch. The latch causes the MCB to turn off by stopping the flow of the current in the circuit. These are an alternative to fuses and are used to protect circuits from excess current. These miniature circuit breakers (MCBs) are automatic switches which open when the current



MCB

SWITCHMODEPOWERSUPPLY

A switched-mode power supply is an electronic power supply that incorporates a switching regulator to convert electrical power efficiently. Like other power supplies an SMPS transfers power from a DC or AC source to DC loads, such as a personal computer, while converting

The advantages of SMPS include:

- The efficiency is as high as 80 to 90 %
- Less heat generation; less power wastage.
- Reduced harmonic feedback in to the supply mains.
- The device is compact and small in size.
- The manufacturing cost is reduced.
- Provision for providing the required number of voltages.



Switch mode power supply

Manual in puts:

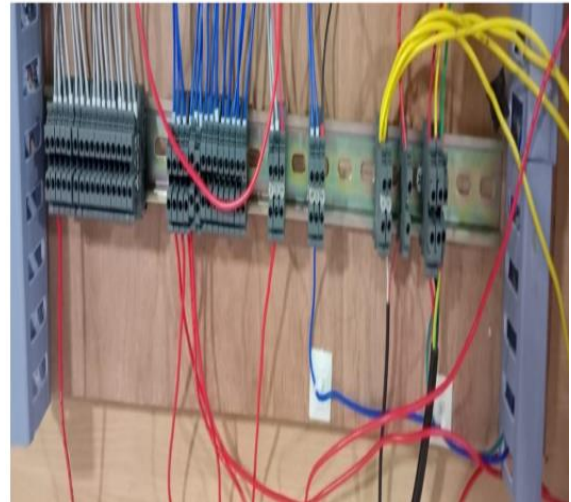
- Following are the Steps to connect the in put
1. The first connection was given to the 24v on/off switch in input X0 terminal.
 2. The remaining red wires given to the connections for output of Y0,Y1,Y2,Y3 terminals.
 3. Supply 24V to one of the input pins
 4. The yellow wires given to the connection for 9V

negative terminals.

Manual outputs:

Following are the Steps to connect the out put

1. The out put Y0 terminal is given to connection container-1
2. Y1 Terminal is given to connection of container-2
3. Y2 Terminal is given to connection of mixer in container-2
4. Y3 Terminal is given to the connection of mixer in container-3
5. The yellow wires given to the connection for 9V negative terminals.



In puts and out puts

Connections from plc to mixing system:

In programmable logic controller they are eight modules present in the system, they are power supply, communication module and three pump motors and one pump dc motor for mixing. The output of the mixing system give connection to the input of plc.



Connections from plc to mixing system

The connections of mixing system is very is easy to connect wiring from plc board to mixing system by the following manual input terminals.

IV. MIXING SYSTEM COMPONENTS

SUB MERSIBLE PUMP MOTOR:

The motor is hermetically sealed and close-coupled to the body of the pump. A submersible pump pushes water to the surface by converting rotary energy in to kinetic energy into pressure energy. Water pressure pushes the water into a submersible pump, thus “saving” a lot of the pump’s energy.



24V-DC Pump motor

DC water pump is a machine that transports liquid or pressurizes liquid. When the water pump is working, the coil and commutator rotate but the magnetic steel and carbon brushes do not rotate. The alternating current direction of the coil is changed by the commutator and brushes that rotate with the motor. In our project it is used to pump the water from one container to other container. We use three pump motors to pump the water. In three containers three motor are placed.

24V-DC motor:

A DC motor is any of a class of rotary electrical motors that converts direct current (DC) electrical energy into mechanical energy. The most common types rely on the forces produced by magnetic fields. Nearly all types of DC motors have some internal mechanism, either electromechanical or electronic, to periodically change the direction of current in part of the motor.



In our project dc motor used for mixing purpose, it is main component to mix both containers liquid in third container.

Containers:

These containers made with plastic. These are used to passing the liquids from one container in to another containers with the help of the water tubes.

The liquid flow into the containers by the ladder diagram (time management).

In this containers we arrange the 3-motor in three containers with water tubes.

We arrange the indicators separately on the top of the containers.

The container 1 is contained colour-1 with indicator.

The container 2 is contained colour-2 with indicator.

The container 3 is a mixer contained with motor for mixing purpose, it is also contained indicators.

The fourth container is output of mixing colours.



Containers

Water Tubes:

The water tubes are helpful to pumping the water one container to another container.

The pipe-1 is placed in first container, which is attached to pump motor-1

The pipe-2 is placed in second container, which is attached to pump motor-2

The pipe-1, pipe-2 is dropped in third container. The pipe-3 is dropped to fourth container.



Water Tube

Rubber Tape

Rubber tapes are designed for use in splicing and terminating wires and cables with options rated up to 69kV. They have excellent physical and electrical properties and are ideal for adding moisture protection and padding to electrical connections and cables.



Indicators Lights:

Indicator lights are a type of illuminating device that is commonly used to signify that equipment is either receiving power or that there is some form of malfunction. We have all seen the red light come on when you power on a device. That is an example of an indicator light. They serve a very basic but very important function, especially when it comes to indicating some type of malfunction. These indicator lights

are designed for panel usage but that does not mean that they cannot be installed in another location.



Indicators

STIRRERFAN:

The stirrer fan is used to stir the water to get well mixed. The stirrer is attached to the 24v DC motor. As it is placed in the third container to mix both colours in the container to give third colour output. It will stir the water up to 75ms by the time management process of ladder diagram.



Stirrer Fan

Electrical wires:

Stranded wire is composed of a number of small wires bundled or wrapped together to form a larger conductor. Stranded wire is more flexible than solid wire of the same total cross-sectional area. Stranded wire is used when higher resistance to metal fatigue is required.



Electrical Wires

METHODOLOGY

STEPBYSTEPFABRICATIONPROCESS:

- The container 1 is contained colour-1 (BLUE) with indicator-1
- The container 2 is contained colour-2 (YELLOW) with indicator-2
- The container 3 is a mixer contained with motor for mixing purpose, it is also contained indicators.
- The container is also contain indicators 3, 4 which supports mixer and output pumping purpose.
- The fourth container is output of mixing colours.
- Container-1 Pump motor -1 will start and pump the liquid third container with colour 1(BLUE) upto100ms.
- Container-2 Pump motor-2 will start and pump the liquid to third container with colour2 (YELLOW) upto100ms.
- Container-3 DC motor will turn on stirrer for mixing both colours upto75ms.
- Container-3 pump motor-3 will start and pump the out put (VIOLET) to fourth container.3 will start and pump the output (VIOLET) to fourth container.

V. OUR MIXING SYSTEM PROJECT



PROGRAMEXECUTION

What is Ladder diagram: Ladder diagrams are specialized schematics commonly used to document industrial control logic systems. They are called “ladder” diagrams because they resemble a ladder, with two vertical rails (supply power) and as many “rungs” (horizontal lines) as there are control circuit store present.

The four components of ladder diagrams are:

- Power Supply (rails).
- Input Devices (components).
- Output Devices (components).
- Conductors (rungs).

VI. LADDER LOGIC

Ladder logic was originally a written method to document the design and construction of relay racks as used in manufacturing and process control. Each device in the relay rack would be represented by a symbol on the ladder diagram with connections between those devices shown. In addition, other items external to the relay rack such as pumps, heaters, and so forth would also be shown on the ladder diagram. Ladder logic has evolved into a programming language that represents a program by a graphical diagram based on the circuit diagrams of relay logic hardware. Ladder logic is used to develop software for programmable logic controllers (PLCs) used in industrial control applications. The name is based on the observation that programs in this language resemble ladders, with two vertical rails and a series of horizontal rungs between them.

ALGORITHM

Stages of Algorithm

STAGE-1 Switch On MCB

STAGE-2 Container-1 Pumpmotor-1 will start and pump the liquid third container with colour-1 upto 100ms.

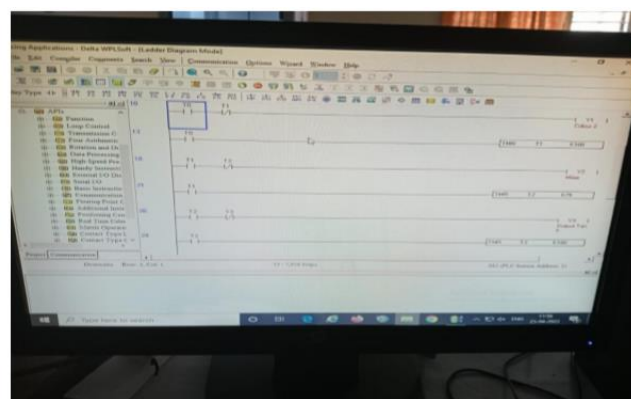
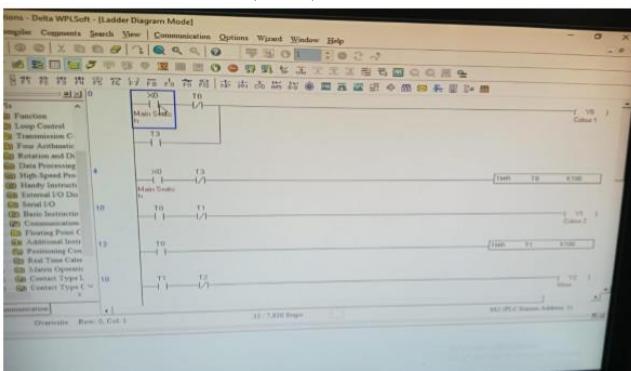
STAGE-3 Container-2 Pumpmotor-2 will start and pump the liquid to third container with colour-2 up to 100ms.

STAGE-4 Container-3 DC motor will turn on stirrer for mixing both colours upto 75ms.

STAGE-5 Container-3 pump motor-3 will start and pump the out putto fourth container upto 100ms.

STAGE-6 The same process will repeat again up tour requirement

LADDER DIAGRAM (LAD)



CONCLUSION

The project ‘Automatic mixing and filling bottle using PLC’ has been successfully designed and executed. This Project has proposed an application of automation illustrating PLC based fully automatic untouched liquid filling and mixing system. The system meets the demand of

high-speed production nosing the least mechanism requirements. The system has proved to work effectively avoiding un necessary spill or wastage of liquids. The system also provides high accuracy and precision in proportion of liquid filling and mixing. Although proposed system illustrates the mixing process of two liquids, any number of liquids may be mixed in varying proportions. It

REFERENCES

- [1] AZMANBIN ABDULRAHMAN, “LIQUID MIXTURE CONTROL SYSTEM USING PLC“ University Tun Hussein Onn Malaysia, May2011
- [2] S.T. Sanamdikar ‘ Color making and mixing process using PLC’ ,IJETTCS ,October2013.
- [3] Mallaradhy HM, KRPrakash "Automatic Liquid Filling To Bottles Of Different eight Using Microcontroller" ,IJMPE,July2013.
- [4] Bipin Mashilkar, Pallavi Khaire and Girish Dalvi “Automatic Bottle Filling System”,IEEE,October2015.
- [5] Prof. Swapnil R. Kurkute, Mr. Akshay S. Kulkarni, Mr. Mahesh V. Gare, Mr. Soham S. Mundada‘ Automatic Liquid Mixing and BottleFilling’,IJREEICE,January2016.
- [6] Shaukat N., “PLC Based Liquid Filling and Mixing System ,”IEEE Multi Topic Conference,2002.
- [7] SIEMENSAG. SIMATICS7-200 “Programmable ControllerManual” ,2004.
- [8] Dr.D.J.Jackson“ProgrammableLogicControllers”,2011.
- [9] K. Gregory, Mc. Millan, M. Douglas. Considine, Process/Industrial Instruments and Controls Handbook Fifth Edition, McGraw-Hill, 1999. 10-Hemant Ahuja, Arika shing, “Automatic Filling Management System for industries” IJETAE,February2014.
- [10] Dr.Vijay Kumar Khatri, Ahsan Javed Ghangro, Jetandar Kumar and Syed Jaad UI Haque. ,”Industrial Data Acquisition and Control System using two PLCs”IEEE,2009.
- [11] Johnson,C.D.,”ProcessControlInstrumentationTechnology”,PrenticeHall,2006.43
- [12] Anderson,J.C.,“Design a flexible industrial controls labmodule” ,32ndAnnualFrontiers in Education,Vol. 1, pp. 17 – 22, Nov 2002. 14- Yang, G., Rasis, Y.,“Teaching PLC in Automation–A Case Study” ,ASEE Annual Conference & Exposition, 2003..

DESIGNING AND MODELING OF GO-KART VEHICLE

Dr.D.Jagadish¹, Shaik Bajan², G.Daniel Raju³, P.Sudarsan Babu⁴

*Professor, Department of Mechanical Engineering, Narasaraopeta Engineering College, Guntur, A.P, India,
Assistant Professor, Department of Mechanical Engineering, Narasaraopeta Engineering College, Guntur, A.P, India,
Student, Department of Mechanical Engineering, Narasaraopeta Engineering College, Guntur, A.P, India*

Abstract - A Go-kart is a small four wheeled vehicle. Go-kart, by definition, has no suspension and no differential. They are usually raced on scaled down tracks, but are sometimes driven as entertainment or as a hobby by non-professionals. Carting is commonly perceived as the stepping stone to the higher and more expensive ranks of motor sports. Kart racing is generally accepted as the most economic form of motor sport available. The drafting and design work of a Go Kart vehicle is carried out as the theme of the project. The initial drawings are prepared and are converted into CAD models and are analysed for stresses and other results of modal analysis. After ensuring the modal analysis the fabrication work is carried out. The fabrication of chassis and other accessories were made

I. INTRODUCTION

Go-kart is a small racing car having a lightweight or skeleton body and powered by a two-stroke engine. Karts may seem like little cars, but there are some defining characteristics that separate them from ATVs or other tiny conveyances. Obviously, size is a big factor, but one major aspect of a kart is its complete lack of a traditional suspension; here the axle is firmly affixed to the frame, there is no differential (both rear tires turn at the same speed), and while things like camber and caster may be adjustable, there are no dampers or springs. Overall kart layout tends to feature a driver sitting beside a low-capacity engine (generally 125cc or less) that uses either chains or gears to drive the rear axle. Traditionally, a kart has a single brake disc on the rear and nothing on the front (though that's not always the case), and the brake pedal is situated to the left of the kart, with the throttle on the right, forcing the driver to either learn left-foot-braking or go hurtling off course. go kart should have a very snug, form-fitting seat and no belts of any kind, and while karts rarely have roll-cages or serious crash structures, that's beginning to change. But despite traditional safety features, karting is considered a very safe form of motorsport with injuries rare and generally non-life-threatening.

II. METHODOLOGY

The carbon content in the steel is very important to determine the hardness, strength, machining and weldability characteristics. Material selection for chassis plays a vital role in building up of entire vehicle in providing reliability, safety and endurance. The steel which has carbon increases the hardness of the material. Aluminium alloy is expensive than steel, in that case steel is the most preferable material for fabricating the chassis.



Fig Go -kart Vehicle

The system fabrication usually started by splitting the work in the areas shown as

1. DESIGN
2. TRANSMISSION
3. BRAKE
4. STEERING
5. ELECTRICALS
6. SAFETY AND ERGONOMICS

Ensuring each part designs are complete then the assembly is done to make a Go-Kart vehicle.

The initial drawings were made with conventional methods to frame the dimensions of the Go- Kart. Having the idea of the shapes of the components from the literature the basic drawings were prepared. Which is followed by drawing in CAD software to prepare for analysis before fabrication.

The chassis has been designed by taking factors like dimensional limits (width, height, length, and weight), operational restrictions, regulatory issues, contractual requirements, financial constraints and human ergonomics as a priority.

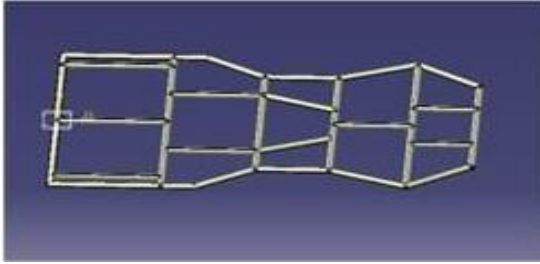


Fig Chassis

The design of chassis was done in Catia V5 software.
 Table 3.1 Chassis Dimensions

Overall length	73 ^{??}
Overall width	48 ^{??}
Overall weight	180 kg
Front track width	36 ^{??}
Rear track width	39 ^{??}
Wheel base	47 ^{??}
Ground clearance	3 ^{??}
Turning radius	2.70 m

III. MATERIAL AND METHODOLOGY

The carbon content in the steel is very important to determine the hardness, strength, machining and weldability characteristics. Material selection for chassis plays a vital role in building up of entire vehicle in providing reliability, safety and endurance. The steel which has carbon increases the hardness of the material. Aluminium alloy is expensive than steel, in that case steel is the most preferable material for fabricating the chassis.

MATERIAL USED AND ITS COMPOSITION

Strength and light weight are the basis of consideration for choosing the chassis material. AISI 4130 is the suitable material to be used for the Go- Kart chassis which is a medium carbon steel having high tensile strength, high machinability and offers good balance of toughness and ductility.

Iron, (Fe)	97.03 – 98.22
Chromium, (Cr)	0.80 – 1.10
Manganese, (Mn)	0.40-0.60
Carbon, (C)	0.280-0.330
Silicon, (Si)	0.15-0.30
Molybdenum, (Mo)	0.15-0.25
Phosphorous, (P)	0.035

DIFFERENT VIEWS OF FULLY DEVELOPED VEHICLE CAD MODEL

Using CATIA the 3D modeling software the images are designed for Go-Kart which are shown below.

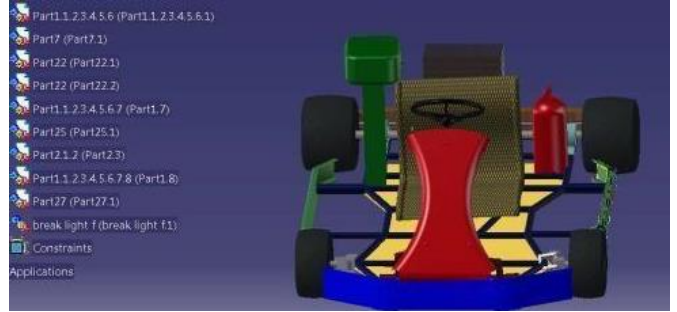


Fig .Front view



Fig Right side view

BRAKE SYSTEM

A brake is a mechanical device which inhibits motion. Its opposite component is a clutch. Brake pedal slows a car to a stop. When you depress your brake pedal, your car transmits the force from your foot to its brakes through a fluid. Since the actual brakes require a much greater force than you could apply with your leg, your car must also multiply the force of your foot. Most brakes commonly use friction between two surfaces pressed together to convert the kinetic energy of the moving object into heat, though other methods of energy conversion may be employed. For example, regenerative braking converts much of the energy to electrical energy, which may be stored for later use. Other methods convert kinetic energy into potential energy in such stored forms as pressurized air or pressurized oil. Eddy current brakes use magnetic fields to convert kinetic energy into electric current in the brake disc, fin, or rail, which is converted into heat. Still other braking methods even transform kinetic energy into different forms, for example by transferring the energy to a rotating flywheel.

IV. SPECIFICATIONS OF GO KART FOR BRAKING

- Mass of the vehicle = 180kg TMC
- Piston diameter = 12.7mm
- Calliper piston diameter = 25.4mm
- Coefficient of friction between tires and road= 0.6

CALCULATIONS:

Let the force on pedal by the driver is 22kg. let the pedal ratio be x: 1

Force applied on the TMC is $F_{mc} = 22 * 9.81 * x = 215.82 * x$ N

Pressure on the brake fluid due to compression of TMC is $P = F_{mc}/A_{mc}$
 $P = 215.82 \text{ N} \times (\pi 4) d^2 = 215.82 \text{ N} \times (\pi 4) (0.0127)^2$

$P_{mc} = 1704739.336 \text{ N/m}^2$

From the evaporator the only condition which produced a steady decrease in temperature throughout the entire duration of the experiments was $t = 110^\circ\text{C}$

STEERING SYSTEM

Function of Steering System

With the help of the steering system, the driver can control the vehicle however

The steering provides stability to the vehicle on the road.

It minimizes tire wear and tear.

It prevents road shocks from reaching to the driver.

The steering provides self-rightening effect after taking a turn.

CALCULATIONS OF STEERING

The experiments whose results are present in process will be recorded in the experimental table. Were such the extended periods of time because their objective is to determine the reference values for the generator temperature which was capable of causing the refrigerator to cooling efficiently.

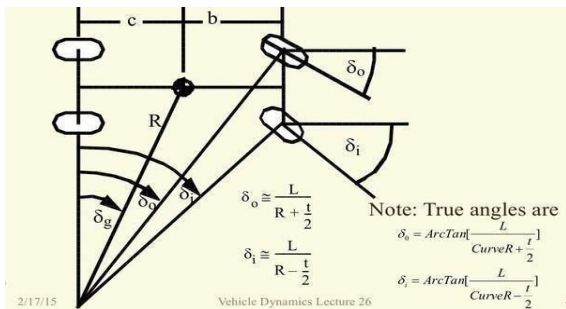


Fig Vehicle dynamic

Inner turning radius

$\tan B = l/(R+d/2)$ $\tan B = 0.34527$ $B = 19.0446^\circ$

Actual turning radius = $d/2 + l \cos(B) = 2.78 \text{ mts}$.

Ackermann = $\tan^{-1}(l / (\tan B - d)) = 25.1453^\circ$

Percentage = $(A/\text{Ackermann}) \times 100 = 80\%$

Wheel base	1.193
	8 Mts
Track width	0.990
	6 Mts
Steering ratio	1:1
Tie rod length	10.4318 Mts
Caster angle	12°
Camber angle	0°
King pin inclination	7°

SAFETY AND ECONOMICS SAFETY EQUIPMENT

Go-karting is a great way to introduce the world of racing to any child. The sport gives them the feel, on a smaller scale, of what drivers experience in real-time in sports like NASCAR and other racing events.

However, like with any sport, there are inherent risks involved, which means youths who are racing should be wearing and using go-kart safety equipment and be compliment by go-kart safety standards.

CONCLUSION

The go-kart dimensions were figured and made drawings. The go-kart was modeled in CAD software. The CAD model of analyzed using Ansys software for determination of deflections and stresses to find out the correct dimensions and material properties. The material suggested was used to make the go-kart model and made trail runs. The braking and steering systems were analyzed in coordination with vehicles norm books.

FUTURE SCOPE

In the present work the go-kart dimensions were obtained and the study was focused on braking and engine system. The total suspension and traction work to fit for competition can be studied as future course of work.

REFERENCES

- [1] Lal K, Design, analysis and fabrication of go-kart, International journal of scientific and engineering research, 2016.
- [2] Pattanshett SV, Design and analysis of GO-KART chassis, International journal of Mechanical and Industrial Technology, 50-164, 2016.
- [3] Chow H Y, Go-Kart's design and construction based on theoretical and experimental findings, University of Malaysia, 2016.
- [4] Michell S, Rajagopal K, MURTY V S S, Harikrishna V, Design of a go kart vehicle, International journal of science, engineering and technology research 2017.
- [5] Hajare K, Shet Y, Khot A, Design and Analysis of a Go-Kart Chassis, International Journal of engineering technology, management and applied science.
- [6] Khan A S, Danish K, Kathola K, Bhonde, G Ghevande, Harshil M, Review on design and analysis of structure of go-kart vehicle, International journal of research in advent technology, Special Issue National Conference 2017, April 9th 2017.
- [7] Nath A, Vikram J C, Nongrum L, Marboh P, Design and fabrication of a Go Kart, International journal of innovative research in science, Engineering and technology, 2015.
- [8] Kelkar K, Gawai S, Suryawanshi T, Ubaid S, Kharat R, Static Analysis of Go-Kart chassis, International journal of research in advent technology, Special Issue National Conference 2017, April 9th 2017.

Experimental observation of Mechanical and microstructure properties of Corn /Coconut Hybrid composites with Alkali Treatment

Ch. Lakshmikanth¹, K. Venkatarao², A. Venkata Jayasri³, S. Nagakumar⁴

^{1,2,4} Prasad V. Potluri Siddhartha Institute of Technology, Kanuru, Vijayawada, Andhra Pradesh.

³ Andhra University, Visakhapatnam, Andhra Pradesh, India

Abstract

This present task focuses on how the mechanical properties and the thermal properties of the regular fiber-built-up composite. For the study, the test samples are made utilizing the different weight rates of the corn and the coconut fiber as support and polyester sap as framework utilizing the hand layup method. The composite which is made of corn and coconut fiber is furthermore blending in with the sap, to hold the example, an impetus to expand the pace of response, and gas pedal to fix the fluid condition of composite material into a strong state. In the project, we involved the Coconut Fiber and the corn fiber as the Reinforcing Fibres. The Tensile Test, Impact Test, and Thermal tests are performed on the specimens. All the test is performed on the samples both treated and untreated by utilizing the heap dislodging diagrams, the properties are been examined. Subsequent to playing out all the Tensile, Impact, and Thermal tests ways of behaving of the composites are examined and the results are finished up by utilizing the charts delivered.

Introduction:

In this paper, the effects of the different parts of the corn stalk, i.e., the stem, ear, husk, cob, and leaf, on the manufacture of corn fiber plastic composites (CFPC) were evaluated. Besides, the mechanical properties of the CFPC were affected by the composition in terms of the cellulose, hemicellulose and lignin fractions, which were also explored herein [1]. This paper deals with corn fiber polypropylene (PP) composites that were fabricated and tested for their mechanical properties. The effect of matrix modification on mechanical properties is investigated. Maleic anhydride grafted polypropylene (MAPP) is added to the matrix and the mechanical properties of MAPP corn fiber composites were found to increase considerably compared with those of PP composites. Experiments were conducted using Taguchi L_{12} orthogonal array considering the two design parameters viz. weight fraction of the fiber and treatment [2]. Corn starch-based composite films were prepared through the solution casting technique using fructose as a plasticizer and different loadings of cornstalk as filler. The physical, thermal, morphological, structural, and mechanical characteristics of the produced bio composite film were investigated [3]. In this work, we developed a novel core-shell nanocomposite from carboxymethylated corn fiber gum (CMCFG) and high nutritious pea protein (PP) for curcumin (Cur) delivery. In the preparation, PP-Cur complexes (PP-Cur) were formed at pH 7.0 and then coated by CMCFG via hydrophobic interactions to form PP-Cur-CMCFG complexes. Our results provide support for the use of plant-derived delivery systems as a strategy for the delivery of chemically unstable hydrophobic Cur [4]. In this work, corn fiber was subjected to alkali and sizing treatments. The treated corn fibers were

used to prepare corn fiber reinforced polylactide (CF/PLA) composites through mechanical mixing and injection molding. Fiber surface, tensile fracture surface, mechanical properties and thermo-mechanical behaviour of various CF/PLA composites were characterized [5]. In this work, we report a novel strategy for improving the interfacial nature in corn fiber/polylactide (CRF/PLA) composites by directly applying a sizing containing silica nanoparticles on the surface of CRFs. This results in enhanced mechanical properties of the CRF/PLA composites. These improvements can be mainly attributed to the presence of silica nanoparticles on CRF-PLA interfaces, which act to resist the crack propagation [6]. In this study, variable amounts of CF and PVA were processed in the presence of both dry and liquid plasticizers, glycerol and pentaerythritol. Corn starch was introduced in the formulation to reduce the cost and to further increase the composition of natural components in the composites [7]. Starch acetate–corn fiber foams were prepared by extrusion. Corn starch was acetylated (DS 2) to introduce thermoplastic properties. Corn stalks were treated with sodium hydroxide to remove the lignin and to obtain purified cellulose fibers. Starch acetate was blended with treated fiber at concentrations of 0, 2, 6, 10, and 14% (w/w) and extruded in a corotating twin-screw extruder with 12 to 18% w/w ethanol content and 5% talc as a nucleating agent [8]. In this work consider the corn fiber with polypropylene resin. The corn fiber is cheaply available in our country, the natural fiber not use in directly adding of polymer resin to improve the strength of the fiber. This present work focused on to prepare corn fiber with polypropylene resin and analysis of the mechanical properties of the fiber efficiently [9]. Bio composites were prepared with corn straw slugging (CSS) and high-density polyethylene (HDPE) at four loading levels (10, 20, 30, and 40 wt %) by extrusion method. CSS/HDPE composites were tested by tension, oxygen index meter, differential scanning calorimetry, X-ray diffraction, and the scanning electron microscopy. The electron microscopy showed that CSS was dispersed uniformly in the HDPE matrix and scanning strong interfacial interaction was achieved, which had an important influence on the tensile strength of the composites [10]. They are planned to produce the test specimens according Taguchi's L_9 orthogonal array concept. The results indicated that the developed models are suitable for prediction of mechanical properties of green coconut fiber reinforced HDPE composite [11]. The study demonstrates that composites with lignin as a compatibilizer possess higher flexural properties as compared to the control composites. The results also show that tensile properties do not improve as lignin is incorporated. Scanning electron

micro copy results (SEM) display some proof of an enhanced compatibility at the interfacial region [12]. In this paper, the mechanical properties and dynamic characteristics of a proposed combined polymer composite which consist of a polyester matrix and coconut fibers are determined. The influence of fibers volume fraction (%) is also evaluated and composites with volumetric amounts of coconut fiber up to 15% are fabricated. In this work, the tensile test was carried out to determine the strength of material, while modal testing was used to obtain the dynamic characteristics of the composite material. Results were found that the strength of the composites tends to decrease with the amount of fiber, which indicates ineffective stress transfer between the fiber and matrix [13]. Composite reinforcement with natural fibers has recently gained attention due to low cost and easy availability. This chapter discusses the use of coir fiber in composites and the current status of research [14]. This work describes the surface treatment of coconut fiber and its application in composite materials for reinforcement of polypropylene. Before testing coconut fiber in composite materials, its susceptibility to chemical treatment was characterized by exposure to the following: (1) hot water; (2) aqueous NaOH 2% (w/v); and (3) a sequence of chemical treatments in hot water, extra 20% (v/v), acetone/water 1:1 (v/v), and aqueous NaOH 10% (w/v). The efficiency of each treatment was evaluated by Fourier transform infrared spectrometry analysis, indicating a reduction in the C=O peak. Besides that, the scanning electron microscope revealed that treatment changed the morphology of the fibers [15].

2. Materials and methods:

The specimens are made according to the weight percentages of Corn fiber and Coconut fiber in Different weight concentrations should be taken to proceed for the examination. Both treated and untreated specimens are made according to weight concentrations of powder and the fiber. We have taken the six different types of specimens with different weight concentrations. The 6 different specimens are shown in the table 1.

Table.1 Composite specimen Preparation weight Percentages:

Tensile Test specimens	Weight percentages of specimens
S1	1 gm corn fiber and 1 gm of coconut fiber (Untreated)
S2	1 gm corn fiber and 1 gm of coconut fiber (Treated)
S3	0.75 gm corn fiber and 0.75 gm of coconut fiber (Untreated)
S4	0.75 gm corn fiber and 0.75 gm of coconut fiber (Treated)
S5	0.25 gm corn fiber and 0.25 gm of coconut fiber (Untreated)
S6	0.25 gm corn fiber and 0.25 gm of coconut fiber (Treated)
S7	Specimen made only with Resin

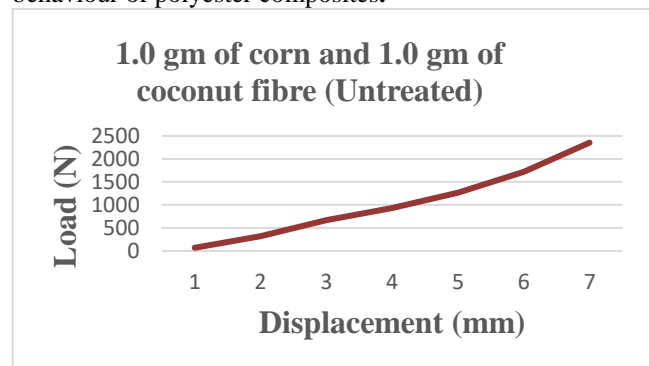
The tensile experiments are performed on universal testing machine with transfer speed of 2 mm/min and the impact study was conducted Izod impact testing machine.



Fig.1 (a) Corn Fiber, (b) Coconut Fiber, (c) Mould preparation, (d) Specimen for Thermal Conductivity Test, (e) Specimen for Impact test (f) Specimen for Tensile test

Results and discussions:

The chemical treatment effect on composites specimens shows an important role in because tensile behaviour of polyester composites and it was gradually increased with increase with reinforcement phase. The higher tensile load bearing capacity was recorded for S4 specimen of excellent bonding strength and combination of corn fiber and coconut fiber. In maximum cases the specimen shows high level strength after chemical treatment because of surface roughness of fiber enhances the superior bonding strength, and it is observed from scanning electronic micrographs. The composite samples exhibited lower-level displacement irrespective of load and chemical treatment. The diminished tensile strength and bearing capacity are noted in the S7 sample. The figures show the load versus displacement curves for a better understanding of the mechanical behaviour of polyester composites.



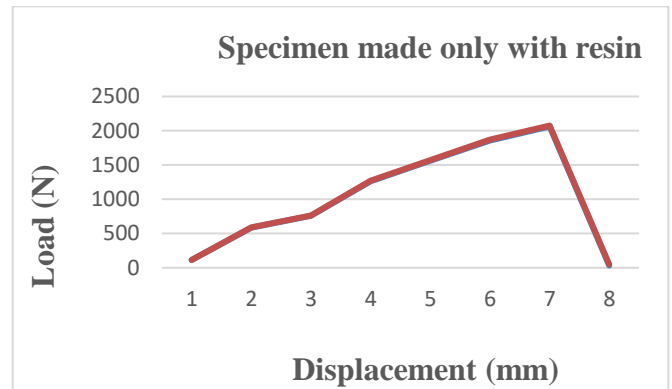
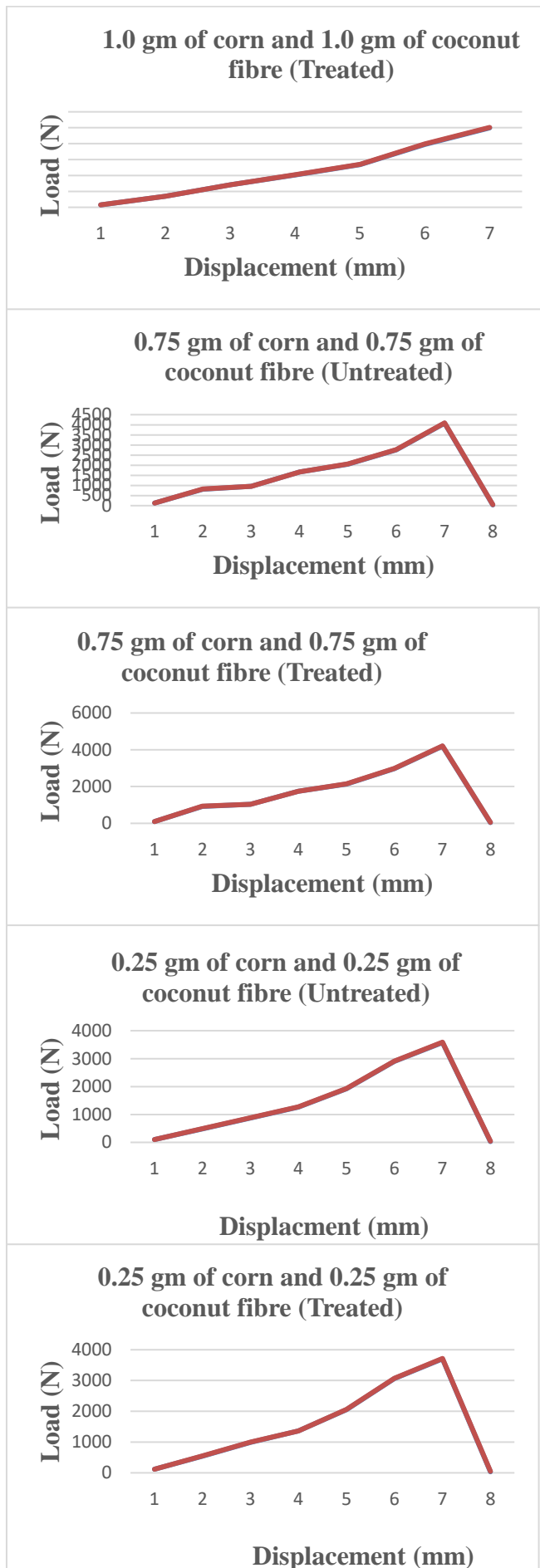


Fig.3 Tensile Behaviour of Composite Specimens

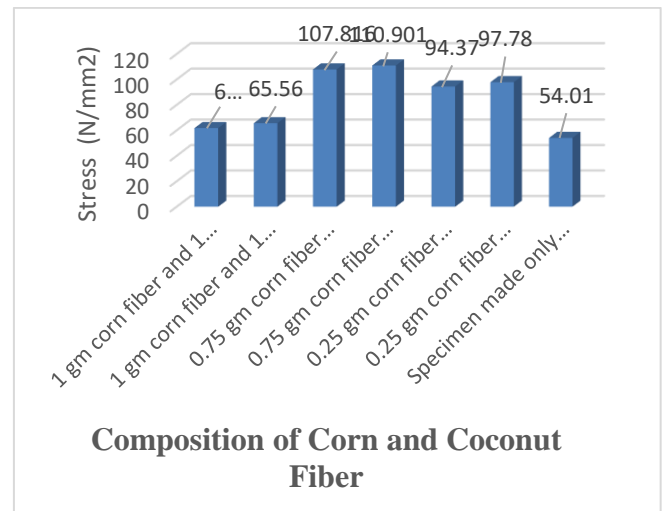


Fig.4 Tensile Behaviour of Composite Specimens

Figure 5 Shows the charpy test specimens were made according to the dimensions of ASTM D 256-M in which the dimension is 60 x 12.5 x 10 mm. One of the main reasons of concern for composites generally is the low values of impact energy. They show relatively low values of impact energy compared to metals.

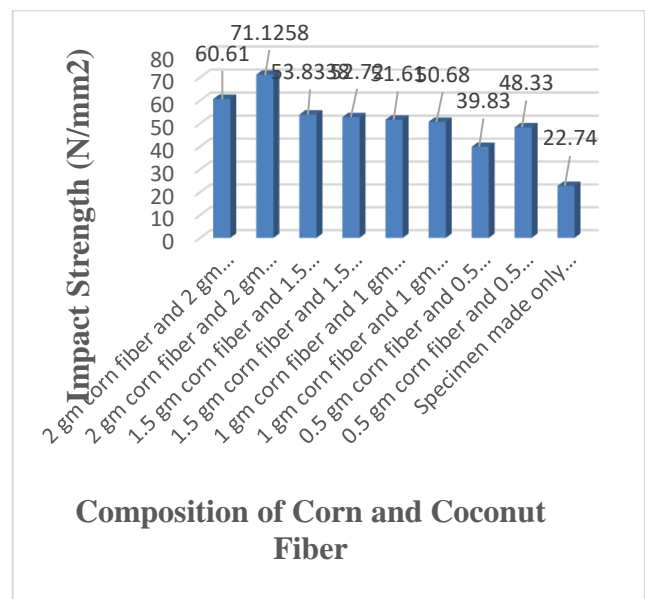


Fig.5. Impact strength of specimens

The ways to increase the impact energy of the composites are being made the major area of research. Figure shows the impact energy variation for fiber reinforced composites. The tests showed that the composites made with 9 sample fiber resin weight percentage were not very good with the impact stress as it showed very low values from the tests performed. Figure 6 shows the Thermal Conductivity of polyester composites. Thermal conductivity refers to the amount/speed of heat transmitted through a material. Heat transfer occurs at a higher rate across materials of high thermal conductivity than those of low thermal conductivity.

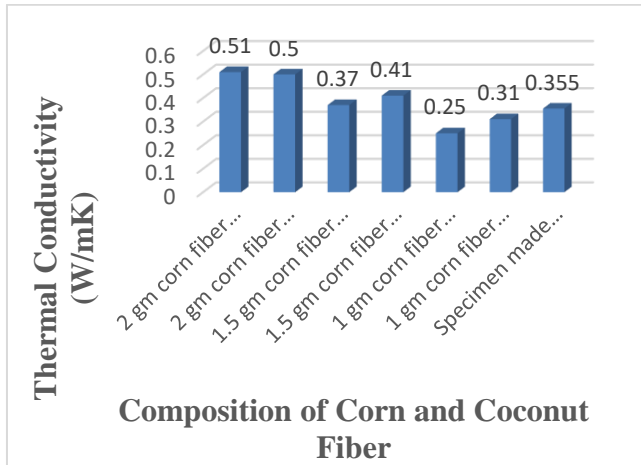


Fig.6. Thermal Conductivity of Composite Specimens

Fracture analysis of Corn – Coconut Fiber reinforced composites:

The fracture surface was examined through the scanning electron microscope micrographs of T1, T6 under tensile loading condition, this micrograph discloses the nature of the failure of the composite specimen. Fig 5a discloses the uniform corn and coconut fiber distribution in the polyester matrix. The internal cracks were noticed from figure 5b due to tensile load and exhibit the brittle failure of the specimen. The fiber pulls out and de-bonding is observed from the figure 5d for tensile specimen T6 under tensile load. The fiber distribution is captured in figure 5c.

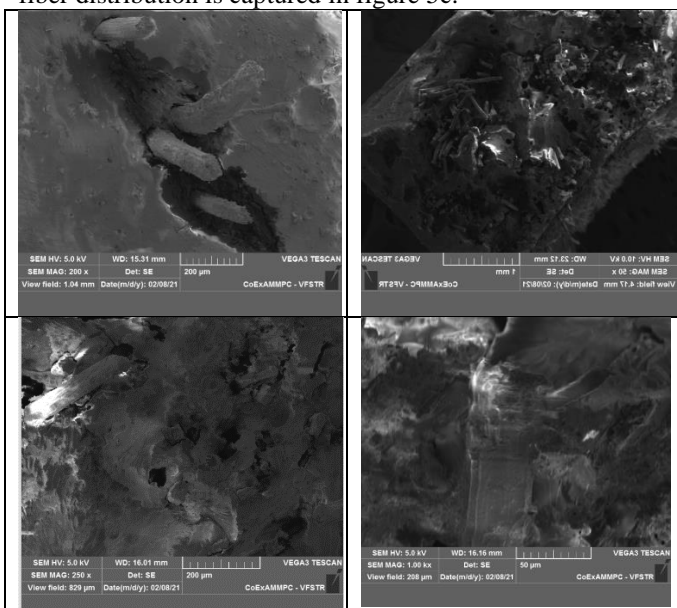


Fig.5. Sem Images of impact and Tensile samples

Conclusion:

By the analysis, the following conclusions were stated:

In this work the fiber-reinforced polyester hybrid composites were prepared as per ASTM standards. The corn fiber and coconut fiber is available abundantly in nature and offer low material density. The Impact strength, Tensile strength of the investigated material composite with the corn and coconut were found to be comparatively higher than novel composite material. The density of the composite decreased with increasing fiber content. Thus, the hybrid composites were found to be light in weight and proposed better mechanical properties and insulating properties. The fracture surface was studied through the SEM images. This work shows corn fiber, coconut fiber, and polymer composites with different fiber weight fractions fabricated by hand lay-up technique. The maximum Tensile strength and Impact strength for the combination of corn and coconut fiber composite are 110.901N/mm² and 71.1258 J/cm² respectively. The thermal conductivity of the composite is 0.25 W/m. K.

References:

- [1] Zhangfeng Luo, PingLi, DiCai, QiuchiChen, PeiyongQin, Tianwei Tan and Hui Cao.(2017), Industrial crops and products 2017 vol.95 pp.52-527
- [2] N.RaviKumar, CH.RangaRao, P.Srikant and B.Raghava Rao,(2015),Mechanical properties of corn fiber reinforced polypropylene composites using taguchi method , doi:10.1016/j.matpr.2015.07.251
- [3] M.I.J.Ibrahim, S.M.Sapuan, E.S.Zainudin, M.Y.M. Zuhri, A.Edhirej, and R.A.Ilyas, (2020), Determination of the tensile properties and biodegradability of cornstarch-based biopolymers plasticized with sorbitol and glycerol , Doi:10.3390/polym13212709
- [4] YueWei, ZhixiangCai, MinWu, YalongGuo, Pengguang Wang, RuiqiLi, AiqinMa and HongbinZhang, (2020), Core-shell pea protein-carboxymethylatecornfiber gum composite nanoparticles as delivery vehicles curcumin. Doi: 10.1016/j.carbpol.2020.116723
- [5] HonglinLuo, GuangyaoXiong, ChunyingMa, Peng Chang, FanglianYao, YongZhu, ChuanyinZhangand YizaoWan, Mechanical and thermo-mechanical behaviors of sizing-treated corn fiber/polylactide composites,Doi: 10.1016/j.polymerfesting.2014.07.014
- [6] Honglin Luo, Zhiwei Yang, Fanglian Yao, Wei Li and YizaoWan, Deenadayalan , Improved properties of corn fiber-reinforced polylactide composites by incorporating silica nanoparticles at interfaces, published august 12, 2019.
- [7] P. Cinelli, E. Chiellini, J. W. Lawton and S. H. Imam, Properties of injection molded composites containing corn fiber and poly (vinyl alcohol) april,2006.
- [8] G.M.Ganjyal,N.Reddy, Y.Q.Yang, M.A.Hanna, Bio degradable packaging foams of starch acetate blended with corn stalk fibers ,published :07 jully 2004 , <https://doi.org/10.1002/app.20843> .
- [9] Sameer A.Agrawal, Ashish M.Umbarkar, Nitin P.Sherie, Ashish M.Dharme and Dharmesh Dhabliya, Statistical study of mechanical properties for corn fiber with reinforced of polypropylene fiber matrix composite , Published:feb,2021, Doi:10.1016/j.matpr.2020.12.1072 .

- [10] Qingfa Zhang, Wenyu Lu, Liang Zhou, Donghong Zhang, Hongzhen Cai, Xiaona Lin, Tensile and flammability characterization of corn straw slagging/high-density polyethylene composites, published april8, 2019.
- [11] Syed Altaf Hussain, Dr.V.Pandurangadu and Dr.K. Palanikuamr, Mechanical properties of green coconut fiber reinforced HDPE polymer composite , Published : nov,2011
- [12] H.D.Rozman, K.W.Tan, R.N.Kumar, A.Abubakar, Z.A. Mohd. and Ishak, H.Ismail, Effect of lignin as a compatibilizer on the physical properties of coconut fiber-polypropylene composites, Published: july, 2000. Doi: 10.1016/S0014-3057(99)00200-1.
- [13] Izzuddin Zaman, Al Emran Ismail and Muhamad Khairudin Awang, In this paper, Influnce of fiber volume fraction on the tensile properties and dynamic characteristics of coconut fiber reinforced composite , Published : jan,2010
- [14] D.Verma and P.C.Gope , Corn fiber reinforcement and application in polymer composite , Published : oct,2012
- [15] R.M.Leao, S.M.Luz, J.A.Araujo and K.Novack , Surface treatment of coconut fiber and its application in composite materials for reinforcement of polypropylene , <https://doi.org/10.1080/15440478.2014.984048> .

Fabrication and analysis of Heliotropic Smart Flower Solar Collector

I Sri Phani Sushma¹, B Bhavana², V Rakesh Ranjan³, S V Pavan Kumar⁴

^{1,2,3,4} Department of Mechanical Engineering, University College of Engineering Narasaraopet JNTUK, Narasaraopet Guntur

ABSTRACT

In the present scenario, everything functions as a result of energy input, and the world depends on some form of energy to operate. Solar energy is undoubtedly one of the most important ways to reduce pollution and save energy, as energy is a current theme that calls for reducing pollution and saving energy. Furthermore, there are concerns regarding insufficient energy production, as well as high energy consumption from stationary solar panels. To prevail over this “Sunflower” based solar panel is instigated to bring out the escalation in efficiency by perpendicular proportionality of the solar panel with the sun rays. In our system we use an Arduino microcontroller, Solar panel, LDR sensor, 10k resistors, servo motor, LI-ION Battery, jumper wires. The project is based on LDR sensing, the solar system automatically waking up through sensing and the Arduino processes the data then rotates the servo motors according to the sun rotation. The project utilizes solar power to its full potential by adjusting the tilt angle of the panels to follow the sun and maximize the absorption. This solar tracking system is a Mechatronics system that integrates electrical and mechanical systems along with computer hardware and software.

Keywords: Photovoltaic (PV), Tracking, Residences, Solar tracking.

1. INTRODUCTION

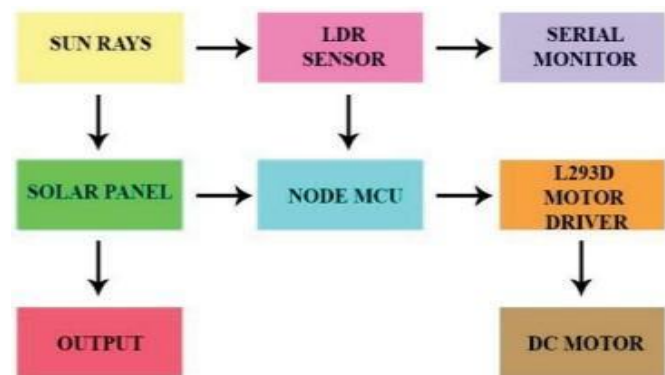
The age of fossil fuels is coming to an end. Alternatives to fossil fuels are being sought to replace them with renewable sources of energy. In the present day, the world has few renewable energy sources and cannot find one that is as efficient as fossil fuel energy. Due to the fact that the working machines are designed to work on the principle of using fossil fuel energy, the world is not able to find the most efficient source of energy to replace it. As a result, the world is not able to transition to renewable energy sources as the systems are adapted to work with fossil fuels. To replace fossil fuels, the entire system should be replaced since the system is designed to produce the desired output via fossil fuels. Instead of looking for renewable energy sources that can replace fossil fuels, we should devise a system that can generate the maximum efficiency out of existing renewable resources, and adapt our machines to work with them. Solar energy is considered to be one of the most abundant and reliable forms of energy. It is superior to all other renewable energy resources on Earth. Because it has universal existence and an indestructible source of energy. This light energy is converted to electrical energy using the photovoltaic effect. Based on this principle, solar cells are designed to convert light into electricity. In order to capture a huge amount of photons with solar cells, we would like to introduce a new system called heliotrope solar collecting system. Solar tracking is implemented with a single axis solar tracking system using Node MCU. Tracking systems for single axis are further classified based on the axes of tracking - Incline

shaft installation, South-North axis, horizontal installation and East-West axis horizontal installation. Its capability to sustain peak voltage over a longer period of time can ensure increased output. By tilting the solar tracker to [2] maximum power can be obtained. This optimum position is known as maximum power point tracking (MPPT) [1]. Solar trackers and their cost effectiveness have been explored in this study, which reviews various types of tracking mechanisms, such as a single-axis tracker and a dual-axis tracker. There are often no noticeable differences in

The position of the sun around the equator for a single axis tracker. Dual axis trackers are necessary for tracking the sun all the day long from east to west and also from east to north and south during the seasons. Shows the advancement in the world regarding the work of solar tracking and highlights the dual axis solar tracking system [2]. Detailed planning and engineering methods for designing a solar tracking system with a fixed dimension of flexibility are presented in this study. A logical and precise approach, similar to incremental refinement in modular programming, was chosen as it ensures a logical and precise approach that is easy to comprehend. Often, this will ensure that any defects are thoroughly investigated and corrected independently. Increasing the illumination level of the photovoltaic system will result in more electricity. It thus paves the way for reducing pollution in the storage of energy harvested from the Sun, and speeds up progress [3].

PROBLEM DESCRIPTION:

Fig 1: Block diagram of Single axis solar tracking system



At present, we use solar panels that are permanently installed in a place where there is no movement and sunrays falling on them are of different intensities and angles. As a result, the output fluctuates and a constant value cannot be achieved. Solar panels are used to utilize solar power in electrical means. They are aligned different arenas to collect maximum solar power.

Though, solar panels can be used to absorb or collect solar power, there work is bounded to certain hours of the day and the sunlight pouring directly on them, i.e. the angle between the sunrays and the panel is orthogonal. While at other hours of the day, the angle of the sunrays is different, hence the amount of the solar power captured is very less. To overcome such pitfalls, and encapsulate the maximum available solar energy the solar tracking systems were introduced. A solar tracking system is designed with the intention of keeping the angle between the sunrays and the solar array 90°. The solar tracking system have three different modules- The mechanism, Driving motors, The tracking controller. The mechanism is accountable to furnish with accurate movements, in the sake of following the footsteps of the sun throughout the day. The prototype of the device is made durable enough to withstand unfavorable weather condition. This mechanism of the solar tracking systems assifies themselves into two segments single axis tracker, dual axis tracker. Single axis tracking can be considered as one of the handy systems or prime solution in terms of small-scale photovoltaic power plants. Single axis tracking can be done using three different arrangements, which are based on the different axes of tracking-Inclined shaft installation, South-North axis horizontal installation, East-West axis horizontal installation. Single axis tracker tracks in a single cardinal direction. The tracker has a single row tracking configuration. The above maintained methods are the different arrangements in which single axis tracker can be implemented. The working mechanism of all the maintained methods is at par with each other. The angle of the sun with the surface of the collector is computed and examined, the collectors are thus charged to track down the movement of the sun to meet the expectations of captivating a greater percentage of solar radiance. In order to overcome this problem, single axis and double axis solar tracking systems have been introduced to increase efficiency. In this article we are proposing a new design of solar panels which are aligned like a sunflower and followed by dual axis solar tracking system Due to the equal distribution of weight, the sunflower petal alignment allows the dual axis solar tracking system to move freely, and the design has a greater exposure to sunlight than the standard one. The opening closing mechanism increases the life span of solar.

3. METHODOLOGY

3.1 Hardware Prototype

Solar panels are arranged to look like sunflower petals for the prototype's hardware design. The cutting of a solar panel is difficult, in this current prototype, we use three- dimensional parts to arrange them in a sun flower petals pattern. A servo motor is installed in the vertical and horizontal positions to drive the entire smart flower in dual axis motion. The servo motors are powered by Arduino Uno boards with ATmega328p microcontrollers. The dual axis solar tracking is achieved by sensing the light by using a set of LDR sensors arranged in a particular pattern. These signals are then used to calculate the angle of the sun at a given moment and the whole system is driven to that angle by the microcontroller System Description

3.1 Software Design

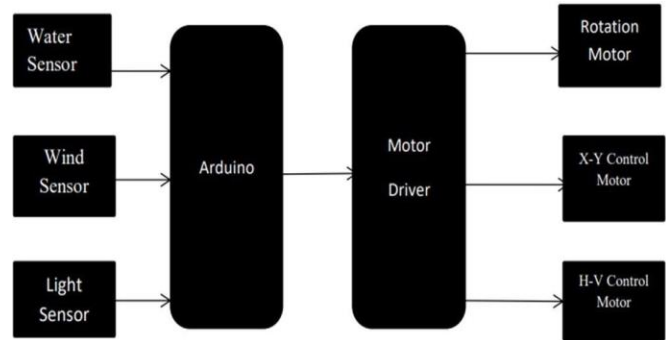


Fig 2: Block Diagram of System

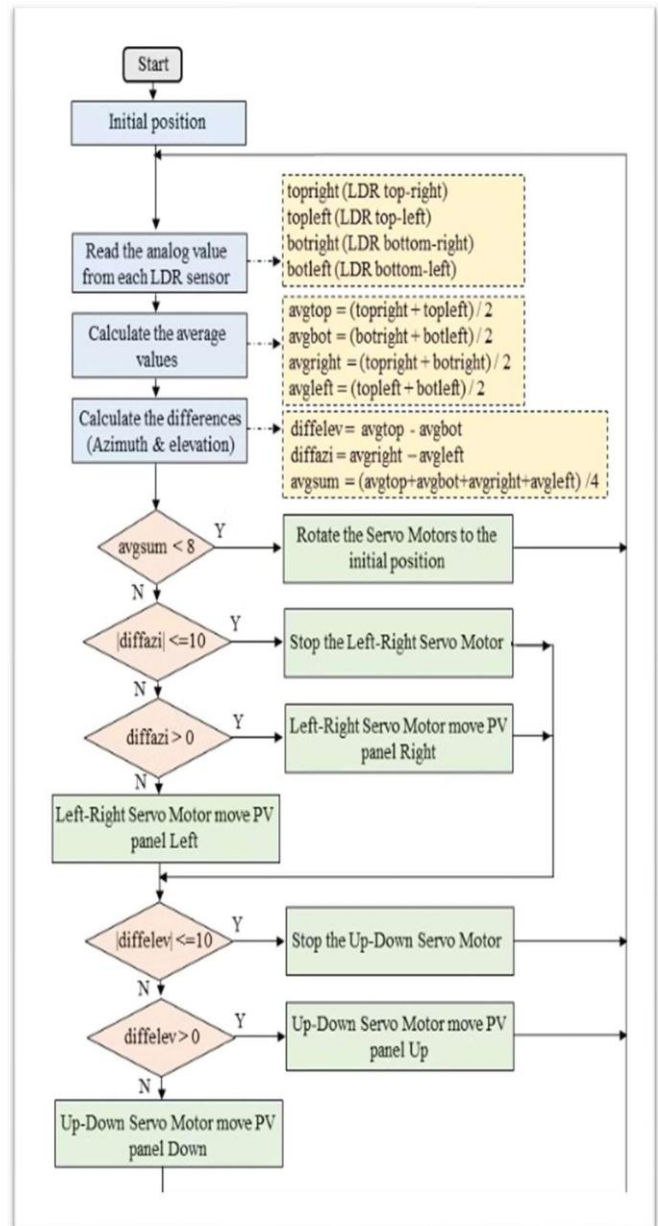


Fig 3: Algorithm

Table 1: Solar panel without tracking:

Time (Hrs)	Voltage (V)	Current(A)	Power (W)
9am	11.6	0.0733	0.8503
10am	11.9	0.128	1.5232
11am	11.8	0.106	1.2508
12 pm	12	0.180	2.16
1 pm	12	0.170	2.04
2 pm	12	0.173	2.076
3 pm	11.9	0.165	1.9635
4 pm	11.6	0.120	1.392
5 pm	10.1	0.070	0.707

4. RESULT AND DISCUSSIONS

4.1 Experiment Results:

The solar tracking system mainly works based on LDR and servo motors. The whole working starts with the intensity of light on the LDR's and there are 4 LDR's connected in the circuit. The LDR's works according to the light, when the light increases the conductance also increases and conductance falls with fall of light. The resistors are connected in the circuit. The LDR resistance drops with light, which causes the current in both resistors to increase, and therefore the voltage across the other increases. So, by this we can estimate that the LDR resistance varies with light. The servo motor contains 3 pins: signal, power, and ground. The power pin is used to supply power to the servo motor. The signal pin is used to receive signal and moves the servo motor accordingly. The analog pins receive voltage from the different LDR's and accordingly the difference from the LDR's signal, the output is given to the digital pin of Arduino board of the circuit. The results for the project were acquired from LDRs for the solar tracking system and the panel that has a fixed position. The results were recorded for four days, recorded and tabulated. The outputs of the LDRs were dependent on the light intensity falling on their surfaces. Arduino has a serial that communicates on digital pins 0 and 1 as well as with the computer through a USB. The LDRs measure the intensity of light and therefore they are a valid indication of the power that gets to the surface of the solar panel. There are two servo motors used in the circuit. One is used to move the solar panels vertically and the other servo motor is used to move the solar panel horizontally. So according to the signals received from the digital pins these servo motors move horizontally and vertically. If the sun position changes the light intensity on the LDR changes and according to the intensity of light the position of the solar panel changes. Thus, the voltage is taken with respect to the time and sun position. Estimation of efficiency is done by the graphical representation of Stationary and Heliotropic solar collector. From the tables and graphs, it can be seen that the maximum sunlight occurs at around mid-day, with maximum values obtained between 12:00 hours and 14:00 hours. In the morning and late evening, intensity of sunlight diminishes and the values obtained are less that those obtained during the day. After sunset, the tracking system is switched off to save energy. It is

switched back on in the morning. 0.36 Watts is the average power obtained from solar panel without tracking and 1.56 Watts power is obtained from solar panel with tracking. 21.64% is the improved efficiency neglecting the power consumption of motor. So, the proposed tracking system presents efficient system to connect solar energy which ensures that consumption of energy is more than the fixed solar panel. In our project the hardware of solar tracking solar panel design and the implementation of the design has been proposed. Our result shows that the solar tracking system increases the efficiency of the solar panel. Solar tracking solar panel is completely automatic and it ensures the minimum low cost. So, it is a dual axis system which maximizes the efficiency and can be obtained over a period of time. Normally a solar panel converts only 30 to 40 percent of the incident solar radiation in to electrical energy. An automated system is required to get a constant output, which should be capable to constantly rotate the solar panel. The sun tracking system was made as a prototype to solve the problem. It will be automatic and keeps the panel in forward- facing of sun until that is visible.

Performance of Solar Panel without Tracking: The below table shows the performance of the solar panel without tracker.

Table 2: Solar panel with tracking:

	Voltage (V)	Current(A)	Power (W)
9am	10.7	0.0194	0.2076
10am	11.3	0.0398	0.4498
11am	11.6	0.0733	0.8529
12 pm	12.0	0.180	2.16
1 pm	11.9	0.128	1.5232
2 pm	11.8	0.106	1.2508
3 pm	11.3	0.038	0.4294
4 pm	11.1	0.0267	0.2964
5 pm	10.7	0.0133	0.1424

Performance of Solar Panel with Tracking: The below table shows the performance of the solar panel with tracking.

4.2 Graphical Representation:

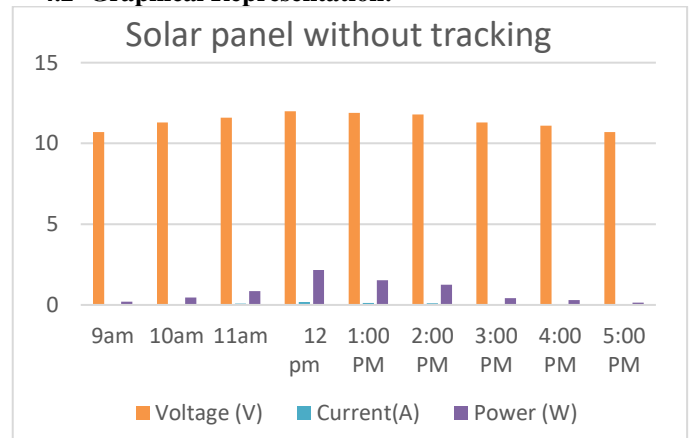


Fig 4: Solar panel without tracking result

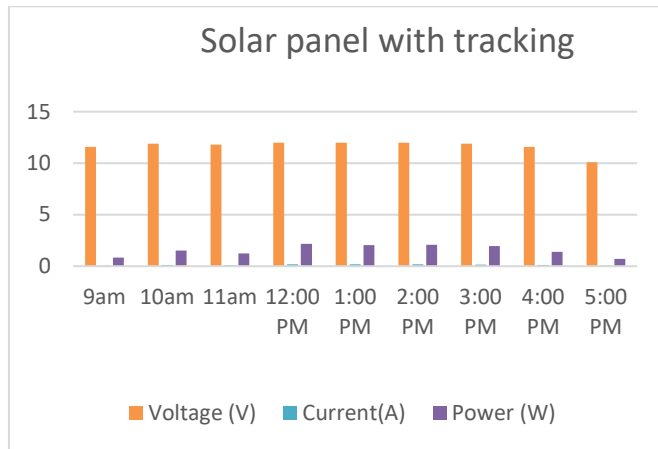


Fig 5: Solar panel with tracking results

5. CONCLUSION

The current project is based on tracking solar panels. These panels change their orientation in relation to solar radiation to increase the efficiency and results in maximum production of energy and helps in getting full benefit of optimal angle between solar panels and solar radiations. The execution of solar tracking system was made clear because of our sufficient research and pre-planning of our goals and objectives. The main agenda of this project was to make simple machinery on low-cost basis. Energy is the fundamental source upon which the whole civilization is based upon. As it is said that energy can neither be created nor be destroyed and, in that response, it can be signified that it can somehow be stored. This project has been endeavored towards unraveling the path of such objectivity. It is quite natural that constant utilization of energies somehow opens the door of scarcity as per as earthly sources are concerned. Sun, in the stand of which, the tallest source, spiked over for age's right from the origin of the whole universe, through which life has been conceived, is the basic and the mother source of all the energies. Considering the very fundamental from the viewpoint of storing such energy, the project has been unraveled. Energies other than from the Sun, are the process from which such are produced through the burning of various materials, involving emission of a large amount of pollution, causing the environment and the atmosphere sick day by day. Trial and error method help us in achieving our goal. We made use of our engineering knowledge in this three-month project and were successful in developing and designing low-cost solar tracking system. Because the issue of global warming must be controlled by making use of alternatives that are environmentally friendly. The very embodiment through which the futuristic conundrum be set aside, is the project called "**Heliotropic Solar Collector**". A trailblazer by its spirit, this system works in its utmost efficiency, whether that be in terms of its pecuniary ability or in terms of its accessibility. In the smoke of the darkness where pollution engulfing every sphere of advancement as an outcome of reducibility, this device in its very efficiency work towards only advancement and development by flushing out the pollution at large.

6. REFERENCES

- [1] Joy Sankha Ghosh, Naiwrita Dey, Pabak Das - Department of AEIE, RCC Institute of Information Technology, Kolkata, India, 27th September 2019.
- [2] 2.Udit Mamodiya, Neeraj Tiwar – Department of Electrical Engineering, Poornima University, Jaipur, India, 14th April 2020
- [3] 3.Dr. V. Shanmugasundaram, Anjali Nighoskar, Sampanthkumar, Dr C Balakrishnan, K. Suresh, Dr Sudharsan Jayabalan – Department of EEE, Sona college of Technology, Salem, Tamil Nadu, 2nd June 2021.
- [4] 4.H. J. Loschi, Department of Communication, The State University of c ampinas,2014
- [5] 5.Gino Alvarado, Carlos Bosquez, Ronald Dominguez, Universidad Politécnica alesiana, Guayaquil, Ecuador, 7th march 2017.
- [6] 6.Reshmi Banerjee, Department of Electrical Engineering, Guru Nanak Institute of Technology, India, March 2015,
- [7] 7.Pavan Badarinath U.G. Student, Department of Electronics and Communication Engineering, BNM Institute of Technology, Bangalore, India, May 2019.
- [8] 8.Mohamad Nur Aiman Mohd Said, Siti Amely Jumaat, Clarence Rimong Anak Jawa, Green and Sustainable Energy Focus Group, Faculty of Electrical and Electronic Engineering, Universiti Tun Hussein Onn Malaysia (UTHM), Malaysia, 11 th November 2019.
- [9] 9.Ms. Priyanka B. Shelar, Mali Abhishek Dattatray, Sarvankar Prathamesh Kishore, Gaikwad Ketan Jitendra, Randive Ravi Devidas, Department of Electrical Engineering, B.R. Harne Institute of Engineering, and Technology At Karav, (West) Tal. Ambarnath, Dist Thane, 6 th June 2020.
- [10] Aman Panchori, Mohit Thakre, Vipul Pande, Department of Electronics and Telecommunication, P. R. Patil College of Engineering and Technology, Amravati, Maharashtra, 2019.

FABRICATION AND PERFORMANCE ANALYSIS OF PORTABLE VERTICAL AXIS WIND TURBINE

Rajana Mani Kumar¹, Rayudu Pranav², Yerugula Jaya Vijay³, Seerapu Subrahmanya Reddy⁴, Valluri Srikar Kumar⁴
^{1,2,3,4} Students (B. Tech, Mechanical Engineering), Raghu Engineering College, Visakhapatnam

ABSTRACT

In the current time environment situation, global warming, pollution caused because of burning fossil fuel and rapid decrease in available amount of fossil fuel, demands for cleaner energy sources are become a viable technology for power generation. Huge researches lead to use of wind energy and wind turbine installations. This paper shows the small research approach of power generation using waste wind energy at ground level with the help of VAWT. The main objective of this attempt is to produce electricity by using the kinetic energy of air that flows at low ground level to generate power. This project involves a fabrication of proto-type for a small scale portable vertical axis wind turbine for charging cellular electronic gadgets.

Key words: vertical axis wind turbine, portable vertical axis wind turbine, waste wind energy, ground level, charging cellular electronic gadgets

1. INTRODUCTION TO WIND TURBINE

As time passes it is getting more and more difficult to use fossil fuel to use it as a source of energy and it increases the pollution of air have compelled many countries to find and use the alternative energy sources, to meet their requirements. Till today our extensive source of primary energy has been fossil fuel for domestic, industrial and for power generation. But it comes with a serious threat of environment pollution and degrading mother earth. There are various types of energy. For example Potential energy in the water stored in a dam, the energy in a coiled spring, and energy stored in molecules (gasoline). Similarly kinetic energy is energy available in the motion of particles such as wind energy. The energy may be categorized as: mechanical, electrical, thermal, chemical, magnetic, nuclear, biological, tidal, geothermal, and so on. Renewable energy is a sustainable future energy resource. The future can be secured with clean energy sources if we prepare for it now. Wind energy is converting wind kinetic energy into mechanical energy, which then can be converted to electrical energy that can be coupled with practical with the help of wind turbines.

Vertical Axis Wind Turbine:

For wind energy generation the wind turbine is the most essential part. Depending on their axis of rotation the turbines can be a horizontal axis wind turbine (HAWT) or a vertical axis wind turbine (VAWT). There has been various occasion we must have encountered HAWT. But there is a bigger issue with HAWT is its size. It needs higher speed of wind to rotate

the huge blades of it, which again space consuming. This type of wind turbine needs a continuous flow of high speed wind to rotate the blades. Also this type of wind turbine needs a large area of flat lands where we can mount.

Because of following advantages of VAWT, we can bring in to use for small power generation.

- The vibration and noise is lesser than horizontal-axis wind turbines
- It can generate electricity irrespective of the wind direction.
- It can produce electrical energy at very low wind speeds unlike HAWT.
- Blade speed is less as the blades are positioned closer to the axis of rotation.
- Can be installed in urban, residential and commercial areas.
- Looks beautiful and pleasing to eye unlike some larger horizontal wind turbines.
- Height of Vertical-axis towers are much less than horizontal-axis wind turbines.

Objective of project:

Being in the coastal area in India, this area faces cyclone every year, as well as in other locations also faces natural disasters time to time, in that case the HAWT get damaged greatly. Also to reduce the space consumption we are fabricating a portable type VAWT prototype which can be disassembled before the disaster.

Also in highway, or in beach area the KE of wind energy get wasted, in those areas we can't mount the HAWT, it will also be suitable for those areas to generate the power to meet the requirement of power for highway.

2. DESIGN AND PRINTING

The design is adapted and modified according to the project objective. The first step is to produce a digital model. Frequently used process of producing digital model is computer-aided design (CAD). STL file is a similar file to stereo-lithography CAD software i.e. developed by 3D systems. Now, a CAD model is converted into an STL file. The STL file then transformed to G-Codes that control the 3D printer automation and check the essential parameters like layers & height.

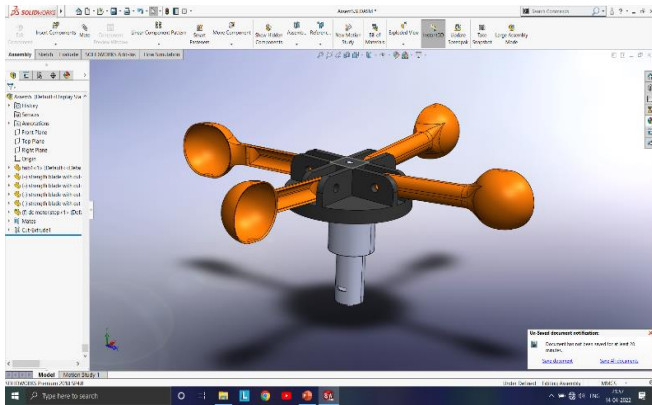


Fig. 1. 3D Model of Wind Turbine

MAJOR COMPONENTS OF VAWT

- Turbine blade.
- HUB.
- Alternator or 12Volt DC motor.
- Battery
- XL6009 DC- DC Adjustable Step up Boost Power Converter Module.
- Diode

3D printed parts:

In additive manufacturing (AM) process a 3D objects is built by adding layers one upon other of specified material using a Computer. Unlike other conventional machining processes, 3D printing or AM can build 3D object using CAD model file, generally by continuous addition of material layer by layer. The 3D printed Model and its assembled structure is shown in following Figure.

ABS Material:

ABS, shot for Acylonitrile Butadiene Styrene, is an oil-based plastic-type. ABS finds many applications in the manufacture of numerous components because it is easy-to-use and has high resistance to high temperatures. ABS might be perfect end-use components, also for functional parts such as those created in 3D printers of 3d printing service. It is a thermoplastic resin and can frequently meet the property requirements for a reasonable price, lying between standard resins like PVC, polyethylene, polystyrene and such more and engineering resins like acrylic, nylon specially(taulman 645 nylon), acetal, and such more.

3. FABRICATION PROCESS

The FDM technology works using a plastic filament or metal wire which is unwound from a coil and supplying material to an extrusion nozzle which can turn the flow on and off. The heated nozzle which melts the material and moves in both horizontal and vertical directions by a NC mechanism, directly controlled by CAM software. The object is produced by extruding melted material to form layers as the material hardens immediately after extrusion from the nozzle. This technology is widely used with following plastic filament materials like ABS (Acrylonitrile Butadiene Styrene) and PLA (Polylactic acid) but more materials are there with properties

like wood filed, conductive, flexible etc. Scott Crump invented FDM in the late 80's. He started the company Stratasys in 1988 after patenting this technology. The software in this technology automatically generates support structures if required.

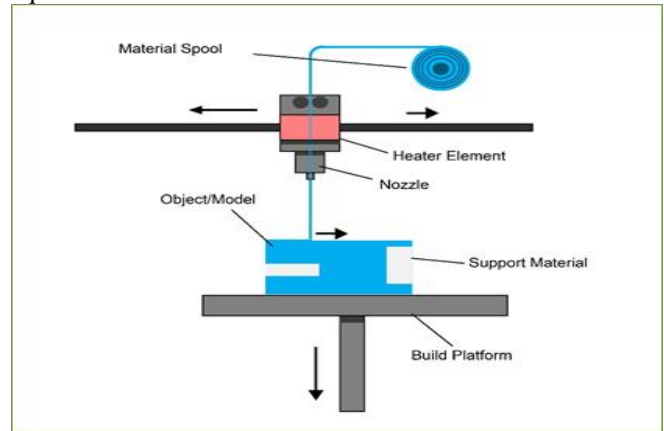


Fig. 2. 3D Printing Process

CREALITY ENDER 3

The Ender 3 Pro is a good printer for beginners because it's easy to set up and use and produces good-quality prints. It is helpful and affordable, which makes an excellent option for beginners in 3D printing. Also, there are many of online/offline tutorials to follow while using this printer.

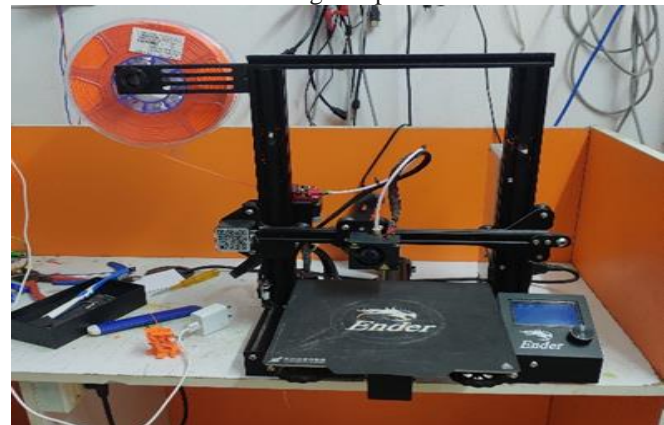


Fig.3 3D printer



Fig. 4 Printing the 3D Object



Fig. 5. Final Prototype of Turbine



Fig. 6. Installed Prototype

4. DATA COLLECTION & CALCULATIONS:

Power in the wind:

Wind turbines generate power by converting the kinetic energy from the wind and transforming it into rotational energy. This is done with the help of a aerodynamic geometry, by creating a pressure difference between the air before the air entering the turbine and after it passed through the turbine. As the air flows gets disrupted by the rotating blades and slowed down them. Since air can be considered incompressible at low velocities, the air pressure is decreased to below atmospheric conditions just after passing through the turbine.

The air pressure remains in equilibrium when the air returns to the surrounding air pressure. As a result, the pressure increases at the cost of a drop in kinetic energy. Eventually, after the stream flows a substantial distance past the turbine it returns to the pressure and velocity of the surrounding air. The exact amount of power of the can be calculated from the wind speed, which need good understanding of fluid dynamics, and airfoil geometry. Yet, a plot between turbine power and various wind speeds can be estimated using simpler calculations based upon the theoretical formula for maximum energy in any given amount of air.

This value can be obtained from Equation.

$$Power = 1/2 \rho A_{swept} v^3$$

Where P equals Power, ρ equals the density of the air at the given atmospheric conditions, A_{swept} is the swept area of the turbine and v is the upstream velocity of the wind. Swept area is total cross sectional area that the blades pass through as they

rotate. The swept area of a Vertical axis turbine, for example, is the area of the circle that connects the four blades together. Since the density of the air is both difficult to change and relatively constant for a given area, the main factor that influences power generation is wind speed. Doubling the turbine’s swept area will only double the turbine's power output. However, doubling the wind speed will provide a significant increase in the turbine's power output. For example, if a turbine generates 1.916W at a wind speed 5.7 m/s.

Coefficient of Power

1. Like all systems, actual turbines do not operate under ideal conditions. The alive of drag, friction and other factors restricts turbine’s power output. The coefficient of power (C_p) is the ratio of total wind power to turbine power.
2. C_p can be calculated using Equation

$$C_p = \frac{Power\ from\ Turbine}{Total\ Power\ from\ Wind} = \frac{Turbine\ Power}{Total\ Power\ from\ Wind}$$
3. The maximum theoretical value for the coefficient of power is 0.092 as determined by the Betz limit.

Tip Speed Ratio:

Rotational velocity of the turbine shaft is essential as it dictate how much mechanical power the turbine produce. Speed Ratio (TSR or λ) is the ratio of blade tip speed to the wind speed, and thus it recount the wind velocity to the angular velocity of the rotor.

$$\lambda = R\omega v$$

In above equation, λ is the TSR, R corresponds to the radius of the turbine, ω is the angular velocity of the turbine blades, and v is the velocity of the wind.

Higher TSRs represents more power, but lesser value for torque, whereas lower TSRs represents higher torque, low angular velocities.

From the above installation highest TSR calculated 0.538 at a wind speed of 5.7 m/s.

S.NO	WIND SPEED	VOLTAGE	RPM
1.	1.9	0.45v	20
2.	2.2	1.02v	45
3.	3.5	1.64v	61
4.	4.4	2.95v	90
5.	5.7	4.51v	161

Table No. 1: Obtained Values

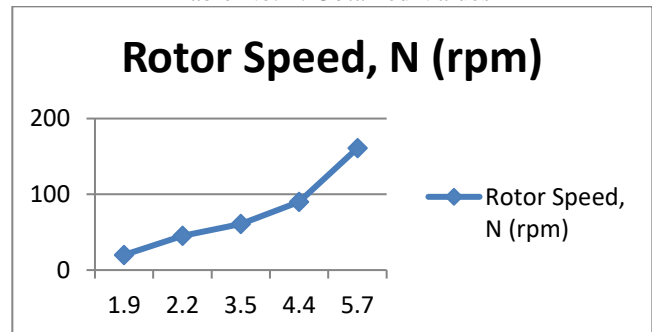


Fig. 7. Graph Between Wind Speed vs Rotor Speed

V (m/s)	N (rpm)	Computed parameters			
		P_a (watts)	P_m (watts)	TSR	C_p
1.9	20	0.011	0.003	0.183	0.063
2.2	45	0.055	0.018	0.346	0.059
3.5	61	0.222	0.056	0.41	0.07
4.4	90	0.881	0.097	0.415	0.071
5.7	161	1.916	0.153	0.538	0.092

Table No. 2 Calculated From the Obtained Values

Given:

Wind Speed, V (m/s)

Rotor Speed, N (rpm)

Power in the wind, P_a (watts)

Mechanical power, P_m (watts)

Tip Speed Ratio, TSR

Power coefficient, C_p

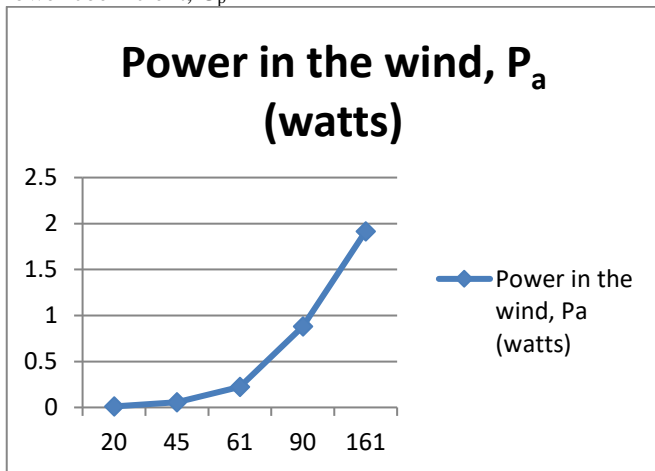


Fig. 8. Graph Between Rotor Speed vs P_a

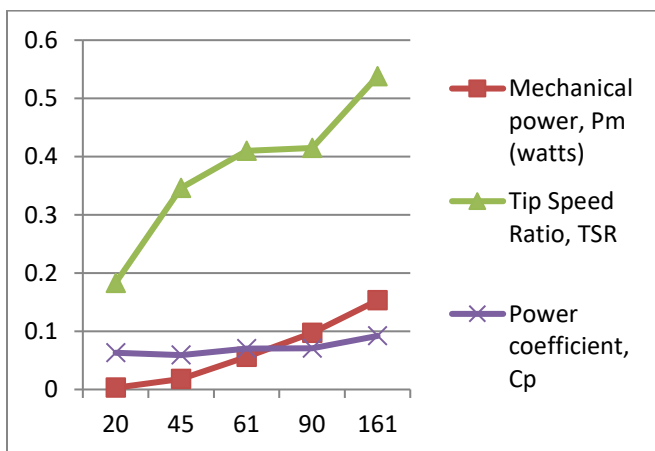


Fig. 8. Graph between Rotor Speed vs P_m , TSR, C_p

In the current attempt, solidity, number of blade, chord length of blade etc. are the basic design consideration for design and development. After the input design parameters, the conceptual model was designed in Solid Works soft ware and fabricated the prototype using 3D Printing process. Here we tried to develop a model which can produce the output even at low wind speed. Parts were fabricated with ABS materials. The testing of the model was the main area towards the success of project and outcome of the project of input decided while designing and development of the product. In the current attempt, minimum beach wind speed is of 1.8 m/s, which is much lower, and generated a power of 0.011 watts, which is sufficient to light Diode LED. So further research can give a more sustainable process of using this type of wind turbine in practical basis to meet the low power requirement of lightening arrangements outdoor such as high way.

REFERENCES

- Hau, E. Wind Turbines, Fundamentals, Technologies, Application, Economics, 2nd ed.; Springer: Berlin, Germany, 2006.
- Dominy, R.; Lunt, P.; Bickerdyke, A.; Dominy, J. Self-starting capability of a darrieus turbine. Proc. Inst. Mech. Eng. Part A J. Power Energy 2007, 221, 111–120.
- Holdsworth, B. Green Light for Unique NOVA Offshore Wind Turbine, 2009. Available online: <http://www.reinforcedplastics.com> (accessed on 8 May 2012).
- Gasch, R.; Twele, J. Wind Power Plants; Solarpraxis: Berlin, Germany, 2002.
- Gorban, A.N.; Gorlov, A.M.; Silantyev, V.M. Limits of the turbine efficiency for free fluid flow. J. Energy Resour. Technol. Trans. ASME 2001, 123, 311–317.
- Burton, T. Wind Energy Handbook; John Wiley & Sons Ltd.: Chichester, UK, 2011. Hull, D.G. Fundamentals of Airplane Flight Mechanics; Springer: Berlin, Germany, 2007.

Effect of Titanium Oxide Nano Lubricant on the Performance of VCR system

Donepudi Jagadish¹, Alladi Naresh², J.Dinesh Kumar Reddy³, K.Srinivasulu⁴,

¹ Professor, Department of Mechanical Engineering, Narasaraopeta Engineering College, Narasaraopet

^{2,3} Student, Department of Mechanical Engineering Narasaraopeta Engineering College, Narasaraopet

⁴ Asst. Professor, Department of BSH, Narasaraopeta Engineering College, Narasaraopet

ABSTRACT

The earth temperature rapidly increases due to releasing of emissions from the vehicles, industrial smoke, Air Conditioners and refrigerators as per the survey of National Ambient Air Quality Standard. Studies revealed that the usage of Nano particles can effectively reduce the harmful pollutant emissions to some extent. The damage caused by refrigerants and lubricants can be reduced by adopting the Nano fluids in the lubrication system of Refrigeration units.

Present work deals with addition of Nano particles to the lubricating oil of a hermetically sealed compressor in order to improve efficiency of compressor. The Nano particles are impregnated into lubricating oil there by enhancing the properties of the same. The nano particles used are Titanium dioxide and Aluminum oxide. The result obtained has directly shown to improve the C.O.P of the refrigeration system, when Nano particles are used as lubricants. Without nano particle addition the C.O.P is 3 and with Nano particle addition of 0.2 g the C.O.P obtained is 3.75 and with addition of 0.4 g the C.O.P obtained is 4.5. The trend showed that with higher additions of Nano particles the C.O.P enhancement is improved.

1. INTRODUCTION

Nano fluids are engineered colloids which consist of a base fluid with Nano sized particles (1-100 nm) suspended within them. Common base fluids include water, organic liquids (e.g. ethylene, tri-ethylene-glycols,

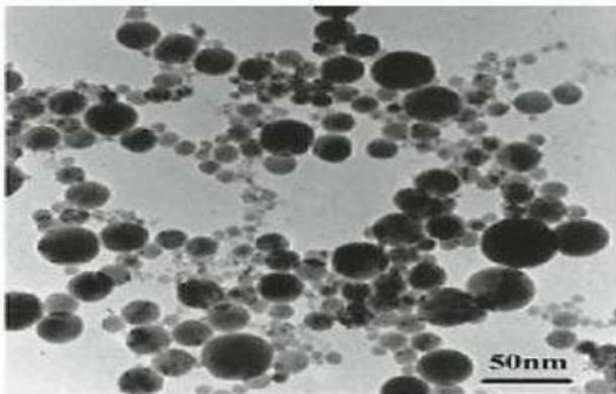


Fig.4.1 micro testing image

Refrigerants, etc.), oils and lubricants, bio-fluids, polymeric solutions and other common liquids. Materials commonly used as nanoparticles include chemically stable metals (e.g., gold, copper), metal oxides (alumina, silica, zirconia, Titanium), oxide ceramics (e.g. Al₂O₃, CuO), metal carbides (e.g. SiC), metal nitrides (e.g. AlN, Si₃N₄),

carbon in various forms (e.g., diamond, graphite, carbon Nano tubes, fullerene) and functionalized nanoparticles. By suspending nanoparticles in conventional heat transfer fluids, the heat transfer performance of the fluids can be significantly improved. As a fluid class, Nano fluids have a unique feature which is quite different from those of conventional solid-liquid mixtures in which millimeter and/or micrometer-sized particles are added. Such particles settle rapidly, clog flow channels, erode pipelines and cause severe pressure drops. All these shortcomings prohibit the application of conventional solid-liquid mixtures to micro channels while Nano fluids instead can be used in micro-scale heat transfer. Heat transfer performance of the Nano fluid is superior to that of the original pure fluid because the suspended ultrafineparticles remarkably increase the thermal conductivity of the mixture and improve its capability of energy exchange.

For this reason, the Nano particles (**TiO₂ oxide**) are added to the compressor lubrication oil it increases efficiency of compressor as well as which impacts on refrigerator entire working and it is the attempt to control the emissions such as less chance to leakage of refrigerant and smooth working of compressor. Finally, our aim is to increase the refrigerator efficiency in terms of applying the Nano particles (**TiO₂ oxide**) to the compressor lubricating oil for smooth working of compressor which impacts on refrigerator performance.

2. EXPERIMENTAL SETUP

The test rig used for this experiment was a domestic refrigerator originally designed to work with R134a refrigerant using Lubricating oil. The R134a refrigerant is used as the base line for the experiment. The system was evacuated with the aid of vacuum flusher. The TiO₂ nanoparticles were used as additive in the Lubricating oil for R134a refrigerant in this project. The TiO₂ nanoparticles were selected because of its properties such good thermal conductivity, large surface area and its anti-wear and anti-corrosion properties. The average size of the nanoparticles was 15-21 nm as stated by the manufacturer. Fig.1 shows the Transmission electron image of the TiO₂ nanoparticles use for the experiment.

The characteristic properties of the PAG oil used to prepare the Nano lubricant for R134a refrigerants. The TiO₂ nanoparticles was prepared with aid of ultrasonicator for 5 hours and magnetic stirrer for uniform

dispersion of the TiO₂ nanoparticles in the lubricant. Fig.1 shows the preparation flow chart of the TiO₂ Nano lubricant.



Fig.2.1. Preparation of TiO₂ Nano lubricant were prepared (0.2g/L, 0.4g/L and 0.6g/L).

A mixture of was selected because hydrocarbon refrigerant they have zero ODP and very GWP compared to R134a. Because the refrigerator was designed to work with 100g charge of R134a, 40g mass charge of R134a was selected for use in TiO₂ nanoparticles PAG oil (polyalkylene Glycol Synthetic Oil). This is also due to lower density of hydrocarbon refrigerants compared to R134a refrigerant.

The refrigerant was charged into the system with aid of digital charging scale. The refrigerator was instrumented at the inlet and outlet of different components (compressor, evaporator, condenser and capillary tube) of the system. K-type thermocouples were used to measure the temperature at the inlet and outlet of each component. Also, pressure gauges (Bourdon type) were connected to suction and discharge of the compressor to measure the suction and discharge pressure of the compressor. The experimental test rig and condition are shown in Figure 1 and Table 2 and 5. The temperature and pressure readings were taken and repeated for five times at intervals of 30 minutes. The outputs of temperature and pressure readings were used to determine the enthalpy and entropy of the refrigerant.

FABRICATION OF EXPERIMENTAL SETUP

The experimental consists of a compressor, fan cooled condenser, expansion device and an evaporator section. Capillary tube is used as an expansion device. The evaporator is of serpentine coil type which is loaded with water. Service ports are provided at the inlet of expansion device and compressor for charging the refrigerant. The mass flow rate is measured with the help of flow meter fitted in the line between expansion device and drier unit. The experimental setup was placed on a platform in a constant room temperature.

MEASUREMENT OF PARAMETERS

The temperatures at different parts of the experimental setup are measured using resistance

thermocouples. 8 numbers of resistance thermocouples were used for the experimentation. The pressure at compressor suction, discharge, condenser outlet and at evaporator outlet is measured with the help of pressure gauges. The power consumption of the system was measures by a digital Watt-hr meter. A digital wattmeter and flow meter were also connected with the experimental setup.



Fig.2.2 Experimental Setup

HOMOGENISING OF NANOPARTICLES IN THE LUBRICANT:

Three lubricants bottles of PAG lubricant was taken 250ml in each beaker. The Nano particles TiO₂ of 0.2g% was taken and added to the beaker containing the lubricant. The same procedure was followed for the rest of the two TiO₂ at .0.4g, 0.6g samples. It is manually stirred first and then closed tightly with a cap and shaken properly to get it mixed well.

Magnetic stirring:

A magnetic stirrer or magnetic mixer is a laboratory device that employs a rotating magnetic field to cause a stir bar immersed in a liquid to spin very quickly, thus stirring it. The rotating field may be created either by a rotating magnet or a set of stationary electromagnets, placed beneath the vessel with the liquid. A stir bar is the magnetic bar placed within the liquid which provides the stirring action. The stir bar's motion is driven by another rotating magnet or assembly of electromagnets in the stirrer device, beneath the vessel containing the liquid.

These are bar shaped and often octagonal in cross-section (sometimes circular), although a variety of special shapes exist for more efficient stirring. Most stir bars have a ridge around the centre (called a pivot ring) on which they rotate. Magnetic stirring was done for 6 hours for each sample of the Nano fluid sample that was prepared earlier.

3. DETERMINATION OF PROPERTIES

Chemical properties

The chemical properties of aluminum oxide nanoparticles are outlined in the following table.

Table.3.1. Chemical Properties of TiO₃

Chemical Data	
Chemical symbol	TiO ₃
CAS No.	1344-28-1
Group	Aluminum13 Oxygen 16
Electronic configuration	Aluminum [Ne]3s ² 3p ¹ Oxygen [He] 2s ² 2p ⁴

Table. 3.2. Chemical Composition of TiO₃

Chemical Composition	
Element	Content (%)
Aluminum	52.92
Oxygen	47.04

Physical properties

The physical properties of aluminum oxide nanoparticles are given in the following table.

Table.3.3.Physical Properties of TiO₃

Properties	Metric	Imperial
Density	3.9 g/cm ³	0.140 lb/in ³
Molar mass	101.96 g/mol	

Thermal properties

The thermal properties of aluminum oxide nanoparticles are provided in the table

MODEL CALUCULATIONS

BEFORE NANO PARTICLES CONCENTRATION:

Initial Readings:

Temperature of water: 29Degrees Energy Meter reading: 48kw/minFlow-Rate: 10LPH
 Current: 1.97AmpVoltage: 230voltsT1:26degrees T2:36 degrees T3:23 degrees T4:-21 degrees T5:15 degrees
 P1:0.6psi P2:100psi

AFTER 45 MINUTES:

Energy Meter reading: 49kw/minFlow-Rate: 13LPH
 T1:19degrees T2:55 degrees T3:22degrees T4:-17 degrees
 T5:15 degrees
 P1:0.68psi = 0.7bar P2:112psi = 7.71bar Ammeter: 1.84
 AmpVolt: 226volts
 Flow-rate: 17LPH
 Energy Meter Reading: 49.3kw/min

AFTER ADDING NANO PARTICLES (Test-1):

P1:1.37bar P2:11.72bar
 T1:17degrees T2:61degrees T3:23degrees T4:-12degrees
 T5:12degrees h1:410kj/kg h2:450kj/kg hf3=h4:230kj/kg

Calculation of C.O.P:

$$C.O.P = (h1-hf3) / (h2-h1)$$

$$=410-230 / 470-410$$

$$=3$$

4. NANOADDITIVES IN PAG OIL

The rapid advances in nanotechnology have led to emerging of new generation heat transfer fluids called as Nano fluids. Suspending Nano sized particles (1-100 nm) in the conventional fluids possess higher thermal conductivity than the base fluid. This concept is being adopted in the work of suspending nanoparticles in the PAG oil used in refrigeration system. The thermophysical properties and convective heat transfer nature of refrigerant determines the performance of refrigeration equipment such as domestic refrigerators and air conditioners. The addition of nanoparticles to the refrigerant results in the improvement of thermo physical properties and efficiency of the compressor and entire VCR system.

NANO ADDITIVE IN VAPOUR COMPRESSION REFRIGERATION SYSTEM:

Nanoparticles can be used in refrigeration system because of its remarkable improvement in thermo physical and heat transfer capabilities to enhance the performance of the refrigeration system. In a vapour compression refrigeration system the nanoparticles can be added to the lubricant oil in the compressor. When the refrigerant is circulated through the compressor it carries traces of lubricant and nanoparticles mixture (Nano lubricant) so that the other heat transfer components will have Nano lubricant refrigerant mixture. Some investigators have conducted studies on the effect of nanoparticles in the refrigerant / lubricant on the system performance. Bi et al. (2011) conducted an experimental

Properties	Metric	Imperial
Melting point	2040°C	3704°F
Boiling point	2977°C	5391°F

Study on the performance of a domestic refrigerator using TiO₂ – R600a Nano refrigerant as working fluid. They reported that the system worked safely and efficiently with an energy saving of 9.6%. They also cited that the freezing velocity of Nano-refrigerating system was more than that of pure R600a system.

Bi et al. (2007) conducted studies on the domestic refrigerator using Nano refrigerant. In their studies they used R134a as the refrigerant. TiO₂ nanoparticles were suspended in the mineral oil of the compressor unit. It was reported that the refrigeration system worked safely without any system modification and the energy consumption reduces by 21.2%.

TABLE: 4.1. Effect of Concentration of Nano additives

Nano-particles concentration (g/lit)	Time for cooling (min)
0	60
0.2	50
0.4	40
0.6	45

TABLE: 4.2.Variation of power consumption with Nano particle concentration

Nano particles concentration (g/lit)	COP
0	0.3
0.1	0.27
0.2	0.2
0.3	0.22

CONCLUSIONS

- Present work deals with addition of Nano particles to the lubricating oil of a hermetically sealed compressor in order to improve efficiency of compressor.
- The Nano particles are impregnated into lubricating oil there by enhancing the properties of the same. The nano particles used are Titanium dioxide and Aluminumoxide.
- The results obtained have directly shown to improve the C.O.P of the refrigeration system, when Nano particles are used as lubricants.
- Without nano particle addition the C.O.P is 3 and with Nano particle addition of 0.2 g the C.O.P obtained is 3.75 and with addition of 0.4 g the C.O.P obtained is 4.5.
- The trend showed that with higher additions of Nano particles the C.O.P enhancement is improved.

REFERENCES

[1] Andrew Giegel (2004), Safety testing of domestic refrigerators using flammable refrigerants, International Journal of Refrigeration 27, 621-628

[2] Bani Agarwal and Vipin shrinivastava (2010) Retrofitting of vapour compression refrigeration trainer by an eco-friendly refrigerant, Indian Journal of Science and Technology Vol. 4 No.4 ISSN 0974-6846.

[3] A.S. Dalkilic., S. Wongwises (2010) A performance comparison of vapour compression refrigeration system using various alternatives refrigerants, International Communications in Heat and mass Transfer 37 1340-1349

[4] Bi S, Guo K and Liu Z (2011), Performance of domestic refrigerator using TiO2R600a nano refrigerant as working fluid, Energy Conservation and Management , Vol.52,No.1, pp 733-737.

[5] Bi S, Shi L and Zhang (2007) Performance study on domestic refrigerator using R134a/mineral oil/nano TiO2 as working fluid, International Journal of Refrigeration, Vol 106, pp 184-190.

[6] Bolaji, B.O. (2010) Experimental Study of R152a and R32 to replace R134a in a domestic refrigerator, International Journal of Energy, Vol. 35, pp 3793- 3798.

[7] B. O. Bolaji, M.A. Akintunde, T. O. Falade.(2011), Comparative Analysis of Performance of Three Ozone-Friends HFC Refrigerants in a Vapour Compression Refrigeration, Journal of Sustainable and Environment, Vol. 2, 61-64.

[8] Ching-Song Jwo, Chen-Ching Ting, Wei-Ru Wang (2012) .Efficiency analysis of home refrigerators by replacing hydrocarbon refrigerators, International Journal of

Measurement, Vol. 42, 697-701.

[9] Ching-Song Jwo. (2008) Experimental Study on Thermal Conductivity of Lubricant containing Nanoparticles, Rev Adv Mater Science, Vol.18, 660-666.

[10] Dossat RJ, Horan TJ (2002) Principles of refrigeration, prentice hall International Inc. New Jersey, USA, 454pp

IoT BASED GAS LEAKAGE DETECTOR ROBOT

Dr.G. Sulochana ¹, Ch.Venkata Prasad ², Sirisha³, Rajeswari⁴

¹Department of Mechanical Engineering, University College of engineering, Narasaraopet, India.

^{2, 3, 4} Department of Mechanical Engineering, Velagapudi Rama Krishna Siddhartha Engineering College, India

ABSTRACT

Gas pipes fulfil vital roles for cities, industries and thus in growing economies. In today’s world, major cities like Mumbai, Thane, Delhi, etc. are getting LPG supply by LPG Pipeline. So, gas leakages lead to threat and create hazardous situations because they can also lead to fire accidents. One of the preventive methods to stop accidents associated with the gas leakage is to install a gas leakage detection kit at vulnerable places by creating an innovative robot that can sense the gas leakage from the outer surface of pipeline and if it detects gas leakage send alert messages to the user with the help of MQ-9 gas sensor, GSM module 800c. The robot or car has wheels, and it will be controlled by the user with a remote controller. The robot has a gas detection system and a GSM module. The robot goes on the surface of pipeline and checks the leakage in the pipeline if any gas leakage is sensed by MQ-9 sensor it will send alert SMS via the help of the GSM module to the respective mobile phone number.

Keywords: IoT, GSM module, MQ-9 gas sensor, robot car, pipe line, leakage

1. INTRODUCTION

1.1 Internet of Things

The Internet of Things (IoT) is a system of interrelated computing devices, mechanical and digital machines, objects, animals, or people that are provided with unique identifiers and the ability to transfer data over a network without requiring human-to-human or human-to-computer interaction. The Internet of Things is a simple concept, it means taking all the physical places and things in the world and connecting them to the internet. On the Internet of Things, all the things that are being connected to the internet can be put into three categories: things that collect information and then send it, things that receive information and then act on it, things that do both, and all three of these have enormous benefits that compound on each other. Key benefits of IoT technology are Technical Optimization, Improved Data Collection, Reduced Waste. Figure 1.1

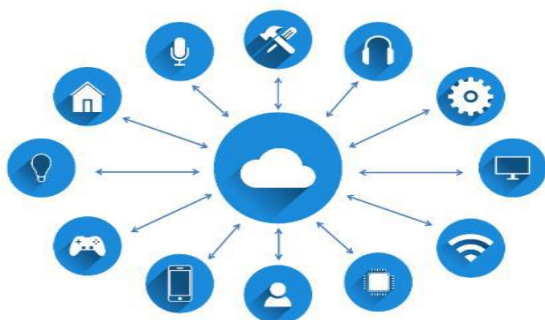


Figure 1.1 Internet of things

A whole industry has sprung up with a focus on filling our homes, businesses, and offices with IoT devices. These smart objects can automatically transmit data to and from the Internet. All these “invisible computing devices” and the technology associated with them are collectively referred to as the Internet of Things.

1.2 Background and Context

Gas leak detection methods became a concern after the effects of harmful gases on human health were discovered. Before modern electronic sensors, early detection methods relied on less precise detectors. Through the 19th and early 20th centuries, coal miners would bring canaries down to the tunnels with them as an early detection system against life-threatening gases such as carbon dioxide, carbon monoxide and methane. According to ABS-CBN news 2017 that from January to June last 2017, the BFP has recorded a total of 2,522 fire incidents. It was traced that LPG is one of the major causes of fire during that year where half of the total which is 1,253 beside from the electrical causes. Arduino has more lifetime because of a reason that thousands of projects from everyday bodies to complicated scientific mechanism. Worldwide societies of scholars, performers, programmers, and specialists have assembled around this open-source program. Their knowledge about the said matter contributions a lot to help the society in this subject area. The project entitled “Gas Leakage Detector Robot using Arduino with SMS Alert and Sound Alarm”, will be a great help in terms of preventing any danger caused by gas leakage. The purpose of this project is to detect the presence of gas leakage as a part of a safety system. Descriptively, we use a gas sensor to monitor the gas if the gas leak reaches beyond the normal level. This project proposed project will trigger the sound alarm. In addition, the authorized person will be informed about the leakage via SMS alert. The people can be saved from a potential explosion caused by gas leakage. Originally, detectors were produced to detect a single gas. Modern units may detect several toxic or combustible gases, or even a combination. Newer gas analysers can break up the component signals from a complex aroma to identify several gases simultaneously. Metal oxide semiconductor sensors (MOS sensors) were introduced in the 1990s. MOS sensors have since become important environmental gas detectors. An LPG gas sensor detector is used to detect the presence of liquid petroleum gas leakage that may be source of risk and help to avoid information sent to fire station being delayed if any accident happened. It will detect the presence of gasses using MQ2 sensor, if the sensor detects the level of gasses is exceeding the normal level it will send an information

through the phone apps through Internet of Thing (IOT). Gas sensor MQ9 is a sensor that detects gases, specifically hydrogen (H₂), Liquid Petroleum Gas (LPG), Methane (CH₄), Carbon Monoxide (CO), Alcohol, Propane, and Smoke at the atmosphere.

1.3 Problem Statement

Liquid Petroleum Gas (LPG) is a highly flammable chemical that consists of mixture of propane and butane. LPG is used for cooking at home, restaurant, and certain use for industry. They have certain weaknesses that make the gas leakage occur. The leakage of gases only can be detected by human nearby and if there are no human nearby, it cannot be detected. But sometimes it cannot be detected by human that has a low sense of smell. Thus, this system will help to detect the presence of gas leakage.



Fig.1.2 Gas leakage in pipes

2. MATERIALS AND METHODOLOGY

2.1 Components of the circuit diagram

- 2.1.1 Arduino Uno 2.1.2 MQ9 gas sensor
- 2.1.3 16*2 LCD Display
- 2.1.4 I2c display module 2.1.5 GSM 800c module
- 2.1.6 Node mcu 2.1.7 L298N motor
- 2.1.8 9V Battery 2.1.9 Servo motor
- 2.1.10 Jumper Wires 2.1.11 Arduino Uno

(Microcontroller: Microchip ATmega328P): Arduino Uno is one of the types of the Arduino Boards. The Arduino consist microcontroller that is used to perform the several operations and handling the other IoT devices like sensors and various modules in figure2.1

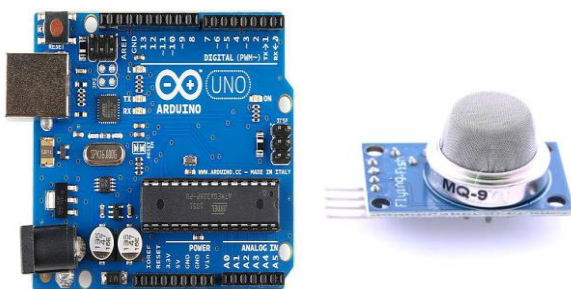


Figure 2.1.Arduino Uno Board & MQ-9 Gas Sensor

2.1.2 MQ-9 Gas Sensor: The MQ-9 sensor is used to detect the gases from the leakage pipeline. The MQ-9 gas sensor is useful for sensing the gas in home as well as in the industrial use. The MQ-9 sensor can be able to detect LPG, CH₄, CO from the air. MQ-9 sensor is highly responsive and sensitive sensor shown in figure.2.2

2.1.3 16X2 LCD Display: The 16X2 is used for displaying the amount of gas present in air in percentage manner in figure.2.3

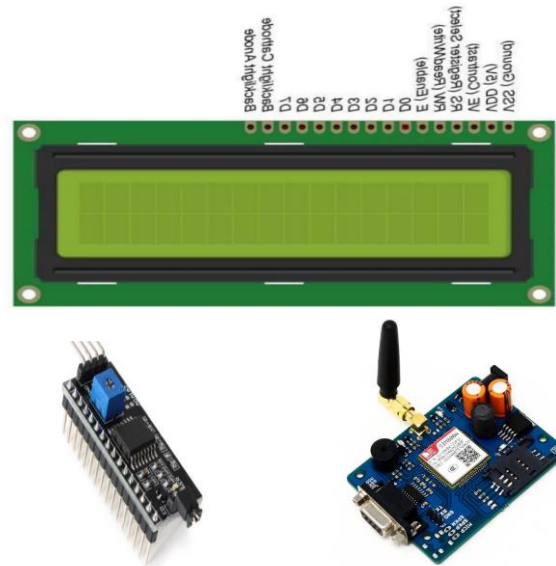


Figure 2.3 16*2LCD Display, I2c display module & GSM800C module

2.1.4 I2c display Module: I2c stands for Inter Integrated Circuit. I2c display module is used to connect 16X2 LCD display to Arduino board in figure.2.4.

2.1.5 GSM 800C Module

The GSM 800C module is used to provide GSM services as well as the GPRS and SMS services. It's used Sim card for transmitting the SMS and GPRS signal from one connection to the other connection. The GSM 800C module works with AT commands and used in 850/900/1800/1900 MHz frequencies. Shown in figure2.5

2.1.6 ESP8266 Node Mcu

Node Mcu is an open source IoT development platform. It has firmware that operates with a Wi-Fi soc Express if Systems, and hardware based on the ESP-12 module. In the figure.2.6

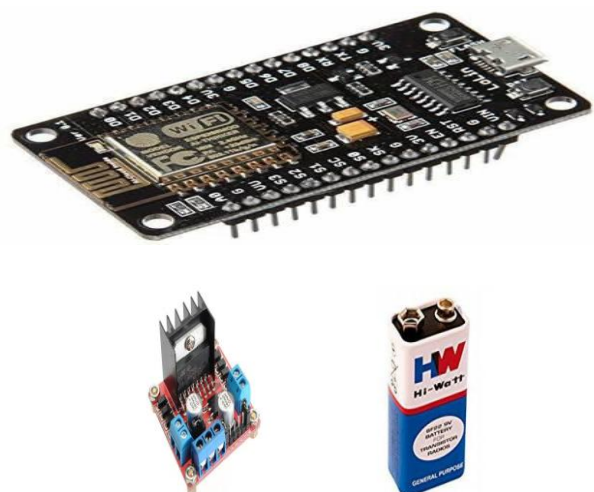


Figure 2.6 Node Mcu, L298N Motor & 9V Battery

2.1.7 L298N Motor driven shield: The L298N motor driven shield which used to control rovers' wheels direction shown in figure.2.7.

2.1.8 9V Battery: 9V Batteries are used for provide power supply to Arduino, GSM module, NodeMcu and L298N motor driven shield shown in figure.2.8.

2.1.9 DC Motor: A DC motor is an electrical machine that converts electrical energy into mechanical energy in figure.2.9.



Figure 2.9 DC Motor & Jumper Wires

2.1.10 Jumper Wires: Jumper wires are used for establish connection between IoT components shown in figure.2.10.

2.2 Methodology

In this, semiconductor sensors are used to detect the gases. An MQ9 semiconductor sensor is used. Sensitive material of the MQ9 gas sensor is SnO₂, which has lower conductivity in clean air. When the target combustible gas exists, the sensor conductivity increases along with the rising gas concentration. The MQ9 gas sensor has a high sensitivity to Propane, Butane, Hydrogen, alcohol vapour and LPG, and response to Natural gas. The sensor could be used to detect different combustible gasses, especially Methane; it is of low cost and is suitable for different applications. The MQ9 can detect gas concentrations anywhere from 200 to 10,000 ppm. The sensor's output is an analogy resistance. Figure 1 shows the block diagram of the gas leakage detection and alert system. Figure.2.11.

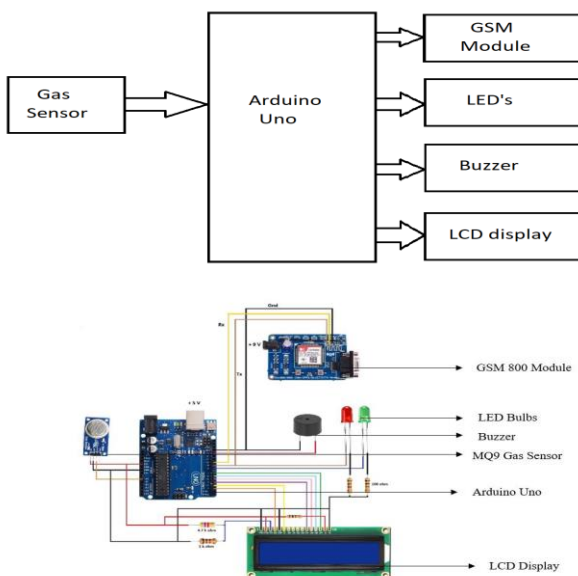


Figure 2.11 Block diagram of gas leakage detection and alert system.

3. EXPERIMENTAL SETUP:

The previous chapter presented the theoretical study relative to the method (hardware and software designs) used in designing of the gas leakage detection system with SMS alert and buzzer sound. This chapter presents relevant results obtained from the theoretical study relative the method used in implementing gas leakage detection system with SMS alert and buzzer sound.

3.1 Arduino Circuit Diagram shown in figure.3.1.

3.2 Working Principle:

Home Gateway, GSM module, buzzer, LED and robot are the main components of the system. The GSM module will send an SMS to a mobile phone number, and the home gateway will manage the signal and interpret the data received from the GSM. The sensor will detect gas leakage once the system is launched, if there is no gas leakage, it will show nothing that means normal condition. If the gas is leaked otherwise, the following scenario will happen. First of all, a signal from the microcontroller will go to the sensor and alert gas leakage message over the mobile then the buzzer will be beeped and the Red LED will be blinked until the gas leakage closed from the source.

3.3. BLOCK DIAGRAM: Shown in figure.3.2.

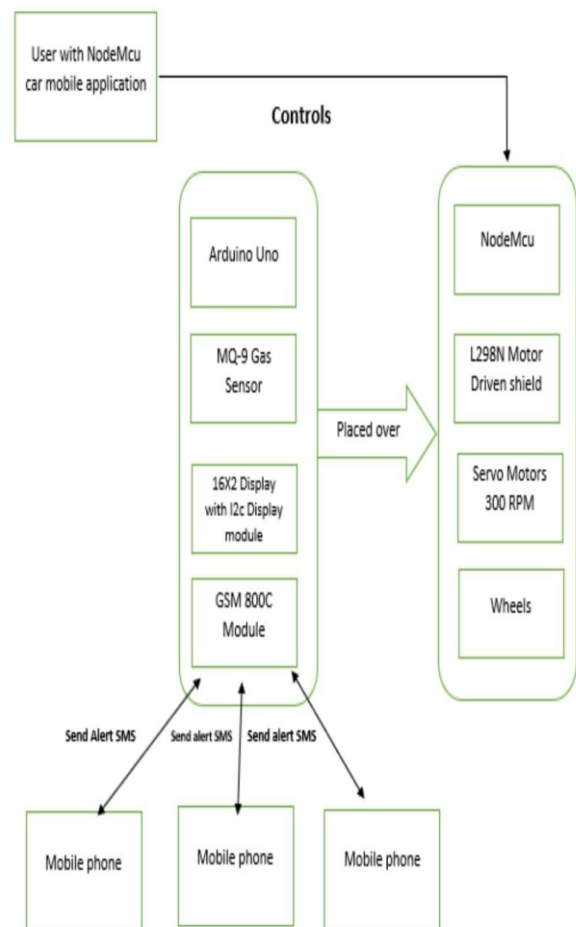


Figure 3.2 Block diagram of gas leakage detection system

4. EXPERIMENTAL CODE

```
#include <LiquidCrystal.h>
LiquidCrystal lcd(2,3,4,5,6,7);
#include <SoftwareSerial.h>
SoftwareSerial mySerial(9, 10);
int gasValue = A0; // smoke / gas sensor connected with
analog pin A1 of the arduino / mega.
int data = 0;
int buzzer = 13;
int G_led = 8; // choose the pin for the Green LED
int R_led = 9; // choose the pin for the Red Led
void setup()
{
pinMode(buzzer,OUTPUT);
pinMode(R_led,OUTPUT); // declare Red LED as output
pinMode(G_led,OUTPUT); // declare Green LED as output
randomSeed(analogRead(0));
mySerial.begin(9600); // Setting the baud rate of GSM
Module
Serial.begin(9600); // Setting the baud rate of Serial Monitor
(Arduino)
lcd.begin(16,2);
pinMode(gasValue, INPUT);
lcd.print (" Gas Leakage ");
lcd.setCursor(0,1);
lcd.print (" Detector Alarm ");
delay(3000);
lcd.clear();
}
void loop()
{
```

Result & Discussion: Gas level displayed is normal and the percentage of the gas is showing on the LCD display. Here the gas level is 89, it means there is no gas leakage. Here we have kept the base value of 100 shown in figure.5.1.



Fig.5.1 Gas Leakage level-Normal

In this case gas level displayed is exceeding and the percentage of the gas is showing on the LCD display .Here the gas leakage level exceeds 100, so the alert message is sent to the user with the help of the GSM module in figure.5.2.&5.3.



Fig.5.2 Gas Leakage level-Hig

5. CONCLUSION AND FUTURE SCOPE:

We implemented Gas Leakage detection system by using Arduino Uno, Node Mcu, MQ-9 gas sensor, LCD Display. While implementing the project we learn lot about Arduino, Gas sensors, Node mcu and many other IoT devices. Gas Leakage leads a huge problem in many industries and households. We are going to design such a robot that can detect Gas Leakages effectively by using a MQ-9 gas sensor and alert user by sending an alert message by using the GSM800C module to the respective mobile phones. Hence our Project will definitely prove to be an important for households and industries. This is a low-cost, low-power, lightweight, safe, user-friendly, efficient, multi-featured, and simple system for detecting gas. A gas detector will not only provide us with significant information for the health department but it will also leads to a significant increase in our economy because when gas leaks, it not only contaminates the atmosphere but also wastes of gases will hurt our economy. The sensor was calibrated, and the program was then run to get the particle per million values. To ensure that the gas levels being detected by the sensor are accurate, the calibration and preheating of the sensor are done. When the system is running, the data from the sensor is uploaded to the webserver. The data collected is in real-time and will display the concentrations of the gases. Buzzer and LED were used as audible and visual alarms. When the concentration of gas crosses a threshold, a buzzer and led will trigger. When the buzzer and LED light up and send out a text alert to the user via smartphone.

6.1. Future scope: In future research we are planning to upgrade project with robotic arm technology that will used for reaching to the heights of pipeline vertically. The camera module and display sensor will also be implemented in the

project so rover can be used for underground and tunnel. One of the significant functions of the system in the future is to add a subsystem that can monitor gas waste and gas usage systems. The system will have a function to notify emergency services if any accidents occur. In the future, a system will be integrated into this one that will provide more safety and relaxation to the users. The proliferation of handheld devices has led to developments in the field of smart gas sensors that have increased their scope of application. Safety will be needed in workplaces, so the market will grow over the coming years.

REFERENCES

- [1] A.Rajendra Prasad, department of ECE, sr engineering college, warangal, india, 1st december 2020.,
- [2] Taimur Ahad, Nila Sultene-Department of CSE, American International University, Bangladesh, April 2022.,
- [3] Juhi chaudhary,Anurag mishra- Guru Gobind Singh Indraprastha University, 2019.
- [4] Humberto Xavier-Program in Computational Systems modeling-Federal University of Tocantins, Brazil, 2019
- [5] Mohammad Manirujjaman Khan-Department of ECE, North south University, Bangladesh, 14th November 2020 ,
- [6] R.Rajesh Sharma-Computer Science and Engineering-Adama Science and Technology University, 2021 Adama, Nazret, Ethiopia,
- [7] Kiyotaka Izumi, Shotaro Ishibashi and Takeshi Tsujimura. Exploring of gas source location using behavioral model of insects., Proceedings of the SICE Annual Conference 2017 September 19-22, 2017, Kanazawa University, Kanazawa, Japan.
- [8] Robot. Prof. Mukesh Mahajan, Vishal Date, Darshan Derle, Swapnil Pawar. IoT Base Gas Pipe Leakage Detection System Using Insect e-ISSN: 2278-067X, pISSN: 2278-800X, Volume 14, Issue 2 (February Ver. I 2018), PP.40-43
- [9] 9.Urvashi Awasthi and Nathi Ram Chauhan. Mobile Robot for Gas Leakage Detection and Source Localization. Journal of Material Science and Mechanical Engineering (JMSME) p-ISSN: 2393-9095; e-ISSN: 2393-9109; Volume 3, Issue 4; April-June, 2016 pp. 262-267
- [10] S. Jeya Anusuya, S. Venkat, R. Elangovan, P. Sunnyteja, M. S. Karthik and E. Jawahar Raj. Under Pipe, Traveling Robot to Detect Gas Line Leakage and Address Navigation to Cloud over IoT. ISSN: 2454-132X Impact factor: 4.295 (Volume 4, Issue 2) 64
- [11] 11.Deepthi Miriyampalli , Ponnuri Anil Kumar , Abdul Khadir Shaik , Ravichandra Vipparla , Komalphanindra Potineni. Gas Leakage Detection based on IoT using Raspberry Pi. ISSN: 2321-9653; IC Value: 45.98; SJ Impact Factor: 6.887 Volume 6 Issue II, February 2018

STERILIZATION OF WATERCOURSE CONTRIVANCE

R.Rambabu¹, N.Hymavathii², D Raghavendra³

¹ Asst. Professor & HOD, Department of Automobile Engineering, Eswar college of Engineering, Narasaraopet

² Asst. Professor, Department of Automobile Engineering, Eswar college of Engineering, Narasaraopet

³ Asst. Professor, Department of Mechanical Engineering, Narasaraopet Engineering College, Narasaraopet

Abstract: River is the important source for water the livelihood. Maintaining its purity is very important. Water pollution is the addition of undesirable substance in water such as inorganic, organic, biological, radiological, heat, which degrades the quality of water so that it becomes unfit for use. Also, on the other hand gutter acts as a channel to divert the waste water from the water source, where it again meets the river at the other end. Hence, maintaining the purity of both the river is very important. However, cleaning of waste water by using man power will causes health problems and diseases occurs. To overcome these types of problems we designed an automatic river cleaning machine by using conveyor. The main objective of this project is to cleaning the river to reduce the man power, and time. In this project we have Automatic River cleaning with the help of mechanical conveyor. This project emphasis on cleaning of water. The work has done looking at the current situation of our national rivers which are dump with core litres of sewage and loaded with pollutants, toxic materials, debris etc. by using conveyor mechanism we can collect all types of unwanted waste from all water bodies with less capital.

1. INTRODUCTION:

Rivers are important part of human lives. But, unfortunately, only few are aware of its importance. The proof tons of trash in rivers and creeks, making it took and smell like a dumpsite. The garbage in rivers is more than just an eyesore because it can possibly contaminate our drinking water, threaten nature, our lives and aquatic animals.

The waste and gases produced from the industries are very harmful to human beings and to the environment. Our proposed system is used to clean and control the water garbage level using automatic conveyor mechanism technique.

The “River cleaning machine” used in that places where there is waste debris in the water body which are to here move. This machine which consists of water wheel driven conveyor mechanism which collects & remove the wastage, garbage & plastic wastages from water bodies. This also reduce the difficulties which we face when collection of debris take place.

A machine will collect the waste debris from the water bodies through the conveyor, this will ultimately result in reduction of water pollution and lastly the aquatic animal’s death to reduce these types of problems. Water bodies for clean the surface water debris from bodies. Similarly, they are lots of problems of water pollution under Ganga River, Godavari River, and Nasik which affect the acoustic, human life & beauty of Ganga River.

1.1. Importance of River Cleaning:

The rivers in India play an important role in the lives of the peoples as following below:

- According to a World Bank report titled ‘Issues and Priorities for Agriculture’, India has about 195 million hectares of land under cultivation.
- Of this, about 63% or nearly 125 million hectares is rain-fed, while remaining 37% or 70 million hectares of the agricultural land depends on irrigation. Generally, rivers around agricultural zones provide much-needed water for irrigation.
- Several wildlife sanctuaries of India are located on banks of rivers and their backwaters.
- They provide potable water, cheap transportation , electricity , and the livelihood for many people nationwide.
- The rivers also have an important role in Hindu Religion and are considered holy by many Hindus in the country
- These national parks are home to several endangered species that feature on Red List of International Union for Conservation of Nature (IUCN). Hence rivers in India are critical to their survival.
- Further, rivers of India also provide livelihood to millions of people including fishermen, sand dredgers and various other professions.

1.2. Causes of Pollution:

1. Oil & Natural Gas Exploration:
2. Chemicals & Effluents:
3. Garbage Dumping:
4. Washing & Sewage:
5. Cremation & Last Rites
6. Sand Dredging:

Possible Consequences of River Water Pollution:

1. Impact on Flora & Fauna:
2. Loss of Livelihood:
3. Food Security:.
4. Drinking Water:
5. Agriculture:
6. Loss of Export Revenue

1.3. Control to Pollution:

Reducing the effluent concentration of the waste input by:

- Wastewater treatment
- Industrial in-plant process control
- Eliminating effluent constituents by pre-treatment prior to discharge to sewer systems or by different product manufacturing for an industry.
- Reducing the upstream concentration by upstream point and non – point source controls.

Reducing the effluent volume by:

- Reduction of direct industrial discharge volumes into the municipal sewer system.
- Reduction in infiltration into municipal sewer systems.

- Reduction of waste volumes through process modifications in industries.
- Increasing the upstream flow by low flow augmentation, i.e., releases from upstream reservoir storage or from diversion from nearby water bodies.
- Water hyacinth (*Eichhornia crassipes*) and other aquatic weeds are used to upgrade wastewater treatment lagoons and treat chemical wastewaters

1.4. Aim &Objective:

The main objective of this project is to clean the rivers and water bodies with less human power and with less time consumption. This machine is fully automated controls which help to drive with less effort. The machine helps to clean all the debris and plastic bodies etc. By using conveyor mechanism, the waste can be collected itself and dumped it into storage tank. This will help to collect large amount of waste at a less period of time.

2. COMPONENTS OF STERILIZATION

2.1. Main Components: There are 2 types of components used in the system they are:

1. Mechanical Components
2. Electrical Components

2.1.1. Mechanical Components: Bevelgear, Conveyor, Hydraulic System, fitting clamps, Shafts, wheels, vane impellers.

Bevel Gear:



Figure 1:Bevel Gear

There are two types of bevel gears used in the system they are

1. Straight bevel gear
2. Spiral bevel gear

1. Straight bevel gear: Straight bevel gears



Figure 2: Straight Bevel Gear

2. Spiral Bevel Gear:



Figure 3: SPIRAL BEVEL GEAR

Conveyor:

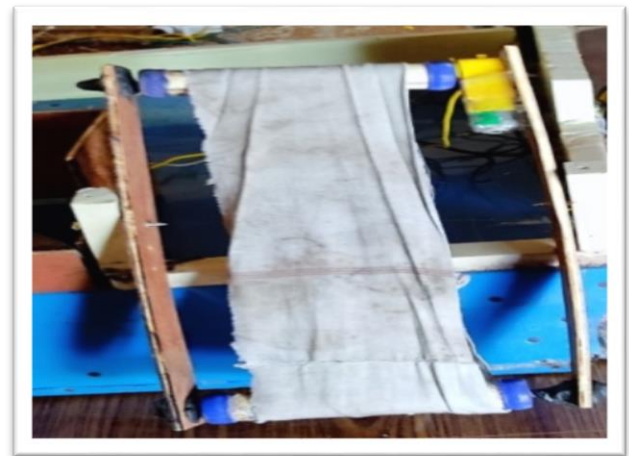


FIG4: CONVEYOR

The following types of conveyors used in this system:

1. Cleated conveyor
2. Forward conveyor
3. Jaw conveyor
4. Amidships conveyor
5. Rear conveyor
6. Chain conveyor
7. Roller conveyor

1. Cleated conveyor:



FIG 5: Cleated conveyor

2. Forward conveyor: A forward conveyor is mounted at the bow portion of the hull and is used for picking up trash from the body of the water and transferring it to the storage conveyor.



FIG6: Forward conveyor

2. Jaw conveyor:



FIG7: Jaw conveyor

This enables the front conveyor to pick up rubbish or waste from a wide area at the front of the vessel. The jaws can be narrowed when loading from a narrow area.

4. Chain conveyor:

A chain conveyor operates on the principle of interconnectivity of chains.

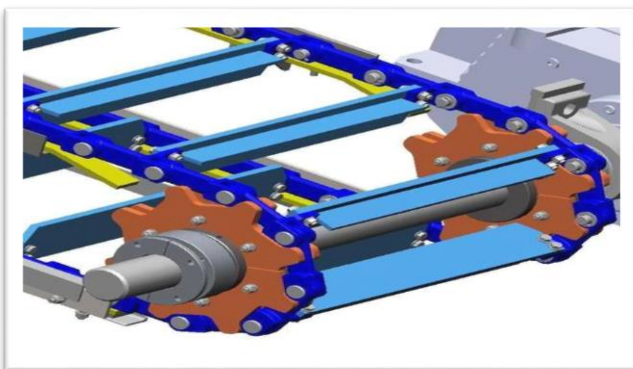


FIG8: chain conveyor

The arrangement is set in such a way that each line carries a single pendant. Conventional steel or multi-flex plastic chains are commonly used in connecting the gears. As a

result, this class of conveyors is best suited for use in transporting products with high load capacity.

5. Roller conveyor:

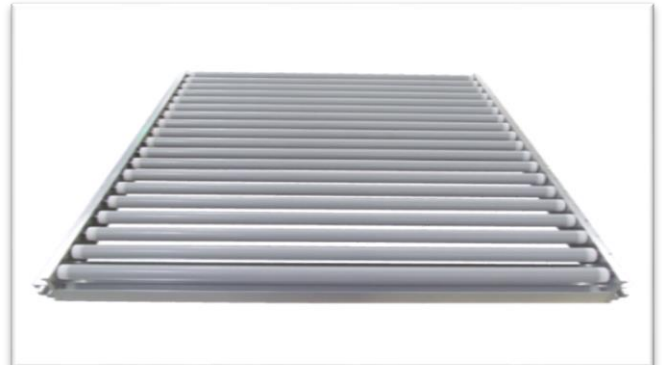


FIG10: Roller conveyor

6 Hydraulic System:

“Hydraulics” is one of drive systems to control machinery and equipment, comparable with pneumatics and electricity.



Fig 11: hydraulic system

Basic components to be used in hydraulic systems are categorized as follows.

1. Reservoir
2. Pump
3. Valves
4. Actuators

2.1.2. Electrical components:

12V4L Battery, 12vdcmotors-4, Speed Regulator, Switch, Connecting Wires.

12V demotor:



Fig 12: DC motor

The chemical reactions in a battery involve the flow of electrons from one material to another, through an external circuit. The flow of electrons provides an electric current that can be used to do work.

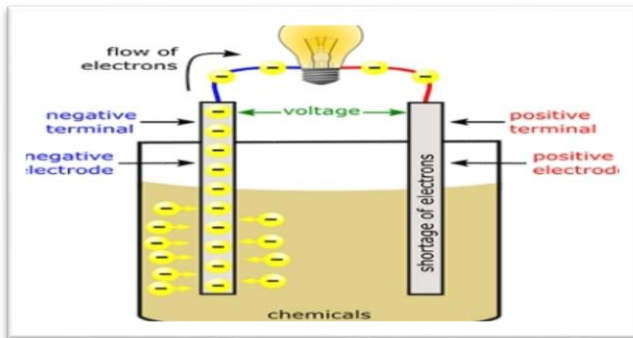


Fig 13: fuel cell

2. Construction:



Fig14: Construction

2.4. Assemble procedure:

3. WORKING

In this project the main aim of this machine is to lift the waste debris from the water surface and dispose them in the tray. The collecting plate and chain drives are rotating continuously by the motor. The collecting plate is coupled between the two chain drives for collect the waste materials from river. The collected wastages are thrown on the collecting tray with the help of conveyer. Our project is having propeller which is used to drive the machine on the river. The propeller is run with the help of four 12V dc motor. The total electrical device is controlled by RF

transmitter and receiver which use to control the machine remotely. Generally our ship completely works on dc motor and battery. Four dc motors are arranged in a series connection for the moment of ship. And another dc motor is connected to the conveyor. Switches have capacity to operate the dc motors. According to our requirement. These are utilized to supply the power source to all dc motors fixed pro-directions. Regulators are used to control speed of conveyor and dc motors. Conveyor is specially designed and it moves backward direction dump the waste disposals from the storage tank. Boat moves in linear direction without any irregular turns. Battery will balance the entire boat without any interruptions caused due to overall weight of the body.



Fig15: working

Conveyor collects the waste disposals from the water and dumped into the storage tank. Storage tank has capacity of 1-2 kg. Collected waste from the storage tank will be dumped outside by using hydraulic pushing.

4 CONCLUSION

During the course of the project study, we tackled many challenges and studied many things. At first, we only started with defining the problem, with a driving motivation to do something about it, which made us to across the growing problem of waste disposal in fresh water sources. Therefore, with keen determination we designed the project, which would overcome this problem.

While doing so we performed various task, which included extensive research on present status of rivers in India, more precisely we selected a river 'Ganga River'. So on the basis of present status of fresh water resources & comparing with it with the past; we can conclude the resources were not always scare or depleted. What caused it was growing population & their lack of awareness in reference to environment & society.

The first thing is to care about the environment that provides us human with so many things. The precise meaning of this is that we should stop pollution the water resources & create awareness about the same in more political & social ways. Then the next step is cleaning the fresh water resources in a technological way, for which we have designed our project.

So the answer to the problem is quite simple, firstly putting a stop to an unsightly mentality of polluting the environment, secondly stopping the pollution itself on the physical grounds by taking suitable measures & lastly cleaning the already polluted water resources in a more technological advance way.

5 FUTURE SCOPE

In future this project can be improved to sort more categories of waste. In this system we can use advance conveyor system and conveyor material for increasing the efficiency of collection of garbage. We can use the solar panel for providing power to the boat instead of battery operation. To modify the size of boat according to its waste collecting capacity is increases. This project makes only for small lake by doing some modification in its size and capacity it can use big lakes and rivers like Ganga, Nasik, etc.

6. REFERENCES

- [1] International Journal of Emerging Technology and Advanced Engineering. (ISSN 2250-2459, ISO 9001: 2008)
- [2] International Journal of Innovative Science and Research Technology(ISSN no :2456-2165).
- [3] Design and fabrication of River Cleaning Machine, Saif Ali Sayyad, Adarsh Dorlikar, Sneha Ratanparkhi, Tanvi Bhagat, RCERT, Chandrapur, India MH.
- [4] Design and Fabrication of River Cleaning Machine, Sheikh MD Shahid MD Rafique, Dr Aakash Langde, Dept of Mechanical, Anjuman college of engineering and technology, Nagpur, Maharashtra.
- [5] <https://learnmech.com/design-and-fabrication-of-river-cleaning-machine/>.
- [6] <https://en.wikipedia.org/wiki/>.
- [7] <https://www.marineinsight.com/naval-architecture/design-of-ships-bottom-structure/s>
- [8] Design, Fabrication and Analysis of Composite Marine Propeller, Dr, P Ravinder Reddy, CBIT, Hyderabad
- [9] www.waterwitch.com
- [10] <https://www.slideshare.net/>

PERFORMANCE MONITORING OF HEAT EXCHANGER USING IOT

Dr.G. Sulochana¹, Ch.Venkata Prasad², Ch. Dhanunjaya³, N. V. Keerthika Chitra⁴

^{1,2} Department of Mechanical Engineering, University College of Engineering, Narasaraopet, India.

^{3,4} Department of Mechanical Engineering, Velagapudi Rama Krishna Siddhartha Engineering College, India

ABSTRACT: An Internet of Things (IoT) is an intelligent approach to connect devices or components to internet and monitor the status of the device. In recent days, many industries connect their equipment's with internet and monitor the status of the same regularly that can help in predicting the failure of the components at the early stage. An IoT platform helps in predictive maintenance by integrating different machines and manufacturing units to internet. Heat exchanger is a component which is used to transfer the heat from one medium to another effectively. Heat exchanger finds application in the field of cryogenics, air-conditioning system, chemical industries, nuclear power plants and surface condenser in power plants. The present work focuses on integrating the counter flow heat exchanger with internet through Arduino UNO microcontroller, temperature and flow rate sensor. An IoT system described in this study, is capable of monitoring the input and output data from the microcontroller. Here we make the device smart enough to calculate its own performances like efficiency, logarithmic mean temperature difference, heat transfer rate, overall heat transfer coefficient and effectiveness of the heat exchanger by using LMTD analysis. By doing this analysis we can find out the performance of heat exchanger.

1. INTRODUCTION

1.1. HEAT EXCHANGER

A heat exchanger is a system used to transfer heat between two or more fluids. These media may be a gas, liquid, or a combination of both. Heat exchangers are used in both cooling and heating processes. The media may be separated by a solid wall to prevent mixing or may be in direct contact. Heat exchangers can improve a system's energy efficiency by transferring heat from systems where it is not needed to other systems where it can be usefully used.

1.2 Types of Heat Exchangers

There are 3 different types of heat exchangers

1.2.1 Concentric tube heat exchanger

It consists of two pipes. Double pipe heat exchangers are the simplest exchangers used in industries. On one hand, these heat exchangers are cheap for both design and maintenance, making them a good choice for small industries. On the other hand, their low efficiency coupled with the high space occupied in large scales. Shown in figure 1.1.

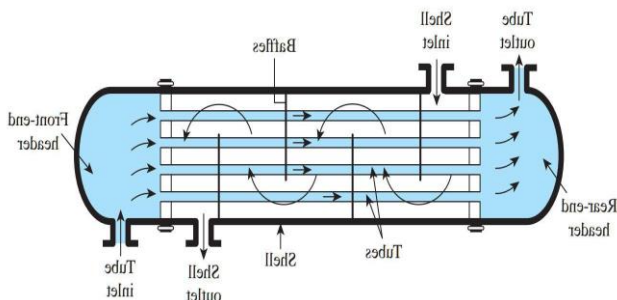


Figure 1.1. Concentric tube heat exchanger



Figure 1.2 Shell and tube heat exchanger

1.2.2 Shell and Tube heat exchanger

The main constituents of this type of heat exchanger seem to be the tube box, shell, the front rear end headers, and baffles or fins. The baffles are used to support the tubes, direct the fluid flow to the tubes in an approximately natural manner, and maximize the turbulence of the shell fluid. There are many various kinds of baffles, and the choice of baffle form, spacing, and geometry depending on the allowable flow rate of the drop in shell-side force, the need for tube support, and the flow-induced vibrations. In figures 1.2 & 1.3.

Flow Types for a Shell and Tube Heat Exchanger

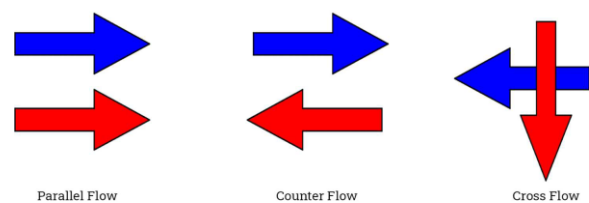


Figure 1.3: Flow types of shell and tube heat exchanger



Figure 1.4. IOT

INTERNET OF THINGS (IOT): The internet of things, or IoT, is a system of interrelated computing devices, mechanical and digital machines, objects, animals or people that are provided with unique identifiers (UID'S) and the ability to transfer data over a network without requiring human-to-human or human-to computer interaction. A thing on the internet of things can be a person with a heart monitor implant, a farm animal with a biochip transponder an automobile that has built-in sensors to alert the driver when tire pressure is low or any other natural or man-made object that can be assigned an Internet Protocol (IP) address and is able to transfer data over a network.

1.3.1 How does IoT work? An IoT ecosystem consists of web-enabled smart devices that use embedded systems, such as processors, sensors and communication hardware, to collect, send and act on data they acquire from their environments. IoT devices share the sensor data they collect by connecting to an IoT gateway or other edge device where data is either sent to the cloud to be analysed or analysed locally. Sometimes, these devices communicate with other related devices and act on the information they get from one another. The devices do most of the work without human intervention, although people can interact with the devices for instance, to set them up, give them instructions or access the data. Shown in figure.1.4.

Dr. R C Sac deva is an ex-professor in mechanical engineering at Delhi College of engineering et al [1]. At present he is director, HMR institute of technology and management, Delhi et al [2]. He is a life fellow member of the institute of engineers and has several publications in the international and national journals. He is the author of "Fundamentals of engineering heat and mass transfer" which was published by New Academic Science in the year 2017. In this book he mentioned about the heat transfer, modes of heat transfer and fins, heat exchangers. From this book we took logarithmic mean temperature difference method of counter flow heat exchanger for our calculations.[1] Min Huang, Zhen Liu, Yang Tao department of software engineering, south China university of technology et al [1] published an article on mechanical fault diagnosis and prediction in IOT based on multi source data fusion in the year 2020. Using multi-source sensing data based on the Internet of Things (IoT) with artificial intelligence and big data processing technology to achieve predictive maintenance of mechanical equipment can remarkably improve the service life of the machine and reduce labour costs when diagnosing mechanical faults, and it has become a highly relevant research topic. In this paper, the multi-source sensing data fusion models and fusion algorithms are studied and discussed.

First, the Joint Directors of Laboratories (JDL) fusion model and the Hierarchical fusion model are compared and analyzed. Then, various types of fusion algorithms based on Neural Networks and Deep Learning, including Dempster-Shafer (D-S) evidence theory and their applications in mechanical fault diagnosis and fault prediction, are studied and compared. The findings reveal that exploring and designing a more intelligent fusion model incorporating the beneficial characteristics of different fusion algorithms are challenging and have a certain value for promoting the development of mechanical fault diagnosis and prediction.

2. EXPERIMENTAL SETUP

2.1. Components used:

- ❖ Counter flow heat exchanger: More rate of heat transfer takes place in counter flow heat exchanger.
- ❖ Arduino Uno board: Arduino Uno microcontroller board based on ATmega328p. It is used to read the code.
- ❖ Flow rate measuring sensor: It is used to measure the flow rate of the fluids.
- ❖ Temperature sensor: It is used to sense the inlet and outlet temperatures of the fluids.
- ❖ Bluetooth module: It is used to control the device.
- ❖ Breadboard: A breadboard allows for easy and quick creation of temporary electronic circuits to carry out experiments.
- ❖ Jumped wires: These are used to connect the breadboard and the Arduino board.
- ❖ USB Cable: It is used for connection.

2.2 Experimental arrangement: In this experiment we have chosen counter flow concentric tube heat exchanger. For the original setup we have added four temperature sensors to the inlet and outlets of the hot and cold fluid and two flow rate sensors to outlets of the cold and hot fluid. As the performance is monitored by IOT the sensors are connected to the read board and Arduino Uno microcontroller using jumped wires. Circuit connection the circuit connections are made in the following way, from the arduino uno microcontroller the supply and ground connection are given to the breadboard. The wires of flow rate sensor one terminal are connected to input and other terminal is connected to ground of the breadboard and in the temperature sensors the three terminals are connected to the breadboard red terminal to the is for ground, black to the ground and the green to the analogy pins of the arduino. Shown in figures.2.1,2.2 &2.3.



Figure 2.1. Experimental setup



Figure 2.2: Circuit connections

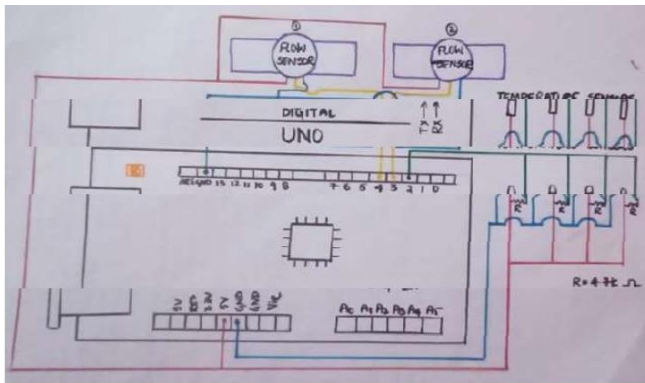


Figure 2.3. Circuit

2.2. Table.1. Specifications of the experimental setup

S. No	Name of the part	Specification	Quantity
01	Diameter of inner tube	12.5mm	1
02	Diameter of outer tube	25mm	1
03	Temperature sensor	-55 O ^c - +125 O ^c	4
04	Flow rate sensor	2.25ml for rotation	2
05	Geyser	3-liter,	1
06	Specimen	Copper tub-7	---
07	Outer shell material	G. I	----

2.3. Experimental procedure

The setup is made by placing the four temperature sensors at the cold and hot fluids and two flow rate sensors at the outlets of the cold and hot fluids. The circuit connections are made from the sensors to the breadboard and Arduino. The code is given to the Arduino board via Bluetooth module. Now the equipment is switched on and left aside for few minutes for efficient heat transfer. Now the temperature sensors and flow rate sensors sense the temperatures and flow rates of the fluids and displayed on the screen. Then the calculations are made automatically. By comparing the efficiencies, the monitor determines the performance and warns if any maintenance is needed. Now switch off the equipment.

2.4. MATERIALS AND METHODOLOGY:

As it is IOT based many electrical components have been used in this project like Arduino microcontroller, sensors, Bluetooth module, breadboard, jumped wires. Sensors a sensor is a device that detects and responds to some type of input from the physical environment. The specific input could be light, heat, motion, moisture, pressure, or any one of a great number of other environmental phenomena.

❖ In the first classification of the sensors, they are divided in to Active and Passive.

Active Sensors are those which require an external excitation signal or a power signal. Passive Sensors, on the other hand, do not require any external power signal and directly generates output response.

The following is a list of different types of sensors that are commonly used in various applications. All these sensors are used for measuring one of the physical properties like

Temperature, Resistance, Capacitance, Conduction, Heat Transfer etc.

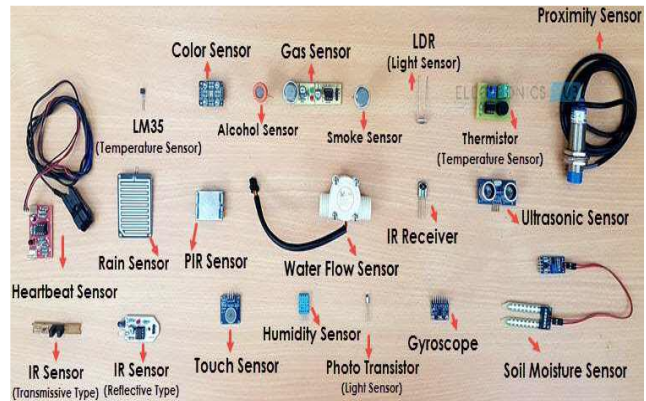


Figure 2.4. Different types of sensors

2.5. Arduino Microcontroller

Arduino is a microcontroller-based open-source electronic prototyping board which can be programmed with an easy-to-use Arduino IDE. The word "Uno" means "one" in Italian and was chosen to mark the initial release of Arduino software. The Uno board is the first in a series of USB-based Arduino boards; it and version 1.0 of the Arduino IDE were the reference versions of Arduino, which have now evolved to newer releases. The ATmega328p on the board comes preprogrammed with a boot loader that allows uploading new code to it without the use of an external hardware programmer.

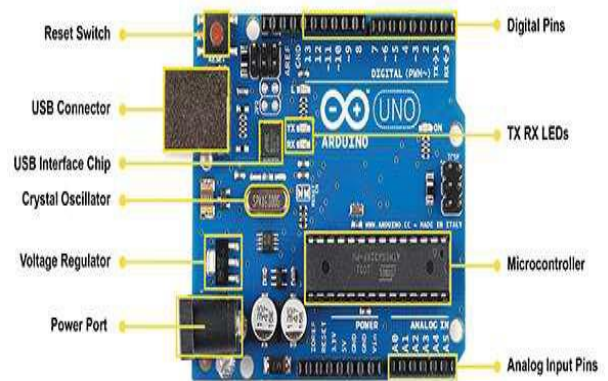


Figure 2.5. Arduino Uno microcontroller



Figure 2.6. Tinker cad logo

2.6. The major components of Arduino UNO board are as follows USB connector Power port Microcontroller Analogy input pins Digital pins Reset switch Crystal oscillator USB interface chip

2.7. Methodology: Heat exchangers are commonly used in practice, and an engineer often finds himself or herself in a position to select a heat exchanger that will achieve a specified temperature change in a fluid stream of known mass flow rate, or to predict the outlet temperatures of the hot and cold fluid streams in a specified heat exchanger. In upcoming sections, we will discuss the methods used in the analysis of heat exchangers. The log mean temperature difference (or LMTD) method is best suited for the knowing the heat transfer rate and the effectiveness we present some general considerations. Heat exchangers usually operate for long periods of time with no change in their operating conditions. Therefore, they can be modelled as steady-flow devices. As such, the mass flow rate of each fluid remains constant, and the fluid properties such as temperature and velocity at any inlet or outlet remain the same. Also, the fluid streams experience little or no change in their velocities and elevations, and thus the kinetic and potential energy changes are negligible. The specific heat of a fluid, in general, changes with temperature. Under these assumptions, the first law of thermodynamics requires that the rate of heat transfer from the hot fluid be equal to the rate of heat transfer to the cold one. That is,

$$Q_c = m_c C_{pc} (T_{co} - T_{ci}) \text{ and } Q_h = m_h C_{ph} (T_{ho} - T_{hi})$$

Where the subscripts c and h stand for cold and hot fluids, respectively, and mc, mh = mass flow rates, Cpc, Cph = specific heats, Tco, Thi = outlet temperatures Tc, in, Th, out = inlet temperatures

2.8. LMTD – Logarithmic mean temperature difference: The LMTD is a logarithmic average of the temperature difference between the hot and cold feeds at each end of the double pipe exchanger. For a given heat exchanger with constant area and heat transfer coefficient, the larger the LMTD, the more heat is transferred.

The total rate of heat transfer: $[Q = UA (Th - Tc)]$

The small amount of heat transfer: $dQ = U dA$

2.9. CODING

2.9.1. **Tinker cad software is used for simulation:** Tinker cad is a free-of-charge, online 3D modelling program that runs in a web browser. Since it became available in 2011 it has become a popular platform for creating models for 3D printing as well as an entry-level introduction to constructive solid geometry in schools. Tinker cad uses a simplified constructive solid geometry method of constructing models. A design is made up of primitive shapes that are either "solid" or "hole". Combining solids and holes together, new shapes can be created, which in turn can be assigned the property of solid or whole. [3] In addition to the standard library of primitive shapes, a user can create custom shape generators using a built-in JavaScript editor. Shapes can be imported in three formats: STL and OBJ for 3D, and 2-dimensional SVG shapes for extruding into 3D shapes. Tinker cad exports models in STL or OBJ formats, ready for 3D printing. Tinker cad also includes a feature to export 3D models to Mine craft Java

Edition, [11] and also offers the ability to design structures using Lego bricks. Shown in figure.2.6

2.10. Code used for monitoring:

```
#include <OneWire.h>
#include <DallasTemperature.h>
#define ONE_WIRE_BUS 4
OneWire oneWire(ONE_WIRE_BUS);
DallasTemperature sensors (&oneWire);
int deviceCount = 0;double tempC[4];int flowPin1 = 2;int flowPin2 = 3;
double flowRate1;double flowRate2;volatile int count1;volatile int count2;
double Qh; double Qc; float Mh; float Mc; double Tci; double Tco;
double Thi; double Tho; double T1; double T2; double Tlm;
double Cp = 4182;
double eff; double Q;double A = 0.1313;// double U.double E;void setup()
{
sensors.begin(); Serial.print("Locating devices...");
Serial.print("Found "); deviceCount =
sensors.getDeviceCount(); Serial.print(deviceCount, DEC);
Serial.println(" devices.");
Serial.println(""); pinMode(flowPin1, INPUT);
pinMode(flowPin2, INPUT);
attachInterrupt(0, Flow1, RISING); attachInterrupt(1, Flow2, RISING); Serial.begin(9600);
}
void loop() {
sensors.requestTemperatures(); for (int i = 0; i < deviceCount; i++) {
tempC[i] = sensors.getTempCByIndex(i); }
Thi = tempC[0]; Tho = tempC[1]; Tci = tempC[2]; Tco = tempC[3];
Serial.println("***** LET'S CALCULATE THE PERFORMANCES *****");
```

3. RESULTS AND DISCUSSION

3.1 RESULT TABLE: In this section evaluation of effectiveness and efficiency of heat exchange process within heat exchanger by integrating device with IoT is observed.

3.2 Simulation Results

When any one of the sensor is not working or there is a connection problem.The following result is shown: Figure 3.1: Result 1When all the sensors are working properly and there is no connection problems, the performance is good. The following result is obtained: Figure 3.2:

S. No	Thi (°C)	Tho (°C)	Tci (°C)	Tco (°C)	R1 (kg/s)	R2 (kg/s)	LMT D (°C)	Q (W)	Uo (W/m²K)	η(%)	ε
1	61	50	34	42	10	20	17.46	652.64	284.7	54.55	0.30
2	47	43	34	37	20	30	9.49	523.22	419.7	70.31	0.23
3	40.90	39.10	33.60	34.80	30	40	5.35	301.85	332.1	66.66	0.19
4	40.80	39.30	33.60	34.90	40	50	5.80	270.66	396.4	90.6	0.18
5	41.30	39.90	34.00	35.20	50	60	4.90	309.53	356.2	93.7	0.17
6	44.20	41.90	34.00	36.00	60	70	8.05	295.13	292.8	96.16	0.20
7	42.30	40.80	34.20	35.70	70	80	6.25	275.93	425.2	93.4	0.19
8	40.80	39.60	34.50	35.60	80	90	5.15	273.86	408.0	91.67	0.17

```

COM3
***** LET'S CALCULATE THE PERFORMANCES *****
Hot water inlet temperature: 54.00 C
Hot water outlet temperature: 48.13 C
Cold water outlet temperature:42.81 C
Cold water inlet temperature: 37.50 C
Mass flow rate of hot water is 0.04 Kg/s
Mass flow rate of cold water is 0.03 Kg/s
Heat gained by the cold water: 917.78 W
Heat lost by the hot water: 676.64 W
Efficiency of the heat exchanger: 135.64 %
LMTD Logarithmic Mean Temperature Difference: 10.90 C
Rate of heat transfer : 797.21 W
Overall heat transfer coefficient : 556.84 W/m2K
Effectiveness of heat exchanger : 0.32

***** LET'S START MONITORING *****

-----> MAL FUNCTIONING <-----
-----> ONCE CHECK TEMPERATURE SENSOR <-----
    
```

Figure.3.1: Result 1

When all the sensors are working properly and there is no connection problems, the performance is good. The following result is obtained:

```

COM3
***** LET'S CALCULATE THE PERFORMANCES *****
Hot water inlet temperature: 54.50 C
Hot water outlet temperature: 46.06 C
Cold water outlet temperature:42.06 C
Cold water inlet temperature: 37.50 C
Mass flow rate of hot water is 0.04 Kg/s
Mass flow rate of cold water is 0.03 Kg/s
Heat gained by the cold water: 788.21 W
Heat lost by the hot water: 971.77 W
Efficiency of the heat exchanger: 81.11 %
LMTD Logarithmic Mean Temperature Difference: 10.38 C
Rate of heat transfer : 879.99 W
Overall heat transfer coefficient : 645.69 W/m2K
Effectiveness of heat exchanger : 0.27

***** LET'S START MONITORING *****

-----> GOOD PERFORMANCE <-----
-----> MAINTENANCE NOT REQUIRED <-----
-----> DEVICE IS WORKING GOOD <-----
    
```

Figure.3.2: Result 2

When there is no sensor setup. The following result is obtained:

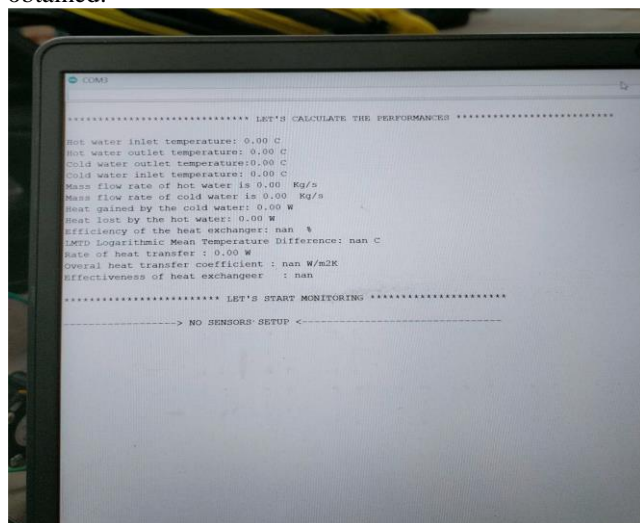


Figure.3.3: Result 3

4. CONCLUSION

- ❖ In this work, we find out the logarithmic mean temperature difference, rate of heat transfer, overall heat transfer coefficient and effectiveness of the heat exchanger by attaching the IoT equipment.
- ❖ The IoT equipment automatically calculated the above-mentioned performances without taking much time.
- ❖ This work will help in testing the mechanical devices and easy way of finding the performance.
- ❖ It will reduce the lead time during the testing.
- ❖ It will help in easy and predictive maintenance.
- ❖ It will compare the performance of heat exchanger steadily and can warn the operator for early maintenance.

5. REFERENCES

- [1] R.C. Sachdeva - “Fundamentals of Engineering Heat and Mass Transfer”.
- [2] Ghani, S., Gamaledin, S. M. A., Rashwan, M. M., &Atieh, M. A. (2020). Experimental
- [3] Investigation of double-pipe heat exchangers in air conditioning applications. Energy and Buildings, 158, 801811.
- [4] Huang, M., Liu, Z., & Tao, Y. (2020). Mechanical fault diagnosis and prediction in IoT
- [5] Based on multi-source sensing data fusion. Simulation Modelling Practice and Theory, 102, 101981.
- [6] Wright, S. J., Dixon-Hardy, D. W., &Heggs, P. J. (2019). Aircraft air conditioning heat
- [7] Exchangers and atmospheric fouling. Thermal Science and Engineering Progress, 7, 184202.
- [8] Yang, X. L., Gong, Y., Tong, Q., & Yang, Z. G. (2020). Failure analysis on abnormal
- [9] bursting of heat transfer tubes in spiral_x0002_wound heat exchanger for nuclear power
- [10] Plant. Engineering Failure Analysis, 108, 104298.
- [11] Nasution, D. M., Idris, M., &Pambudi, N. A. (2019). Room air conditioning performance
- [12] Using liquid-suction heat exchanger retrofitted with R290. Case Studies in Thermal
- [13] Engineering, 13, 100350.
- [14] Zhang, Z., Hou, Y., &Kulacki, F. A. (2018). Theoretical analysis of a transcritical double stage nitrous oxide refrigeration cycle with an internal heat exchanger. Applied Thermal Engineering, 140, 147157.

Mathematical Modeling of Cooling Rates of MangoFruits during Unsteady State Cooling in an ArtificialRipening Chamber

Shaik Shareef ¹, Shaik GouseBasha ², A. Pavan kumar ³

^{1,2} Assistant Professor, *Department of Mechanical Engineering, PACE institute of technology and sciences, Ongole, India*

³ Assistant Professor, *Department of Mechanical Engineering, Narasaraopeta Engineering College, Narasaraopet, India*

Abstract: Mango fruits need to be ripened artificially using ethylene in thermally insulated refrigerated chambers. The present experiments were conducted to determine the kinetics of cooling rates (with respect to time) of mangoes during unsteady state cooling before ripening the fruits. Ethylene based ripening systems becoming popular due to safe and healthy ripening unlike ripening using calcium carbide. Three different lots 4, 6 and 10 Metric Tons of mangoes placed in perforated plastic crates were cooled first to the desired optimum temperature for ripening. Temperature profiles of mangoes were monitored and recorded with a data logger. Time taken for the mangoes to reach the optimum set temperature of 16.8°C is 16, 20 and 26 hours for 4, 6 and 10 MT respectively. During the unsteady state cooling (from approximately 30°C to 16°C), rate of cooling is modeled using three mathematical equations, viz. linear, exponential and polynomial. Experimental data of pre-cooling is fitted to the predicted values. Best fitting models are proposed based on highest R² values for all three different quantities of mangoes pre-cooled. The results will be helpful for deciding the timing for ethylene injection and design of refrigeration equipment for part loads of the ripening chambers.

Keywords: *Mango processing, artificial ripening, cooling rates, mathematical*

I.

INTRODUCTION

Mangoes and bananas need to be artificially ripened before selling in the market. The basic need of ripening arises from the plucking of just matured fruits for enabling them to transport to long distances, otherwise the fruits get ripened in the transit and become unfit for consumption or less acceptable to the customer due to over ripening.

Calcium carbide, which is a carcinogenic substance, is widely used by traders, retailers and farmers for ripening of fruits like banana, mango and citrus fruits in India. This substance is banned by the Government of India for using it as ripening substance. However, traders appearing to be using this material due to its easy availability and non-awareness of its harmful effects in long term on human health (Ramesh Babu et al. 2019)

Alternative technologies are available for ripening fruits artificially using ethylene either from an ethylene generator or gas cylinder or canisters. This technique is much simpler and safer. The important requirements of ripening in a ripening chamber are proper temperature of fruits and ethylene level in the air of the chamber. Typical temperature

ranges are 15°C to 20°C based on variety, origin, growing conditions and maturity level while plucking.

A properly designed ripening chamber consists of an insulated chamber and sealing of the room to ensure maintaining ethylene levels for first 24 hours of ripening cycle. A refrigeration system consists of compressor, condenser, expansion device and cooling unit (Evaporator). This system pre-cools the produce to the desired temperature. Accessories required for a ripening chamber are the perforated plastic crates or ventilated corrugated fiber board (CFB) cartons, ethylene injection system, sensors for temperature & ethylene level measurement and controls.

The objectives of the present experiments are to:

1. Investigate the temperature profiles of mango pulp temperature during pre-cooling stage during artificial ripening of mangoes
2. Model the rate of cooling during un-steady state pre-cooling stage
3. Study the effect of different quantities on the cooling rate
4. Fit the temperature profiles to the mathematical models (kinetics of temperature change with respect to time)

II. LITERATURE OVERVIEW

Narasimha Rao et al. (1992, 1993a, 1993b) have studied the pre-cooling aspects of spherical fruits and modeled the pre-cooling process. They have used hydrair cooling for pre-cooling process. They have used an experimental set up with both air and water spray to pre cool the produce [2-4]. Ramesh Babu et al. (2018) extensively investigated the handling of fruits and reported the incidence of surface damage during handling and loss of texture during storage. However they reported the firmness changes of apples during controlled atmosphere storage. Preserving the fruits in perforated plastic bins has been reported. The time taken for apples to pre-cool is 120 hours (fruit to reach temperature of 10°C from an initial temperature of 25-30°C) Cardenas Perez et al. (2018) evaluated basic parameters concerned with softening of Tommy Atkins mangos during

ripening process. Notify as ripening index (RPI) value and Young's modulus of the primary cell of mango gradually decreases. It leads to physiochemical as well as chemical and mechanical changes. There are three fractions that are isolated with mango cell wall. They are water soluble (WSP), chelator soluble (CSP) and diluted alkali soluble (DASP). Two analysis X-ray and confocal laser scanning microscopy gives the complete information about changes occurred in the mango cell wall during maturation. Finally, a graph between 'E' and 'RPI' gives a linear fit curve Eyarkai Nambi et al (2017) observed the texture and rheological changes of Indian mangos like Banganapalli, Neelam and Alphonso during ripening. There by utilizing logistic models, easily predicts the changes occurring during ripening process. Finally, noticed that pulp exhibits high shear stress and low viscosity. By using Herschel Bulkley model observed that flow behavior index and yield stress gradually decreased. On the other hand, consistency coefficient increases during ripening process. Mango pulp exhibits elastic behavior rather than viscous behavior

Ullah et al. (2016) Provides the information regarding non-invasive assessment of mango during ripening process by using fluorescence spectroscopy. Spectra records from the peel of Dasherri mango using light emitting diode at 460nm as excitation state. Results suggested that carotenoids depicts similar with chlorophyll pigment levels for a fruit maturity. But experiments repeated with a Langra mango, the peel remains green after fully ripening stage. Therefore, carotenoids fluorescence 540 nm may be useful for assessment of mangos during ripening process

Eyarki Nambi et al. (2016) predict a color grade sheets for Indian mangos by classifying the ripening period into different stages. By considering the two Indian mango varieties Banaganpalli and Alphonso measures the physico-chemical properties, external-internal color values and texture characteristics are recorded throughout the ripening period. By introducing Hierarchical method, ripening period of mango is classified into five stages, viz. unripe, early ripe, partially ripe, ripe and over ripe. Based on this stages color grade sheets are developed. The developed grade sheets are useful for non-destructive grading tool at pack houses and packing industries

Vu et al. (2019) reports that changes occurring in the physico-chemicals, chlorophyll and antioxidants of banana peel during ripening with and without usage of ethylene. As the fruit color changes from green to yellow chlorophyll degraded to 90% as well as carotenoids and flavonoids are increased to 50% and 27% respectively. Finally, the banana peel contains higher phenolic content and antioxidants without usage of ethylene than with usage of ethylene

Zulkifli et al. (2019) investigated the potential of laser light back scattering imaging for predicting different ripening stages for a Berangan type banana. In order to investigate the

different stages, a charge coupled device is coupled with a laser emitting diode at a wavelength of 658 nm is used. Grey level intensity and backstage area of the scattering images are used as a parameters for the estimating the quality properties of banana. Finally, a statistical analysis provides successful classification along with their sample ripening stages with a percentage corrected to 94.6%

Campuzano et al. (2018) reported information about physicochemical changes and nutritional characteristics of banana flavor during ripening. At early stages of ripening such as second and third stages, the protein content is gradually increased and decrease in carbohydrate and amylase content. Finally, between these two stages significant decrease in total and resistant starch produced together with an increase in phenolic content and antioxidant activity

Gowda et al. (2001) carried out experiments to determine the qualitative and quantitative changes and physico-chemical changes occurred at the time of ripening process for mangos. By conducting the experiments over a six varieties of mangos, concluded that there is a slight reduction in the fruit weight, volume, fruit length, thickness, firmness, pulp content, starch, vitamin C. On the other hand, there is an increase in peel, TSS, pH, sugar content, carotenoids are relatively high. Finally, the peel color changes from light green to light yellow as well as pulp color is changes from white to pale yellow or yellow to deep yellow and for particular variety mangos pulp color changes from deep yellow to orange color

Maduwanthi et al. (2019) reported that there are many modern methods are available in the market in order to ripen the bananas. Such as ethylene gas, ethephon, ethylene glycol, acetylene, alkyl alcohols etc; whereas burning the leaves and kerosene are used in traditional methods of banana ripening. Here is the interesting point notice that naturally ripe bananas exhibits better sensory characteristics compare to artificially treated fruits

Mayuoni et al. (2011) evaluated the effect of ethylene de-greening on the internal changes of Citrus fruit. Their results show that ethylene de-greens up to 3 days at specific temperature and it does not involve any internal changes in the fruit. Finally, it is concluded that ethylene cannot totally influence the parameter de-greening

Ramesh Babu et al. (2019) reported the process of ripening of mango and banana without using harmful chemicals such as calcium carbide. They reported the consumer awareness on the bad practices and good practices on ripening of fruits. Their report recommended for wider dissemination of ethylene based ripening systems for safe and healthy fruits availability

Ram Deshmukh et al. (2020) reported the importance of sealed chambers for maintaining gas composition in fruit storage chambers. The insulation panels of the fruit pre-

cooling, controlled atmosphere storage need to be gas tight, so that oxygen, carbon dioxide gas levels can be maintained without any leakage.

III. MATERIALS AND METHODS

Ripening process of mango needs proper temperature, RH and Ethylene level management. Proper air flow, temperature during un-steady state and steady state are ensured using electronically controlled refrigeration system, temperature sensors to monitor and control apart from data logging. To determine the cooling rates, arrangement is made with a temperature sensor carefully inserted in the pulp of mango and record the data continuously from chamber sealing time to the steady state temperature achievement. Technical details of instruments used are given below. Data logger: Monitoring the precooling process using a temperature data logger: A temperature data logger is used - Model RC-4, Make: Eli-tech, United Kingdom. The data logger has a temperature range from -40°C to +80°C. The logger recording interval can be set from 10 seconds to 24 hours range. The logger has a capacity to store 16000 data points. It uses a probe to measure the temperature of the pulp. The probe is inserted into the fruit up to the centre (perpendicular to the diameter). The instrument is shown in Figure 1.

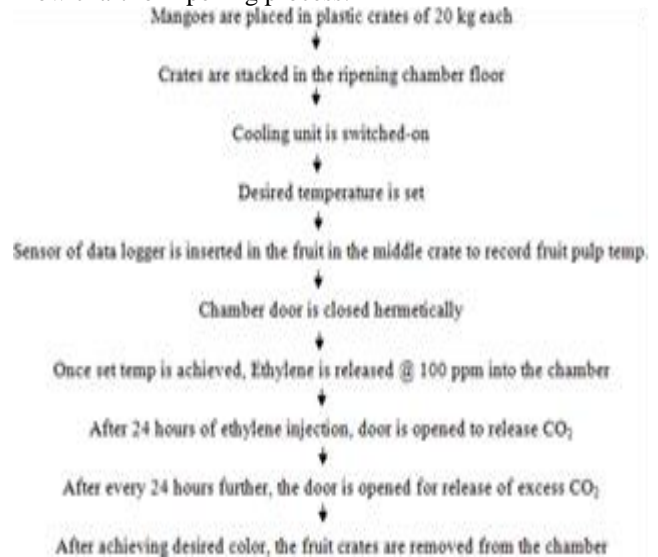
Figure1: Temperature data logger



Monitoring the room air temperature: A digital thermometer is placed at the return air of the cooling unit inside the ripening chamber which records the return air temperature, which is the temperature of the air that picked the heat from the fruits and going to enter the cooling unit for lowering the temperature and to be blown again on to the fruit crates. This instrument has been supplied by the supplier of the equipment, refrigeration unit of the ripening chamber.

Fruits: Mangoes of green colour of uniform size are placed in 20 kg standard perforated plastic crate of Nilkamal make. Stacking of crates is done up to 7 high leaving 2 feet space between top layers of top crate and cooling unit height to allow free flow of air from the cooling unit fans. Stacking pattern is made such that there is no obstruction for the return air from the fruit crates to the cooling coil.

Flow chart for ripening process:



IV. RESULTS AND DISCUSSION

Cooling rates are calculated from the experiments conducted with different tonnage of mango (4MT, 6MT and 10MT). Data logging report is plotted in MS excel for further processing and determining the rate of cooling. As expected the time required to reach the set ripening temperature (which is the steady state temperature also) found to be higher for higher quantities of mangoes.

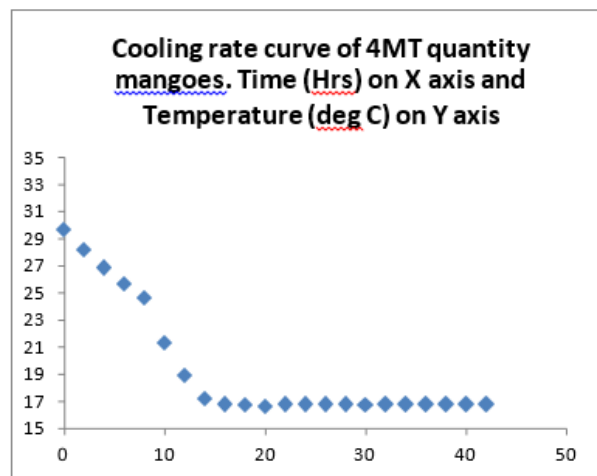


Figure 2: Cooling rate curve of 4MT quantity of mangoes in ripening chamber

It can be seen from Figure 2 that the mangoes are cooled from 30 to 16°C within 16 hours of start of cooling. Further temperature is maintained at 16.8°C to enable the ripening process with ethylene gas. Two distinct regions can be seen in the curve. One is the unsteady state, till the temperature reaches the set value. The second region after reaching set point temperature. The analysis of unsteady state cooling rate has been modeled with different mathematical models at figure 5, 6 and 7.

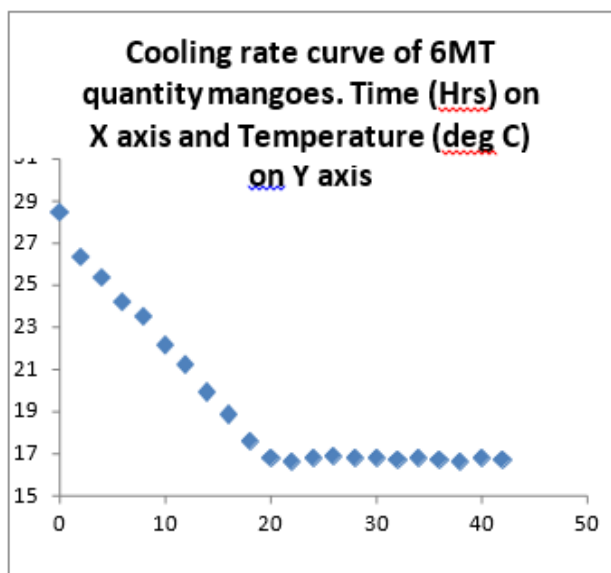


Figure 3: Cooling rate curve of 6 MT quantities of mangoes in ripening chamber

Figure 3 shows the temperature profile of mangoes when the ripening chamber is placed with 6 metric tons of mangoes. Time to achieve the set temperature of 16.8 is 20 hours. Temperature is maintained at 16.8°C till the mangoes are fully ripened. As the quantity increased from 4 to 6 MT, it is seen that time taken to arrive at the set value increased from 16 to 20 hours compared to 4 MT mangoes.

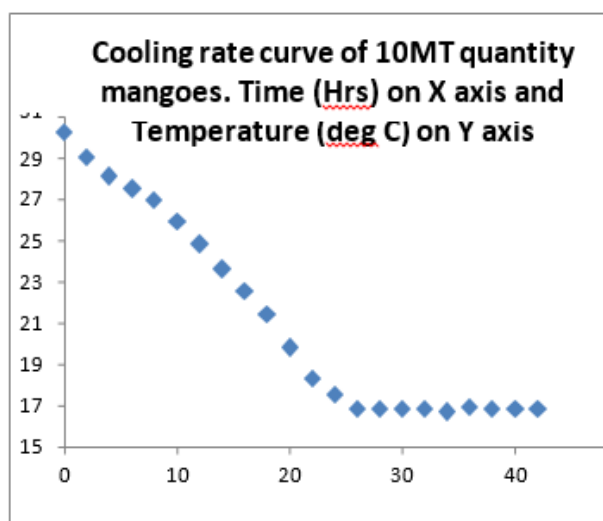


Figure 4: Temperature profile of 10 metric tons of mangoes pre-cooled in the ripening chamber.

The time to reach the set temperature of 16.8 is 26 hours. Further temperature is maintained at the same temperature till the mangoes are ripened and removed from the chamber for marketing. The time to arrive at set value is 26 hours and this is definitely expected to be more due to more sensible and latent heat from the fruits. Sensible heat is due to the fruit temperature and latent heat can be due to the moisture evaporation from the fruit apart from respiration heat

From Figures 2, 3 and 4 it can be seen that the precooling time to the desired temperature of 16.8°C took 16, 20 and 26 hours for 4, 6 and 10 metric tons quantity respectively. It can be interpreted that the ethylene ripening chambers can be successfully utilized for part loads of the chamber.

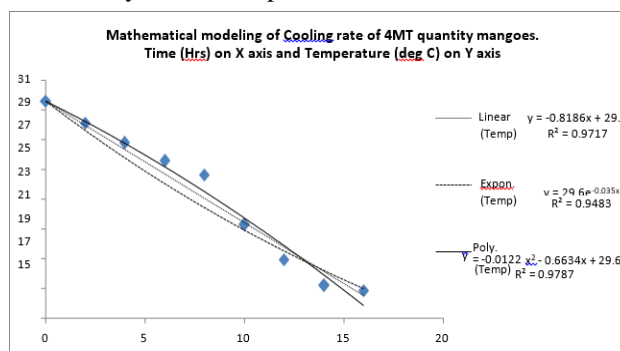


Figure 5: Application of three mathematical models (Linear, Exponential and 2nd order polynomial equations) for the cooling rate of 4 MT mangoes.

V. CONCLUSIONS:

Mangoes of different quantities are subjected to pre-cooling before ripening process with ethylene gas for natural and healthy ripening. Rate of cooling is calculated for 4 MT, 6 MT and 10 MT quantities using mathematical equations, viz. linear, exponential and second order polynomial models. The cooling time for achieving steady state (set temperature for optimum ripening requirements) is found to be 16, 20 and 26 hours for 4, 6 and 10 metric tons respectively. Experimental Vs predicted values of three models resulted to find the best fit equations. For 4 MT and 6 MT quantities, the exponential model fitted the best with 0.978 and 0.971 respectively. For 10 MT quantities, the polynomial second order equation fitted the best with R square value of 0.994. The results of this experiment can be used for the appropriate design of refrigeration equipment for part loads of mango ripening process. Results are also helpful to decide the timing for injection of ethylene based on reaching point of steady state temperature.

VI. REFERENCES

- [1] D. Ramesh Babu, K. V. Narasimha Rao & Syam Kolati (2019) The Design of Refrigeration, Thermal Insulation and an Equipment for Healthy Ripening of Mango and Banana Without Using Harmful Chemicals. International Journal of Mechanical and Production Engineering Research and Development (IJMPERD), ISSN (P): 2249-6890, Vol. 9, Issue 1, Feb 2019, 423-434.
- [2] Narasimha Rao, K. V., Narasimham, G. S. V.L. and Krishna Murthy, M. V. (1992). Analysis of co-current hydraircooling of food products in bulk. Int. J. of Heat and Fluid Flow, 13(3), 300-310. Doi: 10.1016/0142-727x(92)90044-a.
- [3] Narasimha Rao, K. V., Narasimham, G. S. V.L. and Krishna Murthy, M. V. (1993a). Parametric

- study on the bulk hydraircooling of spherical food products. *AICHe Journal*, 39(11), 1870–1884. doi:10.1002/aic.690391114.
- [4] Zulkifli, N., Hashim, N., Abdan, K. and Hanafi, M. (2019). Application of laser- induced back scattering imaging for predicting and classifying ripening stages “Berangan” bananas. *Computers and Electronics in Agriculture* 160 (January), 100 <https://doi.org/10.1016/j.compag.2019.02.031>
- [5] Campuzano, A., Rosell, C. M. and Cornejo, F. (2018). Physicochemical and nutritional characteristics of banana flour during ripening. *Food Chemistry*, 256(February), 11–17. <https://doi.org/10.1016/j.foodchem.2018.02.113>
- [6] Gowda IND, AG Huddar, (2001) Studies on ripening changes in mango (*Mangifera indica* L.) fruits *Journal of food Science and Technology - Mysore*- 38(2):135-137
- [7] Maduwanthi, S. D. T. and Marapana, R. A.U. J. (2019). Induced ripening agents and their effect on fruit quality of banana. *International Journal of Food Science*, 2019. <https://doi.org/10.1155/2019/2520179>.
- [8] Mayuoni, L., Tietel, Z., Patil, B. S. and Porat, R. (2011). Does ethylene de greening affect internal quality of citrus fruit *Postharvest Biology and Technology*, 62(1), 50–58. <https://doi.org/10.1016/j.postharvbio.2011.04.00>
- [9] D Ramesh Babu, Ram Deshmukh, K V Narasimha Rao, M Rajya Laxmi, Kafila, T Sabita (2019). Awareness on Calcium Carbide Ripened Fruits and Recommendations for Toxic Free Artificial Ripening of Fruits. *International Journal of Engineering and Advanced Technology (IJEAT)* ISSN: 2249 – 8958, Volume-9 Issue-2, December, 2019. DOI: 10.35940/ijeat.B4059.129219
- [10] Ram Deshmukh, D Ramesh Babu K V Narasimha Rao (2020) Pressure Testing Results (As A Decision Tool For Deciding E. Ramesh, D. Ramesh Babu and P. Ramchandar Rao (2018) The Impact of Project Management in Achieving Project Success- Empirical Study, *International Journal of Mechanical Engineering and Technology*, 9(13), pp. 237–247, <http://www.iaeme.com/IJMET/issues.asp?JType=IJMET&VType=9&IType=13>
- [11] D Ramesh Babu, Sireesha Koneru, K V Narasimha Rao, B Satish Kumar, Syam Kolati, N Suman Kumar (2019). Identifying Opportunities to start Industries on the Food Production Potential in Telangana and Andhra Pradesh, India. *International Journal of Engineering and Advanced Technology (IJEAT)*, 8 (5), pp. 2189-2193.
- [12] P Sammaiah, D Ramesh Babu, L Radhakrishna, and P Rajendar (2019). Kinetics of Moisture Loss during Dehydration of Drum Stick Leaves (*Moringa Oliefera*) In a Bio-Mass Tray Dryer. *International Journal of Engineering and Advanced Technology (IJEAT)* ISSN: 2249 – 8958, Volume-8 Issue-6, August, 2019.

EFFECT OF ALUMINIUM OXIDE NANO LUBRICANT ON THE PERFORMANCE OF VCR SYSTEM

P.Srinivasarao¹, P.Koteswararao², N.Mallikarjuna³

¹ Assistant professor, *Department of Mechanical Engineering, Narasaraopeta Engineering College, Narasaraopet, India*

^{2,3} Student, *Department of Mechanical Engineering, Narasaraopeta Engineering College, Narasaraopet, India*

Abstract— The earth temperature rapidly increases due to releasing of emissions from the vehicles, industrial smoke, Air Conditioners and refrigerators as per the survey of National Ambient Air Quality Standard. Studies revealed that the usage of Nano particles can effectively reduce the harmful pollutant emissions to some extent. The damage caused by refrigerants and lubricants can be reduced by adopting the Nano fluids in the lubrication system of Refrigeration units.

Present work deals with addition of Nano particles to the lubricating oil of a hermetically sealed compressor in order to improve efficiency of compressor. The Nano particles are impregnated into lubricating oil there by enhancing the properties of the same. The Nano particles used are Aluminum dioxide and Aluminum oxide. The results obtained has directly shown to improve the C.O.P of the refrigeration system, when Nano particles are used as lubricants. Without Nano particle addition the C.O.P is 3 and with Nano particle addition of 0.2 g the C.O.P obtained is 3.75 and with addition of 0.4 g the C.O.P obtained is 4.5. The trend showed that with higher additions of Nano particles the C.O.P enhancement is improved.

Keywords—Nanoparticle's, COP, Nanolubricant, Refrigerant, SiO₂, R-134a.

I. INTRODUCTION

Refrigeration is defined as the process of achieving and maintaining a temperature below that of the surroundings, the aim being to cool some product or space to the required temperature. One of the most important applications of refrigeration has been the preservation of perishable food products by storing them at low temperatures. Refrigeration systems are also used extensively for providing thermal comfort to human beings by means of air conditioning.

The refrigeration and air conditioning sector in India has long history from the early years of last century. India is presently producing R134a, R22, R717 and hydro carbon based refrigeration and air conditioning units in large quantities. The use of CFC refrigerants in new systems was stopped since the year 2002. The factors that dictate the adoption of a particular refrigerant apart from its suitability for the specific application are its availability and cost. The halogenated refrigerants such as R12, R22, R134a and natural refrigerant like R717 are readily available at low prices. The Hydrocarbon (HC) and Hydro Fluoro Carbon (HFC) mixtures (such as R404a, R407, and R410A) are not currently manufactured indigenously and hence have to be imported at a higher cost. This is likely to affect the growth in refrigeration

and air conditioning sector in India and also the total conversion to environmental friendly alternatives in the near future.

Most of commercial freezers like chest freezers, bottle coolers, visa coolers, display cabinets, water coolers and walk in coolers are using R134a and R12 as the refrigerant. Annual production of commercial refrigerated cabins (such as chest freezers, display cabinets, bottle coolers and visa coolers), water coolers and walk in coolers in India were estimated to be about 40,000, 27000, and 500 units respectively. About 80% of these units are manufactured by small and medium enterprises (Ministry of Environment and Forest, 2005). The choice of suitable alternative to R134a in commercial applications is R152a and hydrocarbon mixtures. The estimated population of milk chilling and cold storage in India was about 14,000. Most of the cold storage and milk chilling plants are working on ammonia and some on R502. Ammonia will dominate the industrial refrigeration sector due to its favorable environment properties (zero ODP and GWP). The alternative choice for R502 is 507 and hydrocarbon mixtures for low temperature industrial applications.

Nano fluids are engineered colloids which consist of a base fluid with Nano sized particles (1-100 nm) suspended within them. Common base fluids include water, organic liquids (e.g. ethylene, tri-ethylene-glycols, refrigerants, etc.), oils and lubricants, bio-fluids, polymeric solutions and other common liquids. Materials commonly used as nanoparticles include chemically stable metals (e.g., gold, copper), metal oxides (alumina, silica, zirconia, Titanium), oxide ceramics (e.g. Al₂O₃, CuO), metal carbides (e.g. SiC), metal nitrides (e.g. AlN, SiN), carbon in various forms (e.g., diamond, graphite, carbon Nano tubes, fullerene) and functionalized nanoparticles.

The test rig used for this experiment was a domestic refrigerator originally designed to work with R134a refrigerant using a Lubricating oil. The R134a refrigerant is used as the base line for the experiment. The system was evacuated with the aid of vacuum flusher. The TiO₂ nanoparticles was used as additive in the Lubricating oil for R134a refrigerant in this project. The TiO₂ nanoparticles were selected because of its properties such good thermal conductivity, large surface area and its anti-wear and anti-corrosion properties.

A. Fig.1 Experimental Setup

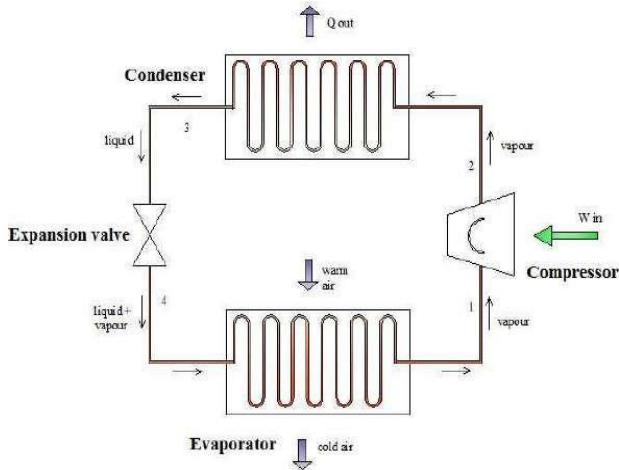


Figure.2 Standard vapour compression refrigeration cycle

The average size of the nanoparticles was 15-21 nm as stated by the manufacturer. Fig.1 shows the Transmission electron image of the TiO₂ nanoparticles use for the experiment.

The characteristic properties of the PAG oil used to prepare the Nano lubricant for R134a refrigerants. The TiO₂ nanoparticles was prepared with aid of ultrasonicator for 5 hours and magnetic stirrer for uniform dispersion of the TiO₂ nanoparticles in the lubricant. Fig.1 shows the preparation flow chart of the TiO₂ Nano lubricant.

A mixture of was selected because hydrocarbon refrigerant they have zero ODP and very GWP compared to R134a. Because the refrigerator was designed to work with 100g charge of R134a, 40g mass charge of R134a was selected for use in TiO₂ nanoparticles PAG oil (polyalkylene Glycol Synthetic Oil). This is also due to lower density of hydrocarbon refrigerants compared to R134a refrigerant.

II. EXPERIMENTAL SETUP

The experimental consists of a compressor, fan cooled condenser, expansion device and an evaporator section. Capillary tube is used as an expansion device. The evaporator is of serpentine coil type which is loaded with water. Service ports are provided at the inlet of expansion device and compressor for charging the refrigerant. The mass flow rate is measured with the help of flow meter fitted in the line between expansion device and drier unit. The experimental setup was placed on a platform in a constant room temperature.



A magnetic stirrer or magnetic mixer is a laboratory device that employs a rotating magnetic field to cause a stir bar immersed in a liquid to spin very quickly, thus stirring it. The rotating field may be created either by a rotating magnet or a set of stationary electromagnets, placed beneath the vessel with the liquid. A stir bar is the magnetic bar placed within the liquid which provides the stirring action. The stir bar's motion is driven by another rotating magnet or assembly of electromagnets in the stirrer device, beneath the vessel containing the liquid.

Compression refrigeration system and the operating cycle on a T-S diagram. As shown in the Fig, the standard single stage, saturated vapour compression refrigeration system consists of the following four processes:

Process 1-2: Isentropic compression of saturated vapour in compressor

Process 2-3: Isobaric heat rejection in condenser

Process 3-4: Isenthalpic expansion of saturated liquid in expansion device

Process 4-1: Isobaric heat extraction in the evaporator

A. ANALYSIS OF VAPOUR COMPRESSION REFRIGERATION CYLCE

A simple analysis of standard vapour compression refrigeration can be carried out by assuming a) steady flow b) negligible kinetic and potential energy changes across each component and c) no heat transfer in connecting pipelines. The steady flow energy equation is applied to each of the four components. The p-h diagram of vapour compression refrigeration

Compressor:

The isentropic work input to compressor (W_{cs} , kJ/s) is expressed as: $W_{cs} = m_r(h_2-h_1)$

Where h_2 is the enthalpy of refrigerant at the outlet of compressor (kJ/kg) the actual compressor work (W_c , kJ/s) is given as

$$W_{cs} = W_c / \eta_s$$

Where η_s is the isentropic efficiency.

Condenser:

The heat rejected by the condenser (Q_{cond} , kJ/s) to the atmosphere is given as

$$Q_{cond} = m_r (h_2 - h_3)$$

Where h_3 is the enthalpy of refrigerant at the outlet of condenser (kJ/kg)

Capillary Tube:

In the capillary tube the enthalpy remains constant (isenthalpic process), therefore,

$$h_3 = h_4$$

Effect produced per unit of work required. It is expressed as:

$$COP = Q_{evap} / W_c$$

III RESULT AND DISCUSSION

Table 1: Variation of power consumption with Nano particle concentration

Nanoparticles concentration (g/lit)	Power consumption (kwh)
0	0.35
0.4	0.26
0.6	0.28

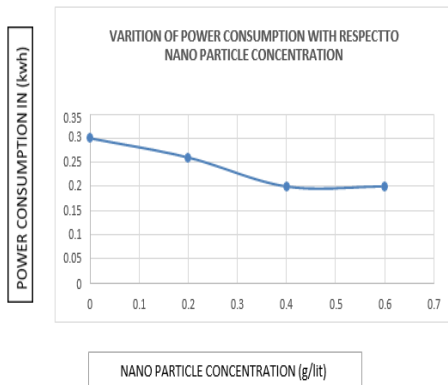


Table 2: Variation of Pressure Ratio work with Nano particle concentration

Nano particles concentration(g/lit)	Pressure ratio (%)
0	10
0.2	8
0.4	6
0.6	5.7

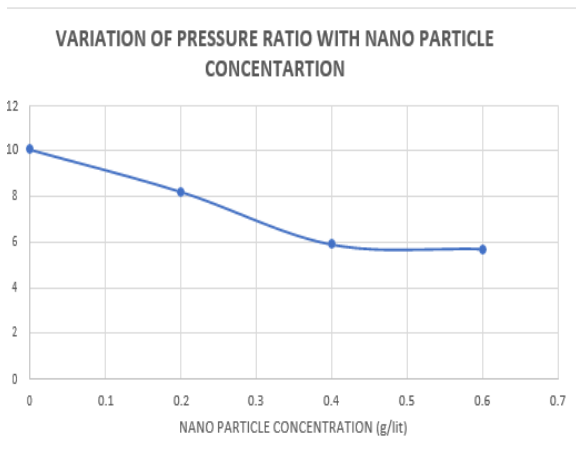
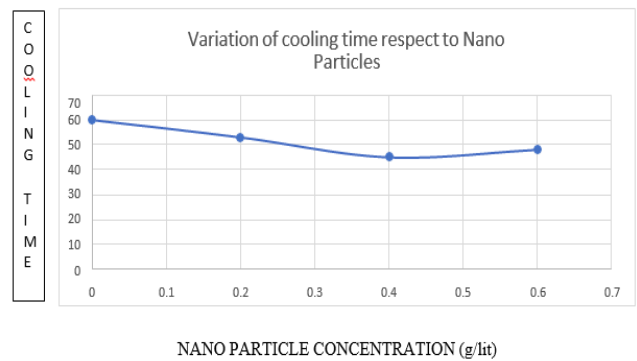


Table 3: Variation of cooling with Nano particle concentration
Variation of cooling time with Nano particle concentration

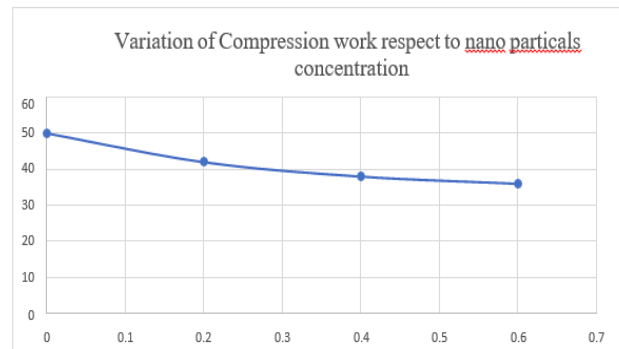
Nanoparticles concentration (g/lit)	Cooling time(min)
0	60
0.2	53
0.4	45
0.6	48

Table 4: Variation compressor work with Nano particle concentration
Variation of compressor work with Nano particle concentration

Nanoparticles concentration (g/lit)	Compressor work(kw)
0	50
0.2	42
0.4	38
0.6	36



The result shows the cooling time of system were improved cooling and efficiency respectively, when the Nano-oil was used instead of pure oil.



NANO PARTICLE CONCENTRATION (g/lit)

IV CONCLUSIONS

- Present work deals with addition of Nano particles to the lubricating oil of a hermetically sealed compressor in order to improve efficiency of compressor.
- The Nano particles are impregnated into lubricating oil there by enhancing the properties of the same. The nano particles used are Titanium dioxide and Aluminum oxide.
- The results obtained have directly shown to improve the C.O.P of the refrigeration system, when Nano particles are used as lubricants.

V. REFERENCES

- [1] Wang, X.-Q., & Mujumdar, A. S. (2008). A Review on Nanofluids - Part I: Theoretical and Numerical Investigations. *Brazilian Journal of Chemical Engineering*, 613 - 630.
- [2] Saidur, R., Kazi, S., Hossain, M., Rahman, M., & Mohammed, H. (2011). A review on the performance of nanoparticles suspended with refrigerants and lubricating oils in refrigeration systems. *Renewable and Sustainable Energy Reviews* 15(1), 310 - 323.
- [3] Ajayi, O.O., Ibia, D.E., Ogbonnaya, M., Attabo, A., & Agarana, M. (2017). CFD analysis of nanorefrigerant through adiabatic capillary tube of vapour compression refrigeration system. *Procedia Manufacturing*, 7, 688 – 695.
- [4] Kostic, M. (2004). *Advanced Flow and Heat Transfer Fluids*. Illinois, Chicago: Department of Mechanical Engineering, Northern Illinois University.
- [5] Vaishali P. Mohod, Nishikant W. Kale (2017). Experimental analysis of vapour compression refrigeration system using nanorefrigerant. *Proceedings of 68th IRF International Conference, 29th January, 90-94 Pune, India*
- [6] Nair V., Tailor P.R., Parekh A.D. (2016). Nanorefrigerants: A comprehensive review on its past, present and future. *International journal of refrigeration*, 67, 290–307.
- [7] Bi S., Shi L. and Zhang L., (2008). Application of Nanoparticles in Domestic Refrigerators. *Applied Thermal Engineering*, 28, 1834 - 1843.
- [8] Omer A. A, Nor A.C, Kherbeet A.Sh. (2015). Nanorefrigerant effects in heat transfer performance and energy consumption reduction: A review. *Int. Com in Heat and Mass Transfer* 69, 76–83
- [9] Babu M., Nallusamy S., Rajan K. (2016). Experimental analysis on vapour compression refrigeration system using nanolubricant with HFC-134a refrigerant. *Nano Hybrids*, 9, 33-43.
- [10] Bi, S., Guo, K., Zhigang, & Wu, J. (2011). Performance of a domestic refrigerator using TiO₂ as working fluid. *Energy Conversion and Management*, 733 - 737.

TRANSIENT THERMAL AND STRUCTURAL ANALYSIS OF DISC BRAKE

R.Rambabu¹, N.Hymavathii², Shaik. Chand MabhuSubhani³

¹ Asst. Professor & HOD, Department of Automobile Engineering, Eswar college of Engineering, Narasarao pet

² Asst. Professor, Department of Automobile Engineering, Eswar college of Engineering, Narasarao pet

³ Asst. Professor, Department of Mechanical Engineering, Eswar college of Engineering, Narasarao pet

Abstract— Braking system is a process which converts the kinetic energy of the vehicle into mechanical energy which must be dissipated into the atmosphere in the form of heat. A brake disc usually made of cast iron or ceramic composites is connected to the wheel and/or the axle. Friction material in the form of brake pads is forced mechanically, hydraulically, pneumatically or electromagnetically against both sides of the disc to stop the wheel. The present analysis “transient thermal and structural analysis of disc brake” deals with the heat generation in the different disc brake materials with varying speeds of the vehicle and the dissipation of heat through these materials and also the deformation and the stresses produced in these materials because of the temperature rise is analysed. A comparative study is made between these materials to suggest the best material for the disc brake in the aspect of the problem considered. Modelling of the disc brake has done using CATIAV5 and the complete analysis is done by using Ansys 16.0.

1. INTRODUCTION

Of all the systems that make car, the brake system is one of the most important. Its function determined the safety of the driver, passenger and also pedestrian. In the olden days it was also one of the simplest. Over the years as improvements have been made, the system that has evolved isn't so simple anymore. Brake system work as hard or harder than any other part of the car, however much energy it takes to get the car up a hill, it takes at least as much energy to stop it at the bottom. In general, there are three main functions of a brake system, to maintain a vehicle's speed when driving downhill, to reduce a vehicle's speed when necessary and to hold a vehicle when in parking. When the brakes were applied, the pads or shoes that press against the brake drum or rotor convert kinetic energy into thermal energy via friction. The cooling of the brakes dissipates the heat and the vehicle slows down. This is all to do with The First Law of Thermodynamics, sometimes known as the law of conservation of energy. This law states that energy cannot be created nor destroyed; it can only be converted from one form to another. In the case of brakes, it is converted from kinetic energy to thermal energy.

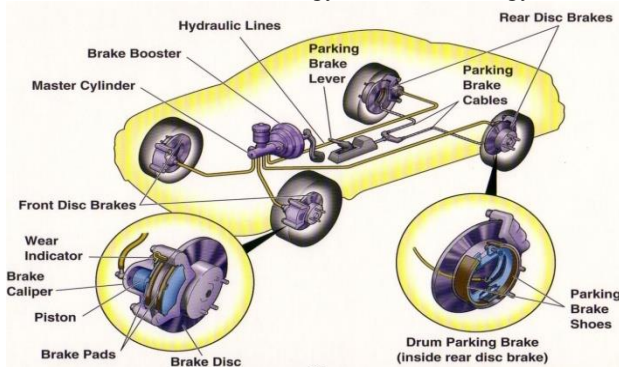


Fig: 1 components of braking system in a car

Typically, there are two types of brakes that were implemented in today's car, drum brake and disc brake. Disc brake is widely used because its design is far superior to that of drum brakes. Disc brakes use a slim disc and small caliper to halt wheel movement. Within the caliper are two brake pads, one on each side of the disc, that clamp together when the brake pedal is pressed. Fluid is used to transfer the movement of the brake pedal into the movement of the brake pads. The disc used in disc brakes is fully exposed to outside air. This exposure works to constantly to cool the disc, greatly reducing its tendency to overheat or cause fading.

1.2 Components of disc brake

A disk brake consists of so many components disk bolted to the wheel hub and a stationary housing called caliper. The caliper is connected to some stationary part of the vehicle like the axle casting or the stub axle as is cast in two parts each part containing a piston. In between each piston and the disc there is a friction pad held in position by retaining pins, spring plates etc. The passages are also connected to another one for bleeding. Each cylinder contains rubber-sealing ring between the cylinder and piston.

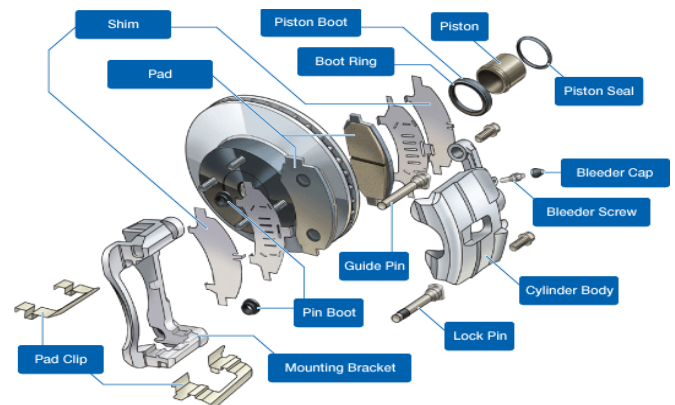


Fig 2: Components of disc brake

The main components of the disk brake are:

- The Brake Pads
- The Caliper which contains the piston
- The Rotor which is mounted to the hub

When the brakes are applied, hydraulically actuated pistons move the friction pads in to contact with the rotating disk, applying equal and opposite forces on the disk. Due to the friction in between disk and pad surfaces, the kinetic energy of the rotating wheel is converted into heat, by which vehicle is to stop after a certain distance. On releasing the brakes the rubbers-sealing rings acts as return spring and retract the pistons and the friction pads away from the disk.

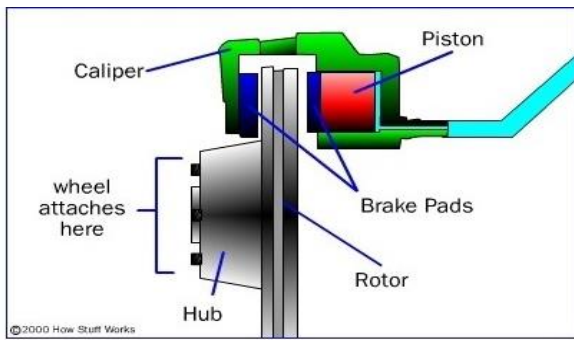


Fig 3: working of disc brake

The caliper is hinged about a fulcrum pin and one of the friction pads is fixed to the caliper. The fluid under pressure presses the other pad against the disk to apply the brake. The reaction on the caliper causes in to move fixed pad inward slightly applying equal pressure to the other side of the pads. The caliper automatically adjusts its position by swinging about the pin.

There are two pistons between which the fluid under pressure is sent which presses one friction pad directly on to the disk where as the other pad is passed indirectly via the caliper.

2. MATERIALS USED

Disc brake systems generate braking force by clamping brake pads onto a rotor that is mounted to the hub. A schematic view of the brake system is shown in Fig. 2. The high mechanical advantage of hydraulic and mechanical disc brakes allows a small lever input force at the handlebar to be converted into a large clamp force at the wheel. This large clamp force pinches the rotor with friction material pads and generates brake power. The higher the coefficient of friction for the pad, the more brake power will be generated. Coefficient of friction can vary depending on the type of material used for the brake rotor.



Fig 4: Brake disc

There are several factors to be considered when selecting a brake disc material. The most important consideration is the ability of the brake disc material to withstand high friction and less abrasive wear. Another requirement is to withstand the high temperature that evolved due to friction. Weight, manufacturing process ability and cost are also important factors those are need to be considered during the design phase. The brake disc must have enough thermal storage capacity to prevent distortion or cracking from thermal stress until the heat can be dissipated. This is not particularly important in a single stop but it is crucial in the case of repeated stops from high speed.

Table 1.1: Materials used for the disc brake

Properties	GCI	ALMM C	Meraging Steel	C-C Composite
Density(kg/m ³)	7200	2700	8100	1800
Young's Modulus(Gpa)	110	70.5	210	95
Poisson's Ratio	0.28	0.3	0.3	0.31
Thermal Conductivity(w /m-k)	52	167	25.5	40
Specific Heat(J/kg-k)	447	980	813	755
Coefficient of friction	0.41	0.35	0.81	0.3

3. SCOPE OF WORK

Braking is an essential phenomenon in engineering applications with the automobiles industry as the chief user. More than 2000 different materials and their variants are currently used in commercial brake components. Braking is a process that converts kinetic energy into mechanical energy and heat energy. The frictional heat generated at the disc-pad interface can lead to high temperatures in this component. In order to achieve a desired property for brake materials, composite materials are compounded to produce a better unit. When the vehicle is moving with a velocity it will have some kinetic energy when the braking is applied this kinetic energy is converted into thermal energy. The heat developed at the interface of the brake disc and pad is mainly depends on the speed of the vehicle and braking time. In this project we are going to analyze the thermal behavior of the different disc brake materials with varying speed and also the braking time. The different materials that we are going to analyze are Gary Cast Iron, Aluminium Metal Matrix Composite, Meraging Steel and Carbon-Carbon Composite. And also by applying the convection to these materials under the same external parameters we are trying to calculate the heat dissipation through the materials after certain time period. Based on the results obtained and by considering the other factors we are trying to suggest the best material for the disc brake among the materials that we have analyzed based on their thermal behavior.

4. MODELING THE COMPONENT

CatiaV5R20 is fully three dimensional, double precision system that allows to accurately describing almost any geometric shape. By combining these shapes, one can design, analyze, and create drawings of products.

The below mentioned are the dimensions of the brake disc and pad that we have used to in the CATIA Version V5R20.

Table 3.1 Parameters of disc brake and pad

PARAMETER	VALUE
Outer disc diameter	0.254 m
Disc thickness	0.020 m
Disc hub inner diameter	0.054 m
Disc hub outer diameter	0.140 m
Pad thickness	0.010 m
Pad area	0.0032 m ²

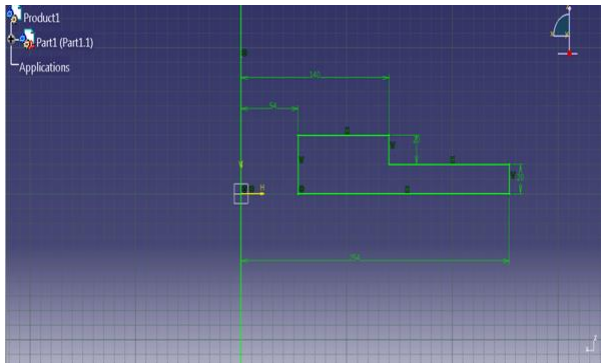


Fig 5: Sketcher view of the disc & its dimensions

The above sketch is drawn in ZX plane in the sketcher module by using various sketcher tools. Dimensions of the brake disc are also can be seen in the figure 3.1. It is then brings back into the part design module and revolved with shaft tool with the angle of revolution of 360° to get the disc as shown above fig. In this the sketch is crested with required measurements. The disc brake pad is also created by following the similar procedure as above but with the angle of revolution as 35° .

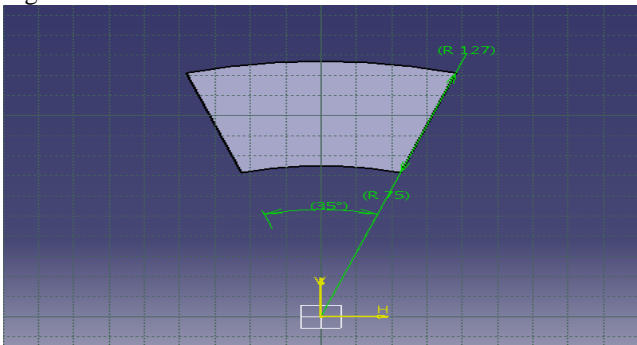


Fig 6:: front view of the pad

The dimensions that are used to create the brake pad are also shown in the figure.

5. FINITE ELEMENT ANALYSIS

Although the ANSYS program has extensive and complex capabilities, its organization and user-friendly graphical user interface makes it easy to learn and use. There are four graphical methods to instruct the ANSYS program.

- Menus.
- Dialog Boxes
- Tool bar.
- Direct input of commands.

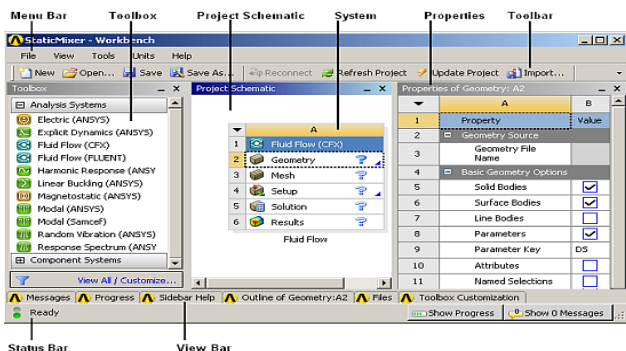


Fig 7: main window of ANSYS 16.0 Workbench
 Now to do the analysis on the geometry that we have imported already now double click on the model it opens the mechanical window with object.

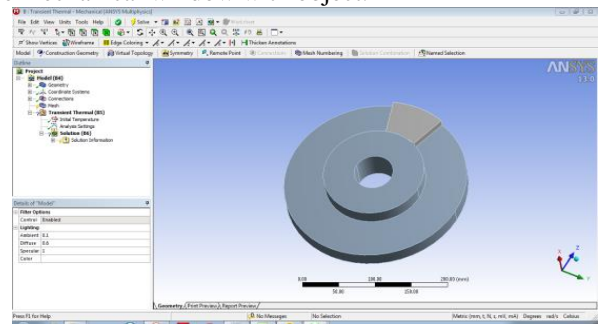


Fig 8: Model with Analysis tools

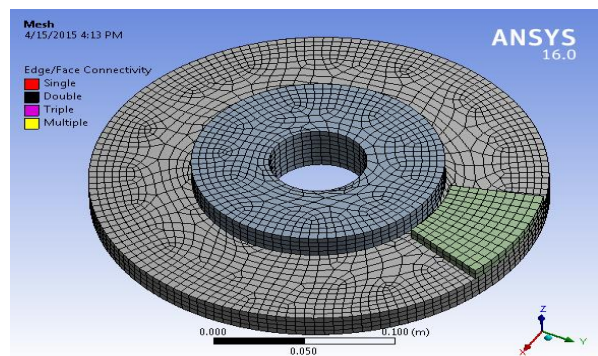


Fig 9: Meshed Geometry brake disc

CASE I:

In this case the analysis is done by assuming that the driver applied the braking for 2 sec and the temperature developed in the four different materials at this time is analyzed by using the ANSYS workbench.

Considerations for the analysis are:

Speed considered is: 80kmph

Set the initial heat flux as: $8.4414e+005 \text{ w/m}^2$

Analysis Settings: step end time 2 Sec

Ambient temperature: 22°C

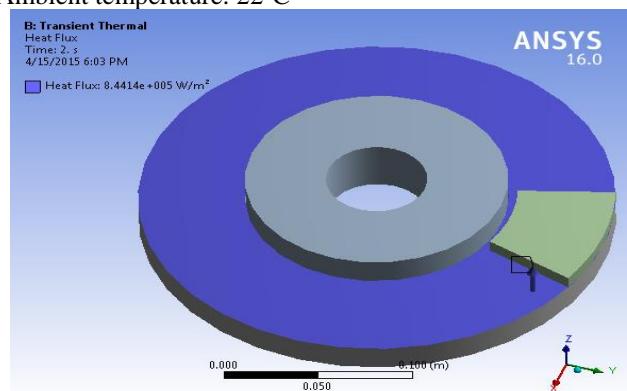


Fig 10: Heat flux at a speed of 80 Kmph

The above fig represents the heat flux value applied to the disc brake and to do give the heat flux value the following steps has to be followed. Right click on Analysis settings – Insert- heat flux – enter the value of heat flux in bottom detailed window with the braking time. To get the solution go to solution and click on solve.

Temperature distribution of various metals at a braking time of 2 sec:

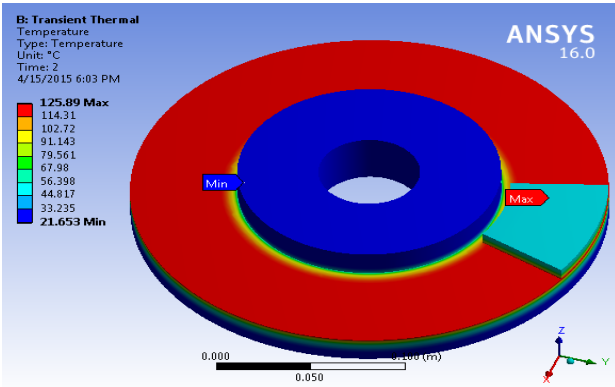


Fig 11(a): GCI

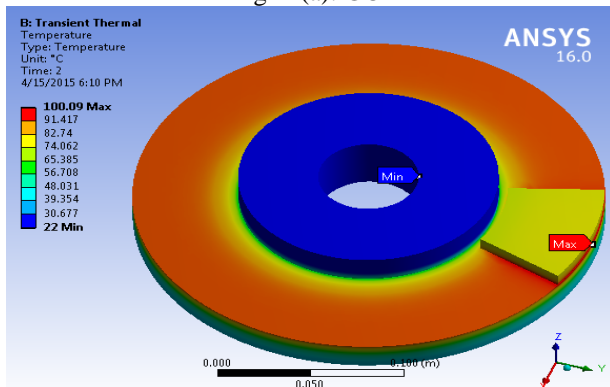


Fig 12(b): ALMMC

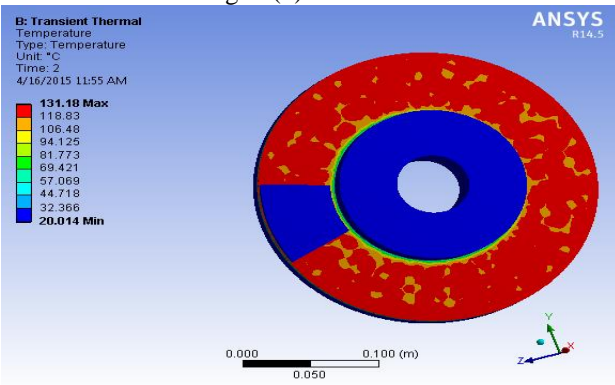


Fig 11(C): Meraging steel

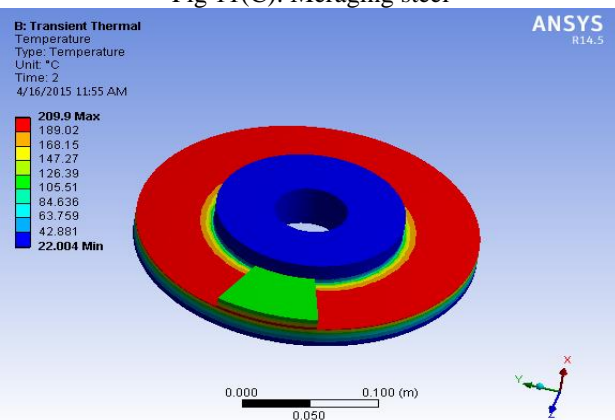


Fig 11(d): C-C composite

As the heat flux value is same with the applied heat flux value and the applied braking time the temperature generated for the different materials are shown in the figs.

The max temperature values in the different materials are 125.09°C for the gray cast iron, 100.09°C for the Aluminium metal matrix composite, and 131.18°C for the material Meraging steel 209.9°C in the material carbon-carbon composite.

CASE II:

In the case I we have shown the heat generated values that are obtained in ANSYS workbench when the input time of 2 sec is given. Now we are calculating the temperature generated values for the different materials with braking time as 4 sec. Here we don't need to assign the heat flux again because we didn't change the speed of the vehicle so by just changing the time in the analysis setting and solve the analysis.

The input parameters for the analysis are:
 Speed considered is: 80kmph
 Set the initial heat flux as: $8.4414e^{+005}$ w/m²
 Analysis Settings: step end time 4 Sec
 Ambient temperature: 22°C
 To solve the problem after giving on the above inputs Right Click on solution – Solve.
 Temperature distribution of various metals at a braking time of 4 sec:

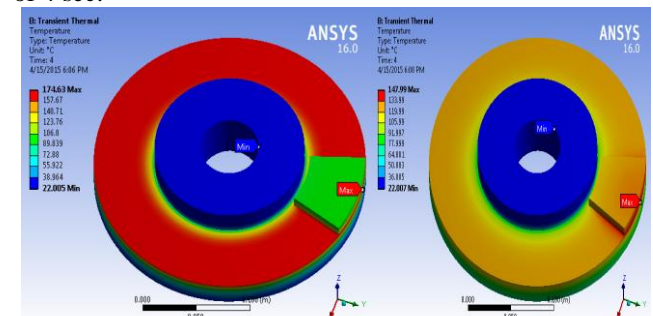


Fig 12(a): GCI

Fig 12(b):

ALMMC

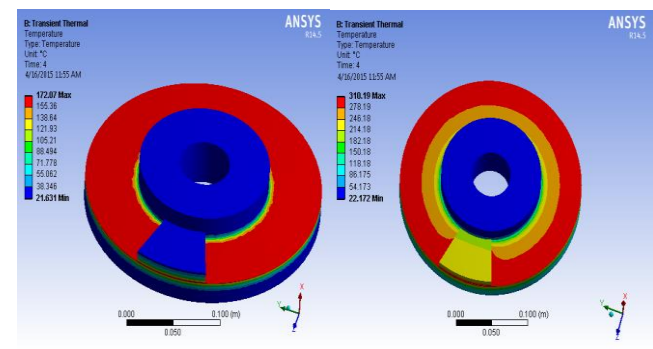


Fig 12(c): Meraging steel

Fig 12(d): C-C Composite

Fig 12:

The maximum temperature values that are generated in the four materials by giving the parameters that are mentioned above are 174.63°C for the GCI and the value for the ALMMC is 147.99°C and 172.87°C for the Meraging Steel and 310.19°C for the material carbon-carbon composite. The further analysis is done by making the speed of the vehicle as 90 Kmph for the varying time as in the above two cases.

6.1 HEAT GENERATED FOR DIFFERENT MATERIALS AT A SPEED OF 90 Km/h:

CASE-I:

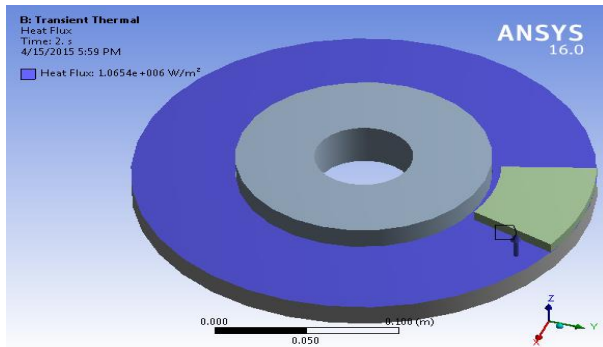


Fig 4.9: Heat flux applied at a speed of 90 Km/h
Below mentioned figures are the temperature distributions of the various materials that are under analysis.

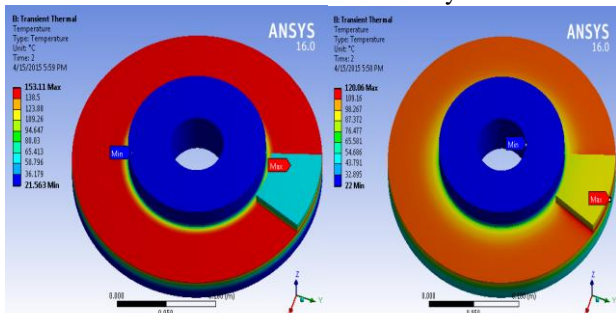


Fig 13(a): GCI Fig 13(b): ALMMC

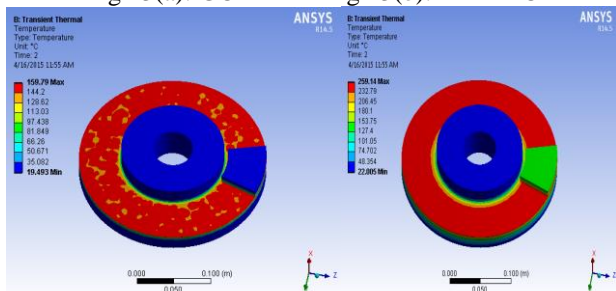


Fig 13(c): Merging steel Fig 13(d): C-C Composite
Fig 13: Temperature distribution of various metals at a braking time of 2 sec

Case II:

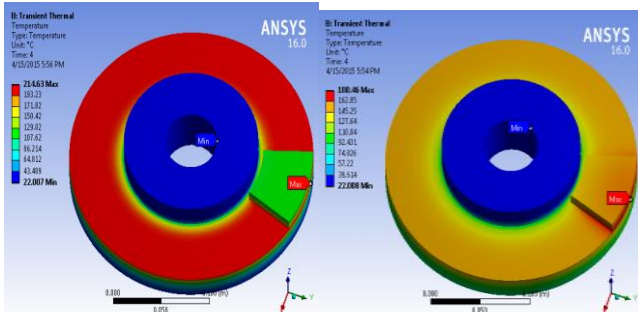


Fig 14(a): GCI Fig 14(b): ALMMC

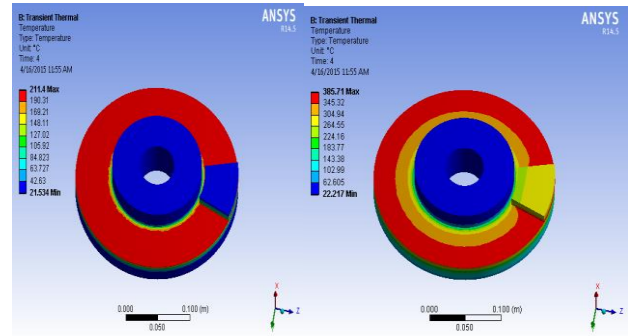


Fig 14(c): Merging steel Fig 14(d): C-C Composite
Fig 14: Temperature distribution of various metals at a braking time of 4 sec

6.2 HEAT GENERATED FOR DIFFERENT MATERIALS AT A SPEED OF 100 Km/h:
Case I:

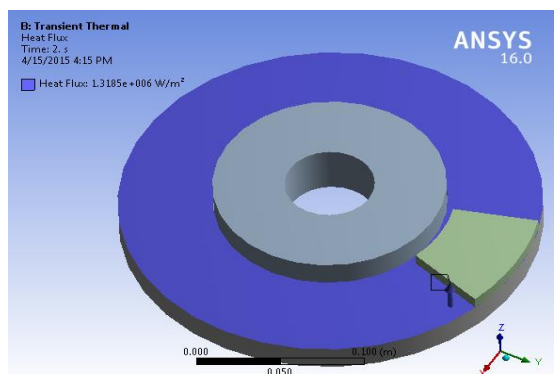


Fig 15: Heat flux applied at a speed of 100 Km/h

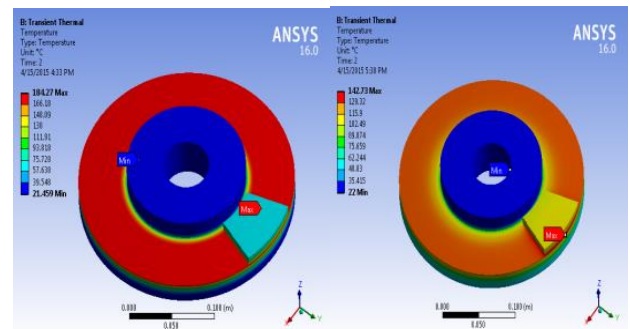


Fig 16(a): GCI Fig 16(b): ALMMC

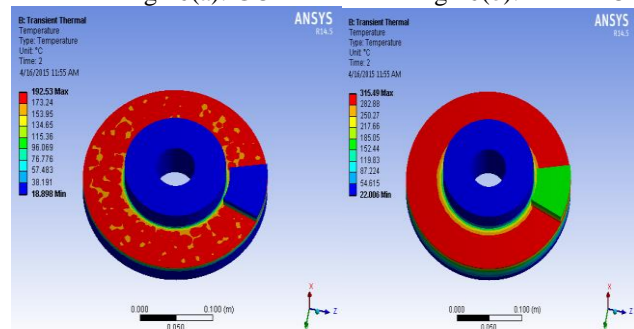


Fig 16(c): Merging Steel Fig 16(d): C-C composite
Fig 16: Temperature distribution of various metals at a braking time of 2 sec.

6.3 COOLING OF DISK BRAKE

by taking a constant temperature of 300°C for all the materials at initial position and same ambient temperature 22°C. By giving the convection value as 14.317 W/m² °C and leaving the disc to a time of 600 sec.

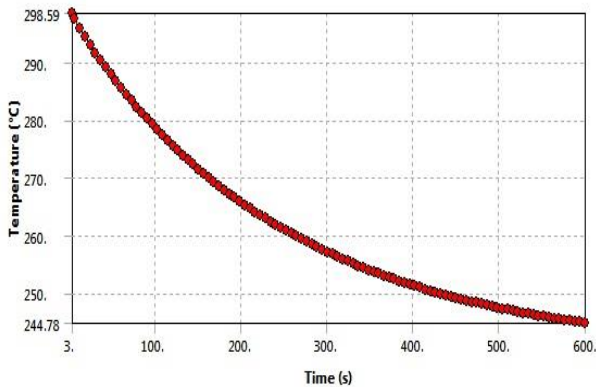


Fig 16: Variation of temperature with time in GCI

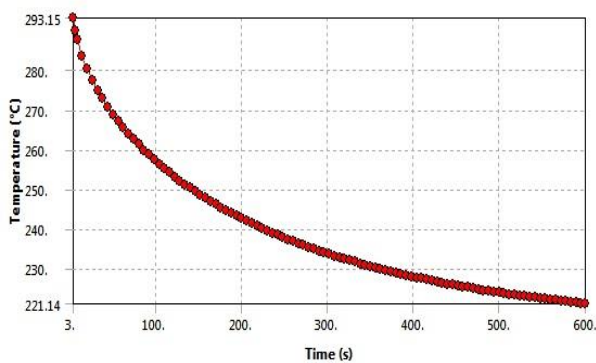


Fig 17: variation of temperature with time in ALMMC

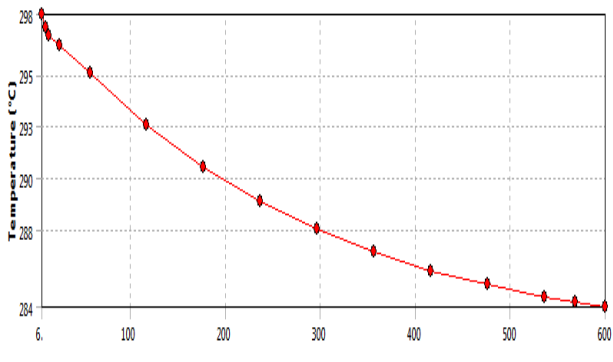


Fig 18: Variation of temperature with time in Meraging Steel

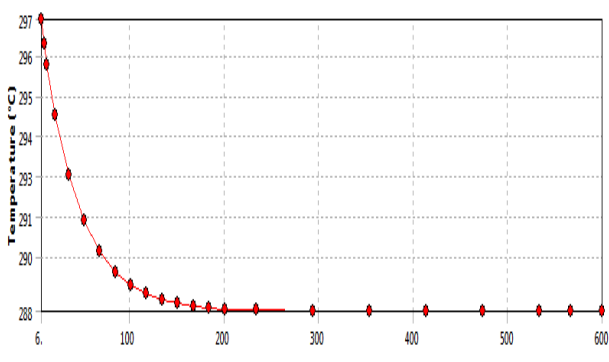


Fig 19: variation of temperature with time in C-C Composite

6.4 Transient Structural analysis:

Transient structural analysis of the disc is used to find out the deformation on the disc due to the temperatures generated and to find out the equivalent von-mises stresses developed in the materials. The results that are generated from the transient thermal analysis are used as the input parameters for this analysis.

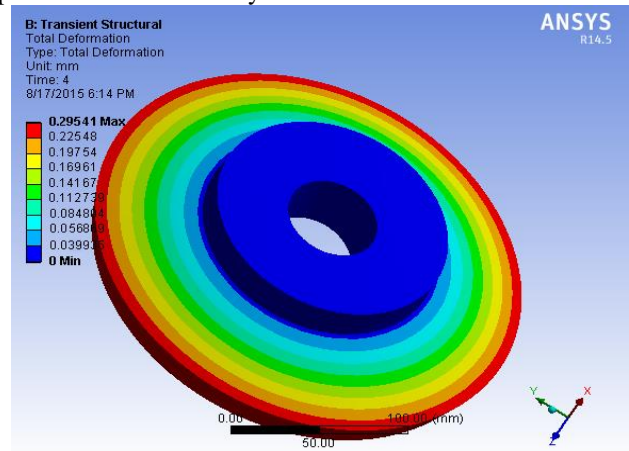


Fig 20: Deformation contour

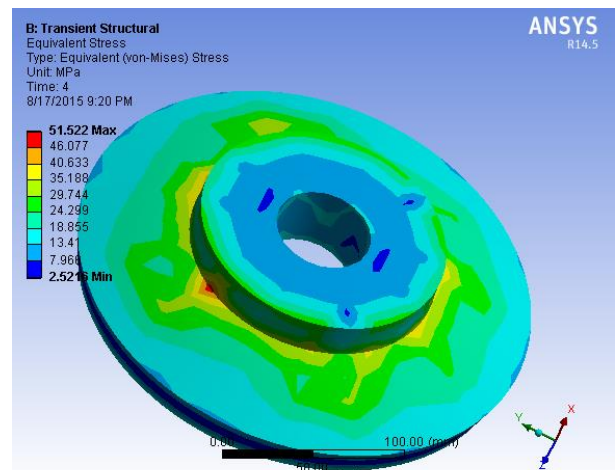


Fig 21: Von-mises stress

7. RESULTS AND DISCUSSIONS

Thermal analysis was done using ANSYS 16.0 Work bench. Different materials were used as the disc brake and did the transient thermal analysis at different speeds and the temperatures developed in different materials are observed and discussed. The effect of braking time on heat generation is also studied at different speed levels of the vehicle and the results are discussed as follows.

7.1 COMPARISON OF THE RESULTS OF VARIOUS MATERIALS

The table 5.1 shows the temperatures that are generated in the materials when the braking is applied for the 2 sec time. The values of the table are plotted in the graph shown in the Fig: 5.1 by taking the temperature on the X- axis and the speed on the Y- axis.

Table 1 Temperature generated in the material at a braking time of 2 sec for different material

Speed	Max. Temperature in the material(in degrees) at 2 sec			
	GCI	ALMMC	Meraging Steel	C-C Composite
80 Kmph	125.09	100.09	131	209.9
90 Kmph	153.11	120.06	159.79	259.14
100 Kmph	184.27	142.73	192.53	315.49

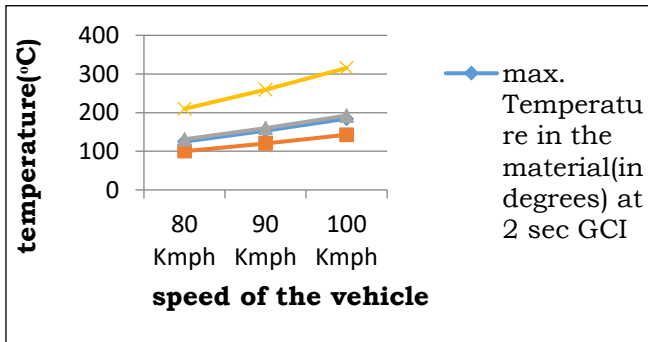


Fig 22 variation in Temperature with speed for the materials at a braking time of 2 sec

By observing the graph shown in the fig 5.1 we can say that the temperature that is developed in the disc brake is maximum for the C-C Composite and the value of the temperature generated in the material ALMMC is minimum. Temperature developed in the materials GCI and in the Meraging steels are nearly same but when we go very accurate the developed temperature in the Meraging steel is more.

Here we can also observe that the Temperature developed varies uniformly with respect to the speed.

Table 2 Temperature generated in the material at a brake time of 4 sec for different speeds

speed	Max. Temperature in the material(in degrees) at 4 sec			
	GCI	ALMMC	Meraging Steel	C-C Composite
80 Kmph	174.63	147.99	172	310.9
90 Kmph	214.63	180.46	211.4	385.71
100 Kmph	260.4	217.2	256.4	472.13

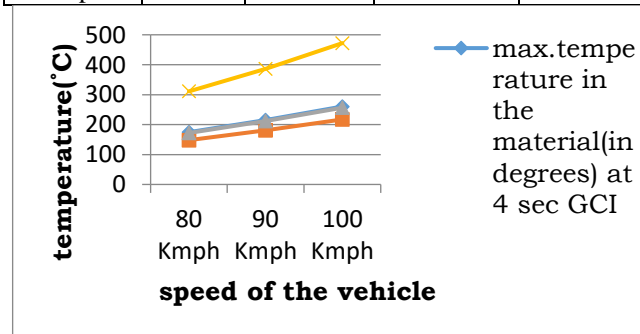


Fig.23 Change in Temperature with speed for the materials at 4 sec

7.2 COOLING CURVE OF THE MATERIALS

We have suggested the material above on the basis of the heat generated in the material and now we are analyzing the value of the temperature reduction in these materials within the stipulated period of time when they are put to the convection in the air.

When the same time and the convection is applied for the different materials their final temperature come to different value after the given time. Below shown is the temperature variation in the different materials with respect to time.

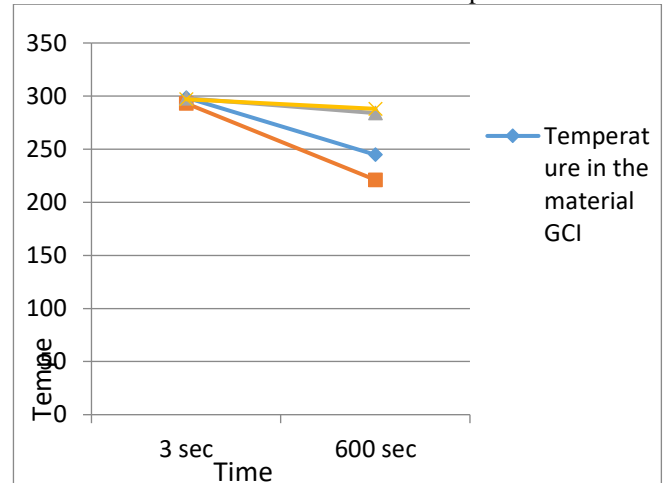


Fig 24 Temperature reduction in the different materials Where weight is specifically required for good performance.

3 TRANSIENT STRUCTURAL ANALYSIS OF DIFFERENT MATERIALS:

Table 3 Stresses and deformation in the materials

Material	Deformation(mm)	Von-mises Stress(Mpa)
GCI	0.295	51.52
ALMMC	0.315	191.71
Meraging Steel	0.354	51.351
C-C Composite	0.473	85.426

From the above results of the deformation and von-mises stress the maximum deflection that is obtained in the material C-C Composite where as the minimum deflection among the four materials is Gray Cast Iron. In the aspect of the von-mises stress the maximum stress is generated in the material ALMMC and the minimum value of the von-mises stresses are almost equal in the materials GCI and Meraging steel.

The stresses produced in the materials are within the allowable stress limit so we can now consider the maximum advantages of the materials and also the deformations produced in the materials are in the safe values. From the above all results we can make a conclusion based on the purpose of the braking used and the loads that may apply on the braking materials. For the different operating conditions different materials show their advantages

8. CONCLUSIONS

The transient thermal analysis of disc brake made of different materials was studied. The different materials considered for the study are Gray cast iron, Al-MMC, Meraging steel and C-C Composite. The heat flux is calculated based on the kinetic energy generated during the time of brake application. The heat flux generated is applied on to the disc for different time instants and temperature rise as the response is studied. Transient structural analysis is done to find out the stresses developed in the materials because of the increase in temperature. The comparative study made between different disc materials. The heat dissipation from the materials is also studied by considering convective heat transfer.

From the above results from the tables and graphs we can say that the temperature developed for ALMMC is low in all the conditions. The temperature developed in C-C Composite is more as compared to the other materials in all the cases. The considered parameters are speed and braking time. The obtained values are peak temperature distribution with these stresses the deformations and the stresses developed in the materials are produced.

From the heat dissipation analysis of the disc brake materials we observed that ALMMC dissipates more heat than the other materials. The Properties of ALMMC also shows improved cooling effect due to its high thermal conductivity when compared to conventional GCI.

From the obtained values of the stresses and the deformation values of the materials GCI and Almmc are the advantage materials among the other materials but the deformation in the Almmc material is less than GCI where as the stress in the GCI is less than the ALMMC. Though the values are within the permissible limit both materials can be used as a disc brakes based on the loading conditions. Both the materials have the pros and cons but the advantages with the ALMMC are more than the GCI.

ALMMC has lower density and higher thermal conductivity as compared to GCI and it results in weight reduction upon 50-60% in brake system as well as improves fuel economy of the vehicle. Because of the heat generation is more in the racing cars ALMMC brake disc cannot with stand those high temperatures so it is suitable to use ALMMC brakes in Consumer cars and in the military transport vehicles. The Rate of heat generation with the speed is less for ALMMC as compared to other materials by considering all the above parameters ALMMC brake is good for brake disc when it is suitable for the loading conditions.

REFERENCES

- [1] Manjunath T V, Dr Suresh P M, "Structural and Thermal Analysis of Rotor Disc of Disc Brake", Vol. 2, Issue 12, December 2013, ISSN: 2319-8753.
- [2] V. Chengal Reddy. "Modeling And Analysis of FSAE Car Disc Brake Using FEM",IJRET (ISSN 2250-2459, ISO 9001:2008 Certified Journal, Volume 3, Issue 9, September 2013).
- [3] Ali Belhocine, "Thermal analysis of a solid brake disc", Applied Thermal Engineering 32 (2012) 59-67.
- [4] Faramarz Talati, "Analysis of heat conduction in a disk brake system", Heat Mass Transfer (2009) 45:1047–1059.

- [5] Subhasis Sarkar, "Modeling and Simulation of Disc Brake to Analyze Temperature Distribution using FEA", IJSRD - Issue 03, 2014 | ISSN (online): 2321-0613.
- [6] NosaIdusuyi, "A Computational Study on the Use of an Aluminium Metal Matrix Composite and Aramid as Alternative Brake Disc and Brake Pad Material". Received 15 May 2014; Accepted 30 July 2014; Published 26 August 2014.
- [7] Guru Murthy Nathi, "Coupled Structural / Thermal Analysis Of Disc" IJRET, ISSN: 2319-1163.
- [8] Belhocine, "Thermal analysis of both ventilated and full disc brake rotors with frictional heat generation", Received 3 March 2014; received in revised form 27 June 2014
- [9] Peter J. Blau, "Compositions, Functions, and Testing of Friction Brake Materials and Their Additives", August 2001
- [10] Paul Wambua, "Natural fibres can they replace glass in fibre reinforced plastics", Accepted 21 February 2003.
- [11] W. Osterle, "Towards a better understanding of brake friction materials", Available online 13 March 2007.
- [12] N. Balasubramanyam, "Design and Analysis of Disc Brake Rotor for a Two Wheeler", October 2013-March 2014.

A STUDY OF BOUNDARY LAYER FLOW OVER BULLET SHAPED OBJECT

R. Mohana Ramana¹, G. Dharmiah², M. Sreenivasa Kumar³.

^{1,2}Department of Mathematics, Narasaraopeta Engineering College, Yellamanda, Narasaraopet, A.P., 522601, INDIA.

³Professor, Department of Mechanical Engineering, Narasaraopeta Engineering College, Yellamanda, Narasaraopet, A.P.,

ABSTRACT: Axisymmetric concerns may be found in a wide variety of various industries and can takes a shape of round toroids, cones, cylinders, and other shapes as well. When it comes to actual applications, they are represented by submarine pressure hulls, offshore drilling rigs, radomes, and other similar objects. The goal of this research is to improve the performance using a heat source and viscous dissipation. The viscous convective flow flowing through a bullet-shaped item is examined. Using similarity transformations, the structure of nonlinear differential equations is transformed into dimensionless ODEs. BVP4C is used to decrypt the findings. An influence of physical entities on velocity and temperature are drawn and briefly described. Physical behavior of skin friction and heat transfer rates are examined. Believing that of the design of this item has an impact on the thermal properties and fluid velocity of the surrounding environment.

KEY WORDS: Viscous dissipation; bvp4c; MHD; Heat Source.

INTRODUCTION

Chen and Smith [1] performed an analytical examination of the steady laminar convective transport flow of nonisothermal flows. A poignant isothermal tiny needle as an analogy for stirring flow, they employed the finite-difference approach in their illustration of the flow utilized by Ishak et al. [2]. Stimulation of nonlinear radiation impact on Casson flow liquid along a tiny needle may be achieved by taking into account double diffusion effects described by Souayah et al. [3]. Nayak et al. [4] researched the influence of changing buoyant force and dissipative influences on the nanoliquids flows via a poignant thin needle by investigating the flow of nanoliquids through a poignant slim needle. Chu et al.[5] explored the role of homogeneous reactions with internally diffusions of particles on a thin surface needle while accounting into consideration heat flow.

The inclusion of dissipation effects in the analyzation of mass and heat transport boundary layer issues opened up a whole new dimension in fluid dynamics research field. The influence of dissipation on fluid flows has also been examined extensively by various scholars. With respect to regular convection in various devices, the influence of viscous dissipation plays a significant part in the process. Viscous dissipation is the term used to describe the process in which work is done by a fluid that is also transformed into heat as a result. When applied to a flow, it represents the connection between its kinetic energy and its enthalpy, and it is used to define the dissipation. Results of a dissipative MHD flow that is stratified thermo-solutal by Murugesan et al. [6]. Sharma and Gupta [7] has shed light on the behavior of dissipative

MHD flow of non-newtonian Nanofluid. Jordan [8] was able to gather information regarding the impacts of dissipation on the flow, using the NSM and solved an unsteady MHD free convection flow. Suneetha et al. [9] have provided excellent papers on hydromagnetic flows that take into consideration viscous dissipation. Earlierly, many authors (Waini et al. [10], Mallick et al. [12], Seth et al [13], Megahed [14]) formulated their research papers on MHD flow through a stretched sheet using dissipative impacts.

Using similarity transformations, the nonlinear structure of the differential equations is transformed into dimensionless ODEs. BVP4C is used to decrypt the findings. The effect of physical entities on velocity and temperature profiles is drawn and briefly described. The Skin friction and the rate of heat transfer are numerical outputs, and the physical behavior is also examined. It is believed that the design of this item has an impact on the thermal properties and fluid velocity of the surrounding environment. The present analysis, concerns may be found in a wide variety of various industries and can take the shape of round cylinders, cones, domes, toroids, and other shapes as well.

MATHEMATICAL MODELING

The steady two-dimensional MHD laminar flow of an incompressible, electrically conducting and viscous fluid over bullet shaped stretching surface in a bulk fluid is described. The schematic illustration of the model is shown in Fig. 1.

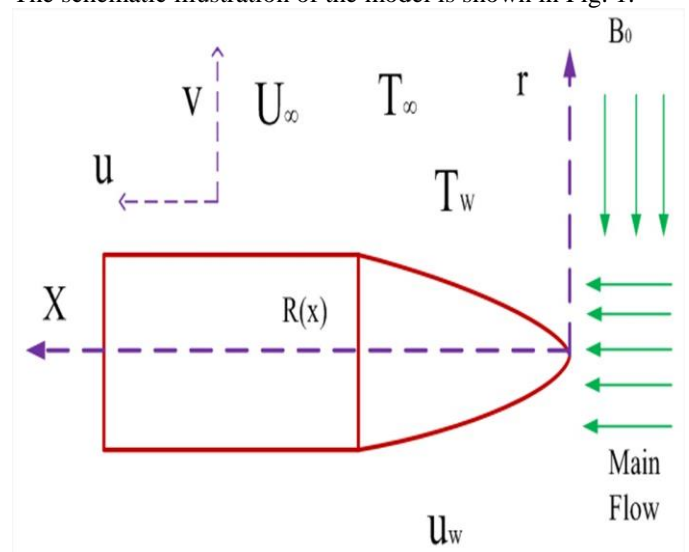


Figure 1: Flow modeling of the problem

The flow assumptions for this problem are:

- The U_∞ and U_w are free stream and the stretching velocities respectively.
- (x, r) – co-ordinates assumed along the bullet surface shaped and the radial direction respectively.
- The T_w & T_∞ are temperature of the surface and free stream temperature respectively.

The surface is an isothermal surface, the temperature T_w such that the temperature differences maintained in the flow are kept to a minimum. When the surface moves at a velocity $U_w(x)$, in opposite or same direction of the free stream velocity $U_\infty(x)$. The velocity of the surface $U_w(x)$, the free stream velocity $U_\infty(x)$ and the temperature of the surface T_w are respectively defined as $U_w(x) = ax^m$, $U_\infty(x) = bx^m$, $T_w(x) = x^{2m-1}$, where a and b ($b > 0$) are the stretching rate of the sheet and straining rate parameters respectively with a > 0 for stretching case and a < 0 for the shrinking case. One thing to keep in mind is that the constant ‘b’ is proportional to the free velocity far away from the surface.

The continuity, momentum and the thermal energy are considered

$$\frac{\partial}{\partial x}(ru) + \frac{\partial}{\partial r}(rv) = 0 \tag{1}$$

$$u \frac{\partial u}{\partial x} + v \frac{\partial u}{\partial r} = U \frac{\partial U}{\partial x} + \frac{v}{r} \left[\frac{\partial u}{\partial r} + r \frac{\partial^2 u}{\partial r^2} \right] + \frac{\sigma B_0^2}{\rho(1+m_1^2)} [U - u] \tag{2}$$

$$u \frac{\partial T}{\partial x} + v \frac{\partial T}{\partial r} = \frac{\alpha}{r} \left[\frac{\partial T}{\partial r} + r \frac{\partial^2 T}{\partial r^2} \right] + \frac{Q^*}{\rho C_p} [T - T_\infty] - \frac{\mu}{\rho C_p} \left[\frac{\partial u}{\partial r} \right]^2 \tag{3}$$

The relative BCs are

$$u = U_w(x), v = 0, T = T_w \quad \text{at} \quad r = R(x) \tag{4}$$

$$u \rightarrow U_\infty(x) = U, T \rightarrow T_\infty \quad \text{as} \quad r \rightarrow \infty \tag{5}$$

The stream function velocity components are

$$u = \frac{1}{r} \frac{\partial \psi}{\partial r} \quad \text{and} \quad v = -\frac{1}{r} \frac{\partial \psi}{\partial x} \tag{6}$$

Transformations for axisymmetric surface are

$$\eta = \frac{Ur^2}{vx}; \quad \psi = vxf(\eta); \quad T = x^{2m-1}\theta(\eta); \quad U_w(x) = ax^m;$$

$$U_\infty(x) = bx^m; \quad T_w(x) = x^{2m-1}; \quad M = \frac{\sigma B_0^2 x}{2\rho U};$$

$$\varepsilon = \frac{U_w}{U}; \quad \text{Pr} = \frac{\nu}{\alpha}; \quad Q^* = \frac{Qx}{\rho U_w C_p}; \quad \text{Ec} = \frac{U_w^2}{C_p(T_w - T_\infty)}; \tag{7}$$

Substituting (7) into (2)-(3) with (4)-(5) we can obtain ODEs

$$\eta f''' + f'' + \frac{1}{2} ff'' + \frac{m}{8}(1-4f'^2) + \frac{M}{8(1+m_1^2)}(1-2f') = 0 \tag{8}$$

$$\eta \theta'' + \frac{1}{2} \theta' + \frac{\text{Pr}}{2}(f\theta' - (2m-1)f'\theta) + \frac{1}{4} \text{Pr} Q\theta - \text{Ec} \text{Pr} f'^2 = 0 \tag{9}$$

The corresponding BCs are

$$f(\eta) = 0, f'(\eta) = \frac{\varepsilon}{2}, \theta(\eta) = 1 \quad \text{at} \quad \eta = s \tag{10}$$

$$f(\eta) \rightarrow \frac{1}{2}, \theta(\eta) \rightarrow 0 \quad \text{at} \quad \eta \rightarrow \infty \tag{11}$$

The skin-friction and the Nusselt number are

$$C_f = \frac{\mu}{\rho U^2} \left[\frac{\partial u}{\partial r} \right]_{r=0} = 4 \sqrt{\frac{\eta}{\text{Re}_x}} f''(\eta) \Rightarrow C_f \sqrt{\text{Re}_x} = 4 \sqrt{\eta} f''(\eta) \tag{12}$$

$$\text{Nu}_x = \frac{xq_w}{\kappa(T_w - T_\infty)} \Rightarrow \text{Nu}_x (\text{Re}_x)^{-\frac{1}{2}} = -2 \sqrt{\eta} \theta'(\eta) \tag{13}$$

METHODOLOGY

The nonlinear non dimensional transformed the equations (8)–(9) along with boundary conditions (10)-(11) has been resolved with MATLAB built-in function bvp4c scheme. It is possible to turn a system of PDEs into a system of first-order ODEs by making use of the variables indicated below.

$$f = f(1); f' = f(2); f'' = f(3); \theta = f(4); \theta' = f(5)$$

Thus, the equations (8)-(9) becomes

$$\frac{d}{d\eta} f(1) = f(2)$$

$$\frac{d}{d\eta} f(2) = f(3)$$

$$\frac{d}{d\eta} f(3) = \frac{1}{\eta} \left[-f(3) - \frac{1}{2} f(1)f(3) - \frac{m}{8}(1-4(f(2))^2) - \frac{M}{8(1+m_1^2)}(1-2f(2)) \right]$$

$$\frac{d}{d\eta} f(4) = f(5)$$

$$\frac{d}{d\eta} f(5) = \frac{1}{\eta} \left[\text{Ec} \text{Pr} (f(3))^2 - \frac{1}{2} f(5) - \frac{1}{2} \text{Pr} (f(1)f(5) - (2m-1)f(2)f(4)) - \frac{1}{4} \text{Pr} Q f(4) \right]$$

RESULTS AND DISCUSSION

The performance of viscous dissipation, and a heat source on the viscous convective flow flowing through a bullet-shaped item is examined. The non-linear ODEs of the problem are solved by using BVP4C. It is shown visually how physical factors affect for BL distributions along with skin friction, heat and mass transfer. This article default factors entire the article is: $S = 0.05$; $M = 1$; $Pr = 0.71$; $m = 1$, $Q = 0.5$; $Ec = 0.01$.

Figure 2 denotes the dimensionless surface thin parameter (S) when $\epsilon < 1.0$ or $= 1$ or > 1.0 with similarity variable η values on velocity profile. Clearly, within the momentum MBL the fluid velocity enhances as $\epsilon < 1.0$ where as the momentum BL thickness decreases $\epsilon > 1.0$ because the velocity surface influences over the free stream velocity. As a result, the velocity boundary layer thickness expands. **Figure 3** denotes the Eckert number Ec when $\epsilon < 1.0$ or $= 1$ or > 1.0 with the finite values of the similarity variable η and with surface thin parameter $S = 0.05$ on velocity profile. Clearly, within the momentum BL the fluid velocity lessens as $\epsilon < 1.0$ where as the momentum BL thickness increases $\epsilon > 1.0$.

Figure 4 shows an influence of the magnetic field when $\epsilon > 1.0$ or $= 1$ or < 1.0 and surface thin parameter $s = 0.05$ on the fluid flow profile. Physically, the velocity profile and BL thickness reduced when $\epsilon < 1.0$ or > 1.0 . **Figures 5** illustrates the variation of viscous fluid temperature profile for the effect of heat generation parameter (Q) for thinner surface ($S = 0.05$), when the stretching ratio parameter $\epsilon > 1$; $= 1$; < 1 , with the surface thickness parameter $S = 0.05$, and $Pr = 0.71$ respectively. From this figure, the variation of Q has an insignificant effect on fluid temperature.

The impact of the hall parameter m_1 on the temperature is discussed in **Figure 6** with the thinner surface parameter $S = 0.05$. It reveals that the increasing values of hall parameter m_1 has an adroit effect on the fluid temperature as it is seen when $\epsilon > 1.0$ or $= 1$ or < 1.0 . **Figure 7** depicts the influence of skin friction as a function of Pr for various values of M . According to what we already know, the drag of skin-friction is in relation to the dimensionless flow gradient. Consequently, skin friction reduces in case of $\epsilon > 1.0$, physically viscous force pre-dominates over the hydromagnetic body force.

The graph of skin friction is plotted for the different values of power law index m in **figure 8**. The results are produced for the case of $\epsilon = 0.2$ and $S = 0.05$. We find that, the Figure describes that an improve in the Darcy-Forchhemier parameter Fr , results in the enhance in the skin-friction. The graph of Nusselt number is plotted for the various values of m in **figure 9**. The results are produced for the case of $\epsilon = 2.0$ and $S = 0.05$. We find that, the Figure describes that a rise in the ‘ m ’ leads to enhance in nusselt number.

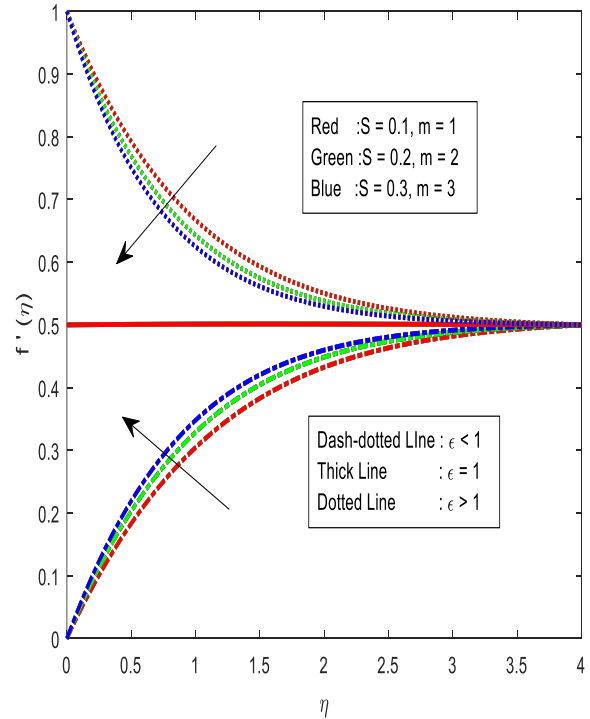


Figure 2. Influences of thinner surface S on velocity

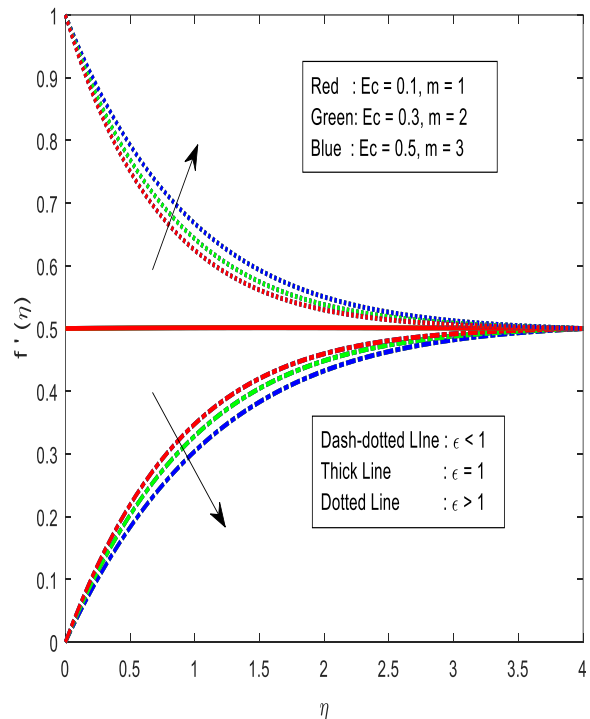


Figure 3. Influences of Eckert number Ec on velocity

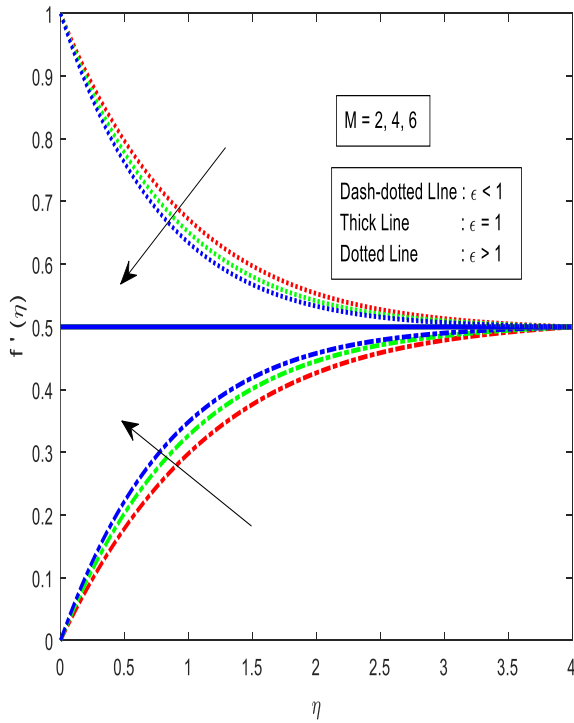


Figure 4. Influences of magnetic parameter M on velocity

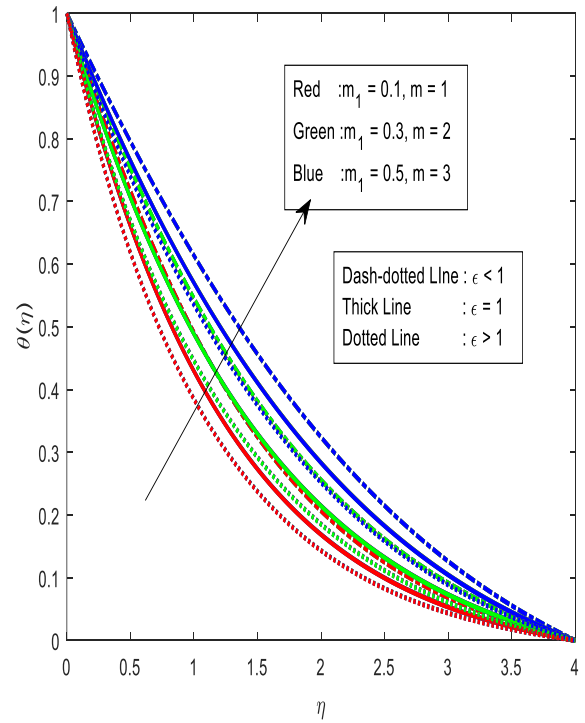


Figure 6. Influences of hall parameter m_1 on temperature

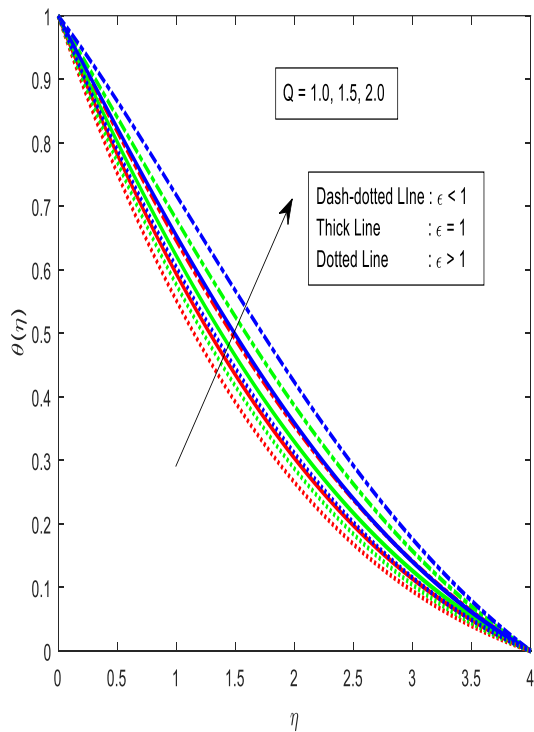


Figure 5. Influences of Heat generation Q on temperature

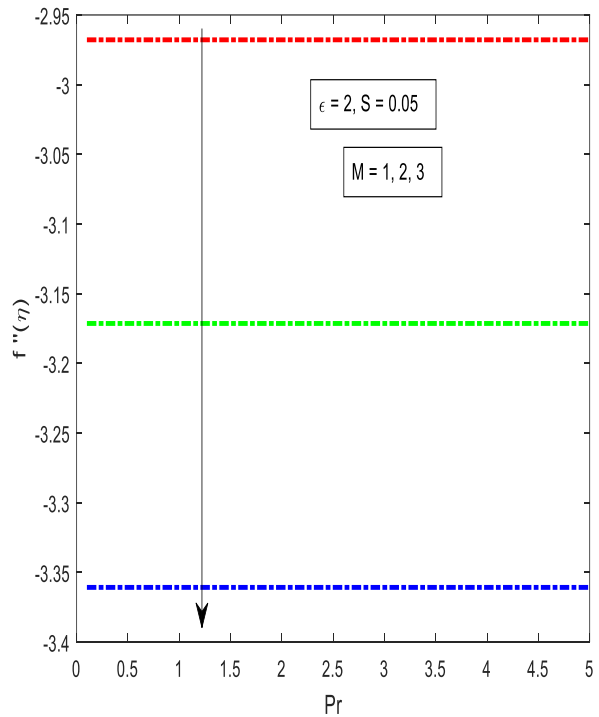


Figure 7. Adaptations of Skin-friction accordant with Pr for several values of M .

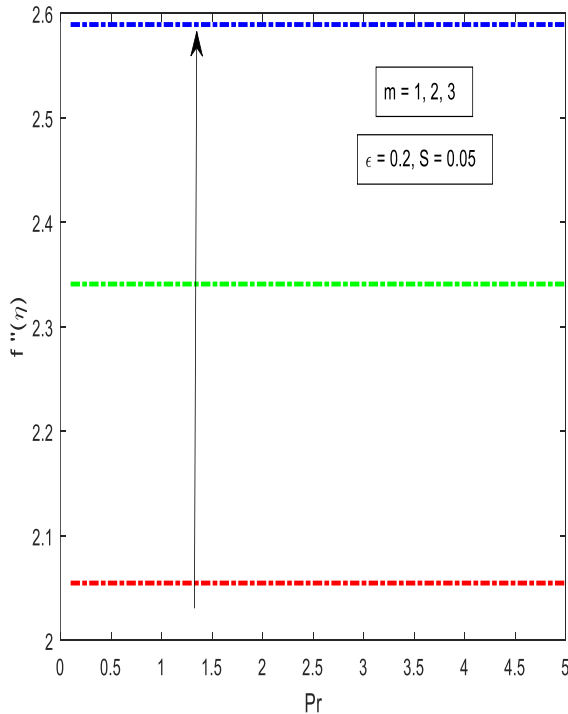


Figure 8. Adaptations of Skin-friction accordant with Pr for several values of m .

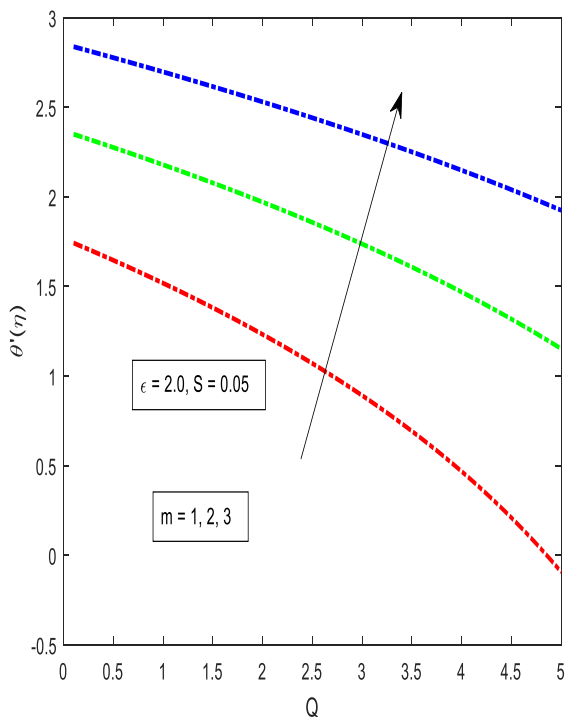


Figure 9. Adaptations of Nusselt number accordant with Q for several values of m .

CONCLUSIONS

The effect of various parameters on MHD laminar boundary layer flow of an incompressible, electrically conducting, and viscous Newtonian fluid past a stretching electrically non-conducting bullet-shaped object with heat transfer has been carried out. The performance of viscous dissipation, and a heat source on velocity and temperature profiles are examined. The non-linear ODEs of the problem are solved by using BVP4C technique. The effect of physical entities on velocity and temperature profiles is drawn and briefly described. The Skin friction and the rate of heat transfer are numerical outputs, and the physical behavior is also examined. The default parameters are: $S = 0.05$; $M = 1$; $Pr = 0.71$; $m = 1$, $Q = 0.5$; $Ec = 0.01$ throughout the problem. Within the momentum BL the fluid velocity increases for dimensionless surface thin parameter (S) as $\epsilon < 1.0$ whereas the momentum BL thickness decreases $\epsilon > 1.0$ because the surface velocity dominates over the free stream velocity. The velocity and thickness of BL lessens for magnetic field parameter when $\epsilon < 1.0$ or > 1.0 . It reveals that the increasing values of power law index m has a halting impact on the fluid temperature as it is seen when $\epsilon > 1.0$ or $= 1$ or < 1.0 . It reveals that the increasing values of ‘ ϵ ’ has a halting effect on the fluid temperature as it is seen when $\epsilon > 1.0$ or $= 1$ or < 1.0 . It reveals that the increasing values of Pr has a halting impact on the fluid temperature as it is seen when stretching ratio $\epsilon > 1.0$ or $= 1$ or < 1.0 . It reveals that the increasing values of hall parameter m_1 has an adroit effect on the fluid temperature as it is seen when stretching ratio $\epsilon > 1.0$ or $= 1$ or < 1.0 . Rise in ‘ M ’ leads to declines in heat transfer rate. Rise in ‘ m ’ leads to enhance in heat transfer rate.

BIBLIOGRAPHY

- [1] [1] J. L. S. Chen and T. N. Smith, “Forced convection heat transfer from nonisothermal thin needles,” *J. Heat Transfer*, vol. 100, no. 2, pp. 358–362, 1978, doi: 10.1115/1.3450809.
- [2] [2] P. I. Ishak, Anuar, Nazar.R, “Boundary Layer flow over a continuously moving thin needle in a parallel free stream,” *Chin.Phys.Letters*, vol. 24, no. 10, pp. 2895–2897, 2007.
- [3] [3] B. Souayah, M. G. Reddy, P. Sreenivasulu, T. Poornima, M. Rahimi-Gorji, and I. M. Alarifi, “Comparative analysis on non-linear radiative heat transfer on MHD Casson nanofluid past a thin needle,” *J. Mol. Liq.*, vol. 284, pp. 163–174, 2019, doi: 10.1016/j.molliq.2019.03.151.
- [4] [4] M. K. Nayak, F. Mabood, and O. D. Makinde, “Heat transfer and buoyancy-driven convective MHD flow of nanofluids impinging over a thin needle moving in a parallel stream influenced by Prandtl number,” *Heat Transf. - Asian Res.*, no. October, 2019, doi: 10.1002/htj.21631.
- [5] [5] Y. M. Chu, M. I. Khan, M. I. Ur Rehman, S. Kadry, and M. K. Nayak, “Flow and thermal management of MHD Cross nanofluids over a thin needle with auto

- catalysis chemical reactions,” *Int. J. Mod. Phys. B*, vol. 2050287, pp. 1–14, 2020, doi: 10.1142/S0217979220502872.
- [6] [6] T. Murugesan and M. D. Kumar, “Viscous dissipation and Joule heating effects on MHD flow of a Thermo-Solutal stratified nanofluid over an exponentially stretching sheet with radiation and heat generation/absorption,” *World Sci. News*, vol. 129, no. May 2019, pp. 193–210, 2019.
- [7] [7] K. Sharma and S. Gupta, “Viscous Dissipation and Thermal Radiation effects in MHD flow of Jeffrey Nanofluid through Impermeable Surface with Heat Generation/Absorption,” *Nonlinear Eng.*, vol. 6, no. 2, pp. 153–166, 2017, doi: 10.1515/nleng-2016-0078.
- [8] [8] J. Z. Jordán, “Network simulation method applied to radiation and viscous dissipation effects on MHD unsteady free convection over vertical porous plate,” *Appl. Math. Model.*, vol. 31, no. 9, pp. 2019–2033, 2007, doi: 10.1016/j.apm.2006.08.004.
- [9] [9] S. Suneetha, N. B. Reddy, and V. R. Prasad, “Thermal Radiation Effects on MHD Free Convection Flow Past an Impulsively Started Vertical Plate with Variable Surface Temperature and Concentration,” *J. Nav. Archit. Mar. Eng.*, vol. 5, no. 2, pp. 57–70, 2009, doi: 10.3329/jname.v5i2.2695.
- [10][10] I. Waini, A. Ishak, and I. Pop, “MHD flow and heat transfer of a hybrid nanofluid past a permeable stretching/shrinking wedge,” *Appl. Math. Mech. (English Ed.)*, vol. 41, no. 3, pp. 507–520, 2020, doi: 10.1007/s10483-020-2584-7.
- [11][11] B. Mallick, J. C. Misra, and A. R. Chowdhury, “Influence of Hall current and Joule heating on entropy generation during electrokinetically induced thermoradiative transport of nanofluids in a porous microchannel,” *Appl. Math. Mech.*, vol. 40, no. 10, pp. 1509–1530, 2019, doi: 10.1007/s10483-019-2528-7.
- [12][12] G. S. Seth, R. Tripathi, and M. K. Mishra, “Hydromagnetic thin film flow of Casson fluid in non-Darcy porous medium with Joule dissipation and Navier’s partial slip,” *Appl. Math. Mech. (English Ed.)*, vol. 38, no. 11, pp. 1613–1626, 2017, doi: 10.1007/s10483-017-2272-7.
- [13][13] A. M. Megahed, “Carreau fluid flow due to nonlinearly stretching sheet with thermal radiation, heat flux, and variable conductivity*,” *Appl. Math. Mech. (English Ed.)*, vol. 40, no. 11, pp. 1615–1624, 2019, doi: 10.1007/s10483-019-2534-6.

OPTIMIZATION OF STEAM TURBINE BLADE AND ITS ANALYSIS

K. Chandra sekhar¹ Dr.B. Sudheer Prem Kumar²

¹Associate Professor, Department of Mechanical engineering, QIS College of engineering and Technology, Ongole, AP, India

²Professor, Department of Mechanical JNT University, Hyderabad, Telangana, India 500085 Email id: bsudheepk@jntu.ac.in

ABSTRACT

A steam turbine is a mechanical device that extracts thermal energy from pressurized steam, and converts it into rotary motion. A system of angled and shaped blades arranged on a rotor through which steam is passed to generate rotational energy. The blades are designed in such a way as to produce maximum rotational energy by directing the flow of the steam along its surface. The blades are made at specific angles in order to incorporate the net flow of steam over it in its favor. The blades may be of stationary or fixed and rotary or moving or types.

The main aim of the project is to suggest the best material with in low cost. The project equipped with the construction and analysis of steam turbine blade with different materials used generally (chrome steel, titanium) and the project improves the mechanical properties like stress, displacement, temperature gradient and thermal flux etc of blade material for which the new material usage is introduced which is cast iron with zirconium coating.

1.0 OPTIMIZATION TECHNIQUES AND SELECTION

Optimization techniques can be classified based on the type of constraints, nature of design variables, physical structure of the problem, nature of the equations involved, deterministic nature of the variables, permissible value of the design variables, separability of the functions and number of objective functions.

2.0 GENERATION OF PRESSURE DISTRIBUTION DATA ON THE BLADE SURFACE:

Last stage blade of steam turbine, which is being analyzed, for stress and vibration is a highly twisted blade due to the variation if the blade speeds across the height of the blade. The deflection in the blade passage also reduces from hub to tip to vary the loading on each section. Thus the pressure distribution on the suction & pressure surface of the blade changes considerably from hub to tip to match the loading at that section. It is known fact that the area of pressure distribution curve representing the blade loading. Hence it has been decided to generate the pressure distribution at all the '17' blade sections.

The following procedure allows to get the blade surface pressure distribution with the help of BladeGen & BladeGen plus package.

1. From the blade coordinate input data file for suction/pressure surface x, y, z, coordinate of surface was generated as a loop with the following notations.

X-along the height of the blade, Y- Meridional direction, Z-along blade to blade

2. Profile curve is generated with above coordinates of all sections placed one below the other is sequence from section (1) to section (5 along the height of the blade. The coordinates between two section separated by '#'.

3. Hub & Shroud boundary is generated at the appropriate heights with -Y negative meridional axis corresponded from LE (Leading edge). And positive distance from meridional distance from TE (Tailing Edge).

4. Hub. Curve file is generated as follows **X, Y, Z**

283.450000	0.000000000	-100.000000
283.450000	0.000000000	0.000000000
283.450000	0.000000000	100.0000000

In between the values Comma is compulsory. (X, Y, Z) A profile contains total 60 points for all '5' sections.

5. Profile. Curve file is generated as follows **X, Y, Z**

```
#
283.45,-5.74,-22.92
283.45,-5.23,-23.25
283.45,-4.46,-23.36
283.45,-3.43,-23.22
283.45,-2.15,-22.82
283.45,-0.66,-22.12
283.45, 1.03,-21.11
283.45, 2.85,-19.72
283.45, 4.74,-17.91
283.45, 6.61,-15.62
283.45, 8.32,-12.78
283.45, 9.66,-9.39
283.45, 10.4,-5.53
283.45, 10.35,-1.43
#442.65, 15.21,-15.51
442.65, 15.64,-15.21
442.65, 15.81,-14.69
442.65, 15.74,-13.95
442.65, 15.44,-12.99
442.65, 14.91,-11.83
442.65, 14.19,-10.49
442.65, 13.26,-8.99
442.65, 12.14,-7.36
442.65, 10.79,-5.66
442.65, 9.23,-3.95
```

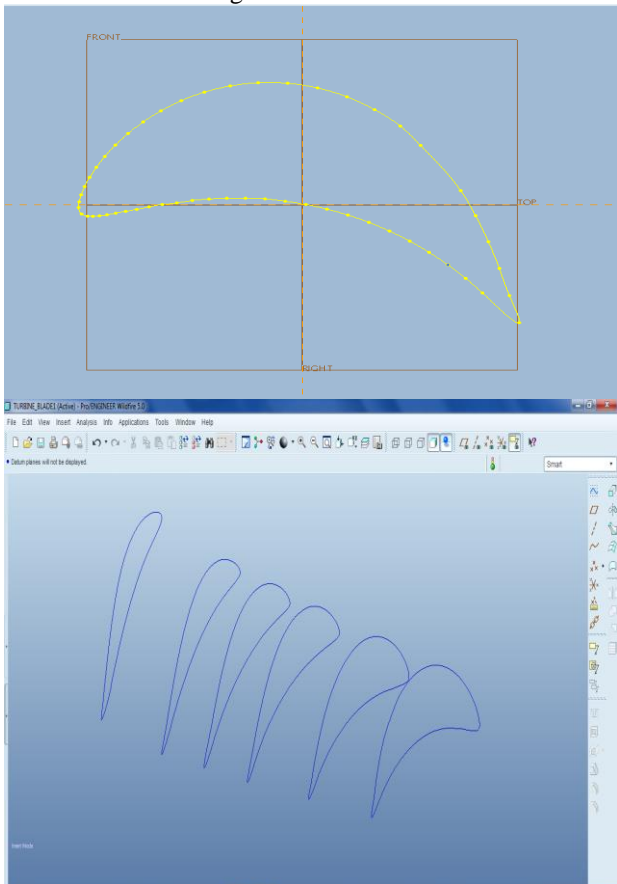
6. Shroud. Curve File is generated as follows:

442.65	0	-100
442.65	0	0
442.65	0	100

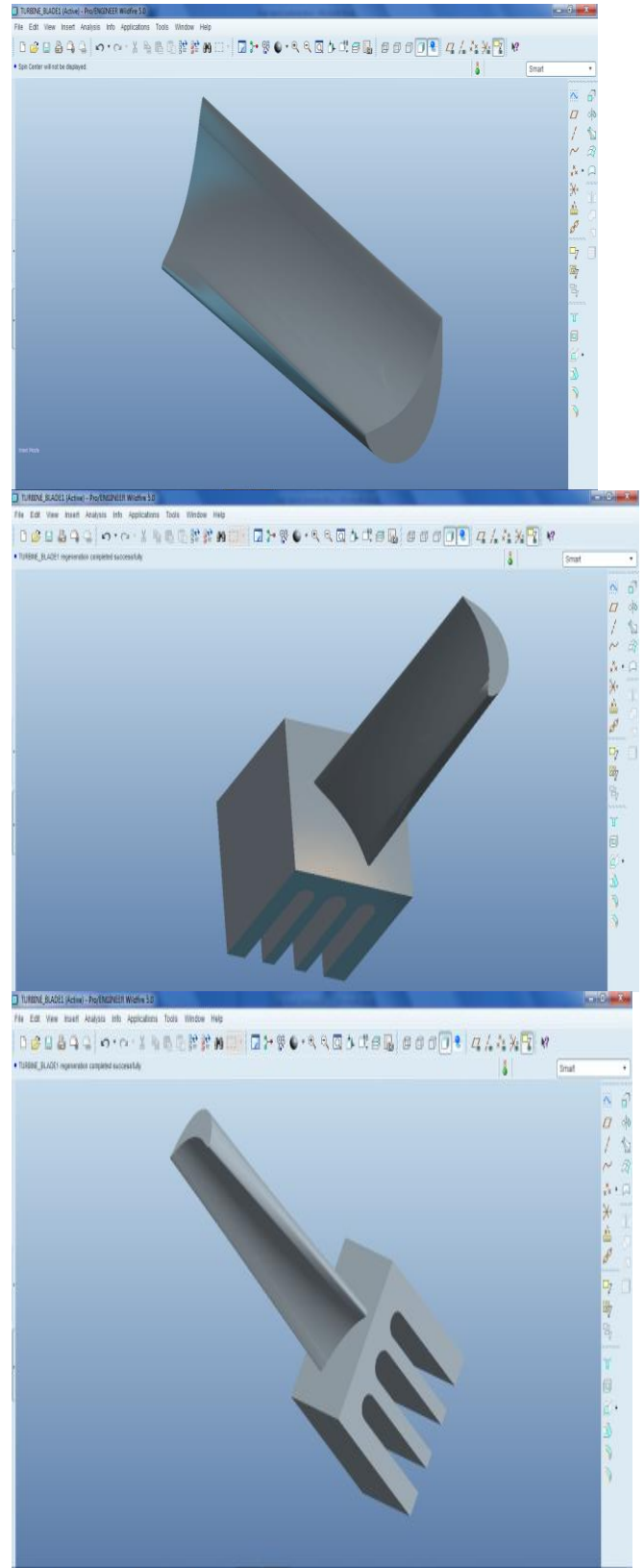
MODEL PREPARATION AND FORMATION

Solid modeling is the first step for doing any analysis and testing and it gives physical picture for new products. FEM models can easily create from solid models, by the process of meshing. FEM models can be made manually, but it is for simple cases only. If the model is of complex shape, only way for preparing FEM model is “meshing the solid model”.

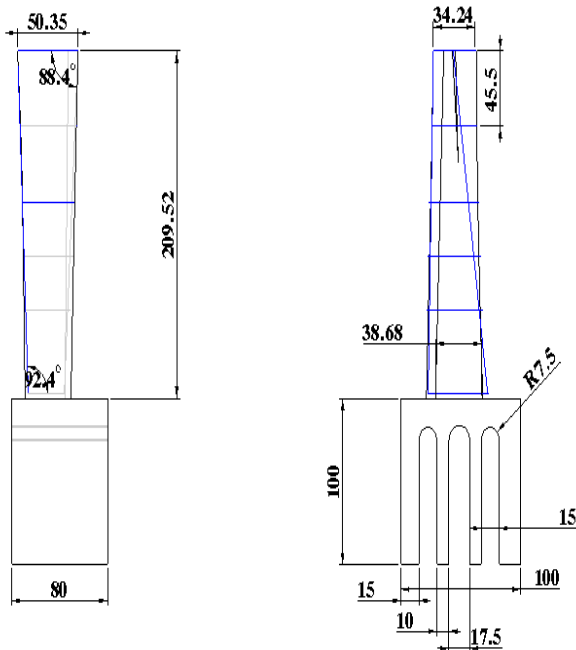
While dealing with complex blade structures such as blades with root or blades with coupling from disc or shroud, development of special purpose finite element packages becomes too involved. In those cases it becomes handy to adopt some well-established finite element codes and couple them with information from aerodynamics and damping models. Some of the important commercial codes available are: NASTRAN, ANSYS, NISA, SDRC, I-DEAS etc. here we will consider the application of ANSYS software to model a Low Pressure last stage turbine blade with its root.



TURBINE BLADE WITH ITS ROOT 3D CURVES



SOLID BLADE FINAL MODEL



ANALYSIS OF STEAM TURBINE BLADE

A wide range of objective functions (variables within the system) are available for minimization or maximization:

- Mass, volume, temperature, Strain energy, stress strain, Force, displacement, velocity, acceleration, Synthetic (User defined)

There are multiple loading conditions which may be applied to a system. Some examples are shown:

- Point, pressure, thermal, gravity, and centrifugal static loads
- Thermal loads from solution of heat transfer analysis
- Enforced displacements
- Heat flux and convection
- Point, pressure and gravity dynamic loads

Each FEA program may come with an element library, or one is constructed over time. Some sample elements are:

- Rod elements
- Beam elements
- Plate/Shell/Composite elements
- Shear panel
- Solid elements
- Spring elements
- Mass elements
- Rigid elements
- Viscous damping elements

Many FEA programs also are equipped with the capability to use multiple materials within the structure such as:

- Isotropic, identical throughout
- Orthotropic, identical at 90 degrees
- General anisotropic, different throughout

Types of Engineering Analysis

Structural analysis consists of linear and non-linear models. Linear models use simple parameters and assume that the material is not plastically deformed. Non-linear models consist of stressing the material past its elastic

capabilities. The stresses in the material then vary with the amount of deformation as in.

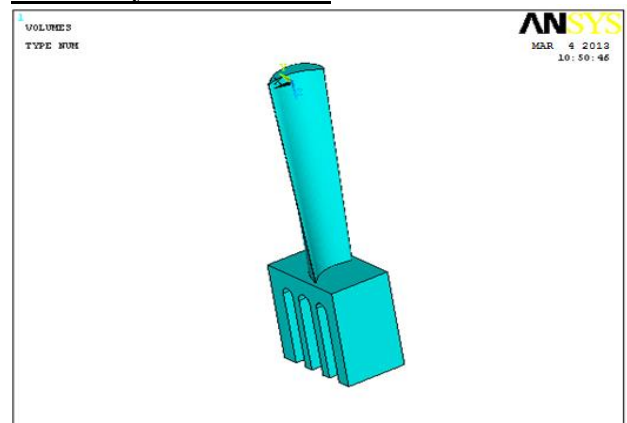
Vibrational analysis is used to test a material against random vibrations, shock, and impact. Each of these incidences may act on the natural vibrational frequency of the material which, in turn, may cause resonance and subsequent failure.

Fatigue analysis helps designers to predict the life of a material or structure by showing the effects of cyclic loading on the specimen. Such analysis can show the areas where crack propagation is most likely to occur. Failure due to fatigue may also show the damage tolerance of the material.

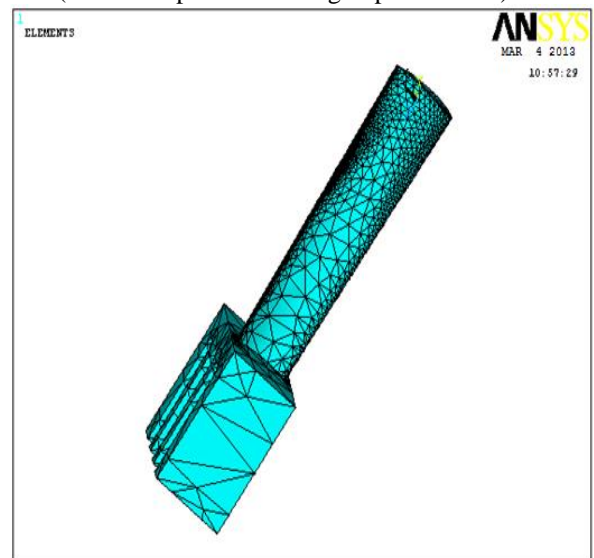
Heat Transfer analysis models the conductivity or thermal fluid dynamics of the material or structure. This may consist of a steady-state or transient transfer. Steady-state transfer refers to constant thermo properties in the material that yield linear heat diffusion.

4.2 ANALYSIS OF BLADES WITH DIFFERENT MATERIALS

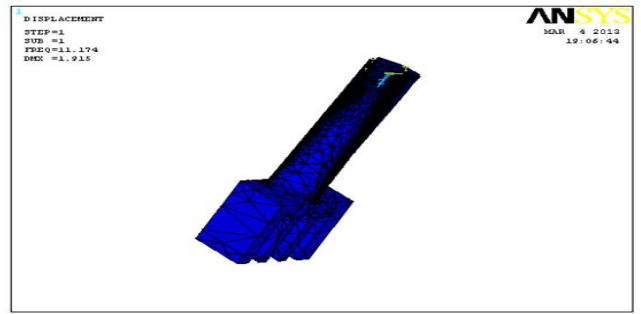
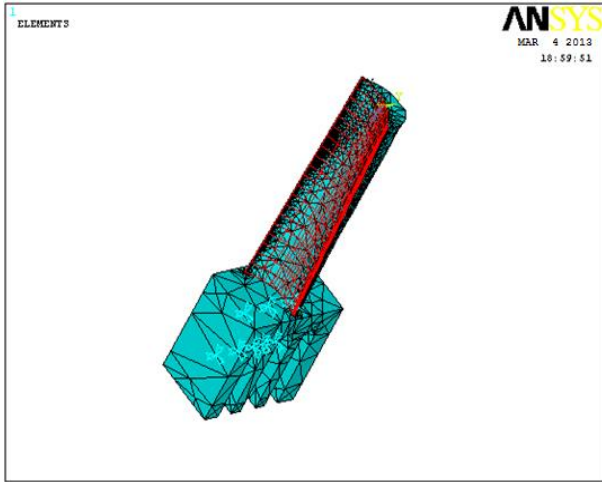
Static analysis Chrome steel:



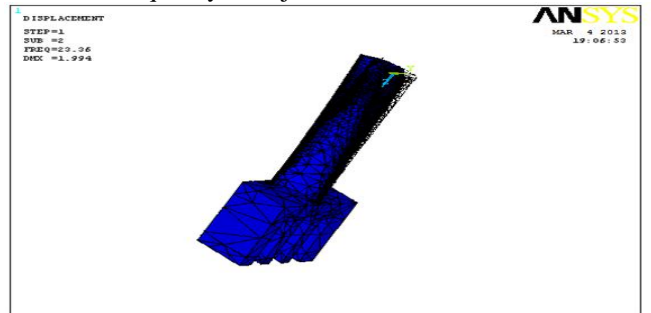
The above image is imported from Pro-e to Ansys using IGES (Initial Graphical Exchange Specification) format.



The above image is showing meshing is used to divide the problem into number of small problems and also to apply the material and element properties.

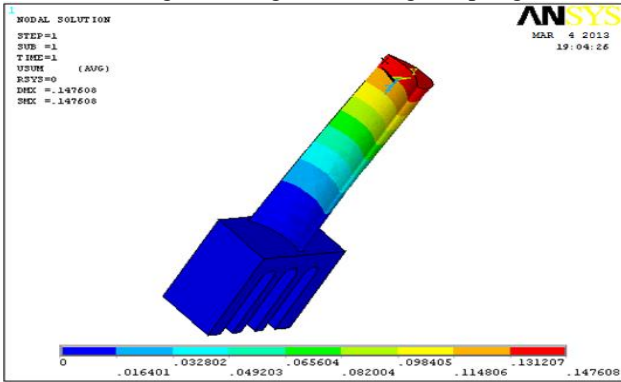


The above image is first mode shape of turbine blade having 11.174 and also the first mode is considered as natural frequency of object.

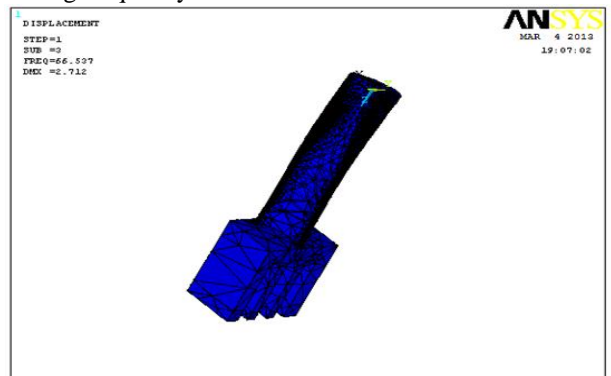


The above image is the second mode shape having frequency 23.56

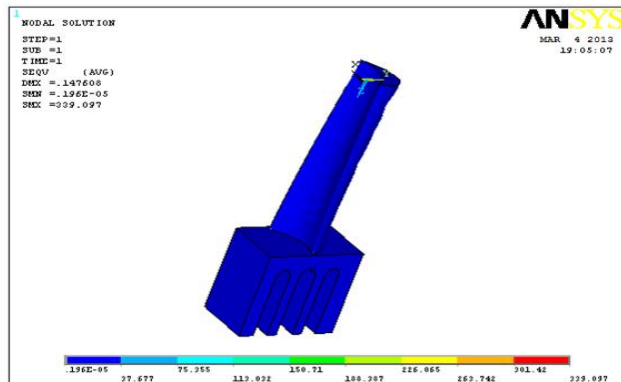
The above image showing loads acting on spring



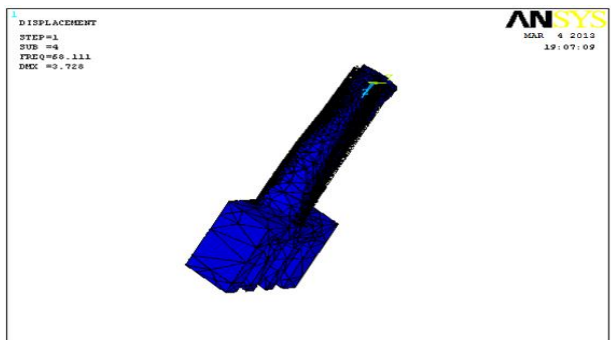
The above image is showing distributed shape or variation of geometry shape after applying loads. The maximum displacement is 0.147608 mm.



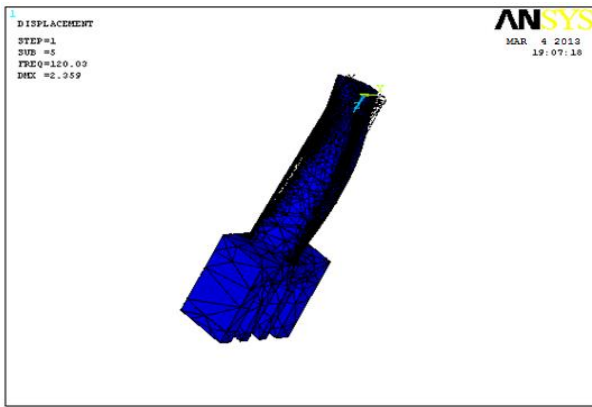
The above image is the third mode shape having frequency 66.537



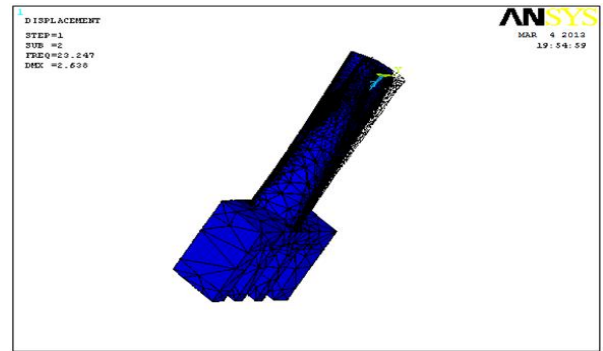
The above image is showing vonmises stress value. Vonmises stress depends on vonmises theory of failure.



The above image is the fourth mode shape having frequency 68.111

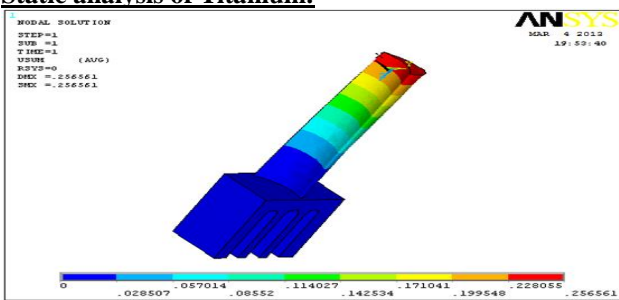


The above image is the fifth mode shape having frequency 120.03

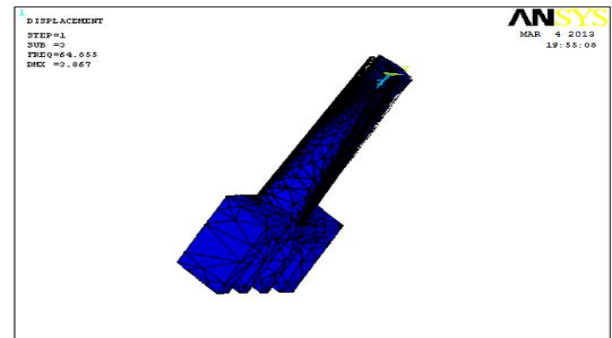


The above image is the second mode shape having frequency 23.247

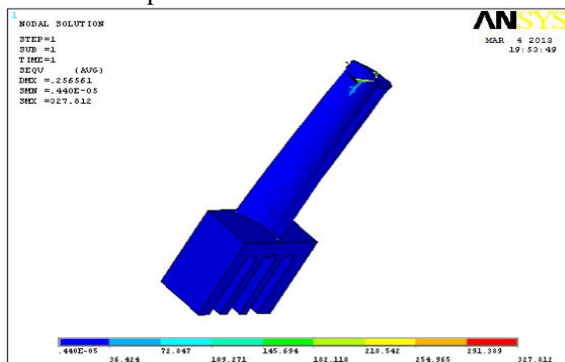
Static analysis of Titanium:



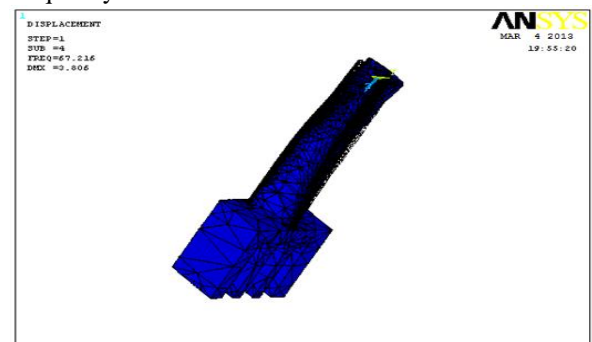
The above image is showing distributed shape or variation of geometry shape after applying loads. The maximum displacement is 0.256561 mm.



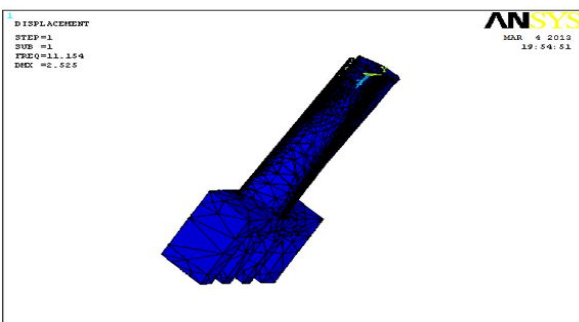
The above image is the third mode shape having frequency 64.855



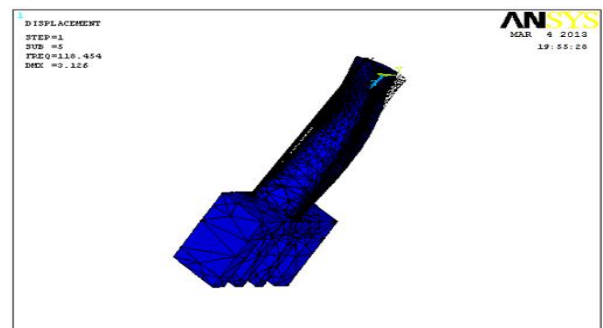
The above image is showing von-mises stress value. Von-mises stress depends on von-mises theory of failure.



The above image is the fourth mode shape having frequency 67.216

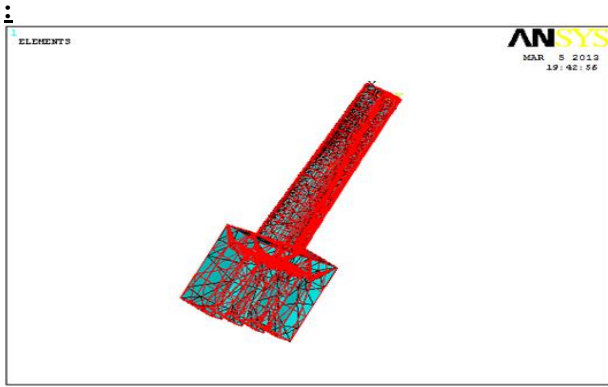


The above image is first mode shape of turbine blade having 11.154 and also the first mode is considered as natural frequency of object.



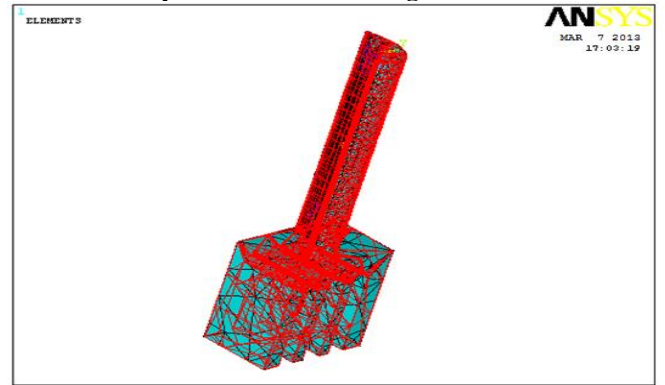
The above image is the fifth mode shape having 118.454

Thermal Analysis of Chrome steel

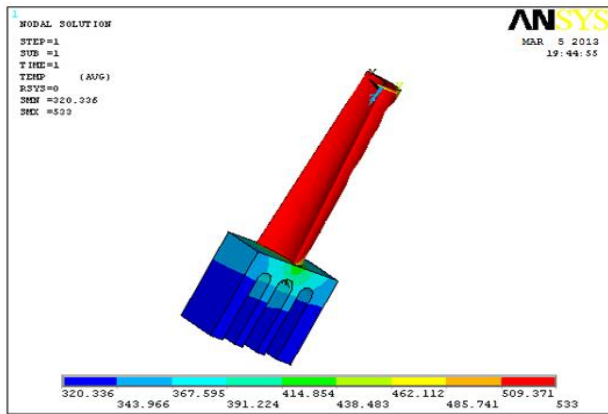


The above image is showing thermal loads.

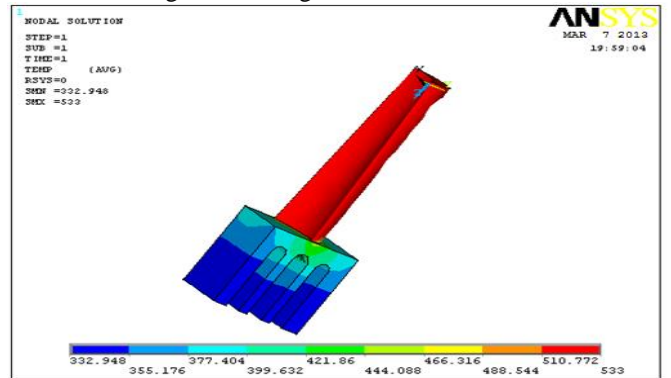
Thermal analysis of ceramic coating:



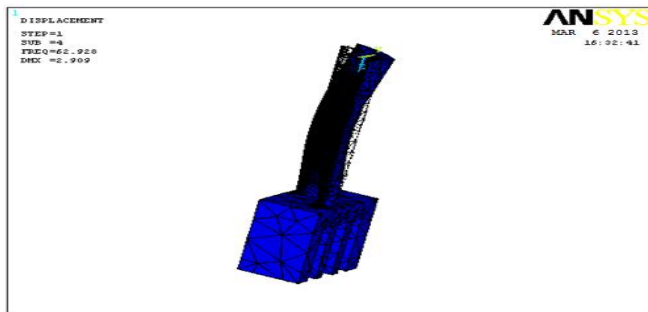
The above image is showing the thermal loads



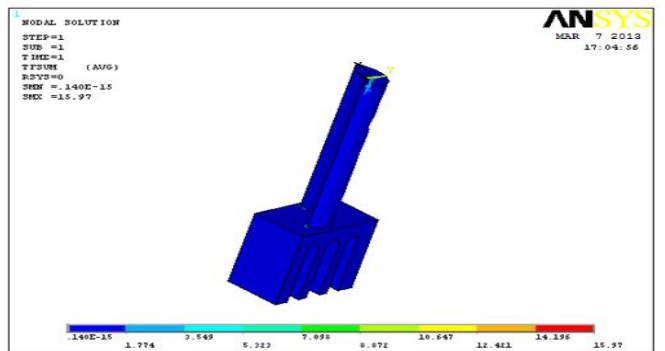
The above image showing the Temperature Distribution.



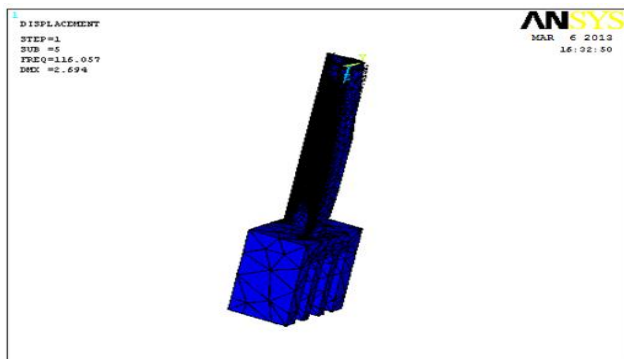
The above image showing the Temperature Distribution.



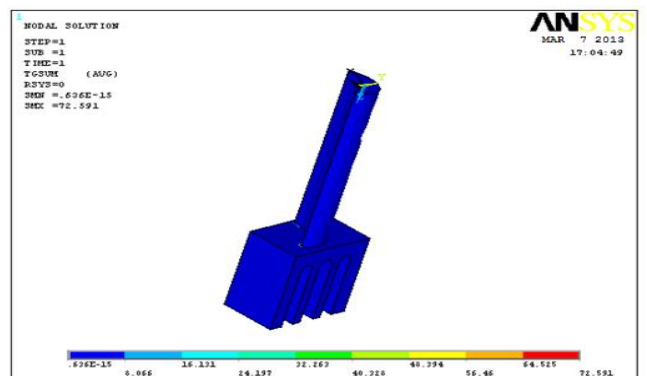
The above image is the fourth mode shape having frequency 52.926



The above image is showing the thermal flux



The above image is the fifth mode shape having mode shape 116.057



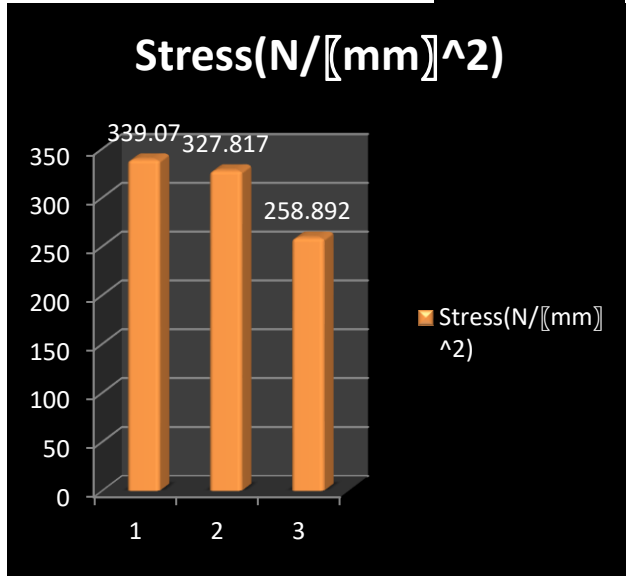
The above image is showing the thermal gradient sum

**RESULTS OF THE ANALYSIS ON BLADES
RESULTS TABLE**

The results table is explained in the below graphs by comparing with each other. The values shown in the above table are taken from the thermal and structural analysis of the blade using ansys software.

The materials are shown in the graphs are listed as like mentioned below.

1. Chrome Steel
2. Titanium
3. Cast Iron coated with Zirconium Stress (N/mm²):



The maximum stress applied on the blade is represented on the graph which will give a brief explanation that

	chrome steel	Titanium	Cast Iron With Zirconium coating
Stress(N/mm ²)	339.07	327.817	258.892
Displacement (mm)	0.147608	0.256561	.0430927
Temperature(°c)	533	533	533
Thermal gradient(°c/m)	715.055	605.119	72.591
Thermal flux(W/mm ²)	11.727	10.287	15.97

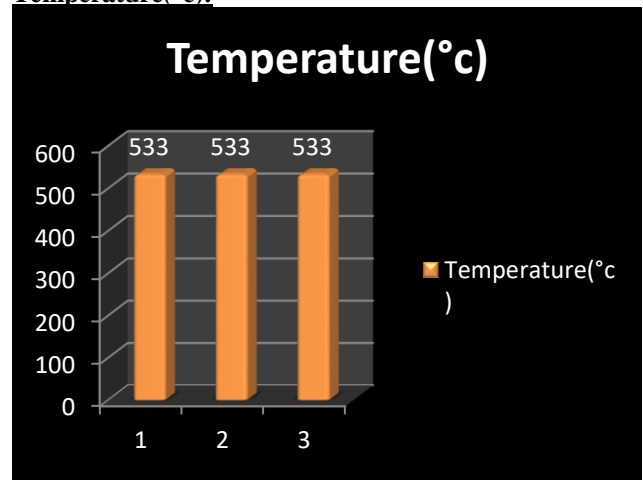
relatively it is low on the applied new material.

Displacement (mm):



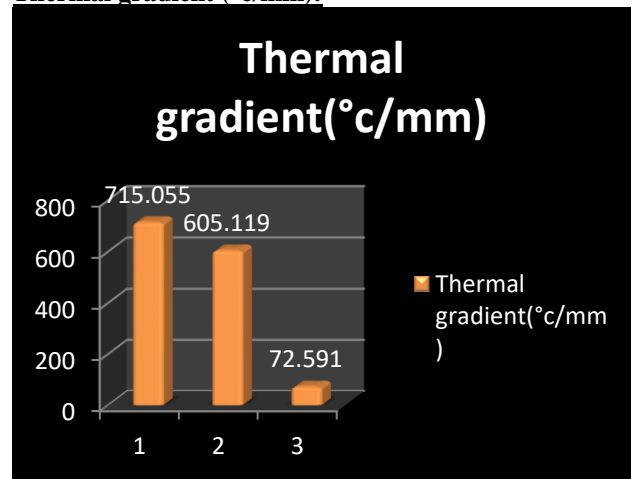
The above chart explains that the displacement due to the stresses is less compared to generally used materials for the applied new material.

Temperature(°c):



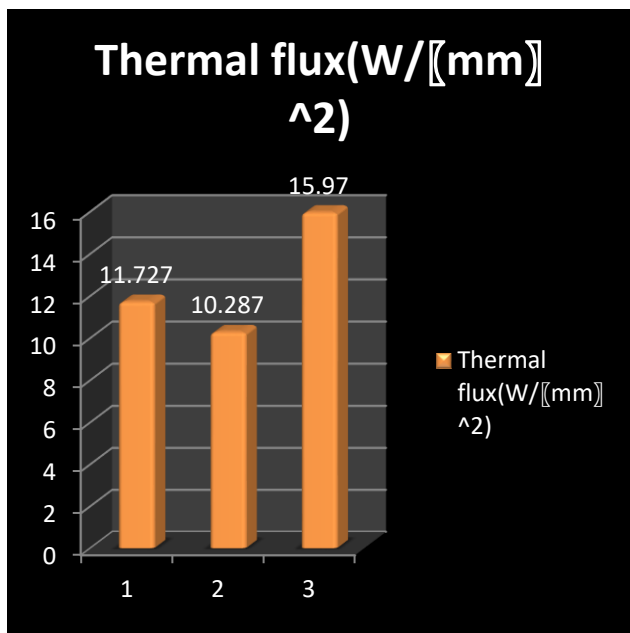
Comparatively the temperature on the surface of the blade is same for all materials. So this shows that there is nothing changed and no loss by introducing new material

Thermal gradient (°c/mm):



Relatively thermal gradient is less for the new applied material. So it is an advantage for intro of zirconium coated cast iron.

Thermal flux(W/mm²):



Relatively the thermal flux is high compared to other general materials. So it is an advantage.

CONCLUSION

In this project we have analyzed previous designs and generals of turbine blade to do further optimization, Finite element results for free standing blades give a complete picture of structural characteristics, which can utilized for the improvement in the design and optimization of the operating conditions.

In the first step we have designed turbine blade using CMM data from existing model.

In the second step we have done the study on different materials which are suitable for the improvement of turbine blade. In the third step we have validated our design using existing materials. In the next step we have applied different materials for turbine blade to suggest best material.

From the above results we can conclude that using cast iron with partially stabilized zirconium coating is more beneficial than previous materials, due to low stress displacement, good thermal strength, low cost and easy to manufacture.

REFERENCES:

[1] Mingyu Zhu, et al., Design and analysis of steam turbine blades, IOP Conf. Series: Journal of Physics: Conf. Series 1300 (2019) 012056, doi:10.1088/1742-6596/1300/1/012056

[2] Md. Abdul Raheem Junaidi et al., Design Optimization and Analysis of a Steam Turbine Rotor Grooves, January 2013, IOSR Journal of Mechanical and Civil Engineering 8(6):66-72, DOI:10.9790/1684-0866672

[3] Ramesh.S. Devarmani A et al., Design and Thermal Analysis of Steam Turbine Blade, International Research Journal of Engineering and Technology (IRJET), Volume: 05 Issue: 08 | Aug 2018

[4] G nagendra Krishna et al., DESIGN AND ANALYSIS OF STEAM TURBINE BLADE AND SHAFT ASSEMBLY, International Journal of Research and Innovation, Volume: II, Issue : II, 2015.

[5] BURAGUMMALABVKISHORE et al., DESIGN AND THERMAL ANALYSIS OF STEAM TURBINE BLADE USING FEM METHOD, Anveshana's International Journal of Research in Engineering and Applied Sciences, VOLUME 3, ISSUE 5 (2018, MAY) (ISSN-2455-6300).

[6] Hui Li et al., Aerodynamic Optimization Design of a Multistage Centrifugal Steam Turbine and Its Off-Design Performance Analysis, Volume 2017.

[7] Jian Zhong Lin et al., The Strength Analysis of the Turbine Blade Based on Finite Element Method Calculation and Optimization, Applied Mechanics and Materials (Volumes 635-637), Pages: 549-554, September 2014.

[8] Prabhunandan G S1 et al., Static and Fatigue Analysis of a Steam Turbine Blade, International Journal of Latest Technology in Engineering, Management & Applied Science (IJLTEMAS) Volume V, Issue X, October 2016 | ISSN 2278-2540.

[9] CHALLA MURALI et al., Thermal Analysis of a Steam Turbine Blade, International Journal of Research, Volume 04 Issue 01 January 2017.

[10] A Junaidi et.al., Design optimization and analysis of a steam turbine rotor grooves, Materials science Engineering, IOSR Journal of Mechanical and Civil Engineering,

PORT FUEL INJECTION WITH FUEL VAPORIZER AND EARLY PILOT INJECTION TECHNIQUES IN HCCI COMBUSTION ENGINE

R.Jyothu Naik^{*1}, K.Thirupathi Reddy² P.Srinivasarao³ Y.Hariprasad Reddy⁴

¹ Assistant Professor, Department of Mechanical Engineering, Rayalaseema University College of Engg., Kurnool A.P, India.

²Professor and Head of Mechanical Engineering, Rajeev Gandhi Memorial college of Engineering and Technology, Nandyal 518501, Kurnool (Dist) A.P, India.

³Assistant Professor, Department of Mechanical Engineering, Narasaraopet Engineering College, Narasaraopeta.

⁴Principal, College of Engineering, Rayalaseema University College of Engineering, Kurnool A.P, India

Abstract: In this investigation we studied the compares of port fuel injection with fuel vaporizer and early pilot injection techniques on the performance combustion and emission characteristics in a HCCI combustion engine. Experiments were carried out in a computerised 4-stroke single cylinder diesel engine was converted into HCCI mode. Homogeneous charge is made by injecting the fuel in the intake and the charge is heated by an air heater with the PFI so as to accomplish HCCI combustion. In early pilot injection technique a homogeneous mixture can likewise be gotten when fuel is injected directly in the combustion chamber throughout the compression stroke a long time before TDC. The experimental results observed that the combustion performance and emissions results were initiate to be of 30.23 % higher RoHR for PFI with Vaporizer compared to early pilot injection technique. The Port fuel injection with fuel vaporizer technique has 5.7 % higher brake thermal efficiency compared to early pilot injection technique. And also found 32.77 % less NO_x emission with PFI with fuel vaporizer compared to early pilot injection technique. But with PFI with fuel vaporizer the UHC (57.14%) and CO (23.07 %) emissions are more compared to early pilot injection technique.

Key words: Port fuel injection, Vaporizer, Early pilot injection, Rate of Heat Release, HCCI

Highlights

Unburned hydrocarbons and carbon moxide was decreased with early pilot injection technique. Extended load condition from low to high with the early pilot injection technique.

1. INTRODUCTION

Under the impact of growing stringent emission rules, the novel combustion approaches were studied to instantaneously decrease NO_x and soot emissions in conventional diesel engine. HCCI is an auspicious alternate combustion technology with more efficiency and low NO_x and soot emissions. Many researcher of HCCI combustion reported a probable for less NO_x and PM emissions (Bendu, 2014; Jyothu, 2018). Nevertheless there are numerous difficulties to be resolved before the marketable use in automotive. Mostly it is challenging to control the combustion timing, extending load and more UHC and CO emissions are presented with PFI-HCCI combustion engine. This effect has been widely studied (Jyothu Naik. and Thirupathi Reddy 2019). Port fuel.injection is the simplest technique for the arrangement of the external blend where the

injector is put in the admission complex close to the admission valve. This methodology progresses fuel delivery and volumetric effectiveness via carburetion. Some of the researchers were used a higher intake air temperature to vaporize the fuel in the intake manifold.Experiments are executed on HCCI engine fuelled with waste plastic pyrolysis oil biodiesel blend with external PFI and Vaporiser method. Experiments were performed by changing the without EGR with 5%, 10% and 15% EGR with a particular true objective to accomplish the steady HCCI combustion. More (BTE) was found to be 37 % free of exhaust gas recirculation (EGR) in WPPO 20% blend of biodiesel. EGR was also found to be the most effective tool for controlling the rate of No_x formation and combustion.This effect has been widely studied (Jyothu Naik. and Thirupathi Reddy 2019). Conducted experiments on HCCI with PFI method by fuel vaporizer with cooled EGR to control the early ignition. The results expressed that at 30% EGR rate arranged low smoke and NO_x outflow. This effect has been widely investigated (Ganesh et al 2014) Developed an atomizer for the arrangement of an outside blend and examined the impact of uncooled EGR, consumption air temperature and engine speed on HCCI combustion. EGR was additionally answered to be the best tool for controlling the pace of NO_x arrangement and combustion.Investigation has been widely reported (Midlam-Mohler, et al.2003).

Recently, Conducted experiments on an advanced combustion idea with split fuel injection techniques, by changing the start of main injection (SoMI) timings (18, 20, 22 and 24° bTDC), start of pilot injection (SoPI) timings (30, 35 and 40° bTDC) and EGR rates (0, 15 and 30 %) at constant fuel injection pressure FIP and engine speed 700 bar and 1500 rpm. From the investigation it is reported that at retarded SoPI timing (30° bTDC), HCCI-DI combustion resulted in slightly more No_x, but at too advanced SoPI timing (40° bTDC), and HCCI-DI combustion found relatively poorer engine performance. This result was stated by Jain, A., et al 2017.used two injection methods in HCCI-DI combustion. The results uncovered that, No_x and smoke emissions were diminished and broadened try by using two injection techniques with blends of n-heptanes and isoctane fuel. It was expressed that the most critical yield is that a two phase's heat release pattern is stated in high cetane fuel. This

effect has been widely investigated (Das, et al 2015). Investigated the single-pilot injection and two pilot injection techniques with wide injection timing, grouping different injection sum proportions and distinctive abide times. The results found that the single-pilot injection is the best technique to diminish the No_x and smoke emissions contrast with other. This result was stated by (Lee,J and Jeon,J.2009).Used DEE as a fuel in HCCI-DI combustion engine. The results observed that the single stage ignition stated by including of premixed DEE fuel, and furthermore expressed that the diminished No_x and soot emissions. This result was stated by (Can cinar et al 2010). Studied the effects of EGR and pilot injection amount on engine performance and emission. The results expressed that, increment the pilot injection sum and low scope of EGR rates diminishes No_x and soot emissions. This effect has been widely studied (Qiang fang et al 2012). Conducted experiments and study of premixed proportion and DI timing. The results found that the expanding the premixed proportions and compelling enhanced the brake, fuel change efficiency at low to medium load and No_x emissions were diminished. This result was stated by (Junjun Ma et al 2008).

From the detailed literature study, it tends to be concluded that the comparison of port fuel injection with vaporizer and early pilot injection techniques in HCCI combustion engine. In this investigation comparison of port fuel injection with vaporizer and early pilot injection techniques in HCCI combustion engine. The experiments conducted and the parameters that have been observed Cylinder Pressure, Heat Release rate (HRR), BTE, EGT, NO_x , CO, UHC and Smoke emission of port fuel injection with vaporizer and early pilot injection techniques in HCCI combustion engine are presented in this paper.

2. EXPERIMENTAL METHODOLOGY

The research engine used was a four strokes, single cylinder, water cooled, DI model Kirloskar TV1 provided by APEX Innovation Ltd at sangli, for investigation resolves the CI engine was efficient to work in HCCI mode. Outside mixture arrangement method (Port Fuel Injection System with a fuel vaporizer) has been presented.The schematic diagram of the experimental setup had shown in figure 1 and the engine specifications are mentioned in table 1.

Table.1. Experimental engine specifications

S.No	Engine specifications	
1	Type	Kirloskar
2	Model	TV1
3	B/L	87.5 mm x 110 mm
4	Swept Volume	661.45 (cc)
5	CR Length	234.00 (mm)
6	Compression Ratio	18:1
7	Rate speed	1500 rpm
8	Cooling method	water

The schematic diagram of the experimental setup had shown in figure 2. In this investigation, two injection techniques were connected in DI diesel engine utilizing regular common-rail injection system. The accompanying strategy was analyzed so as to accomplish the HCCI-DI combustion. The pilot (80%) fuel was injected in the admission stroke of engine cycle to form the premixed fuel-air mixing. The pilot injection timing and pilot injection amount were controlled to accomplish HCCI-DI combustion. The main injection (20%) fuel was injected around compression TDC to control the ignition timing. The main injection timing was varied to optimize the emissions and efficiency.



Figure 1. Photo graphical view of ECU



Figure 2. Photo graphical view of AVL 437 standard smoke meter



Figure 3. Photo graphical view of Airrex 5- gas emission analyzer.

The fuel vaporizer comprises of a heating component, ceramic pipe and stainless steel pipe of diameter 30 mm. The length of the fuel vaporizer is 140 mm and warm-up time is 6 min. The nichrome warming wire is twisted over the ceramic pipe for warming alone. The specifications of the fuel vaporizer are shown in table.2. The Port Fuel Injection (PFI) (up to 4 bars) was climb on the highest point of the fuel vaporizer to supply the right amount of fuel to the vaporizer. The PFI was restrained by an Electronic Control Unit (ECU) and the photographical view shown in figure 3. The Electronic Control Unit (ECU) controls both the timing and amount of the fuel. The exhaust gases were occupied to an examining line for the estimation of emissions without expanding the back pressure in the exhaust pipe. Airrex 5-gas emission analyzer and AVL 437 standard smoke meter are showed in figure 4 & 5. It is used to measure emissions from the engine. All the emissions were consistently estimated for 3 min and the normal outcomes displayed here. Each test was rehashed twice to promise that the outcomes are repeatable inside the experimental uncertainties. The in-cylinder pressure was estimated utilising water-cooled piezo-electric pressure transducer which is fixed flush with the cylinder head. The cylinder pressure history data acquisition and combustion investigation is executed utilizing an engineSoft is Labview based programming package developed by Apex Innovations Pvt.Ltd.In-cylinder pressure was stored for 100 consecutive cycles at 0.5° CA resolution and averaged to estimate the heat release rate and other combustion parameters in this paper. Combustion parameter was finding from the heat release curve. In this investigation, heat release rate was calculated using the following equation.

RESULTS AND DISCUSSION

2.1 Cylinder pressure

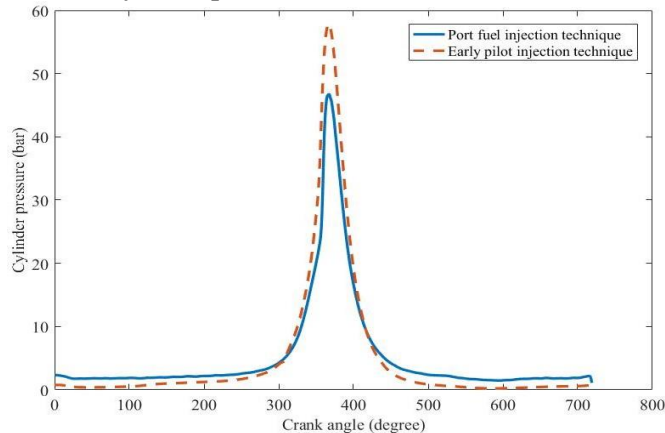


Figure 4. Cylinder Pressure vs. Crank Angle Degree comparison of port fuel injection with vapoizer and early pilot injection at full load condition.

Cylinder pressure rise rates are shown in figure comparison for port fuel injection with vaporizer and early pilot injection technique. From the figure 6 it should be noticed that the early pilot injection technique combustion results in 17.24 %

high in cylinder pressure compared to port fuel injection with fuel vaporizer technique. The ignition rate is higher in the HCCI; the ignition occurs in the total chamber. The Heat Release study is a further illustrative technique for HCCI movement. The HCCI heat discharge strategy differs from existing engines as a result of the synchronous ignition of the homogeneous blend because of compression.

2.2 Heat release rate

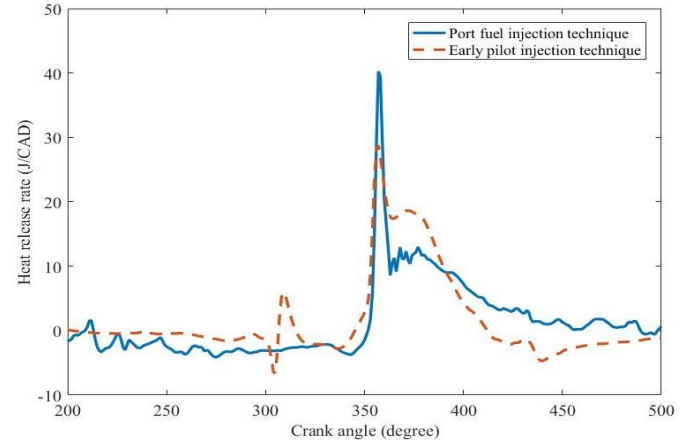


Figure 5. Heat Release Rate vs. Crank Angle Degree comparison of port fuel injection with vaporizer and early pilot injection at full load condition.

Figure.5 shows the variation of Heat Release Rate w.r.t Crank angle comparison for the port fuel injection with vaporizer and early pilot injection in HCCI mode. It is noticed that the port fuel injection with fuel vaporizer technique heat release rates are 30.23 % higher compared to early pilot injection technique. Since longer ignition defers in higher heat release whiles the premixed ignition stage. The superior HRR appear than an expansion in EGT.

PERFORMANCE

4.1 Brake thermal efficiency

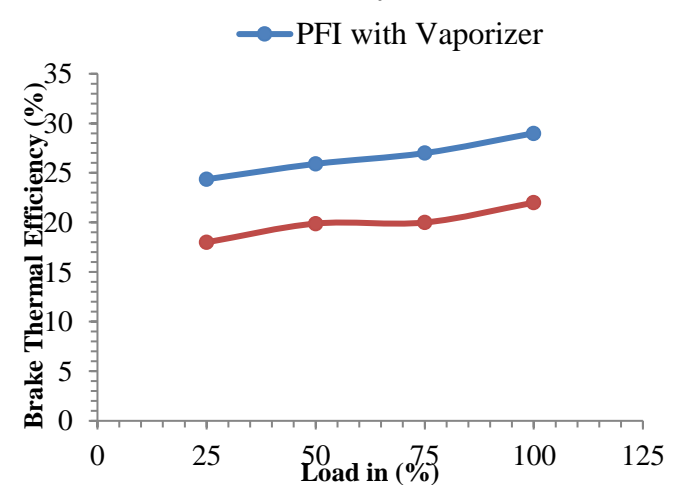


Figure 6. BTE comparison of port fuel injection with vaporizer and early pilot injection at different load conditions.

Figure.6 shows the difference of BTE comparison for the port fuel injection with vaporizer and early pilot injection with various load conditions in HCCI engine. It is noticed that the rising the load conditions increase the BTE in PFI with fuel vaporizer, but decrease the BTE in early pilot injection. The PFI with fuel vaporizer given the high BTE at the full load condition which account of 5.7% increased compare with early pilot injection technique.

Fast combustion leads to better homogeneity of mixtures, resulting in less deposition of soot. The higher combustion temperatures, high Rate of Heat Release (RoHR) and less combustion efficiency are affected by the advance start of combustion because improved emissions and lower LTC.

4.2 Exhaust gas temperature

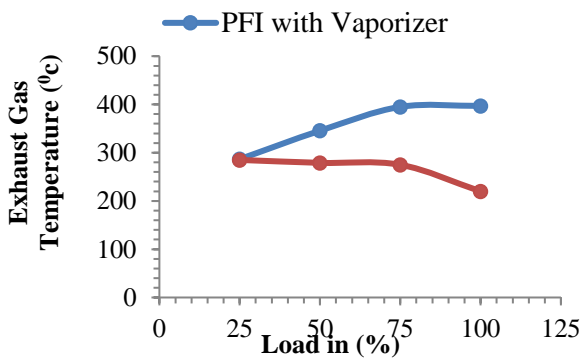


Figure 7. Exhaust gas temperature comparison of port fuel injection with vaporizer and early pilot injection at different load conditions.

Figure 7. Shows the difference of EGT comparison for the port fuel injection with vaporizer and early pilot injection with various load conditions in HCCI engine. It is noticed that the increasing the load conditions increase the EGT in PFI with fuel vaporizer, but decrease the EGT in early pilot injection. The PFI with fuel vaporizer given the 44.58 % high EGT at the initial stage load to full load condition compared with early pilot injection technique..

5. EMISSIONS

5.1 NOx emission

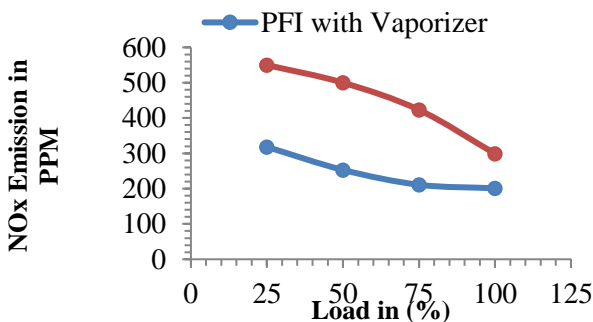


Figure 8. NOx emission comparison of port fuel injection with vaporizer and early pilot injection at different load conditions.

Figure.8 shows the variation of NOx emission comparison for the port fuel injection with vaporizer and early pilot injection with dissimilar load conditions in HCCI mode. It should be clear those PFI with fuel vaporizer NOx emissions levels of around 32.77 % lower than early pilot injection technique. Because depending on the degree of evaporation and homogenization and also homogenization of the combustion, lower peak in-cylinder temperature.

5.1 CO Emission

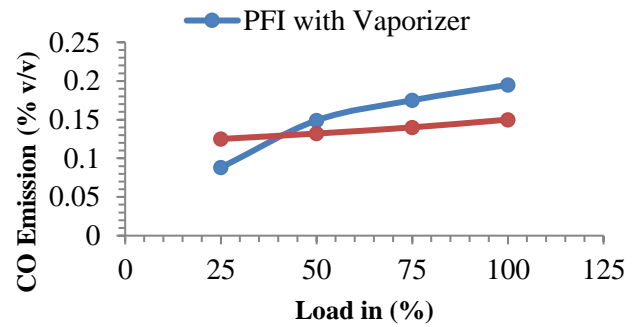


Figure 09. CO emission comparison of port fuel injection with vaporizer and early pilot injection at different load conditions.

Figure 09. Shows the difference of CO emission comparison for the port fuel injection with vaporizer and early pilot injection with various load conditions in HCCI mode. It is clear that the emission of CO tend to be much 23.07 % higher than for early pilot injection technique. Because the level of homogenization. As shown in figure 12, in PFI mode, CO increases as the load increases. CO shows incomplete combustion and it is at the highest point at full load condition; the difference in CO emissions in PFI and early pilot injection modes is the highest at full load and the least difference is at initial stage load condition. In the HCCI engine the formation of CO emissions are created by the insufficient oxidation temperature of the gases.

UHC emission

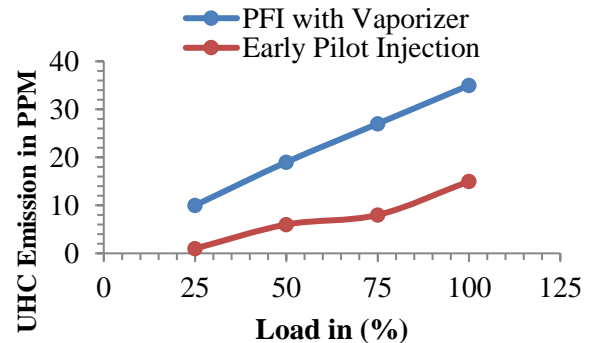


Figure 10. UHC emission comparison of port fuel injection with vaporizer and early pilot injection at different load conditions.

Figure.10 shows the difference of UHC comparison for the port fuel injection with fuel vaporizer and early pilot injection with various load conditions in HCCI engine. It is observed that the rising the load conditions 57.14 % increase the UHC in PFI with fuel vaporizer, but decrease the UHC in early pilot injection. Since fuel is injected throughout the compression stroke, the gas temperature and density are higher than at an admission condition, which enhances the evaporation process and accordingly diminishes the ideal opportunity for setting up the mixture, maintaining a strategic distance from the need to heat up the intake air.

6. CONCLUSION

Based on the results obtained from the experimental investigate, the following conclusions were drawn:

- Only minor modifications are needed to convert from PFI with fuel vaporizer mode of combustion to early pilot injection mode.
- PFI with fuel vaporizer is increasingly reasonable to be worked at low loads and early pilot injection mode is better in higher loads.
- Higher Brake Thermal Efficiency (BTE) was found 29 % with PFI with fuel vaporizer technique.
- PFI with fuel Vaporizer operation at low engine loads has all the earmarks of being exceptionally alluring for enhancing the energy utilization and decreasing NOx emission, yet UHC and CO emissions in PFI with fuel vaporizer mode are high compared with early pilot injection.
- In early pilot injection technique the UHC (57.14 %) and CO (23.07 %) decreased when compared with PFI with fuel Vaporizer technique.

REFERENCES

- [1] Christensen M.2002. "HCCI Combustion—Engine Operation and Emission Characteristics". PhD Thesis, Dept. Heat & Power Eng., Div. of Comb. Engines, Lund University, Sweden ISBN: 91-628-5424-0.
- [2] Cinar, C., Can, Ö. Sahin, F., & Yucesu, H. S. 2010 "Effects of premixed diethyl ether (DEE) on combustion and exhaust emissions in a HCCI-DI diesel engine". *Applied Thermal Engineering*,30:360-365. <https://doi.org/10.1016/j.applthermaleng.2009.09.016>.
- [3] Cinar, C., Can, Ö. Sahin, F., & Yucesu, H. S. 2010 "Effects of premixed diethyl ether (DEE) on combustion and exhaust emissions in a HCCI-DI diesel engine". *Applied Thermal Engineering*,30:360-365. <https://doi.org/10.1016/j.applthermaleng.2009.09.016>.
- [4] Das, P., Subbarao, P.M.V. and Subrahmanyam, J.P. 2015 "Effect of Main Injection Timing for controlling the combustion phasing of a Homogeneous Charge compression ignition engine using a new dual injection strategy". *Energy Conversion and Management*,95:248-258. <https://doi.org/10.1016/j.enconman.2015.02.018>.
- [5] Fang, Q., Fang, J., Zhuang, J., & Huang, Z. 2012 "Influences of pilot injection and exhaust gas recirculation (EGR) on combustion and emissions in a HCCI-DI combustion engine". *Applied Thermal Engineering*, 48:97-104.
- [6] Ganesh, D., Nagarajan, G., & Ganesan, S. 2014 "Experimental investigation of homogeneous charge compression ignition combustion of biodiesel fuel with external mixture formation in a CI engine". *Environmental science & technology*,48:3039-3046.
- [7] Harisankar, B., and Murugan,S. 2014 "Homogeneous charge compression ignition (HCCI) combustion: Mixture preparation and control strategies in diesel engines." *Renewable and Sustainable Energy Reviews*, 38:732-746. <https://doi.org/10.1016/j.rser.2014.07.019>.
- [8] JyothuNaik,R., and ThirupathiReddy,K.. 2018 A review on diesel homogeneous charge compression ignition engine. *Acad. J. Sci. Res*, 321-328. Jyothunaik Ramavathu & Thirupathi Reddy Kota 2019 .Combustion performance and emission characteristics on HCCI engine of waste plastic pyrolysis oil biodiesel blends with external PFI and vaporiser, *International Journal of Sustainable Engineering*,12(5):1-14.
- [9] Jain, A., Singh, A. P., & Agarwal, A. K.2017 Effect of split fuel injection and EGR on NOx and PM emission reduction in a low temperature combustion (LTC) mode diesel engine. *Energy*,122:249-264. <https://doi.org/10.1016/j.energy.2017.01.050>.
- [10] J.B. Heywood. 1988. *Internal Combustion Engine Fundamentals*, McGraw Hill Press, New York, (ISBN-10: 007028637X).
- [11] J.A. Gatowski, E.N. Balles, K.M. Chun, F.E. Nelson, J.A. Ekchian, F.B. Heywood. 1984. A Heat Release Analysis of Engine Pressure Data, SAE paper 841359.
- [12] Lee, J., Jeon, J., Park, J., & Bae, C.2009 Effect of multiple injection strategies on emission and combustion characteristics in a single cylinder direct-injection optical engine, SAE Technical Paper 2009-01-1354, 2009, <https://doi.org/10.4271/2009-01-1354>
- [13] Midlam-Mohler, S., Rizzoni, G., Bargende, M., & Haas, S.2003 Mixed-mode Diesel HCCI with External Mixture Formation: Preliminary Results. The Ohio State University Center for Automotive Research Michael Bargende, Simon Haas FKFS, Universität Stuttgart, Newport Newport.

Investigation of Mechanical, Thermal properties and SEM analysis of Jute/Coconut Hybrid composites with Alkali Treatment

K. Venkatarao¹, A. Venkata Jayasri², Ch. Lakshmikanth³, S. Nagakumar⁴

^{1,3,4} Prasad V. Potluri Siddhartha Institute of Technology, Kanuru, Vijayawada, Andhra Pradesh, India-520007.

² Andhra University, Visakhapatnam, Andhra Pradesh, India

Abstract: This present project focuses on how the mechanical properties and the thermal properties of the natural fiber-reinforced composite. For the study, the test specimens are made using the different weight percentages of the Jute and Coconut Fibers as reinforcement and polyester resin as a matrix using the hand layup technique. The composite which is made of Jute and Coconut Fibers is additionally mixed with the resin, to hold the specimen, a catalyst to increase the rate of reaction, and an accelerator to cure the liquid state of the composite material into a solid state. In the current project, we used the Jute and Coconut Fibers as the reinforcing fibers. The tensile test, Impact test, and Thermal tests are performed on the specimens. All the tests are performed on the specimens both treated and untreated by using the load-displacement graphs, the properties are been analysed. After performing all the Tensile, Impact, and Thermal tests behaviour of the composites are analysed and the results are concluded by using the graphs produced.

1. INTRODUCTION

In this article, the mechanical and tribological portrayal of *Cissus quadrangularis* stem fiber (CQSF)/epoxy pitch particulate with and without coconut shell debris (CSA) powder was done. The materials were created by the hand rest technique. Epoxy and 30 wt. % CQSF with 40 mm fiber length were taken to create the base material, and CSA was independently added at 2.5, 5, 7.5, and 10 wt.%. Along these lines, five materials were created for mechanical and tribological examination. The tribological portrayal was broken down by Response Surface Methodology (RSM) utilizing Design-Expert programming, and a nail-to-plate wear testing machine was utilized to work out the particular wear pace of the materials under various exploratory circumstances [1].

The current work endeavours to make an improvement in the current existing protective cap producing philosophy and materials used to have better mechanical properties as well as to improve the similarity among strands and the framework. The bio-composite are ready with the epoxy gum network and filaments like jute, sisal, coconut, are caalso, banana utilizing hand rest up strategy with fitting extents to bring about head protector shell structure. [2]. This study had as its even handed to research the attributes of the green coconut fiber, from the natural product arranged in the city of Francisco Morato - Sao Paulo, and to contrast them with the qualities from other normal filaments, to check the suitability of use of these strands in the assembling of shoe parts. It was made a natural maceration on the filaments and foothold and

microscopy tests were run. [3]. This study investigated the useful properties of fiber composites loaded up with plant banana fiber furthermore, coconut shells. There are so many plant filaments like banana fiber, bamboo fiber, coconut sheath and sisal fiber which are commonly unloaded aside as waste material have a major capacity of involving it as substitutes as a support material. [4]. This study assesses the warm, morphological and mechanical way of behaving of polypropylene (PP) composite with various regular filaments. The strands utilized were wood, sugarcane, bamboo, babassu, coconut and kenaf with and without coupling specialist. The warm, morphological what's more, mechanical properties were assessed, and a composite PP+GFPP (glass fiber) was utilized as reference. [5].

The primary goal of the current review is the use of jute and coir filaments if support material for the creation of regular composites. To portray the composites what's more, foster a superior comprehension of these composites, the physical and mechanical properties of these composites are assessed to track down hardness, flexural and pliable properties of the jute/coconut coir built up polymer grid composite. [6].

The investigations were arranged according to full factorial plan (FFD) and reaction surface strategy (RSM) based second request numerical models of mechanical properties have been created. Investigation o fluctuation (ANOVA) has been utilized to really take a look at the sufficiency of the created models. From the parametri investigation, it is uncovered that Jute-PP bio-composites display better mechanical properties when contrasted with bio-composites. [7]. In this article, mechanical and tribological portrayal of *Cissus quadrangularis* stem fiber (CQSF)/epoxy tar particulate with and without coconut shell debris (CSA) powder was completed. The materials were created by the hand rest up technique. Epoxy and 30 wt.% CQSF with 40 mm fiber length were taken to create the base material, and CSA was independently added at 2.5, 5, 7.5, and 10 wt.%. [8].

The on-going work deals with the depiction polymer network composites uniting glass fiber and fiber got from coconut. The composite was prepared using hand rest up process and sufficient prudent step has been taken to ensure there is homogeneity. The composite is made out of 60% polyester pitch, 10% glass fiber and 30% coconut fiber. Different mechanical tests like scaled down scale hardness

test, unbending nature, influence quality test has been finished to depict the composite. [9]. This paper assesses the physio-synthetic and mechanical attributes of the strands. The filaments are extricated by us. A progression of examinations is led for this reason: morphological perception with a filtering electron magnifying lens (SEM); thickness assessment with a helium pycnometer, retention rate assessment as per the convention accessible in the writing, Fourier Transform Infrared Spectrometry (FT-IR), compound synthesis assessment as per ASTM 1972 and ASTM 1977 norms, thermogravimetric investigation (TGA) and malleable tests on fiber groups as per NF T25-501-3. [10].

The impact of surface treatment (salt, potassium permanganate, benzoyl chloride and silane) on the mechanical, powerful mechanical and free vibration properties of intra-employ mixture banana/jute woven texture composite has been dissected. Intra-handle woven textures are created by keeping banana yarn in weft course and jute yarn in twist bearing of a bushel type woven texture. [11].

Utilizing polypropylene (PP) as grid and kenaf mat as support, composite tests were created by pressure shaping. From there on, the impact of fiber stacking and basic fiber surface treatment on the mechanical properties were examined. The kena composites were found to have preferable mechanical properties over the polymer matri expected, the interfacial holding between the grid and the filaments improved consider the point when the filaments were exposed to basic treatment. [12]. The current review plans to examine the impacts of stacking succession on physical, mechanical and dampness safe properties of pineapple leaf fiber (PF) and flax fiber (FF) built up composite overlays. The non-crossover and mixture composite covers are created by utilizing vacuum helped sap imbue ment shaping cycle (VARIM) with a between employ arrangement. [13].

In this review, polymer mortars produced with epoxy and unsaturated polyester gums supported with 1%, in weight, of sisal strands were ready. The filaments were synthetically adjusted to work on their similarity with inorganic total, foundry sand, natural fastener, and polymer gum. Sisal filaments were treated with 5% and 10% of NaOH and 20% of acidic corrosive weakened in a fluid arrangement. [14]. This article presents the turn of events and mechanical portrayal of a composite material created from both sustainable assets and biodegradable materials: bamboo woven texture as support and polylactic corrosive (PLA) as sap lattice. The overlay composites were delivered utilizing a film stacking strategy. [15].

2. MATERIALS AND METHODS

The specimens are made according to the weight percentages of Jute fiber and Coconut fiber in Different weight concentrations should be taken to proceed for the examination. Both treated and untreated specimens are made according to the weight concentrations of powder and fiber. We have taken the six different types of specimens

with different weight concentrations. The 6 different specimens are shown in Table 1

Table.1 Composite specimen Preparation weight Percentages

Tensile Test specimens	Weight percentages of specimens
S1	1 gm of Jute fiber and 1 gm of coconut fiber (Untreated)
S2	1 gm of Jute fiber and 1 gm of coconut fiber (Treated)
S3	0.75 gm of Jute fiber and 0.75 gm of coconut fiber (Untreated)
S4	0.75 gm of Jute fiber and 0.75 gm of coconut fiber (Treated)
S5	0.25 gm of Jute fiber and 0.25 gm of coconut fiber (Untreated)
S6	0.25 gm of Jute fiber and 0.25 gm of coconut fiber (Treated)
S7	Specimen made only with Resin

The tensile experiments are performed on a universal testing machine with a transfer speed of 2 mm/min and the impact study was conducted Izod impact testing machine. The thermal testing was performed on the specimen on thermal testing set up for determining the thermal conductivity

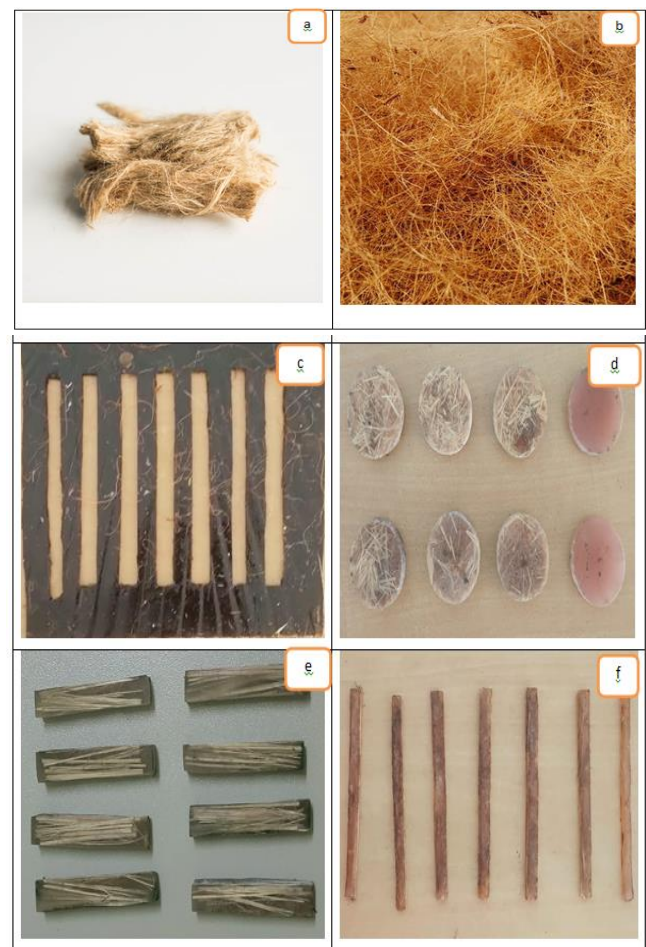


Fig.1 (a) Jute Fiber, (b) Coconut Fiber, (c) Mould preparation, (d) Specimen for Thermal Conductivity Test, (e) Specimen for Impact test (f) Specimen for Tensile test

3. RESULTS AND DISCUSSIONS

The chemical treatment effect on composites specimens shows an important role in because tensile behaviour of polyester composites and it was gradually increased with increase with reinforcement phase. The higher tensile load-bearing capacity was recorded for the S4 specimen of

excellent bonding strength and a combination of Jute fiber and coconut fiber.

In maximum cases the specimen shows high-level strength after chemical treatment because of surface roughness of fiber enhances the superior bonding strength, and it is observed from scanning electronic micrographs. The composite samples exhibited lower-level displacement irrespective of load and chemical treatment. The diminished tensile strength and bearing capacity are noted in the S7 sample. The figures show the load versus displacement curves for a better understanding of the mechanical behaviour of polyester composites.

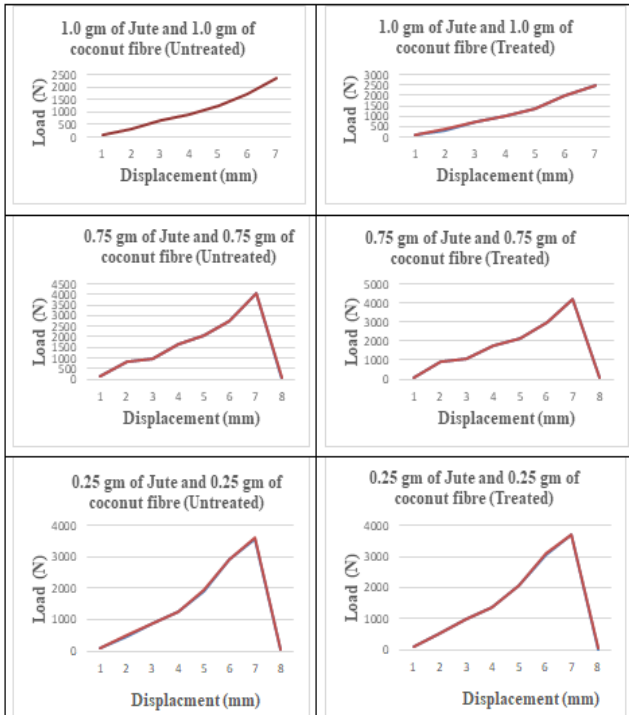


Fig.3 Tensile Behaviour of Composite Specimens

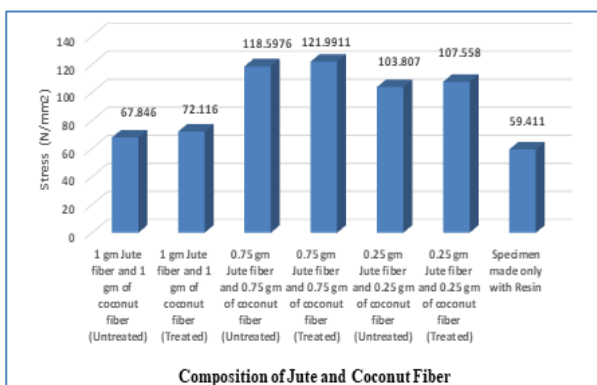


Fig.4 Tensile Behaviour of Composite Specimens

Figure 5 Shows the Charpy test specimens were made according to the dimensions of ASTM D 256-M in which the dimension is 60 x 12.5 x 10 mm. One of the main reasons of concern for composites generally is the low values of impact energy. They show relatively low values of impact energy compared to metals.

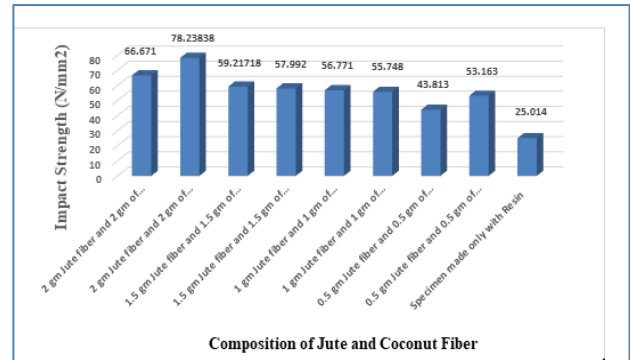


Fig.5. Impact strength of specimens

The ways to increase the impact energy of the composites are being made the major area of research. The figure shows the impact energy variation for fiber-reinforced composites. The tests showed that the composites made with 9 sample fiber resin weight percentage were not very good with the impact stress as it showed very low values from the tests performed.

Figure 6 shows the Thermal Conductivity of polyester composites. Thermal conductivity refers to the amount/speed of heat transmitted through a material. Heat transfer occurs at a higher rate across materials of high thermal conductivity than those of low thermal conductivity.

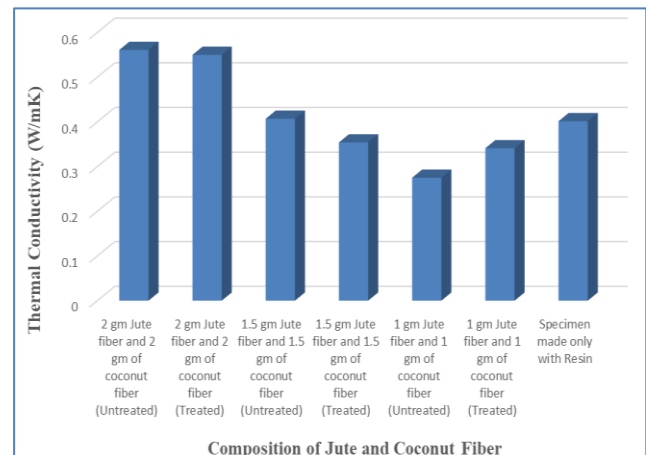


Fig.6. Thermal Conductivity of Composite Specimens

FRACTURE ANALYSIS OF JUTE – COCONUT FIBER REINFORCED COMPOSITES

The fracture surface was examined through the scanning electron microscope micrographs of T1, and T6 under tensile loading condition, these micrographs disclose the nature of the failure of the composite specimen. Fig 7a discloses the uniform teak wood powder distribution in the polyester matrix. The internal cracks were noticed in figure 7b due to tensile load and exhibit the brittle failure of the specimen. The fiber pulls out and de-bonding is observed in figure 5d for tensile specimen T6 under tensile load. The fiber distribution is captured in figure 7c.

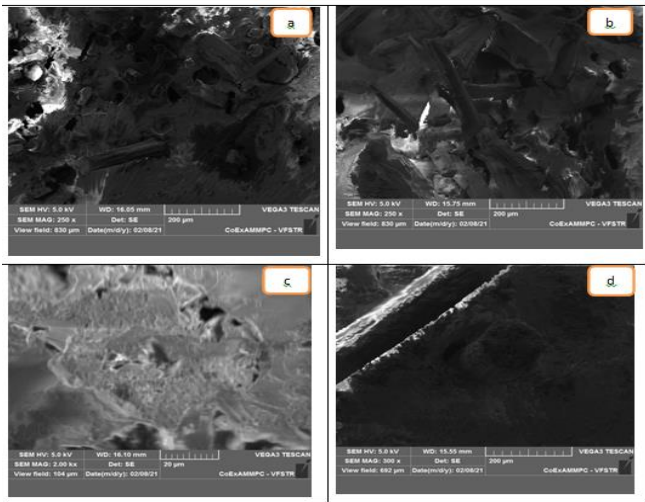


Fig: 5. SEM Images of impact and Tensile samples

4. CONCLUSION

In this work, the fiber-reinforced polyester hybrid composites were prepared as per ASTM standards. Jute fiber and coconut fiber are available abundantly in nature and offer low material density. The impact strength, flexural strength, and tensile strength of the investigated material composite with the jute and coconut were found to be comparatively higher than the novel composite material. The density of the composite decreased with increasing fiber content. Thus, the hybrid composites were found to be light in weight and proposed better mechanical properties and insulating properties. The fracture surface was studied through SEM images. This work shows jute fiber, coconut fiber, and polymer composites with different fiber weight fractions fabricated by hand lay-up technique. The maximum Tensile strength and Impact strength for the combination of corn and coconut fiber composite are 121.9911N/mm^2 and 78.23838 J/cm^2 respectively. The thermal conductivity of the composite is 0.275 W/m.K .

REFERENCES:

- [1] Iyyadurai Jenish, Sathish Gandhi Veeramalai Chinnasamy, Satyappa Basavarajappa, Suyambulingam Indran, D. Divya, Yucheng Liu (2020). <https://doi.org/10.1080/15440478.2020.1838988>.
- [2] B. Bharath, G. Chethan Kumar, G. Shivanna, Syed Sajjad Hussain, B. Chandrashekhar, B.A. Sunil Raj, S. Anand Kumar, C. Girisha (2018). Fabrication and Mechanical Characterization of Bio-Composite Helmet. Volume 5, Issue 1, Part 3, 2018, Pages 2716-2720. <https://doi.org/10.1016/j.matpr.2018.01.053>.
- [3] Célia Regina da Costa, Regina Aparecida Sanches, Júlia Barúque Ramos, Jorge Boueri, Bárbara Maria Gama Guimarães (2013). Mechanical Characterization of the Green Coconut Fiber for Application in the Footwear Industry. Vol. 2 No. 9.
- [4] Santosh Kumar Singh, Manish Kumar Sagar, Rajeev Kumar Upadhyay (2021). Mechanical characterization of plant fortified fiber polymer Composites. Volume 46, Part 20, Pages 11217-11221.
- [5] Alessandra Luiza de Lemos, Pamela Galera Prestes Pires, Marcelo Lopes de Albuquerque, Vagner Roberto Botaro, Jane Maria Faulstich de Paiva, Nei Sebastião Domingues Junior "Biocomposites reinforced with natural fibers: thermal, morphological and mechanical

characterization". Av. Moniz Aragão, 207, 21941-594, Rio de Janeiro, RJ, Brasil.

- [6] Chandra Prakash Singh, Raj Vardhan Patel, Mohd Faizul Hasan, Anshul Yadav, Virendra Kumar, Anil Kumar (2021). Fabrication and evaluation of physical and mechanical properties of jute and coconut coir reinforced polymer matrix composite. Volume 38, Part 5, Pages 2572-2577.
- [7] Tippusultan, V.N. Gaitonde (2015). Preparation and Mechanical Characterization of Jute-PP and CPP Bio-Composites. Pages: 122-132. (Volumes 766-767).
- [8] Iyyadurai Jenish, Sathish Gandhi Veeramalai Chinnasamy, Satyappa Basavarajappa. Tribo-Mechanical characterization of carbonized coconut shell micro particle reinforced with Cissus quadrangularis stem fiber/epoxy novel composite for structural application (2020).
- [9] A. Raji, A. Devaraju, R. Gopi, R. Venkatesh. Fabrication and mechanical characterization of hybrid composite bike safety helmet (2021). Volume 39, Part 1, Pages 892-896.
- [10] Armel Edwige Mewoli, César Segovia, Fabien Betene Ebanda, Atangana Ateba, Pierre Marcel Anicet Noah, Benoit Ndiwe, Abel Emmanuel Njom. Physical-Chemical and Mechanical Characterization of the Bast Fibers of *Triumfetta cordifolia* A.Rich. from the Equatorial Region of Cameroon (2020).
- [11] M Rajesh, Jeyaraj Pitchaimani. Mechanical characterization of natural fiber intra-ply fabric polymer composites: Influence of chemical modifications (2017). <https://doi.org/10.1177/0731684417723084>.
- [12] Sd Jacob Muthu, Ratnam Paskaramoorthy. Mechanical Characterization of Polypropylene Natural Fibre Composites (2011). Pages: 2737-2740. <https://doi.org/10.4028/www.scientific.net/AMR.383-390.2737>.
- [13] Santosh Kumar, Abir Saha. Effects of stacking sequence of pineapple leaf-flax reinforced hybrid composite laminates on mechanical characterization and moisture resistant properties (2021). <https://doi.org/10.1177/09544062211023105>.
- [14] JML Reis, EP Carneiro. Mechanical characterization of sisal fiber reinforced polymer mortars: Compressive and flexural properties (2012). <https://doi.org/10.1177/0731684412462264>.
- [15] A. Porras, A. Maranon. Development and characterization of a laminate composite Material from polylactic acid (PLA) and woven bamboo fabric (2012)., Volume 43, Issue 7, October Pages 2782-2788. <https://doi.org/10.1016/j.compositesb.2012.04.039>.

DESIGN OF GEAR ASSEMBLY USING CATIA V5 SOFTWARE

BOMMERA SHIVAJI¹,

Student, *Department of Mechanical Engineering, Malla Reddy College of Engineering and Technology, India*

Abstract—CATIA V5 (Computer-Aided Three-dimensional Interactive Application) is the product of the highest technological level and represents standard in the scope of designing. Instantaneously, it is the most modern integrated CAD/CAM/CAE software system that can be found on the market for commercial use and scientific-research work. In this paper, the results of the research of three-dimensional (3D) parameter modelling of meshing assembly of spur gears using CATIA V5 software system. Gears modelling by computers are based on geometric and perspective transformation which is not more detail examined in the paper because of their large scope. Parameter modelling application makes possible the control of created 3D gear model through previous defined parameter which is based on relations and geometric constraints (parallelism, perpendicular, etc.). The final shape of gear assembly changes by changing of values of characteristic independent changeable parameters. It is possible to do a control of gear geometry and meshing assembly by use of tools palette Knowledge. Gears modelling were done in Sketcher, Part Design, Generative Shape Design modules and assembly design of CATIA V5 system. As prerequisite for this way of modelling, it is necessary to know modelling methodology in the following CATIA V5 modules, too: Wireframe and Surface Design and Assembly Design.

Keywords—*Catia V5, 2D model, 3D model, circular pattern command, Aerospace.*

I. INTRODUCTION

CATIA V5 (Computer-Aided Three-dimensional Interactive Application) is the product of the highest technological level and represents standard in the scope of designing. Instantaneously, it is the most modern integrated CAD/CAM/CAE software system that can be found on the market for commercial use and scientific-research work. The biggest and well-known world companies and their subcontractors use them. It is the most spread in the car industry (Daimler Chrysler, VW, BMW, Audi, Renault, Peugeot, Citroen, etc.), airplane industry (Airbus, Boeing, etc.), and production of machinery and industry of consumer goods. In the „heart" of the system is the integrated associational data structure for parameter modelling, which makes possible the fact that the changes on model reflects through all related phases of the product development. In that way, time needed for handmade models remodelling cancels. The system makes possible all geometric objects parametering, including solids, surfaces, wireframe models and constructive elements. To obtain the maximum during the work with CATIA V5 system, optimized certificated hardware configurations are recommended.

In addition is shown modelling of characteristic standard catalogue gears: spur gear, bevel gear and worm. It is possible to do a control of gear geometry by use of tools palette Knowledge. Gears modelling were done in Sketcher, Part Design and Generative Shape Design modules of

CATIA V5 system. As prerequisite for this way of modelling, it is necessary to know modelling methodology in the following CATIA V5 modules, too: Wireframe and Surface Design and Assembly Design. Parameter marks and conventional formulas.

Marine engines are among heavy duty machineries, which need to be taken care of in the best way during prototype development stages. These engines are operated at very high speeds which induce large stresses and deflections in the gears as well as in other rotating components. For the safe functioning of the engine, these stresses and deflections have to be minimized. In this work, structural analysis on a high speed helical gear used in marine engines, have been carried out. The dimensions of the model have been arrived at by theoretical methods. The stresses generated and the deflections of the tooth have been analyzed for different materials. Finally the results obtained by theoretical analysis and Finite Element Analysis are compared to check the correctness. A conclusion has been arrived on the material which is best suited for the marine engines based on the results. Basically the project involves the design, modelling and manufacturing of helical gears in marine applications. It is proposed to focus on reduction of weight and producing high accuracy gears.

II. METHODS AND MATERIALS

GEAR TERMINOLOGY

- 1) Pitch circle: Theoretical circle upon which all gear calculations are usually based. Pitch circles of
- 2) Mating gears are tangent to one another.
- 3) Pitch diameter: The diameter of the pitch circle.
- 4) Number of teeth: The number of teeth on the gear.
- 5) Diametric pitch: The number of teeth of a gear per inch of its pitch diameter.
- 6) Module: The ratio of pitch diameter to the number of teeth. It is reciprocal of the diametric pitch.
- 7) The pitch diameter is specified either in inches or millimeters.
- 8) Pressure angle: The angle through which forces are transmitted between meshing gears. It is
- 9) Either 14.5° or 20°. It defines the geometry of the gear tooth and also determines the diameter of the Base circle.
- 10) Addendum: The amount of tooth that protrudes above the pitch circle (from top land to pitch circle)
- 11) Dedendum: The Radial distance from the pitch circle to the bottom of the tooth space.
- 12) Clearance circle: the circle tangent to the addendum circle of the mating gear.
- 13) Clearance: the distance between the tooth top surface and the bottom surface of a mating gear.

III. EXPERIMENTAL SYSTEM DESCRIPTION

HISTORY OF CATIA:

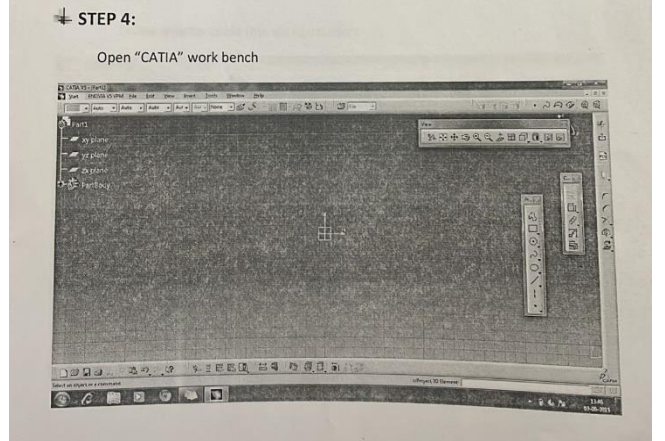
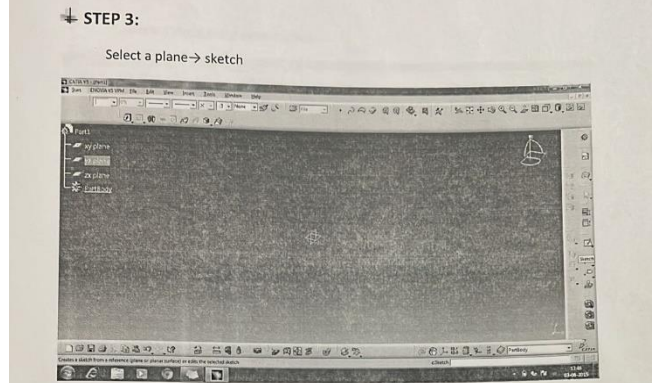
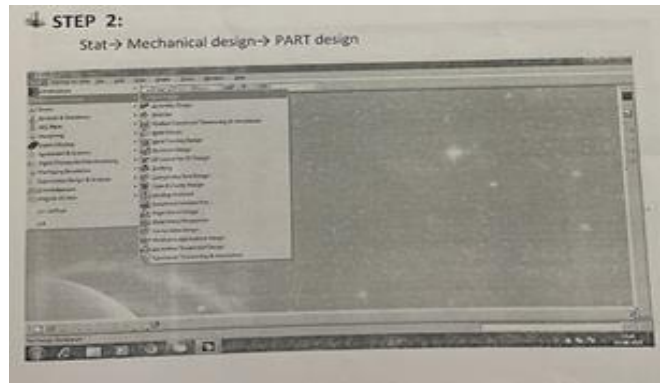
CATIA started as an in-house development in 1977 by French aircraft manufacturer Avions Marcel assault, at that time customer of the CADAM CAD software to develop assault's Mirage fighter jet, then was adopted in the aerospace, automotive, shipbuilding, and other industries. Initially named CATI (Conception Assistée Tridimensionnelle Interactive – French for Interactive Aided Three-dimensional Design) - it was renamed CATIA in 1981, when Dassault created a subsidiary to develop and sell the software, and signed a non-exclusive distribution agreement with IBM. In 1984, the Boeing Company chose CATIA as its main 3D CAD tool, becoming its largest customer.

SUPPORTED OPERATING SYSTEMS AND PLATFORMS:

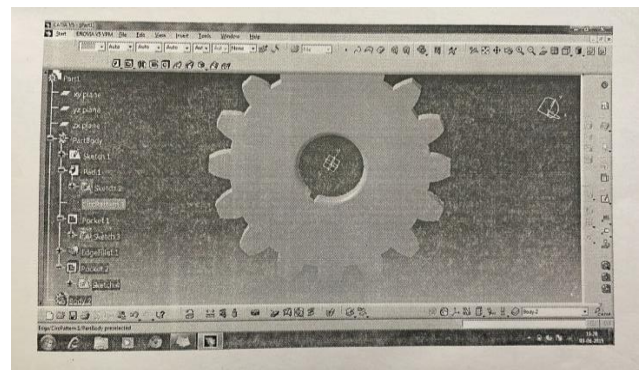
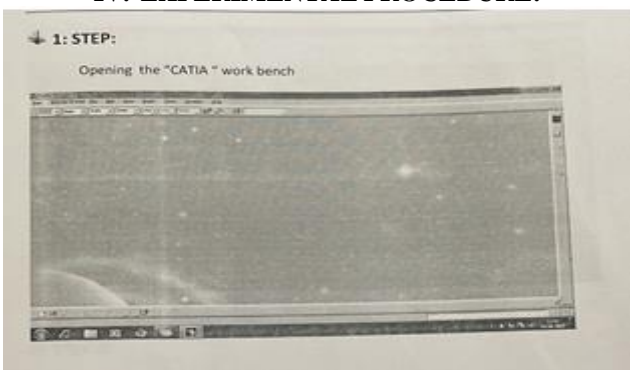
CATIA V6 runs only on Microsoft Windows and Mac OS with limited products. CATIA V5 runs on Microsoft Windows (both 32-bit and 64-bit), and as of Release 18Service Pack4 on Windows Vista 64.IBM AX, Hewlett Packard HP.UX and Sun Microsystems Solaris are supported. CATIA V4 is supported for those Unixes and IBM MVS and VM/MS mainframe platforms up to release 1.7. CATIA V3 and earlier run on the mainframe platforms. NOTABLE INDUSTRIES USING CATIA CATIA can be applied to a wide variety of industries, from aerospace and defense, automotive, and industrial equipment, to high tech, shipbuilding, consumer goods, plant design, consumer packaged goods, life sciences, architecture and construction, process power and petroleum, and services. CATIA V4, CATIA VS, Pro/E, NX (formerly Unigraphics), and Solid Works are the dominant systems.

The Boeing Company used CATIA V3 to develop its 777 airliner, and is currently using CATIA VS for the 787 series aircraft. They have employed the full range of Dassault Systems' 3D PLM products - CATIA, DELMIA, and ENOVIALCA - supplemented by Boeing developed applications. The development of the Indian Light Combat Aircraft has been using CATIA VS. Chinese Xian JH-7 A is the first aircraft developed by CATIA V5, when the design was completed on September 26, 2000. European aerospace giant Airbus has been using CATIA since 2001.. Canadian aircraft maker Bombardier Aerospace has done all of its aircraft design on CATIA The Brazilian aircraft company, EMBRAER, use Catia V4 and VS to build all airplanes.

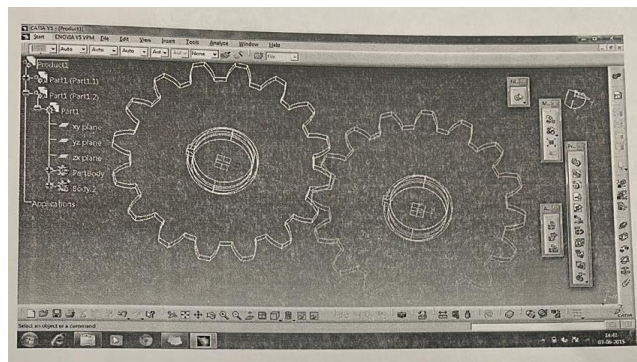
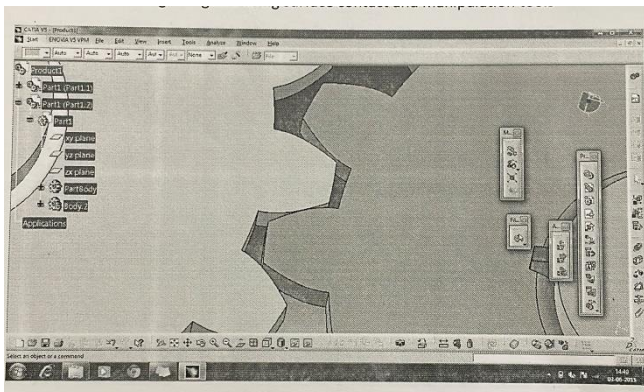
IV. EXPERIMENTAL PROCEDURE:



Draw a circle using sketch tool and then, Divide quarter into six equal parts. Drawing imaginary circles for involute curves. Complete involute circles including tangents. Drawing the involute curve using spline command. Complete the 2D view. Using the circular pattern command. Using the edge fillet command and then draw a kea hole using pocket command.

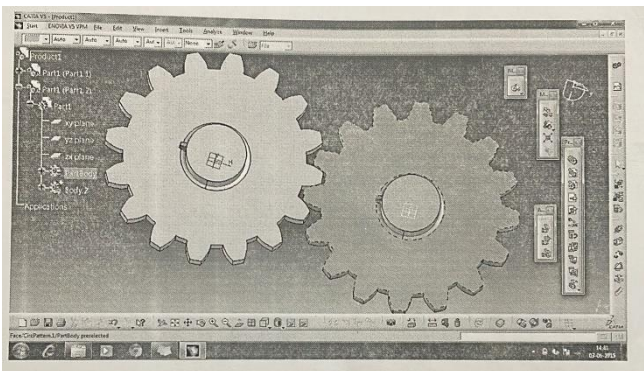


Assembling two gears using surface contact and manipulation tools.



V. RESULTS AND DISSCUSSION

Complete view of Gears



Wave frame view of Gears

CONCLUSIONS

Gears are the moving parts which rotates with reference to its axis and which carries torque in it, while rotating it meshes with another gear which helps in transmitting torque which is inversely proportional to speed. In this project we designed gears using involutes method which is known as one of the accurate arc method for gear teeth. We designed it using CAD tool namely CATIA V5 R20 which is a very advanced design tool. It contains several workbenches, we designed gears using sketcher workbench and added volume using part design workbench which has a large number of command tools. After designing in part design, the gears are imported Assembly workbench for further meshing. While meshing gears many factors should be in main so that its efficiency should not be loss. Meshing Is done using constrain coincidence in assembly workbench and surface constrain.

Optimization of Properties of 3d Printed Abs Material by L₉ Orthogonal Array Method

Mr. Boyapati Chandra Bose¹, Dr. B. Venkata Siva Bathula², Dr. Venkannababu Mendi³

¹ Student, Department of Mechanical Engineering, Narasaraopeta Engineering College (Autonomous), Narasaraopeta - 522601, Guntur District, Andhra Pradesh, India.

² Professor & HOD, Department of Mechanical Engineering, Narasaraopeta Engineering College (Autonomous), Narasaraopeta - 522601, Guntur District, Andhra Pradesh, India.

³ Associate Professor, Department of Mechanical Engineering, Narasaraopeta Engineering College (Autonomous), Narasaraopeta - 522601, Guntur District, Andhra Pradesh, India.

Abstract: Now a day's 3D printing is one of the advance manufacturing processes, also known as Additive manufacturing. Achieving desired strength of 3D printed parts using different materials is still an area of current research. Most of the research are focused on the strength evaluation on ABS material as per ASTM D638 standard. The optimization parameters availability in Cura Software i.e., infill pattern, infill density, layer height and print speed of 3D printer, ABS material by L₉ orthogonal array method. Acrylonitrile butadiene styrene (ABS) has good mechanical properties than PLA material. ABS has toughness, durability and ductility makes it a great material for "wear & tear" application. In this project the specimens are modelled using Fusion 360 software. Tensile specimen is 3D printed as per ASTM D638 standard. It is observed that tensile strength is maximum i.e., "646 N" for 3rd set of experiments, and the Input print settings are Layer Height- 0.2mm, Infill Pattern-Cubic, Infill Density- 25%, Print Speed- 60mm/sec. Hardness is maximum i.e., "174HV" for 7th set of experiments.

1. INTRODUCTION

Additive manufacturing is one of the advances & fast manufacturing process for prototype models. The working of 3D printing is building up layer-by-layer, it refers to a variety of processes in which the material is deposited, solidified under computer guidance to generate a three-dimensional object. First, computer-aided design (CAD) model is designed in any 3D design software, export the model into stereolithography (.STL) file format. Second, the .STL file is imported into 3D printing software for slicing the object and generating the 3D printed code, to process the generation of a body in the printer. In the additive manufacturing process, we have selected Fused Deposition method (FDM) process that gives continues filament of thermoplastic material.

Filament is in the form of spool and is moving to heated nozzle and solid state of material (plastic) is melted into semi-liquid state and gets deposited and solidified to the given shape as input. ABS as the selected filament for printing, it has the good impact resistance, toughness, tensile strength, and rigidity. In this paper we are studying the print setting for the printer to print the object and withstand the good ultimate force and ultimate stress. In 3D printing software to print an object we must specify some of the print settings to slice the object. In the software the system will give default settings to slice the object. In this paper we are changing the print setting and optimizing the values to get best output and obeys the mechanical properties likes tensile strength and ultimate stress & force.

Taguchi method is a robust design technique used in many industries and improves the processing quality, reduces the greater number of experiments, and minimizes the outputs and promotes the best stability in the Taguchi method. I have selected the L₉: Four three-level factor orthogonal array, in this method there are four variables, three values and nine experiments. The four variables are layer height, infill pattern, infill density and print speed. In this work the design of ASTM d638 [dog bone structure] is designed on the Fusion 360 software. It is one of the Computer Aided Design software and a product of Autodesk. It is a cloud-based 3D CAD, CAM, CAE design too. It is one of the parametric software and license-based software. The entire software is cloud based so we can access from any place and in any system.

The main highlights features are:

1. Parametric Modelling
2. Rendering
3. Generative Design
4. Animation
5. Simulation
6. Program manufacturing for CNC machines

2. EXPERIMENTED MATERIALS & METHODS

A. TENSILE DATA

The ASTM D638 is one of the lists in American Society for Testing and Material and used to test the tensile properties of reinforced and non-reinforced plastics. This test is performed by applying tensile forces to the sample and measuring how its properties change under extreme tension (or) stress.

The properties measured by this method are:

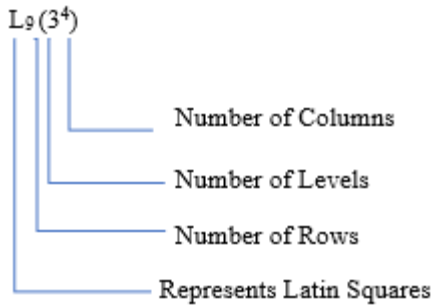
Tensile Force

The amount of force that can be applied on a working sample before it deforms. In this test, the tensile force is the maximum tension can be applied on the working sample. All the tension tests are done on universal machine and this testing machine helps to create a graph containing the recorded force deformation data, and the quantity its maximum resistance or its breaking point.

Taguchi's method (Orthogonal Array)

For the optimization of print settings, we have selected L₉ orthogonal array. This method helps to design of experiments utilizes the robust design, which can be applied to a wide variety of problems. Orthogonal array is a matrix of numbers which are arranged in rows & column the change of factor from experiment to experiment will be

displayed. Each row the state of factor in each experiment will be represented.



From the table the Independent Variables are:

- 1) Layer Height
- 2) Infill Pattern
- 3) Infill Density
- 4) Print Speed

The taken Values are

S. No	Independent variable				Performance
	1	2	3	4	
1	1	1	1	1	P ₁
2	1	2	2	2	P ₂
3	1	3	3	3	P ₃
4	2	1	2	3	P ₄
5	2	2	3	1	P ₅
6	2	3	1	2	P ₆
7	3	1	3	2	P ₇
8	3	2	1	3	P ₈
9	3	3	2	1	P ₉

LAYER HEIGHT

- 1- 0.2mm
- 2-0.15mm
- 3- 0.1mm

INFILL PATTERN

- 1- Lines
- 2-Triangles
- 3- Cubic

INFILL DENSITY

- 1-15%
- 2-20%
- 3-25%

PRINT SPEED

- 1- 50mm/sec
- 2- 55mm/sec
- 3-60mm/sec

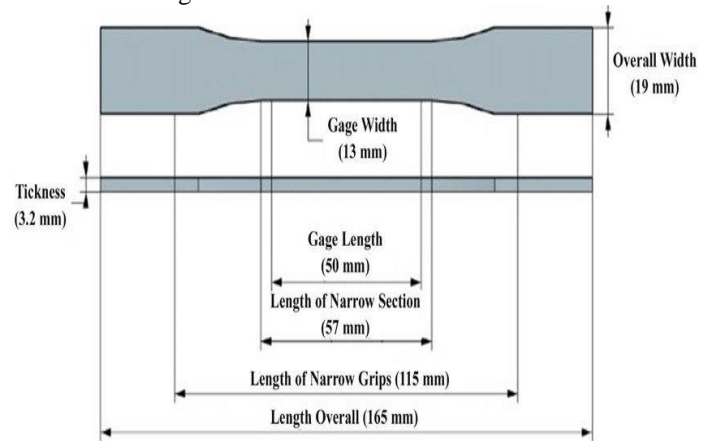
Substitute the values and variable in above orthogonal table.

S. No	Independent variable				Perfor mance
	1(Layer height)	2(Infill pattern)	3(Infill density)	4(Print speed)	
1	0.2mm	Lines	15%	50mm/sec	P ₁
2	0.2mm	Triangles	20%	55mm/sec	P ₂
3	0.2mm	Cubic	25%	60mm/sec	P ₃
4	0.15mm	Lines	20%	60mm/sec	P ₄
5	0.15mm	Triangles	25%	50mm/sec	P ₅
6	0.15mm	Cubic	15%	55mm/sec	P ₆
7	0.1mm	Lines	25%	55mm/sec	P ₇
8	0.1mm	Triangles	15%	60mm/sec	P ₈
9	0.1mm	Cubic	20%	50mm/sec	P ₉

FUSION 360 SOFTWARE

For the design of ASTM d638 (Dog bone Structure) we have selected Fusion 360 software. The steps for designing and export the design into .STL file for printing.

1. At first, we must design the dog bone structure in design work bench according to the given specified dimensions by ASTM d638.
2. Modify the design according to the required dimensions.
3. Next save the file and the export the file in. STL format.
4. The .STL file is used as input for additive manufacturing and especially we are using 3d Printing.



ABS MATERIAL

ABS (Acrylonitrile Butadiene Styrene) material has selected for entire work as infill material in 3D printer. Physical properties like impact resistance, toughness, and rigidity compared to other polymers also strong & cheap. ABS plastic is widely used on mechanical purposes and electric purposes. It is suitable for FDM due to high stability and various post-processing options like sanding, painting, filling etc. For the tensile strength ABS is preferred due to its improved ductility over PLA and have high flexural strength and better elongation before breaking. The surface finishing and past processing of the print layers will be visible after printing in FDM method and is typically print in a matte finish resulting in a glossier finish.

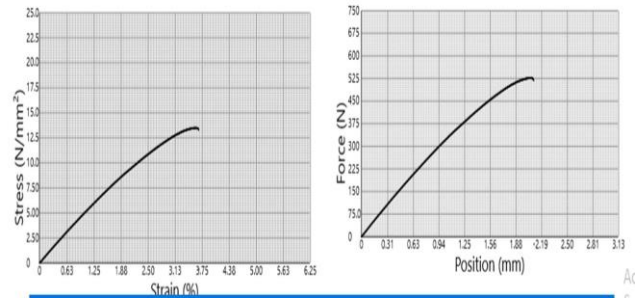
3D PRINTING

For 3D printing of dog bone, we have selected Cura Ultimaker S5 3D printer. It is an open source slicing application.

Steps to follow for printing the component:

- 1) Download the Cura Ultimaker S5 software in your pc.
- 2) Now insert the dog bone component on print bed.
- 3) Now select the material and the nozzle to print.
- 4) According to the table select the print options and slice the component it will generate G-Codes.
- 5) Now save the G-Code file in SD card.
- 6) Repeat the same procedure according to table, we get nine outputs.
- 7) Now insert the SD Card in 3D printer and load the material through selected nozzle.
- 8) Print the nine outputs.

Width mm	Thickness mm	Yield Force N	Yield Stress N/mm ²	Yield Strain mm/mm	Ultimate Force N	Ultimate Stress N/mm ²	Ultimate Strain %	Break Force N	Break Stress N/mm ²	Break Strain %	Total Elongation (Auto) %
13.0	3.00	543	18.1	0.0387	523	17.4	3.87	513	15.2	3.88	3.88

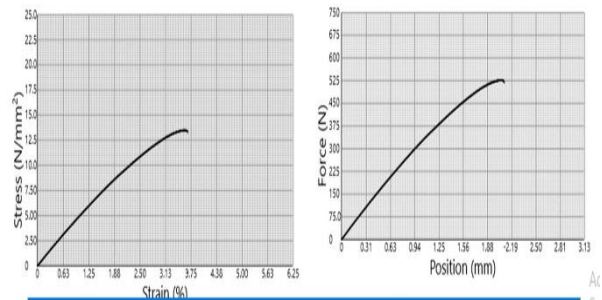


Graph of the output p1

The yield force of the output 1 is 543N.

Performance	1	2	3	4	5	6	7	8	9
Width(mm)	13.0	13.0	13.0	13.0	13.0	13.0	13.0	13.0	13.0
Thickness (mm)	3.00	3.0	3.0	3.00	3.0	3.0	3.0	3.0	3.0
Yield Force(N)	543	572	646	602	632	608	556	523	619
Yield Stress(N/mm ²)	13.9	14.7	16.6	15.4	16.2	15.6	14.3	13.4	15.9
Yield Strain	0.0445	0.0374	0.0399	0.0420	0.0394	0.0401	0.0421	0.0376	0.0429
Ultimate Force(N)	543	572	646	602	632	608	556	523	619
Ultimate Stress(N/mm ²)	13.9	14.7	16.6	15.4	16.2	15.6	14.3	13.4	15.9
Ultimate Strain (%)	4.45	3.74	3.99	4.20	3.94	4.01	4.21	3.76	4.29
Break Force (N)	513	552	591	560	609	513	513	515	561
Break Stress(N/mm ²)	13.1	14.2	15.2	14.4	15.6	13.1	13.1	13.2	14.4
Break Strain (%)	6.72	4.18	5.65	8.38	4.37	6.30	6.03	3.87	5.54
Total elongation (%)	6.72	4.18	5.65	8.38	4.37	6.30	6.03	3.87	5.54

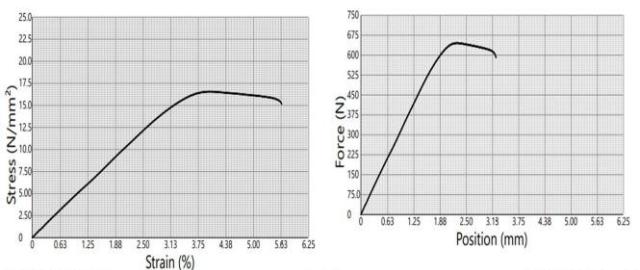
Width mm	Thickness mm	Yield Force N	Yield Stress N/mm ²	Yield Strain mm/mm	Ultimate Force N	Ultimate Stress N/mm ²	Ultimate Strain %	Break Force N	Break Stress N/mm ²	Break Strain %	Total Elongation (Auto) %
13.0	3.00	572	19.1	0.0397	528	18.0	3.97	519	16.3	3.88	3.88



Stress strain of the output graph 2

The yield force of the output 2 is 572N.

Width mm	Thickness mm	Yield Force N	Yield Stress N/mm ²	Yield Strain mm/mm	Ultimate Force N	Ultimate Stress N/mm ²	Ultimate Strain %	Break Force N	Break Stress N/mm ²	Break Strain %	Total Elongation (Auto) %
13.0	3.00	646	21.5	0.0389	640	21.3	3.89	591	18.2	5.65	5.65



Stress Strain Graph of the 3rd output

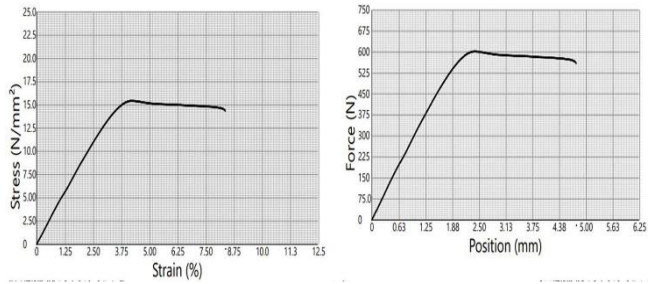
The yield force of the output 3 is 646N.

3. RESULT & DISCUSSIONS

After testing of nine outputs on universal testing machine the values are tabulated.

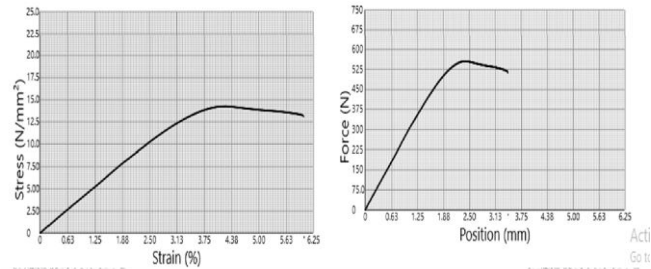
S. No	Independent variable				Performance
	1(Layer height)	2(Infill pattern)	3(Infill density)	4(Print speed)	
1	0.2mm	Lines	15%	50mm/sec	48min/5g/0.69m
2	0.2mm	Triangles	20%	55mm/sec	47min/5g/0.73m
3	0.2mm	Cubic	25%	60mm/sec	47min/5g/0.77m
4	0.15mm	Lines	20%	60mm/sec	56min/5g/0.72m
5	0.15mm	Triangles	25%	50mm/sec	1hr-4min/5g/0.76m
6	0.15mm	Cubic	15%	55mm/sec	56min/5g/0.68m
7	0.1mm	Lines	25%	55mm/sec	1hr-19min/5g/0.73m
8	0.1mm	Triangles	15%	60mm/sec	1hr-9min/5g/0.64m
9	0.1mm	Cubic	20%	50mm/sec	1hr-20min/5g/0.69m

Width mm	Thickness mm	Yield Force N	Yield Stress N/mm ²	Yield Strain mm/mm	Ultimate Force N	Ultimate Stress N/mm ²	Ultimate Strain %	Break Force N	Break Stress N/mm ²	Break Strain %	Total Elongation (Act) %
13.0	3.00	602	19.4	0.0420	692	19.4	4.20	560	14.4	8.39	8.39



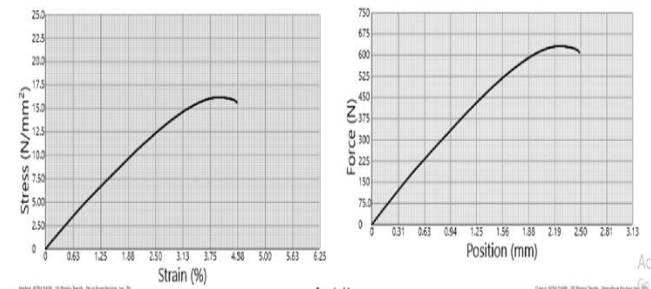
Graph of the 4th output
The yield force of the output 4 is 602N.

Width mm	Thickness mm	Yield Force N	Yield Stress N/mm ²	Yield Strain mm/mm	Ultimate Force N	Ultimate Stress N/mm ²	Ultimate Strain %	Break Force N	Break Stress N/mm ²	Break Strain %	Total Elongation (Act) %
13.0	3.00	556	14.2	0.0421	596	14.3	4.21	513	12.1	8.03	8.03



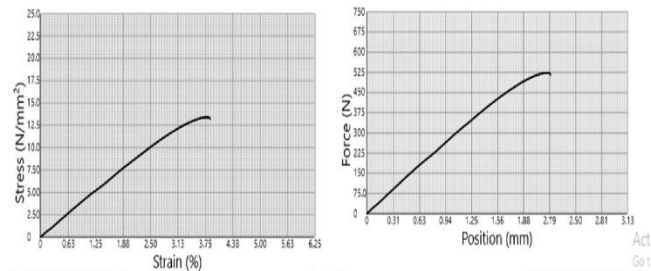
Graph of the 7th output
The yield force of the output 7th is 556N.

Width mm	Thickness mm	Yield Force N	Yield Stress N/mm ²	Yield Strain mm/mm	Ultimate Force N	Ultimate Stress N/mm ²	Ultimate Strain %	Break Force N	Break Stress N/mm ²	Break Strain %	Total Elongation (Act) %
13.0	3.00	632	18.2	0.0344	632	18.2	3.44	609	18.8	4.37	4.37



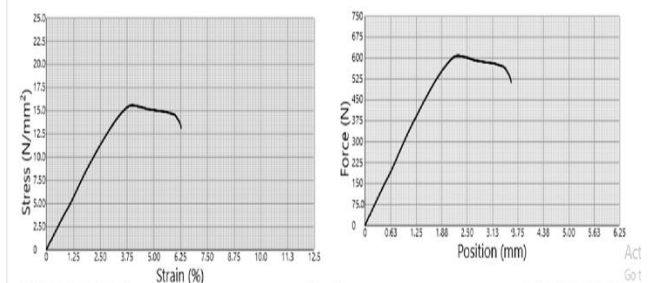
Graph of the 5th output
The yield force of the output 5th is 632N.

Width mm	Thickness mm	Yield Force N	Yield Stress N/mm ²	Yield Strain mm/mm	Ultimate Force N	Ultimate Stress N/mm ²	Ultimate Strain %	Break Force N	Break Stress N/mm ²	Break Strain %	Total Elongation (Act) %
13.0	3.00	523	13.4	0.0376	523	13.4	3.76	510	13.2	3.97	2.87



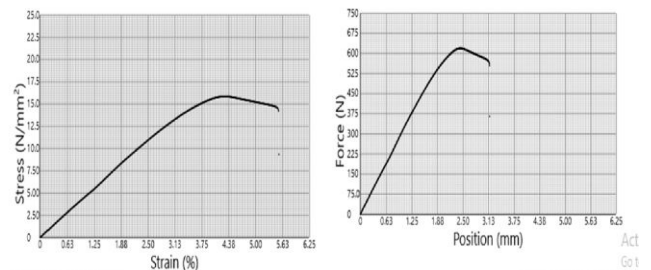
Graph of the 8th output
The yield force of the output 7th is 523N.

Width mm	Thickness mm	Yield Force N	Yield Stress N/mm ²	Yield Strain mm/mm	Ultimate Force N	Ultimate Stress N/mm ²	Ultimate Strain %	Break Force N	Break Stress N/mm ²	Break Strain %	Total Elongation (Act) %
13.0	3.00	608	18.6	0.0401	608	18.6	4.01	513	13.1	8.30	8.30



Graph of the 6th output
The yield force of the output 6th is 608N.

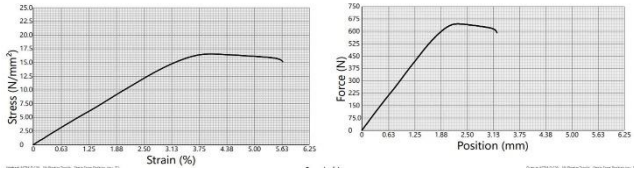
Width mm	Thickness mm	Yield Force N	Yield Stress N/mm ²	Yield Strain mm/mm	Ultimate Force N	Ultimate Stress N/mm ²	Ultimate Strain %	Break Force N	Break Stress N/mm ²	Break Strain %	Total Elongation (Act) %
13.0	3.00	619	18.6	0.0429	619	18.6	4.29	561	14.4	8.54	8.54



Graph of the 9th output
The yield force of the output 7th is 619N.

DISCUSSIONS

Width (mm)	Thickness (mm)	Yield Force (N)	Yield Stress (N/mm ²)	Yield Strain (mm/mm)	Ultimate Force (N)	Ultimate Stress (N/mm ²)	Ultimate Strain (%)	Break Force (N)	Break Stress (N/mm ²)	Break Strain (%)	Total Elongation (Auto) (%)
13.0	3.00	646	16.6	0.0209	646	16.6	3.38	501	15.2	8.80	8.80



Stress Strain Graph of the 3rd output

INPUT PRINT SETTINGS

- Layer Height - 0.2mm
- Infill Pattern -Cubic
- Infill Density - 25%
- Print Speed - 60mm/sec
- Estimated time/material – 47mins
- Material Consumption - /5g/0.77m

ANALYSIS REPORT

- Yield Force - 646N
- Yield Stress - 16.6N/mm²
- Yield Stress - 16.6N/mm²
- Ultimate Force – 646N
- Ultimate Stress – 16.6N/mm²
- Break Stress - 15.2N/mm²

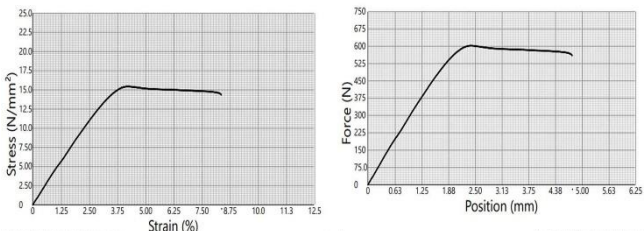
From this work can give a confidence for the good tensile properties of any component you can give these print settings?

1. From the table we observed that 4th output has the highest elongation and 8th output has least elongation form the total 9 outputs.
2. Total elongation of 4th output=8.38% 50.

If a component needs a good elongation, we can give these print settings.

- Layer Height - 0.15mm
- Infill Pattern -Lines
- Infill Density - 20%
- Print Speed - 60mm/sec

Width (mm)	Thickness (mm)	Yield Force (N)	Yield Stress (N/mm ²)	Yield Strain (mm/mm)	Ultimate Force (N)	Ultimate Stress (N/mm ²)	Ultimate Strain (%)	Break Force (N)	Break Stress (N/mm ²)	Break Strain (%)	Total Elongation (Auto) (%)
13.0	3.00	502	15.4	0.0420	602	15.4	4.20	560	14.4	8.38	8.38



Graph of the 4th output

If the component need less elongation to a particular component, you must follow these print settings.

- Total elongation of 8th output=3.87%
- Layer Height - 0.1mm

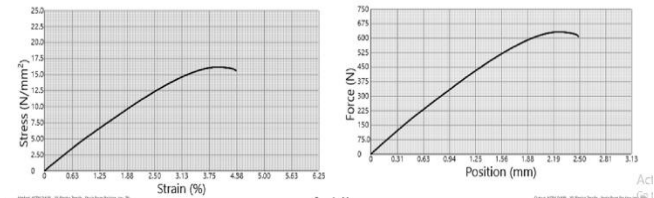
Infill Pattern -Triangles

Infill Density - 15%

Print Speed - 60mm/sec

3. The highest break force is appearing on the 5th output.

Width (mm)	Thickness (mm)	Yield Force (N)	Yield Stress (N/mm ²)	Ultimate Force (N)	Ultimate Stress (N/mm ²)	Break Force (N)	Break Stress (N/mm ²)	Break Strain (%)	Total Elongation (Auto) (%)
13.0	3.00	602	18.2	602	18.2	609	18.8	4.37	4.37



Graph of the 5th output

Break Force=609N, Print settings for the 5th output are:

- Layer Height - 0.15mm, Infill Pattern -Triangles, Infill Density - 25%, Print Speed - 50mm/sec

CONCLUSION

Conclusion of the project clearly says that the below print properties are suitable for certain components like.

1. Tensile strength is maximum i.e. “646 N” at the 3rd set of experiments and the input values for the set are; Layer Height - 0.2mm, Infill Density - 25%, Infill Pattern – Cubic, Print Speed - 60mm/sec
2. Maximum elongation is on 4th set of experiments i.e.” 8.38%” and the input values are; Layer Height - 0.15mm, Infill Density - 20%, Infill Pattern – Lines, Print Speed - 60mm/sec

REFERENCES

- [1] M Rismalia” Infill pattern and density effects on the tensile properties of 3D printed PLA material” 2019.
- [2] N.Shahrudin” An Overview on 3D Printing Technology: Technological, Materials, and Applications” 2019.
- [3] Nagendra G. Tanikella” ensile strength of commercial polymer materials for fused filament fabrication 3D printing” 2017
- [4] jinky C. Pawar “Optimization of 3D Printing Process” March 2019.
- [5] Ramu Murugan” Influence Of Process Parameters on The Mechanical Behaviour And Processing Time Of 3d Printing” 2018.
- [6] David B. Dooner “A Geneva Wheel and a Gear Train” June 2014.
- [7] <https://dergipark.org.tr/en/pub/jnrs/issue/38950/35034>
- [8] <https://amfg.ai/2018/06/29/abs-plastic-3d-printing-all-you-need-to-know/>
- [9] <https://plasticextrusiontech.net/resources/what-is-abs-material/>
- [10] <https://www.instron.com/en-in/testing-solutions/astm-standards/astmd638#:~:text=ASTM%20D638%20is%20the%20most,mechanical%20strength%20of%20their%20materials.>
- [11] Vinod G. Gokhare” A Review paper on 3D-Printing Aspects and Various Processes Used in the 3D-Printing” 2017.

PRODUCTION OF 4 INCH CLEAT GREY IRON CASTING BY FULL MOULD DRY SAND CASTING PROCESS

Srinivasa Reddy Yarram¹, Jabihulla Shariff Md²,

^{1,2} Assitant Professor, Mechanical Engineering, Pace Institute Of Technology & Sciences, Ongole ,India

ABSTRACT: In this project work an attempt is made to produce the 4 inch cleat complexed casting into simple by full mould dry sand-casting process. In this casting all the counter sink multiple holes are produced in as cast compared to drilling in conventional casting process. Undercut is made simple, without core arrangement in this casting for easy assembly in the boiler bed. The elimination of the core box and core making and multiple holes drilling saved the cost. This 4inch cleat is produced in highly productive manner and ready to assemble in the boiler for its erection and usage. Not only time saved but unskilled workmen produced the complexed casting. In this casting production the EPS material is used as pattern material and full moulding is done in dry sand. The melting is done in DBC, liquid grey iron metal is treated with inoculation with low CEV and poured the full moulds to get the castings.

Key Words: complexed cleat 4 inch casting, grey iron melting in DBC, EPS cleats patterns, under cut elimination and no core, multiple counter sink holes as cast and organizational editing before formatting. Please note

DESIGN AND FABRICATION OF INJECTION MOULDING DIE USING WIRE EDM

(With a Comparison of several features on the component produced via
Injection Moulding and 3D Printing)

Penugonda Suresh Babu¹, Suneel Donthamsetty²

¹*Associate Professor, Department of Mechanical Engineering, Narasaraopeta Engineering College (Autonomous),
Narasaraopet - 522601, Guntur District, Andhra Pradesh, India.*

Email: sureshbabudevi.p@gmail.com, Tel: 91-8500857969

²*Vice-Principal & Professor, Department of Mechanical Engineering, Narasaraopeta Engineering College (Autonomous),
Narasaraopet - 522601, Guntur District, Andhra Pradesh, India.*

Email id: viceprincipal@nrtec.in, Tel.: 91-9441895535

Abstract: The importance of injection moulding process is increasing day by day and in this work an attempt is made to fabricate a die which suits for Injection moulding machine to prepare a Key Chain with “NEC logo”. As a case study and for comparing the features of product i.e Key Chain, 3D Printing has been selected to produce same component. Finally costing and other features are compared.

Keywords—Wire EDM, 3D Printing, Injection Moulding, Key Chain.

CONVERSION OF HIGH-DENSITY POLYETHYLENE (HDPE) TO USEFUL MATERIALS

Y.pushpa vardhini ¹, K. Anupama francy ², G. Mahesh ³, S v sai sudheer ⁴

¹ Student, mechanical engineering, vishnu institute of technology, bhimavaram, india

² associate professor, department of mechanical engineering, vishnu institute of technology, bhimavaram, india

³ assistant professor, department of mechanical engineering, vishnu institute of technology, bhimavaram, india

⁴ associate professor, department of mechanical engineering, vishnu institute of technology, bhimavaram, india

Abstract – High density polyethylene (HDPE) is a thermoplastic polymer produced from the monomer ethylene and it is widely used in pipe industry due to high strength-to-density ratio. HDPE is also used in the production of plastic bottles, corrosion-resistant piping, geo-membranes and plastic lumbers. The HDPE components take many years to dissolve in the soil and hence the earth pollution increases. So it's very much need to recycle. While recycling HDPE the number '2' as resin identification code obtained and it can be lucratively used in the plastic components of bottle caps, electrical and plumbing boxes etc. From the perspective of sustainability, researchers have tried to recycle HDPE by mechanical, biological and chemical approaches. However the mechanical approach is a lucrative choice and less harmful. So, in the present work, the process of used HDPE recycle is studied. This study discusses the obstacles of the recycle of HDPE in detail.

Keywords - Recycling, HDPE, grinding wheels, pollution, thermoplastic polymers.

DESIGN AND FABRICATION OF AIR PURIFIER USING HEPA AIR FILTER

Dr. M. Sreenivasa Kumar¹, Dr. M Venkannababu², Mr.K Pedda Vamsi Krishna³

¹ Professor & Principal, Narasaraopeta Engineering College (Autonomous), Narasaraopet – 522601, Andhra Pradesh, India.

² Associate Professor, Department of Mechanical Engineering, Narasaraopeta Engineering College (Autonomous), Narasaraopet - 522601, Guntur District, Andhra Pradesh, India.

³ Student, Department of Mechanical Engineering, Narasaraopeta Engineering College (Autonomous), Narasaraopet - 522601, Guntur District, Andhra Pradesh, India.

Abstract: The air purifier industry has seen a growth in terms of demand and sales lately. All credit goes to massive industrialization in developing countries such as India and China. As a result, a lot of research has been focused into the various methods of purifying air. The most harmful of the pollutants are PM 2.5 particulates and NOx emissions. The aim has been to bring down the costs without compromising on efficiency as efficient air purification is an expensive deal. This article presents a study of the current scenario of the problems of air pollution. Severity of the issues have been highlighted. A compilation of the most common and significant methods of purifying air such as those employing the use of HEPA filters, electrostatic smoke precipitators, activated carbon and UV light has been presented and their use in air purifiers manufactured by OEMs has been mentioned. Some of the most modern methods of purifying air such as those using transparent PAN filters, photochemical materials, soy proteins and silk Nano fibrils have been studied and reviewed. It has been found that these methods provide an attractive and economical pathway of filtering out PM 2.5 when compared to the conventional HEPA filters

THE NUMERICAL ANALYSIS OF BUBBLE GROWTH AND BUBBLE FREQUENCY IN NUCLEATE BOILING

K. Ayyapa Swamy¹, Shaik Nagul Meeravali ²

¹ Ph.D Scholar, Department of Mechanical Engineering, Bits Pillani, Rajasthan, India.

² Assistant Professor, Department of Mechanical Engineering, Narasaraopeta Engineering College, Narasaraopet, India

ABSTRACT: The nucleate boiling phenomena is analysed for TiO₂ and Al₂O₃ aqueous Nanofluids using computational fluid dynamics. The use Nanofluid as a working fluid significantly enhances the boiling critical heat flux (CHF). It has been found that the CHF enhancement in boiling is dependent on the type of Nanofluid as well as its concentration. The present study observed that by increasing the nanoparticles concentration, the bubble frequency increases. Two sets of Nanofluids, viz. Al₂O₃ and TiO₂ with Volume of Fraction (VOF) of 0.05, 0.1, and 0.15 have been considered for the study. The obtained simulation results show that by increasing the nanoparticles concentration, the TSHF and HTC increase proportionally. TiO₂ nanoparticles with various VOF give better results after a time interval of 1.4 s compared to Al₂O₃ and water.

KEYWORDS: Nanofluids, Heat Transfer Coefficient, Total Surface Heat Flux, Critical Heat Flux & Concentration